frontiers | Research Topics

Microbe assisted plant resistance to abiotic stresses

Edited by
Delong Meng, Mengting Maggie Yuan and Juan Li

Published in
Frontiers in Plant Science

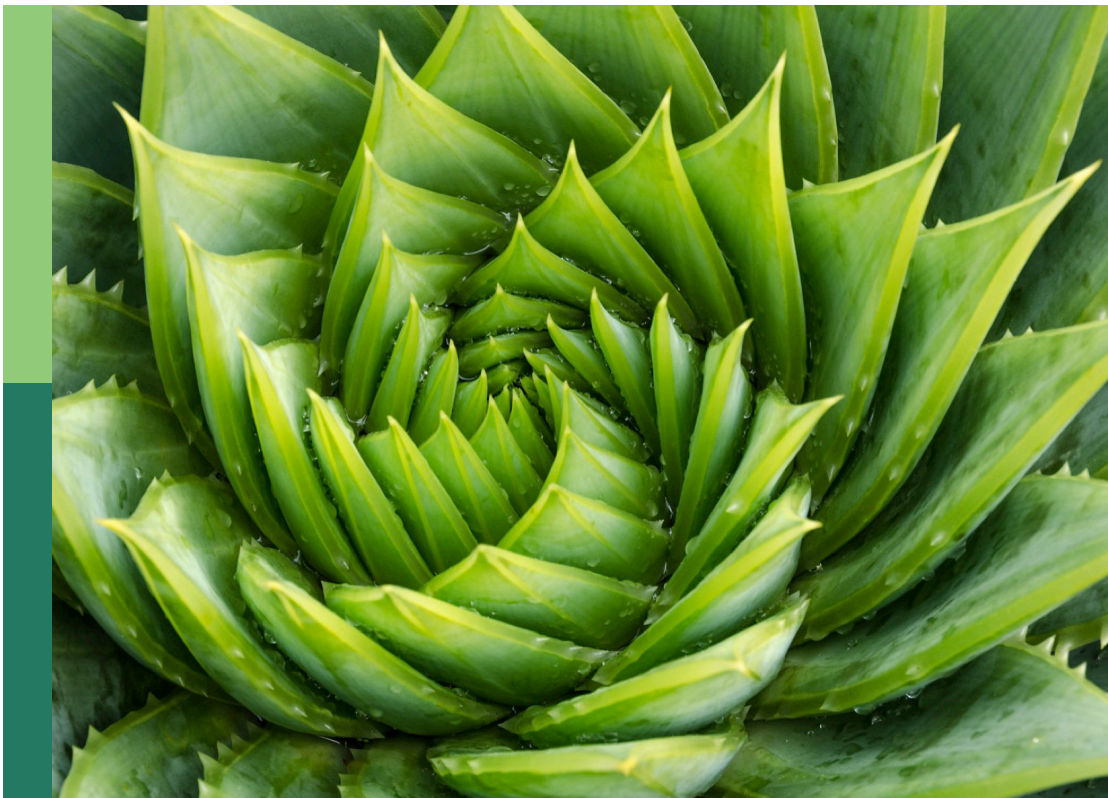

ISSN 1664-8714
ISBN 978-2-8325-3501-1
DOI 10.3389/978-2-8325-3501-1

About Frontiers

Frontiers is more than just an open access publisher of scholarly articles: it is a pioneering approach to the world of academia, radically improving the way scholarly research is managed. The grand vision of Frontiers is a world where all people have an equal opportunity to seek, share and generate knowledge. Frontiers provides immediate and permanent online open access to all its publications, but this alone is not enough to realize our grand goals.

Frontiers journal series

The Frontiers journal series is a multi-tier and interdisciplinary set of open-access, online journals, promising a paradigm shift from the current review, selection and dissemination processes in academic publishing. All Frontiers journals are driven by researchers for researchers; therefore, they constitute a service to the scholarly community. At the same time, the *Frontiers journal series* operates on a revolutionary invention, the tiered publishing system, initially addressing specific communities of scholars, and gradually climbing up to broader public understanding, thus serving the interests of the lay society, too.

Dedication to quality

Each Frontiers article is a landmark of the highest quality, thanks to genuinely collaborative interactions between authors and review editors, who include some of the world's best academicians. Research must be certified by peers before entering a stream of knowledge that may eventually reach the public - and shape society; therefore, Frontiers only applies the most rigorous and unbiased reviews. Frontiers revolutionizes research publishing by freely delivering the most outstanding research, evaluated with no bias from both the academic and social point of view. By applying the most advanced information technologies, Frontiers is catapulting scholarly publishing into a new generation.

What are Frontiers Research Topics?

Frontiers Research Topics are very popular trademarks of the *Frontiers journals series*: they are collections of at least ten articles, all centered on a particular subject. With their unique mix of varied contributions from Original Research to Review Articles, Frontiers Research Topics unify the most influential researchers, the latest key findings and historical advances in a hot research area.

Find out more on how to host your own Frontiers Research Topic or contribute to one as an author by contacting the Frontiers editorial office: frontiersin.org/about/contact

Microbe assisted plant resistance to abiotic stresses

Topic editors

Delong Meng — Central South University, China

Mengting Maggie Yuan — University of California, Berkeley, United States

Juan Li — Hunan Agricultural University, China

Citation

Meng, D., Yuan, M. M., Li, J., eds. (2023). *Microbe assisted plant resistance to abiotic stresses*. Lausanne: Frontiers Media SA. doi: 10.3389/978-2-8325-3501-1

Table of contents

frontiers | Frontiers in Plant Science

TYPE Editorial
PUBLISHED 01 September 2023
DOI 10.3389/fpls.2023.1277682

OPEN ACCESS

EDITED AND REVIEWED BY
Andrea Genre,
University of Turin, Italy

*CORRESPONDENCE
Delong Meng
delong.meng@csu.edu.cn
Mengting Maggie Yuan
maggieyuan@berkeley.edu
Juan Li
adalee619@163.com

RECEIVED 15 August 2023
ACCEPTED 28 August 2023
PUBLISHED 01 September 2023

CITATION
Meng D, Yuan MM and Li J (2023) Editorial: Microbe assisted plant resistance to abiotic stresses. *Front. Plant Sci.* 14:1277682. doi: 10.3389/fpls.2023.1277682

Editorial: Microbe assisted plant resistance to abiotic stresses

Delong Meng[1,2]*, Mengting Maggie Yuan[3]* and Juan Li[4]*

[1]School of Minerals Processing and Bioengineering, Central South University, Changsha, China, [2]Key Laboratory of Biometallurgy, Ministry of Education, Changsha, China, [3]Department of Environmental Science, Policy, and Management, University of California, Berkeley, Berkeley, CA, United States, [4]College of Agronomy, Hunan Agricultural University, Changsha, China

KEYWORDS

abiotic stress, plant resistance, plant microbiome, plant-microbe interaction, bioinformatics

Editorial on the Research Topic
Microbe assisted plant resistance to abiotic stresses

The interaction between microorganisms and plants has emerged as a prominent research area in both microbiology and plant biology. Abiotic stresses, including drought, salinity, and heavy metal, exert substantial impacts on plant growth across the globe. These stressors, whether occurring individually or in combination, can disrupt nutrient uptake and hinder overall plant development (Mushtaq et al., 2023). However, beneficial microbes has shown potential in enhancing plant resilience to such abiotic challenges (Cardarelli et al., 2022; El-Shamy et al., 2022). Certain microorganisms inhabiting the rhizosphere and phyllosphere can facilitate plant water and nutrient acquisition while providing protection against harmful environmental toxins (Degani, 2021; Redondo et al., 2022).

The past decade has witnessed remarkable strides driven by advancements in sequencing and omic technologies, unraveling the intricate mechanisms governing plant-microbe interactions amidst abiotic stresses. These nuanced relationships are progressively being deciphered, providing insights that pave the way for predictive and modulatory strategies. Leveraging plant-microbe interactions to bolster plant adaptation to abiotic stresses holds transformative potential across agricultural productivity, bioremediation strategies, and ecological sustainability.

This research endeavor is aimed at spotlighting the essential role of microorganisms in bolstering plant resistance against abiotic stresses. Within this Research Topic, ten scholarly contributions delve into a variety of mechanisms by which microorganisms assist plants in adapting to environmental fluctuations, safeguarding their growth and survival. The inquiry also delves into the intricate impact of inter-root microbial communities on the broader health of plants. Collectively, these articles provide a comprehensive perspective on how microorganisms contribute to ecosystem functions and the well-being of plants.

Enhancing plant production and survival in response to urgent market demands and severe abiotic stresses has become a central focus of research. Qi et al. utilized RNA interference (RNAi) technology to construct an ihpRNA plant expression vector of the oleic acid desaturase (FAD2) gene, resulting in an elevated oleic acid content and a reduction in levels of linoleic acid and linolenic acid in rapeseed. Notably, the rhizosphere microbial community, employed as an indicator for the safety assessment of genetically

modified plants, remained largely unaffected. This study presents a secure and effective method for enhancing plant production. Fu et al. focused on the impact of high-altitude environments on the endophytic microbial community of Ginkgo biloba. They revealed that altitude could regulate the microbial community structure by modulating Ginkgo biloba metabolites (flavonoids). This research unveiled the intricate interaction between microorganisms and plants, enhancing plant environmental adaptability. Li et al. investigated horizontal gene transfer (HGT) in plant genomes, identifying 235 genes from microbes that conferred abiotic stress resistance. These genes provided plants with defenses against various stressors such as toxic metals, drought, heat, and pollutants. Phylogenetic analysis supported the microbial origin of these genes. The research highlighted the crucial contribution of HGT to enhancing plants' ability to cope with environmental challenges. Moreover, Wang et al. conducted an analysis of the composition and assembly of the microbial community in tobacco leaves. This study aimed to investigate the effects of summer climate and wildfire disease stresses on microorganisms. Their findings shed light on the significant role played by microorganisms in shaping the spatial and temporal patterns, processes, and response mechanisms of plants in their adaptation to environmental stresses. Collectively, these studies promise to not only deepen our comprehension of the contribution of microorganisms to plant adaptation under abiotic stresses, but also to unravel the intricate complexity of the symbiotic relationship between microorganisms and plants.

Plant rhizosphere microorganisms, as essential components of the plant holobiont, play a pivotal role in maintaining plant health and adaptability. This Research Topic illuminated the complex interaction between rhizosphere microbes and the overall health of plants. In the context of collaborative responses to plant diseases, Tang et al. investigated how tobacco bacterial wilt and black shank pathogens modified interactions within the rhizosphere microbial community. At the metabolic level, Actinobacteria strains that secreted antibiotics demonstrated effective pathogen inhibition, underscoring the significance of rhizosphere microbes in sustaining plant health. Similarly, Tao et al. explored how bacterial wilt disease impacts the root-associated microbiomes of tobacco plants. They found that the disease led to distinct changes in the microbiomes of different root compartments. The study highlighted the recruitment of beneficial bacteria and varying sensitivities among root areas. The research provides valuable insights into the responses of root-associated microbiomes to plant diseases. Poria et al. proposed a sustainable solution for remediating marginal land using Plant Growth-Promoting Bacteria (PGPB). They highlighted the role of plants and microorganisms in restoring soil quality in challenging environments. The review covered different phytoremediation methods, focusing on economically important plants and the benefits of PGPB in enhancing plant growth and bioremediation. The authors suggested using PGPB with dual precession technology to improve soil fertility and restore agriculture and native vegetation on marginal lands. In the realm of heavy metal remediation, Xiao et al. investigated how rhizosphere bacteria assisted in phytoremediation within a lead-zinc mining area. They compared the metal accumulation abilities of various plants and identified specific bacteria that influenced metal uptake and soil parameters. Their findings revealed a strong correlation between the composition of plant rhizosphere microorganisms and the plants' capability to absorb heavy metals. The research provided insights into selecting plants for diverse metal remediation scenarios and emphasized the potential of rhizosphere bacteria to enhance multi-metal phytoremediation. Zakrzewska et al. used *Ochrobactrum* sp. POC9 metabolites to counter cadmium toxicity in soil. They investigated the impact of supplementing soil with carbonates-containing metabolites (MCC) on Cd mobility, plant growth, and uptake using *Petroselinum crispum*. MCC acted as a stabilizer for Cd and a stimulant for soil and plants. Li et al. investigated the interplay between rice plant rhizosphere microorganisms and cadmium uptake. The study unveiled significant impacts of specific bacterial strains' inoculation on rice plant cadmium uptake and root endophytic bacterial communities. Furthermore, correlations were identified between the relative abundance of specific bacteria, cadmium content in rice plants, and cadmium enrichment coefficients in roots. These findings underscored the considerable potential of microorganisms in enhancing plant health and promoting sustainable agriculture. In sum, these studies not only deepen our comprehension of the profound connection between rhizosphere microbes and plant health but also unveil the diverse roles of microbes in plant adaptation and restoration capability.

Articles in this Research Topic not only uncovered the significance of microorganisms in aiding plants' adaptation to abiotic stressors and the essential role of rhizosphere microorganisms in plant well-being, but also provide valuable guidance for achieving sustainable agricultural development and ecological preservation. By intensifying in-depth research into the interplay between microorganisms and plants, we aspire to better utilize these interactive relationships in the future, contributing to the sustainable development.

Author contributions

DM: Writing – original draft, Writing – review & editing. MY: Writing – review & editing. JL: Writing – review & editing.

Conflict of interest

The authors declare that the research was conducted in the absence of any commercial or financial relationships that could be construed as a potential conflict of interest.

Publisher's note

References

Cardarelli, M., Woo, S. L., Rouphael, Y., and Colla, G. (2022). Seed treatments with microorganisms can have a biostimulant effect by influencing germination and seedling growth of crops. *Plants (Basel)* 11, 259. doi: 10.3390/plants11030259

Degani, O. (2021). A review: late wilt of maize-the pathogen, the disease, current status, and future perspective. *J. Fungi (Basel)* 7, 989. doi: 10.3390/jof7110989

El-Shamy, M. A., Alshaal, T., Mohamed, H. H., Rady, A. M. S., Hafez, E. M., Alsohim, A. S., et al. (2022). Quinoa response to application of phosphogypsum and plant growth-promoting rhizobacteria under water stress associated with salt-affected soil. *Plants (Basel)* 11, 872. doi: 10.3390/plants11070872

Mushtaq, N. U., Alghamdi, K. M., Saleem, S., Tahir, I., Bahieldin, A., Henrissat, B., et al. (2023). Exogenous zinc mitigates salinity stress by stimulating proline metabolism in proso millet (*Panicum miliaceum* L.). *Front. Plant Sci.* 14. doi: 10.3389/fpls.2023.1053869

Redondo, M. A., Oliva, J., Elfstrand, M., Boberg, J., Capador-Barreto, H. D., Karlsson, B., et al. (2022). Host genotype interacts with aerial spore communities and influences the needle mycobiome of Norway spruce. *Environ. Microbiol.* 24, 3640–3654. doi: 10.1111/1462-2920.15974

frontiers | Frontiers in Plant Science

TYPE Original Research
PUBLISHED 11 August 2022
DOI 10.3389/fpls.2022.982771

OPEN ACCESS

EDITED BY
Juan Li,
Hunan Agricultural University, China

REVIEWED BY
Yonghua Zhu,
Hunan University, China
Qingyun Yan,
Sun Yat-sen University, China

*CORRESPONDENCE
Yili Liang
liangyili6@csu.edu.cn

SPECIALTY SECTION
This article was submitted to Plant Symbiotic Interactions, a section of the journal Frontiers in Plant Science

RECEIVED 30 June 2022
ACCEPTED 19 July 2022
PUBLISHED 11 August 2022

CITATION
Fu S, Deng Y, Zou K, Zhang S, Liu X and Liang Y (2022) Flavonoids affect the endophytic bacterial community in *Ginkgo biloba* leaves with increasing altitude.
Front. Plant Sci. 13:982771.
doi: 10.3389/fpls.2022.982771

Flavonoids affect the endophytic bacterial community in *Ginkgo biloba* leaves with increasing altitude

Shaodong Fu[1,2], Yan Deng[1,2], Kai Zou[3], Shuangfei Zhang[1,2], Xueduan Liu[1,2] and Yili Liang[1,2]*

[1]School of Resource Processing and Bioengineering, Central South University, Changsha, China, [2]Key Laboratory of Biometallurgy, Ministry of Education, Central South University, Changsha, China, [3]College of Advanced Materials Engineering, Jiaxing Nanhu University, Jiaxing, China

Altitude affects plant growth and metabolism, but the effect of altitude on plant endophytic microorganisms is still unclear. In this study, we selected 16 *Ginkgo biloba* trees to study the response of leaves' endophytes to flavonoids and altitude (from 530 m to 1,310 m). HPLC results showed that flavonoids in *Ginkgo biloba* leaves increased by more than 150% with attitude rising from 530 m to 1,310 m, which revealed a positive correlation with altitude. *Ginkgo biloba* might regulate the increased flavonoids in leaves to resist the increasing light intensity. 16S rDNA sequencing results showed that the endophytic bacterial communities of *Ginkgo biloba* at different altitudes significantly differed. *Ginkgo* leaf endophytes' alpha diversity decreased with increasing flavonoids content and altitude. The increased flavonoids might increase the environmental pressure on endophytes and affect the endophytic community in *Ginkgo biloba* leaves. The bacterial network in *Ginkgo biloba* leaves became more complex with increasing altitude, which might be one of the strategies of leaf endophytes to cope with increasing flavonoids. Metagenomes results predicted with PICRUSt showed that the abundance of flavonoid biosynthesis and photosynthesis genes were significantly decreased with the increase of flavonoid contents. High flavonoid content in leaves appeared to inhibit microbial flavonoid synthesis. Our findings indicate that altitude can modulate microbial community structure through regulating plant metabolites, which is important to uncovering the interaction of microbes, host and the environment.

KEYWORDS

***Ginkgo biloba*, flavonoids, endophyte community, network, function genes**

Introduction

Altitude can affect plant growth and metabolism. Previous research showed that flavonoids biosynthesis in ginkgo leaves is affected by altitude (Zou et al., 2019). Endophytes play important roles in plant health and productivity (Leach et al., 2017). Endophytic bacteria spend part or all of their life inside the plant tissues without causing hosts diseases, and they always play positive roles in plant growth (Schulz and Boyle, 2006; White and Torres, 2010). Generally, endophytes are considered as a complement to the plant gene library, helping the hosts adapt to the environment (Vandenkoornhuyse et al., 2015), such as enhancing hosts' stress tolerance (e.g., drought and salinity) (Malinowski et al., 2008), improving hosts' resistance to diseases (Clarke et al., 2006), helping hosts with mineral uptake (Malinowski and Alloush GABelesky, 2000) and promoting hosts growth (Schardl et al., 2004). Besides, endophytes can produce the same bioactive metabolites as the host, like alkaloids, steroids, terpenoids and flavonoids (Tan and Zou, 2010; Deshmukh and Verekar, 2012). Host plants procure an apparent modulation immunity by enriching beneficial microbes (Berendsen et al., 2012). It was generally acknowledged that temperature variation mostly affected the endophytic community formation with the elevation increase (Ju et al., 2006). Thus, deciphering the interaction between plants and endophytes attract much attention in ecology and plant sciences.

The regulation of endophytes by plants is an important part of the relationships between plants and microorganisms. Many factors can affect the community of endophytes in the plant, such as temperature (Ju et al., 2006), precipitation (Brosi et al., 2011) and soil property (Lehtonen et al., 2005). But plant secondary metabolites may have the most immediate effect because of the direct contact with endophyte. Benzoxazinoids, defensive secondary metabolites released by cereals' roots, were reported to alter root-associated fungal and bacterial communities (Saunders and Kohn, 2009; Hu et al., 2018). Sesquiterpenes induced hyphal branching in an arbuscular mycorrhizal fungus (Akiyama et al., 2005). Flavonoids are also essential secondary metabolites in improving plant-microbe interactions (Hassan and Mathesius, 2012; Chin et al., 2018). Previous studies showed that flavonoids could regulate the endophytic microbial community in roots as allelochemicals, nod gene inducers and phytoalexins (Cooper, 2004; Shaw et al., 2006).

Flavonoids are distinguished antioxidants and plant protectants owing to numerous phenolic hydroxyl radicals (Pietta, 2000). They can inhibit the growth of many microorganisms, including *Staphylococcus aureus*, *Escherichia coli*, and many other bacteria (Parvez et al., 2004; Farhadi et al., 2018). Generally, flavonoids (e.g., catechins) show more significant stress on Gram-positive bacteria than Gram-negative bacteria because of different cytoderm structures (Ikigai et al., 1993; Fathima et al., 2016). *Ginkgo* leaves are the main source of flavonoids, so factors that influence the flavonoid content in *Ginkgo* leaves have been investigated extensively. Previous studies revealed that lower temperature promoted the accumulation of flavonoids, but CO_2 and O_3 were important inhibitors of foliar flavonoids in *Ginkgo biloba* (Huang et al., 2010; Wang et al., 2014). Moreover, studies found that UV-B promoted flavonoid synthesis in *Ginkgo biloba* leaves (Zhao et al., 2020). Our recent study observed that the elevation and tree age affect flavonoid biosynthesis, and they attribute it to the light enhancement and gene variations (Zou et al., 2019).

Although flavonoids' influence on microorganisms has gotten much attention, the relationship between flavonoids and endophyte communities in plant leaves is still scarce. In this study, we collected *Ginkgo* leaves with different concentrations of flavonoids at different altitudes. Combining with plant metabolomics and endophyte genomics analysis, we assessed the response of the endophytic community to changes in flavonoids in *Ginkgo* leaves. Our aims were to (i) explore the reasons for the change of flavones with altitude; (ii) analyze the effect of flavonoids on the endophytic community; and (iii) elucidate the mechanism by which flavonoids affect the community.

Materials and methods

Sample collection

We selected 16 *Ginkgo biloba* trees in the Hupingshan Nature Reserve, which were rarely affected by human activities, as the research object (**Table 1**). Ginkgo's leaves were chosen as our object owing to their abundant flavonoids. The average annual temperature in the nature reserve is 9.2°C. The extreme maximum temperature in the sample sites is 38.2°C. The extreme minimum temperature is −15°C. The average annual sunshine in the sample sites is 1,509.9 h, and the annual precipitation is 1,898.5 mm. All trees grew in the same general area and experienced similar growing conditions. The elevation and the diameter at breast height (DBH) were determined by the Global Positioning System (GPS) instrument and a tape measure. All trees were healthy, alone, and had no shade. The leaves of the ginkgo canopy are divided into two parts longitudinally with the trunk as the axis. The sampling height is 5-8 m. The two parts are evenly sampled. Multiple leaves are mixed into one sample. About 200 g of healthy and mature leaves were collected as samples in each part. Leaves in different parts were considered as different samples. All samples were collected aseptically wearing bioclean gloves on a sunny day with the same weather condition. All samples were divided into two parts. One was frozen in liquid nitrogen immediately and then stored at −80°C for metabolome detection and flavonoid extraction. Another was surface disinfected promptly for the microbiological analysis. Leaves were sterilized with 75% ethanol for 5 min, then washed with sterile water, soaked in 8%

NaClO for 2 min and washed with sterile water again (Sahu et al., 2022). After surface sterilizing, dried the leaves surface with sterile filter paper and sterile air on a sterile workbench. All leaves were triturated in liquid nitrogen and stored at −80°C until DNA extraction.

High-performance liquid chromatography

Frozen leaves were dried in an oven at 60°C until the weight was constant (Zhou et al., 1999). Afterward, these leaves were ground into powder smaller than 40 mesh and extracted in a Soxhlet extractor based on Chinese pharmacopeia (2015). 1.000 g dried powder was homogenized in 100 mL chloroform followed by two h reflux at 80°C. The residue was resolved in 50 mL methanol followed by two-hour reflux at 90°C. Then, 20 mL hydrochloride was added to the supernatant, refluxing for 30 min at 90°C and evaporating to dryness. The residue was dissolved in methanol and filtrated through a 0.22 μm membrane for HPLC (Daigle and Conkerton, 1983).

Chromatographic separation was implemented on a Shimadzu LC-20AD Series HPLC system (Shimadzu, Duisburg, Germany) equipped with SIL-20A autosampler, SPD-20A UV-VIS detector. ACQUITY UPLC^{TM} BEH C18 column (217 mm × 2.1 mm, 1.7 μm, Waters, Milford, United States) was connected to the whole detection at 25°C. The mobile phase consisted of 10% 0.05 M sodium acetate (A) and 90% acetonitrile (B). A flow rate of 1.0 mL/min was used. Standard curves were established by a series concentration of the corresponding standard (ChemFaces, Wuhan, China) at 360 nm (Mattila et al., 2000). And the content of total flavonoids was calculated by the formula (Hasler et al., 1992):

$$\text{Total flavonoids} = 2.51quercetin + 2.64kaempferol + 2.39isorhamnetin$$

The data were provided in the (**Supplementary Table 1**).

Deoxyribonucleic acid extraction, sequencing and sequence analysis

The leaf fragments were suspended in TE buffer and homogenized in a sterilized mortar and pestle with liquid nitrogen (Zhang et al., 2016). DNA was extracted from the homogenized leaf material using the DNeasyR Plant Mini Kit (Product of Germany). To get rid of the distractions of DNA of *Ginkgo* leaves, the DNA was polymerase chain reaction (PCR) amplified using a primer pair 799F (5′-AACMGGATTAGATAC CCKG-3′) and 1115R (5′-AGGGTTGCGCTCGTTG-3′) (Leff et al., 2015). The DNA was cleaned by DNA Clean-Up Kit (OMEGA bio-teak, Norcross, Georgia, United States). High-throughput sequencing of the PCR products was conducted on the Illumina Miseq platform (Miseq PE250).

By comparing the NCBI and Greengene databases, we removed the sequence of the chloroplasts. Raw 16S rRNA gene sequences were processed using the Galaxy | Denglab[1]. These steps included: quality filtering, RDP clustering, sequence alignments and community dissimilarities analysis (Wu et al., 2018). Taxonomic assignment of 16S representative sequences was executed with the RDP (Ribosomal Database Project) classifier according to the Greengene database (Desantis et al., 2006). Resampled 16S OTU subsets (1000 sequences per sample) were to compute alpha diversity and beta diversity. The data presented in the study are deposited in the NCBI repository, accession number PRJNA852885.

Data analysis

Alpha-diversity indexes, including Shannon index, Simpson evenness, and Pielou evenness, were calculated at Institute for Environmental Genomics (IEG)[2]. Non-metric multidimensional scaling (NMDS) was calculated to assess the beta diversity. The dissimilarity test identified the difference in bacterial communities. Correlation between bacterial community and flavonoids based on the Mantel test, correlation test, and redundancy analysis (RDA) were completed using the Wekemo Bioincloud[3]. OTUs with an average abundance of more than 0.05% was chosen to construct correlation networks by calculating Spearman's

1 http://mem.rcees.ac.cn:8080/

2 http://ieg.ou.edu/

3 https://www.bioincloud.tech

TABLE 1 Altitude and other information of sampling trees.

Sample	DBH(m)	Latitude	Longitude	Altitude(m)
S1_1	3.00	N 29°57′22″	E 110°48′40″	530
S1_2	4.00	N 29°57′22″	E 110°48′40″	530
S1_3	3.24	N 29°51′59″	E 110°44′59″	560
S1_4	2.18	N 29°51′59″	E 110°44′59″	560
S2_1	2.00	N 29°56′55″	E 110°39′16″	800
S2_2	2.15	N 29°54′12″	E 110°44′33″	820
S2_3	3.10	N 29°54′12″	E 110°44′33″	820
S2_4	3.18	N 29°53′7″	E 110°42′28″	840
S3_1	2.26	N 29°56′7″	E 110°38′28″	1,000
S3_2	1.92	N 29°55′50″	E 110°37′6″	1,020
S3_3	2.59	N 29°52′7″	E 110°37′28″	1,040
S3_4	4.12	N 26°55′13″	E 110°36′16″	1,040
S4_1	2.40	N 30°5′47″	E 110°48′50″	1,260
S4_2	3.00	N 30°6′46″	E 110°46′29″	1,300
S4_3	3.74	N 30°6′7″	E 110°49′2″	1,300
S4_4	2.65	N 30°9′23″	E 110°44′19″	1,310

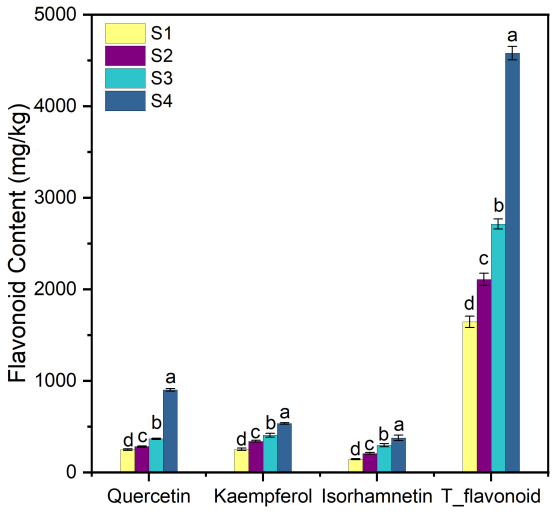

FIGURE 1
The concentration of three flavonols and total flavonoids in *Ginkgo* leaves at different altitudes. The significant difference among the groups is represented by different letters ($p < 0.05$).

rank correlations with Spearman's correlation coefficient ($r > 0.6$, $P < 0.01$) (Steinhauser et al., 2008). We used Gephi to visualize the correlation networks (Bastian et al., 2009).

PICRUSt was used as a bioinformatics tool to predict microflora's abundance of function genes (Langille et al., 2013). In this study, PICRUSt was employed to predict the functions genes of each sample based on 16S rRNA sequencing data. Comparing the sequence data of the 16S Greengene database (Greengenes 13.5), we predicted the community functional gene relative abundance of endophytic microorganisms with reference to the KEGG database.

Results

The content of flavonoids in leaves

HPLC results showed that quercetin, kaempferol and isorhamnetin were the primary flavonoid metabolites of *Ginkgo* leaves. According to the regression equation of the standard curve (**Supplementary Table 2**), the content of total flavonoids was calculated (**Figure 1**). The results showed that the total flavonoids increased by 178.38%, from 1,645.36 mg/kg at S1 to 4580.43 mg/kg at S4 ($p < 0.05$). The three flavonols quercetin, kaempferol and isorhamnetin increase steadily with elevation. The content of quercetin, kaempferol and isorhamnetin in leaves increased by 2.58, 1.11, and 1.71 times from S1 to S4, respectively. The results suggested that Ginkgo flavonoids' content was increased along the altitude gradient.

Endophytic community composition and diversity in ginkgo leaves

After quality filtering, RDP clustering, sequence alignments and other measures, we obtained 312123 high-quality paired 16S rRNA sequences. At the level of 97% similarity, all sequences were assigned to 3,038 OTUs based on the 16S Greengene database. OTU table was provided in the **Supplementary Document**. Alpha diversity represented by the Shannon index (**Figure 2A**) and observed_otus (**Figure 2B**) revealed that alpha diversity decreased significantly with the increase of flavonoids and the elevation. Samples at lower altitudes had higher species richness and diversity. NMDS and PCA results indicated that the bacterial communities in leaves were dynamic. Samples from the same site huddled together, and samples from different altitudes showed a great distance (**Figures 2C,D**).

All reads were affiliated with seven bacterial phyla except 5%∼10% sequences unclassified. The dominant phylum was Proteobacteria, accounting for 90%∼95% of the reads (**Figure 3A**). The samples at lower altitudes had fewer unclassified reads at the phylum level. Bacteria of Actinobacteria and Firmicutes were significantly reduced at higher altitudes. But at the family level, Enterobacteriaceae dominated the bacterial community composition in leaves and remained sequences belonged to 6 families and unclassified family (**Figure 3B**). It was found that samples at higher altitudes have less species richness at the family level.

Factors – bacteria abundance correlations

The Spearman correlation test and RDA analyzed the relationship between endophytic bacterial populations and factors. RDA results showed that the altitude, quercetin, kaempferol, isorhamnetin, and T_flavonoids significantly affected the endophytic bacterial community in ginkgo leaves, and the endophytic bacterial community was slightly affected by the age of Ginkgo (represented by DBH) (**Figure 4A**). VPA revealed that these factors constrained 19.59% of the total community distribution. The flavonoids individually constrained 12.83% of the community distribution, while the altitude and DBH constrained 1.50 and 2.28%, respectively (**Figure 4B**). Besides, flavonoids combined with altitude constrained 5.01% of the community distribution. The heatmap between factors and bacterial abundance was constructed by Spearman correlation values at both the family and genus levels. At the family level, we observed Ruminococcaceae and Porphyromonadaceae were positively correlated with three flavonols and T_flavonoid, while Rhodospirillaceae, Bifidobacteriaceae and Burkholderiaceae were positively correlated with T_flavonoids and one or two flavonols. There was a significant negative correlation

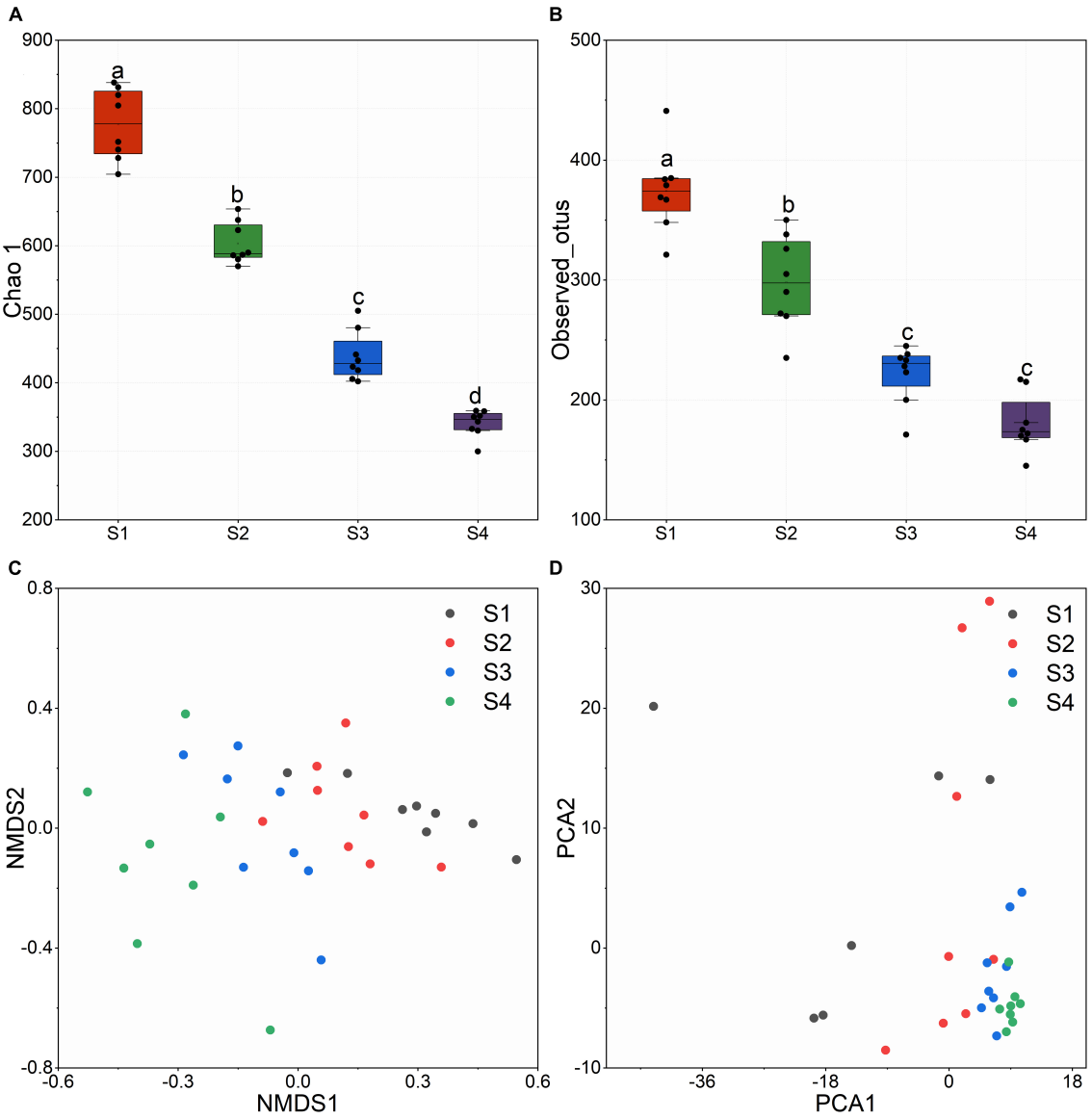

FIGURE 2
(A) Chao 1 index calculated with the OTU table. **(B)** Observed_otus in different sites. **(C)** Non-metric multidimensional scaling (NMDS) based on bray_curtis distance. **(D)** Principal Components Analysis (PCA).

between Bacillaceae and flavonoids (Figure 5A). It was found that endophytes of four genera were significantly positively correlated with flavonoids, including *Oscillibacter, Moraxella, Clostridium* and *Parabacteroides*. Only *Staphylococcus* showed a significant negative correlation with T_flavonoid and kaempferol (Figure 5B).

Functions genes prediction by PICRUSt

Using PICRUSt (Phylogenetic Investigation of Communities by Reconstruction of Unobserved States) as a predictive exploratory tool, we found that seven orthology groups at the level I (KOs in KEGG (Kyoto Encyclopedia of Genes and Genomes)) were observed in the *Ginkgo* endophyte community. Relative abundance of metabolism, genetics information processing and cellular processes tended to be constant in the four samples. Almost half of the significant function genes were classified into multiple metabolism groups. Environmental information processing accounted for nearly 20% of all genes. The difference was the relative abundance of environmental information processing gradually increased from 16.2% in S1 to 17.5% in S4 (Figure 6A). Besides, there were more pronounced changes in function genes at level III. Photosynthetic pathways

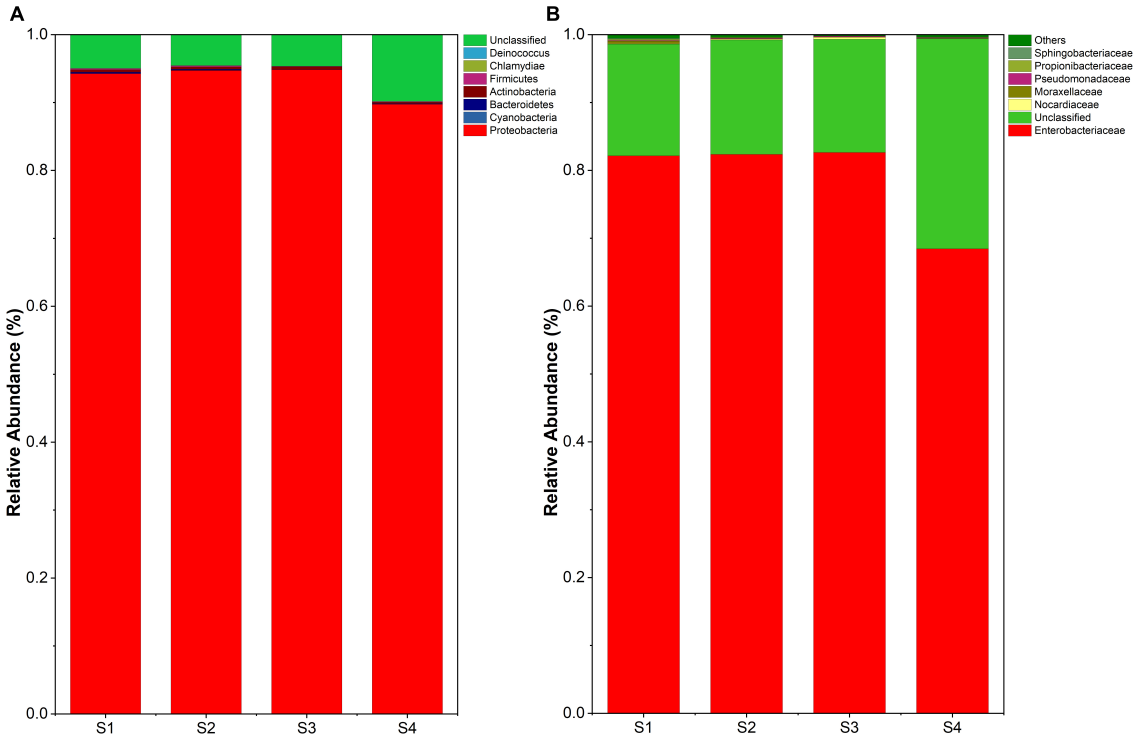

FIGURE 3
(A) Endophyte composition in all samples at the phylum level. **(B)** Endophyte community composition at the family level.

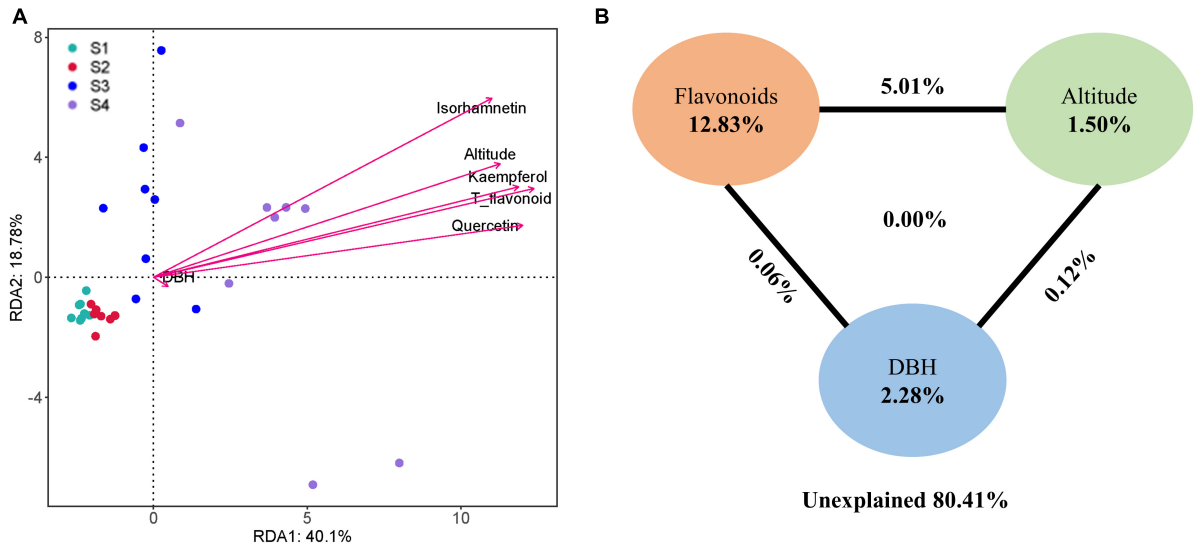

FIGURE 4
(A) Redundancy analysis (RDA) and **(B)** variance partitioning analysis (VPA) of the relationships between endophytic bacterial community and environmental variables in *Ginkgo biloba* leaves.

(including photosynthesis - antenna proteins, photosynthesis proteins, carbon fixation in photosynthetic organisms and photosynthesis) and flavonoids biosynthesis (consisting of phenylalanine, tyrosine and tryptophan biosynthesis, phenylpropanoid biosynthesis and flavonoid biosynthesis) gradually reduced ($p < 0.05$). The relative abundance of function genes of photosynthesis in S1 decreased by two-thirds compared with that in S1 (Figure 6B).

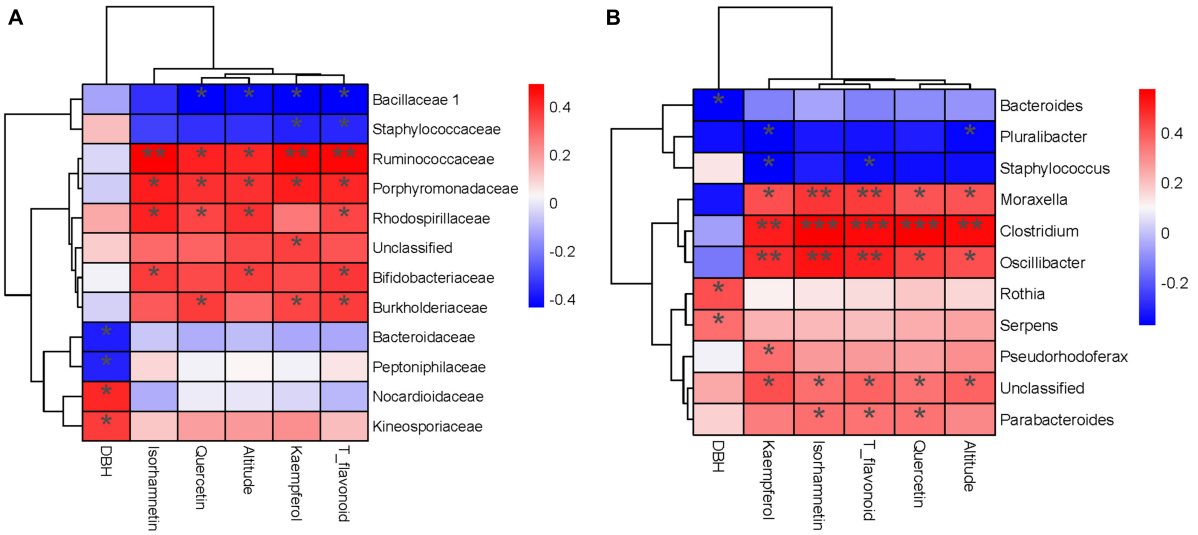

FIGURE 5
Heatmap **(A)** The correlation test between families and factors. **(B)** The correlation test between genera and factors. (***) $p < 0.001$, (**) $p < 0.01$ and (*) $p < 0.05$.

The variation of the endophyte network along with altitude in ginkgo leaves

We further performed network analysis to assess the impact of altitude on ginkgo leaf endophyte. Our results showed that microbial interkingdom network patterns shifted clearly along with the increased altitude (**Figure 7**). Specifically, endophytic networks at lower altitudes had higher network connectivity (i.e., network degree) than networks at higher altitudes. Although there was a near number of nodes contributing to the network construction, the edges of networks gradually increased with the altitude increase. Compared with the network of S1, the number of edges increased by two times at S4. The network's average degree and weighting degree increased from 11.757 and 5.705 to 28.249 and 18.002, respectively (**Figure 7E**).

Discussion

The increase of oxidation activity induced by light might be the key to increasing flavonoid content

In this study, total flavonoids increased significantly with altitude (**Figures 1A,B**). There was not much difference in temperature among the locations of the samples. Meanwhile, it implied that the excess light might be the main reason for the accumulation of flavonoids. Increasing light intensity within a certain range could enhance photosynthesis (Longstreth and Strain, 1977). Another study showed that the strengthening of light intensity could motivate photosynthesis and enhance the oxidative activity in leaves (Ghasemzadeh et al., 2010). As important antioxidants in plants, flavonoids were produced to resist these oxidative active substances like (O_2^-) (Pietta, 2000; Tattini et al., 2010). Thus, we speculated that the accumulation of flavonoids could be an important strategy for plants to protect against cellular damage. With the rise of elevation, the illumination was enhanced, which promoted photosynthesis and increased oxidation activity. *Ginkgo* trees produced more flavonoids to weaken oxidative damage. Our recent study observed that flavonoids and related genes increased with the altitude, attributing it to the enhanced illumination (Zou et al., 2019). The fact that the improvement of illumination intensity could promote the production of flavonoids and accelerate the accumulation of oxidative activity had also been reported in the previous study (Karimi et al., 2013). As an antioxidant, flavonoids protect the plant from light damage (Kumar et al., 2018). Besides, the light was proved to induce the oxidation and degradation of lipids (Sun et al., 2006; Wiswedel et al., 2009). All the above evidence showed that *Ginkgo biloba* increased flavonoid output to resist the accumulation of oxidative activity caused by the elevation and enhanced light.

Flavonoids may regulate the structure of the endophytic community

Many secondary metabolites of plants can affect microbial communities, and flavonoids are no exception. With the

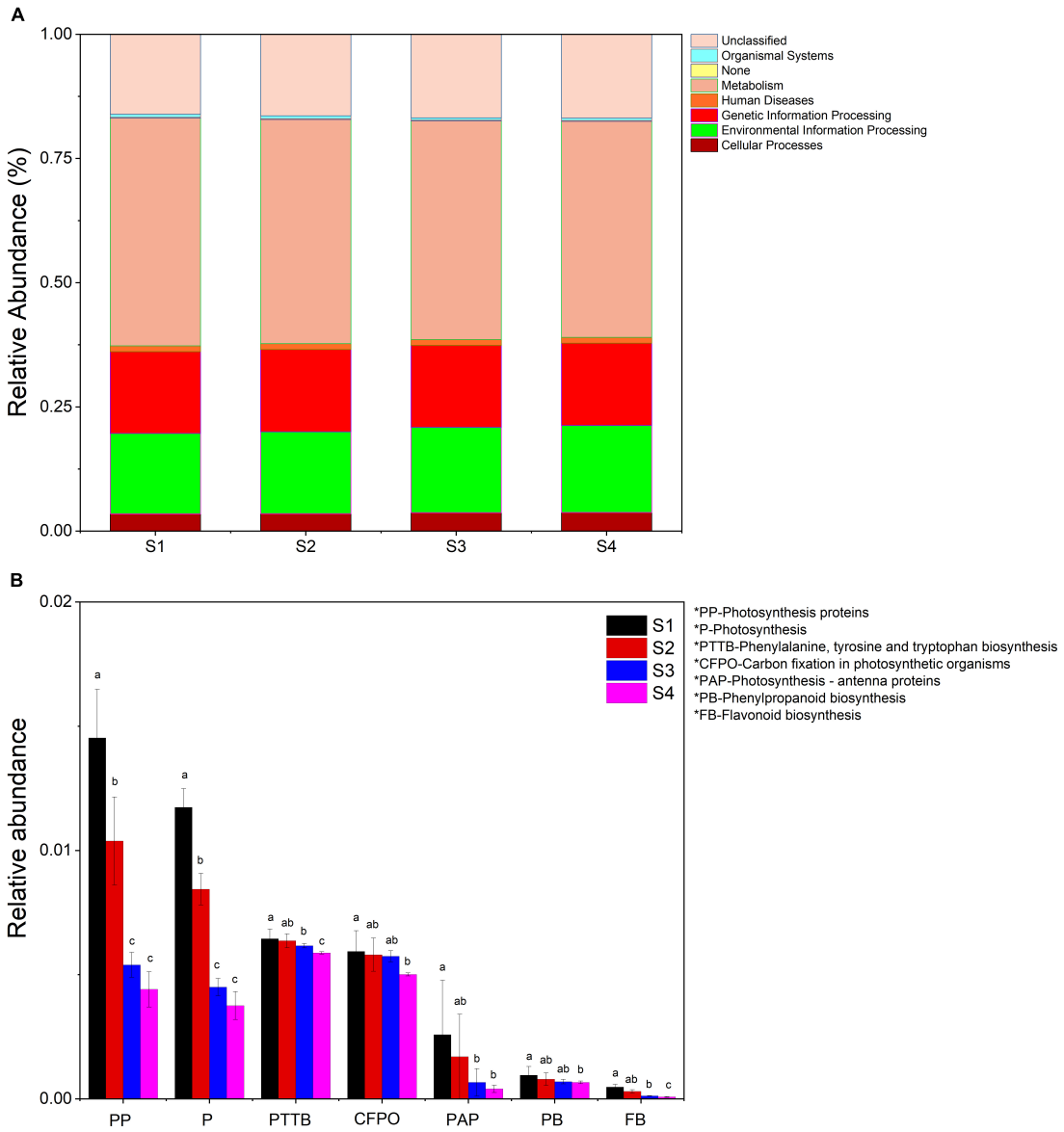

FIGURE 6
(A) Relative abundance of predicted function genes in different levels I samples. **(B)** Changes in the relative abundance of predicted genes in the flavonoid synthesis and photosynthesis pathways in all samples. Samples with different letters indicated significant differences between samples ($p < 0.05$).

increase of flavonoids, alpha diversity and observed_otus of the endophytic community decreased (Figure 2). Besides, we observed gram-negative bacteria accounted for the majority of total microorganisms, and the abundance of gram-negative bacteria increased from S1 to S4 (Figure 3). As the flavonoids increased, some gram-positive bacteria (including Firmicutes and Actinobacteria) decreased. We further analyzed the influencing factors of the microbial community in leaves by analyzing the correlation between the microbial community and factors such as flavonoid content and altitude (Figure 4). Flavonoids and altitude were proven to regulate the endophytic bacterial community in *Ginkgo biloba* leaves. Flavonoids are known to be antibacterial agents. Studies showed that the accumulation of flavonoids affected the symbiosis of endophytic bacteria and plants (Abdel-Lateif et al., 2012). Thus, flavonoids may be a key factor in the loss of diversity.

Furthermore, we found some microbiomes positively correlated with flavonoids, such as *Oscillibacter, Moraxella, Clostridium* and *Parabacteroides*. Microbes of *Clostridium* were proved to be flavonoid-degrading bacterium (Gupta et al., 2019). *Parabacteroides* were also found to increase with the addition of flavonoids in the gut microbiome (Zhang et al., 2022).

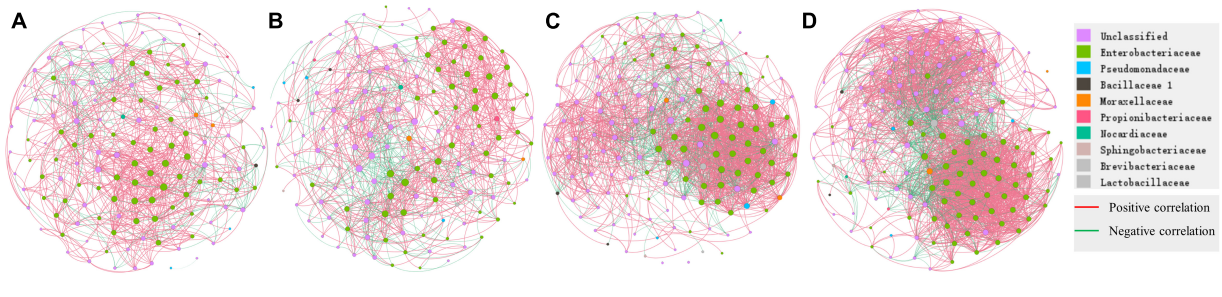

E

	S1	S2	S3	S4
Number of Nodes	148	153	152	151
Number of Edges	870	1022	1832	2284
Average degree	11.757	13.359	24.105	28.249
Average weighting degree	5.705	5.313	10.749	18.002
Network diameter	7	6	6	7
Network density	0.08	0.088	0.16	0.202
Network modularity	0.743	1.023	0.873	0.764
Clustering coefficient	0.444	0.45	0.561	0.635
Positive correlation	82.12%	76.17%	75.66%	79.38%
Negative correlation	17.88%	23.83%	24.34%	20.62%

FIGURE 7
Network of different sites **(A)** Network of bacterial community at S1. **(B)** Network of S2. **(C)** Network of S3. **(D)** Network of S4. **(E)** Details of networks in different sites.

In contrast, *Oscillibacter* and *Moraxella* decreased with the addition of flavonoids in the gut microbiome (Goulart et al., 2019; He et al., 2021; Cao et al., 2022). This difference might be because these microorganisms in Ginkgo leaves already live in an environment with high flavonoid content and have developed the resistance to flavonoids. Staphylococcus showed a significant negative correlation with T_flavonoid and kaempferol, the same as our previous study (Deng et al., 2021). Thus, we indicated that flavonoids could affect the community's composition and structure in *Ginkgo* leaves.

Microorganisms facing stress need to develop some resistant strategies for survival. Our results showed that the network of endophytic bacteria in ginkgo leaves became more complex with the increasing altitude. Thus, it can be inferred that the adjustment of microbial interactions could be a strategy for microbes to resist enhancing environmental stresses, such as the increase of flavonoid content, altitude, and light intensity.

Flavonoids regulated the physiological activities of endophytic microorganisms in leaves

In general, the environmental selection of microorganisms is mainly reflected in the collection of functions (Hammesfahr et al., 2011). The environmental information processing of endophytic bacteria in leaves significantly improved along with the increase of flavonoid content (**Figure 5A**), which also proved that the increase of altitude and flavonoids increased the environmental stress on endophytic bacteria in *Ginkgo biloba* leaves. *Ginkgo* leaves needed more environmental information processing genes to deal with the greater pressure caused by more flavonoids and more light with increased altitude. The analogical finding deemed environmental stress to be the momentous reason for enriching environmental information processing in early inquiry (Debroas et al., 2009). Furthermore, the abundance of genes on the photosynthetic pathway decreased with the flavonoids (**Figure 5B**). Microorganisms of Cyanobacteria were the dominating photosynthetic organisms in the endophytic communities. So the decrease of photosynthetic genes might attribute to the decreasing Cyanobacteria. We also observed genes related to flavonoid biosynthesis dropped with higher flavonoids. *In vitro*, flavonoid biosynthesis was inevitably inhibited by flavonoids' accumulation by feedback inhibition (Yin et al., 2012). So we hypothesized that flavonoids could also inhibit the accumulation of microorganisms that could produce flavonoids in leaves. In conclusion, flavonoids played an essential role in coordinating endophytic community functions in *Ginkgo* leaves.

Conclusion

In this study, the effects of altitude and flavonoids on the community of endophytic microorganisms in *Ginkgo biloba*

were revealed by combining the analysis of plant metabolites and genomics of endophytic microorganisms. HPLC results expounded that the output of flavonoids in *Ginkgo* leaves improved with elevation. The enhancement of photosynthesis and accumulation of oxidative activity caused by altitude elevation might account for the increase of flavonoids. It was not difficult to find that flavonoids could regulate the overall function of the microbial community by selectively inhibiting or promoting certain microorganisms and function genes. The network of endophytes in *ginkgo* leaves also became more complex with increasing altitude and flavonoids. It may be the strategy of ginkgo endophytic bacteria to respond to environmental changes. These results would benefit the studies on the endophytic microbiome of plants and the cultivation of *Ginkgo biloba*. It can also help to clarify the interactions between the environment, plants and the plant microbiome. Nevertheless, some other unmonitored conditions might have been overlooked in terms of flavonoid synthesis and community structure. There must be further research on the effects of flavonoids and altitude on the endophytic microorganisms in *Ginkgo biloba*.

Data availability statement

The data presented in this study are deposited in the NCBI repository, accession number: PRJNA852885.

Author contributions

SF performed the experiments and wrote the manuscript. KZ helped with the sample collection. SZ assisted in performing some experiments. YD and YL revised the manuscript. All authors approved the submitted manuscript.

Funding

This work was supported by the following grants: the National Natural Science Foundation of China (31570113) and the Graduate Research and Innovation Project (2018zzts772) in Central South University, China.

Acknowledgments

We thank James W. Voordeckers for his suggestions and grammar corrections on this manuscript.

Conflict of interest

The authors declare that the research was conducted in the absence of any commercial or financial relationships that could be construed as a potential conflict of interest.

Publisher's note

Supplementary material

The Supplementary Material for this article can be found online at: https://www.frontiersin.org/articles/10.3389/fpls.2022.982771/full#supplementary-material

References

Abdel-Lateif, K., Bogusz, D., and Hocher, V. (2012). The role of flavonoids in the establishment of plant roots endosymbioses with arbuscular mycorrhiza fungi, rhizobia and Frankia bacteria. *Plant Signal. Behav.* 7, 636–641. doi: 10.4161/psb.20039

Akiyama, K., Matsuzaki, K., and Hayashi, H. (2005). Plant sesquiterpenes induce hyphal branching in arbuscular mycorrhizal fungi. *Nature* 435, 824–827. doi: 10.1038/nature03608

Bastian, M., Heymann, S., and Jacomy, M. (2009). "Gephi: An open source software for exploring and manipulating networks," in *Proceedings of the international AAAI conference on web and social media*, Vol. 3, 361–362.

Berendsen, R. L., Pieterse, C. M. J., and Bakker, P. A. (2012). The rhizosphere microbiome and plant health. *Trends Plant Sci.* 17, 478–486.

Brosi, G. B., Mcculley, R. L., Bush, L. P., Nelson, J. A., Classen, A. T., and Norby, R. J. (2011). Effects of multiple climate change factors on the tall fescue-fungal endophyte symbiosis: Infection frequency and tissue chemistry. *N. Phytol.* 189, 797–805.

Cao, X., Guo, X., Fang, X., Ru, S., and Li, E. (2022). Effects of Poncirin, a Citrus Flavonoid and Its Aglycone, Isosakuranetin, on the Gut Microbial Diversity and Metabolomics in Mice. *Molecules* 27:3641.

Chin, S., Behm, C., and Mathesius, U. (2018). Functions of Flavonoids in Plant–Nematode Interactions. *Plants* 7:85. doi: 10.3390/plants7040085

Clarke, B. B., White, J. F. Jr., Hurley, R. H., Torres, M. S., Sun, S., and Huff, D. R. (2006). Endophyte-Mediated Suppression of Dollar Spot Disease in Fine Fescues. *Plant Dis.* 90, 994–998. doi: 10.1094/PD-90-0994

Cooper, J. E. (2004). Multiple Responses of Rhizobia to Flavonoids During Legume Root Infection. *Adv. Bot. Res.* 41, 1–62. doi: 10.1128/AEM.01268-20

Daigle, D. J., and Conkerton, E. J. (1983). Analysis of Flavonoids by HPLC. *J. Liquid Chromatograph.* 6, 105–118.

Debroas, D., Humbert, J. F., Enault, F., Bronner, G., Faubladier, M., and Cornillot, E. (2009). Metagenomic approach studying the taxonomic and

functional diversity of the bacterial community in a mesotrophic lake (Lac du Bourget–France). *Environ. Microbiol.* 11, 2412–2424. doi: 10.1111/j.1462-2920.2009.01969.x

Deng, Y., Huang, H., Lei, F., Fu, S., Zou, K., Zhang, S., et al. (2021). Endophytic Bacterial Communities of Ginkgo biloba Leaves During Leaf Developmental Period. *Front. Microbiol.* 12:698703. doi: 10.3389/fmicb.2021.698703

Desantis, T. Z., Hugenholtz, P., Larsen, N., Rojas, M., Brodie, E. L., Keller, K., et al. (2006). Greengenes, a chimera-checked 16S rRNA gene database and workbench compatible with ARB. *Appl. Environ. Microbiol.* 72, 5069–5072. doi: 10.1128/AEM.03006-05

Deshmukh, S. K., and Verekar, S. A. (2012). Fungal endophytes: A potential source of antifungal compounds. *Front. Biosci.* 4, 2045–2070. doi: 10.3390/jof4030077

Farhadi, F., Khameneh, B., Iranshahi, M., and Iranshahy, M. J. P. R. (2018). Antibacterial activity of flavonoids and their structure-activity relationship: An update review. *Phytother. Res.* 33, 13–40.

Fathima, A., Rao, J. R. J. A. M., and Biotechnology. (2016). Selective toxicity of Catechin—a natural flavonoid towards bacteria. *Appl. Microbiol. Biotechnol.* 100, 6395–6402. doi: 10.1007/s00253-016-7492-x

Ghasemzadeh, A., Jaafar, H. Z., Rahmat, A., Wahab, P. E., and Halim, M. R. (2010). Effect of different light intensities on total phenolics and flavonoids synthesis and anti-oxidant activities in young ginger varieties (Zingiber officinale Roscoe). *Int. J. Mol. Sci.* 11, 3885–3897. doi: 10.3390/ijms11103885

Goulart, M. C., Cueva-Yesquén, L. G., Attili-Angelis, D., and Fantinatti-Garboggini, F. (2019). "Endophytic Bacteria from *Passiflora incarnata* L. Leaves with Genetic Potential for Flavonoid Biosynthesis," in *Microbial Probiotics for Agricultural Systems: Advances in Agronomic Use*, eds D. Zúñiga-Dávila, F. González-Andrés, and E. Ormeño-Orrillo (Cham: Springer International Publishing), 127–139.

Gupta, A., Dhakan, D. B., Maji, A., Saxena, R. P. K., Mahajan, S., and Bordenstein, S. (2019). Association of Flavonifractor plautii, a Flavonoid-Degrading Bacterium, with the Gut Microbiome of Colorectal Cancer Patients in India. *mSystems* 4:e438–e419. doi: 10.1128/mSystems.00438-19

Hammesfahr, U., Bierl, R., and Thiele-Bruhn, S. (2011). Combined effects of the antibiotic sulfadiazine and liquid manure on the soil microbial-community structure and functions. *J. Plant Nutr. Soil Sci.* 174, 614–623. doi: 10.1002/jpln.201000322

Hasler, A., Sticher, O., and Meier, B. (1992). Identification and determination of the flavonoids from Ginkgo biloba by high-performance liquid chromatography. *J. Chromatograph.* 605, 41–48.

Hassan, S., and Mathesius, U. (2012). The role of flavonoids in root-rhizosphere signalling: Opportunities and challenges for improving plant-microbe interactions. *J. Exp. Bot.* 63, 3429–3444. doi: 10.1093/jxb/err430

He, B., Jiang, J., Shi, Z., Wu, L., Yan, J., Chen, Z., et al. (2021). Pure total flavonoids from citrus attenuate non-alcoholic steatohepatitis via regulating the gut microbiota and bile acid metabolism in mice. *Biomed. Pharmacother.* 135:111183. doi: 10.1016/j.biopha.2020.111183

Hu, L., Robert, C. A. M., Cadot, S., Zhang, X., Ye, M., Li, B., et al. (2018). Root exudate metabolites drive plant-soil feedbacks on growth and defense by shaping the rhizosphere microbiota. *Nat. Commun.* 9:2738. doi: 10.1038/s41467-018-05122-7

Huang, W., He, X., Liu, C., and Li, D. (2010). "Effects of elevated carbon dioxide and ozone on foliar flavonoids of *Ginkgo biloba*," in *Advanced materials research*, Vol. 113–116, eds Z. Du and X. B. Sun (Freienbach: Trans Tech Publications, Ltd), 165–169. doi: 10.4028/www.scientific.net/AMR.113-116.165

Ikigai, H., Nakae, T., Hara, Y., and Shimamura, T. J. B. E. B. A. (1993). Bactericidal catechins damage the lipid bilayer. *Biochim. Biophys. Acta* 1147, 132–136.

Ju, H.-J., Hill, N. S., Abbott, T., and Ingram, K. T. (2006). Temperature Influences on Endophyte Growth in Tall Fescue. *Crop Sci.* 46, 404–412. doi: 10.2135/cropsci2005.0282

Karimi, E., Jaafar, H. Z. E., Ghasemzadeh, A., and Ibrahim, M. H. (2013). Light intensity effects on production and antioxidant activity of flavonoids and phenolic compounds in leaves, stems and roots of three varieties of Labisia pumila Benth. *Aus. J. Crop Sci.* 7, 1016–1023.

Kumar, V., Suman, U., and Rubal, Y. S. K. (2018). "Flavonoid Secondary Metabolite: Biosynthesis and Role in Growth and Development in Plants," in *Recent Trends and Techniques in Plant Metabolic Engineering*, eds S. Yadav, V. Kumar, and S. Singh (Singapore: Springer), 19–45. doi: 10.1007/978-981-13-2251-8_2

Langille, M. G., Zaneveld, J., Caporaso, J. G., McDonald, D., Knights, D., Reyes, J. A., et al. (2013). Predictive functional profiling of microbial communities using 16S rRNA marker gene sequences. *Nat. Biotechnol.* 31, 814–821. doi: 10.1038/nbt.2676

Leach, J. E., Triplett, L. R., Argueso, C. T., and Trivedi, P. (2017). Communication in the Phytobiome. *Cell* 169, 587–596. doi: 10.1016/j.cell.2017.04.025

Leff, J. W., Del Tredici, P., Friedman, W. E., and Fierer, N. (2015). Spatial structuring of bacterial communities within individual Ginkgo biloba trees. *Environ. Microbiol.* 17, 2352–2361. doi: 10.1111/1462-2920.12695

Lehtonen, P., Helander, M., and Saikkonen, K. (2005). Are endophyte-mediated effects on herbivores conditional on soil nutrients? *Oecologia* 142, 38–45. doi: 10.1007/s00442-004-1701-5

Longstreth, D. J., and Strain, B. R. (1977). Effects of salinity and illumination on photosynthesis and water balance of Spartina alterniflora Loisel. *Oecologia* 31, 191–199. doi: 10.1007/BF00346920

Malinowski, D. P., and Alloush GABelesky, D. P. (2000). Leaf endophyte Neotyphodium coenophialum modifies mineral uptake in tallfescue. *Plant Soil* 227, 115–126.

Malinowski, D. P., Belesky, D. P., and Lewis, G. C. (2008). "Abiotic Stresses in Endophytic Grasses," in *Neotyphodium in Cool Season Grasses*, eds C. A. Roberts, C. P. West, and D. E. Spiers (Ames, IA: Blackwell Publishing Professional), 187–199.

Mattila, P., Astola, J., and Kumpulainen, J. (2000). Determination of flavonoids in plant material by HPLC with diode-array and electro-array detections. *J. Agric. Food Chem.* 48, 5834–5841. doi: 10.1021/jf000661f

Parvez, M. M., Tomita-Yokotani, K., Fujii, Y., Konishi, T., and Iwashina, T. J. (2004). Effects of quercetin and its seven derivatives on the growth of Arabidopsis thaliana and Neurospora crassa. *Biochem. Syst. Ecol.* 32, 631–635.

Pietta, P. G. (2000). Flavonoids as antioxidants. *J. Natural Produc.* 63:1035.

Saunders, M., and Kohn, L. M. (2009). Evidence for alteration of fungal endophyte community assembly by host defense compounds. *N. Phytol.* 182, 229–238. doi: 10.1111/j.1469-8137.2008.02746.x

Schardl, C. L., Leuchtmann, A., and Spiering, M. J. (2004). Symbioses of grasses with seedborne fungal endophytes. *Annu. Rev. Plant Biol.* 55, 315–340. doi: 10.1146/annurev.arplant.55.031903.141735

Schulz, B., and Boyle, C. (2006). "What are Endophytes?," in *Microbial Root Endophytes. Soil Biology*, Vol. 9, eds B. J. E. Schulz, C. J. C. Boyle, and T. N. Sieber (Berlin: Springer), doi: 10.1007/3-540-33526-9_1

Sahu, P. K., Tilgam, J., Mishra, S., Hamid, S., Gupta, A., Jayalakshmi, K., et al. (2022). Surface sterilization for isolation of endophytes: Ensuring what (not) to grow. *J. Basic Microbiol.* 62, 647–668. doi: 10.1002/jobm.202100462

Shaw, L. J., Morris, P., and Hooker, J. E. (2006). Perception and modification of plant flavonoid signals by rhizosphere microorganisms. *Environ. Microbiol.* 8, 1867–1880. doi: 10.1111/j.1462-2920.2006.01141.x

Steinhauser, D., Krall, L., Müssig, C., Büssis, D., and Usadel, B. (2008). "Correlation networks," in *Analysis of biological networks*, Vol. 305, eds B. H. Junker and F. Schreiber (Hoboken, NJ: Wiley), 333.

Sun, M., Finnemann, S. C., Febbraio, M., Shan, L., Annangudi, S. P., Podrez, E. A., et al. (2006). Light-induced oxidation of photoreceptor outer segment phospholipids generates ligands for CD36-mediated phagocytosis by retinal pigment epithelium: A potential mechanism for modulating outer segment phagocytosis under oxidant stress conditions. *J. Biol. Chem.* 281, 4222–4230. doi: 10.1074/jbc.M509769200

Tan, R. X., and Zou, W. X. (2010). ChemInform Abstract: Endophytes: A Rich Source of Functional Metabolites. *Cheminform* 18, 448–459. doi: 10.1039/b100918o

Tattini, M., Galardi, C., Pinelli, P., Massai, R., Remorini, D., and Agati, G. (2010). Differential Accumulation of Flavonoids and Hydroxycinnamates in Leaves of Ligustrum vulgare under Excess Light and Drought Stress. *N. Phytol.* 163, 547–561. doi: 10.1111/j.1469-8137.2004.01126.x

Vandenkoornhuyse, P., Quaiser, A., Duhamel, M., Le Van, A., and Dufresne, A. (2015). The importance of the microbiome of the plant holobiont. *N. Phytol.* 206, 1196–1206. doi: 10.1111/nph.13312

Wang, G., Cao, F., Li, C., Guo, X., and Jian, W. (2014). Temperature has more effects than soil moisture on biosynthesis of flavonoids in Ginkgo (Ginkgo biloba L.) leaves. *New For.* 45, 797–812.

White, J. F. Jr., and Torres, M. S. (2010). Is plant endophyte-mediated defensive mutualism the result of oxidative stress protection? *Physiol. Plant* 138, 440–446. doi: 10.1111/j.1399-3054.2009.01332.x

Wiswedel, I., Gardemann, A., Storch, A., Peter, D., and Schild, L. (2009). Degradation of phospholipids by oxidative stress—Exceptional significance of cardiolipin. *Free Radic. Res.* 44, 135–145. doi: 10.3109/10715760903352841

Wu, Y., Yang, Y., Cao, L., Yin, H., Xu, M., Wang, Z., et al. (2018). Habitat environments impacted the gut microbiome of long-distance migratory swan geese but central species conserved. *Sci. Rep.* 8:13314. doi: 10.1038/s41598-018-31731-9

Yin, R., Messner, B., Faus-Kessler, T., Hoffmann, T., Schwab, W., Hajirezaei, M. R., et al. (2012). Feedback inhibition of the general phenylpropanoid and flavonol biosynthetic pathways upon a compromised flavonol-3-O-glycosylation. *J. Exp. Bot.* 63, 2465–2478. doi: 10.1093/jxb/err416

Zhang, S.-K., Wang, Y., Li, Z.-K., Xue, H.-J., Zhou, X.-D., and Huang, J.-H. (2022). Two Apriona Species Sharing a Host Niche Have Different Gut Microbiome Diversity. *Microb. Ecol.* 83, 1059–1072. doi: 10.1007/s00248-021-01799-4

Zhang, Y., Yang, Q., Ling, J., Van Nostrand, J. D., Shi, Z., Zhou, J., et al. (2016). The Shifts of Diazotrophic Communities in Spring and Summer Associated with Coral Galaxea astreata. Pavona decussata, and Porites lutea. *Front. Microbiol.* 7:1870. doi: 10.3389/fmicb.2016.01870

Zhao, B., Wang, L., Pang, S., Jia, Z., Wang, L., Li, W., et al. (2020). UV-B promotes flavonoid synthesis in Ginkgo biloba leaves. *Industr. Crops Produc.* 151:112483. doi: 10.1016/j.indcrop.2020.112483

Zhou, K., Ye, C., and Ye, Z. (1999). Determination of total amount of flavonoids in Ginkgo biloba L. leaves during different growing periods. *J. Mountain Agric. Biol.* 18, 1–7.

Zou, K., Liu, X., Zhang, D., Yang, Q., Fu, S., Meng, D., et al. (2019). Flavonoid Biosynthesis Is Likely More Susceptible to Elevation and Tree Age Than Other Branch Pathways Involved in Phenylpropanoid Biosynthesis in Ginkgo Leaves. *Front. Plant Sci.* 10:983. doi: 10.3389/fpls.2019.00983

frontiers | Frontiers in Plant Science

TYPE Original Research
PUBLISHED 16 September 2022
DOI 10.3389/fpls.2022.1023837

OPEN ACCESS

EDITED BY
Mengting Maggie Yuan,
University of California, Berkeley,
United States

REVIEWED BY
Pingzhi Zhao,
Institute of Microbiology, Chinese Academy of Sciences (CAS), China
R. K. Govindarajan,
South China Agricultural University, China

*CORRESPONDENCE
Peijian Cao
peijiancao@163.com

†These authors have contributed equally to this work

SPECIALTY SECTION
This article was submitted to Plant Symbiotic Interactions, a section of the journal Frontiers in Plant Science

RECEIVED 20 August 2022
ACCEPTED 02 September 2022
PUBLISHED 16 September 2022

CITATION
Tao J, Yu S, Jin J, Lu P, Yang Z, Xu Y, Chen Q, Li Z and Cao P (2022) The wilt pathogen induces different variations of root-associated microbiomes of plant.
Front. Plant Sci. 13:1023837.
doi: 10.3389/fpls.2022.1023837

The wilt pathogen induces different variations of root-associated microbiomes of plant

Jiemeng Tao[1†], Shizhou Yu[2†], Jingjing Jin[1], Peng Lu[1], Zhixiao Yang[2], Yalong Xu[1], Qiansi Chen[1], Zefeng Li[1] and Peijian Cao[1*]

[1]China Tobacco Gene Research Center, Zhengzhou Tobacco Research Institute of CNTC, Zhengzhou, China, [2]Molecular Genetics Key Laboratory of China Tobacco, Guizhou Academy of Tobacco, Guiyang, China

Root-associated compartments, including the rhizosphere, rhizoplane, and endosphere, live with diverse microbial communities which profoundly affect plant growth and health. However, a systematic understanding of the microbiome assembly across the rhizosphere, rhizoplane, and endosphere under pathogen invasion remains elusive. Using 16S high-throughput sequencing, we studied how bacterial wilt disease affected the variation and assembly of the three continuous root-associated microbiomes of tobacco. The results indicated that microorganisms were gradually filtered from the rhizosphere to the endosphere. With the pathogen invasion, the rhizosphere, rhizoplane and endosphere microbiomes selected and recruited different beneficial bacterial taxa. Some recruited bacteria were also identified as keystone members in networks (i.e., *Bosea* in the endosphere). The microbiomes of endosphere and rhizoplane were more sensitive to plant disease than the rhizosphere microbiome. Still, response strategies of the rhizoplane and endosphere to disease were obviously different. Microbial networks of the rhizoplane became complex in diseased samples and genes involved in sporulation formation and cell cycle were enriched. However, microbial networks of the diseased endosphere were disrupted, and functional genes related to nitrogen utilization and chemotaxis were significantly increased, indicating the importance of nitrogen resources supply of plants for the endosphere microbiome under pathogen invasion. Our results provide novel insights for understanding the different responses of the root-associated microbiomes to plant disease.

KEYWORDS

root-associated microbiomes, bacterial wilt disease, disease suppression, microbiome assembly, microbial networks

Introduction

In nature, plants do not grow as solitary organisms but harbor a high diversity of microorganisms. These microorganisms, which inhabit the rhizosphere, rhizoplane, phyllosphere, and endosphere, form microbial communities and are collectively called plant microbiomes (Turner et al., 2013; Müller et al., 2016). The plant microbiomes coevolve with their host and profoundly impact a range of aspects of plant performance (Simon et al., 2019; Trivedi et al., 2020), including nutrient availability (Martin et al., 2017), abiotic stress tolerance (de Vries et al., 2020), and disease suppression (Mendes et al., 2011; Carrión et al., 2019). Therefore, understanding the plant microbiomes will have important implications for plant health, productivity, and ecosystem function (Sessitsch and Mitter, 2015).

Soil is the largest known reservoir of microbial diversity (Torsvik et al., 2002), and the root is a critical zone for plant-microbiome interactions. The root zone can be separated into three rhizocompartments: the rhizosphere (soil close to the root surface), rhizoplane (root surface), and endosphere (root interior), each of which was found to harbor a distinct microbiome (Edwards et al., 2015). Recently, a three-step enrichment model was proposed to demonstrate the forming process of the three compartments at the soil-root interface (Reinhold-Hurek et al., 2015). The suitable physicochemical environment and rich nutrient conditions of the roots can recruit microorganisms migrating from the bulk soil to the roots. In this process, a portion of microorganisms is enriched in the soil close to the roots and forms the rhizosphere microbiome. Then, a specialized community is further enriched on the root surface and forms the rhizoplane microbiome. Finally, some microorganisms which have higher compatibility with plants enter and occupy niches within plant roots and establish the endosphere microbiome to greatly influence plant growth and health (Reinhold-Hurek et al., 2015). It is believed that the microbial communities inhabiting the three rhizocompartments are mainly derived from the bulk soil and gradually filtered at different compartment niches (Xiong et al., 2021). However, whether the enrichment process of the three root-associated microbiomes is affected by biotic stresses such as disease remains elusive.

Previous studies have suggested that changes in plant microbiomes are not just passive responses of plants but rather the result of coevolution, and plants may actively seek help from microbes to relieve stresses (Liu et al., 2020). The recruitment of microbes upon biotic or abiotic stresses is likely a survival strategy conserved across the plant kingdom, known as the "cry for help" strategy (Gao et al., 2021; Liu et al., 2021). Plants can recruit some beneficial microbes from surrounding soils, and the structure and function of plant microbiomes change and then reassemble (Xiong et al., 2021). For example, *Stenotrophomonas rhizophila* (SR80) was enriched in both the rhizosphere and root endosphere of *Fp*-infected wheat, and re-inoculation of SR80 in soils could enhance both plant health and disease suppression (Liu et al., 2021). Fusarium wilt disease greatly influenced the bacterial and fungal community assembly of the root and stem microbiomes and potentially beneficial bacteria such as *Pseudomonas*, *Streptomyces*, and *Bacillus* were enriched in diseased pepper plants (Gao et al., 2021). Microbial community assembly is mainly influenced by the host, environmental factors, and potential interactions among microbial individuals (van der Heijden and Hartmann, 2016; Durán et al., 2018). The cooperative and competitive interactions among different microbes across different habitats can be characterized using microbial co-occurrence network analysis (Feng et al., 2019). A growing number of studies have provided evidence that keystone members (e.g., connectors, module hubs, and network hubs) in microbial networks are crucial for predicting plant growth and fitness (Tao et al., 2017; Hu et al., 2020; Tao et al., 2021). However, most previous studies often focused on the rhizosphere microbiome, and a systematic understanding of the microbiome assembly across the rhizosphere, rhizoplane, and endosphere under pathogen invasion remains unclear.

Bacterial wilt disease is caused by *Ralstonia* species which infect a wide variety of *Solanaceae* crops, such as tobacco, tomato, and eggplant (Jiang et al., 2017). The *Ralstonia* pathogen survives in soils, enters the plant through root wounds, and destroys the vascular bundle system of the host, leading to the wilting and death of the host plant (Li et al., 2017). To reveal the structure, variation, and assembly of the three continuous root-associated microbiomes with *Ralstonia* invasion, soil and root samples were collected from healthy or diseased fields with tobacco plants. Using 16S rRNA gene sequencing, we aim to (i) describe the taxonomic and functional shifts in the three root-associated microbiomes under bacterial wilt disease, (ii) investigate which members in different microbiomes conferred positive effects on the plant upon pathogen attack, and (iii) compare the networks of healthy and diseased root-associated microbiomes to offer insights into the stability of communities.

Materials and methods

Sample collection and processing

All samples were collected from the main tobacco-growing regions in Tianzhu (26°58'15'' N, 109°15'34'' E), Guizhou province in China. The annual mean temperature in Tianzhu is 16.1°C, and the average annual precipitation was between 1200 mm to 1380 mm. The tobacco cultivar planted was Yunyan 87, and sample collections were performed on 4th September

2021. There were two adjacent plots in which tobacco plants displayed considerably different wilt symptoms. Tobaccos in the healthy field showed healthy conditions, and those in the diseased field showed severe wilt symptoms (infection grade 5–9). Six replicates of both soils and roots were taken from healthy and diseased fields, respectively. Each replicate was a composite sample formed by mixing two individual samples.

The bulk soil was collected 20 cm away from the root at 0–15 cm depth. The three rhizocompartments were gradually collected according to previous studies with some modifications. The whole plant was uprooted from the soil. The loosely attached soil was manually shaken from the roots, and the rhizosphere soil was collected by gently brushing the remaining soil on the roots (Zhang et al., 2017). The roots with the rhizosphere compartment removed were placed in a 50 mL tube with 15 mL of sterile Phosphate Buffered Saline (PBS) solution. After sonicating at 40 kHz for 1 min, the PBS was transferred into a new clean tube. Refilled PBS in the sonicated roots and repeated the same sonication procedure until no cells in the supernatant could be detected by microscopy. The mixed PBS solution was centrifuged at 12,000 × g for 10 min to collect rhizoplane microbes (Edwards et al., 2015). The sonicated roots were stored at -80°C for endosphere DNA extraction.

DNA extraction and amplicon sequencing

Each plant sample was divided into four compartments: the bulk soil, the rhizosphere soil, the rhizoplane, and the endosphere. A total of 0.5 g bulk soil, rhizosphere soil, or rhizoplane microbial enrichment were used to extract DNA using a Mag-Bind® Soil DNA Kit (Omega Biotek Inc., Doraville, GA, USA) following the manufacturer's instructions. For the root endosphere, about 5 g sonicated sample as above was surface sterilized by consecutive immersion for 5 min in 75% ethanol, 5 min in 1% sodium hypochlorite solution, and 30 s in 75% ethanol and finally washed with sterile H_2O for three times. The sterilized roots were ground using sterile mortars and pestles with liquid nitrogen, and then DNA was extracted from the 0.4 g resulting powder using the Mag-Bind® Soil DNA Kit. The DNA concentration was evaluated using a NanoDrop® 1000 spectrophotometer (Thermo Scientific), and the DNA quality was assessed by 1.0% agarose gel. The V3-V4 region (341F/805R) and V5-V7 region (799F/1193R) of bacterial 16S rRNA gene were amplified for epiphytic and endophytic microbes, respectively. Primer sequences and PCR amplification conditions are shown in Table S1. PCR was conducted in 25 μL mixtures containing 12.5 μL TaqMaster Mix (Vazyme, Piscataway, NJ, USA), 2.5 μL of forward/reverse primers (1 μM), 2.0 μL DNA (~25 ng/μL), and DNase-RNase-Free deionized water to adjust the volume. PCR products were purified using the E.Z.N.A. TM Gel Extraction Kit (OMEGA Biotek Inc., Doraville, GA, USA). Purified PCR products were pooled in equimolar concentrations for library construction. High-throughput sequencing was performed on the MiSeq platform (Illumina, San Diego, CA, USA).

Amplicon sequencing data processing

The 16S rRNA gene sequences were processed using QIIME 2 (Quantitative Insights Into Microbial Ecology 2, version 2019.7) (Bolyen et al., 2019) and USEARCH v10.0 (Edgar, 2010). DATA2 (Callahan et al., 2016) was used for quality control, chimeric filtering, and to infer unique sample sequences (amplicon sequence variants, ASVs) from the sequencing data. The ASVs were subsequently assigned to taxonomy groups by comparisons with the SILVA v138 prokaryotic database (Yilmaz et al., 2014). Alpha diversity indices (Shannon, Chao1, and Simpson) and beta diversity metrics (Bray-Curtis) of the bacterial community were calculated in QIIME 2 through the diversity plugin (q2-diversity). To eliminate the influences of different sequencing depths, the bacterial ASV tables were rarefied to 29,546 reads for alpha diversity index estimates. The Phylogenetic Investigation of Communities by Reconstruction of Unobserved States (PICRUSt2) was applied to predict potential functional profiles of the bacterial community using 16S rRNA gene data (Douglas et al., 2020).

Statistical analysis

All statistical analyses were performed using specific packages in R version 3.6.3 (The R Foundation for Statistical Computing, Vienna, Austria). Alpha diversity indices (Shannon index, Chao1 index, and Simpson index) of the bacterial community were calculated in QIIME 2. The beta diversity of bacterial communities was assessed by computing Bray-Curtis distance matrices and visualized using Principal coordinate analysis (PCoA) plots. The relative contribution of different factors to community dissimilarity was evaluated by Permutational multivariate analysis of variance (PERMANOVA) statistical tests using the Adonis function (R package "*vegan*"). The effects of bacterial wilt disease in single rhizocompartments were also assessed by PERMANOVA. One-way analysis of variance (ANOVA) followed by Tukey's test was used to determine the statistical significance among groups. Venn diagram and heatmap analyses were performed using the "*venndiagram*" and "*pheatmap*" packages in R. The Ternary plots were visualized by calculating the mean relative abundances of ASVs of each compartment using the "*vcd*" package in R. The SourceTracker model was applied to predict the relative contributions of different microbial compartments in the enrichment process from bulk soil communities to root endosphere communities. The percentage

values were calculated with the functions "*sourcetracker*" and "*predict*" packages in R (Knights et al., 2011).

Random matrix theory based molecular ecology networks

Molecular ecological networks for root-associated microbiomes under both healthy and diseased conditions were constructed *via* the online pipeline (http://ieg2.ou.edu/MENA/). For each network, ASVs (relative abundance > 0.01%)) presented in at least 4 out of the 6 biological replicates were included for network analysis. The value of *St* was automatically determined by a random matrix theory (RMT) based approach that observed the transition point of nearest-neighbor spacing distribution of eigenvalues from Gaussian to Poisson distribution (Zhou et al., 2011). The networks were visualized using the interactive platforms Gephi and Cytoscape. Nodes represent the individual ASVs, and edges represent the pairwise correlations between the nodes in the microbiome network, indicating biologically or biochemically meaningful interactions. Node topologies could be classified into four categories based on the value of within-module connectivity (*Zi*) and among-module connectivity (*Pi*): peripheral nodes ($Zi \leq 2.5$ and $Pi \leq 0.62$), connectors ($Zi \leq 2.5$ and $Pi > 0.62$), module hubs ($Zi > 2.5$ and $Pi \leq 0.62$), and network hubs ($Zi > 2.5$ and $Pi > 0.62$) (Olesen et al., 2007).

Results

Both niches and disease affect the distribution and source of root-associated microbiomes

A total of 2,800,052 bacterial 16S rRNA high-quality sequences were obtained from 48 samples (average: 58,334; range: 44,904–75,018 reads per sample). After removing the chimeric and organelle sequences with USEARCH, 14,416 ASVs were identified from these reads. The results showed that the root-associated microbiomes have different patterns of community structure and microbial diversity among the rhizosphere, rhizoplane, and root endosphere compartments (Figures 1, S2, S3). PCoA of Bray–Curtis distance revealed that the bulk soil and root-associated microbiomes formed three distinct clusters regardless of plant health conditions (Figure 1A). PERMANOVA analysis was performed to evaluate the relative contribution of rhizocompartment niche and bacterial wilt disease to the structures of root-associated microbiomes. The calculation results indicated that compartment niche explained a large source of variation within the microbiome data (63.54%, $P < 0.001$), and bacterial wilt disease showed a relatively little effect on the differences of root-associated microbiomes (6.85%, $P < 0.001$). PCoA of each compartment microbiome showed that bacterial wilt disease caused significant differences in the community

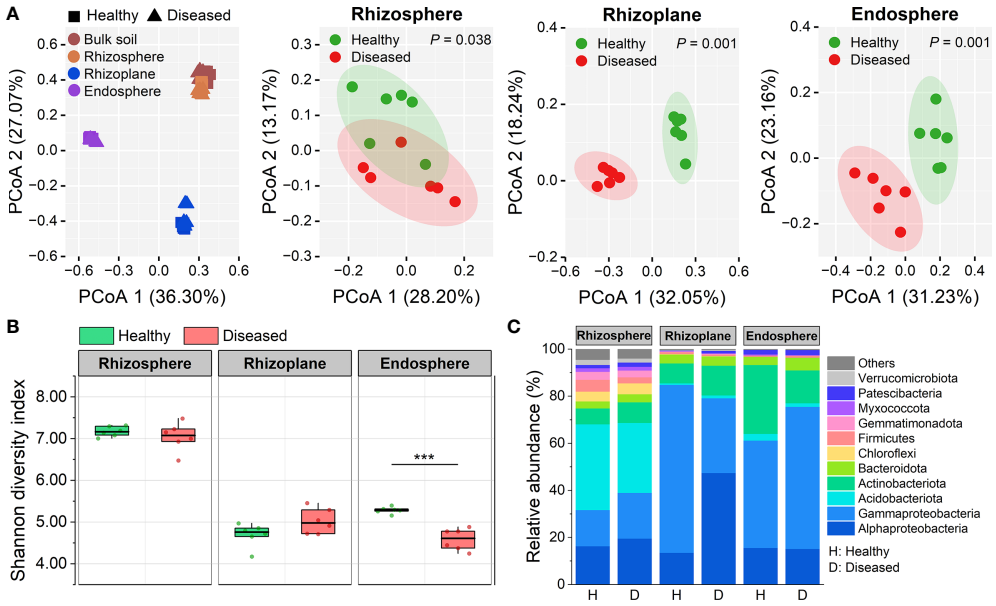

FIGURE 1
Community assembly of root-associated microbiomes. **(A)** Principal coordinate analysis (PCoA) of Bray–Cutis dissimilarity matrices showing effects of compartment niche and bacterial wilt disease on the community structure of the rhizosphere, rhizoplane and endosphere microbiomes. **(B)** Shannon diversity index of bacterial communities in root-associated microbiomes of healthy and diseased plants Asterisks denote significant differences (***$P < 0.001$). **(C)** Stacked bar chart showing phylum composition in the three rhizocompartments of healthy and diseased plants based on relative abundance data.

structures of the rhizosphere, rhizoplane, or root endosphere (PERMANOVA; $P < 0.001$) (Figure 1A), but the structure of the bulk soil community was not significantly affected by the disease (PERMANOVA; $P = 0.105$) (Figure S1).

Measures of the alpha diversity (Shannon index, Chao1 richness, and Simpson index) showed an obvious downtrend from the rhizosphere to the endosphere (Figures 1B, S2). The bacterial alpha diversity in the rhizosphere and rhizoplane compartments was not affected by bacterial wilt disease (ANOVA; $P > 0.05$). However, the alpha diversity in the diseased endosphere was significantly lower than those in the healthy one in terms of Shannon diversity index and Simpson index (ANOVA; $P < 0.001$) (Figures 1B, S2). Taxonomic classification showed that both bacterial phyla and genera varied distinctly across compartment niches (Figures 1C, S3). The rhizoplane and endosphere had a significantly greater proportion of Gammaproteobacteria, Actinobacteria, and Bacteroidota than the rhizosphere, whereas Acidobacteria, Chloroflexi, Firmicutes, Gemmatimonadota, and Verrucomicrobiota were mostly depleted in the rhizoplane and endosphere compared with the rhizosphere (Figure 1C). The composition differences among the three rhizocompartments differed more significantly at the genus level (Figure S3). The three compartments shared only 138 genera and the rhizosphere had the largest number of distinct genera (165), followed by the rhizoplane (110). Besides, the taxonomic classification of each compartment showed that different compartments changed distinct members under bacterial wilt disease, and the rhizoplane and endosphere were more affected by the disease than the rhizosphere (Figures 1C, S3). For example, *Allorhizobium-Neorhizobium-Pararhizobium-Rhizobium*, *Ensifer*, and *Sphingomonas* were significantly enriched in diseased rhizoplane, while *Pseudomonas* and *Stenotrophomonas* were significantly enriched in diseased endosphere.

To understand better how the bacterial wilt disease influenced the bacterial community, the specifically enriched ASVs in each compartment and the microbial sources of each compartment across healthy and diseased samples were compared (Figure 2). Ternary plots showed that more specific ASVs were enriched in the rhizosphere than the rhizoplane and endosphere under both healthy and diseased conditions. Compared with healthy samples (489 and 302 enriched ASVs in the rhizosphere and endosphere, respectively), there were significantly more ASVs were enriched in the diseased rhizosphere (579) and endosphere (387), while the

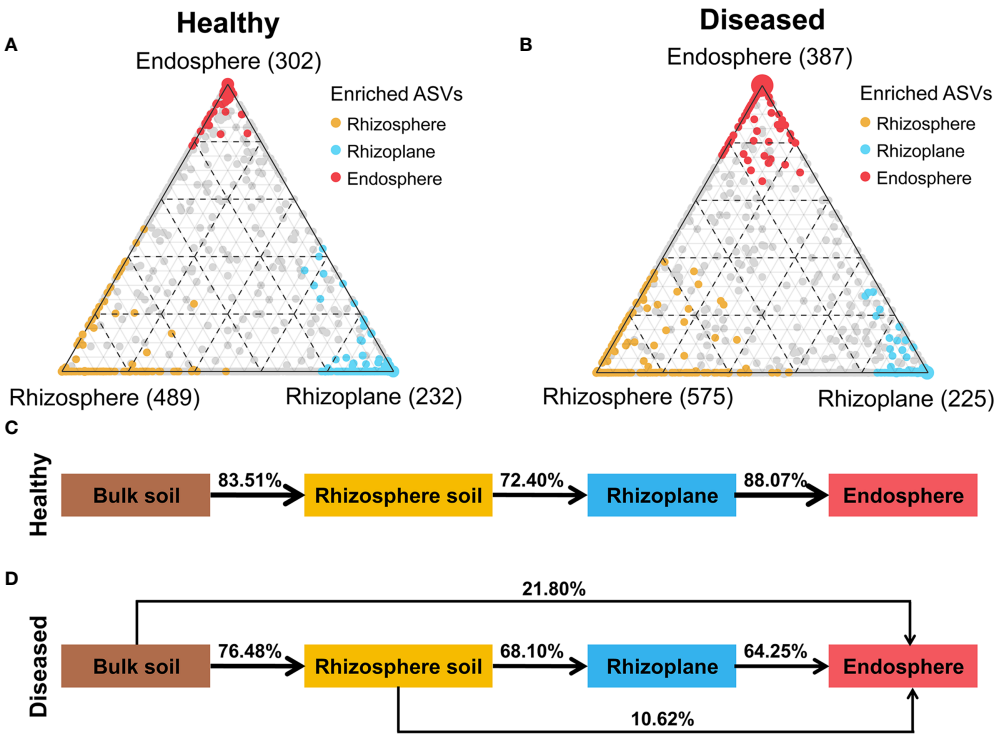

FIGURE 2
Distribution of ASVs across different compartments. **(A, B)** Ternary plots depicting bacterial ASVs significantly enriched in three root-associated microbiomes (FDR, $p < 0.01$) under healthy and diseased conditions. Each circle represents one ASV, and the size of each circle represents its relative abundance. Different colors represent different compartments. **(C)** Source-tracking analysis showing the sources of the rhizosphere, rhizoplane and endosphere microbiomes in healthy plants. **(D)** Source-tracking analysis showing the sources of the rhizosphere, rhizoplane and endosphere microbiomes in diseased plants.

specific ASVs in rhizoplane showed a slight decrease (from 232 to 225) (Figures 2A, B). SourceTracker analysis showed that root-associated microorganisms were mainly derived from the bulk soil, but the trends differed in healthy and diseased samples (Figures 2C, D). In healthy samples, the majority of the rhizosphere microbial members (83.51%) were derived from the bulk soil, then the microorganisms were gradually filtered at the rhizoplane and endodphere compartments. Most of the endosphere members (88.07%) were migrated from the rhizoplane and no microorganisms were from the rhizosphere or bulk soil (Figure 2C). In diseased samples, the rhizosphere microorganisms (76.48%) were also primarily derived from the bulk soil and gradually filtered at different plant compartment niches. However, for the root endosphere microorganisms in diseased samples, the bulk soil (21.80%) and the rhizosphere (10.62%) were also important sources of the endosphere microbiome except for the rhizoplane (64.25%) (Figure 2D).

All the above results showed that pathogen invasion could affect the distribution of root-associated microbiomes and promote the plant root system to expand the ecological range of recruiting microorganisms.

Three Rhizo-compartments enriched significantly different OTUs under disease

Given the recruitment strategy of plants for beneficial microbes, we identified enriched or depleted ASVs (relative abundance > 0.01%) in each rhizocompartment of diseased samples using Manhattan plots (Figure 3). In the three compartments, ASVs enriched in diseased samples belonged to a wide range of bacterial phyla, including Actinobacteriota, Bacteroidta, Patescibacteria, Proteobacteria (mainly Alphaproteobacteria and Gammaproteobacteria), and WPS-2 (FDR adjusted $P < 0.05$, Wilcoxon rank sum test; Figures 3A–C). The rhizosphere and endosphere of diseased samples enriched the same number of ASVs (42). Among them, *Dyadobacter* ASV_6201, *Ochrobactrum* ASV_530 and *Pseudomonas* ASV_4114 in the rhizosphere and *Shinella* ASV_8061 in the endosphere were the "new microbes" in diseased samples, which were present in ≥ 50% diseased samples and in none healthy samples (Figures 3A, C and Tables S2, S4). In comparison, the diseased rhizoplane enriched for more ASVs (mainly belonging to

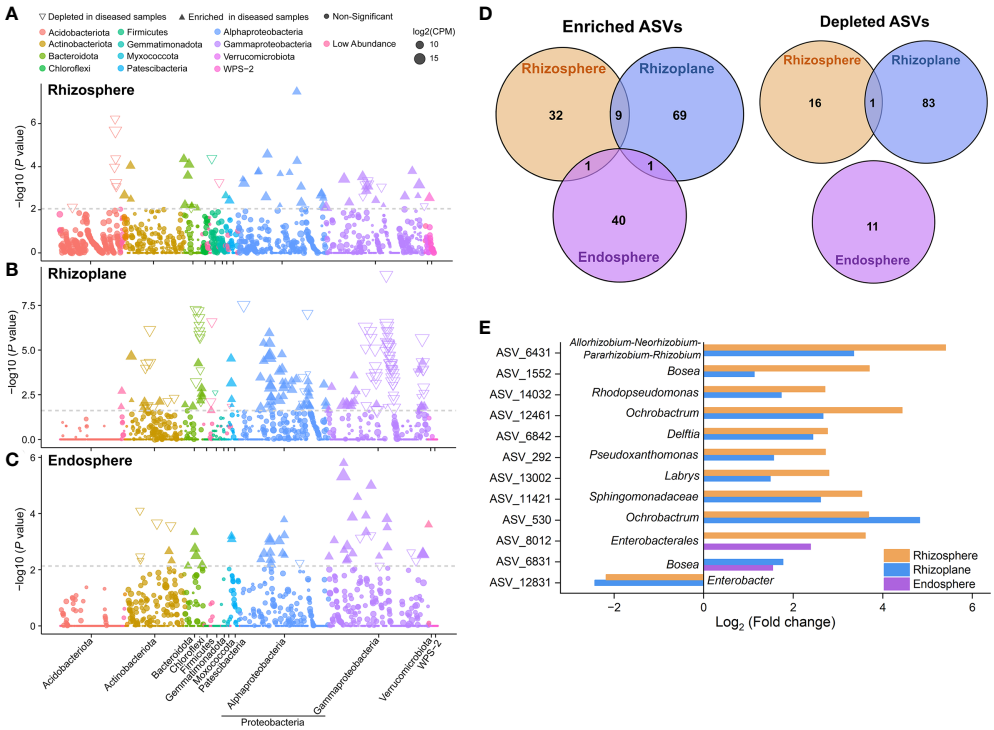

FIGURE 3
Taxonomic characteristics of differential bacteria of root-associated microbiomes between healthy and diseased plants. **(A–C)** Manhattan plots showing ASVs enriched or depleted in the diseased rhizosphere, rhizoplane, and endosphere, respectively. Each circle or triangle represents a single ASV. ASVs enriched or depleted in the diseased samples are represented by filled or empty triangles, respectively (ASVs abundance > 0.01%, $P < 0.05$). **(D)** Venn diagram depicting number of enriched or depleted ASVs in each compartment of diseased plants. **(E)** The genus classification (if not annotated to specific genera, using higher-level taxa to represent) of the shared enriched or depleted ASVs between the microbiomes of diseased rhizosphere, rhizoplane, and endosphere.

Alphaproteobacteria) while simultaneously depleting a larger proportion of ASVs (79 vs. 84) (Figure 3D). Moreover, the rhizoplane of diseased samples presented a large number of distinct ASVs (new microbes) unique to healthy samples, which was distinctly different from the endosphere community (Figure S4). Among the enriched ASVs of the rhizoplane, *Mycobacterium* ASV_11679 and *Saccharimonadales* ASV_12660 represented "new microbes" in diseased samples (Figure 3B and Table S3). In terms of enriched ASVs, none was shared by the three compartments, and only 11 ASVs were shared by two of them (Figure 3D). The shared ASVs were assigned to different genera, such as *Allorhizobium-Neorhizobium-Pararhizobium-Rhizobium*, *Bosea*, *Rhodopseudomonas*, *Ochrobactrum*, *Pseudoxanthomonas*, *Labrys* and so on (Figure 3E). For depleted ASVs, only one ASV belonging to *Enterobacte*r was shared by the rhizosphere and rhizoplane. The above results indicated that different ASVs were enriched in different compartments with pathogen invasion.

Molecular ecological networks of root-associated microbiomes are influenced by disease

Molecular ecological networks (MENs) were constructed to unravel how bacterial wilt disease affected the microbial interactions across the three rhizocompartments under healthy and diseased conditions (Figure 4). The topological properties of the six networks were shown in Supplementary Table S5. The same threshold values were chosen for each compartment (0.94 for the rhizosphere, 0.93 for the rhizoplane and 0.94 for the endosphere). The node and link numbers of the rhizosphere networks were significantly higher than those of the rhizoplane and endosphere networks (Table S5). For healthy plants, the networks of the rhizosphere (1659 links) and endosphere (1774 links) were more complex than the rhizoplane network (198 links). However, under diseased conditions, the links within networks showed a clear downward trend from the rhizosphere (2110 links) to endosphere (406 links), and the network of the rhizoplane presented a higher number of connections per node (average degree = 5.892) than that of the rhizosphere (3.764) and endosphere (2.115), indicating a highly connected microbial community of the diseased rhizoplane (Figures 4A, B and Table S5). For different compartments, networks of the rhizoplane and endosphere were significantly affected by the disease (based on the average degree) (Figure 4C). In addition, we identified the keystone nodes (connectors and module hubs) in each network based on the values of within-module connectivity (*Zi*) and among-module connectivity (*Pi*), and found 24 connectors (healthy: 9, diseased:15) and 34 module hubs (healthy: 18, diseased: 16) in the rhizosphere networks, 8 connectors (diseased: 8) and 1 module hub (diseased: 1) in the rhizoplane networks, and 14 connectors (healthy: 13, diseased: 1) and 10 module hubs (healthy: 7, diseased: 3) in the endosphere networks (Figure 4C and Tables S6–S8).

Considering the high abundance of *Ralstonia* in the root endosphere (Figure S3), we further constructed the endosphere subnetworks of the interactions among pathogenic *Ralstonia* and other microbial members to identify key organisms (Figure 4D). The results showed that more bacterial members directly connected to *Ralstonia* in the diseased root than those in the healthy one. For the diseased endosphere, most of the bacterial members relating to *Ralstonia* tended to co-exclude (negative correlations, red lines) rather than co-occur (positive correlations, blue lines) (Figure 4D). A variety of bacterial genera such as *Allorhizobium-Neorhizobium-Pararhizobium-Rhizobium, Streptomyces, Burkholderiales, Achromobacter, Bosea and Flavobacterium* were negatively correlated with the pathogenic *Ralstonia* in the diseased root endophytic communities. Among these nodes, *Bosea* ASV_6831 was significantly enriched (FDR adjusted $P < 0.05$) in diseased root endosphere, which provided evidence that plant recruited some microorganisms to suppress the expansion of pathogenic *Ralstonia*. Only two positive correlations between bacterial genera (*Xenophilus* and an unclassified genus of Gammaproteobacteria) and the pathogen were found in the root endosphere. One node (ASV_8652) belonging to *Gammaproteobacteria* and positively correlating to *Ralstonia* was detected in both the healthy and diseased networks of the endosphere, indicating its importance in facilitating the colonization and development of the pathogen (Figure 4D).

Collectively, molecular ecological networks of each compartments were influenced by bacterial wilt disease, but the variation trends were significantly between them.

The function profiles of root-associated microbiomes are influenced by disease

In order to investigate the effects of disease on the community functions of different compartments, metagenomes of bacterial communities were predicted using PICRUSt2 and then annotated by referring to the KEGG database. A total of 7,986 KOs (KEGG Orthologs) were predicted in the three root-associated communities. Our results showed that the endosphere microbiome in the diseased roots possessed significantly lower KO diversity (i.e. Chao1 richness) than those in the healthy roots (ANOVA; $P < 0.01$). However, the diseased rhizoplane microbiome showed a higher KO diversity than the healthy one (ANOVA; $P < 0.05$) (Figure 5A). PCoA analysis at the KO level showed that community functions of the three compartments significantly differed from each other ($R^2 = 0.548$, $P < 0.001$), and the bacterial wilt disease also had a significant effect on microbiome functions for the three

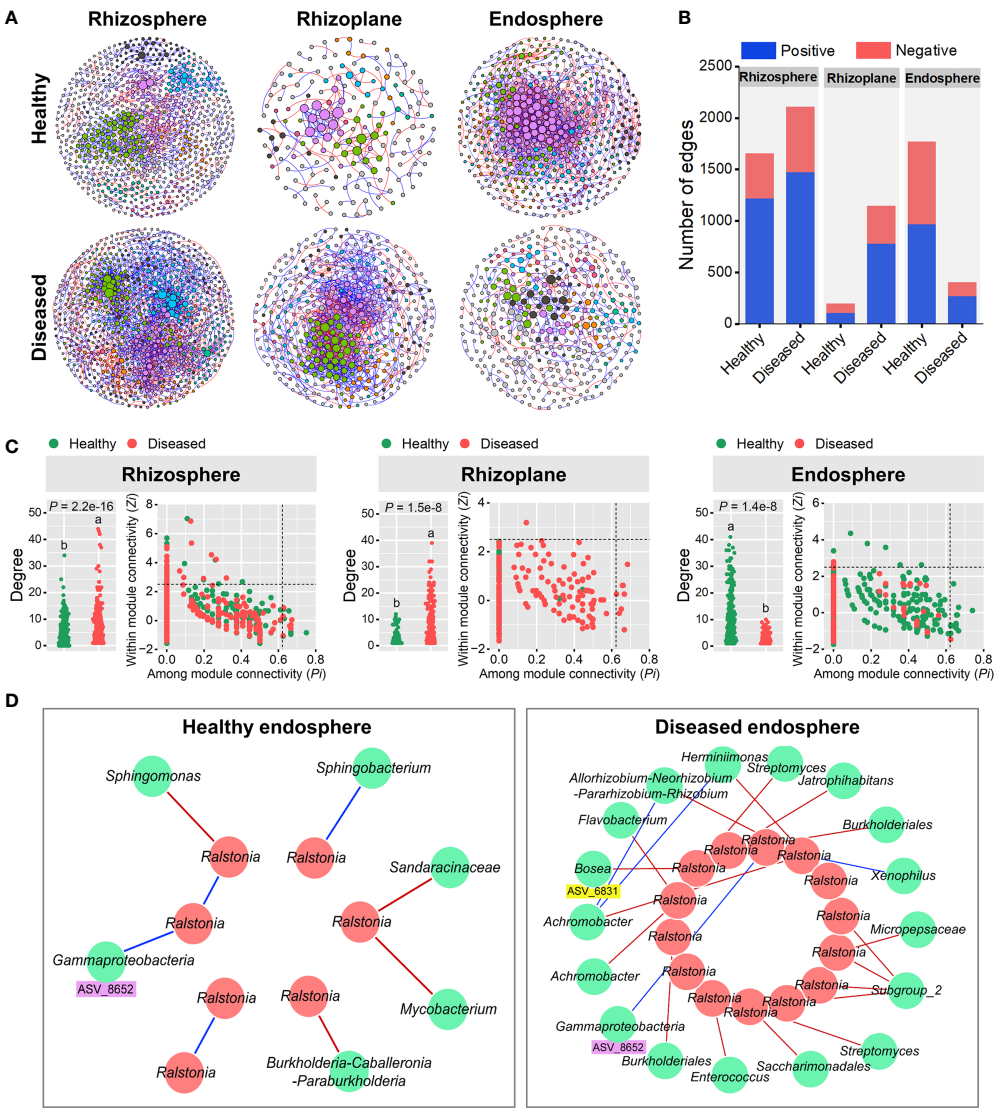

FIGURE 4
Random matrix theory (RMT)-based molecular ecology networks. **(A)** Bacterial co-occurrence networks of the rhizosphere, rhizoplane and endosphere in healthy and diseased plants. Each node represents an ASV. The size of each node is proportional to the number of connections (that is, degree) and the colors of nodes represent different modules. The links between the nodes indicate strong and significant ($P < 0.01$) correlations. A red line indicates a positive interaction between two individual nodes, while a blue line indicates a negative interaction. **(B)** The number and types (positive or negative) of edges in the rhizosphere, rhizoplane and endosphere networks of healthy and diseased plants. **(C)** Node degree and classification for each root-associated microbiome of healthy and diseased plants. Different letters indicate a significant difference determined by ANOVA test. Each symbol represents an ASV. The topological role of each ASV was determined according to the scatter plot of within-module connectivity (*Zi*) and among-module connectivity (*Pi*). Module hubs have *Zi*> 2.5, whereas connectors have *Pi* > 0.62. **(D)** Subnetworks of the pathogen (*Ralstonia*) and related bacterial species in the root endosphere microbiomes of healthy and diseased plants. Each node represents an ASV. A red line indicates a positive interaction between two individual nodes, while a blue line indicates a negative interaction.

compartments ($R^2 = 0.125$, $P < 0.001$) (Figure 5B). Several C, N and P cycling related genes showed a varied pattern among three root-associated communities (Figure 5C). Specifically, functional genes involved in Nitrification (e.g. *amo*A, *amo*B, and *amo*C) and P transport (e.g. *pst*A, *pst*B *pst*C, and *pst*S) were more abundant in the rhizosphere microbiome, genes related to C degradation (e.g. *xyl*A and *xyl*B) and Denitrification (e.g. *nor*C, *nir*S, and *nos*Z) were more abundant in the rhizoplane microbiome, and N reduction genes (e.g. *nar*G, *nar*H, *nar*I, *nas*A, *nas*B, and *nir*D) and N fixation genes (e.g. *nif*H, *nif*D, and *nif*K) were more abundant in the endosphere microbiome (Figure 5C). For individual compartment, disease presented more significant effects on the rhizoplane and endosphere than those on the rhizosphere. For the rhizoplane and endosphere

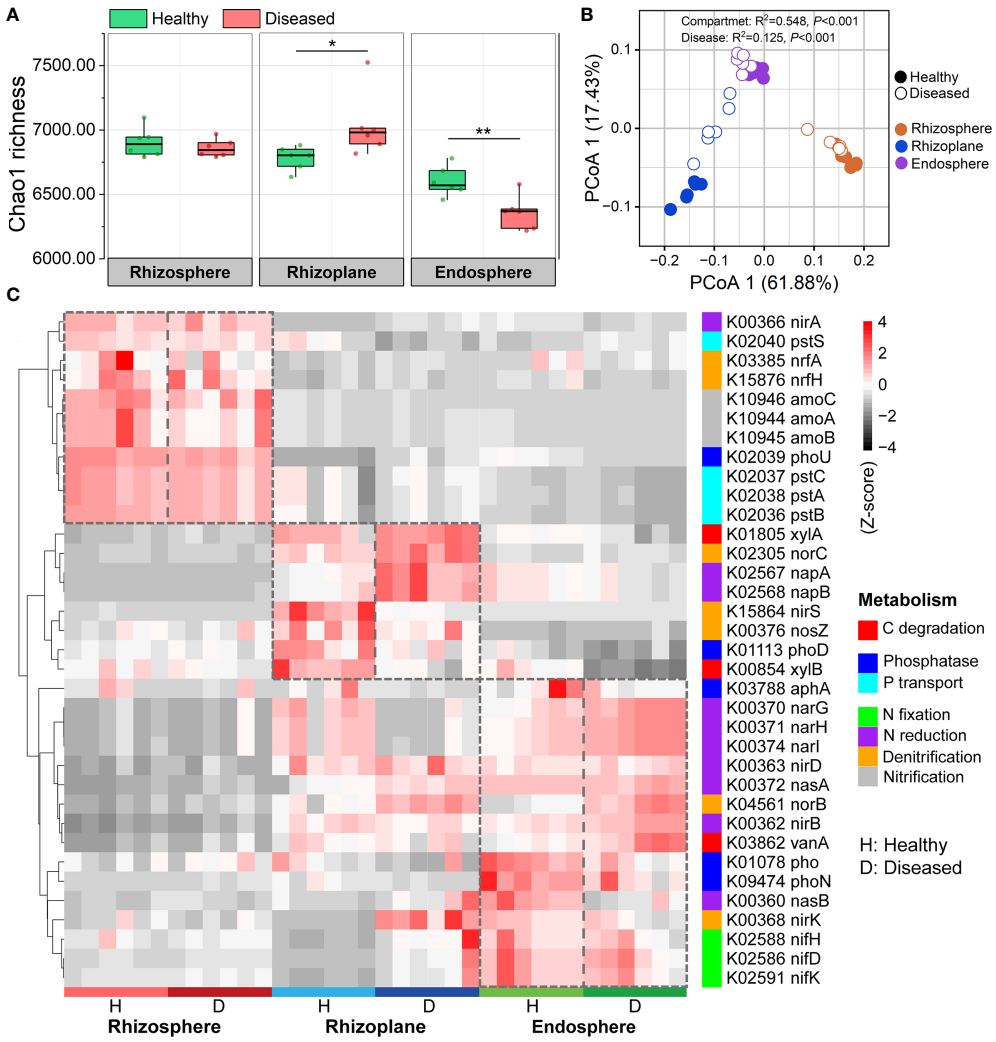

FIGURE 5
PICRUSt predicted metagenome functions at KO level. **(A)** Functional diversity of KO profiles of the rhizosphere, rhizoplane and endosphere microbiomes in healthy and diseased plants. Asterisks denote significant differences (*$P < 0.05$; **$P < 0.01$). **(B)** PCoA analysis of functional genes based on Bray–Curtis distance matrices of KO. **(C)** Heatmap exhibiting the relative abundance of functional genes (based on KO) involved in C, N, and P cycling which varied among three root-associated microbiomes.

microbiomes, the genes involved in N reduction were enriched and P transport genes were depleted in diseased samples (Figure 5C).

We further compared the functional genes involved in plant-microbiome signaling pathways (e.g. signal transduction) (Figure S5, Figure 6). The distributions of signal transduction genes were obviously different across the three root-associated microbiomes, and the microbiomes of the rhizoplane and endosphere were more susceptible to disease (Figure S5). For instance, the relative abundance of genes associated with cell cycle family and sporulation family was significantly increased in the diseased rhizoplane microbiome (ANOVA; $P < 0.05$), compared with the healthy plant (Figure 6A). The relative abundance of the functional genes involved in chemotaxis family (e.g. K03406: methyl-accepting chemotaxis), NtrC family and NarL family was significantly abundant in the microbiome of the diseased root endosphere (ANOVA; $P < 0.05$), compared with the healthy plant (Figure 6B).

All the above results indicated that the community function of endosphere and rhizoplane were significantly changed with pathogen invasion, but.

Discussion

Uncovering the changes of the structure and assembly of plant-associated microbiomes with plant disease invasion is essential to advance the co-evolutionary theory of plant-

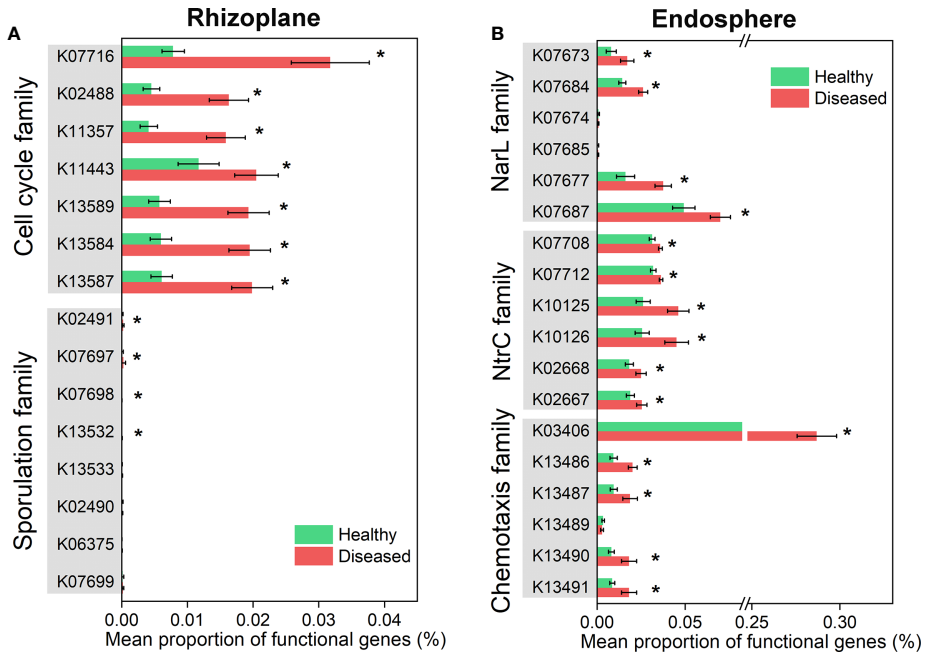

FIGURE 6
Differential abundance analysis of microbiome functional genes involved in plant-microbiome signaling pathways which varied significantly in healthy and diseased rhizoplane or endosphere. **(A)** Functional genes in cell cycle and sporulation families showing significantly different between healthy and diseased rhizoplane microbiomes. **(B)** Functional genes in NarL, NtrC and chemotaxis families showing significantly different between healthy and diseased endosphere microbiomes. Asterisks denote significant differences (*$P < 0.05$).

microbiome interactions (Liu et al., 2020). In this study, we characterized the compositions of three distinct rhizocompartments—the rhizosphere, rhizoplane, and endosphere, and gained insights into the effects of plant disease on each of these compartments. Our results demonstrated that the community assembly of the three root-associated microbiomes was simultaneously influenced by compartment niche and bacterial wilt disease. The microbiomes in or close to the plant's root (endosphere and rhizoplane) were more sensitive to the plant disease than the rhizosphere microbiome in terms of multiple microbial attributes (i.e. alpha-diversity, community structure, microbial networks, and community functions). However, the response strategies of the endosphere and rhizoplane microbiomes were obviously different.

Previous studies have demonstrated that the plant compartment was a crucial factor affecting the assembly of plant-associated microbiomes (Cregger et al., 2018; Gao et al., 2021). Similar to these reports, our results showed that the three rhizocompartments formed distinct microbial communities regardless of plant health conditions (Figure 1A). Microbial diversity (Shannon index, Chao1 richness, and Simpson index) patterns showed an obvious gradient from the rhizosphere to the endosphere (Figure 1B), indicating the filter effect of plant hosts on the closely associated microbiome assembly (Reinhold-Hurek et al., 2015). We noted that the proportion of Proteobacteria is more abundant in the rhizoplane and endosphere compartments compared with the rhizosphere and that the relative abundances of Acidobacteria and Gemmatimonadota were higher in the rhizosphere (Figure 1C), which were similar to the microbial composition of other plant species, such as *Arabidopsis* (Schlaeppi et al., 2014), rice (Edwards et al., 2015) and citrus (Zhang et al., 2017). Therefore, we inferred that the distribution of different bacterial phyla associated with the plant roots might be similar for most land plants. Further, functional analysis in our study revealed that the functional diversity and enriched functional traits in microbial communities varied across the three rhizocompartments (Figure 5). We demonstrated that the genes involved in nitrate reduction (*nar*G, *nar*H, and *nar*I) and N assimilation gene (*nas*A and *nas*B) were enriched from the rhizosphere to the endosphere (Figure 5C), further suggesting the importance of nitrogen resources supply of plants for rhizo-microbiomes.

We found that bacterial wilt disease had different effects on communities of the three rhizocompartments, in which the endosphere was more sensitive to the disease (Figure 1). Generally, the low microbial diversity of the microbial community was beneficial for the pathogen invasion (Locey and Lennon, 2016). Indeed, in our study, the endosphere, which held the lowest diversity indexes of Shannon, Chao1, and

Simpson (Figure 1B), showed a significantly higher abundance of the pathogen (*Ralstonia*) (Figure S3). With the success of pathogen invasion, the endosphere microbiome was disrupted and the community structure and function were clearly altered (Wei et al., 2017). Previous studies have demonstrated that the root-associated bacterial assemblage is mostly derived from the highly diverse soil microbiome surrounding roots (Zgadzaj et al., 2016). Here, we found the bacterial source of the endosphere community was also influenced by the pathogen invasion. In healthy plants, rare microorganisms were observed from the rhizosphere or bulk soil to the endosphere, while the bulk soil (21.80%) and the rhizosphere (10.62%) became important sources of the endosphere microbiome in diseased samples (Figure 2C, D). The results were in accordance with a recent study that endophytic communities of the infected plants were also derived from soil communities (Hu et al., 2020). The pathogenic *Ralstonia* enriched in the endosphere may begin in the soils and transfer to the plant root.

Faced with complex environments, plants may actively seek help from microbes to relieve stresses. Previous studies have evidenced that plants with pathogen invasion could use a variety of chemical stimuli to recruit beneficial microbes/traits from the environment (Liu et al., 2021). The beneficial microbes attracted by plants acted as key members of plant microbiomes and enhanced plant resistance to disease by interacting directly with pathogens (e.g., competition and antibiosis) (Woo et al., 2006) or by modulating plant defense responses (Mejía et al., 2014). For example, plant roots of sugar beet enriched for Chitinophagaceae and Flavobacteriaceae in the root endosphere, and the reconstruction of a consortium of *Chitinophaga* and *Flavobacterium* consistently suppressed fungal root disease (Carrión et al., 2019). Here, the enriched bacterial members across three root-associated microbiomes were significantly different (Figure 3), indicating microbial colonization in plant-associated niches is not a passive process and that plants had the ability to select for certain microbial members or that different microbes tended to enrich in the favorable colonizing niches (Edwards et al., 2015). Among these enriched microbes, most of them were enriched from the native community and distributed in a variety of bacterial genera. Besides, in the diseased plants, some new microbes (at ASV level) appeared in each rhizocompartment (Figures 3 and Tables S2–S4). For example, compared to the healthy samples, *Dyadobacter* ASV_6201, *Ochrobactrum* ASV_530, and *Pseudomonas* ASV_4114 in the rhizosphere, *Mycobacterium* ASV_11679 and *Saccharimonadales* ASV_12660 in the rhizoplane and *Shinella* ASV_8061 in the endosphere represented the "new microbes" in the three diseased compartments. These new ASVs may carry new microbial functions to help plants to resist the invasion of pathogenic bacteria. For example, *Pantoea* asv90 and *Methylobacterium* asv41 were identified as "recruited new microbes" in citrus leaves and exhibited antagonistic activities to the melanose pathogen *Diaporthe citri* (Li et al., 2022).

Except for analyzing changes in microbial taxa, changes in microbial interactions and functional profiles can further provide useful information to the effects of microbiome changes on plant health. Our study here revealed that networks of the rhizoplane and endosphere were significantly affected by the disease (based on links and the average degree) (Figure 4), which may be related to the low bacterial diversity in the rhizoplane and endosphere microbiomes (Figure 1B). However, the variation patterns of the rhizoplane and endosphere networks were greatly different. The rhizoplane microbiome of diseased samples presented a more intense microbial network than that of healthy samples, but the endosphere microbiome showed exactly the opposite variation. It has been suggested that highly connected networks could occur when microbes faced environmental pressures, such as pathogen invasion (Faust and Raes, 2012). The complex soil microbial community networks, rather than the simple ones, benefit plants (Yang et al., 2017). Therefore, the complex networks observed in the diseased rhizoplane might be a beneficial signal for plant defense. Although the endosphere network of diseased samples was simple as a whole, more microbes negatively connected to *Ralstonia* were identified in the diseased root than those in the healthy root (Figure 4D). The microbes having positive or negative connections with pathogen were considered as "pathogen antagonists" or "pathogen facilitators", respectively (Tao et al., 2021). Therefore, the microbes belonging to the genera of *Allorhizobium-Neorhizobium-Pararhizobium-Rhizobium*, *Streptomyces, Burkholderiales, Achromobacter, Bosea, and Flavobacterium* might act as 'pathogen antagonists' (Figure 4D). Notably, *Bosea* ASV_6831, a potential 'pathogen antagonist', was significantly enriched (FDR adjusted $P < 0.05$) in diseased root endosphere, might play a crucial role in suppressing the growth of pathogenic *Ralstonia*. *Bosea* spp. are Gram-negative, rod-shaped aerobic bacteria and are frequently isolated from various environments, including soils, sediments, root nodules of plants and digester sludge (Ouattara et al., 2003; De Meyer and Willems, 2012; Safronova et al., 2015). Several studies have reported that *Bosea* could protect plants against phytopathogen fungi, such as *Botrytis cinerea* and *Penicillium expansum* (Khoury et al., 2021). Here, our results indicated that *Bosea* ASV_6831 might also be a potential new 'pathogen antagonist' to phytopathogen bacteria, in accordance with a recent study that *Bosea minatitlanensis* SSB-9 had plant growth-promoting and antibacterial activities against *Ralstonia solanacearum* (Yuan et al., 2022). At present, there are few studies on the antagonistic mechanism of *Bosea* against plant pathogens, and future studies should focus on the potential interactions between *Bosea* and pathogens.

Analysis of community function indicated that microbiome functional genes involved in sporulation family and cell cycle family were enriched in the diseased rhizoplane and those involved in chemotaxis family, NtrC family, and NarL family

were more abundant in the diseased endosphere when compared to those genes in healthy samples. With the pathogen invasion, microbes in the rhizoplane community might take measures to increase their growth rate and promote sporulation formation to enhance their competitiveness with the pathogen. It has become evident that the production of bacterial toxins was controlled by the pathway regulating sporulation initiation (Bongiorni et al., 2007). The toxins produced by microbes could inhibit the growth of pathogens to a certain extent. The increase of genes in NarL and NtrC families in the diseased root endosphere indicated that nitrogen availability might be an important limiting factor for the plant under pathogenic *Ralstonia* invasion. Among the functional genes involved in chemotaxis, the gene (K03406) encoding MCPs (methyl-accepting chemotaxis proteins) was significantly enriched in the microbiome of diseased root endosphere, which was in accordance with a recent study on the Fusarium wilt disease of chili pepper (Gao et al., 2021). Under pathogen invasion, plants can recruit distant beneficial microbes by actively releasing some specific secondary metabolites (Schulz-Bohm et al., 2018; Yuan et al., 2018), which might cause the enrichment of microbial MCP genes in diseased plants. Some bacteria could use MCPs to detect specific concentrations of plant metabolic compounds in the extracellular matrix, enabling the directional accumulation of the bacteria to the plant (Gao et al., 2021).

Data availability statement

The data presented in the study are deposited in the Genome Sequence Archive in Beijing Institute of Genomics repository (https://bigd.big.ac.cn/gsa), accession number CRA007832.

Author contributions

PC, JT and JJ designed the experiments. JT, SY, ZY and QC performed the experiments. PL, JJ, YX and ZL analyzed the data. JT and SY wrote the manuscript. JJ and PC reviewed the manuscript. All authors contributed to the article and approved the submitted version.

Funding

This project was funded by China Postdoctoral Science Foundation (Grant/Award number: 2021M693511) and the Scientific and Technological Project of Henan Province (Grant/Award number: 222102110224 and 212102110257).

Conflict of interest

The authors declare that the research was conducted in the absence of any commercial or financial relationships that could be construed as a potential conflict of interest.

Publisher's note

All claims expressed in this article are solely those of the authors and do not necessarily represent those of their affiliated organizations, or those of the publisher, the editors and the reviewers. Any product that may be evaluated in this article, or claim that may be made by its manufacturer, is not guaranteed or endorsed by the publisher.

Supplementary material

The Supplementary Material for this article can be found online at: https://www.frontiersin.org/articles/10.3389/fpls.2022.1023837/full#supplementary-material

References

Bolyen, E., Rideout, J. R., Dillon, M. R., Bokulich, N. A., Abnet, C. C., Al-Ghalith, G. A., et al. (2019). Reproducible, interactive, scalable and extensible microbiome data science using QIIME 2. *Nat. Biotechnol.* 37 (8), 852–857. doi: 10.1038/s41587-019-0209-9

Bongiorni, C., Stoessel, R., and Perego, M. (2007). Negative regulation of *Bacillus anthracis* sporulation by the Spo0E family of phosphatases. *J. Bacteriol.* 189 (7), 2637–2645. doi: 10.1128/jb.01798-06

Callahan, B. J., McMurdie, P. J., Rosen, M. J., Han, A. W., Johnson, A. J., and Holmes, S. P. (2016). DADA2: High-resolution sample inference from illumina amplicon data. *Nat. Methods* 13 (7), 581–583. doi: 10.1038/nmeth.3869

Carrión, V. J., Perez-Jaramillo, J., Cordovez, V., Tracanna, V., de Hollander, M., Ruiz-Buck, D., et al. (2019). Pathogen-induced activation of disease-suppressive functions in the endophytic root microbiome. *Science* 366 (6465), 606–612. doi: 10.1126/science.aaw9285

Cregger, M. A., Veach, A. M., Yang, Z. K., Crouch, M. J., Vilgalys, R., Tuskan, G. A., et al. (2018). The populus holobiont: dissecting the effects of plant niches and genotype on the microbiome. *Microbiome* 6 (1), 31. doi: 10.1186/s40168-018-0413-8

De Meyer, S. E., and Willems, A. (2012). Multilocus sequence analysis of *Bosea* species and description of *Bosea lupini* sp. nov., *Bosea lathyri* sp. nov. and *Bosea robiniae* sp. nov., isolated from legumes. *Int. J. Syst. Evol. Microbiol.* 62 (Pt 10), 2505–2510. doi: 10.1099/ijs.0.035477-0

de Vries, F. T., Griffiths, R. I., Knight, C. G., Nicolitch, O., and Williams, A. (2020). Harnessing rhizosphere microbiomes for drought-resilient crop production. *Science* 368 (6488), 270–274. doi: 10.1126/science.aaz5192

Douglas, G. M., Maffei, V. J., Zaneveld, J. R., Yurgel, S. N., Brown, J. R., Taylor, C. M., et al. (2020). PICRUSt2 for prediction of metagenome functions. *Nat. Biotechnol.* 38 (6), 685–688. doi: 10.1038/s41587-020-0548-6

Durán, P., Thiergart, T., Garrido-Oter, R., Agler, M., Kemen, E., Schulze-Lefert, P., et al. (2018). Microbial interkingdom interactions in roots promote *Arabidopsis* survival. *Cell* 175 (4), 973–983.e914. doi: 10.1016/j.cell.2018.10.020

Edgar, R. C. (2010). Search and clustering orders of magnitude faster than BLAST. *Bioinformatics* 26 (19), 2460–2461. doi: 10.1093/bioinformatics/btq461

Edwards, J., Johnson, C., Santos-Medellín, C., Lurie, E., Podishetty, N. K., Bhatnagar, S., et al. (2015). Structure, variation, and assembly of the root-associated microbiomes of rice. *Proc. Natl. Acad. Sci. U.S.A.* 112 (8), E911–E920. doi: 10.1073/pnas.1414592112

Faust, K., and Raes, J. (2012). Microbial interactions: from networks to models. *Nat. Rev. Microbiol.* 10 (8), 538–550. doi: 10.1038/nrmicro2832

Feng, K., Zhang, Y., He, Z., Ning, D., and Deng, Y. (2019). Interdomain ecological networks between plants and microbes. *Mol. Ecol. Resour.* 19 (6), 1565–77. doi: 10.1111/1755-0998.13081

Gao, M., Xiong, C., Gao, C., Tsui, C. K. M., Wang, M. M., Zhou, X., et al. (2021). Disease-induced changes in plant microbiome assembly and functional adaptation. *Microbiome* 9 (1), 187. doi: 10.1186/s40168-021-01138-2

Hu, Q., Tan, L., Gu, S., Xiao, Y., and Deng, Y. (2020). Network analysis infers the wilt pathogen invasion associated with non-detrimental bacteria. *NPJ Biofilms Microbiomes* 6 (1), 8. doi: 10.1038/s41522-020-0117-2

Jiang, G., Wei, Z., Xu, J., Chen, H., Zhang, Y., She, X., et al. (2017). Bacterial wilt in China: History, current status, and future perspectives. *Front. Plant Sci.* 8, 1549. doi: 10.3389/fpls.2017.01549

Khoury, E., Abou Fayad, A., Karam Sarkis, D., Fahs, H., Gunsalus, K. C., and Kallassy Awad, M. (2021). The microbiome of the Lebanese wild apple, *Malus trilobata*, is a rich source of potential biocontrol agents for fungal post-harvest pathogens of apples. *Curr. Microbiol.* 78 (4), 1388–1398. doi: 10.1007/s00284-021-02397-w

Knights, D., Kuczynski, J., Charlson, E. S., Zaneveld, J., Mozer, M. C., Collman, R. G., et al. (2011). Bayesian Community-wide culture-independent microbial source tracking. *Nat. Methods* 8 (9), 761–763. doi: 10.1038/nmeth.1650

Li, S., Liu, Y., Wang, J., Yang, L., Zhang, S., Xu, C., et al. (2017). Soil acidification aggravates the occurrence of bacterial wilt in south China. *Front. Microbiol.* 8. doi: 10.3389/fmicb.2017.00703

Liu, H., Brettell, L. E., Qiu, Z., and Singh, B. K. (2020). Microbiome-mediated stress resistance in plants. *Trends Plant Sci.* 25 (8),733–743. doi: 10.1016/j.tplants.2020.03.014

Liu, H., Li, J., Carvalhais, L. C., Percy, C. D., Prakash Verma, J., Schenk, P. M., et al. (2021). Evidence for the plant recruitment of beneficial microbes to suppress soil-borne pathogens. *New Phytol.* 229 (5), 2873–2885. doi: 10.1111/nph.17057

Li, P. D., Zhu, Z. R., Zhang, Y., Xu, J., Wang, H., Wang, Z., et al. (2022). The phyllosphere microbiome shifts toward combating melanose pathogen. *Microbiome* 10 (1), 56. doi: 10.1186/s40168-022-01234-x

Locey, K. J., and Lennon, J. T. (2016). Scaling laws predict global microbial diversity. *Proc. Natl. Acad. Sci. U.S.A.* 113 (21), 5970–5975. doi: 10.1073/pnas.1521291113

Martin, F. M., Uroz, S., and Barker, D. G. (2017). Ancestral alliances: Plant mutualistic symbioses with fungi and bacteria. *Science* 356 (6340),eaad4501. doi: 10.1126/science.aad4501

Mejía, L. C., Herre, E. A., Sparks, J. P., Winter, K., García, M. N., Van Bael, S. A., et al. (2014). Pervasive effects of a dominant foliar endophytic fungus on host genetic and phenotypic expression in a tropical tree. *Front. Microbiol.* 5. doi: 10.3389/fmicb.2014.00479

Mendes, R., Kruijt, M., de Bruijn, I., Dekkers, E., van der Voort, M., Schneider, J. H., et al. (2011). Deciphering the rhizosphere microbiome for disease-suppressive bacteria. *Science* 332 (6033), 1097–1100. doi: 10.1126/science.1203980

Müller, D. B., Vogel, C., Bai, Y., and Vorholt, J. A. (2016). The plant microbiota: Systems-level insights and perspectives. *Annu. Rev. Genet.* 50, 211–234. doi: 10.1146/annurev-genet-120215-034952

Olesen, J. M., Bascompte, J., Dupont, Y. L., and Jordano, P. (2007). The modularity of pollination networks. *Proc. Natl. Acad. Sci.* 104 (50), 19891–19896. doi: 10.1073/pnas.0706375104

Ouattara, A. S., Assih, E. A., Thierry, S., Cayol, J. L., Labat, M., Monroy, O., et al. (2003). *Bosea minatitlanensis* sp. nov., a strictly aerobic bacterium isolated from an anaerobic digester. *Int. J. Syst. Evol. Microbiol.* 53 (Pt 5), 1247–1251. doi: 10.1099/ijs.0.02540-0

Reinhold-Hurek, B., Bünger, W., Burbano, C. S., Sabale, M., and Hurek, T. (2015). Roots shaping their microbiome: global hotspots for microbial activity. *Annu. Rev. Phytopathol.* 53, 403–424. doi: 10.1146/annurev-phyto-082712-102342

Safronova, V. I., Kuznetsova, I. G., Sazanova, A. L., Kimeklis, A. K., Belimov, A. A., Andronov, E. E., et al. (2015). *Bosea vaviloviae* sp. nov., a new species of slow-growing rhizobia isolated from nodules of the relict species *Vavilovia formosa* (Stev.) fed. *ANTON LEEUW. Int. J. G.* 107 (4), 911–920. doi: 10.1007/s10482-015-0383-9

Schlaeppi, K., Dombrowski, N., Oter, R. G., Ver Loren van Themaat, E., and Schulze-Lefert, P. (2014). Quantitative divergence of the bacterial root microbiota in *Arabidopsis thaliana* relatives. *Proc. Natl. Acad. Sci. U.S.A.* 111 (2), 585–592. doi: 10.1073/pnas.1321597111

Schulz-Bohm, K., Gerards, S., Hundscheid, M., Melenhorst, J., de Boer, W., and Garbeva, P. (2018). Calling from distance: attraction of soil bacteria by plant root volatiles. *Isme J.* 12 (5), 1252–1262. doi: 10.1038/s41396-017-0035-3

Sessitsch, A., and Mitter, B. (2015). 21st century agriculture: integration of plant microbiomes for improved crop production and food security. *Microb. Biotechnol.* 8 (1), 32–33. doi: 10.1111/1751-7915.12180

Simon, J. C., Marchesi, J. R., Mougel, C., and Selosse, M. A. (2019). Host-microbiota interactions: from holobiont theory to analysis. *Microbiome* 7 (1), 5. doi: 10.1186/s40168-019-0619-4

Tao, J., Cao, P., Xiao, Y., Wang, Z., Huang, Z., Jin, J., et al. (2021). Distribution of the potential pathogenic *Alternaria* on plant leaves determines foliar fungal communities around the disease spot. *Environ. Res.* 200, 111715. doi: 10.1016/j.envres.2021.111715

Tao, J., Liu, X., Liang, Y., Niu, J., Xiao, Y., Gu, Y., et al. (2017). Maize growth responses to soil microbes and soil properties after fertilization with different green manures. *Appl. Microbiol. Biotechnol.* 101 (3), 1289–1299. doi: 10.1007/s00253-016-7938-1

Torsvik, V., Øvreås, L., and Thingstad, T. F. (2002). Prokaryotic diversity–magnitude, dynamics, and controlling factors. *Science* 296 (5570), 1064–1066. doi: 10.1126/science.1071698

Trivedi, P., Leach, J. E., Tringe, S. G., Sa, T., and Singh, B. K. (2020). Plant-microbiome interactions: from community assembly to plant health. *Nat. Rev. Microbiol.* 18 (11), 607–621. doi: 10.1038/s41579-020-0412-1

Turner, T. R., James, E. K., and Poole, P. S. (2013). The plant microbiome. *Genome Biol.* 14 (6), 209. doi: 10.1186/gb-2013-14-6-209

van der Heijden, M. G., and Hartmann, M. (2016). Networking in the plant microbiome. *PloS Biol.* 14 (2), e1002378. doi: 10.1371/journal.pbio.1002378

Wei, Z., Hu, J., Gu, Y. A., Yin, S., Xu, Y., Jousset, A., et al. (2017). *Ralstonia solanacearum* pathogen disrupts bacterial rhizosphere microbiome during an invasion. *Soil Biol. Biochem.* 118 (1), 8–17. doi: 10.1038/s41522-020-0117-2

Woo, S. L., Scala, F., Ruocco, M., and Lorito, M. (2006). The molecular biology of the interactions between *Trichoderma* spp., phytopathogenic fungi, and plants. *Phytopathology* 96 (2), 181–185. doi: 10.1094/phyto-96-0181

Xiong, C., Singh, B. K., He, J. Z., Han, Y. L., Li, P. P., Wan, L. H., et al. (2021). Plant developmental stage drives the differentiation in ecological role of the maize microbiome. *Microbiome* 9 (1), 171. doi: 10.1186/s40168-021-01118-6

Yang, H., Li, J., Xiao, Y., Gu, Y., Liu, H., Liang, Y., et al. (2017). An integrated insight into the relationship between soil microbial community and tobacco bacterial wilt disease. *Front. Microbiol.* 8. doi: 10.3389/fmicb.2017.02179

Yilmaz, P., Parfrey, L. W., Yarza, P., Gerken, J., Pruesse, E., Quast, C., et al. (2014). The SILVA and "All-species living tree project (LTP)" taxonomic frameworks. *Nucleic Acids Res.* 42 (Database issue), D643–D648. doi: 10.1093/nar/gkt1209

Yuan, W., Ruan, S., Qi, G., Wang, R., and Zhao, X. (2022). Plant growth-promoting and antibacterial activities of cultivable bacteria alive in tobacco field against *Ralstonia solanacearum*. *Environ. Microbiol.* 24 (3), 1411–1429. doi: 10.1111/1462-2920.15868

Yuan, J., Zhao, J., Wen, T., Zhao, M., Li, R., Goossens, P., et al. (2018). Root exudates drive the soil-borne legacy of aboveground pathogen infection. *Microbiome* 6 (1), 156. doi: 10.1186/s40168-018-0537-x

Zgadzaj, R., Garrido-Oter, R., Jensen, D. B., Koprivova, A., Schulze-Lefert, P., and Radutoiu, S. (2016). Root nodule symbiosis in *Lotus japonicus* drives the establishment of distinctive rhizosphere, root, and nodule bacterial communities. *Proc. Natl. Acad. Sci. U.S.A.* 113 (49), E7996–e8005. doi: 10.1073/pnas.1616564113

Zhang, Y., Xu, J., Riera, N., Jin, T., Li, J., and Wang, N. (2017). Huanglongbing impairs the rhizosphere-to-rhizoplane enrichment process of the citrus root-associated microbiome. *Microbiome* 5 (1), 97. doi: 10.1186/s40168-017-0304-4

Zhou, J., Deng, Y., Luo, F., He, Z., and Yang, Y. (2011). Phylogenetic molecular ecological network of soil microbial communities in response to elevated CO_2. *mBio* 2 (4),e00122–11. doi: 10.1128/mBio.00122-11

frontiers | Frontiers in Plant Science

TYPE Review
PUBLISHED 21 October 2022
DOI 10.3389/fpls.2022.999866

OPEN ACCESS

EDITED BY
Mengting Maggie Yuan,
University of California, Berkeley,
United States

REVIEWED BY
Muhammad Yahya Khan,
University of Agriculture, Faisalabad,
Pakistan
Giovana Slanzon,
University of Hawaii, United States

*CORRESPONDENCE
Kumar Pranaw
kpranaw@gmail.com;
k.pranaw@uw.edu.pl

SPECIALTY SECTION
This article was submitted to
Plant Symbiotic Interactions,
a section of the journal
Frontiers in Plant Science

RECEIVED 21 July 2022
ACCEPTED 04 October 2022
PUBLISHED 21 October 2022

CITATION
Poria V, Dębiec-Andrzejewska K,
Fiodor A, Lyzohub M, Ajijah N, Singh S
and Pranaw K (2022) Plant Growth-
Promoting Bacteria (PGPB)
integrated phytotechnology:
A sustainable approach for
remediation of marginal lands.
Front. Plant Sci. 13:999866.
doi: 10.3389/fpls.2022.999866

Plant Growth-Promoting Bacteria (PGPB) integrated phytotechnology: A sustainable approach for remediation of marginal lands

Vikram Poria[1], Klaudia Dębiec-Andrzejewska[2], Angelika Fiodor[2], Marharyta Lyzohub[2], Nur Ajijah[2], Surender Singh[1] and Kumar Pranaw[2]*

[1]Department of Microbiology, Central University of Haryana, Mahendergarh, India, [2]Department of Environmental Microbiology and Biotechnology, Institute of Microbiology, Faculty of Biology, University of Warsaw, Warsaw, Poland

Land that has little to no utility for agriculture or industry is considered marginal land. This kind of terrain is frequently found on the edge of deserts or other arid regions. The amount of land that can be used for agriculture continues to be constrained by increasing desertification, which is being caused by climate change and the deterioration of agriculturally marginal areas. Plants and associated microorganisms are used to remediate and enhance the soil quality of marginal land. They represent a low-cost and usually long-term solution for restoring soil fertility. Among various phytoremediation processes (viz., phytodegradation, phytoextraction, phytostabilization, phytovolatilization, phytofiltration, phytostimulation, and phytodesalination), the employment of a specific mechanism is determined by the state of the soil, the presence and concentration of contaminants, and the plant species involved. This review focuses on the key economically important plants used for phytoremediation, as well as the challenges to plant growth and phytoremediation capability with emphasis on the advantages and limits of plant growth in marginal land soil. Plant growth-promoting bacteria (PGPB) boost plant development and promote soil bioremediation by secreting a variety of metabolites and hormones, through nitrogen fixation, and by increasing other nutrients' bioavailability through mineral solubilization. This review also emphasizes the role of PGPB under different abiotic stresses, including heavy-metal-contaminated land, high salinity environments, and organic contaminants. In our opinion, the improved soil fertility of marginal lands using PGPB with economically significant plants (e.g., *Miscanthus*) in dual precession technology will result in the reclamation of general agriculture as well as the restoration of native vegetation.

KEYWORDS

phytoremediation, plant growth-promoting bacteria (PGPB), marginal land, biodegradation, heavy metals (HMs), organic pollutants

1 Introduction

Marginal lands are increasing at an alarming rate due to various anthropogenic activities. Marginal lands are defined as having inferior soil with inadequate agricultural attributes and crop yield that is occasionally polluted. The state of the world's land and water resources for food and agriculture is associated with the condition of our productive land and ecosystems and reflects problematic trends in resource consumption (FAO, 2022). A rapid decline in natural and seminatural ecosystems over the last centuries and severe climatic changes along with increasing human pressure have led to more frequent extreme weather events, higher rates of land degradation, and potential habitat losses. Furthermore, excessive use of fertilizer impacts the health of soil negatively. Thus, remedial actions are needed to prevent land degradation, on which 98% of the world's food is produced.

The degradation of land, soil, and water resources as a result of human activity diminishes their production potential, biodiversity, and environmental services that support healthy and resilient livelihoods. Energy crops planted in these regions can aid in land reclamation and significantly reduce greenhouse gas emissions (Zhuang et al., 2011; Schröder et al., 2018). Overgrazing (35%), intensive agriculture (28%), deforestation (30%), manufacturing fuel wood (7%), and industrialization (4%) are the main drivers of soil deterioration (Schröder et al., 2018). Land might be marginal for a variety of reasons, including a lack of water supply, low chemical and/or microbiological soil quality, pollution from previous industrial activity, topographic obstacles such as an extreme slope, or when inaccessible or very remote from transportation networks. Most marginal lands are also characterized by heavy metal (HM) contamination, organic pollutants, strong acidification or alkalization, high salinity, limited water, etc. (Jiang et al., 2021; Shahane and Shivay, 2021). According to Fan et al. (2020), for energy crop production, about 43.75 million hectares (Mha) of marginal land is available in South China, 11.36 Mha in the US, 1.4 Mha in the UK, and almost 45 Mha in Europe. On the other hand, Jiang et al. (2021) assessed the total marginal land worldwide suitable for the cultivation of the energy crop *Pistacia chinensis* using a machine learning method and reported that a total of 1311.85 Mha of marginal land is mostly distributed in Southern Africa, the southern part of North America, the western part of South America, Southeast Asia, Southern Europe, and the east and southwest coasts of Oceania.

Plant growth is adversely affected by increased salinity or HM concentration, too high or low pH, low water availability, and the presence of other contaminants. Wilting and abscission of leaves, decreased leaf regions, and decreased water loss through transpiration are all physiological responses to stress in plants. Reduced turgor pressure under stress is one of the most delicate physiological mechanisms that allows cells to develop in a stressed environment. Drought stress disrupts water passage from the xylem to surrounding elongating cells in higher plants resulting in cell elongation suppression. In addition, drought leads to a reduction in leaf area, plant height, and plant development as cell elongation, mitosis, and spreading are impaired. Osmotic modification, which supports the active accumulation of solutes in the cytoplasm to maintain the cell's water balance, can reduce the negative effects of stress (Yadav et al., 2020).

Plants employ various mechanisms, such as escape, avoidance, and tolerance, to counteract various stresses, and many plants have been described for their soil remediation ability. Plants can remove or immobilize various pollutants from the soil by employing different phytoremediation strategies, such as phytodegradation, phytoextraction, phytostabilization, etc. (Yan et al., 2020). PGPB also helps to improve the remediation ability of plants by stimulating plant growth through the secretion of various types of metabolites and hormones, solubilizing minerals, fixing nitrogen, and protecting plants against pathogens. PGPB also helps in alleviating various other types of biotic and abiotic stresses faced by plants (Backer et al., 2018). In this review, various phytoremediation strategies and the role of PGPB in enhancing the plant's potential for phytoremediation have been discussed. In addition, a number of plant growth-promoting activities of PGPB have also been reported.

2 Phytoremediation

Phytoremediation is a decontamination technique wherein plants, such as grasses, shrubs, and trees, help to clean up the environment by degrading, accumulating, or stabilizing the contaminants. Phytoremediation techniques generate very little secondary waste while removing contaminants from the environment in an environmentally friendly way and at a very low cost (Shah and Daverey, 2020).

2.1 Types of phytoremediation and their mechanisms

Based on the soil conditions, pollutants, and plant species, phytoremediation of HM-contaminated soils includes many methods and processes such as phytodegradation (phytotransformation), phytofiltration, phytoextraction (phytoaccumulation), phytostabilization, rhizodegradation, phytodesalination, and phytovolatilization, as shown in Figure 1 (Saleem et al., 2020b; Nedjimi, 2021; Sabreena et al., 2022). The most extensively employed phytoremediation methods in the remediation of HM-contaminated soils are phytostabilization, phytoextraction, phytovolatilization, and phytofiltration, whereas strategies like phytodegradation and rhizodegradation are used for

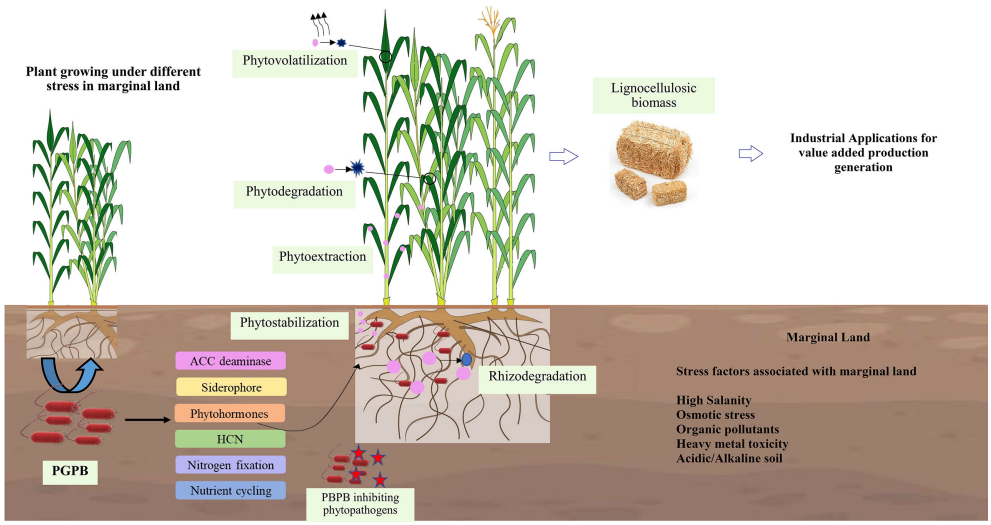

FIGURE 1
Phytoremediation methods and the role of PGPB in assisting plants for the remediation of marginal lands.

the degradation of organic pollutants (Yan et al., 2020). The effectiveness of phytoremediation depends primarily on the plant species used for contaminant removal. Plant species with high metal tolerance and high extraction or immobilization ability are very effective and are usually used for phytoremediation (Visconti et al., 2022). There are several newly emerged phytoremediation techniques such as phytoremediation buffers, phytoremediation vegetation, phytoremediation caps, phytoremediation plantings, and percolation and phytoremediation (Riaz et al., 2022).

2.1.1 Phytostabilization or Phytoimmobilization

Phytostabilization is a cost-effective and less invasive phytotechnology that stabilizes hazardous contaminants such as HMs in the rhizosphere or roots by using tolerant plants that bind the contaminants in soil reducing their mobility within ecosystems and food chains (Shackira and Puthur, 2019). It involves a temporary accumulation of contaminants by plants in their belowground parts, which only immobilize and deactivate toxic metal ions instead of permanently removing them from the contaminated soil by forming metal complexes with root exudates, cell wall bonds, precipitates, or reducing HMs in the rhizosphere, which are sequestered in the vacuoles of root cells with the help of microorganisms (Zgorelec et al., 2020; Kafle et al., 2022). For effective phytostabilization, the selection of suitable plant species is very important. The plant should be HM tolerant and have a dense root system because roots play an important role in HM immobilization, stabilizing the soil structure, and preventing soil erosion (Shackira and Puthur, 2019; Zine et al., 2020). In addition, plant species and varieties characterized by low translocation factors are also highly desirable (Huang et al., 2021).

2.1.2 Phytodegradation

Phytodegradation is the degradation of contaminants taken up by plants through metabolic processes, or the degradation of pollutants outside the plant by enzymes (such as dehalogenases, nitro reductases, and peroxidases) released by roots (Jhilta et al., 2021; Nedjimi, 2021). Rhizosphere microorganisms perform most of the phytodegradation activities in a favorable rhizosphere environment. The ability of plants to modify the rhizospheric microbial community composition (Poria et al., 2021b) and microbial interaction within it has a significant impact on the degradation of pollutants. There are many reports which suggest that plants promote the degradation of contaminants by rhizospheric effects (Kotoky and Pandey, 2020a;Kotoky and Pandey, 2020b; Nebeská et al., 2021).

2.1.3 Phytoextraction or phytoaccumulation

Contaminants from soil or water are taken up by plants and permanently accumulated in above-ground biomass through translocation during phytoextraction or phytoaccumulation (Ali et al., 2020). Phytoextraction involves several steps, starting with HM mobilization in the rhizosphere, followed by uptake by plant roots and translocation to above-ground parts of the plant. The final step is the immobilization and compartmentalization of HM ions in the aerial tissues of the plant (Yan et al., 2020).

2.1.4 Phytovolatilization

In this phytoremediation strategy, plants release volatile forms of HMs by transpiration through the leaves after absorbing HMs from the soil and converting them to less toxic volatile forms (Bortoloti and Baron, 2022). Compared to other

phytoremediation strategies, phytovolatilization is more beneficial as it removes contaminants without harvesting and disposing of the plants and converts them to gaseous compounds (Yan et al., 2020).

2.1.5 Phytofiltration

In this strategy, reclamation of soil and water with a low content of contaminants is carried out using seedlings (blastofiltration), shoots (caulofiltration), or roots (rhizofiltration). In rhizofiltration, HMs are either adsorbed on the root surface or absorbed by the roots. Root exudates can alter the pH of rhizosphere, resulting in HM precipitation at plant roots and a reduction in HM transport to subsurface water. Plants used for rhizofiltration are first cultivated in clean water (hydroponics) to establish an extensive root system, and then contaminated water is utilized to acclimate the plants. These plants are then transferred to the contaminated site for HM removal. The roots are removed and discarded once they become soaked with HMs (Ashraf et al., 2019).

2.1.6 Rhizodegradation or phytostimulation

Rhizodegradation is the biodegradation of organic pollutants in the soil, which involves the secretion of certain enzymes by rhizospheric microorganisms that degrade or convert heavily polluted organic pollutants into less harmful substances. The rhizodegradation process is accelerated by microbes that take up nutrients (amino acids, carbohydrates, etc.) from the root secretions of the plant, increasing its efficiency and accelerating the extraction and removal of contaminants (Ashraf et al., 2019; Sabreena et al., 2022). Dissolution of the pollutant at the source is a key element of rhizodegradation, which focuses on the complete mineralization of the organic pollutant by transferring it to the plant or atmosphere. Soil type and plant species has an effect on rhizodegradation. *Bacillus*, *Burkholderia*, *Pseudomonas*, *Agrobacterium*, *Alcaligenes*, *Arthrobactor*, and *Micrococcus* are bacteria frequently reported to be involved in rhizodegradation, as are mycorrhizal fungi such as *Glomus* (P.P and Puthur, 2021).

2.1.7 Phytodesalination

Phytodesalination is the most widely used method to decontaminate saline soils and uses halophytic plants. In comparison to other phytoremediation approaches, knowledge about this strategy is still poor. Halophytes are thought to be naturally well-adapted to live in HM- contaminated surroundings in contrast to most glycophyte plants. The plant's ability to desalinate soil is determined by the species, as well as soil properties like salinity, sodicity, and porosity, as well as other climatic elements like rainfall (Sabreena et al., 2022).

Several new sustainable phytoremediation techniques are also being used for soil remediation. Such a technique can be used to remediate areas like brownfields, mine wastes, and landfill trash that have low to moderate levels of contamination. Known as phytoremediation buffers, the technique uses buffer strips in conjunction with riparian corridors where appropriate plant species are planted in the stripes along stream channels to remove toxins from surface water and groundwater flowing into rivers. This method is incredibly useful in preventing the further spread and mixing of water pollutants into groundwater supplies. Phytoremediation can result in contaminants entering the food chain, and some phytoremediation techniques do not completely remove contaminants from the environment. To reduce this risk of environmental and food contamination, another combined technique, percolation, along with phytoremediation, can be used to remove and percolate contaminants from the polluted soils. Using infiltration and percolation through vegetative covers, this technique is designed to remove soil pollutants. Phytoremediation caps also serve the purpose of reducing contaminant input to natural resources by reducing infiltration and precipitation and improving cap integrity. To reduce the spread of contaminants from their active hotspots, phytoremediation vegetation cover systems are used to establish barriers and prevent the further spread of contaminants. This is an economically feasible system because it is self-regenerating and can control soil erosion (Riaz et al., 2022)

2.2 Major economically important plants used for phytoremediation

Phytoremediation is a cost-effective and ecologically sound method of removing contaminants from soil and water. Adsorption, transport and translocation, hyperaccumulation or transformation, and mineralization are all processes that plants use to remove HMs from the environment (Pandey et al., 2015). Phytoremediation has already been documented for *Festuca arundinacea*, *Hordeum vulgare*, *Thlaspi caerulescens*, *Linum usitatissimum*, *Pteris vittata*, and *Brassica juncea*, among other economically important plants (Saleem et al., 2020a). Marginal lands are suitable for the growth of numerous energy crops, such as *Arundo donax*, *Brassica juncea*, *Jatropha curcas*, *Miscanthus species*, *Ricinus communis*, and *Salix* spp., which have been used to remediate polluted areas (P.P and Puthur, 2021).

Plants with a high degree of ecological adaptability and economic value are selected for their phytoremediation capacity so that, in addition to removing contaminants, they offer other social, environmental, and economic prospects, such as carbon sequestration, increasing soil's organic biomass, promoting microbial biodiversity, biomass for value-added products such as bioenergy production, platform chemicals, fragrances and flavorings, construction and soundproofing materials for houses, and raw material for the paper pulp industry, etc. These plants, which include *Saccharum munja*, *Saccharum spontaneum*, *Vetiveria*

zizanioides, *Cymbopogon flexuosus*, *Ocimum basilicum*, *Ricinus communis*, *Jatropha curcas*, *Miscanthus giganteus* (Pandey et al., 2015), *Cyperus alternifolius*, *Amaranthus retroflexus*, *Celosia cristata*, and *Bambusa vulgaris*, have been reported for their bioremediation and phytodesalination activity (Ameri Siahouei et al., 2020). A list of some economically important plants for phytoremediation is presented in Table 1.

TABLE 1 A list of economically significant plants for phytoremediation.

Plant name	Purpose	Contaminant removed	Phytoremediation strategy	Reference
Amorpha fruticosa	Phytoremediation ability, N_2-fixation, stress-tolerant, and tap root system	Pb and Zn	Phytostabilization	Sikdar et al. (2020)
Helianthus petiolaris	Bioenergy crop and phytoremediation ability	Pb and Cd	Phytostabilization	Saran et al. (2020a)
Thymus kotschyanus, *Phleum pratense*, and *Achillea millefolium*	Phytoremediation ability	Cu	Phytoextraction and phytostabilization	Ghazaryan et al. (2018)
Atriplex nummularia	Phytoremediation and stress tolerating ability	Zn, Cu, Cd, and Pb	Phytostabilization	Eissa (2019)
Pennisetum purpureum cv. Mott	Bioenergy crop and phytoremediation ability	As and Mn	Phytostabilization	Kowitwiwat and Sampanpanish (2020)
Azolla filiculoides	Phytoremediation ability and N_2-fixation	Sodium dodecyl benzene sulfonate	Phytodegradation	Masoudian et al. (2020)
Andropogon tectorum	Phytoremediation ability	Petroleum hydrocarbon	Phytodegradation	Jude et al. (2019)
Acacia farnesiana	Bioenergy crop and phytoremediation ability	Crude oil	Phytodegradation	Ahmed et al. (2021)
Calophyllum brasiliense, Hymenaea courbaril	Phytoremediation ability	Hexazinone	Phytodegradation and Rhizodegradation	Dos Santos et al. (2018)
Salix interior and *Trifolium pratense*	Phytoremediation ability and N_2-fixation	As, Cu, Cr, and pentachlorophenol	Phytoextraction	Lachapelle et al. (2021)
Cotton	Bioenergy crop and phytoremediation ability	Cd	Phytoextraction	Ramana et al. (2021)
Linum usitatissimum	Bioenergy crop and phytoremediation ability	Cu	Phytoextraction	Saleem et al. (2020c)
Sedum plumbizincicola	Phytoremediation ability	Cd	Phytoextraction	Zhou et al. (2020)
Pteris vittata L. and *Morus alba* L. or *Pteris vittata* L. and *Broussonetia papyrifera* L.	Bioenergy crop and phytoremediation ability	As, Cd, Pb, and Zn	Phytoextraction	Zeng et al. (2019)
Pteris multifida	Bioenergy crop and phytoremediation ability	As, Pb, and Cd	Phytofiltration	Rahman et al. (2018)
Trifolium alexandrinum L.	Green manure and phytoremediation ability	Cr, Co, and Ni	Phytofiltration	Abuzaid et al. (2021)
Helichrysum arenarium	Phytoremediation ability	Au and Ag	Phytoextraction, phytostabilization, and phytoremediation	Vural and Safari (2022)
Oryza sativa	Phytoremediation ability	2,4-dibromophenol (2,4-DBP) and 2,4-dibromoanisole (2,4-DBA)	Phytovolatilization	Zhang et al. (2020)
Cajanus cajan	Legume (N_2-fixation) and phytoremediation ability	Petroleum Oily Sludge	Rhizodegradation	Allamin et al. (2020)
Sorghum x *drummondii*	Bioenergy crop and phytoremediation ability	Polycyclic aromatic hydrocarbons	Rhizodegradation	Dominguez et al. (2020)
Daucus carota L.	Vegetable and phytoremediation ability	2,2′,4, 4′-tetrabrominated diphenyl ether	Rhizodegradation	Xiang et al. (2018)
Ipomoea aquatica, *Alternanthera philoxeroides*, and *Ludwigia adscendens*	Vegetable, fodder, and phytoremediation ability	Sodium	Phytodesalination	Islam et al. (2019)
Puccinellia nuttalliana and *Typha latifolia*	Phytoremediation ability	Landfill leachate	Phytodesalination	Xu et al. (2019)
Triticum aestivum and *Chenopodium quinoa*	Salinity tolerant and phytoremediation ability	Ca, Mg, Na, K, and Cl	Phytodesalination	Hoseini et al. (2022)

2.3 Factors limiting plant growth and phytoremediation potential

Phytoremediation is a potential method for removing contaminants from soil, but it has several drawbacks. Decontamination using plants is a time-consuming process due to its complete dependence upon the type and amount of particular contaminants in soil and the plant variety. The majority of plants with phytoremediation potential are slow growing and have lower biomass, limiting their efficacy. Some pollutants are found in soil in a very tightly bound state, limiting their bioavailability and making mobilization difficult. Because plants are not tolerant to extremely high levels of pollutants, phytoremediation is only successful in low-to- moderately contaminated soil/water. Moreover, other soil properties like pH, clay content, and organic matter also limit phytoremediation efficiency (Jaskulak et al., 2020). Effective phytoremediation also necessitates favorable weather and climatic conditions for plants. Storage, handling, and correct disposal of metal-derived phyto-biomass are also difficult due to the constraints mentioned above. Compaction and composting of phyto-biomass reduce bulk and transportation costs while increasing dissolved metal-organic compound leaching. As a result, a key concern with phytoremediation is the long-term disposal of phyto-biomass (Shah and Daverey, 2020). Because plant roots can only uptake contaminants in their immediate proximity and cannot reach deep layers of soil, phytoremediation has a major drawback: It only removes a fraction of the contaminants from the soil. Furthermore, soil may contain many contaminants at the same time, and the plants used to remediate the soil may not be tolerant or hyperaccumulators for all of the chemicals, rendering the process less effective (Pathak et al., 2020).

These challenges can be overcome by increasing the phytoremediation potential of plants by using various breeding techniques to improve their stress tolerance. Plants contain many genes responsible for stress tolerance to metals and are involved in the uptake and transport of these metals. Breeding techniques transfer these genes to increase the potential of plants to thrive under metal stress conditions. Using these techniques, many resistant varieties have been bred such as Parang 401 (Fe chlorosis resistant rice), BRRI-29, BR-26, and BR-14 (As tolerant commercial rice), Pirsabak 2004 (Pb tolerant wheat variety), Micro-Tom (Cd tolerant tomato), and Strongfield (Cd tolerant wheat variety). It has also been reported that complementary interaction of different groups of non-allelic genes provides stress tolerance. In rice, the complementary interaction of two groups of non-allelic genes (Ic1 and Ic2; Ic3 and Ic4) is responsible for Fe uptake. Ic1 is complementary with Ic3 and Ic2 with Ic4 and shows tolerance to Fe chlorosis (Elango et al., 2022). Overexpression of these genes may also contribute to increasing the phytoremediation efficiency of various plants. Heavy metal ATPases such as HMA3 and HMA4 are also responsible for the accumulation and tolerance of Zn and Cd. Overexpression of heavy metal ATPase 3 (TcHMA3) in *Noccaea caerulea* improved tolerance to Zn and Cd (Sorour et al., 2022).

Another alternative to overcome these challenges is the use of different additives that can help to increase the phytoremediation efficiency of different plants. In one study, different organic fertilizers, including leonardite, bone meal, vermicompost, chicken manure, and bat manure, were employed individually and in combination to test their inoculation effect on phytoremediation efficiency of *Acacia mangium*, *Jatropha curcas*, and *Manihot esculenta*. *Acacia mangium* and *Manihot esculenta* reportedly grew better when treated with bone meal and bat dung and with leonardite and bat dung amendments, respectively, while *Jatropha curcas* reportedly grew better when treated with bone meal, which improved the phytoremediation properties of Cd (Taeprayoon et al., 2022). Biochar can immobilize heavy metals and, therefore, can be used to remediate contaminated soil. Under non-flooded conditions, bamboo biochar boosted Cd and Zn transport from roots to aboveground parts by 68.85% and 102.27%, respectively, compared to no BBC amendment (Li et al., 2022). The use of multi-stress tolerant PGPB with high bioremediation ability against various contaminants in combination with different plants can also be explored.

3 PGPB and their role in mitigating abiotic stresses

Agricultural productivity is affected by various environmental stress factors, which are divided into abiotic and biotic stresses. Abiotic stress contributes to a 50% loss in productivity and biotic stress to 30% (Kumar and Verma, 2018). Salinity, drought, flooding, HM contamination, extreme temperatures, and pH are major abiotic stress factors. PGPBs are well-known for their ability to mitigate the negative effects of stress on plants by influencing processes related to their stress response. In the natural environment, plants coexist with various microorganisms (microbiota), belonging to different domains and kingdoms: Archaea, bacteria, fungi, other eukaryotes, and viruses. The rhizosphere provides nutrients and ecological niches for the growth of microbiota, while microorganisms (PGPB) provide beneficial compounds, including phytohormones, which defend plants from diseases and pathogens (Schirawski and Perlin, 2018; Singh et al., 2019; Poria et al., 2021a). The application of PGPB formulations is beneficial for plant development and a way to transform damaged and uncultivable land into healthy soil (Gouda et al., 2018).

3.1 PGPB as a salinity tolerant agent

It is estimated that up to 33% of total agricultural land worldwide is salinized (Otlewska et al., 2020). The main mechanism which contributes to salinity tolerance in plants is the translocation of sodium to vacuoles, thus reducing the amount of sodium in the cytoplasm. Research shows that PGPB treatment is associated with increased expression of genes encoding the Salt Overly Sensitive 1 (SOS1) exchanger located in the plasma membrane and other genes connected with the SOS pathway. The main consequence of salinity stress is the increase in the production of phytohormones such as abscisic acid, salicylic acid, and ethylene, which are responsible for activating the signaling cascade of various genes that are involved in enhancing salt tolerance (Ramakrishna et al., 2020). Studies suggest that soil inoculation with specific PGPB strains (*Bacillus aryabhattai* H19-1 and *B. mesonae* H20-5) is linked to increased antioxidant enzyme activity, metabolism of abscisic acid, and proline accumulation, under salinity stress (Sung-Je et al., 2019).

Production of ACC deaminase by PGPB is the best-studied mechanism that contributes to salinity tolerance in plants. Ali et al. (2014) observed that in the presence of PGPB *Pseudomonas* spp., tomato plants under 165 mM of salt stress have shown a 2.5- to 3.5-fold increase in dry weight compared to uninoculated controls and treatments inoculated with *Pseudomonas* spp. mutants that were deficient in ACC deaminase. Another important mechanism to combat salinity stress is the production of exopolysaccharides (EPS) and biofilm formation. Inoculation of chickpea with *Halomonas variabilis* HT1 and *Planococcus rifietoensis* RT4 strains improved fresh weight by 153% and 177%, respectively, under a NaCl concentration of 100 mM (Qurashi and Sabri, 2012).

3.2 PGPB as a HM-tolerant agent

Approximately 20 Mha of land around the globe is affected by HM contamination (Liu et al., 2018). HMs occur naturally in the Earth's crust, and their overuse in industrial production has resulted in the contamination of large areas of land (Liu et al., 2018). In plants and other biological organisms, contact with HMs can affect components of cellular organelles and important enzymes. PGPB can mitigate the effects of exposure to HMs in plants and increase biomass production (Tchounwou et al., 2012; Ma et al., 2016b). The HM-polluted environment can be restored for crop production by either eliminating it or converting it to a non-bioavailable form (Tak et al., 2013).

Microbial populations exposed to HMs develop the resistance for these HMs to survive. These PGPB may become tolerant to HMs due to their biological properties or use direct detoxification and, therefore, become resistant (Ledin, 2000). Such mechanisms developed by PGPB include metal-protein complex formation, biotransformation, methylation, and demethylation (Tak et al., 2013). For instance, *Bacillus thuringiensis* strain GDB - 1 enhanced the metal removal activities of *Alnus firma* by acting on Pb, Zn, As, Cd, Cu, and Ni or reducing their toxicity by accumulating those metals in the seedlings of *Alnus firma* (Babu et al., 2013). Another study showed that maize inoculated with *Proteus mirabilis* T2Cr and CrP450 reduced Cr toxicity and increased Cr tolerance. It was found that the fresh weight in maize increased by 114% compared to the uninoculated control (Islam et al., 2016). In one study, the metal tolerant PGPR *Pseudomonas* and *Bacillus* increased the hyperaccumulation capacity of *Helianthus annuus* L. and caused a 1.7–2.5-fold accumulation of Zn and Cd in *Helianthus annuus* L. shoots (Sorour et al., 2022). The uptake, localization, intracellular transport, and efflux of Zn are regulated by Zn-related transporters, which include the yellow stripe-like (YSL) transporter, the copper transporter (COPT/Ctr), the P1B-type heavy metal ATPase (HMA), the cation efflux (CE) transporter, the Zn- and Fe-regulated transporter-like protein (ZIP), and the Zn-induced facilitator1 (ZIF1) transporter family. ZNTs are zinc-resistant transporters and iron-resistant transporter-like protein (ZIP) family micronutrient transporters. These transporters can be targeted for improving the resistance of plants against heavy metals. Similarly, Arbuscular mycorrhiza fungi (AMF) increased the resistance of *E. grandis* to high-Zn stress by improving nutrient uptake and regulating Zn uptake at the gene transcription level. With AMF symbiosis under high-Zn conditions, 10 genes (ZNT:4, COPT/Ctr:2, YSL:3, CE:1) were upregulated, while 19 genes (ZNT:9, COPT/Ctr:2, YSL:3, ZIFL:4, CE:1) were downregulated (Wang et al., 2022).

3.3 PGPB as a drought-tolerant agent

Drought affects more than 160 Mha of rain-fed land used to grow cereals and legumes. Moreover, due to climate change, water deficiency will affect even more lands, as global warming is projected to increase by around 0.2 to 0.5 each decade in Asian regions and by up to 1.6 in South Africa (Berger et al., 2016).

Drought triggers a signaling pathway that accumulates reactive oxygen species (ROS) in plants, which can damage cell membranes, proteins, and DNA in the absence of detoxification mechanisms (Saikia et al., 2018; Yang and Guo, 2018). These mechanisms may be enzymatic involving enzymes such as catalase (CAT), peroxidase (POD), and superoxide dismutase (SOD), or non-enzymatic, relying on antioxidant compounds such as polyphenols and ascorbic acid (Tiepo et al., 2020). Inoculation with PGPB also enhances the antioxidant response of plants. For instance, inoculation of *Urochloa ruziziensis* leaves with *Azosprillum brasilense* increased the content of CAT and POD in plant tissues, which may have contributed to increased drought tolerance (Bulegon

et al., 2016). PGPB can also help the plant endure drought stress by secreting exopolysaccharides (Sun et al., 2020) and by ACC deaminase synthesis. In one study, a consortium of three PGPB strains was shown to improve chlorophyll content in drought-stressed black gram plants by more than 100% and garden pea plants by up to 280% (Saikia et al., 2018).

4 PGPB's role in phytoremediation

Phytoremediation is one of the few universal methods that can be used to treat almost all types of marginal land due to the diversity and high remedial ability of different plants (Thijs et al., 2017). However, in some marginal lands, especially with highly toxic contaminants, or other stressed environments, the efficiency of phytoremediation may be lower. One way to improve the effectiveness of phytoremediation is by the employment of microorganisms which can support the growth of plants under such stressed environments and contribute to the mobility of contaminants in soil (Yan et al., 2020). Soil bioaugmentation with an exogenous/endogenous pool of microbes or stimulations of the activities of autochthonic microbiota, which can establish beneficial relationships with plants, can improve the phytoremediation abilities of these plants (Baneshi et al., 2014; Ferrarini et al., 2021; Rabani et al., 2022). The role of different PGPBs in the phytoremediation of several contaminants is illustrated in Table 2.

4.1 PGPB enhanced plant growth on marginal land under HM contamination conditions

The microbial enhancement of the phytoremediation of marginal soils contaminated with HMs may be the result of (i) promoting the growth of plants (Saleem et al., 2019; Debiec-Andrzejewska et al., 2020; Zainab et al., 2021), (ii) increasing plant tolerance against the metal's toxicity (Khan and Bano, 2018), (iii) increasing the solubility and mobility of HMs (Ferrarini et al., 2021), or (iv) biotransformation of metals to less toxic chemical compounds (Karthik et al., 2017; Debiec-Andrzejewska et al., 2020). Most PGPBs are characterized by more than one plant growth-promoting property; thus, enhancement in the phytoremediation efficiency of HM-contaminated areas is usually complex and is a result of the synergistic effect of various plant-beneficial properties of bacteria (Ahemad, 2015; Sansinenea, 2019; Debiec-Andrzejewska et al., 2020).

Various phytoremediation strategies are used depending on many factors, such as (i) type of HM contamination (one or many metals), (ii) its concentrations, as well as the (iii) availability of plants and microbes species in the contaminated areas (Ullah et al., 2015). Phytoextraction is a commonly used method for HM-contaminated environments. The efficiency of phytoextraction in highly contaminated areas depends largely on the presence of plants and bacteria with high resistance to HMs (Girolkar et al., 2021). PGPBs seem to be highly beneficial for the phytoextraction process since their presence contributes to the additional increase of plant tolerance to HMs. For example, three bacterial strains resistant to Cu, *Burkholderia cepacia* J62, *Pseudomonas thivervalensis* Y1-3-9, and *Microbacterium oxydans* JYC17, contributed significantly to an increase in the biomass of *Brassica napus* L. and the Cu enrichment in the above-ground part by up to 63.4%, 55.3%, and 63.4%, respectively, compared to uninoculated soil (Ren et al., 2019). In other studies, endophytic and Cd resistance *Pseudomonas fluorescens* Sasm05 promoted the growth of *Sedum alfredi* and significantly increased their ability to accumulate Cd by increasing production of IAA and by the upregulation of the gene expression responsible for the uptake and transport of Cd by plants (Chen et al., 2017a; Wu et al., 2020a). The IAA production by metal-resistant *Pseudomonas libanensis* TR1 and *Pseudomonas reactans* Ph3R3 enhanced plant growth and Cu and Zn accumulation by *Brassica oxyrrhina* under HMs and drought stress (Ma et al., 2016b). Lead-tolerant *Bacillus altitudinis* KP14 enhanced the biomass of *Miscanthus* x *giganteus* (MxG) by up to 77%, due to its ability to solubilize phosphorus and produce IAA, ACC deaminases, ammonia, siderophores, and hydrogen cyanide, as well as its high antifungal activity (Pranaw et al., 2020).

The role of microorganisms in phytoextraction was also confirmed in the case of Ni (Ma et al., 2011; Durand et al., 2016; Chen et al., 2017b), Pb (He et al., 2020; Konkolewska et al., 2020), Cd (He et al., 2020), Mn (Huang et al., 2020; Li et al., 2020), Cr (Ahemad, 2015), and As (Debiec-Andrzejewska et al., 2020). Soil bioaugmentation with nickel-resistant bacterium *Psychrobacter* sp. SRS8 resulted in significant growth promotion of *R. communis* and *H. annuus* and doubled nickel phytoextraction efficiency (Ma et al., 2010). PGPB activity increased Ni bioaccumulation in plant tissues by improving their Ni resistance (Chen et al., 2017b). The improved *Solanum nigrum* growth along with greater tolerance to Pb and Cd stress was observed after inoculation with *Bacillus* sp. QX8 and QX13 (He et al., 2020). Similarly, the inoculation of *Bacillus cereus* HM5 and *B. thuringiensis* HM7 increased the absorption of Mn by *B. papyrifera* by promoting plant root function maintenance and by reducing oxidative stress (Huang et al., 2020). Phytoextraction may also be facilitated by HM stress mitigation for plants by the activity of PGPB (Ahemad, 2015). This mechanism was confirmed in the case of Cr soil contamination (by the microbial Cr(IV)-reducing potential) (Ahemad, 2015) and As (microbial As(III)-oxidizing potential) (Debiec-Andrzejewska et al., 2020).

The choice of HM phytoremediation strategy also depends on the ability of plants to translocate the metal from roots to aboveground parts of plants. This is the so-called translocation

TABLE 2 Depiction of PGPB role in phytoremediation of different pollutants.

Plant name	PGPB	Role of PGPB	Contaminant removed	Reference
Medicago sativa	Co-inoculation of *Paenibacillus mucilaginosus* and Cu resistant rhizobia *Sinorhizobium meliloti*	Increased the phytostabilization of Cu and prevented toxic metals from entering the food chain, increased shoot and root biomass, increased total nitrogen, available potassium, and soil organic matter content, microbial community structure, and increased soil enzymatic activity.	Cu	Ju et al. (2020)
Robinia pseudoacacia L.	*Enterobacter* sp. YG-14 combined with sludge biochar	Increased Cd stabilization through chelation, increased shoot and root biomass, and biochar amendment increased the survivability of PBPB in harsh environments.	Cd	Zhang et al. (2021)
Corn	*Pseudomonas putida* in combination with EDTA	Microbial inoculation increased phytostabilization efficiency.	Cd, Pb, and Zn	Hamidpour et al. (2020)
Helianthus petiolaris	*Bacillus* spp.	Increased shoot biomass and lowered HM uptake.	Pb, Cd	Saran et al. (2020b)
Zea mays	*Providencia* sp. and *Proteus mirabilis*	Reduced Cr accumulation in the shoot by reducing Cr translocation from root to shoot.	Cr	Vishnupradeep et al. (2022)
Ryegrass	*Bacillus* spp.	Immobilized Cu and Cd, phosphate solubilization, IAA production, increased root and shoot biomass of plant, and increased stressed mitigation ability.	Cu and Cd	Ke et al. (2021a)
Lolium perenne	*Rhodococcus erythropolis Rhizobium* sp.	Increased effectiveness of photodegradation through enzyme secretion.	Petroleum Hydrocarbons	Pawlik et al. (2020)
Phragmites australis	*Acinetobacter*	Increased plant growth and pyridine degradation.	Pyridine	Karaghool (2022)
Celosia argentea	*Bacillus megaterium*	PGPB increased the shoot biomass significantly and increased the shoot Cd extraction amount. It enhanced phytoextraction as well as increased soil enzyme activities of the contaminated soil.	Cd	Yu et al. (2020)
Triticum aestivum L.	*Streptomyces pactum*	Increased metal uptake, increased wheat growth, decreased soil pH, and/or increased metal chelation and production of indole acetic acid and siderophores, decreased antioxidant activity and lipid peroxidation in wheat.	Cd, Cu, and Zn	Ali et al. (2021)
Lolium perenne L.	*Bacillus* spp.	Increased biomass yield, phytoextraction efficiency, and Cu extraction efficiency. Increased soil Cu bioavailability by secreting siderophores and organic acid.	Cu	Ke et al. (2021b)
Glycine max L.	*Kocuria rhizophila*	Enhanced plant biomass by about 38.73% and the accumulation of Cd, Cr, Cu, and Ni.	Cd, Cr, Cu and Ni	Hussain et al. (2019)
Jatropha curcas	*Bacillus cereus*	Enhanced metal mobilizing activity and increased plant growth by different PGP activities, such as nitrogen fixation, phosphate solubilization, etc.	Bauxite waste	Narayanan et al. (2021)
Medicago sativa L.	*Bacillus subtilis*	PGPB decreased malondialdehyde (MDA) amount and improved activities of plant antioxidant enzymes which led to increased plant biomass. Inoculation also increased Cd bioavailability and Cd removal efficiency.	Cd	Li et al. (2021)
Arundo donax L.	*Stenotrophomonas maltophilia* and *Agrobacterium* sp.	Leaf and stem biomass increased. The bioaccumulation factor doubled in the presence of PGPB.	As	Guarino et al. (2020)
Tagetes erecta L.	*Klebsiella pneumoniae*	Improved plant growth and increased root length, dry root weight, shoot length, and dry shoot weight in the presence of PGPB. Enhanced relative abundance of Firmicutes and Acidobacteria in the presence of PGPB.	Pyrene	Rajkumari et al. (2021)
Melia azedarach	*Serratia marcescens* S2I7	Rhizodegradation increased in the presence of PGPB. PBPB enhanced plant growth.	Benzo (A) pyrene and Cd	Kotoky and Pandey (2020a)
Zea Mays L.	*Piriformospora Indica*	PGPB enhanced the degradation of petroleum hydrocarbons in the root zone and increased root and shoot biomass.	Petroleum	Zamani et al. (2018)
Melia azedarach	*Bacillus flexus Paenibacillus* sp.	Rhizodegradation increased in the presence of PGPB	Benzo (A) pyrene	Kotoky and Pandey (2020b)
Lepironia articulata	*Pseudomonas toyotomiensis Microbacterium resistens Bacillus pumilus*	Enhanced removal of Polycyclic aromatic hydrocarbons.	Polycyclic aromatic hydrocarbons	Al Sbani et al. (2021)

factor (TF). Plants species with a TF above 1 are considered a good candidate for phytoextraction, but plants characterized with a TF below 1 are considered appropriate phytostabilizors (Ma et al., 2015). Phytostabilization is usually applied when the HM concentration in soil is relatively low and their potential release to other environments does not present too much risk. This phytoremediation method was used for the stabilization of Zn by *Brassica juncea* and *Ricinus communis* inoculated with *Psychrobacter* sp. SRS8 and *Pseudomonas* sp. A3R3 (Ma et al., 2015). Surprisingly, Fe and Ni in these plants-microbial

partnerships were phytoextracted too. Another study revealed that Cd and Zn rhizoaccumulation by *Sedum plumbizincicola* enhanced by E6S strain homologous to *Achromobacter piechaudii* (Ma et al., 2016c). The main mechanism of the microbial enhancement of phytostabilization is the reduced solubility and/or mobility of HMs both in the soil and inside plants. Among these processes are adsorption, biosorption, bioaccumulation, biotransformation, (bio)precipitation and complexation of HMs, and alkalization of soil (Manoj et al., 2020). The key role in adsorption is played by anionic-charged EPS and extracellular membrane functional groups, which can adsorb cationic-charged metals (Wang et al., 2010; Karthik et al., 2017). Biosorption and bioaccumulation processes are directly correlated with passive or active transport to microbial cells, and after that, metals are intracellularly immobilized by precipitation, accumulation, sequestration, and/or transformation (Ma et al., 2016a). Microbes are also able to biotransform HMs, thus decreasing their mobility and bioavailability.

The last commonly used method for the phytoremediation of HM-contaminated lands is phytovolatilization. This method is used in the case of HMs that can be biotransformed to less toxic volatile compounds. Phytovolatilization is, therefore, mainly used to treat lands contaminated with As, Se, and Hg, and the efficiency of this method may be also strengthened by the activity of PGPB. Plant-beneficial strains *Stenotrophomonas maltophilia* and *Agrobacterium* sp. were useful in effective phytovolatilization of As during the investigation of phytoremediation technology with the use of *Arundo donax* L (Yan et al., 2020). The mechanism for As phytovolatilization depends on the As-speciation in soil, but generally, it relies on the intracellular reduction of As(V) to As(III) by plants, the addition of methyl groups to As(III), and then further reduction of the methylated form of As (Chen et al., 2017c). Assisting microorganisms in this process relies on an increase in the As uptake efficiency from the soil, which causes more As to phytovolatilize (Guarino et al., 2020). Microbial enhancement of phytovolatilization was also confirmed in the case of Se contamination. Phytovolatilization relies on the transformation of toxic Se (as selenate) to the less toxic dimethyl selenide gas (Pivetz, 2001). An example of the enhanced Se phytovolatilization was the activity of environmental isolates BJ2 and BJ15, which supported the uptake and evaporation of selenium by *Brassica juncea* L. It was shown that bacteria contributed to the high efficiency of volatilization and accumulation of Se in plant tissues, which were enhanced by 35% and 70%, respectively (De Souza et al., 1999). The microbial enhancement of Hg phytovolatilization efficiency is based on decreasing the toxicity of this element by reduction of organomercurials to Hg(II) (Matsui et al., 2016) or Hg(II) to less toxic and volatile Hg(0) (Silver and Hobman, 2007). *Zea mays* inoculation by endophytic bacteria *Serratia marcescens* BacI56 and *Pseudomonas* sp. BacI38 increased Hg volatilization by 47.16% and 62.42%, respectively (Mello et al., 2020). Despite the confirmed cases of microbial-assisted Hg phytovolatilization, knowledge about molecular and physiological aspects of this mechanism is still poor (Tiodar et al., 2021).

4.2 PGPB-enhanced plant growth on marginal land with high salinity

Marginal land can have high salt concentration due to a variety of reasons, and sources of this high salinity can be natural resulting from (i) salt accumulation over a long time, (ii) weathering of rocks and minerals that release soluble salts including chloride, sulfates, and carbonates of sodium, calcium, and magnesium, or (iii) deposition of oceanic salt carried by wind and rain (Mukhopadhyay and Maiti, 2010). Anthropogenic sources are the result of the (i) replacement of perennial vegetation with annual crops, (ii) inappropriate fertilization or soil irrigation with salt-rich water, or (iii) insufficient drainage systems (Mukhopadhyay and Maiti, 2010). High salinity in soil contributes to ion imbalance and hyperosmotic pressure, leading to oxidative stress in plants (Heydarian et al., 2016). High salt concentrations may also decrease the availability of essential nutrients in the soil which leads to a reduced uptake of some nutrients by the plants (Pankaj et al., 2019). High salinity environments have been shown to elevate ethylene concentration, which is a typical reaction of plants under stress conditions (Heydarian et al., 2016). PGPB helps plants to alleviate salinity stress in marginal lands by reducing ethylene precursors through the production of ACC-deaminase (Ali et al., 2014; Sofy et al., 2021) and the production of biofilms covering the surface of the roots, limiting the physical contact of roots with contaminants (Kasim et al., 2016). PGPB also increases water use efficiency by transpiration regulation, stomatal conductance, and reduction of reactive oxygen species concentrations in inoculated plants (Amaresan et al., 2020).

Application of ACC deaminase-producing *Pseudomonas* spp. on barley and oat for phytoremediation of marginal lands with high salinity resulted in promotion of the growth of barley and oats roots in saline soil by 200% and 50%, respectively, and contributed to an increase in the shoot's biomass by 100%–150%. This significantly increased plant biomass was able to accumulate higher amounts of salt (Chang et al., 2014). Similarly, *Pseudomonas putida* KT2440 and *Novosphingobium* sp. HR1a promoted the growth of *Citrus macrophylla*. The strain HR1a contributed to increased accumulation of IAA in leaves, while the strain KT2440 inhibited root chloride and proline accumulation under salt stress (Vives-Peris et al., 2020). Spinach (*Spinacia oleracea* L) inoculated with halotolerant (*Pseudomonas* sp., *Thalassobacillus* sp., and *Terribacillus* sp.) and chitinolytic (*Pseudomonas* spp., *Sanguibacter* spp., *Bacillus* spp.) bacterial strains with high antifungal activity resulted in better plant growth and reduced salinity (Anees et al., 2020).

4.3 PGPB enhanced plant growth on marginal lands contaminated with organic compounds

Due to the strong hydrophobic characteristics of many organic contaminants, phytoextraction efficiency is usually lower than that of phytodegradation or phytostimulation (Schwitzguébel, 2017). Bacteria use the metabolites secreted by the plant as carbon sources to stimulate their biodegradation ability, which, in turn, reduces the stress effect of the contaminant and promotes the growth and development of plants (Girolkar et al., 2021).

Among PGPB useful in phytostimulation are highly resistant microbes to hydrocarbons, which can degrade organic contaminants aerobically. Particularly desirable are strains capable of degrading crude oil hydrocarbon, the most pervasive class of environmental organic contaminants worldwide (Ławniczak et al., 2020). The source of PGPB in phytostimulation methods is usually autochthonic microbiota, whose activity is stimulated by plants. Soil bioaugmentation with an exogenous pool of microorganisms as well as combined methods is also applied (Schwitzguébel, 2017; Girolkar et al., 2021).

Acinetobacter, *Alcanivorax*, *Bacillus*, *Corynebacterium*, *Gordonia*, *Hahella*, *Immundisolibacter*, *Luteimonas*, *Marinobacter*, *Mycobacterium*, *Ochrobactrum*, *Pseudomonas*, *Rhodococcus*, and *Sphingomonas* are some of the reported genera capable of degrading organic pollutants effectively (Kukla et al., 2014; Oliveira et al., 2014; Fatima et al., 2015; Pawlik et al., 2017). Despite the high diversity of these strains, the rhizosphere microorganisms are regarded as the most effective in hydrocarbon degradation (Ruley et al., 2020). Biosurfactant production by these bacterial strains helps in increasing the bioavailability of petroleum compounds, which plays an important role in biodegradation (Ławniczak et al., 2020).

The positive effect of PGPB was observed in the phytoremediation of Ni-pyrene-contaminated soil with the use of *Scripus triqueter* (Chen et al., 2017b). Although PGPB presence decreased the plant's biomass, their activity facilitated the increase in the plant's resistance to pyrene and promotion of pyrene degradation (Chen et al., 2017b). High efficiency of the phytostimulation was achieved in crude petroleum oil-contaminated soil with the use of *Bassia scoparia* supported by associated rhizosphere microorganisms (Moubasher et al., 2015). A similar effect of PGPB was observed in the case of petroleum hydrocarbon degradation by Italian ryegrass (Hussain et al., 2018), petroleum oily sludge phytoremediation with the use of legumes plant *Cajanus cajan*, and rhizospheric microorganisms (Allamin et al., 2020), and diesel contaminant degradation by *Zea mays* L. supported by alkane-degrading bacterial strains (Ummara et al., 2021).

Phytostimulation may also be used as an additional strategy for the remediation of organic compounds on contaminated lands. For example, in the polychlorinated biphenyl (PCB) removal by switchgrass (*Panicum virgatum*), phytostimulation with the use of plant-beneficial bacteria *Burkholderia xenovorans* LB400 was an additional strategy to the main treatment mechanism – phytoextraction. In this case, a quite effective translocation of PCB was confirmed, but enhanced microbial activity in the rhizosphere was also observed (Liang et al., 2014).

Numerous biotechnological strategies that promote plant tolerance and metal accumulation, such as the modification of HM transporter genes and their uptake systems, along with the improvement of HM ligand production, can also be used to improve phytoremediation (Bhat et al., 2022). Overexpression of HM transporter gene in *Arabidopsis thaliana* (YCF1 gene) improved tolerance to and accumulation of Pb and Cd. Similarly, transgenic plants that overexpressed the *Nicotiana tabacum* NtCBP4 protein displayed enhanced Pb hypersensitivity and accumulation. HM-binding ligands, phytochelatins, glutathione, and cystine-rich peptides, such as metallothioneins, are utilized for HM detoxification. In peas, due to the overexpression of the metallothioneins gene PsMTA, significant Cu buildup in roots was detected. Similarly, transgenic *Brassica juncea* with overexpression of *E. coli* GSH synthetase gene showed improved Cd tolerance (Bhat et al., 2022).

5 Economic perspectives of bioremediation and marginal land utilization for biomass production

The global bioremediation market was valued at USD 105.68 billion in 2019 and is expected to grow at a compound annual growth rate (CAGR) of 15.5% to reach USD 334.70 billion by 2027. In light of contemporary green technologies to improve waste management, awareness of bioremediation is growing. Due to their affordability and ease of use, microbiological counterparts to bioremediation are being utilized more frequently than other environmentally friendly techniques. Growing urbanization causes land to become marginalized, or less suited for agricultural, in many regions of industrialized and developing countries. The phytoremediation segment held the majority of the market share in 2019. Plants are extensively used to kickstart the process and are driving the growth of the segment. In terms of market share, North America accounted for approximately 41.8% of the global bioremediation market in 2019. The global microbial bioremediation market is quite fragmented, with a few large and medium-sized market players accounting for most of the revenue. The major players are implementing a variety of strategies, including mergers and acquisitions, strategic agreements and contracts, and the

development, testing, and deployment of more effective microbial bioremediation systems. As governments across the globe are trying to attempt to focus on environmental protection, the market for bioremediation technology and services is expected to grow significantly during the forecast period. The bioremediation market is expected to reach new heights by 2030. This is due to the above-mentioned factors as well as the tremendous growth in research and development activities throughout the world (Emergen Research, 2022).

The global microbial bioremediation market is segmented into bacteria, fungi, and archaea. Bacteria are the most used organisms in the bioremediation process. Table 3 shows the United States Environmental Protection Agency's national contingency plan for planned bioremediation products (EPA, 2022).

Another economic aspect of bioremediation is the use of contaminated soil for the production of industrially important raw materials such as biomass while carrying out remediation. Global economic growth and industrialization require a continuous supply of energy, which dramatically decreases natural energy resources. Therefore, an intense search for alternative and renewable energy sources to meet the demands of an ever-evolving world is underway (Mehmood et al., 2017). The latest estimates show that about 19% of global energy demand is met by renewable sources, of which biomass accounts for 9.3% (Edrisi and Abhilash, 2016). Among the renewable energy sources currently available, plant biomass is regarded as one of the most promising (Mehmood et al., 2017). In comparison to fossil fuels, the primary benefit of biomass as an energy source is its beneficial effect on the global CO_2 balance in the atmosphere, since more CO_2 is absorbed by plants during photosynthesis than is emitted to the atmosphere during biofuel combustion (Baumgarten et al., 2017). Bioenergy derived from a plant's biomass also has a considerable influence on the

TABLE 3 Commercial microbial inoculants (culture formulation) for bioremediation in soil.

Tradename	Manufacturer	Product form	Application method	Type of contamination	Shelf life
BET BIOPETRO	BioEnviro Tech	Powder	–	Heavy refined and crude hydrocarbon contaminants	More than 3 years
BIOREM-2000 OIL DIGESTER™	Clift Industries, Inc., Charlotte, US	–	Spray	Oil	2 years
BioWorld BHTP	BioWorld USA, Inc., US	Liquid or dry form	Directly into the soil or mix with water before use	Hydrocarbons	Max 3 years
DRYLET™ MB BIOREMEDIATION	DryLet, LLC, Houston, US	–	Applied by the usual methods of aerial or manual broadcast spreading	Oil	Min 5 years
DUALZORB®	LBI Renewable, Buffalo, US	Dehydrated product	Applied by hand, mechanical spreaders, portable mixer or blown onto a surface using an air conveyor	Hydrocarbons	5 years
ERGOFIT MICROMIX AQUA	Evadine Technologies, LLC, New Braunfels, US	Liquid	Spray	Hydrocarbons	5 years
MICRO-BLAZE EMERGENCY LIQUID SPILL CONTROL	Verde Environmental, Inc., Houston, US	Liquid formulation	Spray	Organics and hydrocarbons in soil and water as well as control odors	Min 10 years
MUNOX SR®	Osprey Biotechnics, Sarasota, US	Stabilized liquid form or after the freeze-dried form is hydrated	Spray	Fresh and weathered crude oil and refined products	1 year
OPPENHEIMER FORMULA (The OPPENHEIMER FORMULA I, MICROSORB SC)	Oppenheimer Biotechnology, Inc., Pflugerville, US	Powder seeding	Spray	Oil	5 years
SOIL RX	3 Tier Technologies LLC Worldwide Headquarters, Stanford, US	Liquid	Sprayed after dilution	Organics and hydrocarbons	2 years
STEP ONE	B & S Research, Inc., Embarrass, US	–	Spray	Most hydrocarbons, including crude and refined petroleum products, pesticides	Over 3 years
SYSTEM E.T. 20	Environmental Restoration Services, Windsor, US	–	–	Broad range of hydrocarbon compounds	2 years
WMI-2000	WMI International, Inc., Houston, US	–	Spray	–	2 years

mitigation of various environmental problems; e.g., high-yielding plants may be used for the phytoremediation of contaminated soils. Thus, bioenergy plant cultures may constitute an additional possibility for marginal land restoration (Edrisi and Abhilash, 2016).

The availability of land for biofuel production is limited (arable lands cannot be considered due to the high demand for food production). More and more frequently, the utilization of marginal and degraded lands is a viable solution to meet the energy needs of the people (Pancaldi and Trindade, 2020). The total world surface area of marginal lands is estimated at 13.1 Gha, of which 152 Mha (14% of the total marginal land area in the world) are available only in China. It is also estimate, that out of this 152 Mha, 60% may be utilized for bioenergy crop plantation. The current bioenergy potential of plants growing on marginal lands may range from 30 to 1000 Exa-Joule (EJ; 1 EJ=1018 J) of primary energy per year (Haberl et al., 2010). Considering the imperatives of sustainable economic development, it is estimated that the bio-energy potential by 2050 will be in the range of 130 - 270 EJ per year (Hoogwijk et al., 2009).

Several bioenergy crops are characterized by having high resistance to stressful environmental conditions and achieving high biomass in poor soils without special fertilization or other agricultural inputs (Hood, 2016). The most promising energy crop is *Miscanthus* species, which is regarded as a second-generation biofuel plant capable of producing high amounts of biomass due to effective photosynthesis and high water and nutrient usage efficiencies (Lewandowski et al., 2019; Pidlisnyuk et al., 2020). Plants such as *Agave* spp., *Cynara cardunculus* (cardoon), *Panicum virgatum* L. (switchgrass), *Phalaris arundinacea* L. (reed canarygrass), *Sida hermaphrodita* (sida), *Ulmus pumila* (Siberian elm), *Sorghum bicolor* L. (sweet sorghum), and *Salix* spp. (willow) are also considered good candidates for bioenergy crops (Saballos, 2008; Soldatos, 2015; Mehmood et al., 2017). Some of them are more adaptive to changing environmental conditions, but all of them have shown high potential for effective biomass production (Soldatos, 2015; Mehmood et al., 2017). Table 4 shows some important bioenergy crops and their yields.

Despite the high potential and diversity of bioenergy crops, the cost of cultivation and biofuel production is one of the most important factors in deciding their successful commercialization (Mehmood et al., 2017). Current studies indicate that bioenergy produced from the plant's biomass is still more costly than fossil fuel production; e.g., the cost of cellulosic ethanol is three times higher than the current price of gasoline on an energy equivalent basis (Carriquiry et al., 2011).

Economic analysis showed that the profitability of the cultivation of *Miscanthus* in Europe and the USA depended largely on uncertain assumptions such as environmental factors. Depending on environmental conditions like the amount of rainfall or temperature, *Miscanthus* yield may vary from 10–48 t dry matter per ha. The significant differences in yield have a direct influence on biomass prices, which may vary in the range of 48–134 €/t dry matter, and thus on the price of bioenergy, which increases in direct proportion. Depending on the species and environmental conditions, the lifespan of plants plays an important role in the profitability of *Miscanthus* cultures and is estimated at 10–20 years (Witzel and Finger, 2016).

In terms of cost, biomass production can depend on many factors, including the species of cultivated plants. For example, in the case of switchgrass, the biomass production cost ranged from $40–61 Mg to $53–74 Mg in Tennessee and Oklahoma in the USA, respectively. Furthermore, the target cost for the commercial production of alcohols from biomass was

TABLE 4 Some important bioenergy crops with their yield in contaminated land.

Bioenergy crop	Contaminants removed	Yield	Reference
Helianthus annuus and *Zea mays*	Cr, Cu, Pb, and Cd	84-87% increase in biomass	Iram et al. (2019)
Manihot esculenta	Cu, Pb, and Zn	Fresh tuber yield of 23.13–26.22 t/ha	Shen et al. (2020)
Canola, oat, and wheat	Cd	159.37%, 179.23% and 111.34% increase in biomass	Zhang et al. (2013)
Phragmites australis, *Arundo donax*, and *Piptatherum miliaceum*	Zn, As, Cd, and Pb	Heating values of biomass 16.03–18.75 MJ/Kg	Bernal et al. (2021)
Miscanthus × *giganteus*	Cd and Hg	6.3–13.9 t/ha	Zgorelec et al. (2020)
Brassica napus L.	Cd	109 g/plant	Wu et al. (2020b)
Lantana camara L.	Cd	12.8 g/pot	Liu et al. (2019)
Brassica juncea L.	Cd	14.4 g/pot	Dhaliwal et al. (2020)
Lolium multiflorum Lam	Cd	1656.6 kg/km^2	Hu et al. (2020)
Miscanthus floridulus	Pb	22.4 t/ha	Cheng et al. (2016)
Sorghum bicolor L.	Cd	27.9 t/ha	Xiao et al. (2021)

estimated at US$ 38 Mg. Modeling studies on the commercialization of switchgrass found that the US$ 11–27 Mg expenditure on switchgrass biomass production is justifiable if losses due to sedimentation and soil erosion caused by plant roots are reduced (Mehmood et al., 2017). Another example showed that the cost of the production of biomass in the case of giant reed was up to US$85 per ton, and this species was regarded as the most profitable among two other bioenergy plants, *Miscanthus* and switchgrass (Soldatos, 2015).

There are many barriers to growing energy crops on marginal lands. These include (i) the lack of solid and established markets for trade, (ii) the high cost of crop establishment and uncertainty about crop quality, (iii) unstable prices over the long term (Saballos, 2008; Soldatos, 2015; Mehmood et al., 2017; Pancaldi and Trindade, 2020). Farmers can receive direct or indirect support in the form of subsidies to make the cultivation of energy crops on marginal lands more lucrative in the long run. Unfortunately, the current level of support varies widely across countries and is often insufficient (Mehmood et al., 2017). The cultivation of energy crops on marginal lands to produce alternative fuels is a highly promising option keeping in view the increasing demand for fuel and the decline in arable land. To fully leverage the potential of bioenergy crops, we need to better understand the environmental impact of large-scale production of energy crops using marginal lands worldwide.

Two aspects influence the economics of phytoremediation: application potential and cost compared to traditional treatments (Wan et al., 2016). Using conventional methods involving excavation and filling or ex-situ cleaning of the soil would cost approximately €280,000 and € 680,000 per hectare, respectively, compared with the economic value of phytoremediation of €14,850 and €14,600 per hectare, respectively, as determined by hedonic price analysis and substitution costs. The conventional method generally reduces soil fertility because soil is either landfilled or washed away during the cleaning process (Lewandowski et al., 2006). The plants used for phytoremediation can be used for metal recovery, bioenergy production, packaging materials, and house and furniture construction. However, some phytoremediation techniques are not able to remove the contaminants from soil, such as phytostabilization, and in most of these techniques, the concentration of contaminants in the plant exceeds critical limits so that they can enter the food chain (Parveen et al., 2022). Therefore, contaminants such as HMs can be extracted from plants after remediation using various industrial techniques (phytomining), and high profits can be made due to the costly nature of certain HMs (Riaz et al., 2022).

6 Future research directions

Plants used in bioremediation can provide several benefits, including efficient utilization of polluted biomass to produce various value-added products like pigments, platform chemicals, etc., and energy production through cogeneration. Moreover, metals recovered from plant combustion can be utilized as raw materials in industrial processes. Several future areas of research are waiting to be explored. First is estimating the influence of various contaminants on each other's dynamics and their toxicity to soil microbial populations in the presence of selective plant species such as *Miscanthus* sp. The use of genetically modified plants may provide additional benefits, but their use should be carefully considered on a case-by-case basis and not generalized. Special care should be taken to explore genetically modified bacteria supporting phytoremediation and improving soil health, organic carbon dynamics, and soil biodiversity. This allows the use of plants that previously could not be used in contaminated soils due to their high sensitivity to a particular metal. This is especially important with regard to plants that have other outstanding properties, such as very rapid growth. So far, the impact of climatic change on the dynamics of various contaminants in plants and associated microbial metabolites has been overlooked.

7 Conclusion

Plants and bacteria both provide phytoremediation of hazardous pollutants, but bacteria also protect plants from a variety of stresses (HM toxicity, osmotic stress, salinity stress, etc.) and promote plant growth through numerous PGP processes (hormones and siderophores secretion, mineral solubilization, nitrogen fixation, etc.). Despite decades of research, phytoremediation is still considered a relatively new option because there are few long-term field trials. Microorganisms play an important role in the phytoremediation of soils by directly degrading or biotransforming contaminants and indirectly improving the growth of phytoremediated plants. In particular, the study of bacteria that have evolved to be resistant to high metal/pollutant concentrations and their host linkages can add a new dimension to existing phytoremediation techniques. Soil inoculation with PGPB and metal-solubilizing microbes show a lot of potential for boosting hyperaccumulators' health, biomass yield, and metal accumulation capabilities. Further research is needed on the effectiveness of microbe-assisted phytoremediation under abiotic stresses such as climate change-induced drought and salinity. Furthermore, more research is needed to better understand the interactions between microbes and their host plants in metal-contaminated ecosystems.

Author contributions

Conceptualization, KP. Writing—original draft preparation, VP, KD-A, AF, ML, and NA. Writing—review and editing, KP and SS. Supervision, KP. All authors have read and agreed to the published version of the manuscript.

Funding

This research was funded by the grant from the project "The Fly Ash as the Precursors of Functionalized Materials for Applications in Environmental Engineering, Civil Engineering and Agriculture" (no. POIR.04.04.00-00-14E6/18-00), carried out within the TEAM-NET programme of the Foundation for Polish Science co-financed by the European Union under the European regional development fund.

Acknowledgments

VP acknowledges the DBT-JRF fellowship (award letter no. DBTHRDPMU/JRF/BET-22/I/2022-23/45) provided by the Department of Biotechnology, Government of India.

Conflict of interest

The authors declare that the research was conducted in the absence of any commercial or financial relationships that could be construed as a potential conflict of interest.

Publisher's note

All claims expressed in this article are solely those of the authors and do not necessarily represent those of their affiliated organizations, or those of the publisher, the editors and the reviewers. Any product that may be evaluated in this article, or claim that may be made by its manufacturer, is not guaranteed or endorsed by the publisher.

References

Abuzaid, A. S., Jahin, H. S., Asaad, A. A., Fadl, M. E., Abdelrahman, M., and Scopa, A. (2021). Accumulation of potentially toxic metals in Egyptian alluvial soils, berseem clover (*Trifolium alexandrinum* l.), and groundwater after long-term wastewater irrigation. *Agriculture* 11. doi: 10.3390/agriculture11080713

Ahemad, M. (2015). Enhancing phytoremediation of chromium-stressed soils through plant-growth-promoting bacteria. *J. Genet. Eng. Biotechnol.* 13, 51–58. doi: 10.1016/j.jgeb.2015.02.001

Ahmed, R., Taha, Y.-E., and Ali, H. M. A. (2021). Phytoremediation of crude oil contaminated soil by *Acacia farnesiana* l. willd. and spraying glutathione. *Univ. Thi-Qar J. Sci.* 8, 59–66. doi: 10.32792/utq/utjsci/v8/1/10

Ali, S., Abbas, Z., Rizwan, M., Zaheer, I. E., Yavaş, İ., Ünay, A., et al. (2020). Application of floating aquatic plants in phytoremediation of heavy metals polluted water: A review. *Sustainability* 12. doi: 10.3390/su12051927

Ali, S., Charles, T. C., and Glick, B. R. (2014). Amelioration of high salinity stress damage by plant growth-promoting bacterial endophytes that contain ACC deaminase. *Plant Physiol. Biochem.* 80, 160–167. doi: 10.1016/j.plaphy.2014.04.003

Ali, A., Guo, D., Li, Y., Shaheen, S. M., Wahid, F., Antoniadis, V., et al. (2021). *Streptomyces pactum* addition to contaminated mining soils improved soil quality and enhanced metals phytoextraction by wheat in a green remediation trial. *Chemosphere* 273, 129692. doi: 10.1016/j.chemosphere.2021.129692

Allamin, I. A., Halmi, M. I. E., Yasid, N. A., Ahmad, S. A., Abdullah, S. R. S., and Shukor, Y. (2020). Rhizodegradation of petroleum oily sludge-contaminated soil using *Cajanus cajan* increases the diversity of soil microbial community. *Sci. Rep.* 104094. doi: 10.1038/s41598-020-60668-1

Al Sbani, N. H., Abdullah, S. R. S., Idris, M., Hasan, H. A., Halmi, M. I. E., Jehawi, O. H., et al. (2021). PAH-degrading rhizobacteria of *Lepironia articulata* for phytoremediation enhancement. *J. Water Process Eng.* 39, 101688. doi: 10.1016/j.jwpe.2020.101688

Amaresan, N., Murugesan, S., Kumar, K., and Sankaranarayanan, A. (2020). Microbial mitigation of stress response of food legumes. *CRC Press* Boca Raton, 300. doi: 10.1201/9781003028413

Ameri Siahouei, R., Zaeimdar, M., Moogouei, R., and Jozi, S. A. (2020). Potential of *Cyperus alternifolius*, *Amaranthus retroflexus*, *Closia cristata* and *Bambusa vulgaris* to phytoremediate emerging contaminants and phytodesalination; insight to floating beds technology. *Caspian J. Environ. Sci.* 18, 309–317. doi: 10.22124/cjes.2020.4277

Anees, M., Qayyum, A., Jamil, M., Rehman, F. U., Abid, M., Malik, M. S., et al. (2020). Role of halotolerant and chitinolytic bacteria in phytoremediation of saline soil using spinach plant. *Int. J. Phytoremediation* 22, 653–661. doi: 10.1080/15226514.2019.1707160

Ashraf, S., Ali, Q., Zahir, Z. A., Ashraf, S., and Asghar, H. N. (2019). Phytoremediation: Environmentally sustainable way for reclamation of heavy metal polluted soils. *Ecotoxicol. Environ. Saf.* 174, 714–727. doi: 10.1016/j.ecoenv.2019.02.068

Babu, A. G., Kim, J.-D., and Oh, B.-T. (2013). Enhancement of heavy metal phytoremediation by *Alnus firma* with endophytic *Bacillus thuringiensis* GDB-1. *J. Hazard. Mater.* 250-251, 477–483. doi: 10.1016/j.jhazmat.2013.02.014

Backer, R., Rokem, J. S., Ilangumaran, G., Lamont, J., Praslickova, D., Ricci, E., et al. (2018). Plant growth-promoting rhizobacteria: Context, mechanisms of action, and roadmap to commercialization of biostimulants for sustainable agriculture. *Front. Plant Sci.* 9. doi: 10.3389/fpls.2018.01473

Baneshi, M. M., Rezaei Kalantary, R., Jonidi Jafari, A., Nasseri, S., Jaafarzadeh, N., and Esrafili, A. (2014). Effect of bioaugmentation to enhance phytoremediation for removal of phenanthrene and pyrene from soil with *Sorghum* and *Onobrychis sativa*. *J. Environ. Health Sci. Eng.* 12, 24. doi: 10.1186/2052-336X-12-24

Baumgarten, W., Ivanina, V., and Hanzhenko, O. (2017). ""Biomass production on marginal lands-catalogue of bioenergy crops"," in *EGU general assembly conference abstracts* Germany: European Geosciences Union, 7904.

Berger, J., Palta, J., and Vadez, V. (2016). Review: An integrated framework for crop adaptation to dry environments: Responses to transient and terminal drought. *Plant Sci.* 253, 58–67. doi: 10.1016/j.plantsci.2016.09.007

Bernal, M. P., Grippi, D., and Clemente, R. (2021). Potential of the biomass of plants grown in trace element-contaminated soils under Mediterranean climatic conditions for bioenergy production. *Agronomy* 11. doi: 10.3390/agronomy11091750

Bhat, S. A., Bashir, O., Ul Haq, S. A., Amin, T., Rafiq, A., Ali, M., et al. (2022). Phytoremediation of heavy metals in soil and water: An eco-friendly, sustainable and multidisciplinary approach. *Chemosphere* 303, 134788. doi: 10.1016/j.chemosphere.2022.134788

Bortoloti, G. A., and Baron, D. (2022). Phytoremediation of toxic heavy metals by *Brassica* plants: A biochemical and physiological approach. *Environ. Adv.* 8, 100204. doi: 10.1016/j.envadv.2022.100204

Bulegon, L., Guimarães, V., and Laureth, J. (2016). *Azospirillum brasilense* affects the antioxidant activity and leaf pigment content of *Urochloa ruziziensis* under water stress. *Pesquisa Agropecuaria Trop.* 46, 343–349. doi: 10.1590/1983-40632016v4641489

Carriquiry, M. A., Du, X., and Timilsina, G. R. (2011). Second generation biofuels: Economics and policies. *Energy Policy* 39, 4222–4234. doi: 10.1016/j.enpol.2011.04.036

Chang, P., Gerhardt, K. E., Huang, X.-D., Yu, X.-M., Glick, B. R., Gerwing, P. D., et al. (2014). Plant growth-promoting bacteria facilitate the growth of barley and oats in salt-impacted soil: Implications for phytoremediation of saline soils. *Int. J. Phytoremediation* 16, 1133–1147. doi: 10.1080/15226514.2013.821447

Cheng, S.-F., Huang, C.-Y., Chen, K.-L., Lin, S.-C., and Lin, Y.-C. (2016). Phytoattenuation of lead-contaminated agricultural land using *Miscanthus floridulus*–an *in situ* case study. *Desalination Water Treat* 57, 7773–7779. doi: 10.1080/19443994.2015.1033477

Chen, Y., Han, Y.-H., Cao, Y., Zhu, Y.-G., Rathinasabapathi, B., and Ma, L. Q. (2017c). Arsenic transport in rice and biological solutions to reduce arsenic risk from rice. *Front. Plant Sci.* 8. doi: 10.3389/fpls.2017.00268

Chen, X., Liu, X., Zhang, X., Cao, L., and Hu, X. (2017b). Phytoremediation effect of *Scirpus triqueter* inoculated plant-growth-promoting bacteria (PGPB) on different fractions of pyrene and Ni in co-contaminated soils. *J. Hazard. Mater.* 325, 319–326. doi: 10.1016/j.jhazmat.2016.12.009

Chen, B., Luo, S., Wu, Y., Ye, J., Wang, Q., Xu, X., et al. (2017a). The effects of the endophytic bacterium *Pseudomonas fluorescens* Sasm05 and IAA on the plant growth and cadmium uptake of *Sedum alfredii* hance. *Front. Microbiol.* 8. doi: 10.3389/fmicb.2017.02538

Debiec-Andrzejewska, K., Krucon, T., Piatkowska, K., and Drewniak, L. (2020). Enhancing the plants growth and arsenic uptake from soil using arsenite-oxidizing bacteria. *Environ. Pollut.* 264, 114692. doi: 10.1016/j.envpol.2020.114692

De Souza, M. P., Chu, D., Zhao, M., Zayed, A. M., Ruzin, S. E., Schichnes, D., et al. (1999). Rhizosphere bacteria enhance selenium accumulation and volatilization by Indian Mustard1. *Plant Physiol.* 119, 565–574. doi: 10.1104/pp.119.2.565

Dhaliwal, S. S., Taneja, P. K., Singh, J., Bhatti, S. S., and Singh, R. (2020). Cadmium accumulation potential of *Brassica* species grown in metal spiked loamy sand soil. *Soil Sediment Contam.: Int. J.* 29, 638–649. doi: 10.1080/15320383.2020.1758031

Dominguez, J. J. A., Inoue, C., and Chien, M.-F. (2020). Hydroponic approach to assess rhizodegradation by sudangrass (*Sorghum x drummondii*) reveals pH- and plant age-dependent variability in bacterial degradation of polycyclic aromatic hydrocarbons (PAHs). *J. Hazard. Mater.* 387, 121695. doi: 10.1016/j.jhazmat.2019.121695

Dos Santos, N. M. C., Da Costa, V., De Araújo, F. V., Alencar, B. T. B., Ribeiro, V. H. V., Okumura, F., et al. (2018). Phytoremediation of Brazilian tree species in soils contaminated by herbicides. *Environ. Sci. Pollut. Res.* 25, 27561–27568. doi: 10.1007/s11356-018-2798-0

Durand, A., Piutti, S., Rue, M., Morel, J. L., Echevarria, G., and Benizri, E. (2016). Improving nickel phytoextraction by co-cropping hyperaccumulator plants inoculated by plant growth promoting rhizobacteria. *Plant Soil* 399, 179–192. doi: 10.1007/s11104-015-2691-2

Edrisi, S. A., and Abhilash, P. C. (2016). Exploring marginal and degraded lands for biomass and bioenergy production: An Indian scenario. *Renewable Sustain. Energy Rev.* 54, 1537–1551. doi: 10.1016/j.rser.2015.10.050

Eissa, M. A. (2019). Effect of compost and biochar on heavy metals phytostabilization by the halophytic plant old man saltbush [*Atriplex nummularia* lindl]. *Soil Sediment Contam.: Int. J.* 28, 135–147. doi: 10.1080/15320383.2018.1551325

Elango, D., Devi, K. D., Jeyabalakrishnan, H. K., Rajendran, K., Thoomatti Haridass, V. K., Dharmaraj, D., et al. (2022). Agronomic, breeding, and biotechnological interventions to mitigate heavy metal toxicity problems in agriculture. *J. Agric. Food Res.* 10, 100374. doi: 10.1016/j.jafr.2022.100374

Emergen Research (2022) *Microbial bioremediation market, by pollutants (Organic pollutants and inorganic pollutants), by organisms, by type, by technology, by application, by end-use, and by region forecast to 2030*. Available at: https://www.emergenresearch.com/industry-report/microbial-bioremediation-market (Accessed 15th September 2022).

EPA (2022), 260–2342. U.S. Environmental Protection Agency National Contingency Plan Product Schedule. NCP Product Schedule Manager, U.S. Environmental Protection Agency, Office of Land and Emergency Management (OLEM), Office of Emergency Management (OEM) and Regulations Implementation Division (RID). NCP Subpart J Information Line, at (202).

Fan, P., Hao, M., Ding, F., Jiang, D., and Dong, D. (2020). Quantifying global potential marginal land resources for switchgrass. *Energies* 13. doi: 10.3390/en13236197

FAO (2022). *The state of the world's land and water resources for food and agriculture – systems at breaking point* (Rome, Italy: FAO). doi: 10.4060/cb9910en

Fatima, K., Afzal, M., Imran, A., and Khan, Q. M. (2015). Bacterial rhizosphere and endosphere populations associated with grasses and trees to be used for phytoremediation of crude oil contaminated soil. *Bull. Environ. Contam. Toxicol.* 94, 314–320. doi: 10.1007/s00128-015-1489-5

Ferrarini, A., Fracasso, A., Spini, G., Fornasier, F., Taskin, E., Fontanella, M. C., et al. (2021). Bioaugmented phytoremediation of metal-contaminated soils and sediments by hemp and giant reed. *Front. Microbiol.* 12. doi: 10.3389/fmicb.2021.645893

Ghazaryan, K. A., Movsesyan, H. S., Khachatryan, H. E., Ghazaryan, N. P., Minkina, T. M., Sushkova, S. N., et al. (2018). Copper phytoextraction and phytostabilization potential of wild plant species growing in the mine polluted areas of Armenia. *Geochemist.: Exploration Environ. Anal.* 19, 155–163. doi: 10.1144/geochem2018-035

Girolkar, S., Thawale, P., and Juwarkar, A. (2021). ""Chapter 12 - bacteria-assisted phytoremediation of heavy metals and organic pollutants: challenges and future prospects,"," in *Bioremediation for environmental sustainability*. Eds. V. Kumar, G. Saxena and M. P. Shah (USA: Elsevier), 247–267. doi: 10.1016/B978-0-12-820318-7.00012-5

Gouda, S., Kerry, R. G., Das, G., Paramithiotis, S., Shin, H.-S., and Patra, J. K. (2018). Revitalization of plant growth promoting rhizobacteria for sustainable development in agriculture. *Microbiol. Res.* 206, 131–140. doi: 10.1016/j.micres.2017.08.016

Guarino, F., Miranda, A., Castiglione, S., and Cicatelli, A. (2020). Arsenic phytovolatilization and epigenetic modifications in *Arundo donax* l. assisted by a PGPR consortium. *Chemosphere* 251, 126310. doi: 10.1016/j.chemosphere.2020.126310

Haberl, H., Beringer, T., Bhattacharya, S. C., Erb, K.-H., and Hoogwijk, M. (2010). The global technical potential of bio-energy in 2050 considering sustainability constraints. *Curr. Opin. Environ. Sustain.* 2, 394–403. doi: 10.1016/j.cosust.2010.10.007

Hamidpour, M., Nemati, H., Abbaszadeh Dahaji, P., and Roosta, H. R. (2020). Effects of plant growth-promoting bacteria on EDTA-assisted phytostabilization of heavy metals in a contaminated calcareous soil. *Environ. Geochemist. Health* 42, 2535–2545. doi: 10.1007/s10653-019-00422-3

He, X., Xu, M., Wei, Q., Tang, M., Guan, L., Lou, L., et al. (2020). Promotion of growth and phytoextraction of cadmium and lead in *Solanum nigrum* l. mediated by plant-growth-promoting rhizobacteria. *Ecotoxicol. Environ. Saf.* 205, 111333. doi: 10.1016/j.ecoenv.2020.111333

Heydarian, Z., Yu, M., Gruber, M., Glick, B. R., Zhou, R., and Hegedus, D. D. (2016). Inoculation of soil with plant growth promoting bacteria producing 1-Aminocyclopropane-1-Carboxylate deaminase or expression of the corresponding acdS gene in transgenic plants increases salinity tolerance in *Camelina sativa*. *Front. Microbiol.* 7. doi: 10.3389/fmicb.2016.01966

Hood, E. E. (2016). Plant-based biofuels. *F1000Research* 5, Rev–1185. doi: 10.12688/f1000research.7418.1

Hoogwijk, M., Faaij, A., De Vries, B., and Turkenburg, W. (2009). Exploration of regional and global cost–supply curves of biomass energy from short-rotation crops at abandoned cropland and rest land under four IPCC SRES land-use scenarios. *Biomass Bioenergy* 33, 26–43. doi: 10.1016/j.biombioe.2008.04.005

Hoseini, S., Moogouei, R., Borghei, M., Abedi, Z., and Ramezani, M. (2022). Potential of wheat (*Triticum aestivum*) and quinoa (*Chenopodium quinoa*) for phytodesalination of calcium, magnesium, sodium, potassium and chlorine under different water salinity stresses. *J. Iranian Plant Ecophysiol. Res.* 17, 38–53. doi: 10.30495/iper.2022.690262

Huang, W. X., Chen, X. W., Wu, L., Yu, Z. S., Gao, M. Y., Zhao, H. M., et al. (2021). Root cell wall chemistry remodelling enhanced arsenic fixation of a cabbage cultivar. *J. Hazard. Mater.* 420, 126165. doi: 10.1016/j.jhazmat.2021.126165

Huang, H., Zhao, Y., Fan, L., Jin, Q., Yang, G., and Xu, Z. (2020). Improvement of manganese phytoremediation by *Broussonetia papyrifera* with two plant growth promoting (PGP) *Bacillus* species. *Chemosphere* 260, 127614. doi: 10.1016/j.chemosphere.2020.127614

Hussain, F., Hussain, I., Khan, A. H. A., Muhammad, Y. S., Iqbal, M., Soja, G., et al. (2018). Combined application of biochar, compost, and bacterial consortia with Italian ryegrass enhanced phytoremediation of petroleum hydrocarbon contaminated soil. *Environ. Exp. Bot.* 153, 80–88. doi: 10.1016/j.envexpbot.2018.05.012

Hu, Z., Wang, Y., Fang, Z., Shi, G., Lou, L., Ren, K., et al. (2020). Italian Ryegrass–rice rotation system for biomass production and cadmium removal from contaminated paddy fields. *J. Soils Sediments* 20, 874–882. doi: 10.1007/s11368-019-02470-9

Hussain, A., Kamran, M.A., Javed, M.T., Hayat, K., Farooq, M.A., Ali, N., et al. (2019). Individual and combinatorial application of Kocuria rhizophila and citric acid on phytoextraction of multi-metal contaminated soils by Glycine max L. *Environmental and Experimental Botany* 159, 23–33. doi: 10.1016/j.envexpbot.2018.12.006

Iram, S., Basri, R., Ahmad, K. S., and Jaffri, S. B. (2019). Mycological assisted phytoremediation enhancement of bioenergy crops *Zea mays* and *Helianthus annuus* in heavy metal contaminated lithospheric zone. *Soil Sediment Contam.: Int. J.* 28, 411–430. doi: 10.1080/15320383.2019.1597011

Islam, M. S., Hosen, M. M. L., and Uddin, M. N. (2019). Phytodesalination of saline water using ipomoea aquatica, *Alternanthera philoxeroides* and *Ludwigia adscendens*. *Int. J. Environ. Sci. Technol.* 16, 965–972. doi: 10.1007/s13762-018-1705-z

Islam, F., Yasmeen, T., Arif, M. S., Riaz, M., Shahzad, S. M., Imran, Q., et al. (2016). Combined ability of chromium (Cr) tolerant plant growth promoting bacteria (PGPB) and salicylic acid (SA) in attenuation of chromium stress in maize plants. *Plant Physiol. Biochem.* 108, 456–467. doi: 10.1016/j.plaphy.2016.08.014

Jaskulak, M., Grobelak, A., and Vandenbulcke, F. (2020). Modelling assisted phytoremediation of soils contaminated with heavy metals – main opportunities, limitations, decision making and future prospects. *Chemosphere* 249, 126196. doi: 10.1016/j.chemosphere.2020.126196

Jhilta, P., Dipta, B., and Rana, A. (2021). ""Phytoremediation of heavy metals and radionuclides: Sustainable approach to environmental management,"," in *Phytoremediation for environmental sustainability*. Ed. R. Prasad (Singapore: Springer Nature Singapore). doi: 10.1007/978-981-16-5621-7_5

Jiang, C., Guan, K., Khanna, M., Chen, L., and Peng, J. (2021). Assessing marginal land availability based on land use change information in the contiguous united states. *Environ. Sci. Technol.* 55, 10794–10804. doi: 10.1021/acs.est.1c02236

Jude, K., Tanee, F. B. G., and Mensah, S. I. (2019). Enhancing phytoremediation potential of *Andropogon tectorum* (Schumach & thonn) in petroleum hydrocarbon contaminated soil using cassava peel. *Scientia Africana* 18, 23–36. Available at: https://www.ajol.info/index.php/sa/article/view/199472.

Ju, W., Jin, X., Liu, L., Shen, G., Zhao, W., Duan, C., et al. (2020). Rhizobacteria inoculation benefits nutrient availability for phytostabilization in copper contaminated soil: Drivers from bacterial community structures in rhizosphere. *Appl. Soil Ecol.* 150, 103450. doi: 10.1016/j.apsoil.2019.103450

Kafle, A., Timilsina, A., Gautam, A., Adhikari, K., Bhattarai, A., and Aryal, N. (2022). Phytoremediation: Mechanisms, plant selection and enhancement by natural and synthetic agents. *Environ. Adv.* 8, 100203. doi: 10.1016/j.envadv.2022.100203

Karaghool, H. (2022). ""The employment of endophytic bacteria for phytodegradation of pyridine"," in *IOP conference series: Earth and environmental science* (Baghdad, Iraq: IOP Publishing).

Karthik, C., Barathi, S., Pugazhendhi, A., Ramkumar, V. S., Thi, N. B. D., and Arulselvi, P. I. (2017). Evaluation of Cr(VI) reduction mechanism and removal by *Cellulosimicrobium funkei* strain AR8, a novel haloalkaliphilic bacterium. *J. Hazard. Mater.* 333, 42–53. doi: 10.1016/j.jhazmat.2017.03.037

Kasim, W. A., Gaafar, R. M., Abou-Ali, R. M., Omar, M. N., and Hewait, H. M. (2016). Effect of biofilm forming plant growth promoting rhizobacteria on salinity tolerance in barley. *Ann. Agric. Sci.* 61, 217–227. doi: 10.1016/j.aoas.2016.07.003

Ke, T., Guo, G., Liu, J., Zhang, C., Tao, Y., Wang, P., et al. (2021a). Improvement of the Cu and cd phytostabilization efficiency of perennial ryegrass through the inoculation of three metal-resistant PGPR strains. *Environ. Pollut.* 271, 116314. doi: 10.1016/j.envpol.2020.116314

Ke, T., Zhang, J., Tao, Y., Zhang, C., Zhang, Y., Xu, Y., et al. (2021b). Individual and combined application of Cu-tolerant *Bacillus* spp. enhance the Cu phytoextraction efficiency of perennial ryegrass. *Chemosphere* 263, 127952. doi: 10.1016/j.chemosphere.2020.127952

Khan, N., and Bano, A. (2018). ""Role of PGPR in the phytoremediation of heavy metals and crop growth under municipal wastewater irrigation,"," in *Phytoremediation: Management of environmental contaminants*, vol. 6 . Eds. A. A. Ansari, S. S. Gill, R. Gill, G. R. Lanza and L. Newman (Cham: Springer International Publishing), 135–149. doi: 10.1007/978-3-319-99651-6_5

Konkolewska, A., Piechalak, A., Ciszewska, L., Antos-Krzemińska, N., Skrzypczak, T., Hanć, A., et al. (2020). Combined use of companion planting and PGPR for the assisted phytoextraction of trace metals (Zn, Pb, cd). *Environ. Sci. pollut. Res.* 27, 13809–13825. doi: 10.1007/s11356-020-07885-3

Kotoky, R., and Pandey, P. (2020a). Rhizosphere assisted biodegradation of benzo(a)pyrene by cadmium resistant plant-probiotic *Serratia marcescens* S2I7, and its genomic traits. *Sci. Rep.* 105279. doi: 10.1038/s41598-020-62285-4

Kotoky, R., and Pandey, P. (2020b). Rhizosphere mediated biodegradation of benzo (A)pyrene by surfactin producing soil bacilli applied through *Melia azedarach* rhizosphere. *Int. J. Phytoremediation* 22, 363–372. doi: 10.1080/15226514.2019.1663486

Kowitwiwat, A., and Sampanpanish, P. (2020). Phytostabilization of arsenic and manganese in mine tailings using *Pennisetum purpureum* cv. Mott supplemented with cow manure and acacia wood-derived biochar. *Heliyon* 6, e04552. doi: 10.1016/j.heliyon.2020.e04552

Kukla, M., Płociniczak, T., and Piotrowska-Seget, Z. (2014). Diversity of endophytic bacteria in *Lolium perenne* and their potential to degrade petroleum hydrocarbons and promote plant growth. *Chemosphere* 117, 40–46. doi: 10.1016/j.chemosphere.2014.05.055

Kumar, A., and Verma, J. P. (2018). Does plant–microbe interaction confer stress tolerance in plants: A review? *Microbiol. Res.* 207, 41–52. doi: 10.1016/j.micres.2017.11.004

Lachapelle, A., Yavari, S., Pitre, F. E., Courchesne, F., and Brisson, J. (2021). Co-Planting of *Salix interior* and *Trifolium pratense* for phytoremediation of trace elements from wood preservative contaminated soil. *Int. J. Phytoremediation* 23, 632–640. doi: 10.1080/15226514.2020.1847034

Ławniczak, Ł., Woźniak-Karczewska, M., Loibner, A. P., Heipieper, H. J., and Chrzanowski, Ł. (2020). Microbial degradation of hydrocarbons–basic principles for bioremediation: A review. *Molecules* 25. doi: 10.3390/molecules25040856

Ledin, M. (2000). Accumulation of metals by microorganisms — processes and importance for soil systems. *Earth-Science Rev.* 51, 1–31. doi: 10.1016/S0012-8252(00)00008-8

Lewandowski, I., Bahrs, E., Dahmen, N., Hirth, T., Rausch, T., and Weidtmann, A. (2019). Biobased value chains for a growing bioeconomy. *GCB Bioenergy* 11, 4–8. doi: 10.1111/gcbb.12578

Lewandowski, I., Schmidt, U., Londo, M., and Faaij, A. (2006). The economic value of the phytoremediation function – assessed by the example of cadmium remediation by willow (*Salix* ssp). *Agric. Syst.* 89, 68–89. doi: 10.1016/j.agsy.2005.08.004

Liang, Y., Meggo, R., Hu, D., Schnoor, J. L., and Mattes, T. E. (2014). Enhanced polychlorinated biphenyl removal in a switchgrass rhizosphere by bioaugmentation with *Burkholderia xenovorans* LB400. *Ecol. Eng.* 71, 215–222. doi: 10.1016/j.ecoleng.2014.07.046

Li, X., Cao, Y., Xiao, J., Salam, M. M. A., and Chen, G. (2022). Bamboo biochar greater enhanced Cd/Zn accumulation in salix psammophila under non-flooded soil compared with flooded. *Biochar* 4, 7. doi: 10.1007/s42773-022-00139-0

Li, Y., Lin, J., Huang, Y., Yao, Y., Wang, X., Liu, C., et al. (2020).). bioaugmentation-assisted phytoremediation of manganese and cadmium co-contaminated soil by polygonaceae plants (*Polygonum hydropiper* l. and *Polygonum lapathifolium* l.) and *Enterobacter* sp. FM-1. *Plant Soil* 448, 439–453. doi: 10.1007/s11104-020-04447-x

Liu, S., Ali, S., Yang, R., Tao, J., and Ren, B. (2019). A newly discovered cd-hyperaccumulator *Lantana camara* l. *J. Hazard. Mater.* 371, 233–242. doi: 10.1016/j.jhazmat.2019.03.016

Liu, L., Li, W., Song, W., and Guo, M. (2018). Remediation techniques for heavy metal-contaminated soils: Principles and applicability. *Sci. Total Environ.* 633, 206–219. doi: 10.1016/j.scitotenv.2018.03.161

Li, Q., Xing, Y., Fu, X., Ji, L., Li, T., Wang, J., et al. (2021). Biochemical mechanisms of rhizospheric *Bacillus subtilis*-facilitated phytoextraction by alfalfa under cadmium stress – microbial diversity and metabolomics analyses. *Ecotoxicol. Environ. Saf.* 212, 112016. doi: 10.1016/j.ecoenv.2021.112016

Manoj, S. R., Karthik, C., Kadirvelu, K., Arulselvi, P. I., Shanmugasundaram, T., Bruno, B., et al. (2020). Understanding the molecular mechanisms for the enhanced phytoremediation of heavy metals through plant growth promoting rhizobacteria: A review. *J. Environ. Manage.* 254, 109779. doi: 10.1016/j.jenvman.2019.109779

Ma, Y., Oliveira, R. S., Freitas, H., and Zhang, C. (2016a). Biochemical and molecular mechanisms of plant-Microbe-Metal interactions: Relevance for phytoremediation. *Front. Plant Sci.* 7. doi: 10.3389/fpls.2016.00918

Ma, Y., Prasad, M. N. V., Rajkumar, M., and Freitas, H. (2011). Plant growth promoting rhizobacteria and endophytes accelerate phytoremediation of metalliferous soils. *Biotechnol. Adv.* 29, 248–258. doi: 10.1016/j.biotechadv.2010.12.001

Ma, Y., Rajkumar, M., Rocha, I., Oliveira, R. S., and Freitas, H. (2015). Serpentine bacteria influence metal translocation and bioconcentration of *Brassica juncea* and *Ricinus communis* grown in multi-metal polluted soils. *Front. Plant Sci.* 5. doi: 10.3389/fpls.2014.00757

Ma, Y., Rajkumar, M., Vicente, J., and Freitas, H. (2010). Inoculation of Ni-resistant plant growth promoting bacterium psychrobacter sp. strain SRS8 for the improvement of nickel phytoextraction by energy crops. *Int. J. Phytoremediation* 13, 126–139. doi: 10.1080/15226511003671403

Ma, Y., Rajkumar, M., Zhang, C., and Freitas, H. (2016b). Inoculation of *Brassica oxyrrhina* with plant growth promoting bacteria for the improvement of heavy metal phytoremediation under drought conditions. *J. Hazard. Mater.* 320, 36–44. doi: 10.1016/j.jhazmat.2016.08.009

Masoudian, Z., Salehi-Lisar, S. Y., and Norastehnia, A. (2020). Phytoremediation potential of *Azolla filiculoides* for sodium dodecyl benzene sulfonate (SDBS) surfactant considering some physiological responses, effects of operational parameters and biodegradation of surfactant. *Environ. Sci. pollut. Res.* 27, 20358–20369. doi: 10.1007/s11356-020-08286-2

Matsui, K., Yoshinami, S., Narita, M., Chien, M.-F., Phung, L. T., Silver, S., et al. (2016). Mercury resistance transposons in bacilli strains from different geographical regions. *FEMS Microbiol. Lett.* 363, fnw013. doi: 10.1093/femsle/fnw013

Ma, Y., Zhang, C., Oliveira, R. S., Freitas, H., and Luo, Y. (2016c). Bioaugmentation with endophytic bacterium E6S homologous to *Achromobacter piechaudii* enhances metal rhizoaccumulation in host *Sedum plumbizincicola*. *Front. Plant Sci.* 7. doi: 10.3389/fpls.2016.00075

Mehmood, M. A., Ibrahim, M., Rashid, U., Nawaz, M., Ali, S., Hussain, A., et al. (2017). Biomass production for bioenergy using marginal lands. *Sustain. Prod. Consump.* 9, 3–21. doi: 10.1016/j.spc.2016.08.003

Mello, I. S., Targanski, S., Pietro-Souza, W., Frutuoso Stachack, F. F., Terezo, A. J., and Soares, M. A. (2020). Endophytic bacteria stimulate mercury phytoremediation by modulating its bioaccumulation and volatilization. *Ecotoxicol. Environ. Saf.* 202, 110818. doi: 10.1016/j.ecoenv.2020.110818

Moubasher, H. A., Hegazy, A. K., Mohamed, N. H., Moustafa, Y. M., Kabiel, H. F., and Hamad, A. A. (2015). Phytoremediation of soils polluted with crude petroleum oil using *Bassia scoparia* and its associated rhizosphere

microorganisms. *Int. Biodeterior. Biodegradation* 98, 113–120. doi: 10.1016/j.ibiod.2014.11.019

Mukhopadhyay, S., and Maiti, S.K.J.T.B. (2010). Natural mycorrhizal colonization in tree species growing on the reclaimed coalmine overburden dumps: Case study from jharia coalfields, India. *Annu. Rev. Plant Biol.* 3, 761–770. doi: 10.1146/annurev.arplant.59.032607.092911

Narayanan, M., Kandasamy, G., He, Z., Kandasamy, S., Alfarhan, A. H., and Pugazhendhi, A. (2021). Phytoextraction competence of *J. curcas* l. @ on ore waste dump of the bauxite mine under the influence of multi potential *Bacillus cereus*. *Environ. Technol. Innovation* 21, 101221. doi: 10.1016/j.eti.2020.101221

Nebeská, D., Trögl, J., Ševců, A., Špánek, R., Marková, K., Davis, L., et al. (2021). *Miscanthus* x *giganteus* role in phytodegradation and changes in bacterial community of soil contaminated by petroleum industry. *Ecotoxicol. Environ. Saf.* 224, 112630. doi: 10.1016/j.ecoenv.2021.112630

Nedjimi, B. (2021). Phytoremediation: a sustainable environmental technology for heavy metals decontamination. *SN Appl. Sci.* 3, 286. doi: 10.1007/s42452-021-04301-4

Oliveira, V., Gomes, N. C. M., Almeida, A., Silva, A. M. S., Simões, M. M. Q., Smalla, K., et al. (2014). Hydrocarbon contamination and plant species determine the phylogenetic and functional diversity of endophytic degrading bacteria. *Mol. Ecol.* 23, 1392–1404. doi: 10.1111/mec.12559

Otlewska, A., Migliore, M., Dybka-Stępień, K., Manfredini, A., Struszczyk-Świta, K., Napoli, R., et al. (2020). When salt meddles between plant, soil, and microorganisms. *Front. Plant Sci.* 11. doi: 10.3389/fpls.2020.553087

Pancaldi, F., and Trindade, L. M. (2020). Marginal lands to grow novel bio-based crops: A plant breeding perspective. *Front. Plant Sci.* 11. doi: 10.3389/fpls.2020.00227

Pandey, V. C., Pandey, D. N., and Singh, N. (2015). Sustainable phytoremediation based on naturally colonizing and economically valuable plants. *J. Cleaner Prod.* 86, 37–39. doi: 10.1016/j.jclepro.2014.08.030

Pankaj, U., Singh, G., and Verma, R. K. (2019). ""Chapter 20 - microbial approaches in management and restoration of marginal lands,"," in *New and future developments in microbial biotechnology and bioengineering*. Ed. J. S. Singh (USA: Elsevier), 295–305. doi: 10.1016/B978-0-12-818258-1.00020-0

Parveen, S., Bhat, I. U. H., Khanam, Z., Rak, A. E., Yusoff, H. M., and Akhter, M. S. (2022). Phytoremediation: *In situ* alternative for pollutant removal from contaminated natural media: A brief review. *Biointerface Res. Appl. Chem.* 12, 4945–4960. doi: 10.33263/BRIAC124.49454960

Pathak, S., Agarwal, A. V., and Pandey, V. C. (2020). ""1 - phytoremediation–a holistic approach for remediation of heavy metals and metalloids,"," in *Bioremediation of pollutants*. Eds. V. C. Pandey and V. Singh (USA: Elsevier), 3–16. doi: 10.1016/B978-0-12-819025-8.00001-6

Pawlik, M., Cania, B., Thijs, S., Vangronsveld, J., and Piotrowska-Seget, Z. (2017). Hydrocarbon degradation potential and plant growth-promoting activity of culturable endophytic bacteria of lotus corniculatus and *Oenothera biennis* from a long-term polluted site. *Environ. Sci. pollut. Res.* 24, 19640–19652. doi: 10.1007/s11356-017-9496-1

Pawlik, M., Płociniczak, T., Thijs, S., Pintelon, I., Vangronsveld, J., and Piotrowska-Seget, Z. (2020). Comparison of two inoculation methods of endophytic bacteria to enhance phytodegradation efficacy of an aged petroleum hydrocarbons polluted soil. *Agronomy* 10. doi: 10.3390/agronomy10081196

Pidlisnyuk, V., Mamirova, A., Pranaw, K., Shapoval, P. Y., Trögl, J., and Nurzhanova, A. (2020). Potential role of plant growth-promoting bacteria in *Miscanthus* x *giganteus* phytotechnology applied to the trace elements contaminated soils. *Int. Biodeterior. Biodegradation* 155, 105103. doi: 10.1016/j.ibiod.2020.105103

Pivetz, B. E. (2001). *"Ground water issue: phytoremediation of contaminated soil and ground water at hazardous waste sites"* (USA: National Risk Mannagement Research Lab ADA Ok).

Poria, V., Rana, A., Kumari, A., Grewal, J., Pranaw, K., and Singh, S. (2021a). Current perspectives on chitinolytic enzymes and their agro-industrial applications. *Biology* 10. doi: 10.3390/biology10121319

Poria, V., Singh, S., Nain, L., Singh, B., and Saini, J. K. (2021b). ""Rhizospheric microbial communities: Occurrence, distribution, and functions,"," in *Microbial metatranscriptomics belowground*. Eds. M. Nath, D. Bhatt, P. Bhargava and D. K. Choudhary (Singapore: Springer Singapore), 239–271. doi: 10.1007/978-981-15-9758-9_12

P.P, S., and Puthur, J. T. (2021). Heavy metal phytoremediation by bioenergy plants and associated tolerance mechanisms. *Soil Sediment Contam.: Int. J.* 30, 253–274. doi: 10.1080/15320383.2020.1849017

Pranaw, K., Pidlisnyuk, V., Trögl, J., and Malinská, H. (2020). Bioprospecting of a novel plant growth-promoting bacterium *Bacillus altitudinis* KP-14 for enhancing *Miscanthus* × *giganteus* growth in metals contaminated soil. *Biology* 9. doi: 10.3390/biology9090305

Qurashi, A. W., and Sabri, A. N. (2012). Bacterial exopolysaccharide and biofilm formation stimulate chickpea growth and soil aggregation under salt stress. *Braz. J. Microbiol. [publication Braz. Soc. Microbiol.* 43, 1183–1191. doi: 10.1590/S1517-838220120003000046

Rabani, M. S., Hameed, I., Mir, T. A., A. Wani, B., Gupta, M. K., Habib, A., et al. (2022). ""Chapter 5 - microbial-assisted phytoremediation," in phytoremediation,". *Phytoremediation: Biotechnological Strategies for Promoting Invigorating Environs* Eds. R. A. Bhat, F. M. P. Tonelli, G. H. Dar and K. Hakeem (UK: Academic Press), 91–114. doi: 10.1016/B978-0-323-89874-4.00006-6

Rahman, F., Sugawara, K., Huang, Y., Chien, M.-F., and Inoue, C. (2018). Arsenic, lead and cadmium removal potential of *Pteris multifida* from contaminated water and soil. *Int. J. Phytoremediation* 20, 1187–1193. doi: 10.1080/15226514.2017.1375896

Rajkumari, J., Choudhury, Y., Bhattacharjee, K., and Pandey, P. (2021). Rhizodegradation of pyrene by a non-pathogenic *Klebsiella pneumoniae* isolate applied with *Tagetes erecta* l. and changes in the rhizobacterial community. *Front. Microbiol.* 12. doi: 10.3389/fmicb.2021.593023

Ramakrishna, W., Rathore, P., Kumari, R., and Yadav, R. (2020). Brown gold of marginal soil: Plant growth promoting bacteria to overcome plant abiotic stress for agriculture, biofuels and carbon sequestration. *Sci. Total Environ.* 711, 135062. doi: 10.1016/j.scitotenv.2019.135062

Ramana, S., Tripathi, A. K., Kumar, A., Singh, A. B., Bharati, K., Sahu, A., et al. (2021). Potential of cotton for remediation of cd-contaminated soils. *Environ. Monit. Assess.* 193, 186. doi: 10.1007/s10661-021-08976-5

Ren, X.-M., Guo, S.-J., Tian, W., Chen, Y., Han, H., Chen, E., et al. (2019). Effects of plant growth-promoting bacteria (PGPB) inoculation on the growth, antioxidant activity, Cu uptake, and bacterial community structure of rape (*Brassica napus* l.) grown in Cu-contaminated agricultural soil. *Front. Microbiol.* 10. doi: 10.3389/fmicb.2019.01455

Riaz, U., Athar, T., Mustafa, U., and Iqbal, R. (2022). ""Chapter 23 - economic feasibility of phytoremediation,"," in *Phytoremediation*. Eds. R. A. Bhat, F. M. P. Tonelli, G. H. Dar and K. Hakeem (USA: Academic Press). doi: 10.1016/B978-0-323-89874-4.00025-X

Ruley, J. A., Tumuhairwe, J. B., Amoding, A., Westengen, O. T., and Vinje, H. (2020). Rhizobacteria communities of phytoremediation plant species in petroleum hydrocarbon contaminated soil of the sudd ecosystem, south Sudan. *Int. J. Microbiol.* 2020, 6639118. doi: 10.1155/2020/6639118

Saballos, A. (2008). ""Development and utilization of sorghum as a bioenergy crop,"," in *Genetic improvement of bioenergy crops*. Ed. W. Vermerris (New York, NY: Springer New York). doi: 10.1007/978-0-387-70805-8_8

Sabreena, H.S., Bhat, S. A., Kumar, V., Ganai, B. A., and Ameen, F. (2022). Phytoremediation of heavy metals: An indispensable contrivance in green remediation technology. *Plants* 11. doi: 10.3390/plants11091255

Saikia, J., Sarma, R. K., Dhandia, R., Yadav, A., Bharali, R., Gupta, V. K., et al. (2018). Alleviation of drought stress in pulse crops with ACC deaminase producing rhizobacteria isolated from acidic soil of northeast India. *Sci. Rep.* 83560. doi: 10.1038/s41598-018-21921-w

Saleem, M. H., Ali, S., Hussain, S., Kamran, M., Chattha, M. S., Ahmad, S., et al. (2020a. Flax (*Linum usitatissimum* l.): A potential candidate for phytoremediation? biological and economical points of view. *Plants* 9. doi: 10.3390/plants9040496

Saleem, M. H., Ali, S., Rehman, M., Hasanuzzaman, M., Rizwan, M., Irshad, S., et al. (2020b). Jute: A potential candidate for phytoremediation of metals–a review. *Plants* 9. doi: 10.3390/plants9020258

Saleem, M. H., Kamran, M., Zhou, Y., Parveen, A., Rehman, M., Ahmar, S., et al. (2020c). Appraising growth, oxidative stress and copper phytoextraction potential of flax (*Linum usitatissimum* l.) grown in soil differentially spiked with copper. *J. Environ. Manage.* 257, 109994. doi: 10.1016/j.jenvman.2019.109994

Saleem, M. U., Naeem Asghar, H., Ahmad Zahir, Z., and Shahid, M. (2019). EVALUATION OF LEAD TOLERANT PLANT GROWTH PROMOTING RHIZOBACTERIA FOR PLANT GROWTH AND PHYTOREMEDIATION IN LEAD CONTAMINATION. *Rev. Internacional Contaminación Ambiental* 35, 999–1009. doi: 10.20937/rica.2019.35.04.18

Sansinenea, E. (2019). ""Bacillus spp.: As plant growth-promoting bacteria,"," in *Secondary metabolites of plant growth promoting rhizomicroorganisms: Discovery and applications*. Eds. H. B. Singh, C. Keswani, M. S. Reddy, E. Sansinenea and C. García-Estrada (Singapore: Singapore: Springer), 225–237. doi: 10.1007/978-981-13-5862-3_11

Saran, A., Fernandez, L., Cora, F., Savio, M., Thijs, S., Vangronsveld, J., et al. (2020a). Phytostabilization of Pb and cd polluted soils using *Helianthus petiolaris* as pioneer aromatic plant species. *Int. J. Phytoremediation* 22, 459–467. doi: 10.1080/15226514.2019.1675140

Saran, A., Imperato, V., Fernandez, L., Gkorezis, P., D'haen, J., Merini, L. J., et al. (2020b). Phytostabilization of polluted military soil supported by bioaugmentation with PGP-trace element tolerant bacteria isolated from *Helianthus petiolaris*. *Agronomy* 10, 459–467. doi: 10.3390/agronomy10020204

Schirawski, J., and Perlin, M. H. (2018). Plant–microbe interaction 2017–the good, the bad and the diverse. *Int. J. Mol. Sci.* 19. doi: 10.3390/ijms19051374

Schröder, P., Beckers, B., Daniels, S., Gnädinger, F., Maestri, E., Marmiroli, N., et al. (2018). Intensify production, transform biomass to energy and novel goods and protect soils in Europe–a vision how to mobilize marginal lands. *Sci. Total Environ.* 616-617, 1101–1123. doi: 10.1016/j.scitotenv.2017.10.209

Schwitzguébel, J.-P. (2017). Phytoremediation of soils contaminated by organic compounds: hype, hope and facts. *J. Soils Sediments* 17, 1492–1502. doi: 10.1007/s11368-015-1253-9

Shackira, A. M., and Puthur, J. T. (2019). ""Phytostabilization of heavy metals: Understanding of principles and practices,"," in *Plant-metal interactions*. Eds. S. Srivastava, A. K. Srivastava and P. Suprasanna (Cham: Springer International Publishing), 263–282. doi: 10.1007/978-3-030-20732-8_13

Shahane, A. A., and Shivay, Y. S. (2021). Soil health and its improvement through novel agronomic and innovative approaches. *Front. Agron.* 3. doi: 10.3389/fagro.2021.680456

Shah, V., and Daverey, A. (2020). Phytoremediation: A multidisciplinary approach to clean up heavy metal contaminated soil. *Environ. Technol. Innovation* 18, 100774. doi: 10.1016/j.eti.2020.100774

Shen, S., Chen, J., Chang, J., and Xia, B. (2020). Using bioenergy crop cassava (*Manihot esculenta*) for reclamation of heavily metal-contaminated land. *Int. J. Phytoremediation* 22, 1313–1320. doi: 10.1080/15226514.2020.1768512

Sikdar, A., Wang, J., Hasanuzzaman, M., Liu, X., Feng, S., Roy, R., et al. (2020). Phytostabilization of Pb-zn mine tailings with *Amorpha fruticosa* aided by organic amendments and triple superphosphate. *Molecules* 25. doi: 10.3390/molecules25071617

Silver, S., and Hobman, J. L. (2007). ""Mercury microbiology: Resistance systems, environmental aspects, methylation,and human health,"," in *Molecular microbiology of heavy metals*. Eds. D. H. Nies and S. Silver (Berlin, Heidelberg: Springer Berlin Heidelberg), 357–370. doi: 10.1007/7171_2006_085

Singh, D., Ghosh, P., Kumar, J., and Kumar, A. (2019). ""Plant growth-promoting rhizobacteria (PGPRs): Functions and benefits,"," in *Microbial interventions in agriculture and environment: Volume 2: Rhizosphere, microbiome and agro-ecology*. Eds. D. P. Singh, V. K. Gupta and R. Prabha (Singapore: Springer Singapore), 205–227. doi: 10.1007/978-981-13-8383-0_7

Sofy, M. R., Aboseidah, A. A., Heneidak, S. A., and Ahmed, H. R. (2021). ACC deaminase containing endophytic bacteria ameliorate salt stress in *Pisum sativum* through reduced oxidative damage and induction of antioxidative defense systems. *Environ. Sci. Pollut. Res.* 28, 40971–40991. doi: 10.1007/s11356-021-13585-3

Soldatos, P. (2015). Economic aspects of bioenergy production from perennial grasses in marginal lands of South Europe. *Bioenergy Res.* 8, 1562–1573. doi: 10.1007/s12155-015-9678-y

Sorour, A. A., Khairy, H., Zaghloul, E. H., and Zaghloul, H. (2022). Microbe-plant interaction as a sustainable tool for mopping up heavy metal contaminated sites. *BMC Microbiol.* 22, 174. doi: 10.1186/s12866-022-02587-x

Sung-Je, Y., Weon, H.-Y., Song, J., and Sang, M. K. (2019). Induced tolerance to salinity stress by halotolerant bacteria *Bacillus aryabhattai* H19-1 and *B. mesonae* H20-5 in tomato plants. *J. Microbiol. Biotechnol.* 29, 1124–1136. doi: 10.4014/jmb.1904.04026

Sun, L., Yang, Y., Wang, R., Li, S., Qiu, Y., Lei, P., et al. (2020). Effects of exopolysaccharide derived from *Pantoea alhagi* NX-11 on drought resistance of rice and its efficient fermentation preparation. *Int. J. Biol. Macromolecules* 162, 946–955. doi: 10.1016/j.ijbiomac.2020.06.199

Taeprayoon, P., Homyog, K., and Meeinkuirt, W. (2022). Organic amendment additions to cadmium-contaminated soils for phytostabilization of three bioenergy crops. *Sci. Rep.* 12, 13070. doi: 10.1038/s41598-022-17385-8

Tak, H. I., Ahmad, F., and Babalola, O. O. (2013). ""Advances in the application of plant growth-promoting rhizobacteria in phytoremediation of heavy metals,"," in *Reviews of environmental contamination and toxicology*. Ed. D. M. Whitacre (New York, NY: Springer New York), 33–52. doi: 10.1007/978-1-4614-5577-6_2

Tchounwou, P. B., Yedjou, C. G., Patlolla, A. K., and Sutton, D. J. (2012). ""Heavy metal toxicity and the environment," in molecular, clinical and environmental toxicology," in *Environmental toxicology*, vol. 3 . Ed. A. Luch (Basel: Springer Basel), 133–164. doi: 10.1007/978-3-7643-8340-4_6

Thijs, S., Sillen, W., Weyens, N., and Vangronsveld, J. (2017). Phytoremediation: State-of-the-art and a key role for the plant microbiome in future trends and research prospects. *Int. J. Phytoremediation* 19, 23–38. doi: 10.1080/15226514.2016.1216076

Tiepo, A. N., Constantino, L. V., Madeira, T. B., Gonçalves, L. S. A., Pimenta, J. A., Bianchini, E., et al. (2020). Plant growth-promoting bacteria improve leaf antioxidant metabolism of drought-stressed Neotropical trees. *Planta* 251, 83. doi: 10.1007/s00425-020-03373-7

Tiodar, E. D., Văcar, C. L., and Podar, D. (2021). Phytoremediation and microorganisms-assisted phytoremediation of mercury-contaminated soils: Challenges and perspectives. *Int. J. Environ. Res. Public Health* 18. doi: 10.3390/ijerph18052435

Ullah, A., Heng, S., Munis, M. F. H., Fahad, S., and Yang, X. (2015). Phytoremediation of heavy metals assisted by plant growth promoting (PGP) bacteria: A review. *Environ. Exp. Bot.* 117, 28–40. doi: 10.1016/j.envexpbot.2015.05.001

Ummara, U., Noreen, S., Afzal, M., and Ahmad, P. (2021). Bacterial bioaugmentation enhances hydrocarbon degradation, plant colonization and gene expression in diesel-contaminated soil. *Physiologia Plantarum* 173, 58–66. doi: 10.1111/ppl.13171

Visconti, D., Ventorino, V., Fagnano, M., Woo, S. L., Pepe, O., Adamo, P., et al. (2022). Compost and microbial biostimulant applications improve plant growth and soil biological fertility of a grass-based phytostabilization system. *Environ. Geochemist. Health*. doi: 10.1007/s10653-022-01235-7

Vishnupradeep, R., Bruno, L. B., Taj, Z., Karthik, C., Challabathula, D., et al. (2022). Tripti, Kumar, a Plant growth promoting bacteria improve growth and phytostabilization potential of *Zea mays* under chromium and drought stress by altering photosynthetic and antioxidant responses. *Environ. Technol. Innovation* 25, 102154. doi: 10.1016/j.eti.2021.102154

Vives-Peris, V., De Ollas, C., Gómez-Cadenas, A., and Pérez-Clemente, R. M. (2020). Root exudates: from plant to rhizosphere and beyond. *Plant Cell Rep.* 39, 3–17. doi: 10.1007/s00299-019-02447-5

Vural, A., and Safari, S. (2022). Phytoremediation ability of *Helichrysum arenarium* plant for au and Ag: Case study at demirören village (Gümüşhane, Turkey). *Gold Bull* 55, 129-136. doi: 10.1007/s13404-022-00313-z

Wang, X., Liang, J., Liu, Z., Kuang, Y., Han, L., Chen, H., et al. (2022). Transcriptional regulation of metal metabolism- and nutrient absorption-related genes in eucalyptus grandis by arbuscular mycorrhizal fungi at different zinc concentrations. *BMC Plant Biol.* 22, 76. doi: 10.1186/s12870-022-03456-5

Wang, S., Teng, S., and Fan, M. (2010) "Interaction between heavy metals and aerobic granules" in *Environmental management* Ed. S. Sarkar. UK: IntechOpen. doi: 10.5772/10106

Wan, X., Lei, M., and Chen, T. (2016). Cost–benefit calculation of phytoremediation technology for heavy-metal-contaminated soil. *Sci. total Environ.* 563, 796–802. doi: 10.1016/j.scitotenv.2015.12.080

Witzel, C.-P., and Finger, R. (2016). Economic evaluation of *Miscanthus* production – a review. *Renewable Sustain. Energy Rev.* 53, 681–696. doi: 10.1016/j.rser.2015.08.063

Wu, Y., Ma, L., Liu, Q., Vestergård, M., Topalovic, O., Wang, Q., et al. (2020a). The plant-growth promoting bacteria promote cadmium uptake by inducing a hormonal crosstalk and lateral root formation in a hyperaccumulator plant *Sedum alfredii*. *J. hazard. mater.* 395, 122661. doi: 10.1016/j.jhazmat.2020.122661

Wu, Y., Wang, M., Yu, L., Tang, S.-W., Xia, T., Kang, H., et al. (2020b). A mechanism for efficient cadmium phytoremediation and high bioethanol production by combined mild chemical pretreatments with desirable rapeseed stalks. *Sci. Total Environ.* 708, 135096. doi: 10.1016/j.scitotenv.2019.135096

Xiang, L., Song, Y., Bian, Y., Liu, G., Herzberger, A., Gu, C., et al. (2018). Manure amendment reduced plant uptake and enhanced rhizodegradation of 2,2′,4, 4′-tetrabrominated diphenyl ether in soil. *Biol. Fertility Soils* 54, 807–817. doi: 10.1007/s00374-018-1304-7

Xiao, M.-Z., Sun, R., Du, Z.-Y., Yang, W.-B., Sun, Z., and Yuan, T.-Q. (2021). A sustainable agricultural strategy integrating cd-contaminated soils remediation and bioethanol production using sorghum cultivars. *Ind. Crops Products* 162, 113299. doi: 10.1016/j.indcrop.2021.113299

Xu, Q., Renault, S., and Yuan, Q. (2019). Phytodesalination of landfill leachate using *Puccinellia nuttalliana* and *Typha latifolia*. *Int. J. Phytoremediation* 21, 831–839. doi: 10.1080/15226514.2019.1568383

Yadav, S., Modi, P., Dave, A., Vijapura, A., Patel, D., and Patel, M. (2020). ""Effect of abiotic stress on crops,"," in *Sustainable crop production*. Eds. M.C.M.T.F.M. Hasanuzzaman, M. Fujita, T. Assis and R. Nogueira (London: IntechOpen). doi: 10.5772/intechopen.88434

Yang, Y., and Guo, Y. (2018). Unraveling salt stress signaling in plants. *J. Integr. Plant Biol.* 60, 796–804. doi: 10.1111/jipb.12689

Yan, A., Wang, Y., Tan, S. N., Mohd Yusof, M. L., Ghosh, S., and Chen, Z. (2020). Phytoremediation: A promising approach for revegetation of heavy metal-polluted land. *Front. Plant Sci.* 11. doi: 10.3389/fpls.2020.00359

Yu, G., Jiang, P., Fu, X., Liu, J., Sunahara, G. I., Chen, Z., et al. (2020). Phytoextraction of cadmium-contaminated soil by *Celosia argentea* linn.: A long-term field study. *Environ. Pollut.* 266, 115408. doi: 10.1016/j.envpol.2020.115408

Zainab, N., Amna,, Khan, A. A., Azeem, M. A., Ali, B., Wang, T., et al. (2021). "PGPR-mediated plant growth attributes and metal extraction ability," in *Industrially contaminated soils*, vol. 11 . Ed. L. Sesbania sesban (Basel, Switzerland: Agronomy). doi: 10.3390/agronomy11091820

Zamani, J., Hajabbasi, M. A., Mosaddeghi, M. R., Soleimani, M., Shirvani, M., and Schulin, R. (2018). Experimentation on degradation of petroleum in contaminated soils in the root zone of maize (*Zea mays* l.) inoculated with *Piriformospora indica*. *Soil Sediment Contam.: Int. J.* 27, 13–30. doi: 10.1080/15320383.2018.1422693

Zeng, P., Guo, Z., Xiao, X., Peng, C., Feng, W., Xin, L., et al. (2019). Phytoextraction potential of *Pteris vittata* l. co-planted with woody species for as, cd, Pb and zn in contaminated soil. *Sci. Total Environ.* 650, 594–603. doi: 10.1016/j.scitotenv.2018.09.055

Zgorelec, Z., Bilandzija, N., Knez, K., Galic, M., and Zuzul, S. (2020). Cadmium and mercury phytostabilization from soil using *Miscanthus* × *giganteus*. *Sci. Rep.* 106685. doi: 10.1038/s41598-020-63488-5

Zhang, Q., Kong, W., Wei, L., Wang, Y., Luo, Y., Wang, P., et al. (2020). Uptake, phytovolatilization, and interconversion of 2,4-dibromophenol and 2,4-dibromoanisole in rice plants. *Environ. Int.* 142, 105888. doi: 10.1016/j.envint.2020.105888

Zhang, H., Tian, Y., Wang, L., Zhang, L., and Dai, L. (2013). Ecophysiological characteristics and biogas production of cadmium-contaminated crops. *Bioresource Technol.* 146, 628–636. doi: 10.1016/j.biortech.2013.07.148

Zhang, X., Yu, J., Huang, Z., Li, H., Liu, X., Huang, J., et al. (2021). Enhanced cd phytostabilization and rhizosphere bacterial diversity of *Robinia pseudoacacia* l. by endophyte *Enterobacter* sp. YG-14 combined with sludge biochar. *Sci. Total Environ.* 787, 147660. doi: 10.1016/j.scitotenv.2021.147660

Zhou, J.-W., Li, Z., Liu, M.-S., Yu, H.-M., Wu, L.-H., Huang, F., et al. (2020). Cadmium isotopic fractionation in the soil–plant system during repeated phytoextraction with a cadmium hyperaccumulating plant species. *Environ. Sci. Technol.* 54, 13598–13609. doi: 10.1021/acs.est.0c03142

Zhuang, D., Jiang, D., Liu, L., and Huang, Y. (2011). Assessment of bioenergy potential on marginal land in China. *Renewable Sustain. Energy Rev.* 15, 1050–1056. doi: 10.1016/j.rser.2010.11.041

Zine, H., Midhat, L., Hakkou, R., El Adnani, M., and Ouhammou, A. (2020). Guidelines for a phytomanagement plan by the phytostabilization of mining wastes. *Sci. Afr.* 10, e00654. doi: 10.1016/j.sciaf.2020.e00654

frontiers | Frontiers in Plant Science

TYPE Original Research
PUBLISHED 02 November 2022
DOI 10.3389/fpls.2022.1025122

OPEN ACCESS

EDITED BY
Juan Li,
Hunan Agricultural University, China

REVIEWED BY
Qiming Wang,
Hunan Agricultural University, China
Yun Fang,
Wuhan Institute of Technology, China
Qingyun Yan,
Sun Yat-sen University, China

*CORRESPONDENCE
Huaqun Yin
yinhuaqun_cs@sina.com
Yongjun Liu
Vincentliu2020@163.com

SPECIALTY SECTION
This article was submitted to Plant Symbiotic Interactions, a section of the journal Frontiers in Plant Science

RECEIVED 22 August 2022
ACCEPTED 07 September 2022
PUBLISHED 02 November 2022

CITATION
Li L, Peng S, Wang Z, Zhang T, Li H, Xiao Y, Li J, Liu Y and Yin H (2022) Genome mining reveals abiotic stress resistance genes in plant genomes acquired from microbes *via* HGT. *Front. Plant Sci.* 13:1025122. doi: 10.3389/fpls.2022.1025122

Genome mining reveals abiotic stress resistance genes in plant genomes acquired from microbes *via* HGT

Liangzhi Li[1,2], Shuguang Peng[3], Zhenhua Wang[4], Teng Zhang[1,2,5], Hongguang Li[3], Yansong Xiao[6], Jingjun Li[6], Yongjun Liu[3]* and Huaqun Yin[1,2]*

[1]School of Minerals Processing and Bioengineering, Central South University, Changsha, China, [2]Key Laboratory of Biometallurgy of Ministry of Education, Central South University, Changsha, China, [3]Hunan Tobacco Science Institute, Changsha, China, [4]Zhangjiajie Tobacco Company of Hunan Province, Zhangjiajie, China, [5]Hunan Urban and Rural Environmental Construction Co., Ltd, Changsha, China, [6]Chenzhou Tobacco Company of Hunan Province, Chenzhou, China

Colonization by beneficial microbes can enhance plant tolerance to abiotic stresses. However, there are still many unknown fields regarding the beneficial plant-microbe interactions. In this study, we have assessed the amount or impact of horizontal gene transfer (HGT)-derived genes in plants that have potentials to confer abiotic stress resistance. We have identified a total of 235 gene entries in fourteen high-quality plant genomes belonging to phyla *Chlorophyta* and *Streptophyta* that confer resistance against a wide range of abiotic pressures acquired from microbes through independent HGTs. These genes encode proteins contributed to toxic metal resistance (e.g., ChrA, CopA, CorA), osmotic and drought stress resistance (e.g., Na^+/proline symporter, potassium/proton antiporter), acid resistance (e.g., PcxA, ArcA, YhdG), heat and cold stress resistance (e.g., DnaJ, Hsp20, CspA), oxidative stress resistance (e.g., GST, PoxA, glutaredoxin), DNA damage resistance (e.g., Rad25, Rad51, UvrD), and organic pollutant resistance (e.g., CytP450, laccase, CbbY). Phylogenetic analyses have supported the HGT inferences as the plant lineages are all clustering closely with distant microbial lineages. Deep-learning-based protein structure prediction and analyses, in combination with expression assessment based on codon adaption index (CAI) further corroborated the functionality and expressivity of the HGT genes in plant genomes. A case-study applying fold comparison and molecular dynamics (MD) of the HGT-driven CytP450 gave a more detailed illustration on the resemblance and evolutionary linkage between the plant recipient and microbial donor sequences. Together, the microbe-originated HGT genes identified in plant genomes and their participation in abiotic pressures resistance indicate a more profound impact of HGT on the adaptive evolution of plants.

KEYWORDS

abiotic stress resistance, plant, microbe, horizontal gene transfer, phylogeny

Introduction

Plants, the most profoundly distributed lineage on earth, possess the remarkable abilities to convert solar energy into bio-matter and produce oxygen while consume the greenhouse gas carbon dioxide. At the same time, plants have to face the frequent offense of inhospitable abiotic stresses caused by the constant fluctuations of global climate since plants cannot "run away" from them. The challenging conditions like drought, radiation, nutrient deficiencies, temperature extremes (cold and heat), metal ion toxicity, salinity and organic pollution are typical abiotic stress factors that plants frequently encounter (Zhang et al., 2022). These abiotic factors have drastically influenced plant distribution and growth status globally (Nolan et al., 2018). It is long known that beneficial microbes are helping plants to overcome climate change and other adverse conditions through a variety of ways (Schützendübel and Polle, 2002; Haney et al., 2015; Murali et al., 2021). For example, microbes can increase the activity of plant antioxidant defense enzyme (Mastouri et al., 2012), release beneficial volatile organic compounds (VOCs) that trigger resistance response (Liu and Zhang, 2015), and modulate the expression of plant metal transporters against the accumulation of heavy metals (Zhou et al., 2020). However, many aspects of the plant-microbe interactions for mutual benefits are still in the "black box" and lack in-depth mechanism analysis.

Horizontal gene transfer (HGT), referring to the exchange of genetic material between distant lineages, is considered as an effective mechanism to spread evolutionary success in both prokaryotes and eukaryotes (Huang, 2013; Daubin and Szöllősi, 2016). Studies on HGT genes introduced into eukaryotic taxa have been expanding fast in the last twenty years as next-generation sequencing technology has made large-scale genome data available (Soucy et al., 2015). Recent researches have demonstrated that genes in plant genomes important for the function of specific plant activities, including the biosynthesis of plant structure components and hormones, plant defense, nitrogen recycling and stress resistance, can be obtained *via* the omnipresent HGT process (Yue et al., 2012). It is strongly proposed in a recent review that HGTs possess the potency to drastically influence plant evolutionary path by imparting selective advantages (Wickell and Li, 2020). Here are some examples illustrating the importance of microbe-derived HGTs in plants that confer adaptive benefits. Firstly, it is found that the ancestor of land plants acquired a phenylalanine ammonia lyase (PAL), the entry point of the phenylpropanoid pathway, through HGT during symbioses with soil bacteria and fungi (Emiliani et al., 2009); The second case is that *Physcomitrella patens* is suggested to acquire from bacteria acyl-activating enzyme 18 (AAE18)/flavin monooxygenase (YUC3) for auxin biosynthesis, guanine deaminase, allantoate amidohydrolase and ureidoglycolate amidohydrolase associated with purine degradation, as well as subtilases for protein degradation (Yue et al., 2012). Besides, Li et al. (2018) detected that the squalene-hopene cyclase (SHC) encoding genes in three plant clades (mosses, liverworts and lycophytes/ferns) are interspersing with bacterial SHCs, suggesting the occurrence of independent and repeated HGT events for enhanced adaption since the product of SHC, hopanoid, constitutes plant cell membrane important for maintaining cell integrity. Lastly, it is reported that the adaptive genes in *Zygnematophyceae*, GRAS and PYR/PYL/RCAR that enhance resistance to abiotic stresses (e.g., desiccation), were obtained through HGT from nearby soil bacteria (Cheng et al., 2019). However, many of these previous investigations focused mainly on individual plant lineage or limited HGT events on important economic aspects such as the valuable plant metabolism pathways. Despite these efforts, we still have little knowledge on the amount or impact of HGT-derived genes in plants that have potentials to confer resistance against a wide range of abiotic stresses (e.g., low pH, osmotic pressure, heat and cold stress) and hence promote the growth of plants in extreme conditions. It is still an open question that if there is microbe-originated HGT(s) that has facilitated plant to adapt such abiotic stresses. And if there are such HGT genes, what are their functions in combating abiotic stresses and to what extent are they distributed in the plant genomes?

Against such background, in this study, we have chosen fourteen high-quality plant genomes covering major plant taxa (Clade *Viridiplantae*) within Phyla *Chlorophyta* and *Streptophyta*, and tried to uncover and scrutinize putative microbe-originated HGT genes that are associated with abiotic stress resistance in these genomes employing a combination of methods previously showed to be highly effective in identifying HGT between distantly related species (Schönknecht et al., 2014), including BLASTP-based searches and gene tree reconciliation. To further testify the expression potential of the detected HGT genes, we supply codon adaption index calculation, deep-learning-driven protein structure prediction, fold alignment, and molecular dynamics to assess the expression potential and functionality of the abiotic stress resistance genes acquired by plants from microbial lineages. Our findings indicated that the HGT events in beneficial microbes putatively colonizing plant might be an important source of acquisitions of genes that help enhance plant tolerance against abiotic stresses. This study has also advanced our understanding on plant-microbe interactions and the adaptive evolution of plants to encounter adverse conditions.

Results

General information

Detailed information of the fourteen high-quality eukaryotic plant genomes covering major plant taxa (clade *Viridiplantae*) within phyla *Chlorophyta* and *Streptophyta* chosen for

downstream analyses is provided in Table 1. Putative microbe-originated HGT genes in these genomes employing the BLASTP-based IMGAP pipeline (Markowitz et al., 2010), followed by manual pickup of microbe-originated genes that are associated with abiotic stress resistance. These processes eventually produce a total of 235 gene entries, as listed in Table 2 and Supplementary Tables S1A and S1B at https://doi.org/10.6084/m9.figshare.20530083.v1. Detailed descriptions are provided in the following subsections.

HGT genes for metal resistance

The accumulation of toxic metals in contaminated soils stands for a serious environmental challenge, which negatively affects plant health and growth. As a possible solution, it has been reported that metal-resistant bacteria/fungi inhabiting plant-related sphere have the ability to promote plant growth and tolerance upon the attack of toxic metal stress (Mishra et al., 2017; Zhou et al., 2020), forming plant-microbe interactions which might also provide an opportunity for plants to acquire metal-resistant genes originated from nearby microbial taxa. In accordance, we identified eleven HGT gene entries for metal resistance in the tested plant genomes (Table 2), most of which are metal ion transport proteins (e.g., ChrA, CopA, CorA) that facilitate the efflux of cytosolic excessed toxic metal ions. Other HGT genes related to metal resistance might include phosphatase (Table 2), which might be secreted to increase soil phosphorus availability and immobilize toxic metal ions by forming complex compounds with them (Bechtaoui et al., 2021).

To confirm the HGT origin of the mentioned plant metal resistance genes, we selected and built the phylogenetic trees with three representative genes as queries: chromate transporters (ChrA) of *Ricinus communis*, copper homeostasis protein (CutC) of *Chlamydomonas reinhardtii*, and magnesium and cobalt transport protein (CorA) of *Volvox carteri*. As expected, all these suggested HGT genes in plant genomes are clustering with homologues of cross-phylum microbial taxa (putative HGT donors). To be specific, it is illustrated in the well-supported phylogenetic tree constructed with not-exclusive top BLASTP hit entries that: ChrA of *Ricinus communis* (eudicots) and several green algae (e.g., *Chlorella* spp., *Chlamydomonas* spp., *Coccomyxa* spp.) bear significant resemblance to the homologues of vast *Proteobacteria* and *Firmicutes* lineages (e.g., *Methylophilus* spp., *Pseudomonas* spp., and *Bacillales*) (Figure 1A); CutC homologues of green algae (e.g., *Chlamydomonas* spp., *Volvox* spp., *Klebsormidium nitens*) are completely nested within in bacterial taxa (e.g., *Verrucomicrobiales, Bacteroidales, Rhizobiaceae*), a pattern indicative of cross-kingdom HGT (Figure 1B); besides, CorA homologues of green algae (e.g., *Chlamydomonas* spp., *Scenedesmus* spp., *Volvox* spp.) are closely clustering with fungal lineages (e.g., *Colletotrichum* spp., *Spizellomyces* spp., *Kwoniella* spp.) (Figure 1C). Lastly, phosphatase homologues of green algae (e.g., *Chlamydomonas* spp., *Ostreobium* spp., *Micromonas* spp.) are clustering adjacent to bacterial taxa (e.g., *Sphingomonas* spp., *Zoogloea* spp., *Pseudomonadales*), indicating strong HGT signals (Figure 1D).

Osmotic and drought stress resistance

Salinization and drought of arable land stand for major challenges to agriculture production worldwide. Salt accumulation and water scarcity would cause osmotic and water-deficit stress that restrict plant growth by affecting nutrient uptake and cell physiology (Bashir et al., 2014; Hanin et al., 2016). Acquisitions of osmotic and drought stress resistance genes from nearby microbes to enhance self-resistance might be an alleviating approach for plants. Accordingly, we found ten gene entries that putatively confer osmotic stress resistance in five tested plant genomes (Table 2): eight ion/solute transporter (e.g., sodium/potassium ATPase, Na^+/proline symporter, chloride channel protein and potassium/proton antiporter) and two organic osmolyte biosynthesis enzymes (choline dehydrogenase BetA and sarcosine oxidase SoxA). These genes are correspondent to two mechanisms of osmotic stress resistance: maintaining cellular ion homeostasis and recruitment of compatible solutes (e.g., proline, betaine, sarcosine) to stabilize proteins. These compatible solutes can also protect against drought, heat or cold stresses (Bashir et al., 2014; Hanin et al., 2016). Other putative HGT and osmotic/drought resistance genes detected in plants, as listed in Table 2, may include: trehalose 6-phosphate synthase and trehalose hydrolase, and dTDP-D-glucose 4,6-dehydratase (RmlB), involving in the biosynthesis of protective sugar; cellulose synthase, significant for enhanced cell wall (Behr et al., 2015). Besides, we have found in the plant genomes HGT-driven malate synthase and isocitrate lyase of the glyoxylate cycle, which were reported to be highly expressed under drought conditions (Todaka et al., 2015; Kim et al., 2020); Lastly, transaldolase, an upstream enzyme controlling erythritol (protectant) production, which was found up-regulated upon exposure to short-term drought stress (Liu et al., 2015) and hyper-osmotic stress (Iwata et al., 2015; Yang et al., 2015).

To further verify the occurrence of HGT on the plant stress resistance genes mentioned above, we chose and built the phylogenetic trees of three representative genes: sodium/proton antiporter (CPA1) from *Chlamydomonas reinhardtii*, Na^+/solute symporter from *Arabidopsis thaliana*, chloride channel protein (ClcA) and dTDP-D-glucose 4,6-dehydratase (RmlB) from *Chlorella variabilis* (Figure 2). As observed from the well-supported phylogenetic tree of CPA1, homologues from *Chlamydomonas* spp. are tightly clustering with CPA1 from fungi (e.g., *Basidiobolus, Rhizophagus,*

TABLE 1 High-quality eukaryotic plant genomes covering major plant taxa (clade *Viridiplantae*) within phyla *Chlorophyta* and *Streptophyta* chosen for microbe-originated horizontal gene transfer (HGT) detection in this study.

Genome name	Phylum	NCBI bioproject	NCBI genbank ID	IMG genome ID	Sequencing depth	Sequencing quality	Sequencing status	Genome size (bp)	Scaffold count	Gene count	GC %
Chlamydomonas reinhardtii CC-503 cw92 mt+	*Chlorophyta*	PRJNA12260	ABCN00000000	649410502	10x	Level 2: High-Quality Draft	Complete	120404952	1558	14546	63.87
Volvox carteri f. nagariensis 69-1b	*Chlorophyta*	PRJNA13109	ACJH00000000	2507525017	8x	Level 2: High-Quality Draft	Complete	137835555	1265	14542	55.97
Chlorella variabilis NC64A	*Chlorophyta*	PRJNA45853	ADIC00000000	2507525016	8.9x	Level 1: Standard Draft	Complete	46159515	414	9791	67.14
Arabidopsis thaliana Columbia	*Streptophyta*	PRJNA13190	GCA_000211275	639560100		Level 6: Finished	Complete	119707899	7	31370	36.06
Physcomitrella patens patens (Moss)	*Streptophyta*	PRJNA13064	ABEU00000000	649410504	8.63x	Level 2: High-Quality Draft	Complete	477845029	1992	35938	33.58
Glycine max cultivar Williams 82 (Soybean)	*Streptophyta*	PRJNA19861	ACUP00000000	2507525014	8.5x	Level 2: High-Quality Draft	Complete	973344380	1168	55787	34.75
Populus balsamifera trichocarpa (Balsam poplar)	*Streptophyta*	PRJNA10772	AARH00000000	649410505	7.5x	Level 2: High-Quality Draft	Complete	480871302	20644	40566	33.55
Zea mays mays cv. B73 (Maize)	*Streptophyta*	PRJNA10769	CM000786, CM000777, GK000031	2507525013	6x	Level 6: Finished	Complete	2065722704	11	106044	46.89
Arabidopsis lyrata lyrata MN47	*Streptophyta*	PRJNA41137	ADBK00000000	649410501	8x	Level 2: High-Quality Draft	Complete	206667935	695	32549	36.08
Vitis vinifera PN40024 (Grape Vines)	*Streptophyta*	PRJNA34679	CAAP00000000	649410508	12x	Level 2: High-Quality Draft	Complete	791124756	3535	24954	34.51
Ricinus communis Hale (Castor bean)	*Streptophyta*	PRJNA16585	AASG00000000	649410506	2.45x	Level 2: High-Quality Draft	Complete	350458699	25762	31894	33.84
Sorghum bicolor BTx623	*Streptophyta*	PRJNA13876	ABXC00000000	2507525011	4x	Level 2: High-Quality Draft	Complete	738540932	3304	29448	43.93
Solanum tuberosum DM 1-3 516 R44 (Potato)	*Streptophyta*	PRJNA63145	AEWC00000000	2507525040	114x	Level 2: High-Quality Draft	Complete	727424546	66254	24377	34.8
Fragaria vesca Hawaii 4 (Woodland strawberry)	*Streptophyta*	PRJNA60037	AEMH00000000	2507525039	49x	Level 2: High-Quality Draft	Complete	214219504	3254	7931	38.4

10.3389/fpls.2022.1025122

TABLE 2 Microbe-originated HGT genes identified in tested plant genomes that associated with miscellaneous abiotic stress resistance.

Plant recipient	Recipient gene accession (IMG)	Gene function	Donor gene accession (IMG)	Microbial donor	Donor taxon
Metal resistance					
Chlorella variabilis NC64A	2507982899	Magnesium-translocating P-type ATPase MgtA	646357403	*Escherichia coli O111:H 11128*	*Bacteria; Proteobacteria*
Chlamydomonas reinhardtii CC-503 cw92 mt+	649485460	Magnesium and cobalt transport protein	2508406796	*Spizellomyces punctatus DAOM BR117*	*Eukaryota; Chytridiomycota*
Chlamydomonas reinhardtii CC-503 cw92 mt+	649493513	Copper homeostasis protein CutC	2506487166	*Emticicia oligotrophica GPTSA100-15*	*Bacteria; FCB group*
Physcomitrella patens patens	649531133	Copper resistance protein CopC	648722241	*Paenibacillus curdlanolyticus YK9*	*Bacteria; Firmicutes*
Ricinus communis Hale	649585425	Chromate transporter ChrA	649771835	*Methylovorus* sp. *MP688*	*Bacteria; Proteobacteria*
Arabidopsis thaliana Columbia	639572405	Copper-transporting ATPase	645867480	*Talaromyces marneffei ATCC 18224*	*Eukaryota; Ascomycota*
Arabidopsis thaliana Columbia	639588060	P-type copper ATPase	645729519	*Aspergillus clavatus NRRL 1*	*Eukaryota; Ascomycota*
Volvox carteri f. nagariensis 69-1b	2507995811	Magnesium and cobalt transport protein	2508406796	*Spizellomyces punctatus DAOM BR117*	*Eukaryota; Chytridiomycota*
Vitis vinifera PN40024	649546378	Ca^{2+}-transporting atpase	2509695751	*Schizophyllum commune H4-8*	*Eukaryota; Opisthokonta; Fungi*
Physcomitrella patens patens	649501412	Acid phosphatase	2509205796	*Batrachochytrium dendrobatidis JEL423*	*Eukaryota; Chytridiomycota; Chytridiomycetes*
Osmotic and drought stress resistance					
Physcomitrella patens patens	649496502	Choline dehydrogenase BetA	2509380569	*Ensifer aridi TW10*	*Bacteria; Proteobacteria; Deltaproteobacteria*
Volvox carteri f. nagariensis 69-1b	2508002683	Chloride intracellular channel 6	639857298	*Stigmatella aurantiaca DW4/3-1*	*Bacteria; Proteobacteria; Deltaproteobacteria*
Volvox carteri f. nagariensis 69-1b	2507995432	Potassium/proton antiporter	645972328	*Streptomyces* sp. *SPB78*	*Bacteria; Actinobacteria; Actinomycetia*
Chlorella variabilis NC64A	2507981403	Sarcosine oxidase SoxA	646435156	*Sphaerobacter thermophilus 4ac11, DSM 20745*	*Bacteria; Chloroflexi; Thermomicrobia*
Chlorella variabilis NC64A	2507981739	Na^+/proline symporter	2508394518	*Allomyces macrogynus ATCC 38327 (fungus)*	*Eukaryota; Blastocladiomycota; Blastocladiomycetes*
Chlorella variabilis NC64A	2507982753	Chloride channel protein ClcA	637771792	*Synechococcus* sp. *CC9902*	*Bacteria; Cyanobacteria; Synechococcales*
Arabidopsis thaliana Columbia	639580571	Na^+/solute symporter	646259962	*Oxalobacter formigenes HOxBLS*	*Bacteria; Proteobacteria; Betaproteobacteria*
Arabidopsis thaliana Columbia	639566001	Na/K ATPase alpha 1 subunit, putative	645866880	*Talaromyces marneffei ATCC 18224*	*Eukaryota; Ascomycota; Eurotiomycetes*
Chlamydomonas reinhardtii CC-503 cw92 mt+	649489365	Sodium/calcium exchanger	649408713	*Perkinsus marinus PmCV4CB5 2B3 D4*	*Eukaryota; Perkinsozoa; Perkinsida*
Chlamydomonas reinhardtii CC-503 cw92 mt+	649487367	Sodium/proton antiporte, CPA1	637235733	*Nostoc* sp. *PCC 7120*	*Bacteria; Cyanobacteria; Nostocales*

(Continued)

TABLE 2 Continued

Plant recipient	Recipient gene accession (IMG)	Gene function	Donor gene accession (IMG)	Microbial donor	Donor taxon
Chlamydomonas reinhardtii CC-503 cw92 mt+	649492246	Zinc-nutrition responsive transporter, ZIP family	649337865	*Phaeodactylum tricornutum CCAP1055/1*	*Eukaryota; Bacillariophyta; Bacillariophyceae*
Glycine max cultivar Williams 82	2507918029	Maltooligosyl trehalose hydrolase (EC 3.2.1.141)	651457131	*Xanthomonas vesicatoria Maraite, ATCC 35937*	*Bacteria; Proteobacteria; Gammaproteobacteria*
Arabidopsis thaliana Columbia	639571770	Trehalose 6-phosphate synthase (EC 2.4.1.15)	646433456	*Thermanaerovibrio acidaminovorans Su883, DSM 6589*	*Bacteria; Synergistetes; Synergistia*
Arabidopsis thaliana Columbia	639573047	Teichoic acid biosynthesis protein B	646070519	*Staphylococcus aureus A9635*	*Bacteria; Firmicutes; Bacilli*
Chlamydomonas reinhardtii CC-503 cw92 mt+	649484689	Cellulose synthase (UDP-forming)	637692951	*Cupriavidus pinatubonensis JMP134*	*Bacteria; Proteobacteria; Betaproteobacteria*
Chlorella variabilis NC64A	2507980628	dTDP-D-glucose 4,6-dehydratase RmlB	641205904	*Acanthocystis turfacea Chlorella virus 1*	*Viruses; dsDNA viruses, no RNA stage; Megaviricetes*
Physcomitrella patens patens	649498952	Capsular exopolysaccharide family	2505768802	*Fischerella thermalis JSC-11*	*Bacteria; Cyanobacteria; Synechococcales*
Chlorella variabilis NC64A	2507978560	Malate synthase (EC 2.3.3.9)	641353162	*Sorangium cellulosum So ce 56*	*Bacteria; Proteobacteria; Deltaproteobacteria*
Chlorella variabilis NC64A	2507978803	Malate synthase (EC 2.3.3.9)	641353162	*Sorangium cellulosum So ce 56*	*Bacteria; Proteobacteria; Deltaproteobacteria*
Chlorella variabilis NC64A	2507978611	Isocitrate lyase (EC 4.1.3.1)	643430771	*Anoxybacillus flavithermus WK1, DSM 2641*	*Bacteria; Firmicutes; Bacilli*
Physcomitrella patens patens	649526838	Transaldolase/Fructose-6-phosphate aldolase	647578161	*Synechococcus* sp. *PCC 7335*	*Bacteria; Cyanobacteria; Synechococcales*
Heat and cold stress					
Glycine max cultivar Williams 82	2507922078	Stromal 70 kDa chaperone protein DnaK	643477038	*Rippkaea orientalis PCC 8801*	*Bacteria; Cyanobacteria; Chroococcales*
Chlorella variabilis NC64A	2507984527	DnaJ-class molecular chaperone with C-terminal Zn finger domain	645858879	*Pyrenophora tritici-repentis Pt-1C-BFP*	*Eukaryota; Ascomycota; Dothideomycetes*
Chlorella variabilis NC64A	2507978787	DNA-binding protein HU	644676974	*Bacillus thuringiensis sv. monterrey BGSC 4AJ1*	*Bacteria; Firmicutes; Bacilli*
Chlorella variabilis NC64A	2507982059	DnaJ-class molecular chaperone with C-terminal Zn finger domain	2507660422	*Phytophthora ramorum Pr102, UCD Pr4*	*Eukaryota; Oomycota; Peronosporales*
Chlorella variabilis NC64A	2507982566	Chaperonin GroEL (HSP60 family)	2509191772	*Ectocarpus siliculosus Ec 32 (CCAP 1310/04)*	*Eukaryota; Phaeophyceae; Ectocarpales*
Chlorella variabilis NC64A	2507983822	Small heat shock protein (HSP20) family	641146850	*Marinobacter algicola DG893*	*Bacteria; Proteobacteria; Gammaproteobacteria*
Chlorella variabilis NC64A	2507983994	DnaJ molecular chaperone homology domain	2507660422	*Phytophthora ramorum Pr102, UCD Pr4*	*Eukaryota; Oomycota; Peronosporales*
Chlorella variabilis NC64A	2507984993	Heat shock protein 70	2509695036	*Schizophyllum commune H4-8*	*Eukaryota; Opisthokonta; Fungi*
Volvox carteri f. nagariensis 69-1b	2507993038	DnaJ-class molecular chaperone with C-terminal Zn finger domain	642750380	*Hydrogenobaculum* sp. *Y04AAS1*	*Bacteria; Aquificae; Aquificae*

(Continued)

TABLE 2 Continued

Plant recipient	Recipient gene accession (IMG)	Gene function	Donor gene accession (IMG)	Microbial donor	Donor taxon
Fragaria vesca Hawaii 4	2508472453	Heat shock protein 70KD	638270255	*Guillardia theta*	*Eukaryota; Cryptophyceae; Pyrenomonadales*
Arabidopsis thaliana Columbia	639560148	Heat shock protein. Metallo peptidase. MEROPS family M48B	639002844	*Nitrococcus mobilis Nb-231*	*Bacteria; Proteobacteria; Gammaproteobacteria*
Chlamydomonas reinhardtii CC-503 cw92 mt+	649482610	Heat shock factor binding protein 1	639628046	*Trypanosoma brucei brucei 927/4 GUTat10.1*	*Eukaryota; Euglenozoa; Kinetoplastea*
Ricinus communis Hale	649563104	Chaperone clpb, heat shock protein	637065254	*Escherichia coli O157:H7 EDL933 (EHEC)*	*Bacteria; Proteobacteria; Gammaproteobacteria*
Ricinus communis Hale	649583866	Molecular chaperone	2509190845	*Ectocarpus siliculosus Ec 32 (CCAP 1310/04)*	*Eukaryota; Phaeophyceae; Ectocarpales*
Ricinus communis Hale	649584950	Cold-shock DNA-binding protein CspA	642599004	*Paraburkholderia phymatum STM815*	*Bacteria; Proteobacteria; Betaproteobacteria*
Volvox carteri f. nagariensis 69-1b	2507995359	Chitinase	650773356	*Burkholderia gladioli BSR3*	*Bacteria; Proteobacteria; Betaproteobacteria*
Chlamydomonas reinhardtii CC-503 cw92 mt+	649491057	Chitinase family 18 (EC:3.2.1.14)	637922967	*Saccharophagus degradans 2-40*	*Bacteria; Proteobacteria; Gammaproteobacteria*
Chlamydomonas reinhardtii CC-503 cw92 mt+	649492930	Chitinase	2508410311	*Spizellomyces punctatus DAOM BR117*	*Eukaryota; Chytridiomycota; Chytridiomycetes*
Ricinus communis Hale	649570195	Ribulose 1,5-bisphosphate carboxylase large subunit (EC 4.1.1.39)	647109286	*Raphidiopsis brookii D9*	*Bacteria; Cyanobacteria; Nostocales*
Chlamydomonas reinhardtii CC-503 cw92 mt+	649488017	Mitochondrial carbonic anhydrase, beta type	648186377	*Gloeothece verrucosa PCC 7822*	*Bacteria; Cyanobacteria; Chroococcales*
Chlamydomonas reinhardtii CC-503 cw92 mt+	649410718	Photosystem II protein VI	648390068	*Limnospira indica PCC 8005*	*Bacteria; Cyanobacteria; Oscillatoriales*
Chlamydomonas reinhardtii CC-503 cw92 mt+	649410720	Photosystem II cytochrome *b6/f* complex subunit V	637799911	*Synechococcus elongatus PCC 7942*	*Bacteria; Cyanobacteria; Synechococcales*
Oxidative stress resistance					
Volvox carteri f. nagariensis 69-1b	2507998527	Peroxin-13	645816130	*Coprinopsis cinerea okayama7#130*	*Eukaryota; Basidiomycota; Agaricomycetes*
Volvox carteri f. nagariensis 69-1b	2507998720	Haem peroxidase	2506751490	*Thiothrix nivea JP2, DSM 5205*	*Bacteria; Proteobacteria; Gammaproteobacteria*
Chlorella variabilis NC64A	2507978793	Glutathione S-transferase	2504722272	*Pseudomonas fluorescens HK44*	*Bacteria; Proteobacteria; Gammaproteobacteria*
Chlorella variabilis NC64A	2507980056	Peroxiredoxin Q/BCP	645811546	*Coprinopsis cinerea okayama7#130*	*Eukaryota; Basidiomycota; Agaricomycetes*
Physcomitrella patens patens	649527966	Cysteine synthase A	640878576	*Parvibaculum lavamentivorans DS-1*	*Bacteria; Proteobacteria; Alphaproteobacteria*

(Continued)

TABLE 2 Continued

Plant recipient	Recipient gene accession (IMG)	Gene function	Donor gene accession (IMG)	Microbial donor	Donor taxon
Chlorella variabilis NC64A	2507979706	Glutaredoxin	2509193249	*Ectocarpus siliculosus Ec 32 (CCAP 1310/04)*	*Eukaryota; Phaeophyceae; Ectocarpales*
Chlamydomonas reinhardtii CC-503 cw92 mt+	649493089	Glutaredoxin, CGFS type	2508453811	*Saprolegnia parasitica CBS 223.65*	*Eukaryota; Oomycota; Saprolegniales*
Physcomitrella patens patens	649517225	L-glutamine synthetase (EC 6.3.1.2)	2505791185	*Runella slithyformis LSU4, DSM 19594*	*Bacteria; FCB group; Bacteroidetes*
Volvox carteri f. nagariensis 69-1b	2507994380	Homocysteine/selenocysteine methylase (S-methylmethionine-dependent)	651485911	*Rubrivivax benzoatilyticus JA2*	*Bacteria; Proteobacteria; Betaproteobacteria*
Zea mays mays cv. *B73*	2507869489	Glutamate synthase (NADPH/NADH)	649510728	*Physcomitrella patens patens*	*Eukaryota; Streptophyta; Bryopsida*
Glycine max cultivar Williams 82	2507946040	Glutamate synthase (NADH) large subunit (EC 1.4.1.14)	638941273	*Vibrio* sp. *MED222*	*Bacteria; Proteobacteria; Gammaproteobacteria*
Volvox carteri f. nagariensis 69-1b	2507995895	Folylpolyglutamate synthase	2508319981	*Micromonas pusilla NOUM17, RCC 299*	*Eukaryota; Chlorophyta; Mamiellophyceae*
Arabidopsis thaliana Columbia	649593200	Glutamate synthase (ferredoxin) (EC 1.4.7.1)	637875655	*Synechococcus* sp. *JA-2-3B'a(2-13)*	*Bacteria; Cyanobacteria; Synechococcales*
Arabidopsis thaliana Columbia	649604117	Glutamate synthase (ferredoxin) (EC 1.4.7.1)	640085243	*Prochlorococcus marinus NATL1A*	*Bacteria; Cyanobacteria; Synechococcales*
Chlamydomonas reinhardtii CC-503 cw92 mt+	649485827	Thiol-disulfide isomerase and thioredoxins	2508407653	*Spizellomyces punctatus DAOM BR117*	*Eukaryota; Chytridiomycota; Chytridiomycetes*
Populus balsamifera trichocarpa	649557489	Cytochrome-c oxidase	645666500	*Talaromyces marneffei ATCC 18224*	*Eukaryota; Ascomycota; Eurotiomycetes*
Ricinus communis Hale	649585270	Electron transfer flavoprotein beta subunit	646832083	*Methylotenera versatilis 301, JCM 17579*	*Bacteria; Proteobacteria; Betaproteobacteria*
Volvox carteri f. nagariensis 69-1b	2507995502	Ubiquinol-cytochrome *c* reductase cytochrome *b* subunit	640951028	*Rickettsia canadensis McKiel*	*Bacteria; Proteobacteria; Alphaproteobacteria*
Volvox carteri f. nagariensis 69-1b	2508002619	Menaquinol-cytochrome c reductase iron-sulfur subunit precursor	639801009	*Paenarthrobacter aurescens TC1*	*Bacteria; Actinobacteria; Actinomycetia*
Physcomitrella patens patens	649529911	*c*-type cytochrome synthesis protein Ycf5	641534169	*Microcystis aeruginosa NIES-843*	*Bacteria; Cyanobacteria; Chroococcales*
Arabidopsis thaliana Columbia	639588215	Cytochrome c oxidase assembly protein	639887067	*Synechococcus* sp. *BL107*	*Bacteria; Cyanobacteria; Synechococcales*
Chlorella variabilis NC64A	2507979399	Phytoene dehydrogenase	641347970	*Sorangium cellulosum So ce 56*	*Bacteria; Proteobacteria; Deltaproteobacteria*
Arabidopsis thaliana Columbia	639581518	Isocitrate dehydrogenase, NADP-dependent	637833532	*Hahella chejuensis KCTC 2396*	*Bacteria; Proteobacteria; Gammaproteobacteria*
Chlorella variabilis NC64A	2507984961	Thiamine biosynthesis protein ThiC	2509194402	*Ectocarpus siliculosus Ec 32 (CCAP 1310/04)*	*Eukaryota; Phaeophyceae; Ectocarpales*

(Continued)

TABLE 2 Continued

Plant recipient	Recipient gene accession (IMG)	Gene function	Donor gene accession (IMG)	Microbial donor	Donor taxon
Volvox carteri f. nagariensis 69-1b	2508000640	Thiamine pyrophosphate enzyme	651583914	*Sphingomonas* sp. *S17*	*Bacteria; Proteobacteria; Alphaproteobacteria*
Arabidopsis thaliana Columbia	639576678	Thiamine pyrophosphate protein	646441210	*Thermobaculum terrenum YNP1, ATCC BAA-798*	*Bacteria; Chloroflexi; Thermobaculum*
Chlorella variabilis NC64A	2507979588	Thiamine monophosphate synthase	2502685596	*Pontibacter actiniarum DSM 19842*	*Bacteria; FCB group; Bacteroidetes*
Chlorella variabilis NC64A	2507980977	Selenocysteine lyase	646501278	*Conexibacter woesei ID131577, DSM 14684*	*Bacteria; Actinobacteria; Thermoleophilia*
Chlorella variabilis NC64A	2507981240	Selenocysteine lyase	2508443779	*Saprolegnia parasitica CBS 223.65*	*Eukaryota; Oomycota; Saprolegniales*
Volvox carteri f. nagariensis 69-1b	2507997145	Selenocysteine lyase	2509158209	*Entamoeba histolytica HM-1:IMSS*	*Eukaryota; Evosea; Mastigamoebida*
Chlamydomonas reinhardtii CC-503 cw92 mt+	649484656	Selenophosphate synthase	2507499783	*Crocosphaera subtropica BH63E*	*Bacteria; Terrabacteria group; Cyanobacteria*
Chlorella variabilis NC64A	2507981440	Cobalamin synthesis protein cobW	640895065	*Roseiflexus castenholzii HLO8, DSM 13941*	*Bacteria; Chloroflexi; Chloroflexia*
Chlamydomonas reinhardtii CC-503 cw92 mt+	649491021	Cobalamin synthesis protein cobW	640596696	*Roseiflexus* sp. *RS-1*	*Bacteria; Chloroflexi; Chloroflexia*
Physcomitrella patens patens	649500991	Cobalamin synthesis protein cobW	649849043	*Pantoea* sp. *At-9b*	*Bacteria; Proteobacteria; Gammaproteobacteria*
Acid resistance					
Sorghum bicolor BTx623	2507715021	Spermidine/putrescine transporter	2509391205	*Rhizobium leguminosarum bv. trifolii WSM597*	*Bacteria; Proteobacteria;*
Volvox carteri f. nagariensis 69-1b	2508000101	Arginine deiminase ArcA (EC 3.5.3.6)	639619926	*Dictyostelium discoideum AX4*	*Eukaryota; Evosea; Eumycetozoa*
Chlamydomonas reinhardtii CC-503 cw92 mt+	649410730	Proton extrusion protein PcxA	640014237	*Lyngbya* sp. *PCC 8106*	*Bacteria; Cyanobacteria; Oscillatoriales*
Chlamydomonas reinhardtii CC-503 cw92 mt+	649494337	Arginine deiminase ArcA (EC 3.5.3.6)	649376570	*Naegleria gruberi NEG-M (Amoeba)*	*Eukaryota; Heterolobosea; Vahlkampfiidae*
Chlorella variabilis NC64A	2507979843	Carbamate kinase (EC 2.7.2.2)	643475399	*Rippkaea orientalis PCC 8801*	*Bacteria; Cyanobacteria; Chroococcales*
Chlamydomonas reinhardtii CC-503 cw92 mt+	649494190	Polyamine transporter 3	649064649	*Nannizzia gypsea CBS 118893*	*Eukaryota; Ascomycota; Eurotiomycetes*
Physcomitrella patens patens	649499876	Basic amino acid/polyamine antiporter, APA family/ solute carrier family 7 (L-type amino acid transporter), member 9	639684312	*Candidatus Solibacter usitatus Ellin6076*	*Bacteria; Acidobacteria; Acidobacteriia*
Physcomitrella patens patens	649531109	Argininosuccinate lyase	651569762	*Paenibacillus* sp. *HGF7*	*Bacteria; Firmicutes; Bacilli*
Ricinus communis Hale	649573998	Spermidine/putrescine transport system	2508732231	*Microvirga lupini Lut6*	*Bacteria; Proteobacteria;*
Ricinus communis Hale	649590952	Argininosuccinate synthase (EC 6.3.4.5)	640876950	*Parvibaculum lavamentivorans DS-1*	*Bacteria; Proteobacteria; Alphaproteobacteria*

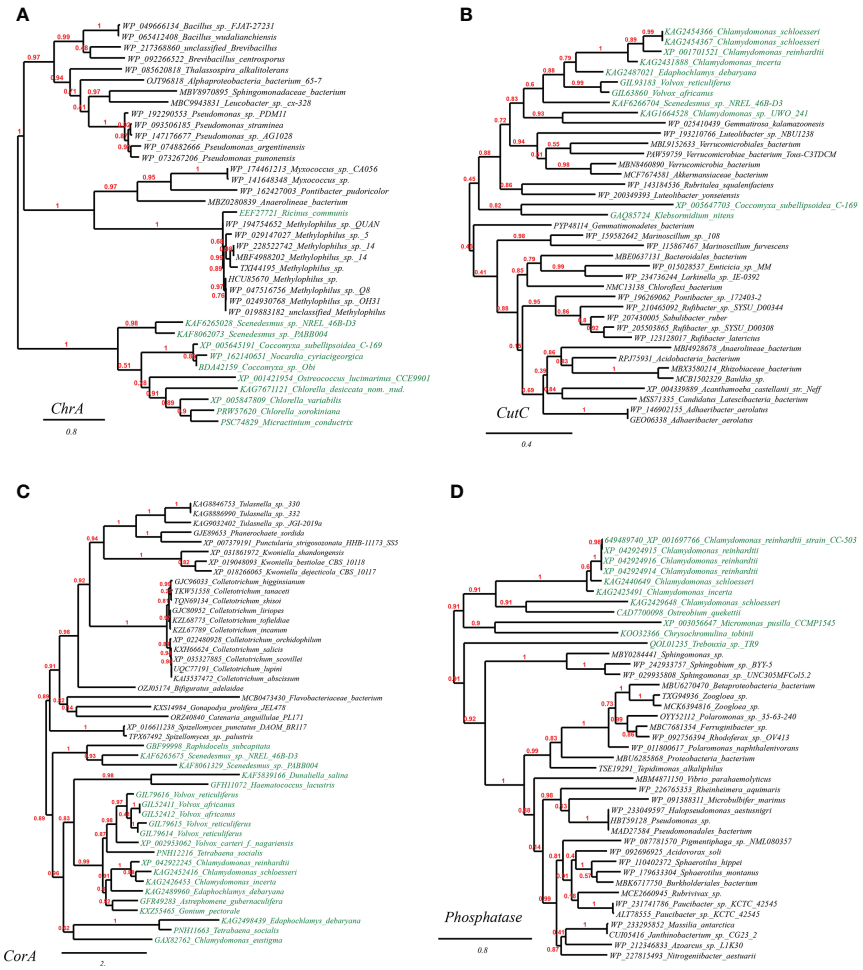

FIGURE 1
Phylogenetic tree of metal resistance proteins in plant genomes originated from microbial taxa. The phylogeny construction was conducted based on gene-translating protein sequences using PhyML program with the Maximum Likelihood (ML) method and 1,000 bootstrap replicates (with bootstrap values in red showing on respective branches). Branches leading to plant taxa are marked by green color, whereas those belonging to microbial lineages are in black: **(A)** chromate transporters (ChrA); **(B)** copper homeostasis protein (CutC); **(C)** magnesium and cobalt transport protein (CorA). **(D)** phosphatase.

Actinomortierella), and remotely with CPA1 from cyanobacteria and actinobacteria (Figure 2A). Likewise, the well-supported phylogenetic tree of Na^+/solute symporter placed green algae/plant homologues (e.g., *Scenedesmus*, *Coccomyxa*, and *Klebsormidium*) in the vicinity of those of fungi (e.g., *Batrachochytrium, Podila, Mortierella*) (Figure 2B). Similarly, in the well-supported phylogenetic tree of ClcA (Figure 2C), homologues from *Chlorella* spp. (green algae) clustering with several homologues of other green algae (e.g., *Chlamydomonas*, *Micractinium*), are embedded in branches derived from archaeal taxa of phylum Euryarchaeota (*Methanobacteriales, Methanomassiliicoccales*) and high G+C Gram-positive bacterial taxa (e.g., *Pseudonocardia* spp., *Mumia* spp. and *Microbacterium* spp.), suggesting the occurrence of cross-phylum HGT. Finally, the phylogenetic tree of RmlB indicates that *Chlorella virus Acanthocystis turfacea* has facilitated the transitions of RmlB encoding genes (Figure 2D), in consistence with previous studies (Parakkottil et al., 2010).

HGT genes in response to heat and cold stress

Large fluctuations in environmental temperature caused by inconstant global climate also render severe abiotic impacts (heat and cold stress) on plants. To cope with such conditions, gene inventions and expansions of heat/cold shock factor gene families into plant genomes are constantly happening during adaptive evolution (Wang et al., 2018; Li et al., 2021). In this study, we have also detected in tested plant genomes a wide

range (26 gene entries) of microbial-originated HGT gene families related to heat/cold shock response (Table 2), which mainly function as transcription factors and molecular chaperones regulated by the former, working corporately to maintain cellular protein homeostasis (Andrási et al., 2021). In addition, it is reported that chitinase is also involved in plants' cold and osmotic stress responses (Cao et al., 2019), and correspondingly, HGT gene entries encoding chitinases are also detected (Table 2). In addition, we have discovered HGT genes encoding ribulose 1,5-bisphosphate carboxylase large subunit (Rubisco), carbonic anhydrase (CA), and photosystem II proteins putatively acquired from Bacteria (Table 2). It is possible that plants might depend on generating more photosynthesis-related protein copies as a remedy strategy to cope with the impaired CO_2-fixing efficiency resulted from malfunction of heat-liable Rubisco under heat-stress conditions (Nouri et al., 2015).

As before, we chose and performed phylogenetic analyses on several such genes to illustrate the likely evolutionary path. The first gene query is heat-shock protein DnaJ, which is reported to protect Rubisco activity under heat stress (Wang et al., 2015). As expected, we found that DnaJ proteins from a group of green algae (e.g., *Chlamydomonas*, *Tetrabaena, Edaphochlamys*, *Volvox*) and eudicots (*Erigeron canadensis*) (Figure 3A, marked with green color) are placed just next to homologues from bacterial lineages (e.g., *Phycisphaerae, Anaerolineae, Pseudanabaenaceae*). The second tested gene is heat shock protein Hsp20 (Figure 3B). Likewise, a group of green algae (e.g., *Chlorella*, *Micractinium, Scenedesmus*) is located in the well-supported tree of Hsp20 next to various bacterial taxa (e.g., *Marinobacter* spp., *Marinimicrobia*, *Nitrospirae*). The final case present the phylogeny of typical cold-shock protein CspA that promotes the correct folding of RNA molecules (Rennella et al., 2017). We found that several CspA-like proteins from eudicots

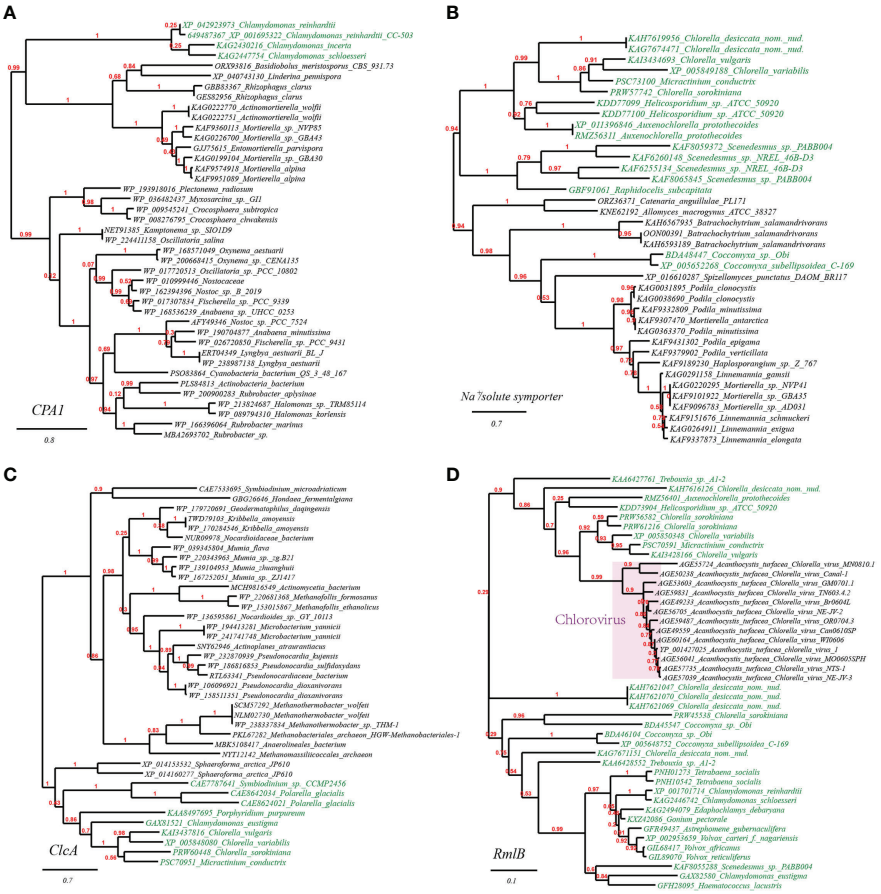

FIGURE 2
Phylogenetic tree of osmotic and drought stress resistance proteins in plant genomes originated from microbial taxa. The phylogeny construction was conducted based on gene-translating protein sequences using PhyML program with the Maximum Likelihood (ML) method and 1,000 bootstrap replicates (with bootstrap values in red showing on respective branches). Branches leading to plant taxa are marked by green color, whereas those belonging to microbial lineages are in black. **(A)** sodium/proton antiporter (CPA1); **(B)** Na^+/solute symporter; **(C)** chloride channel protein (ClcA); **(D)** dTDP-D-glucose 4,6-dehydratase (RmlB).

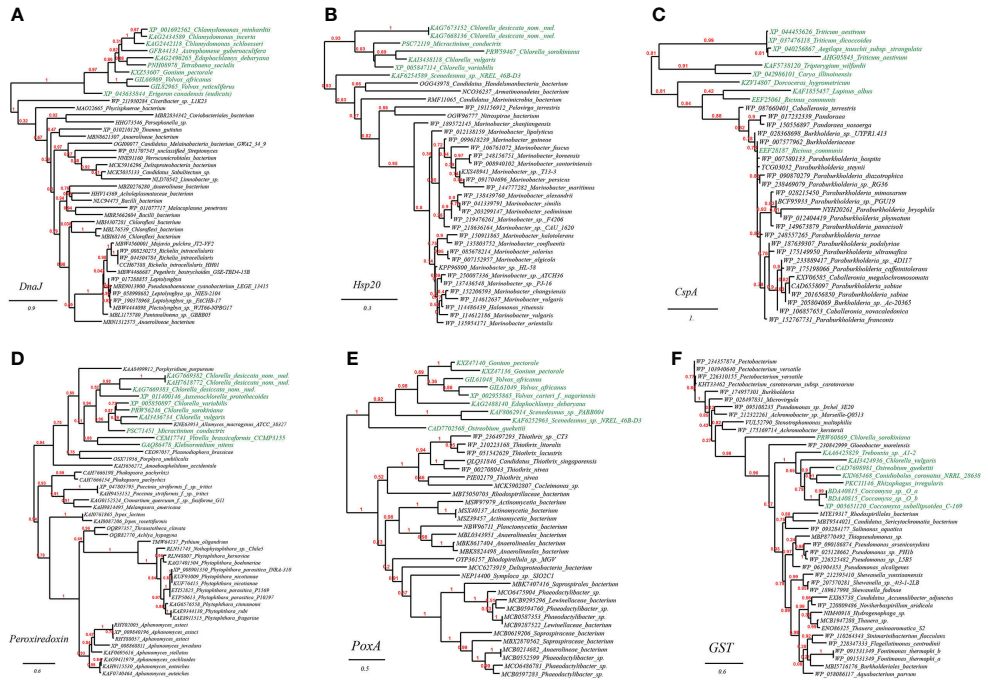

FIGURE 3
Phylogenetic tree of heat and cold stress as well as oxidative stress resistance proteins in plant genomes originated from microbial taxa. The phylogeny construction was conducted based on gene-translating protein sequences using PhyML program with the Maximum Likelihood (ML) method and 1,000 bootstrap replicates (with bootstrap values in red showing on respective branches). Branches leading to plant taxa are marked by green color, whereas those belonging to microbial lineages are in black: **(A)** heat-shock protein DnaJ; **(B)** heat shock protein Hsp20; **(C)** cold-shock protein CspA; **(D)** peroxiredoxin; **(E)** heme peroxidase (PoxA); **(F)** glutathione S-transferase (GST).

(e.g., *Ricinus communis*, Lupinus albus) are in close homology to CspA proteins from *Betaproteobacteria* lineages (e.g., *Burkholderiaceae, Methylophilaceae*) (Figure 3C). Together, these phylogenetic relations might be existing molecular evidence supporting the HGT origins of plant abiotic resistance genes.

HGT genes resisting oxidative stress

Oxidative stress resulting from the excessive generation of reactive oxygen species (ROS) that damage cellular biomolecules, including proteins, DNA, lipids, and carbohydrates, is the usual consequence of miscellaneous abiotic stresses in plants mentioned above (e.g., drought (Niu et al., 2021), osmotic pressure (Cai-Hong et al., 2005), toxic metal stress (Schützendübel and Polle, 2002)). As illustrated in our results (Table 2), it seems a potential strategy for plants to cope with the omnipresent oxidative stresses by obtaining directly from nearby microorganisms relevant resistance genes belonging to the canonical antioxidant machinery (e.g., hame peroxidase, glutaredoxin, thioredoxin, peroxin, peroxiredoxin, glutathione-S-transferase, cysteine synthase and glutamate/glutamine synthase) (Gill and Tuteja, 2010; Hasanuzzaman et al., 2019). Furthermore, miscellaneous HGT genes encoding components of oxidative electron transfer chain such as cytochrome oxidase (an oxygen-reducing reducing proton-pump) were also discovered (Table 2), which are suggested to be involved in oxidative stress and acid stress tolerance (de la Garza-García et al., 2021). In addition, also discovered in tested plant genomes were bacteria/fungi-originated genes encoding an isocitrate dehydrogenase (in *Arabidopsis thaliana*), which might supply reductant NADPH to defend against oxidative stress (Komatsu et al., 2014), a phytoene dehydrogenase (in *Chlorella variabilis*) that converts phytoene into antioxidant carotene, a homocysteine S-methyltransferase (in *Volvox carteri*) that generates antioxidant methionine, as well as genes related to biosynthesis of antioxidant vitamins thiamine and cobalamin in multiple plants (Rosado-Souza et al., 2020; Vásquez et al., 2022), as well as selenophosphate synthase and selenocysteine lyase putatively conferring oxidative stress protection (Costa et al., 2011) (Table 2).

As verified through phylogenetic analysis, the tested HGT genes in plants are all faithfully clustering with distant microbial taxa (the HGT donors), showing strong HGT signs (Figure 3). To be specific, in the well-supported phylogenetic tree of

peroxiredoxin, homologues from the green algae (e.g., *Chlorella, Auxenochlorella, Micractinium*) and charophytic algae *Klebsormidium* are embedded in those from fungi (e.g., *Phakopsora, Puccinia, Irpex*), which indicated that the green algae might have gained peroxiredoxin genes through gene exchange from nearby fungi (Figure 3D); Similarly, as seen from the reconstructed phylogeny of heme peroxidase (PoxA), a group of green algae (e.g., *Gonium, Volvox, Scenedesmus, Ostreobium*) is placed in the vicinity of multiple bacterial lineages (e.g., *Thiothrix, Rhodospirillaceae, Anaerolineales*) (Figure 3E); Lastly, in the phylogeny of glutathione S-transferase (GST), homologues from the green algae (e.g., *Chlorella*, *Rhizophagus, Coccomyxa*) are enveloped by those from multiple bacterial lineages (e.g., *Pseudomonas, Achromobacter, Burkholderiales*), again, suggesting the cross-kingdom HGT of GST genes among such taxa (Figure 3F).

HGT genes contributed to pH homeostasis

Environmental pH is considered as an important factor for plants since it influences soil physical, chemical properties and nutrient availability and thereby affects plant inner homeostasis and growth (Zhou et al., 2022). Interestingly, we have excavated seven microbe-derived gene entries linking with pH homeostasis maintenance and acid stress resistance in five tested plant genomes (Table 2): two basic amino acid/spermidine/putrescine transporter and a proton extrusion protein (PcxA) encoding genes acquired from Bacteria, and genes within the arginine deiminase pathway (argininosuccinate synthase, argininosuccinate lyase, carbamate kinase and arginine deiminase) derived from Bacteria and Amoeba, which might conduct pH regulation by neutralization of proton with base substrates like ammonia, arginine and polyamine. Besides, the mentioned osmotic stress resistance ion/proton transporter above might also take part in adaptive responses to pH perturbation.

We further selected and constructed the phylogeny of two representative HGT genes, which encode arginine deiminase (ArcA) in *Volvox carteri* (chlorophyte algae) and basic amino acid/polyamine antiporter (YhdG) in *Physcomitrella patens* (mosses), to test the reliability of the HGT inference (Figure 4). Consistency, the well-supported phylogenetic tree constructed with not-exclusive top hit entries showed that ArcA homologues of *Volvox* spp. are clustering with those of several green algae affiliations like *Scenedesmus* spp., *Chlamydomonas* spp., and *Chlorella* spp. etc. (Figure 4A, marked with green color), which are wholly embedded in homologous sequences from protist (e.g., *Carpediemonas, Fonticula, Plasmodiophora* and *Naegleria* etc.), the most likely cross-phylum HGT donor(s), and also, remotely associated with a cluster of Bacteria (e.g., *Desulfobacterales*). Likewise, the well-supported phylogenetic tree of YhdG showed that homologues of *Physcomitrella*, closely clustering with homologues of other mosses (e.g., *Sphagnum* spp., *Ceratodon purpureus*), liverworts (*Marchantia* spp.), and a green plant (*Klebsormidium nitens*), are nested within homologues of fungi (e.g., *Mucor* spp. and *Aspergillus* spp.) and bacteria (e.g., *Acidobacteria*, *Aminicenantes* and *Solimonas*), strongly indicating that cross-phylum HGTs might contribute to the spread of YhdG from microbes to plants (Figure 4B).

HGT genes contribute to ultraviolet light damage resistance

The plant DNA can be damaged by various abiotic factors such as chemical mutagens or ultraviolet (UV) light radiation due to long-term sun exposure, which would induce oxidative damage and cross-links (DNA–protein or DNA–DNA). The accumulation of such damages in the plant would ultimately cause genomic instability and cell death (Tuteja et al., 2009). Apart from cellular DNA-damage response pathways encoded by plants themselves, our results suggested that many plants have also recruited plenty of genes with functions related to DNA repair/replication/recombination (68 gene entries, see Table S1A at https://doi.org/10.6084/m9.figshare.20530083.v1). For example, we have also found in the reconstructed phylogeny of UvrD, a DNA helicase involved in excision repair of UV-induced DNA damage, that green algae homologues (e.g., *Micractinium*, *Chlorella*, *Raphidocelis*) are placed in the vicinity of homologues from cross-phylum *Streptomyces* spp. (fungi), which indicated the occurrence of HGT event (Figure 4C); Likewise, we found that several green algae (e.g., *Volvox*, *Chlorella*, *Chlamydomonas*) contain Rad25, a DNA helicase required for DNA repair and RNA polymerase II transcription, which is in close sequence homology to that from fungi (e.g., *Podila, Lactarius, Auriculariopsis*) (Figure 4D).

HGT genes contribute to organic pollutant resistance

Organic soil pollution discharged by anthropogenic processes like herbicides overuse and chemical waste mismanagement can threaten the life of plants, and the association of endophytic or mycorrhizal microbes with host plants can reduce the harmful effect of organic pollutants to plant (Sun et al., 2015; Rajtor and Piotrowska-Seget, 2016). Interestingly, we found that plants have integrated various enzymes related to organic pollutant catabolism and several multidrug transport proteins into their genomes, such as cytochrome P450s, laccase, beta-lactamase, alkanesulfonate monooxygenase, haloperoxidase, most likely through HGT from nearby microbes (81 gene entries, see Table S1B at https://doi.org/10.6084/m9.figshare.20530083.v1). The most

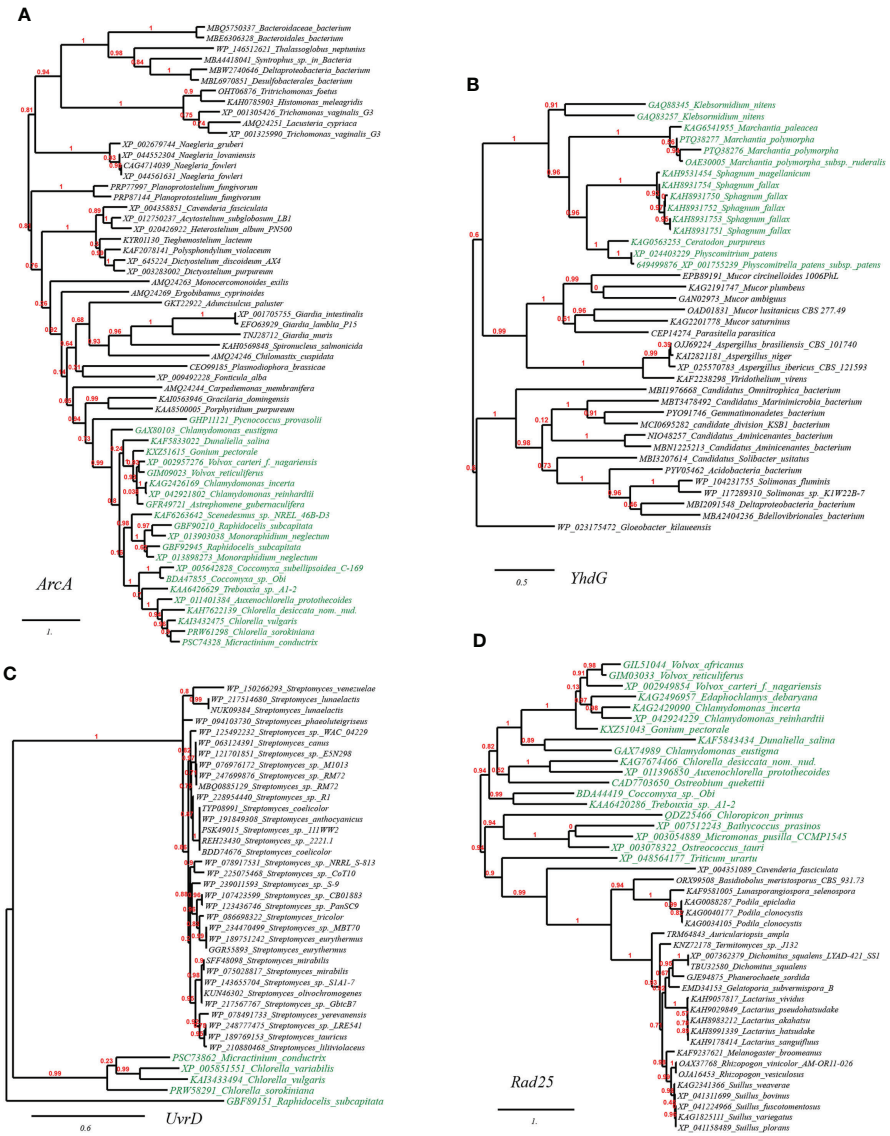

FIGURE 4
Phylogenetic tree of acid resistance and DNA damage resistance proteins in plant genomes originated from microbial taxa. The phylogeny construction was conducted based on gene-translating protein sequences using PhyML program with the Maximum Likelihood (ML) method and 1,000 bootstrap replicates (with bootstrap values in red showing on respective branches). Branches leading to plant taxa are marked by green color, whereas those belonging to microbial lineages are in black. **(A)** arginine deiminase (ArcA); **(B)** basic amino acid/polyamine antiporter (YhdG); **(C)** chloride channel protein (ClcA); **(D)** dTDP-D-glucose 4,6-dehydratase (RmlB).

commonly-seen HGT enzyme of these, cytochrome P450 (CytP450, six gene entries), is a group of oxygenase enzymes that can catalyze the catabolism of a wide range of organic pollutants using oxygen as the electron acceptor, undergoing various detoxification reaction, including hydroxylation, N-, O-, S-dealkylation, sulfurization, epoxidation, deamination, desulfurization, dehalogenation, peroxidation, and N- oxide reduction (Lin et al., 2022). In addition to microbial CytP450, two laccases for removal of phenolic pollutants (Asadgol et al., 2014) were found in the genomes of *Chlamydomonas reinhardtii* and *Arabidopsis thaliana*, respectively, putatively acquired from fungi. While other organic degradation oxidases we found acquired by plants from microorganisms might target more specific organic compounds, such as alkanesulfonate, amine and beta-lactams (see Table S1B at https://doi.org/10.6084/m9.figshare.20530083.v1).

As before, the HGT possibility was tested on representative genes. In the well-supported phylogenetic tree using CytP450 from *Chlamydomonas reinhardtii* (XP_001698815) as query and constructed with not-exclusive top 100 BLASTP hit entries

showed that CytP450 homologues of green algae (e.g., *Chlamydomonadales, Trebouxiales, Chlorellales, Sphaeropleales*), along with several homologues from eudicots (*Pentapetalae*), are placed in the neighborhood of homologues from cyanobacteria (e.g., *Synechococcales, Nostocales, Pseudanabaenales*), clearly indicating the occurrence of cross-kingdom HGT events that have facilitated the acquisitions and spread of organic pollutant catabolism enzyme CytP450 from lower-grade microbial lineages to various plant taxa (Figure 5A).

Assessment of the functionality of HGT genes

To assess if the above-mentioned abiotic resistance genes in plants are functioning normally in plants, we resorted to protein structure analysis methods to assess fold reasonability on one hand and codon adaption index (CAI) calculation for prediction on gene expression potential of the abiotic stress resistance genes on the other hand.

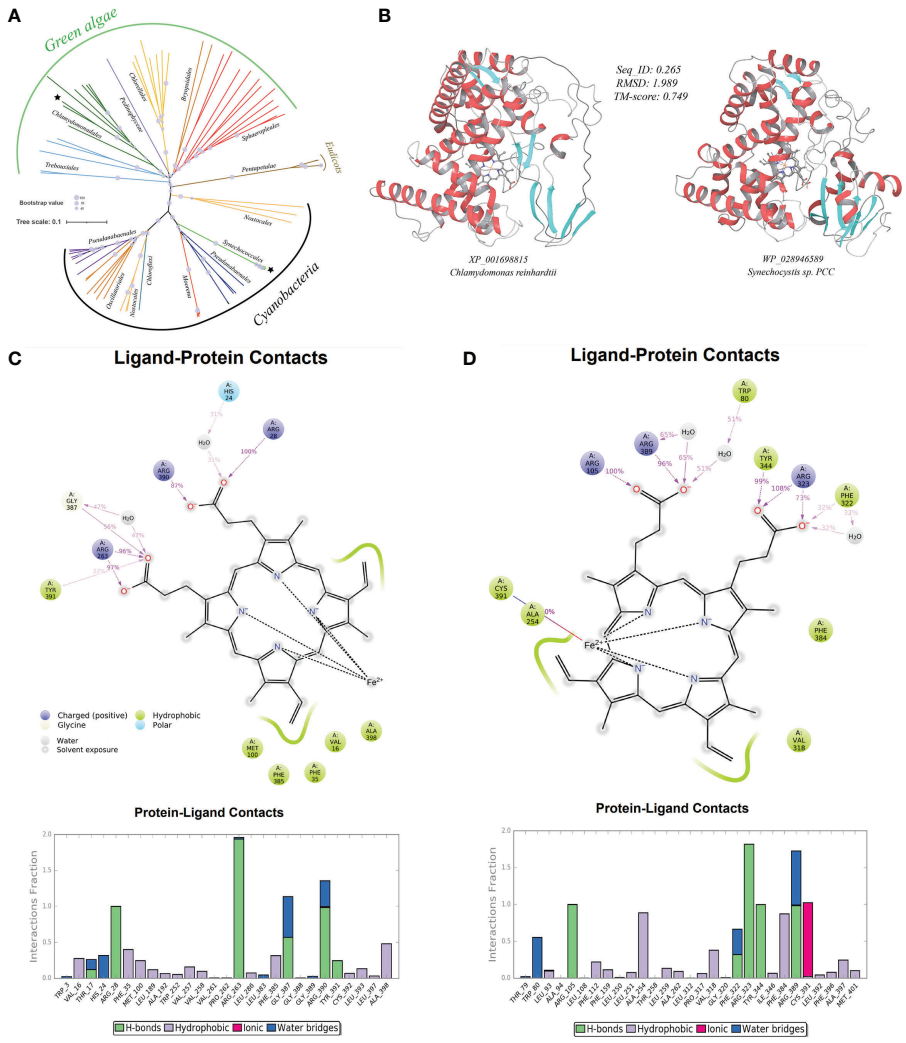

FIGURE 5
A case-study of microbe-originated plant cytochrome P450 and its donor protein. **(A)** Phylogenetic tree of the organic pollutant catabolism protein cytochrome P450 constructed by PhyML program with the Maximum Likelihood (ML) method and 1,000 bootstrap replicates (with bootstrap values shown by size of symbols); **(B)** structure perdition (deep-learning-driven) and comparison of representative recipient plant cytochrome P450 (left, *Chlamydomonas reinhardtii*: XP_001698815) and its putative microbial donor (right, *Synechocystis* sp. PCC: WP_028946589); **(C)** ligand-protein simulation diagram (5 ns classical molecular dynamics) of cytochrome P450 from *Chlamydomonas reinhardtii* (XP_001698815) showing key residues in proteins interacting with the hame prothetic group (ligand). Interactions that occur more than 30.0% of the simulation time in the selected trajectory (0.0 through 5.0 ns), are shown; **(D)** ligand-protein simulation diagram (5 ns classical molecular dynamics) of the cytochrome P450 from donor *Synechocystis* sp. PCC (WP_028946589) showing key residues in proteins interacting with the hame prothetic group (ligand) for comparison.

We first tested if proteins encoded by such HGT-originated abiotic stress resistance genes in plant genomes can fold themselves into reasonable three-dimensional (3D) structures conveying acknowledged molecular functions. With the aid of the excellent deep-learning-driven structure prediction programs, AlphaFold2 (Jumper et al., 2021) and RoseTTAFold (Baek et al., 2021), we have generated full-length structure predictions of proteins encoded by all detected microbe-originated HGT genes in plants related to abiotic stress resistance in this study. The outcoming models of both methods in this test are available at https://doi.org/10.6084/m9.figshare.20530026.v1. The TM-align-based comparison showed that the predicted models from both methods (AlphaFold2 and RoseTTAFold) agreed well with each other, giving an average pairwise TM-score of 0.80 (TM-score > 0.5 indicates similar fold), indicating that our protein structural models are very reliable. We further used such protein models as inputs of the deep-learning-driven structure-based protein functional annotation program DeepFRI (Gligorijević et al., 2021) for functional assessment. Results showed that about 68.5% molecular function annotations of these HGT-driven proteins have reliable confident scores above the DeepFRI significance cutoff score of 0.5 (see Table S1C at https://doi.org/10.6084/m9.figshare.20530083.v1), strongly indicating that most of the aforementioned HGT-originated abiotic stress resistance proteins can fold themselves into a correct, recognizable, and functional 3D topology. Furthermore, TM-align-based structural alignments of the 3D models of protein homologue from corresponding microbial donors built by the same deep-learning method (The outcoming models are available at https://doi.org/10.6084/m9.figshare.20530026.v1) to the plant HGT-driven abiotic stress resistance proteins also reveal similar fold with a relatively high average pairwise TM-score of 0.72 (see Table S1D at https://doi.org/10.6084/m9.figshare.20530083.v1). To give more impression, we provided here a case study of the above-mentioned CytP450 from *Chlamydomonas reinhardtii* (Figure 5B). Comparisons of the CytP450 protein structure from the plant representative with that from the predicted microbial donor representative (*Synechocystis* sp. PCC) reveal a pair of folds showing highly identical topology with pairwise TM-score of 0.75 and average root mean square deviations (RMSD) of 1.99 Angstrom (Å). Resemblance was further found as we compared ligand-protein interaction patterns of these two structures by conducting classical molecular dynamics for 5 ns (Figures 5C, D). Results showed that both proteins used conserved residues like positively charged Arg and aromatic Tyr, Phe for ligand interactions throughout the simulation, suggesting strong evolutionary connection and reaction feasibility. Similar fold resemblances were found in structures derived from other pairs of HGT genes (see Figure S1 at https://doi.org/10.6084/m9.figshare.21008905.v1).

Due to translational selection, genes with high expression level generally have a stronger codon bias than those expressed at lower levels (Hiraoka et al., 2009; Zhou et al., 2013). The codon adaption index (CAI) initially proposed by Sharp and Li (1987) can measure synonymous codon usage bias for a tested gene sequence by comparing the similarity between the synonymous codon usage of a gene and the synonymous codon frequency of validated highly expressed reference gene sets. CAI value ranges from 0 and 1, with higher value indicating higher synonymous codon usage similarity with the reference/higher expression level (Puigbò et al., 2008). The CAI method has been successfully used in various areas, such as the predictions on expression likelihood (Puigbò et al., 2007; Puigbò et al., 2008) and level (Li et al., 2019) of heterologous/HGT gene, and deduction of lifestyles based on genomic data (Willenbrock et al., 2006). In this study, the expression levels of all predicted HGT genes conferring abiotic stress resistance in the plant genomes were assessed utilizing the codon adaption index (CAI) as a numerical estimator. Results showed that many HGT-driven abiotic stress resistance genes in plant genomes possess relatively high CAI values (Figure 6): averagely, metal resistance (0.683), osmotic and drought stress resistance (0.682), acid resistance (0.712), heat and cold stress resistance (0.697), UV light damage resistance (0.702), and organic pollutant resistance (0.681). The HGT genes related with pH homeostasis and DNA repair have relative higher CAI values, which might indicate that the pH turbulence and UV light radiation are the most commonly encountered abiotic stresses.

Together, it means that the strategy of acquisitions of abiotic stress resistance genes by plants from microbes to enhance adaption might be successful and significant as far as our results corroborate.

Discussion

In this study, we have discovered an abundant repertoire of putative microbial-originated genes in 14 tested plant genomes that confer resistance to a wide range of abiotic stresses commonly encountered by plants, with the putative microbial HGT donors spanning from viruses, bacteria, fungi to protists (Table 2 and see Table S1 at https://doi.org/10.6084/m9.figshare.20530083.v1). We have also applied in-silico approaches to verify the accuracy of blast-based HGT inference (phylogenetic analyses), the functionality of the 3D protein fold encoded by such HGT genes (deep-learning-driven protein structure prediction, fold alignment, molecular dynamics etc.), and the expression potential of HGT genes (codon adaption index calculation).

The emergence and mechanism of HGT events ("Why does lateral transfer occur in so many species and how?") is recommended as a still-pending and significant scientific question worthy of more in-depth ivestigations by the editorial of the journal Science in the article "So much more to know" (American Association for the Advancement of Science, 2005), and we prudently considered that the present research might have supplied some hints for this question. HGT can serve as a

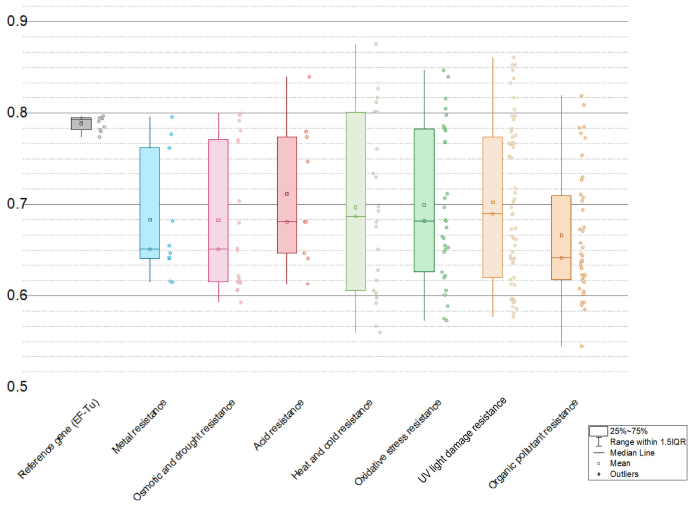

FIGURE 6
Ranges of codon adaption index (CAI) values of different kinds of abiotic resistance genes with EF-Tu gene as a reference.

significant force that supplies species with genetic innovations and regulation flexibility that guarantees successful migration into novel niches. In our results, we found that the most commonly seen microbial HGT donor taxon for acquisition of resistance genes is *Burkholderiaceae* (n=10). Members of *Burkholderiaceae* are characterized as plant-associated, which usually constitute the core floral community (Massoni et al., 2021). Besides, we found that *Chlorophyta* taxa (e.g. *Chlorella variabilis* NC64A, n=42) generally have more HGT resistance genes than lower-grade *Streptophyta* taxa (e.g. *Physcomitrella patens patens* (moss), n=21), which outnumber those from high-grade land plant (e.g. *Ricinus communis Hale* (castor bean), n=14). Such richness of HGT genes associated with abiotic stress resistance especially those within the transition-stage lineages might have reflected a ring linking to the early adaption processes of plant to accomplish the colonization of land environment from aquatic. These HGT genes seem well-suited to combat abiotic factors more frequently encountered in land environments (e.g., desiccation, fluctuations of temperature, UV radiation), in consistence with previous studies (de Vries et al., 2016; Pennisi, 2019; Bowles et al., 2020). The mechanism leading to such abundant cross-lineage gene transfer into plant genomes might be explained by the "weak-link model" (Huang, 2013). Namely, foreign DNA fragments (e.g., from microbes) could be naturally imported into the plant receptors at the susceptible stages in plant lifecycle, such as the single-cell/preliminary stages (germline cells, embryos, etc.) or dedifferentiation/asexual reproduction stages. The microbe-plant HGT processes can be promoted by intimate or direct physical contact through symbiosis, parasitism, infection, or other associations, especially when the weakly-protected cells are exposed to the environment. Once getting into the cell, fixation of HGT genes to the recipient genome can be facilitated by the still undergoing organellar DNA fragment integrations into the nuclear chromosome in the developing cells, followed by vertical transfer of integrated HGT genes to offspring cells *via* mitosis (Huang, 2013).

Concerns regarding such cross-lineage HGT genes might be the authenticity of both HGT direction and identification during the inference and the functionality of such HGT genes in the plant genomes. It has been argued that some of such HGT genes in the eukaryotic genome might result from endosymbiotic origin or contamination (Koutsovoulos et al., 2016).

To alleviate these concerns, we have integrated into our study the "gold standard" verification for the detected HGT genes: that a particular gene has been gained through HGT from a different lineage would be phylogenetic incongruence, where an evolutionary tree for a specific protein family is distinct from the established organismal phylogeny (Schönknecht et al., 2014). For example, the well-supported phylogenetic tree of chromate transporters (ChrA) (Fig. 1a) shows the protein sequence from *Ricinus communis* and green algae embedded within bacterial sequences. The most parsimonious explanation for this phylogenetic distribution is HGT from bacteria. Regarding the direction of the gene acquisition (microbe to plant instead of the reverse), it is ensured through the HGT detection pipeline IMGAP v.5.0 that only selects HGT candidate genes showing the best hits outside the taxonomic lineage of the tested genome (i. e. from distant phylum, class, etc.), but with lower-scoring or no hits within the lineage of the tested genome. The precise method for identification of HGTs by the IMGAP pipeline has been expatiated by Markowitz et al. (2010).

Furthermore, our supplemented phylogenetic analyses have also supported the direction of the predicted HGTs. As for

excluding the possibility of false positive induced by contamination, we included in our analyses only high-quality complete (or near-complete) genome assemblies of plants (Table 1), and our phylogenetic analyses further indicate that the historical HGT events not only occurred once but also can be confidently identified in cases in related plant taxa. For example, in the well-supported phylogenetic tree of copper homeostasis protein (CutC), the HGT-driven homologues were detected in a range of different green algae (from *Chlamydomonas* on the top of the tree to *Coccomyxa* inserted in the middle of the tree), again intertwined with branches leading to bacteria taxa. This suggested that such HGT events should be very likely actual since the probability that the said green algae's genome sequences happen to contaminate simultaneously the same kind of DNA fragments in lab is minor.

As for the functionality of the HGT genes in the plant genomes, we have resorted to multiple methods (e.g., structure analysis and codon adaption index calculation) to illustrate the functionality of the HGT genes related to plant abiotic stress resistance. In line with our results, previous studies have experimentally verified that many horizontally transferred genes in plants *Orobanchaceae, Cuscuta* and *Rafflesia* are being expressed (Xi et al., 2012; Yang et al., 2016; Vogel et al., 2018; Yang et al., 2019). What's even more surprising is that twelve of the HGT genes in *Alloteropsis semialata* (grass) genome have a higher expression level than their native homologues, and in one case, the native copy was replaced by the foreign one (Dunning et al., 2019). In consistence, our CAI calculation results also supported relatively high expression levels across the microbe-originated abiotic stress resistance genes in plants, which emphasized their significant functions in supporting the growth of the plant host in the face of harsh abiotic conditions.

In summary, the microbe-originated HGT genes in plant genomes identified in our analyses and their participation in resistance against diverse abiotic pressures commonly encountered in land environments indicate a widespread and profound impact of HGT on the evolution of plants and other eukaryotes. Still, our analysis presented here is not exhaustive. We believe that the microbe-to-plant HGT cases discovered by far stand for only the tip of the profound evolutionary iceberg. As more and more genomic sequences of superior quality become available for wider lineage branches in the tree of plants, it is foreseeable that future research will provide us with a more exciting panorama illustrating both the extent and the evolutionary significance of HGT in plants thoroughly.

Materials and methods

Fourteen high-quality eukaryotic plant genomes covering major plant taxa (clade *Viridiplantae*) within phyla *Chlorophyta* and *Streptophyta*, as listed in Table 1 were chosen and downloaded from the public database (Genbank/IMG) for downstream analyses. Identification of horizontally transferred genes in the genomes of plant genomes was conducted through the Integrated Microbial Genomes Annotation Pipeline (IMGAP) v.5.0 (Markowitz et al., 2010), which defined genes in tested plant genomes as having been horizontally transferred from a distant lineage with the principle: genes that have the best BLASTP hits (highest bit scores) or >90% of the best hits found outside the taxonomic lineage of the tested genome (i.e., from distant phylum, class, etc.) and with lower-scoring hits or no hits within the lineage.

The phylogeny of different kinds of abiotic resistance gene was constructed based on gene-translating protein sequences using PhyML program (Guindon et al., 2010) at http://www.phylogeny.fr/simple_phylogeny.cgi with the Maximum Likelihood (ML) method and 1,000 bootstrap replicates (with bootstrap values in red showing on respective branches) and visualized with iTOL (Letunic and Bork, 2021) at https://itol.embl.de/. Sequences were aligned with MUSCLE (Edgar, 2004) and trimmed with Gblocks (Talavera and Castresana, 2007) prior to tree construction.

AlphaFold2 (Jumper et al., 2021) and RoseTTAFold (Baek et al., 2021) were applied to generate the full-length 3D structure of proteins encoded by targeted HGT genes in plant genomes and their suggested donors, following guidance from https://github.com/deepmind/alphafold and https://github.com/RosettaCommons/RoseTTAFold. Docking of ligands into respective protein structure was conducted with AutoDock Vina v.1.2.0 (Trott and Olson, 2010). Molecular dynamics (MD) simulations for the targeted protein-ligand complex were performed using the Desmond Molecular Dynamics System, version 3.6, (D. E. Shaw Research, New York, NY, 2008) with OPLS_2005 force field (with default parameters) and visualized by Visual Molecular Dynamics (VMD) software v.1.9.4 and LigPlot+ (Laskowski and Swindells, 2011). DeepFRI (Gligorijević et al., 2021) was further applied for reliable structure-based functional annotation verify recognizable functional folds in the proteins encoded by the HGT genes related to abiotic pressure resistance in plant genomes.

Codon adaption index (CAI) was used as a numerical estimator of gene expression level (Hiraoka et al., 2009; Zhou et al., 2013), and correspondingly, the webserver CAIcal (Puigbò et al., 2008) (http://genomes.urv.es/CAIcal/calc.php) was applied to calculate respective CAI values of HGT genes in plant genomes participating in resistance of diverse abiotic pressures with the EF-Tu gene (the elongation factors) as refence, which is supposed to be highly expressed across most organisms (Puigbò et al., 2008), as conducted previously (Li et al., 2019). Besides, the Origin Pro 2020 software (OriginLab, Northampton, MA, USA) was used for data analysis and figure creation.

Data availability statement

The data presented in the study are available in the Genbank and IMG repositories under accession numbers provided in Table 1.

Author contributions

LL, and HY conceived and designed the research. LL, SP, ZW, TZ, HL, YX, JL and YL analyzed the data. LL wrote the manuscript. All authors contributed to the article and approved the submitted version.

Funding

This research was supported by the key project of Science and Technology of Hunan Branch of China National Tobacco Corporation (202104, XX2022-2024Aa01, HN2021KJ05, 20-22A02, HN2020KJ02), the key research and development program of Hunan Province (grants no. 2020WK2022, 2022SK2076), the National Natural Science Foundation of China (NSFC) (No. 41807332), Fundamental Research Funds for the Central Universities of Central South University (no. 2022ZZTS0420) and Hunan International Scientific and Technological Cooperation Base of Environmental Microbiome and Application (No. 2018WK4019).

Acknowledgments

We are grateful for resources from the High-Performance Computing Center of Central South University.

Conflict of interest

Author ZW is employed by Zhangjiajie Tobacco Company of Hunan Province. Author TZ is employed by Hunan Urban and Rural Environmental Construction Co., Ltd. Authors YX and JL are employed by Chenzhou Tobacco Company of Hunan Province.

The remaining authors declare that the research was conducted in the absence of any commercial or financial relationships that could be construed as a potential conflict of interest.

The authors declare that this study received funding from Science and Technology of Hunan Branch of China National Tobacco Corporation. The funder was not involved in the study design, collection, analysis, interpretation of data, the writing of this article, or the decision to submit it for publication.

Publisher's note

All claims expressed in this article are solely those of the authors and do not necessarily represent those of their affiliated organizations, or those of the publisher, the editors and the reviewers. Any product that may be evaluated in this article, or claim that may be made by its manufacturer, is not guaranteed or endorsed by the publisher.

Supplementary Material

The Supplementary Material for this article can be found online at: https://doi.org/10.6084/m9.figshare.20530083.v1

References

András, N., Pettkó-Szandtner, A., and Szabados, L. (2021). Diversity of plant heat shock factors: Regulation, interactions, and functions. *J. Exp. Bot.* 72, 1558–1575. doi: 10.1093/jxb/eraa576

Asadgol, Z., Forootanfar, H., Rezaei, S., Mahvi, A. H., and Faramarzi, M. A. (2014). Removal of phenol and bisphenol-a catalyzed by laccase in aqueous solution. *J. Environ. Health Sci. Eng.* 12, 93. doi: 10.1186/2052-336X-12-93

Baek, M., DiMaio, F., Anishchenko, I., Dauparas, J., Ovchinnikov, S., Lee, G. R., et al. (2021). Accurate prediction of protein structures and interactions using a three-track neural network. *Science* 373, 871–876. doi: 10.1126/science.abj8754

Bashir, A., Hoffmann, T., Smits, S. H., and Bremer, E. (2014). Dimethylglycine provides salt and temperature stress protection to bacillus subtilis. *Appl. Environ. Microbiol.* 80, 2773–2785. doi: 10.1128/AEM.00078-14

Bechtaoui, N., Rabiu, M. K., Raklami, A., Oufdou, K., Hafidi, M., and Jemo, M. (2021). Phosphate-dependent regulation of growth and stresses management in plants. *Front. Plant Sci.* 12, 679916. doi: 10.3389/fpls.2021.679916

Behr, M., Legay, S., Hausman, J. F., and Guerriero, G. (2015). Analysis of cell wall-related genes in organs of medicago sativa l. under different abiotic stresses. *Int. J. Mol. Sci.* 16, 16104–16124. doi: 10.3390/ijms160716104

Bowles, A. M. C., Bechtold, U., and Paps, J. (2020). The origin of land plants is rooted in two bursts of genomic novelty. *Curr. Biol.* 30, 530–536. doi: 10.1016/j.cub.2019.11.090

Cai-Hong, P., Su-Jun, Z., Zhi-Zhong, G., and Bao-Shan, W. (2005). NaCl Treatment markedly enhances H2O2-scavenging system in leaves of halophyte suaeda salsa. *Physiol. Plantarum* 125, 490–499. doi: 10.1111/j.1399-3054.2005.00585.x

Cao, S., Wang, Y., Li, Z., Shi, W., Gao, F., Zhou, Y., et al. (2019). Genome-wide identification and expression analyses of the chitinases under cold and osmotic stress in ammopiptanthus nanus. *Genes (Basel)* 10. doi: 10.3390/genes10060472

Cheng, S., Xian, W., Fu, Y., Marin, B., Keller, J., Wu, T., et al. (2019). Genomes of subaerial zygnematophyceae provide insights into land plant evolution. *Cell* 179, 1057–1067. doi: 10.1016/j.cell.2019.10.019

Costa, F. C., Oliva, M. A., de Jesus, T. C., Schenkman, S., and Thiemann, O. H. (2011). Oxidative stress protection of trypanosomes requires selenophosphate synthase. *Mol. Biochem. Parasitol.* 180, 47–50. doi: 10.1016/j.molbiopara.2011.04.007

Daubin, V., and Szöllősi, G. J. (2016). Horizontal gene transfer and the history of life. *Cold Spring Harb. Perspect. Biol.* 8, a18036. doi: 10.1101/cshperspect.a018036

de la Garza-García, J. A., Ouahrani-Bettache, S., Lyonnais, S., Ornelas-Eusebio, E., Freddi, L., Al, D. S., et al. (2021). Comparative genome-wide transcriptome analysis of brucella suis and brucella microti under acid stress at pH 4.5: Cold shock protein CspA and dps are associated with acid resistance of b. microti. *Front. Microbiol.* 12, 794535. doi: 10.3389/fmicb.2021.794535

de Vries, J., Stanton, A., Archibald, J. M., and Gould, S. B. (2016). Streptophyte terrestrialization in light of plastid evolution. *Trends Plant Sci.* 21, 467–476. doi: 10.1016/j.tplants.2016.01.021

Dunning, L. T., Olofsson, J. K., Parisod, C., Choudhury, R. R., Moreno-Villena, J. J., Yang, Y., et al. (2019). Lateral transfers of large DNA fragments spread functional genes among grasses. *Proc. Natl. Acad. Sci. U.S.A.* 116, 4416–4425. doi: 10.1073/pnas.1810031116

Edgar, R. C. (2004). MUSCLE: Multiple sequence alignment with high accuracy and high throughput. *Nucleic Acids Res.* 32, 1792–1797. doi: 10.1093/nar/gkh340

Emiliani, G., Fondi, M., Fani, R., and Gribaldo, S. (2009). A horizontal gene transfer at the origin of phenylpropanoid metabolism: A key adaptation of plants to land. *Biol. Direct* 4, 7. doi: 10.1186/1745-6150-4-7

Gill, S. S., and Tuteja, N. (2010). Reactive oxygen species and antioxidant machinery in abiotic stress tolerance in crop plants. *Plant Physiol. Biochem.* 48, 909–930. doi: 10.1016/j.plaphy.2010.08.016

Gligorijević, V., Renfrew, P. D., Kosciolek, T., Leman, J. K., Berenberg, D., Vatanen, T., et al. (2021). Structure-based protein function prediction using graph convolutional networks. *Nat. Commun.* 12, 3168. doi: 10.1038/s41467-021-23303-9

Guindon, S., Dufayard, J. F., Lefort, V., Anisimova, M., Hordijk, W., and Gascuel, O. (2010). New algorithms and methods to estimate maximum-likelihood phylogenies: Assessing the performance of PhyML 3.0. *Syst. Biol.* 59, 307–321. doi: 10.1093/sysbio/syq010

Haney, C. H., Samuel, B. S., Bush, J., and Ausubel, F. M. (2015). Associations with rhizosphere bacteria can confer an adaptive advantage to plants. *Nat. Plants* 1 (6). doi: 10.1038/nplants.2015.51

Hanin, M., Ebel, C., Ngom, M., Laplaze, L., and Masmoudi, K. (2016). New insights on plant salt tolerance mechanisms and their potential use for breeding. *Front. Plant Sci.* 7, 1787. doi: 10.3389/fpls.2016.01787

Hasanuzzaman, M., Bhuyan, M., Anee, T. I., Parvin, K., Nahar, K., and Mahmud, J. A. (2019). Regulation of ascorbate-glutathione pathway in mitigating oxidative damage in plants under abiotic stress. *Antioxid. (Basel)* 8. doi: 10.3390/antiox8090384

Hiraoka, Y., Kawamata, K., Haraguchi, T., and Chikashige, Y. (2009). Codon usage bias is correlated with gene expression levels in the fission yeast schizosaccharomyces pombe. *Genes to Cells* 14, 499–509. doi: 10.1111/j.1365-2443.2009.01284.x

Huang, J. (2013). Horizontal gene transfer in eukaryotes: The weak-link model. *BioEssays* 35, 868–875. doi: 10.1002/bies.201300007

Iwata, H., Mizushima, D., Kobayashi, Y., Ookura, T., Ogihara, J., Kato, J., et al. (2015). Two transaldolase isogenes from moniliella megachiliensis behave in a different way depending on the stress class. *J. Biosci. Bioeng* 119, 148–152. doi: 10.1016/j.jbiosc.2014.07.002

Jumper, J., Evans, R., Pritzel, A., Green, T., Figurnov, M., Ronneberger, O., et al. (2021). Highly accurate protein structure prediction with AlphaFold. *Nature* 596, 583–589. doi: 10.1038/s41586-021-03819-2

Kim, Y., Chung, Y. S., Lee, E., Tripathi, P., Heo, S., and Kim, K. H. (2020). Root response to drought stress in rice (Oryza sativa l.). *Int. J. Mol. Sci.* 21. doi: 10.3390/ijms21041513

Komatsu, S., Kamal, A. H., and Hossain, Z. (2014). Wheat proteomics: Proteome modulation and abiotic stress acclimation. *Front. Plant Sci.* 5. doi: 10.3389/fpls.2014.00684

Koutsovoulos, G., Kumar, S., Laetsch, D. R., Stevens, L., Daub, J., Conlon, C., et al. (2016). No evidence for extensive horizontal gene transfer in the genome of the tardigrade hypsibius dujardini. *Proc. Natl. Acad. Sci. U.S.A.* 113, 5053–5058. doi: 10.1073/pnas.1600338113

Laskowski, R. A., and Swindells, M. B. (2011). LigPlot+: Multiple ligand-protein interaction diagrams for drug discovery. *J. Chem. Inf Model.* 51, 2778–2786. doi: 10.1021/ci200227u

Letunic, I., and Bork, P. (2021). Interactive tree of life (iTOL) v5: An online tool for phylogenetic tree display and annotation. *Nucleic Acids Res.* 49, W293–W296. doi: 10.1093/nar/gkab301

Li, F., Brouwer, P., Carretero-Paulet, L., Cheng, S., de Vries, J., Delaux, P., et al. (2018). Fern genomes elucidate land plant evolution and cyanobacterial symbioses. *Nat. Plants* 4, 460–472. doi: 10.1038/s41477-018-0188-8

Li, X. T., Feng, X. Y., Zeng, Z., Liu, Y., and Shao, Z. Q. (2021). Comparative analysis of HSF genes from secale cereale and its triticeae relatives reveal ancient and recent gene expansions. *Front. Genet.* 12, 801218. doi: 10.3389/fgene.2021.801218

Li, L., Liu, Z., Meng, D., Liu, X., Li, X., Zhang, M., et al. (2019). Comparative genomic analysis reveals the distribution, organization, and evolution of metal resistance genes in the genus acidithiobacillus. *Appl. Environ. Microbiol.* 85, e2118–e2153. doi: 10.1128/AEM.02153-18

Lin, S., Wei, J., Yang, B., Zhang, M., and Zhuo, R. (2022). Bioremediation of organic pollutants by white rot fungal cytochrome P450: The role and mechanism of CYP450 in biodegradation. *Chemosphere* 301, 134776. doi: 10.1016/j.chemosphere.2022.134776

Liu, H., Sultan, M. A., Liu, X. L., Zhang, J., Yu, F., and Zhao, H. X. (2015). Physiological and comparative proteomic analysis reveals different drought responses in roots and leaves of drought-tolerant wild wheat (Triticum boeoticum). *PloS One* 10, e121852. doi: 10.1371/journal.pone.0121852

Liu, X. M., and Zhang, H. (2015). The effects of bacterial volatile emissions on plant abiotic stress tolerance. *Front. Plant Sci.* 6, 774. doi: 10.3389/fpls.2015.00774

Markowitz, V. M., Chen, I. A., Palaniappan, K., Chu, K., Szeto, E., Grechkin, Y., et al. (2010). The integrated microbial genomes system: An expanding comparative analysis resource. *Nucleic Acids Res.* 38, D382–D390. doi: 10.1093/nar/gkp887

Massoni, J., Bortfeld-Miller, M., Widmer, A., and Vorholt, J. A. (2021). Capacity of soil bacteria to reach the phyllosphere and convergence of floral communities despite soil microbiota variation. *Proc. Natl. Acad. Sci. U.S.A.* 118, e2100150118. doi: 10.1073/pnas.2100150118

Mastouri, F., Björkman, T., and Harman, G. E. (2012). Trichoderma harzianum enhances antioxidant defense of tomato seedlings and resistance to water deficit. *Mol. Plant Microbe Interact.* 25, 1264–1271. doi: 10.1094/MPMI-09-11-0240

Mishra, J., Singh, R., and Arora, N. K. (2017). Alleviation of heavy metal stress in plants and remediation of soil by rhizosphere microorganisms. *Front. Microbiol.* 8, 1706. doi: 10.3389/fmicb.2017.01706

Murali, M., Naziya, B., Ansari, M. A., Alomary, M. N., AlYahya, S., Almatroudi, A., et al. (2021). Bioprospecting of rhizosphere-resident fungi: Their role and importance in sustainable agriculture. *J. Fungi (Basel)* 7. doi: 10.3390/jof7040314

Niu, T., Zhang, T., Qiao, Y., Wen, P., Zhai, G., Liu, E., et al. (2021). Glycinebetaine mitigates drought stress-induced oxidative damage in pears. *PloS One* 16, e251389. doi: 10.1371/journal.pone.0251389

Nolan, C., Overpeck, J. T., Allen, J., Anderson, P. M., Betancourt, J. L., Binney, H. A., et al. (2018). Past and future global transformation of terrestrial ecosystems under climate change. *Science* 361, 920–923. doi: 10.1126/science.aan5360

Nouri, M. Z., Moumeni, A., and Komatsu, S. (2015). Abiotic stresses: Insight into gene regulation and protein expression in photosynthetic pathways of plants. *Int. J. Mol. Sci.* 16, 20392–20416. doi: 10.3390/ijms160920392

Parakkottil, C. M., Duncan, G. A., Armirotti, A., Abergel, C., Gurnon, J. R., Van Etten, J. L., et al. (2010). Identification of an l-rhamnose synthetic pathway in two nucleocytoplasmic large DNA viruses. *J. Virol.* 84, 8829–8838. doi: 10.1128/JVI.00770-10

Pennisi, E. (2019). Algae suggest eukaryotes get many gifts of bacteria DNA. *Science* 363, 439–440. doi: 10.1126/science.363.6426.439-b

Puigbò, P., Bravo, I. G., and Garcia-Vallve, S. (2008). CAIcal: A combined set of tools to assess codon usage adaptation. *Biol. Direct* 3, 38. doi: 10.1186/1745-6150-3-38

Puigbò, P., Guzmán, E., Romeu, A., and Garcia-Vallvé, S. (2007). OPTIMIZER: A web server for optimizing the codon usage of DNA sequences. *Nucleic Acids Res.* 35, W126–W131. doi: 10.1093/nar/gkm219

Puigbò, P., Romeu, A., and Garcia-Vallvé, S. (2008). HEG-DB: A database of predicted highly expressed genes in prokaryotic complete genomes under translational selection. *Nucleic Acids Res.* 36, D524–D527. doi: 10.1093/nar/gkm831

Rajtor, M., and Piotrowska-Seget, Z. (2016). Prospects for arbuscular mycorrhizal fungi (AMF) to assist in phytoremediation of soil hydrocarbon contaminants. *Chemosphere* 162, 105–116. doi: 10.1016/j.chemosphere.2016.07.071

Rennella, E., Sára, T., Juen, M., Wunderlich, C., Imbert, L., et al. (2017). RNA Binding and chaperone activity of the e. coli cold-shock protein CspA. *Nucleic Acids Res.* 45, 4255–4268. doi: 10.1093/nar/gkx044

Rosado-Souza, L., Fernie, A. R., and Aarabi, F. (2020). Ascorbate and thiamin: Metabolic modulators in plant acclimation responses. *Plants (Basel)* 9. doi: 10.3390/plants9010101

Schönknecht, G., Weber, A. P., and Lercher, M. J. (2014). Horizontal gene acquisitions by eukaryotes as drivers of adaptive evolution. *Bioessays* 36, 9–20. doi: 10.1002/bies.201300095

Schützendübel, A., and Polle, A. (2002). Plant responses to abiotic stresses: Heavy metal-induced oxidative stress and protection by mycorrhization. *J. Exp. Bot.* 53, 1351–1365. doi: 10.1093/jxb/53.372.1351

Sharp, P. M., and Li, W. H. (1987). The codon adaptation index–a measure of directional synonymous codon usage bias, and its potential applications. *Nucleic Acids Res.* 15, 1281–1295. doi: 10.1093/nar/15.3.1281

Soucy, S. M., Huang, J., and Gogarten, J. P. (2015). Horizontal gene transfer: Building the web of life. *Nat. Rev. Genet.* 16, 472–482. doi: 10.1038/nrg3962

Sun, K., Liu, J., Gao, Y., Sheng, Y., Kang, F., and Waigi, M. G.. (2015). Inoculating plants with the endophytic bacterium pseudomonas sp. Ph6-gfp to reduce phenanthrene contamination. *Environ. Sci. pollut. Res. Int.* 22, 19529–19537. doi: 10.1007/s11356-015-5128-9

Talavera, G., and Castresana, J. (2007). Improvement of phylogenies after removing divergent and ambiguously aligned blocks from protein sequence alignments. *Syst. Biol.* 56, 564–577. doi: 10.1080/10635150701472164

American Association for the Advancement of Science. (2005). So much more to know. *Science* 309, 78–102. doi: 10.1126/science.309.5731.78b

Todaka, D., Shinozaki, K., and Yamaguchi-Shinozaki, K. (2015). Recent advances in the dissection of drought-stress regulatory networks and strategies for development of drought-tolerant transgenic rice plants. *Front. Plant Sci.* 6. doi: 10.3389/fpls.2015.00084

Trott, O., and Olson, A. J. (2010). AutoDock vina: Improving the speed and accuracy of docking with a new scoring function, efficient optimization, and multithreading. *J. Comput. Chem.* 31, 455–461. doi: 10.1002/jcc.21334

Tuteja, N., Ahmad, P., Panda, B. B., and Tuteja, R. (2009). Genotoxic stress in plants: Shedding light on DNA damage, repair and DNA repair helicases. *Mutat. Res./Rev. Mutat. Res.* 681, 134–149. doi: 10.1016/j.mrrev.2008.06.004

Vásquez, L., Parra, A., Quesille-Villalobos, A. M., Gálvez, G., Navarrete, P., Latorre, M., et al. (2022). Cobalamin cbiP mutant shows decreased tolerance to low temperature and copper stress in listeria monocytogenes. *Biol. Res.* 55, 9. doi: 10.1186/s40659-022-00376-4

Vogel, A., Schwacke, R., Denton, A. K., Usadel, B., Hollmann, J., Fischer, K., et al. (2018). Footprints of parasitism in the genome of the parasitic flowering plant cuscuta campestris. *Nat. Commun.* 92515. doi: 10.1038/s41467-018-04344-z

Wang, G., Kong, F., Zhang, S., Meng, X., Wang, Y., and Meng, Q. (2015). A tomato chloroplast-targeted DnaJ protein protects rubisco activity under heat stress. *J. Exp. Bot.* 66, 3027–3040. doi: 10.1093/jxb/erv102

Wang, X., Shi, X., Chen, S., Ma, C., and Xu, S. (2018). Evolutionary origin, gradual accumulation and functional divergence of heat shock factor gene family with plant evolution. *Front. Plant Sci.* 9. doi: 10.3389/fpls.2018.00071

Wickell, D. A., and Li, F. W. (2020). On the evolutionary significance of horizontal gene transfers in plants. *New Phytol.* 225, 113–117. doi: 10.1111/nph.16022

Willenbrock, H., Friis, C., Juncker, A. S., and Ussery, D. W. (2006). An environmental signature for 323 microbial genomes based on codon adaptation indices. *Genome Biol.* 7, R114. doi: 10.1186/gb-2006-7-12-r114

Xi, Z., Bradley, R. K., Wurdack, K. J., Wong, K., Sugumaran, M., Bomblies, K., et al. (2012). Horizontal transfer of expressed genes in a parasitic flowering plant. *BMC Genomics* 13, 227. doi: 10.1186/1471-2164-13-227

Yang, L. B., Dai, X. M., Zheng, Z. Y., Zhu, L., Zhan, X. B., and Lin, C. C. (2015). Proteomic analysis of erythritol-producing yarrowia lipolytica from glycerol in response to osmotic pressure. *J. Microbiol. Biotechnol.* 25, 1056–1069. doi: 10.4014/jmb.1412.12026

Yang, Z., Wafula, E. K., Kim, G., Shahid, S., McNeal, J. R., Ralph, P. E., et al. (2019). Convergent horizontal gene transfer and cross-talk of mobile nucleic acids in parasitic plants. *Nat. Plants* 5, 991–1001. doi: 10.1038/s41477-019-0458-0

Yang, Z., Zhang, Y., Wafula, E. K., Honaas, L. A., Ralph, P. E., Jones, S., et al. (2016). Horizontal gene transfer is more frequent with increased heterotrophy and contributes to parasite adaptation. *Proc. Natl. Acad. Sci. U.S.A.* 113, E7010–E7019. doi: 10.1073/pnas.1608765113

Yue, J., Hu, X., Sun, H., Yang, Y., and Huang, J. (2012). Widespread impact of horizontal gene transfer on plant colonization of land. *Nat. Commun.* 3, 1152. doi: 10.1038/ncomms2148

Zhang, H., Zhu, J., Gong, Z., and Zhu, J. (2022). Abiotic stress responses in plants. *Nat. Rev. Genet.* 23, 104–119. doi: 10.1038/s41576-021-00413-0

Zhou, Y., Fan, Y., Lu, G., Zhang, A., Zhao, T., Sun, G., et al. (2022). Assessment of soil quality for guided fertilization in 7 barley agro-ecological areas of China. *PloS One* 17, e261638. doi: 10.1371/journal.pone.0261638

Zhou, M., Guo, J., Cha, J., Chae, M., Chen, S., Barral, J. M., et al. (2013). Non-optimal codon usage affects expression, structure and function of clock protein FRQ. *Nature* 495, 111–115. doi: 10.1038/nature11833

Zhou, J., Li, P., Meng, D., Gu, Y., Zheng, Z., Yin, H., et al. (2020). Isolation, characterization and inoculation of cd tolerant rice endophytes and their impacts on rice under cd contaminated environment. *Environ. pollut.* 260, 113990. doi: 10.1016/j.envpol.2020.113990

frontiers | Frontiers in Plant Science

TYPE Original Research
PUBLISHED 01 December 2022
DOI 10.3389/fpls.2022.953476

OPEN ACCESS

EDITED BY
Sofia I.A. Pereira,
Universidade Católica Portuguesa, Portugal

REVIEWED BY
Dandan Hu,
Henan Agricultural University, China
Mohammad Sayyar Khan,
University of Agriculture, Peshawar, Pakistan
Kun Lu,
Southwest University, China

*CORRESPONDENCE
Wai chin Li
waichin@eduhk.hk
Weisong Pan
panweisong@hunau.edu.cn

†These authors have contributed equally to this work

SPECIALTY SECTION
This article was submitted to Plant Symbiotic Interactions, a section of the journal Frontiers in Plant Science

RECEIVED 26 May 2022
ACCEPTED 20 October 2022
PUBLISHED 01 December 2022

CITATION
Qi Y, Wang Q, Xie Q, Wu C, Xu M, Han S, Zhou T, Li J, Xia L, Li Wc and Pan W (2022) Safety evaluation of *FAD2* RNAi transgenic *Brassica napus* L. based on microbial diversity and metabonomic analysis. *Front. Plant Sci.* 13:953476. doi: 10.3389/fpls.2022.953476

Safety evaluation of *FAD2* RNAi transgenic *Brassica napus* L. based on microbial diversity and metabonomic analysis

Yanting Qi[1,2†], Qiming Wang[1†], Qingxuan Xie[1†], Chuan Wu[2,3], Minhui Xu[1], Shaofan Han[1], Ting Zhou[1], Juan Li[4], Libing Xia[1], Wai chin Li[3*] and Weisong Pan[1*]

[1]College of Bioscience and Biotechnology, Hunan Agricultural University, Changsha, China, [2]School of Metallurgy and Environment, Central South University, Changsha, China, [3]Department of Science and Environmental Studies, The Education University of Hong Kong, Tai Po, Hong Kong SAR, China, [4]College of Agronomy, Hunan Agricultural University, Changsha, China

Oleic acid desaturase (*FAD2*) is the key enzyme that produces polyunsaturated fatty acids in rapeseed (*Brassica napus* L), which is one of the main oil crops. RNA interference (RNAi) is an emerging technique that provides new opportunities for the generation of new traits in plants. To increase oleic acid content and reduce linoleic and linolenic acid content in rapeseed, we constructed an ihpRNA plant expression vector of the *FAD2* gene and obtained transgenic plants for multiple generations by stable inheritance. In this study, third-generation transgenic plants (T3), seventh-generation transgenic plants (T7), and wild-type plants (WT) were used. The differences in microbial community diversity between transgenic plants and wild-type plants and the up- and downregulation of rhizosphere metabolite contents were investigated. In conclusion, the results showed that the soil microbial community structure was stable, the general microbial community structure was not changed by the transgenic rhizosphere exudates, and no significant harmful root exudate of transgenic rapeseed on the environment was found through the microbial community and metabolomics analysis. This work may provide an understanding of the impact of RNAi on plant metabolites and a safety evaluation method for transgenic plants and a reference for rapeseed breeding.

KEYWORDS

safety evaluation, *FAD2* RNAi, *Brassica napus* L., microbial community, metabonomic

Introduction

Rapeseed (*Brassica napus* L.) is one of the main oil crops in China and provides approximately 5.2 million tons of high-quality edible oil every year; rapeseed oil accounts for 47% of Chinese vegetable oil (Liu et al., 2019). Vegetable oil from rapeseed (*B. napus*) is one of the most commonly used vegetable oils in the world, and its oleic acid content is moderately high (approximately 65%) (Jung et al., 2011). Rapeseed oil contains high polyunsaturated fatty acid contents, such as linoleic acid and linolenic acid. These fatty acids are very unstable in terms of their chemical properties and are easily oxidized to form substances that are harmful to the human body. Oleic acid is a monounsaturated fatty acid with complex chemical properties. Studies have shown that oleic acid has good nutrition and healthcare functions by alleviating acute cadmium poisoning in mice (Chen et al., 2009; Yang et al., 2009; Guan et al., 2016; Wang et al., 2019). Therefore, reducing the content of polyunsaturated fatty acids, especially linolenic acid, and increasing the content of oleic acid have become important objectives of oil crop quality breeding (Sivaraman et al., 2004).

Oleic acid desaturase (*FAD2*) is the key enzyme for synthesizing polyunsaturated fatty acids in plants. *FAD2* is located in the endoplasmic reticulum (ER), and it is desaturated by catalysis of the formation of the double bond of oleic acid (18:1) at δ12 and plays a vital role in the formation of linoleic acid (18:2) (Lee et al., 2013). Seed oil with the largest change in fatty acid composition is produced by oil crops with high oleic acid, in which *FAD2* gene expression is inhibited (Lee et al., 2013).

RNA interference (RNAi) provides new opportunities to develop new traits in transgenic plants (Ramon et al., 2014). RNAi is an innovative gene-blocking technology, and RNAi has become a current functional genomic and genetic tool that is broadly applied to study gene functions by "knock-down" of cognate gene targets (Fishilevich et al., 2016). Compared with traditional transgenes, RNAi has the characteristics of high specificity, high efficiency, persistence, and signal conductivity, which can simply and efficiently inhibit the expression of specific genes. Therefore, RNAi has become an important field in the research and development of new transgenic plants. We found some studies on the ecological safety aspects of transgenic plants through a literature search in the early stage of the study (Chen et al., 2017; Cui et al., 2019; Tian et al., 2020). In regard to the application of genetically modified organisms (GMOs) in agriculture, discussions on this aspect have focused on consumer safety and the impact of genetically modified (GM) crops on the environment. Controlled on-site release and commercial applications of GMOs are regulated by risk assessment procedures in many countries. In the European Union, these procedures are guided by Directives 90/220/EEC and 94/15/EC (Pascher and Gollmann, 1999). China has not yet developed a special safety assessment guide for RNAi transgenic plants. Therefore, we can argue that if there is no change in the nutritional composition, nutritional value, and proposed use of GM crops, they can be considered basically equivalent to nongenetically modified crops (OECD, 1993). In addition, RNAi GM crops should be managed by classification according to the principle of case analysis and still need to be managed according to GM plants.

Comparing transgenic crops with their parents based on molecular characteristics is an effective method to evaluate the safety of transgenic crops, and it has been used in many studies on transgenic plants. Montero et al. (2011) found that approximately 0.40% of transcripts were differentially expressed in conventional rice varieties, and half of the difference between transgenic resistant rice and conventional rice was related to transgenic rice. Coll et al. (2009) compared widely used commercial GM-BT transgenic maize with nontransgenic varieties through transcriptome analysis, and they found differential expression of a small number of sequences in GM-BT maize. Wang et al. (2018) obtained stacked transgenic maize 12-5xIE034 that contained insecticidal *cry* and glyphosate tolerance *G10-epsps* genes by crossing of transgenic maize varieties 12-5 and IE034, and did transcriptome and metabolome analyses for different maize varieties; the results showed that the nine maize varieties had obvious differences in gene expression.

The microbial community is one of the important constituents of the ecosystem, and the long-term result of its influence is a change in soil quality. Root exudates of transgenic crops may have an impact on environmental safety because they interact with microorganisms in the soil, resulting in changes in microbial communities (Xiong et al., 2020). Therefore, it is necessary to study the change in soil microorganisms of transgenic *B. napus* L. under the dynamics of root exudates. Kremer et al. (2005) pointed out that the abundance of *Pseudomonas* in glyphosate-resistant soybean rhizosphere soil changed significantly. Means et al. (2007) studied the large-scale application of glyphosate and noted that transgenic glyphosate-resistant soybeans could have a significant impact on the composition and structure of soil microorganisms in this case. Saxena and Stotzky (2000) noted that planting transgenic crops did not cause significant changes in soil microorganisms. However, the soil environment is affected by various factors (Rajendran et al., 2019). In addition, the relationship between secretions from the roots of transgenic crops and microorganisms in the soil is also influenced by many study factors, such as the different materials used in the test; weather, moisture, and other environmental conditions during the test; and the artificial management. He et al. (2019) concluded that corresponding GM subrice and japonica rice had different effects on soil bacteria compared with their corresponding sister conventional rice. However, these differences in composition and abundance occurred only in a few genera and had no effect on the primary genera, and soil properties were mainly

responsible for these differences. Khan et al. (2017) used 16S–23S rRNA intergenic spacer amplification to evaluate the genotypic diversity of soil microorganisms to assess the potential impact of transgenes, and they concluded that the NiC *B. napus* strain may not affect microbial enzyme activities and community structure in rhizosphere soils. The difference in varieties may be the reason for the slight variation in the test parameters. Lee et al. (2022) evaluated the effects of soybean (*Glycine max L.*) and hot pepper (*Capsicum annuum L.*) on soil microbial community structure, and the results showed that soil microbial communities were not significantly different between GM and non-GM strains. The results indicated that the soil microbial community structure was not significantly affected. Arshad et al. (2022) compared the rhizosphere bacterial populations, root exudates, and soil enzyme activities of nontransgenic and AVP1 genes in transgenic wheat. The results showed that the AVP1 gene in transgenic wheat had no obvious adverse effects on the soil environment and different bacterial communities. However, bacterial communities depend on several factors other than just the genetic makeup of the host plant.

In this study, to investigate whether RNAi transgenic plants have an impact on ecological environmental systems through changes in rhizosphere microbial diversity and metabolites, the soil samples and plant tissues of *FAD2* RNAi transgenic rapeseed were evaluated by using Illumina MiSeq sequencing technology and UPLC–MS/MS metabolomics technology. Comparative metabonomic analysis was conducted to obtain differential metabolites between transgenic rapeseed and the parent rapeseed, and the metabolic pathway changes caused by RNAi were also analyzed. This study provides a new basis for evaluating the safety of *FAD2* RNAi transgenic rapeseed from the molecular characteristics of metabolic terminals.

Materials and methods

Soil sample collection

FAD2 RNAi transgenic *B. napus* L. was obtained through RNAi technology (Zhou et al., 2021b), and multiple generations of GM plants were obtained through stable inheritance. The phenotype of transgenic *B. napus L.* analyzed in this study and the specific planting and seed treatment procedures can be found in a previous study (Zhou et al., 2021b). T3, T7, and WT plants were used in this study (Zhou et al., 2021b). WT is wild-type *B. napus* L., and T3 and T7 are different generations of transgenic *B. napus* L., corresponding to the third generation and seventh generation, respectively. The two genotypes were provided by Jiangsu Academy of Agricultural Sciences (Zhou et al., 2021). Rapeseed plants were planted in a paddy field at Hunan Agricultural University, and the latitude and longitude were 28.18°CN and 113.08°CE, respectively. The sampling time was the summer season in 2018. We used a five-point sampling method. The soils for the experiments were collected at five points in each plot from the rapeseed field (1–30 cm depth) and mixed into one sample. The loose soil of the root system around the surface was shaken off the roots, and the soil that adhered strongly to the roots was carefully brushed from the roots and kept as rhizosphere soil. Stones and debris were removed manually and combined into one sample. Four composite soil samples were collected for each treatment, totalling 12 soil samples. Three treatments were designed, and each experimental treatment was replicated four times and repeated four times. Samples were stored at −80°C until pretreatment. Among the samples, Samples 1 to 4 were wild-type rapeseed (WT), Samples 5 to 8 were the third generation of *FAD2* RNAi transgenic *B. napus* L. (T3), and Samples 9 to 12 were the seventh generation of *FAD2* RNAi transgenic *B. napus* L. (T7).

Microbial DNA extraction and illumina sequencing

Microbial community genomic DNA was extracted from the collected samples using the E.Z.N.A.® soil DNA Kit (Omega Bio-Tek, Norcross, GA, USA) according to the manufacturer's instructions. The hypervariable region ITS of the fungal gene was amplified with the primer pairs ITS3F (5'-GCATCGATGA AGAACGCAGC-3') and ITS4R (5'-TCCTCCGCTT ATTGATATGC-3'), and the hypervariable region V3–V4 of the bacterial 16S rRNA gene was amplified with the primer pairs 338F (5'-ACTCCTACGGGAGGCAGCAG-3') and 806R (5'-GGACTACHVGGGTWTCTAAT-3') (Toju et al., 2012; Liu et al., 2016). PCR reactions of the 16S rRNA gene and ITS gene, containing 25 μl of 2× Premix Taq (Takara Biotechnology, Dalian Co. Ltd., China), 1 μl of each primer (10 μM), and 3 μl of DNA (20 ng/μl) template in a volume of 50 μl, were amplified by thermocycling: 5 min at 94°C for initialization; 30 cycles of 30 s denaturation at 94°C, 30 s annealing at 52°C, and 30 s extension at 72°C; followed by 10 min final elongation at 72°C. The PCR instrument was Bio-Rad S1000 (Bio-Rad Laboratory, CA, USA). The PCR product was extracted from a 1% agarose gel, purified using the E.Z.N.A. Gel Extraction Kit (Omega, USA), according to the manufacturer's instructions and quantified using a Quantus™ Fluorometer (Promega, USA) (Zuo et al., 2018). Sequencing libraries were generated using NEBNext® Ultra™ II DNA Library Prep Kit for Illumina® (New England Biolabs, MA, USA) and index codes were added. The library quality was assessed on the Qubit@ 2.0 Fluorometer (Thermo Fisher Scientific, MA, USA). Lastly, purified amplicons were pooled in equimolar amounts and paired-end sequenced on an Illumina Nova6000 platform and 250-bp paired-end reads were generated (Guangdong Magigene Biotechnology Co., Ltd. Guangzhou, China).

Metabolite extraction and metabolomic analysis

Fifty milligrams of soil sample was accurately weighed, and the metabolites were extracted using a 400-μl methanol:water (4:1, v/v) solution. The mixture was allowed to settle at −20°C and treated by a high-throughput tissue crusher (Wonbio-96c, Shanghai Wanbo Biotechnology Co., Ltd) at 50 Hz for 6 min, followed by vortexing for 30 s and ultrasound at 40 kHz for 30 min at 5°C. The samples were placed at −20°C for 30 min to precipitate proteins after centrifugation at 4°C for 15 min. The supernatant was transferred to sample vials for LC–MS/MS analysis (Wang and Xie, 2020).

Multivariate statistical analysis was performed by using the ropls R package (Version 1.6.2, http://bioconductor.org/packages/release/bioc/html/ropls.html). Principal component analysis (PCA) using an unsupervised method was applied to obtain an overview of the metabolic data. All metabolite variables were scaled to unit variances prior to conducting the PCA. Partial least squares discriminate analysis (PLS-DA) was used for statistical analysis. All metabolite variables were scaled to Pareto scaling prior to conducting the PLS-DA. The model validity was evaluated from model parameters R^2 and Q^2, which provide information for interpretability and predictability, respectively, and avoid the risk of overfitting (Wang et al., 2021). Variable importance in the projection (VIP) was calculated in the PLS-DA model, and p-values were estimated with paired Student's t-test on single-dimensional statistical analysis. The variables with significant differences of $p < 0.05$ and VIP values > 1 were defined as key metabolites.

The raw 16S rRNA gene-sequencing reads and raw ITS gene-sequencing reads were demultiplexed, quality-filtered by fastp Version 0.20.0, and merged by FLASH Version 1.2.7. Operational taxonomic units (OTUs) with a 97% similarity cutoff were clustered using UPARSE Version 7.1 (Edgar, 2013), and chimeric sequences were identified and removed. QIIME software and R language tools were used to analyze the community structure of samples at different classification levels. The taxonomy of each OTU representative sequence was analyzed by RDP Classifier Version 2.2 against the 16S rRNA database (silva132/16s_bacteria) and ITS database (unite7.2/its_fungi) using a confidence threshold of 0.7 (Wang et al., 2007).

Statistical analysis

Statistical analyses were performed by SPSS 19.0 and summarized as the means ± standard errors (SE). The level of significance of various treatments was set at $p < 0.05$ using one-way analysis of variance (ANOVA).

Results and discussion

Microbial composition of the rhizosphere microbial community of wild-type and transgenic rapeseed plants

The number of common and specific OTUs of groups is displayed in Figure 1 to show the overlaps of OTUs among the rhizosphere soil from WT, T3, and T7 plants. The OTUs of bacteria and fungi totalled 4,526 and 1,453 in the rhizosphere soil of WT, respectively. The OTUs of bacteria and fungi totalled 4,631 and 1,624 in the rhizosphere soil of T3, respectively, and the OTUs of bacteria and fungi totalled 4,540 and 1,335 in the rhizosphere soil of T7, respectively. Compared with that of the WT, the number of genera in the root soil of T7 decreased relatively, while the number of genera in T3 increased relatively. The number of common OTUs of bacteria and fungi in root soil was 4,004 among WT, T3, and T7, representing 66.97%, 64.01%, and 68.15% of the total number of OTUs in WT, T3, and T7, respectively. The composition of the microbial communities of WT, T3, and T7 is shown in Figure 2. There was rarely any difference in rhizosphere microbial abundance between wild-type and transgenic plants. *Bacteroidia*, *Gammaproteobacteria*, *Ascomycota*, and *Sordariomymycetes* were found in high proportions in each sample. Moreover, *Ascomycota* accounted for a very high proportion of the fungal communities. In addition, the abundance of *Bacteroidia* in sample No. 7 of T3 (T3_7) was as high as 44%, and the abundance of *Sordariomymycetes* in this sample was also high. There was no difference in the composition of microbial species at the class level in the samples, but the abundance of microbial species was slightly different. Zhou et al. (2021a) found that Bt corn residues had no direct effect on soil bacterial communities compared with the decomposition time and environment. The functional diversity and metabolic activity of the microbial community indicated that there was no significant difference between Bt maize IE09S034 and the control group. A study found differences in microbial community structures between Bt and non-Bt maize fields, and there were also variations between the chemical and biochemical properties of rhizosphere soils under Bt and non-Bt maize cultivation; they concluded that these differences could be related to agricultural practices and varieties (van Wyk et al., 2017).

In Figure 3, the dominant species with high abundance at the genus level of rhizosphere bacteria in wild-type and transgenic plant were *Proteobacteria* and *Bacteroidia*. At the genus level of rhizosphere fungi in wild-type and transgenic plant, the dominant species was *Ascomycota*. They had a high percentage in all samples. All other soil samples of T3, T7, and WT at the genus level showed very small differences in microbial abundance. As shown in Figure 3, the abundance of *Proteobacteria, Bacteroidetes, Acidobacteria, Verrucomicrobia,*

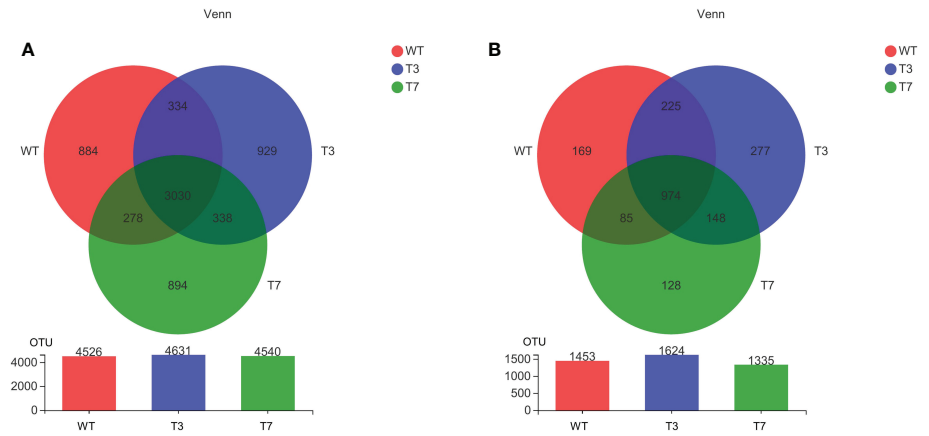

FIGURE 1
Venn diagram of the microbial community at the OTU level of wild-type and transgenic rapeseed plants (**A**, bacteria; and **B**, fungi). Note: The number of overlapping parts represents the number of species common to multiple groups, and the number of nonoverlapping parts represents the number of species unique to the corresponding group.

Chloroflexi, and *Ascomycota* was relatively high at the genus level. Some studies have used *Proteobacteria* and *Acidobacteria* as indicators of land use change and soil pollution (Schneider et al., 2017; Kim et al., 2021). Members of the class *Bacteroidia* are Gram-negative, non-spore-forming, mostly anaerobic bacteria that decompose organic substances, and they thrive in diverse environments, such as soils and subsurface sediments (Garcia-Lopez et al., 2019; Podosokorskaya et al., 2020). *Ascomycota* is by far the largest group in the fungal kingdom. Ecologically important mutualistic associations, such as mycorrhizae and lichens, have evolved in this species and are regarded as pivotal innovations that supported the evolution of land plants (Beimforde et al., 2014). These results showed that the soil microbial community structure was stable, and the general microbial community structure of rhizosphere soil was not changed by the transgenic plants. Zou et al. found that 5-year-old transgenic Poplar 741 could not cause ecological risk and could not affect the microbial community structure or functional diversity (Zou et al., 2018). Fan et al. (2020) analyzed the effects of transgenic poplar on related bacterial communities from various aspects, including bacterial OTU composition, alpha and beta diversity, gene function, and differences among groups. Overall, transgenic poplar did not significantly affect endophytic or soil bacteria. Our results on the structural composition and diversity of the microbial community are consistent with these studies. Therefore, we preliminarily concluded that transgenic *B. napus* L. had no harmful effects on microbial communities in the environment.

Alpha diversity analysis of the rhizosphere microbial community of wild-type and transgenic rapeseed plants

Alpha diversity refers to the diversity in a specific region or ecosystem. The commonly used indicators to characterize alpha

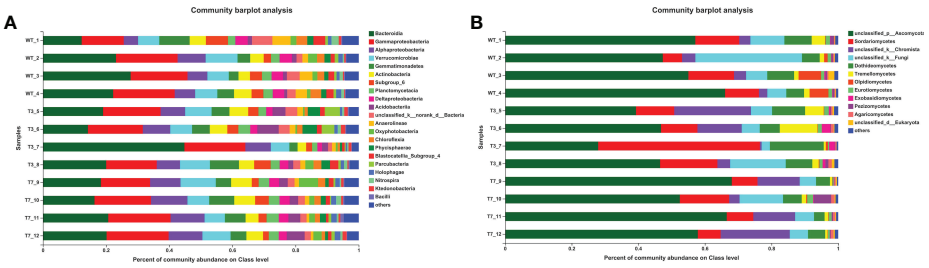

FIGURE 2
Percent of community abundance at the class level of wild-type and transgenic rapeseed plants (**A**, bacteria; and **B**, fungi). Note: The different colors of the column represent different species, and the length of the column represents the size of the proportion of the species.

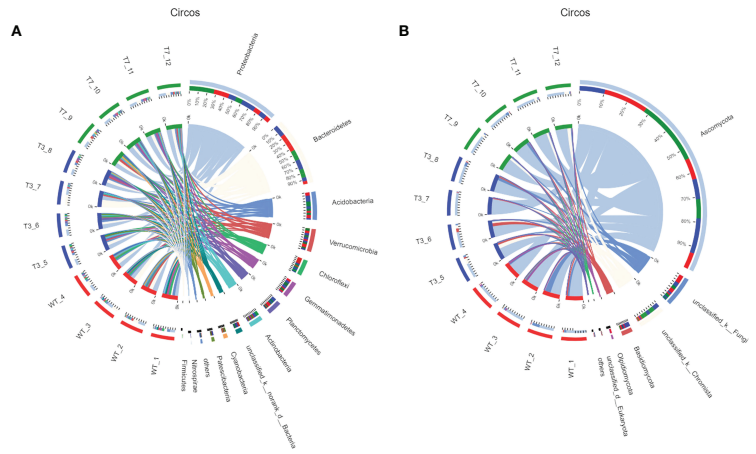

FIGURE 3
Circos diagram of bacteria and fungi at the genus level in different generations (**A**, bacteria; **B**, fungi). Note: The small semicircle (left half circle) represents the species composition in the sample. The large semicircle (right half circle) represents the distribution ratio of species in different samples at the taxonomic level.

diversity are Chao, ACE, and Shannon. The ACE index, Chao index, and Shannon index were obtained at a 97% similarity level using Mothur software. The Shannon index measures the average degree of uncertainty in predicting to what species a randomly selected individual from a set of S species and N individuals will belong to, and the value increases as the number of species increases and individuals become evenly distributed among species (Pylro et al., 2014). The ACE index and Chao1 index reflect the number of species in the community. Figure 4 shows the alpha diversity analysis of the microbial community and significance difference test. The results of some samples showed fluctuations but few changes within a certain range, and the diversity indicators of WT, T3, and T7 were close to each other. Compared with transgenic plants and wild-type plants, the ACE index value and Chao index showed little difference between transgenic plants and wild-type plants, indicating that the transgenic plants did not cause obvious changes in the richness of the bacterial community. The Chao index of the fungal community from T7 was slightly smaller than that of WT and T3, indicating that the fungal community had higher richness in WT and T3. By comparing the two indicators, no obvious difference in bacterial community diversity between transgenic plants and wild-type plants was found, while the fungal community diversity of T7 was slightly smaller than that of the WT and T3. Overall, there was no significant difference in the alpha diversity of the fungal community and bacterial community.

Zhang et al. (2015) detected no OsrHSA protein in the roots of OsrHSA transgenic rice and concluded that OsrHSA transgenic rice and the rHSA protein produced by transgenic rice did not change the functional diversity of rhizosphere microbial communities. Another study also confirmed that microbial community diversity was not significantly influenced by the presence of GM plants (Riglietti et al., 2006). Our results were similar to these studies. In summary, through RNAi technology, *B. napus* L. had no obvious effect on the richness and diversity of the rhizosphere bacterial community and fungal community.

Microbial abundance analysis of the rhizosphere microbial community of wild-type and transgenic rapeseed plants

As shown in Figure 5, the heatmap graph color represents the size and proportion of data in a two-dimensional matrix or table, thus showing the composition and structure of the microbiome and reflecting the similarity and differences of the community composition of different groups or different samples at each classification level. In the heatmap of bacterial and fungal abundance, the abundance of each microbial species in WT, T3, and T7 was similar. *Flavobacterium* in T3 was significantly more than that in WT and T7, and *Ascomycota* was abundant in WT, T3, and T7, which was consistent with the above analysis. The dominant genus and proportion between transgenic rapeseed plants and wild plants were consistent with the structural analysis at the genus level. A study found that compared with the parental line, the transgenic strain had no obvious effect, and for all evaluated microbial communities, soil type and the year of planting maize were the dominant factors affecting their structures, and no difference in the total number of bacteria between the rhizospheres of GM and parental plant lines was observed (Saxena and Stotzky, 2001). Chun et al. (2012) found no difference between transgenic rice and its parental

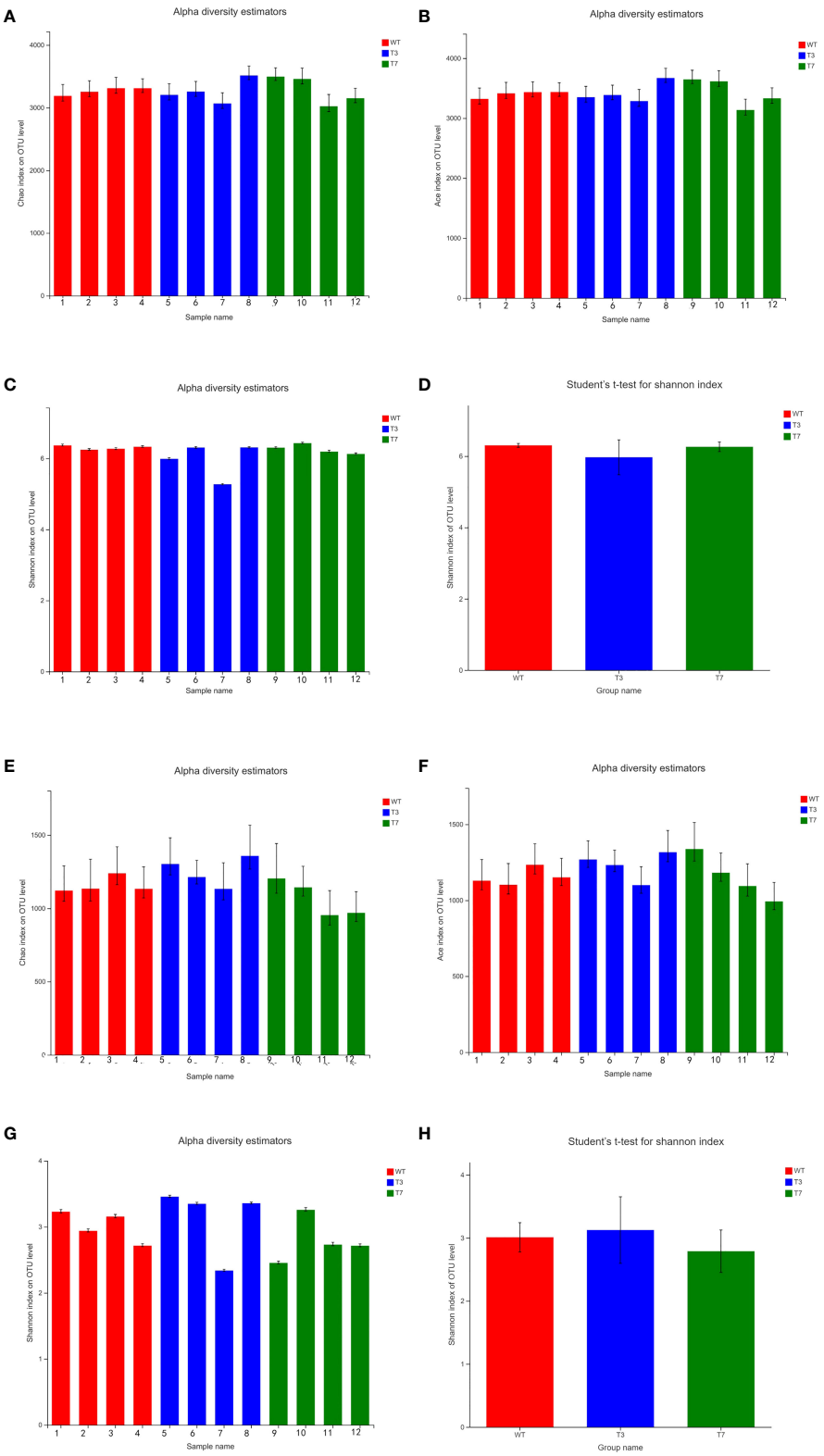

FIGURE 4
Alpha diversity index bar graph and alpha diversity significance difference test of interrooted prokaryotic and eukaryotic microbes (**A–D**, bacteria; **E–H**, fungi). Note: Student's *t*-test was used to calculate the difference between the two groups, and the two groups were marked with significant differences ($0.01 < p \leq 0.05$ was marked with *, $0.001 < p \leq 0.01$ was marked with **, and $p \leq 0.001$ was marked with ***).

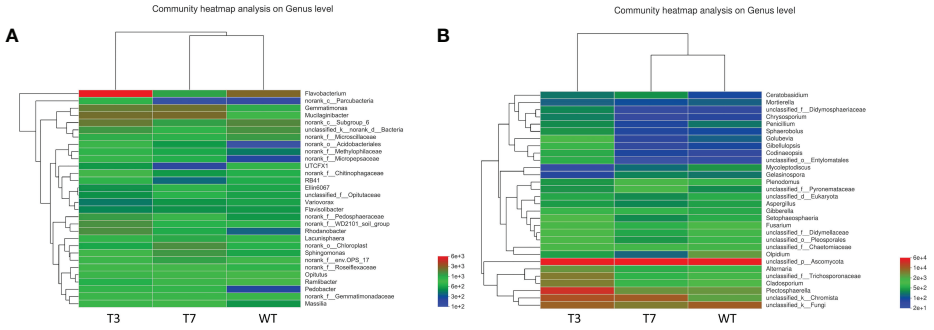

FIGURE 5
Heatmap of microbial communities at the genus level of wild-type and transgenic rapeseed plants (**A**, bacteria; **B**, fungi). Note: The variation in the abundance of different species in the sample is displayed through the color gradient of the color block.

nontransgenic counterpart (cultivar Dongjin) in the diversity index and community composition of the microbial community. In contrast, this change in the microbial community depended strongly on the growth stage and year. Therefore, they did not observe the adverse effects of these transgenic rice crops on the microbial community in paddy soils.

Comparative analysis of metabolites in wild-type and transgenic rapeseed plants

PLS-DA can maximize the intergroup distinction and is conducive to finding differential metabolites, and it belongs to beta diversity approaches. PLS-DA obtained two principal components: the contribution rate of Principal Component 1 was 56.40%, the contribution rate of Principal Component 2 was 13.70%, $R^2X = 0$, $R^2Y = 0.9721$, and $Q^2 = 0.6466$. PLS-DA was verified for alignment ($n = 200$, i.e., 200 alignment experiments). In the model verification (Figure 6B), the horizontal line corresponds to R^2Y and Q^2 of the original model, and the red dot and blue dot represent R^2Y' and $Q^{2'}$ of the model after replacement of y, respectively. R^2Y' and $Q^{2'}$ were both smaller than R^2Y and Q^2 of the original model; i.e., the corresponding points did not exceed the corresponding lines, which indicated that the model was meaningful and that its differential metabolites could be screened according to VIP value analysis. According to the PLS-DA model (Figure 6A), 726 metabolome data points were analyzed. The samples of RNAi-T3 were distributed on the left side of the confidence interval, and the samples of WT were distributed on the right side of the confidence interval. The distinguishing effects of the two samples were abundant and obvious.

The root exudates of rapeseed mainly included alcohols, hydrocarbons, acids, and esters, and the contents of alcohols and hydrocarbons were relatively high. Hydrocarbons, esters, and acids or secondary metabolites have certain chemical influences, including the inhibition or stimulation of seed germination in other crops and an influence on microorganisms in the soil, in keeping with the results of Yang (2006).

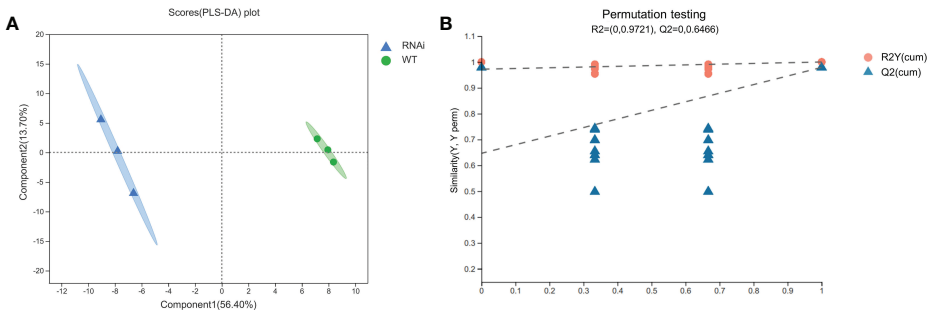

FIGURE 6
PLS-DA scoring models **(A)** and permutation test **(B)** of wild-type and transgenic rapeseed plants. Note: Component 1 denotes the first principal component interpretation degree, and Component 2 denotes the second principal component interpretation degree. The contribution rate of Principal Component 1 is 56.40%, and the contribution rate of Principal Component 2 is 13.70%.

Differential metabolite analysis of wild-type and transgenic rapeseed plants

Comparing the multiple changes in quantitative information for metabolic components in WT and RNAi samples, log2 treatment was carried out on the difference multiple. The top 20 differentially expressed metabolic components with changes are shown in Figure 7. Compared with WT plants, five types of amino acids and their derivatives [proline, L-(+)-arginine, N-(3-indolylacetyl)-L-alanine, Nα-acetyl-L-glutamine, and L-phenylalanine], one aldehyde and its derivatives (4-hydroxy-3,5-diisopropylbenzaldehyde), one amide and its derivatives (N, N-dimethylformamide), one chalcone (4,2',4',6'-tetrahydroxychalcone), one alcohol and its derivatives (caffeyl alcohol and sclareol), one ketone and its derivatives (α-lonone), one glycoside and its derivatives (deoxyguanosine), one pyrimidine and its derivatives (thymidine), and two others [acid orange 20 and MAG(18:1) isomer1] increased in relative content in RNAi-T plants. However, one guanidine and its derivatives (1-dimethylbiguanide), one polyether and its derivatives (salicin), one alcohol and its derivatives (chrysoeriol), two glycosides and their derivatives [O-glucuronic acid-O-hexoside and delphinidin 3-O-rutinoside (Tulipanin)], and one aldehyde and its derivatives (1 p-coumaricaldehyde) were reduced in relative content in RNAi-T plants.

Based on the PLS-DA results, the VIP of the PLS-DA model was analyzed from the obtained multivariate analysis. A total of 88 upregulated differential metabolites were detected, namely, 19 amino acids and their derivatives; 15 organic acids and their derivatives; 14 lipids; 6 nucleotides and their derivatives; 5 flavanones; 4 alkaloids; 3 phenylpropanoids, flavonoids, and flavonols; 2 alcohols, polyphenols, and procyanidins; 1 phenolamine, terpenoid, and vitamin and their derivatives; 1 indole and its derivatives; and 6 other metabolites. A total of 24 downregulated differential metabolites were detected, namely, 10 phenylpropanoids, 3 lipids, 3 flavonols, 2 polyphenols, 2 organic acids and their derivatives, 1 amino acid and its derivatives, 1 phenolamine, 1 nucleotide and its derivatives, and 1 vitamin. A volcano map was used to visualize the differential data for observation and analysis. It was found that there were both upregulated and downregulated substances with significant differences. Metabolites with upregulated expression were more abundant than metabolites with downregulated expression. However, there was no significant change in the expression of most metabolites.

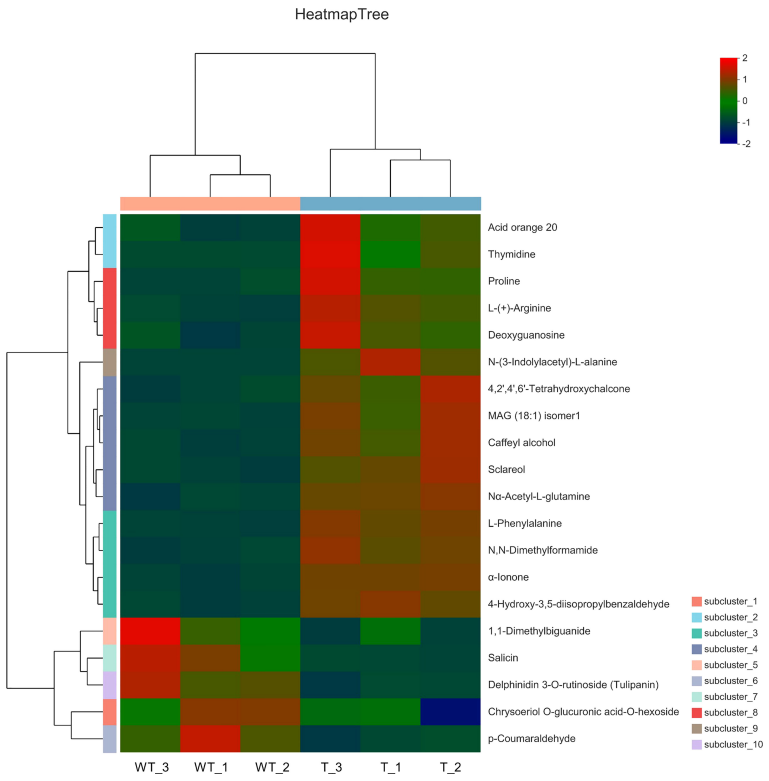

FIGURE 7
Heatmap of metabolic differences of the top 20 substances between wild-type and transgenic rapeseed plants. Note: Metabolites with fold change ≥2 or fold change ≤0.5 have significant differences.

All metabolites were analyzed by *t*-test and two-tailed test, and the differences in metabolites were plotted (Figure 8). A point represented a metabolite, and a horizontal coordinate represented a pair of values. As shown in Figure 8, only a few metabolites showed significant differences. The expression levels of more differential metabolites increased in GM rapeseed than in wild-type rapeseed, and the expression levels of some metabolites were reduced. Specifically, there were six metabolites with significantly upregulated and downregulated changes. The main metabolites significantly upregulated were quinic acid O-glucuronic acid, N-(3-indolylacetyl)-L-alanine, L-tyramine, and phenylacetyl-L-glutamine. There were two significantly downregulated differential metabolites, homovanilloyl quinic acid and N-caffeoyl agmatine. It was necessary to demonstrate that the presence of these metabolites and expressed changes were not harmful to the environment based on relevant studies. Alanine is an amino acid with a neutral charge that can be sorbed into soil particles by (1) cation exchange, (2) anion exchange, or (3) ligand exchange (Apostel et al., 2017). Alanine is also the richest amino acid in soluble organic substances (Fischer et al., 2007). Therefore, this kind of metabolite is common in the environment. In addition, a study found that feruloyl tyramine, feruloyl tryptamine, and feruloyl dopamine were effective against *S. aureus* 209 and *S. pyogenes*, and the MIC was between 190 and 372 μM (Georgiev et al., 2012). Glutamine affected the level of other amino acids utilized by microorganisms, and the addition of glutamine reduced ($P<0.05$) the use of alanine and glycine by *E. coli* while stimulating ($P<0.05$) the use of threonine in the bacteria (Dai et al., 2013). Aromatic compounds are produced by microorganisms in the synthesis of the aromatic components of their own cellular materials. In addition to these anabolic syntheses, some microorganisms produce aromatic metabolites in the process of oxidative assimilation of nonaromatic materials. Quinic acid (1,3,4,5-tetrahydroxycyclohexanecarboxylic acid) was attacked by Micrococcus chinicus, resulting in protocatechuic acid (Rogoff, 1958). In *Neurospora crassa* and *Aspergillus nidulans*, the exogenous supply of quinic acid as a growth carbon source led to the production of three enzymes that were essential for the catabolism of quinic acid into protocatechuic acid (Watts et al., 2002). Such acids can be used by microorganisms and do not harm the environment. Polyamines play a variety of roles in every living organism, including physiological responses to pathogens in plants (Jiménez-Bremont et al., 2014). In fungi, they are involved in

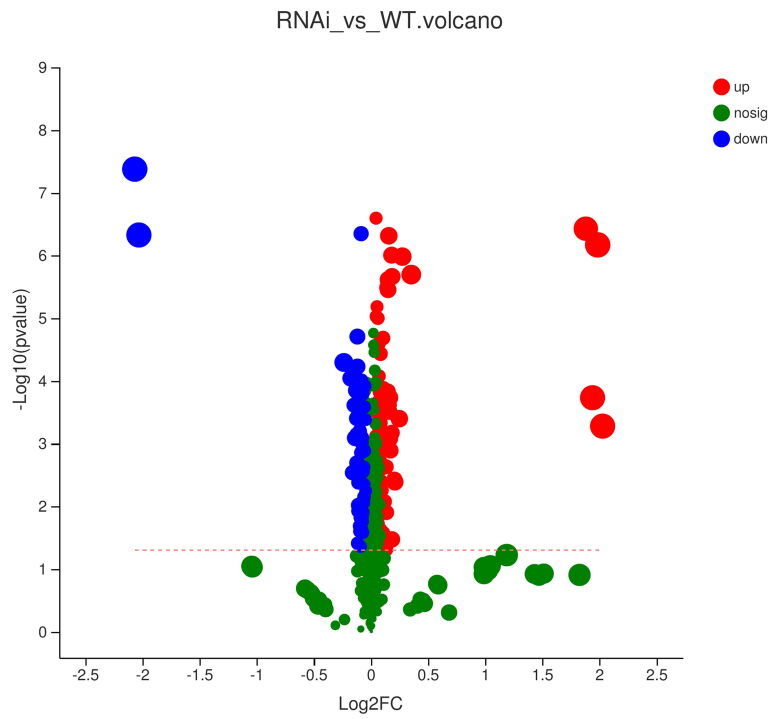

FIGURE 8
Volcano map of metabolic differences of wild-type and transgenic rapeseed plants (RNAi vs. WT). Note: Each dot in the figure represents a specific metabolite, and the size of the dot indicates the VIP value (the importance of the independent variable *x* in explaining the dependent variable *y*). The blue dots on the left are differentially downregulated metabolites, and the red dots on the right are differentially upregulated metabolites. The more dots on the left and right there are, the more significant the differences, and the higher the ordinate value is, the more significant the expression difference.

metabolism, regulation (Valdés-Santiago et al., 2012), and stress-coping functions (Valdés-Santiago and Ruiz-Herrera, 2014), and they also do not cause harm to the environment. In conclusion, the metabolites with variable expression levels were not harmful to the environment.

Conclusion

In summary, the microbial community analysis showed that transgenic plants caused no significant changes in microbial (both bacterial and fungal) community composition and did not cause obvious changes in microbial community diversity, which indicated that transgenic *B. napus* L. might have no specific impacts on the rhizosphere microbial community abundance in rhizosphere soils and no risk to the environment. Root exudates were either upregulated or downregulated in transgenic *B. napus* L., and there were six differential metabolites with very significant changes. The main differential metabolites significantly upregulated were quinic acid O-glucuronic acid, N-(3-indolylacetyl)-L-alanine, L-tyramine, and phenylacetyl-L-glutamine. The main significantly downregulated differential metabolites were homovanilloyl quinic acid and N-caffeoyl agmatine. Relevant studies have shown that none of these metabolites are harmful to the environment. Therefore, based on the research results, we can basically infer that no harm to the ecological environment based on the dynamics of microbial diversity and metabonomic analysis was detected in transgenic plants cultivated in fields. Therefore, transgenic rapeseed has the potential for application. However, its safety needs to be further evaluated. Therefore, the future assessment of ecological safety in transgenic plants needs further study.

Data availability statement

The data presented in the study are deposited in the NCBI repository, accession number SRR17344596-SRR17344612.

Author contributions

The overarching research goals were developed by WP, QW, and YQ carried out experiments and conducted the first draft of the manuscript. WL guided the study and reviewed the manuscript. CW reviewed the manuscript and proposed some important advice. YQ: Experiment; Data curation; Formal analysis; Software; Visualization; Writing - review & editing. QW: Experiment; Data curation; Writing - review & editing. CW: Methodology; Resources; Writing - review & editing. WP: Funding; Conceptualization; Resources. QX: Experiment; Data curation; Writing - review & editing. MX: Experiment; Data curation. SH: Experiment; Data curation. TZ: Experiment; Data curation. LX: Experiment; Data curation. JL: Review & editing. WL: Review & editing. All authors contributed to the article and approved the submitted version.

Funding

Financial support from the Research Foundation of Education Bureau of Hunan Province, China (No. 20A246), the Natural Science Foundation of Hunan Province of China (No. 2021JJ30340), the National Natural Science Foundation of China (No. 42177392), and the Dean's Research Fund [Project code: 04626 (2020/21) and 04730 (2021/22)] of the Education University of Hong Kong is gratefully acknowledged.

Conflict of interest

The authors declare that the research was conducted in the absence of any commercial or financial relationships that could be construed as a potential conflict of interest.

Publisher's note

References

Apostel, C., Dippold, M. A., Bore, E., and Kuzyakov, Y. (2017). Sorption of alanine changes microbial metabolism in addition to availability. *Geoderma* 292, 128–134. doi: 10.1016/j.geoderma.2017.01.016

Arshad, M., Naqqash, T., Tahir, M., Leveau, J. H., Zaheer, A., Tahira, S. A., et al. (2022). Comparison of bacterial diversity, root exudates and soil enzymatic activities in the rhizosphere of AVP1-transgenic and non-transgenic wheat (*Triticum aestivum* l.). *J. Appl. Microbiol* 133 (5), 3094–3112. doi: 10.1111/jam.15751

Beimforde, C., Feldberg, K., Nylinder, S., Rikkinen, J., Tuovila, H., Dorfelt, H., et al. (2014). Estimating the phanerozoic history of the ascomycota lineages: Combining fossil and molecular data. *Mol. Phylogenet. Evol.* 78, 386–398. doi: 10.1016/j.ympev.2014.04.024

Chen, S., Pu, H. M., Zhang, J. F., Gao, J. Q., Chen, F., Long, W. H., et al. (2009). Identification of high oleic acid germplast from the T2 progeny of the transgenic *B. napus* l. *Jiangsu J. Agric. Sci.* 25 (06), 1234–1237.

Chen, G. H., Tian, X. L., Wang, D. D., Ling, J., Mao, Z. C., Yang, Y. H., et al. (2017). Expression of mitogen-activated protein kinase double-stranded RNA in cucumber has no apparent effect on the diversity of rhizosphere archaea. *J. Integr. Agric.* 16 (10), 2239–2245. doi: 10.1016/S2095-3119(16)61594-0

Chun, Y. J., Kim, H. J., Park, K. W., Jeong, S. C., Lee, B., Back, K., et al. (2012). Two-year field study shows little evidence that PPO-transgenic rice affects the structure of soil microbial communities. *Biol. Fertility Soils* 48 (04), 453–461. doi: 10.1007/s00374-011-0626-5

Coll, A., Nadal, A., Collado, R., Capellades, G., Messeguer, J., Mele, E., et al. (2009). Gene expression profiles of MON810 and comparable non-GM maize varieties cultured in the field are more similar than are those of conventional lines. *Transgenic Res.* 18, 801–808. doi: 10.1007/s11248-009-9266-z

Cui, M. Q., Wu, C., Jiang, X. X., Liu, Z. Y., and Xue, S. G. (2019). Bibliometric analysis of research on soil arsenic during 2005–2016. *J. Cent. South Univ.* 26 (02), 479–488. doi: 10.1007/s11771-019-4020-z

Dai, Z. L., Li, X. L., Xi, P. B., Zhang, J., Wu, G. Y., and Zhu, W. Y. (2013). L-glutamine regulates amino acid utilization by intestinal bacteria. *Amino Acids* 45 (03), 501–512. doi: 10.1007/s00726-012-1264-4

Edgar, R. C. (2013). UPARSE: highly accurate OTU sequences from microbial amplicon reads. *Nat. Methods* 10 (10), 996–998. doi: 10.1038/NMETH.2604

Fan, J. M., Dong, Y., Yu, X. Y., Yao, L. Z., Li, D. M., Wang, J. M., et al. (2020). Assessment of environmental microbial effects of insect–resistant transgenic *Populus×euramericana* cv. *'74/76'* based on high–throughput sequencing. *Acta Physiologiae Plantarum* 42 (11). doi: 10.1007/s11738-020-03148-3

Fischer, H., Meyer, A., Fischer, K., and Kuzyakov, Y. (2007). Carbohydrate and amino acid composition of dissolved organic matter leached from soil. *Soil Biol. Biochem.* 39 (11), 2926–2935. doi: 10.1016/j.soilbio.2007.06.014

Fishilevich, E., Vélez, A. M., Storer, N. P., Li, H., Bowling, A. J., Rangasamy, M., et al. (2016). RNAi as a management tool for the western corn rootworm, diabrotica virgifera. *Pest Manage. Sci.* 72 (09), 1652–1663. doi: 10.1002/ps.4324

Garcia-Lopez, M., Meier-Kolthoff, J. P., Tindall, B. J., Gronow, S., Woyke, T., Kyrpides, N. C., et al. (2019). Analysis of 1,000 type-strain genomes improves taxonomic classification of *Bacteroidetes*. *Front. Microbiol.* 10. doi: 10.3389/fmicb.2019.02083

Georgiev, L., Chochkova, M., Ivanova, G., Najdenski, H., Ninova, M., and Milkova, T. (2012). Radical scavenging and antimicrobial activities of cinnamoyl amides of biogenic monoamines. *Rivista Italiana Delle Sostanze Grasse* 89 (02), 91–102.

Guan, M., Chen, H., Xiong, X. H., Lu, X., Li, X., Huang, F. H., et al. (2016). A study on triacylglycerol composition and the structure of high-oleic rapeseed oil. *Engineering* 2 (02), 233–242. doi: 10.1016/J.ENG.2016.02.004

He, M. D., Zhang, J. C., Shen, L. B., Xu, L. X., Luo, W. J., Li, D., et al. (2019). High-throughput sequencing analysis of microbial community diversity in response to indica and japonica bar-transgenic rice paddy soils. *PloS One* 14 (9). doi: 10.1371/journal.pone.0222191

Jiménez-Bremont, J. F., Marina, M., Guerrero-González, M. L., Rossi, F. R., Sánchez-Rangel, D., and Rodriguez-Kessler, M. (2014). Physiological and molecular implications of plant polyamine metabolism during biotic interactions. *Front. Plant Sci.* 5. doi: 10.3389/fpls.2014.00095

Jung, J. H., Kim, H., Go, Y. S., Lee, S. B., Hur, C. G., Kim, H. U., et al. (2011). Identification of functional *BrFAD2-1* gene encoding microsomal delta-12 fatty acid desaturase from *Brassica rapa* and development of *B. napus* containing high oleic acid contents. *Plant Cell Rep.* 30 (10), 1881–1892. doi: 10.1007/s00299-011-1095-x

Khan, M. S., Sadat, S. U., Jan, A., and Munir, I. (2017). Impact of transgenic brassica napus harboring the antifungal synthetic chitinase (NiC) gene on rhizosphere microbial diversity and enzyme activities. *Front. Plant Sci.* 8). doi: 10.3389/fpls.2017.01307

Kim, H. S., Lee, S. H., Jo, H. Y., Finneran, K. T., and Kwon, M. J. (2021). Diversity and composition of soil *Acidobacteria* and *Proteobacteria* communities as a bacterial indicator of past land-use change from forest to farmland. *Sci. Total Environ.* 797. doi: 10.1016/j.scitotenv.2021.148944

Kremer, R. J., Means, N. E., and Kim, S. (2005). Glyphosate affects soybean root exudation and rhizosphere micro-organisms. *Int. J. Environ. Analytical Chem.* 85, 1165–1174. doi: 10.1080/03067310500273146

Lee, K. R., In Sohn, S., Jung, J. H., Kim, S. H., Roh, K. H., Jong, B., et al. (2013). Functional analysis and tissue-differential expression of four *FAD2* genes in amphidiploid *B. napus* derived from *Brassica rapa* and *Brassica oleracea*. *Gene* 531 (02), 253–262. doi: 10.1016/j.gene.2013.08.095

Lee, H., Yoon, J., and Kim, D. U. (2022). Molecular analysis of soil bacterial community structures for environmental risk assessment with varieties of genetically modified soybean and hot pepper. *Processes* 10 (5). doi: 10.3390/pr10051037

Liu, C., Feng, Z. C., Xiao, T. H., Ma, X. M., Zhou, G. S., Huang, F. H., et al. (2019). Development, potential and adaptation of Chinese rapeseed industry. *Chin. J. Oil Crop Sci.* 41 (04), 485–489. doi: 10.7505/j.issn.1007-9084.2019.04.001

Liu, C. S., Zhao, D. F., Ma, W. J., Guo, Y. D., Wang, A. J., Wang, Q. L., et al. (2016). Denitrifying sulfide removal process on high-salinity wastewaters in the presence of halomonas sp. *Appl. Microbiol. Biotechnol.* 100 (3), 1421–1426. doi: 10.1007/s00253-015-7039-6

Means, N. E., Kremer, R. J., and Ramsier, C. (2007). Effects of glyphosate and foliar amendments on activity of microorganisms in the soybean rhizosphere. journal of environmental science and health - part b pesticides. *Food Contaminants Agric. Wastes* 42, 125–132. doi: 10.1080/03601230601123227

Montero, M., Coll, A., Nadal, A., Messeguer, J., and Pla, M. (2011). Only half the transcriptomic differences between resistant genetically modified and conventional rice are associated with the transgene. *Plant Biotechnol. J.* 9, 693–702. doi: 10.1111/j.1467-7652.2010.00572.x

OECD (1993). "Traditional crop breeding practices," in *An historical review to serve as a baseline for assessing the role of modern biotechnology* (Paris: Organization for Economic Co-operation and Development (OECD)).

Pascher, K., and Gollmann, G. (1999). Ecological risk assessment of transgenic plant releases: An Austrian perspective. *Biodiver. Conserv.* 8 (09), 1139–1158. doi: 10.1023/A:1008904525713

Podosokorskaya, O. A., Kochetkova, T. V., Novikov, A. A., Toshchakov, S. V., Elcheninov, A. G., and Kublanov, I. V. (2020). *Tenuifilum thalassicum* gen. nov., sp. nov., a novel moderate thermophilic anaerobic bacterium from a kunashir island shallow hot spring representing a new family *Tenuifilaceae* fam. nov. in the class *Bacteroidia*. *Systematic Appl. Microbiol.* 43 (5). doi: 10.1016/j.syapm.2020.126126

Pylro, V. S., Roesch, L. F. W., Morais, D. K., Clark, I. M., Hirsch, P. R., and Totola, M. R. (2014). Data analysis for 16S microbial profiling from different benchtop sequencing platforms. *J. Microbiological Methods* 107, 30–37. doi: 10.1016/j.mimet.2014.08.018

Rajendran, M., An, W. H., Li, W. C., Perumal, V., Wu, C., Sahi, S. V., et al. (2019). Chromium detoxification mechanism induced growth and antioxidant responses in vetiver 107(*Chrysopogon zizanioides*(L.) roberty). *J. Cent. South Univ.* 26 (02), 489–500. doi: 10.1007/s11771-019-4021-y

Ramon, M., Devos, Y., Lanzoni, A., Liu, Y., Gomes, A., Gennaro, A., et al. (2014). RNAi-based GM plants: food for thought for risk assessors. *Plant Biotechnol. J.* 12 (09), 1271–1273. doi: 10.1111/pbi.12305

Riglietti, A., Ruggiero, P., and Crecchio, C. (2006). Investigating the influence of transgenic tobacco plants codifying a protease inhibitor on soil microbial community. *Soil Biol. Biochem.* 40 (12), 2928–2936. doi: 10.1016/j.soilbio.2008.07.027

Rogoff, M. H. (1958). An aromatic intermediate in the bacterial oxidation of quinic acid. *J. Gen. Microbiol.* 19 (02), 330–339. doi: 10.1099/00221287-19-2-330

Saxena, D., and Stotzky, G. (2000). Insecticidal toxin from *Bacillus thuringiensis* is released from roots of transgenic *Bt* corn *in vitro* and in situ. *FEMS Microbiol. Ecol.* 33, 35–39. doi: 10.1016/S0168-6496(00)00041-6

Saxena, D., and Stotzky, G. (2001). *Bt* corn has a higher lignin content than non-*Bt* corn. *Am. J. Bot.* 88 (09), 1704–1706. doi: 10.2307/3558416

Schneider, A. R., Gommeaux, M., Duclercq, J., Fanin, N., Conreux, A., Alahmad, A., et al. (2017). Response of bacterial communities to Pb smelter pollution in contrasting soils. *Sci. Total Environ.* 605-606, 436–444. doi: 10.1016/j.scitotenv.2017.06.159

Sivaraman, I., Arumugam, N., Sodhi, Y. S., Gupta, V., Mukhopadhyay, A., Pradhan, A. K., et al. (2004). Development of high oleic and low linoleic acid transgenic in a zero erucic acid *Brassica juncea* l. (Indian mustard) line by antisense suppression of the *fad2* gene. *Mol. Breed.* 13 (04), 365–375. doi: 10.1023/B:MOLB.0000034092.47934.d6

Tian, W. H., Yi, X. L., Liu, S. S., Zhou, C., and Wang, A. Y. (2020). Effect of transgenic cotton continuous cropping on soil bacterial community. *Ann. Microbiol.* 70 (1). doi: 10.1186/s13213-020-01602-8

Toju, H., Tanabe, A. S., Yamamoto, S., and Sato, H. (2012). High-coverage ITS primers for the DNA-based identification of ascomycetes and basidiomycetes in environmental samples. *PloS One* 7 (7). doi: 10.1371/journal.pone.0040863

Valdés-Santiago, L., Cervantes-Chávez, J. A., León-Ramírez, C. G., and Ruiz-Herrera, J. (2012). Polyamine metabolism in fungi with emphasis on phytopathogenic species. *J. Amino Acids* 2012, 1–13. doi: 10.1155/2012/837932

Valdés-Santiago, L., and Ruiz-Herrera, J. (2014). Stress and polyamine metabolism in fungi. *Front. Chem.* 2. doi: 10.3389/fchem.2013.00042

van Wyk, D. A. B., Adeleke, R. R., Owen, H. J., Bezuidenhout, C. C., and Mienie, C. (2017). Ecological guild and enzyme activities of rhizosphere soil microbial communities associated with *Bt*-maize cultivation under field conditions in north West province of south Africa. *J. Basic Microbiol.* 57 (09), 781–792. doi: 10.1002/jobm.201700043

Wang, J. W., Chen, Z. N., Gao, J., Wang, Y. L., Fang, Z. J., Sun, L. J., et al. (2019). Effect of oleic acid on acute cadmium poisoning and cadmium residue in mice. *J. Biol.* 36 (04), 50–54. doi: 10.3969 /j. issn.2095-1736.2019.04.050

Wang, Q., Garrity, G. M., Tiedje, J. M., and Cole, J. R. (2007). Naive Bayesian classifier for rapid assignment of rRNA sequences into the new bacterial

taxonomy. *Appl. Environ. Microbiol.* 73 (16), 5261–5267. doi: 10.1128/AEM.00062-07

Wang, J. Q., Wen, X. F., Zhang, Y. Y., Zou, P. P., Cheng, L., Gan, R. Y., et al. (2021). Quantitative proteomic and metabolomic analysis of *Dictyophora indusiata* fruiting bodies during post-harvest morphological development. *Food Chem.* 339. doi: 10.1016/j.foodchem.2020.127884

Wang, X. Y., and Xie, J. (2020). Assessment of metabolic changes in *Acinetobacter johnsonii* and *Pseudomonas fluorescens* co-culture from bigeye tuna (*Thunnus obesus*) spoilage by ultra-high-performance liquid chromatography-tandem mass spectrometry. *Lwt-Food Sci. Technol.* 123. doi: 10.1016/j.lwt.2020.109073

Wang, X. J., Zhang, X., Yang, J. T., and Wang, Z. X. (2018). Effect on transcriptome and metabolome of stacked transgenic maize containing insecticidal *cry* and glyphosate tolerance *epsps* genes. *Int. J. Lab. Hematol.* 38, 42–49. doi: 10.1111/ijlh.12426

Watts, C., Si-Hoe, S. M., Lamb, H. K., Levett, L. J., Coggins, J. R., and Hawkins, A. R. (2002). Kinetic analysis of the interaction between the QutA and QutR transcription-regulating proteins. *Proteins: Structure Funct. Genet.* 48 (2), 161–168. doi: 10.1002/prot.10157

Xiong, Y. W., Li, X. W., Wang, T. T., Gong, Y., Zhang, C. M., Xing, K., et al. (2020). Root exudates-driven rhizosphere recruitment of the plant growth-promoting rhizobacterium *Bacillus flexus* KLBMP 4941 and its growth-promoting effect on the coastal halophyte *Limonium sinense* under salt stress. *Ecotoxicol. Environ. Saf.* 194. doi: 10.1016/j.ecoenv.2020.110374

Yang, R. J. (2006). Allelopathic effects of rape root exudates on growth of seedlings of different crops. *Ecol. Environ.* 15 (05), 1062–1066. doi: 10.16258/j.cnki.1674-5906.2006.05.034

Yang, Q. L., Min, P., Cao, Y. L., Li, H. X., and Yu, S. L. (2009). Effect of high-oleate peanut on serum lipids level in rats. *J. Peanut Sci.* 38 (03), 6–9. doi: 10.14001/j.Issn.1002-4093.2009.03.002

Zhang, X. B., Wang, X. J., Tang, Q. L., Li, N., Liu, P. L., Dong, Y. F., et al. (2015). Effects of cultivation of OsrHSA transgenic rice on functional diversity of microbial communities in the soil rhizosphere. *Crop J.* 3 (2), 163–167. doi: 10.1016/j.cj.2014.11.001

Zhou, X. L., Liang, J. G., Luan, Y., Song, X. Y., and Zhang, Z. G. (2021a). Characterisation of *Bt* maize IE09S034 in decomposition and response of soil bacterial communities plant. *Soil Environ.* 67 (05), 286–298. doi: 10.17221/629/2020-PSE

Zhou, C., Pan, W. S., Peng, Q., Chen, Y. C., Zhou, T., Wu, C., et al. (2021b). Characteristics of metabolites by seed-specific inhibition of *FAD2* in *B. napus* l. *J. Agric. Food Chem.* 69 (19), 5452–5462. doi: 10.1021/acs.jafc.0c06867

Zou, Q., An, W. H., Wu, C., Li, W. C., Fu, A. Q., Xiao, R. Y., et al. (2018). Red mud –modified biochar reduces soil arsenic availability and changes bacterial composition. *Environ. Chem. Lett.* 16 (2), 615–622. doi: 10.1007/s10311-017-0688-1

Zuo, L. Z., Yang, R. L., Zhen, Z. X., Liu, J. X., Huang, L. S., and Yang, M. S. (2018). A 5-year field study showed no apparent effect of the *Bt* transgenic 741 poplar on the arthropod community and soil bacterial diversity. *Sci. Rep.* 8 (01), 1–13. doi: 10.1038/s41598-018-20322-3

frontiers | Frontiers in Plant Science

TYPE Original Research
PUBLISHED 21 December 2022
DOI 10.3389/fpls.2022.1050967

OPEN ACCESS

EDITED BY
Juan Li,
Hunan Agricultural University, China

REVIEWED BY
Yi Cheng,
Chinese Academy of Agricultural Sciences (CAAS), China
Fenliang Fan,
Chinese Academy of Agricultural Sciences (CAAS), China

*CORRESPONDENCE
Huaqun Yin
yinhuaqun_cs@sina.com
Liangzhi Li
205601006@csu.edu.cn

SPECIALTY SECTION
This article was submitted to Plant Symbiotic Interactions, a section of the journal Frontiers in Plant Science

RECEIVED 22 September 2022
ACCEPTED 08 November 2022
PUBLISHED 21 December 2022

CITATION
Wang Z, Fu C, Tian J, Wang W, Peng D, Dai X, Tian H, Zhou X, Li L and Yin H (2022) Responses of the bacterial community of tobacco phyllosphere to summer climate and wildfire disease.
Front. Plant Sci. 13:1050967.
doi: 10.3389/fpls.2022.1050967

Responses of the bacterial community of tobacco phyllosphere to summer climate and wildfire disease

Zhenhua Wang[1], Changwu Fu[1], Jinyan Tian[1], Wei Wang[1], Deyuan Peng[1], Xi Dai[1], Hui Tian[1], Xiangping Zhou[2], Liangzhi Li[3,4]* and Huaqun Yin[3,4]*

[1]Zhangjiajie Tobacco Company of Hunan Province, Zhangjiajie, China, [2]Yongzhou Tobacco Company of Hunan Province, Yongzhou, China, [3]School of Minerals Processing and Bioengineering, Central South University, Changsha, China, [4]Key Laboratory of Biometallurgy of Ministry of Education, Central South University, Changsha, China

Both biotic and abiotic factors continually affect the phyllospheric ecology of plants. A better understanding of the drivers of phyllospheric community structure and multitrophic interactions is vital for developing plant protection strategies. In this study, 16S rRNA high-throughput sequencing was applied to study how summer climatic factors and bacterial wildfire disease have affected the composition and assembly of the bacterial community of tobacco (*Nicotiana tabacum* L.) phyllosphere. Our results indicated that three time series groups (T1, T2 and T3) formed significantly distinct clusters. The neutral community model (NCM) and beta nearest taxon index (betaNTI) demonstrated that the overall bacterial community assembly was predominantly driven by stochastic processes. Variance partitioning analysis (VPA) further showed that the complete set of the morbidity and climatic variables together could explain 35.7% of the variation of bacterial communities. The node numbers of the molecular ecological networks (MENs) showed an overall uptrend from T1 to T3. Besides, *Pseudomonas* is the keystone taxa in the MENs from T1 to T3. PICRUSt2 predictions revealed significantly more abundant genes of osmoprotectant biosynthesis/transport in T2, and more genes for pathogenicity and metabolizing organic substrate in T3. Together, this study provides insights into spatiotemporal patterns, processes and response mechanisms underlying the phyllospheric bacterial community.

KEYWORDS

tobacco, phyllosphere, bacterial community, high-throughput sequencing, molecular ecological networks, neutral community model

Introduction

The leaf surface on which microorganisms inhabit is called phyllosphere, which is an independent microhabitat of plant foliar surface. Bacteria, fungi, algae and other microorganisms living in these regions are called phyllospheric microorganisms, the structure of which is affected by a range of abiotic and biotic factors, including space (Rastogi et al., 2012) , growth season (Copeland et al., 2015) , climate variation (Medina-Martínez et al., 2015) , solar radiation (Truchado et al., 2017) and disease severities (Zheng et al., 2022) . The phyllospheric area has long been considered an unfavorable habitat for microbial colonization due to long time exposure to solar/ultraviolet radiation, severe diurnal temperature, desiccation, fluctuation of humidity, scouring rainfall, and the scarcity of available nutrients. Recent high-throughput sequencing technologies have enabled the characterization exhaustively the spatio-temporal structure of phyllosphere microbiome. It has also been found that there are a large number of microorganisms inhabiting the phyllosphere, with a density as high as 10^6-10^7 cells per square centimeter with multiple biological functions, such as improving plant disease resistance, biocontrol of phytopathogens, enhancing nitrogen fixation, decomposing toxic and harmful substances, and producing plant hormones, volatile organic compounds (VOCs) to promote plant growth (Vorholt, 2012; Xu et al., 2022) . Besides, the phyllosphere also stands for a suitable model system for testing basic principles in ecology since it is amenable for experiments and visual inspection. Such research has implications for fields like plant health and environmental chemistry (Redford and Fierer, 2009; Remus-Emsermann and Schlechter, 2018) .

A thorough understanding of the ecological drivers of phyllospheric community assembly and multitrophic interactions is vital to develop strategies for plant protection. However, many research aspects of phyllospheric microbiome still lag behind in comparison with rhizospheric studies.

Tobacco (*Nicotiana tabacum* L.), is a model plant and important economic crop, and an ideal research object to study plant-microbe interactions under multiple stresses (Xiang et al., 2022). Tobacco is usually grown in summer and harvested at the end of August. Tobacco's leaves are continually subjected to excessive strong sunlight on summer days, which makes it an ideal material to study the mechanism of bacterial community assembly and succession in the face of strong abiotic stresses (i.e., UV radiation, desiccation and heat), accompanied with pathogen invasion (Bringel and Couée, 2015; Xing et al., 2022). Dai et al. (2022) investigated the spatiotemporal variation of the community tobacco leaves affected by brown spot disease and found that the relative abundance of *Pseudomonas, Sphingomonas*, and *Methylobacterium* increased as tobacco leaves aging gradually. Besides, Liu et al. (2022) found that the inoculation of *Bacillus velezensis* SYL-3 could increase the abundance of beneficial bacteria, (*Pseudomonas* and *Sphingomonas*), while suppress the pathogens *Alternaria alternata* and tobacco mosaic virus (TMV).

In the current study, we have tried to (i) elucidate successions of the taxonomic and functional profile in the phyllospheric bacterial community under abiotic and biotic stresses of three time periods T1, T2 and T3 in summer (corresponding to the June, July and August of the year 2021), (ii) investigate which members in different bacterial community conferred positive effects on the plant upon abiotic and biotic stresses, and (iii) compare the networks of different period to provide insights into the key taxa of communities.

Results and discussion

Bacterial community composition and diversity in tobacco phyllosphere

A total of 2,302,148 high-quality paired 16S rRNA sequences and 3,276 operational taxonomic units (OTU) were obtained from 36 tobacco phyllospheric bacterial DNA samples, (average: 63,949; range: 47,651–79,418 reads per sample). The ternary phase diagrams (Figure 1A) show the relative abundance and relationships of the different taxonomic categories in the three time series groups (T1, T2 and T3), with the circle's size and vicinity to the vertex proportional to relative abundance in the respective group. We found that the phylum *Proteobacteria*, class *Gammaproteobacteria* and orders *Pseudomonadales* and *Enterobacteriales* made up the majority of phyllospheric bacterial taxa (Figures 1A, B). In comparison, the phyllosphere of other species from the solanaceous family such as tomato (*Lycopersicon esculentum*) is also additionally dominant by *Rhizobium*, *Methylobacterium*, and *Xanthomonas* (Ottesen et al., 2013; Toju et al., 2019).

Principal coordinate analysis (PCoA) of Bray–Curtis distance (Figure 1C) revealed that the microbiome from three time series groups (T1, T2 and T3) formed three significantly distinct clusters, indicating that phyllospheric microbiome from different time periods exhibited distinct community compositions. The first three axes together explained 75.4% of the cumulative variation (ANOISM analysis, $p < 0.001$, $R = 0.597$). A total of 556 OTUs are shared across three groups (Figure 1D), and T3 group comparatively has more unique OTUs (795), followed by T2 group (628) and T1 group (591). Alpha diversity indexes, including Richness, Shannon, Simpson, Pielou, and invsimpson showed an obvious uptrend from the T1 group to T3 group (Figure 2).

To determine the changes in bacterial community composition across time series, LEfSe analysis was applied to find the differential taxa in each group. The linear discriminant analysis (LDA) score is positively correlated with the significance of bacterial biomarkers in each group (Figure 3). Comparatively, T1 group shows enrichment of bacterial families like *Enterobacteriaceae* (LDA =5.89) and *Haliangiaceae* (LDA =3.12), genra *Azorhizobium* (LDA =3.37)

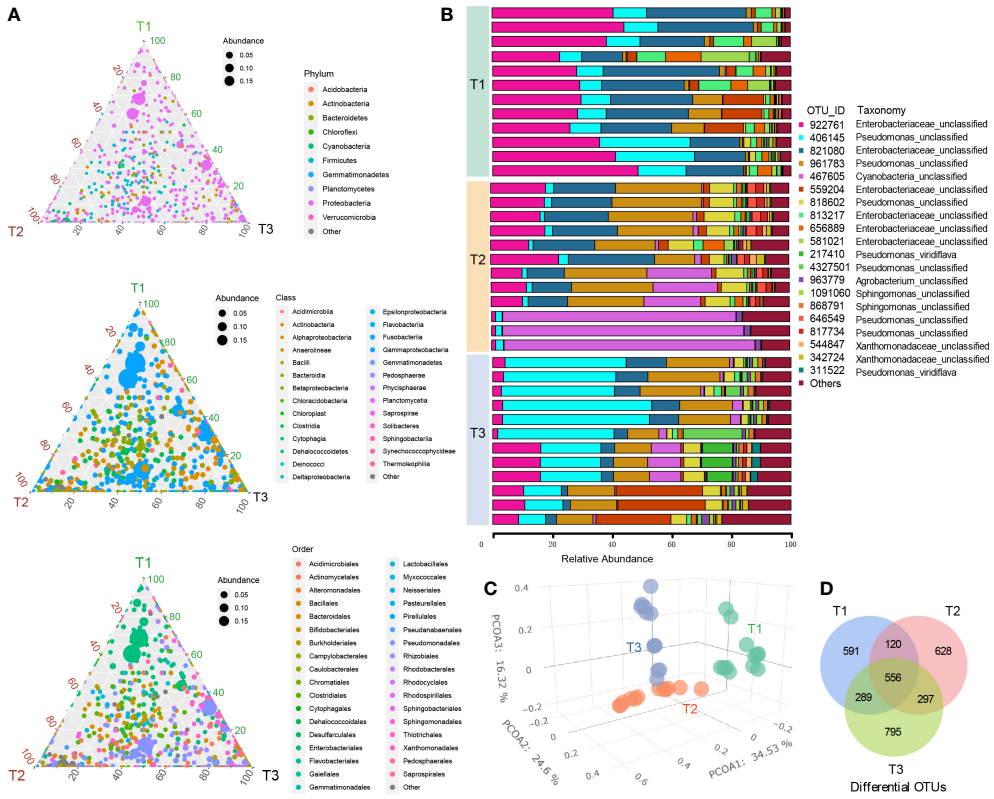

FIGURE 1
Bacterial community composition and diversity in tobacco phyllosphere. **(A)** The ternary phase diagrams showing the relative abundance and relationships of the different taxonomic categories (top, phylum; middle, class; bottom, order) in the three time series groups (three vertices, T1, T2 and T3). The size of each circle is proportional to relative abundance; the closer the circle is to the vertex, the higher the relative abundance of the group in that group. **(B)** Stack bar chart showing the twenty most abundant OUT taxa in each sample. **(C)** Principal coordinate analysis (PCoA) of Bray–Curtis dissimilarity matrices showing effects of time series (T1, T2 and T3 groups) on the tobacco phyllospheric bacterial community structure. **(D)** Venn diagram depicting number of shared or unique OTUs in each time series group (T1, T2 and T3).

and *Bradyrhizobium* (LDA =3.34), and species *Azorhizobium doebereinerae* (LDA =3.34). Members of *Enterobacteriaceae* in plant phyllosphere are sensitive to abiotic or biotic stresses (Erlacher et al., 2015), whose population sizes decline upon desiccation stress on leaves (Brandl and Mandrell, 2002; Brandl, 2006; Whipps et al., 2008), and they contribute to the overall phyllospheric resistome (Cernava et al., 2019).

At the same time, T2 group shows enrichment of bacterial phylum *Cyanobacteria* (LDA =5.13), *Firmicutes* (LDA =3.37) and *Actinobacteria* (LDA =3.09), class like *Alphaproteobacteria* (LDA =3.59), orders like *Burkholderiales* (LDA =3.57) and *Oceanospirillales* (LDA =3.23). In previous studies, *Firmicutes* (represented by *Bacillus* sp.) and *Cyanobacteria* were considered beneficial to plant growth and pathogen control (Priya et al., 2015; Han et al., 2016; Liu et al., 2022), indicating that plant host might have induced the enrichment of these pathogen antagonists in the phyllosphere during T2 to rescue itself from disease invasion.

Whereas the T3 group shows strong enrichment of genra including *Pseudomonas* (LDA =5.29), *Sphingomonas* (LDA =4.19), *Agrobacterium* (LDA =3.82), and family like *Xanthomonadaceae* (LDA =3.94). Most *Pseudomonas* species are beneficial for plants, producing phytohormones and siderophores to the inhibit pathogens (McSpadden et al., 2001; Hsu and Micallef, 2017) and induce host systemic resistance to improve morphological and biochemical traits of plants at the same time (Kumar et al., 2021). Besides, the abundance of *Pseudomonas* was negatively correlated with the disease index caused by pathogens *Alternaria alternate* (leaf spot or blight disease) tobacco mosaic virus (TMV) both in tobacco (Liu et al., 2022) and tomato (Gupta et al., 2021). Likewise, *Sphingomonas* sp., is a kind of gram-negative, aerobic foliar and phytohormone-producing bacterium capable of protecting plants from foliar diseases caused by *Pseudomonas syringae* (wildfire disease pathogen) *via* substrate competition (Vogel et al., 2012) and various pathogenic fungi (e.g., *Alternaria* and *Arthrinium*) (Enya et al., 2007; Vogel et al., 2012; Luo et al., 2019) and improving plant growth during stress conditions (Asaf et al., 2020). The enrichment of *Pseudomonas* and *Sphingomonas* in T3 might be a"cry for help" strategy of tobacco for the recruitment

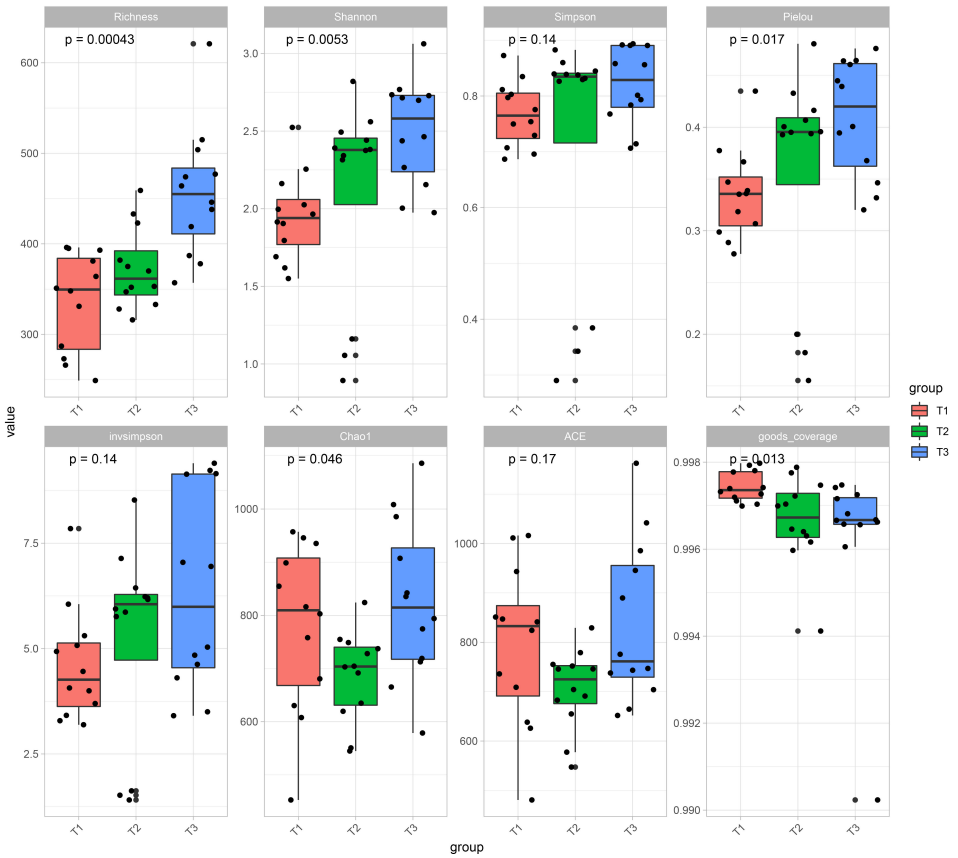

FIGURE 2
Alpha diversity indexes including Richness, Shannon, Simpson, Pielou, invsimpson, Chao1, ACE, and goods coverage of tobacco phyllospheric bacterial communities in each time series group (T1, T2 and T3).

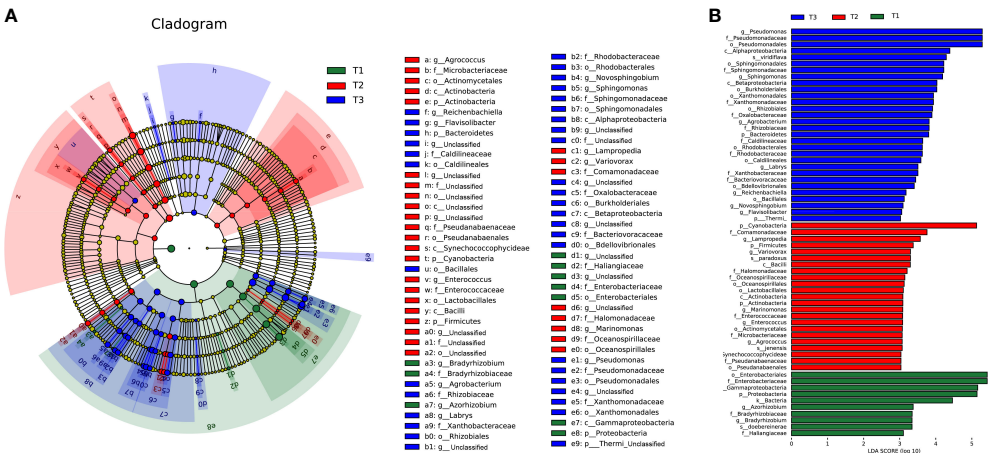

FIGURE 3
The linear discriminant analysis effect size (LEfSe) analysis at species level of bacterial communities (with LDA score >3.1 and $p < 0.05$) among T1, T2 and T3 groups presented by **(A)** cladogram **(B)** and distribution histogram.

of microbes upon biotic (pathogen invasion) and abiotic stresses (drought and heat) (Wang and Song, 2022).

The neutral community model (NCM) is a validated method for deducing stochastic processes related to community assembly, which has been helpful in explaining various ecological phenomena (Roguet et al., 2015) . This model could quantify the significance of processes that are not easy to observe directly but might have a great impact on microbial communities (i.e., dispersal and ecological drift). In our study, the neutral community model (NCM) has successfully predicted a large fraction of the relation between the occurrence frequency of OTUs and the relative abundance (Figure 4A), with 72.1%, 70.8%, 71.6% and 71.5% of explained community variance for T1, T2, T3 groups and overall, respectively, indicating similar responses of species in different groups to stochastic processes. Besides, the Nm value is relatively higher for T2 group (Nm = 38,332) than T1 group (Nm = 24,237) and T3 group (Nm = 25,770), indicating that the species dispersal was higher in T2 group. Consistently, the majority of betaNTI values of these tobacco phyllospheric bacterial communities fall within -2 and +2 (stochastic process) in all groups (Figure 4B). The distributions of betaNTI shifted with a downtrend from higher betaNTI in T1 showing more deterministic community assembly processes (betaNTI > 2) to lower betaNTIs in T2 and T3 predominant with stochastic community assembly processes (-2 < betaNTI < +2). Besides, the estimated niche width of T3 group is significantly greater than that of T2 and T1 (Figure 4C). These results suggested that stochasticity was more important than determinism in influencing the tobacco phyllospheric bacterial community

It has been demonstrated that environmental factors (e.g., water, temperature, nutrient and metal concentrations) affect the microbial community composition, which further impact the relative abundance and occurrence frequency of microbes in the neutral or non-neutral distribution . (Liu et al., 2013; Logares et al., 2013; Zhang et al., 2018) Rainfall always concentrates in the summer season in the subtropical area of China. Zhangjiajie region (the sample collection site) generally has the annual precipitation peak in July (corresponding to T2), according to data from national meteorological center of China (http://www.nmc.cn/). Such rainfall abounding conditions, along with accompanying high aerial humidity, could increase the air retention time of microbe (pathogen) and facilitate their passive dispersal across space with higher immigration rate and spores germination on the leaf surface. This might explain why the T2 group has the highest Nm-value in the neutral community model, similar to what have observed in previous studies (Chen et al., 2019) .

Relationship between bacterial populations and environmental factors

Redundancy analysis (RDA) was further applied to reveal the relationship between phyllospheric bacterial populations and factors (Figure 4D). RDA results showed that morbidity variables, including wildfire disease incidence rate (IR) and disease index (DI), are positively correlated with temperature (TEMP) and OTU406145 (*Pseudomonas syringae*, the pathogen of bacterial wildfire disease), whereas they negatively correlated with OTU467605 (*Cyanobacteria*), indicating that *Cyanobacteria* is the potential disease biocontrol agent. Consistently, a previous study also indicated that *Cyanobacteria* was a major phylum on the leaf of tobacco (Xing et al., 2021) and *Cyanobacteria* may play a major role in nutrient cycling and water storage in the phyllosphere (Fürnkranz et al., 2008). Besides, humidity (HM) and rainfall capacity (RC) are consistently and positively correlated with *Enterobacteriaceae* (OTU559204, OTU581021, OTU813217, OTU656889, OTU922761). This is consistent with previous reports that members of *Enterobacteriaceae* in the phyllosphere are capable of rapid reproduction and formation of aggregates under high moisture conditions and are sensitive to fluctuations in water availability on plant surfaces (Brandl and Mandrell, 2002; Brandl, 2006; Whipps et al., 2008).

Overall, the morbidity (IR, DI) and climatic factors (TEMP, HM, RC) have significantly affected the phyllospheric bacterial community. Variance partitioning analysis (VPA) further showed that the complete set of the morbidity and climatic variables together could explain 35.7% of the variation of tobacco phyllospheric bacterial communities, with climatic variables contributing most (Figure 4E). Still, the high proportion of unexplained variation in VPA also suggested the potential importance of neutral or stochastic processes during community assembly.

Molecular ecological networks of phyllospheric bacterial community

Molecular ecological networks (MENs) were constructed to unravel how the combinations of bacterial wildfire disease and climatic factors have affected microbial interactions across the three time periods (Figure 5). The topological properties of the three sub networks were shown in Table 1. The node numbers of the phyllosphere networks showed an overall uptrend from T1 to T3. Whereas link numbers increase sharply from T1 (639) to T2 (14,401), followed by a rapid decrease to T3 (3,533). Similar trend is also found in MEN properties like the average number of neighbors, network density (comparison between the edges available in a graph and a graph with all possible edges), network centralization (measure of how much the degree of every node is far from the degree of the highest degree node), and connected components (a maximal set of nodes such that each pair of nodes is connected by a path). This indicated that T2 was more complex, with abundant interactions in a highly connected microbial community, which might also be explained by the rainfall peak at T2 that has provided great growth opportunity for microbes to multiply and make connections as mentioned

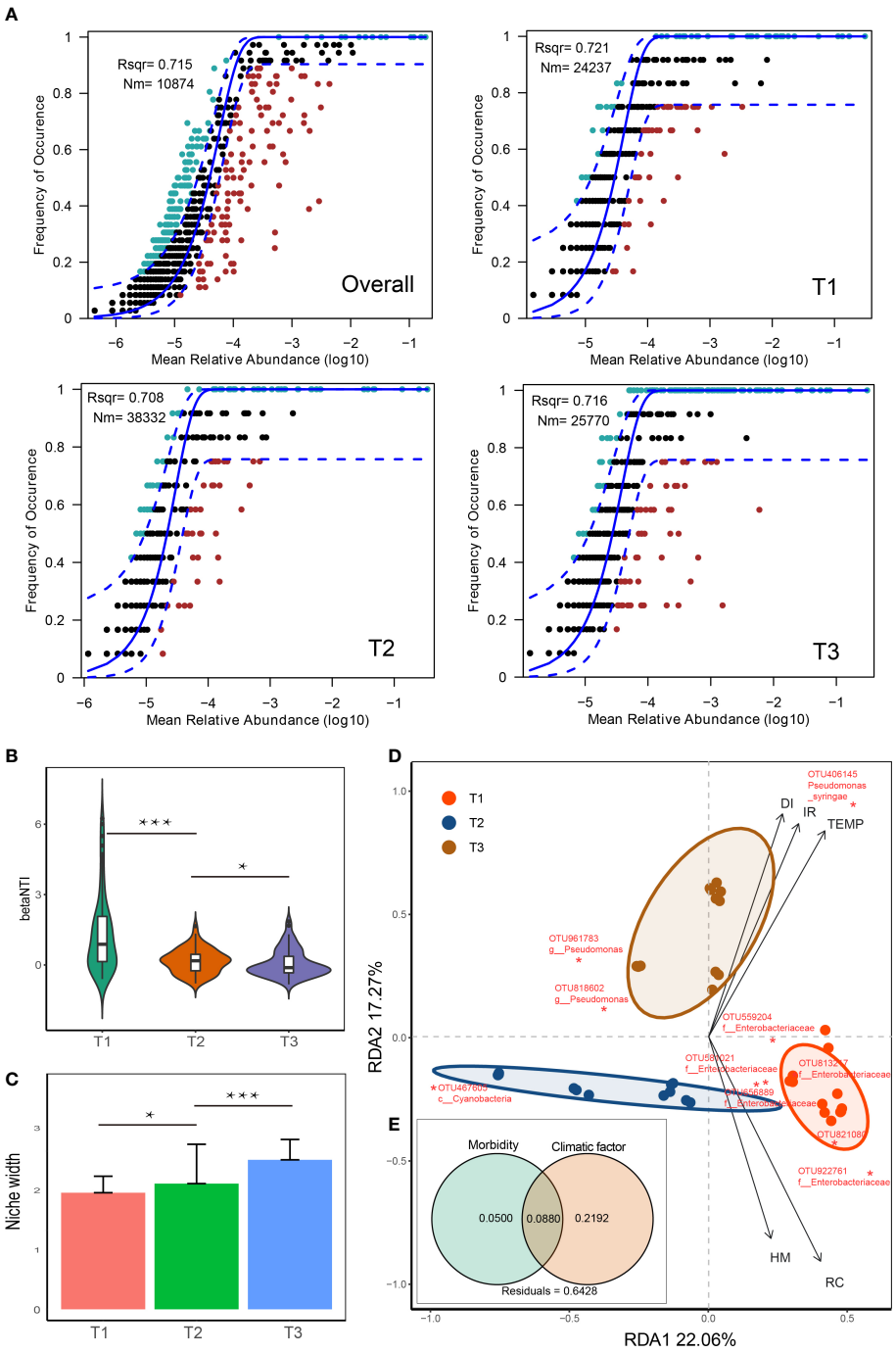

FIGURE 4
Analyses on factors that impacted the relative abundance and occurrence frequency of microbes in tobacco phyllosphere. **(A)** Fit of the neutral community model (NCM) of community assembly. The OTUs more frequently present than predicted are in cyan, whereas those less frequently are in red. The blue dashed lines represent 95% confidence intervals around the model prediction and the OTUs fallen into the confidence intervals are regarded as neutrally distributed. Nm indicates the meta-community size times immigration, Rsqr indicates the fit to the neutral model. Neutral processes are the part within 95% confidence interval (red) while non-neutral are the parts including above and below prediction (dark green); **(B)** beta nearest taxon index (betaNTI) comparison; **(C)** niche breadth comparison; **(D)** redundancy analysis (RDA) of the relationships between bacterial community in tobacco leaves and environmental variables, including morbidity variables (disease incidence rate: IR, and disease index: DI) and climatic factors (temperature: TEMP, humidity: HM, and rainfall capacity: RC), **(E)** variance partitioning analysis (VPA) showing contributions of morbidity and climatic variables to tobacco phyllospheric bacterial community variation. Asterisks indicate significance; *, $p < 0.05$; ***, $P< 0.001$.

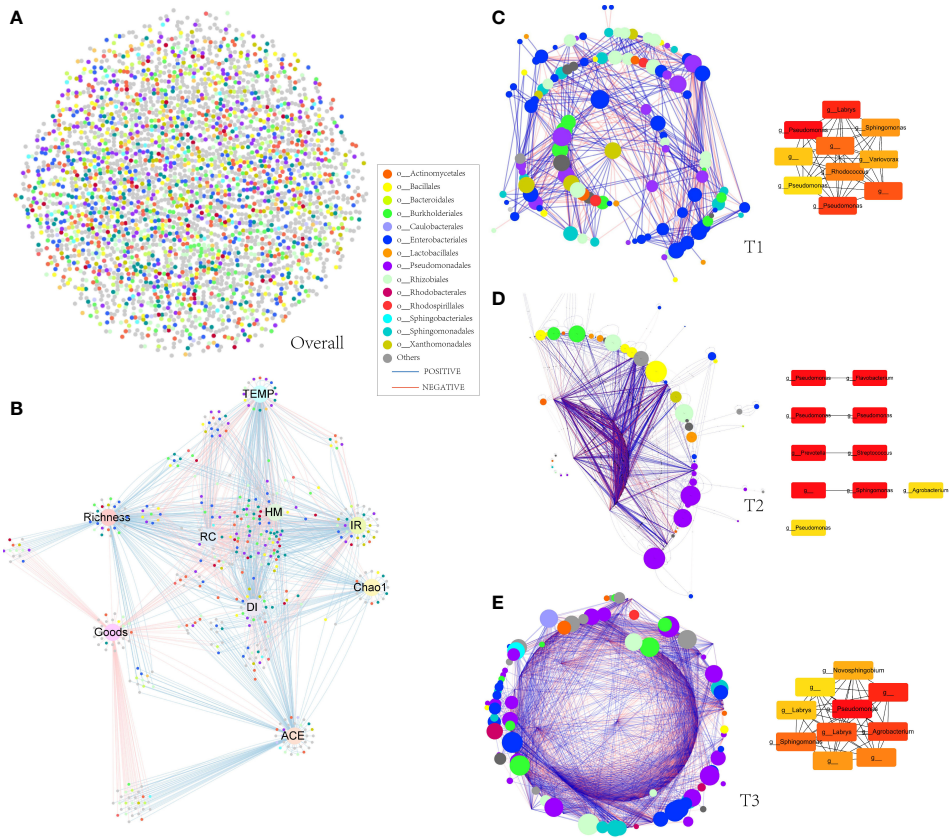

FIGURE 5
Molecular ecological networks of phyllospheric bacterial community. Each node represents an OTU. The size of each node is proportional to the number of connections (that is, degree) and the colors of nodes represent different order. The links between the nodes indicate strong and significant ($P < 0.01$) correlations. A red line indicates a negative interaction between two individual nodes, while a blue line indicates a positive interaction. **(A)** Overall molecular ecological network; **(B)** spearman correlation between environmental factor, alpha diversity index, and OTUs. **(C)** molecular ecological network of T1 group (left) and predicted keystone nodes (right); **(D)** molecular ecological network of T2 group (left) and predicted keystone nodes (right); **(E)** molecular ecological network of T3 group (left) and predicted keystone nodes (right).

TABLE 1 Molecular ecological network properties of the three groups.

	T1	T2	T3
Number of nodes	117	191	200
Number of edges	639	14401	3533
Positive link	0.574	0.527	0.536
Negative link	0.425	0.472	0.463
Avg- number of neighbors	10.923	45.73	35.33
Network diameter	6	7	5
Network radius	4	7	3
Characteristic path length	2.677	2.154	2.181
Clustering coefficient	0.409	0.691	0.637
Network density	0.094	0.249	0.178
Network heterogeneity	0.659	0.806	0.64
Network centralization	0.141	0.331	0.206
Connected components	1	7	1

above. A similar phenomenon of relatively higher connections was also observed in the wilt diseased rhizoplane of tobacco (Tao et al., 2022) . The percentage of positive correlation follow largely a downtrend from T1 (57.4%) to T3 (53.6%), indicating the decrease of cooperative relation. Besides, it is predicted by the program cytoHubba (Chin et al., 2014) that *Pseudomonas* is the keystone taxa and is present in the top 10 important nodes in the MENs from T1 to T3 (Figure 5). Other frequently present keystone taxa includes *Sphingomonas* and *Labrys*. These taxa are reported to be dominant in plant phyllosphere and might play important roles in inhibiting plant disease (Liu et al., 2021; Liu et al., 2022).

The function profiles of phyllospheric bacterial community

To assess the putative effect of stress factors on the bacterial community functions of different time periods, metagenome of tobacco phyllospheric bacterial communities were predicted with PICRUSt2 (Douglas et al., 2020) followed by annotation in referring to the KEGG database. A total of 7,557 KOs (KEGG Orthologs) were predicted across three groups, and some of them are significantly different among groups (Figures 6A, B). For example, biosynthesis/transport genes of osmoprotectant against osmotic stress (*opuA, opuBD, treA, otsA*) in T2 were predicted to be more abundant than T3 (Figure 6B). At the same time, the relative abundance of genes encoding resistance–nodulation–division (RND) type cobalt–zinc–cadmium resistance protein, periplasmic protein TonB, sirohydrochlorin ferrochelatase, twitching motility protein PilU and several metabolic genes for organic substrate (*atoB, paaH, prnA, prpB, ctpA, pepO, aguA, abfA*) is significantly increased in T3. We proposed that these genes enriched in the T3 group were related with the deterioration of wildfire disease, since previous studies have found RND efflux pumps of plant-pathogenic *P. syringae* pathovars essential for *in planta* reproduction and evasion of the host native immune response (Stoitsova et al., 2008) . Besides, TonB-dependent receptor is regarded as a feature shared by phytopathogenic bacteria for the uptake of various carbohydrates under environmental conditions (Blanvillain et al., 2007) . Motility can help wildfire disease pathogen search for favorable sites, facilitate spreading and locate the most preferred site (Haefele and Lindow, 1987) . Toxin such as syringomycin produced by *Pseudomonas syringae* is responsible for pore formation and nutrient leakage through the host cell membrane (Pritchard et al., 2009) , Besides, plants generally produce phenolic substances to counteract increased stress levels (Lucas et al., 2022). This might explain the significant enrichment of organic metabolic genes in the T3 group community.

Collectively, this study has contributed to improving the understanding of the spatiotemporal patterns of tobacco phyllospheric microbiome and shed light on the putative underlying mechanism.

Materials and methods

Disease incidence of bacterial wildfire disease

The standards used to examine tobacco bacterial wildfire disease were based on the tobacco pest classification and survey methods (GB/T 23222–2008), P.R. China. Disease incidence was calculated by the percentage of diseased tobacco in each field. Disease index was calculated using the formula:

$$Disease\ \ index\ \ (DI)\ \ =\ \ \left[\sum(r \times N)/(n \times R)\right]\ \ \times\ \ 100$$

r is the disease severity; N is the number of infected tobaccos with a rating of r; n is the total number of tobaccos tested, and R is the value of the highest disease severity in each field. Meteorological data were retrieved from the National Meteorological Center of China (http://www.nmc.cn/).

Sample collection

The tobacco leaf samples were collected in Gaofeng Town, Cili County, Zhangjiajie City, Hunan Province (29°28′5″N, 110° 57′53″E), China, at June (T1), July (T2) and August (T3) of 2021. In the test areas, tobacco fields having typical and serious bacterial wildfire disease levels were selected. In the same plot, with similar conditions, plants with typical symptoms of bacterial wildfire disease were sampled, with three plants per group. The experiment adopted a random block design with three duplicates; the plot area was 90 m^2. Other field management measures were carried out in accordance with local planting practices. A total of 18 plants were randomly selected from each plot, and the middle leaves of every sixth plant were taken as a sample, which was kept at 4°C and brought back to the laboratory for subsequent foliar microbial DNA extractions.

DNA extraction and high-throughput sequencing

Fifteen grams of leaf samples obtained from various parts of the leaf surface (avoiding the main and branch veins) using a sterile puncher were added to 50 mL of 0.1% Tween-80 bacterial phosphate buffer (pH 7.0). The samples were then shaken for 30 min at 170 revolutions/min (rpm) and 28°C. The bacterial suspension was then collected, and the leaf samples were washed twice more. The collected suspensions were centrifuged

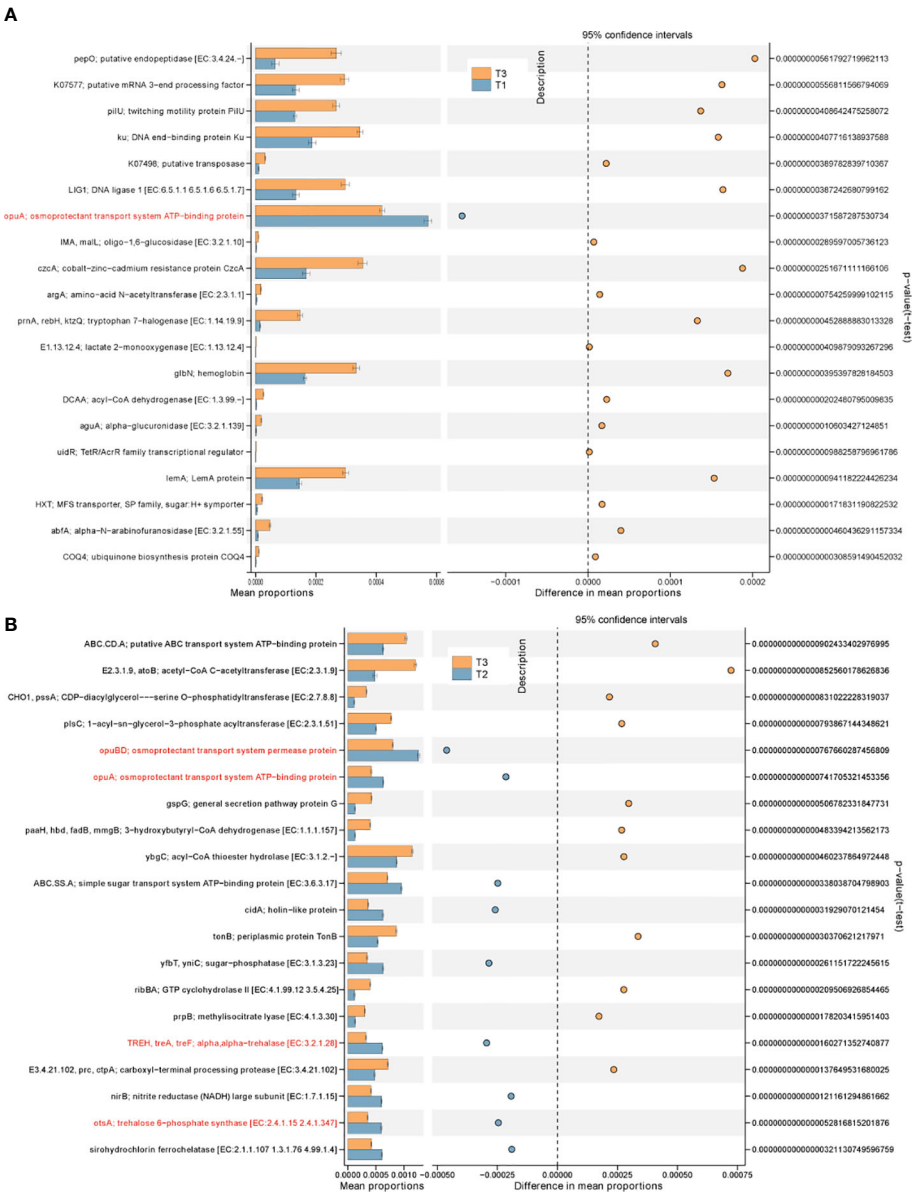

FIGURE 6
PICRUSt predicted metagenome functions with significant difference in abundance between groups at KO level. **(A)** T1 vs. T3; **(B)** T2 vs. T3.

for 15 min (4°C, 10,000 rpm) to pellet the microorganisms. The pellet was suspended in sterile water and washed three times. Finally, the microorganisms were resuspended with 1 mL of sterile water for subsequent DNA extraction. Genomic DNA extraction of foliar microorganisms was performed using the Plant Genomic DNA Kit (Plant Genomic DNA Kit), following the manufacturer's protocol. We used the primer pair 341F (5'-CCT ACG GGN GGC WGC AG-3') and 805R (5'-GAC TAC HVG GGTATC TAA TCC-3') of V3/V4 regions to amplify the 16S rRNA. Amplicons were sequenced by Illumina NovaSeq PE250 platform (LC-Bio Technology Co., Ltd, Hang Zhou, Zhejiang Province, China). The raw sequencing data were deposited in the European Nucleotide Archive database under accession number PRJEB56205.

Sequencing processing and statistical analyses

Raw sequences were split into sample libraries with perfect matches to barcodes. Low-quality sequences with QC < 20 over a 5-bp window size were trimmed using Btrim (Kong, 2011) , and sequences with a length of < 100 bp were removed. Then, the

forward and reverse sequences were spliced together. Any sequences containing ambiguous bases or the incorrect length were removed, and the remaining sequences were compared against the UNITE v8.2 database (Kõljalg et al., 2005) to remove possible chimeras. The length of the sequencing fragment was 200–400 bp. Then, UPARSE (Edgar, 2013) was used to cluster and produce operational taxonomic units (OTUs) at 97% similarity level. To ensure the authenticity of the data, we removed OTUs that were represented by only one sequence in overall data (global singletons). All statistical analyses and calculations were carried out using the R (v 3.6.3) statistical platform (www.r-project.org).

Network construction

To construct a microbial association network, correlations between pairwise OTUs that were present in more than half of the samples were calculated using the SparCC method (Friedman and Alm, 2012). Only edges with a significant correlation higher than 0.5 ($p < 0.01$) were retained for network construction. Cytoscape v.3.9.1 (https://cytoscape.org) was used for network visualization. Cytoscape plugin cytoHubba (Chin et al., 2014) with Maximal Clique Centrality (MCC) method was used to predict essential/keystone nodes in the network.

To determine the potential importance of stochastic processes on community assembly, we adopted a neutral community model (NCM) to predict the relationship between OTU detection frequencies and their relative abundance across the wider metacommunity, performed using R (version 3.6.3). The assembly processes of bacterial and fungal communities were evaluated by calculating the nearest taxon index and beta nearest taxon index (betaNTI) using the "picante" package. A betaNTI value < 2 indicates that the contribution is a stochastic process, and when betaNTI > 2 the shifts in community composition were considered to be shaped by deterministic processes.

The Phylogenetic Investigation of Communities by Reconstruction of Unobserved States (PICRUSt2) (Douglas et al., 2020) was applied to predict potential functional profiles of the bacterial community using 16S rRNA gene data.

Data availability statement

The datasets presented in this study can be found in online repositories. The names of the repository/repositories and accession number(s) can be found below: https://www.ebi.ac.uk/ena, PRJEB56205.

Author contributions

LL and HY conceived and designed the research. ZW, CF, JT, WW, DP, XD, HT and XZ conducted the experiment and analyzed the data. LL wrote the manuscript. All authors read and approved the manuscript.

Funding

This research was supported by the key project of Science and Technology of Hunan Branch of China National Tobacco Corporation (202104, HN2020KJ02).

Acknowledgments

We are grateful for resources from the High-Performance Computing Center of Central South University.

Conflict of interest

Author ZW, CF, JT, WW, DP, XD and HT are employed by Zhangjiajie Tobacco Company of Hunan Province. Author XZ is employed by Yongzhou Tobacco Company of Hunan Province.

The remaining authors declare that the research was conducted in the absence of any commercial or financial relationships that could be constructed as a potential conflict of interest.

The authors declare that this study received funding from Science and Technology of Hunan Branch of China National Tobacco Corporation. The funder was not involved in the study design, collection, analysis, interpretation of data, the writing of this article, or the decision to submit it for publication.

Publisher's note

References

Asaf, S., Numan, M., Khan, A. L., and Al-Harrasi, A. (2020). Sphingomonas: From diversity and genomics to functional role in environmental remediation and plant growth. *Crit. Rev. Biotechnol.* 40, 138–152. doi: 10.1080/07388551.2019.1709793

Blanvillain, S., Meyer, D., Boulanger, A., Lautier, M., Guynet, C., Denancé, N., et al. (2007). Plant carbohydrate scavenging through tonB-dependent receptors: A feature shared by phytopathogenic and aquatic bacteria. *PloS One* 2, e224. doi: 10.1371/journal.pone.0000224

Brandl, M. T. (2006). Fitness of human enteric pathogens on plants and implications for food safety. *Annu. Rev. Phytopathol.* 44, 367–392. doi: 10.1146/annurev.phyto.44.070505.143359

Brandl, M. T., and Mandrell, R. E. (2002). Fitness of salmonella enterica serovar Thompson in the cilantro phyllosphere. *Appl. Environ. Microbiol.* 68, 3614–3621. doi: 10.1128/AEM.68.7.3614-3621.2002

Bringel, F., and Couée, I. (2015). Pivotal roles of phyllosphere microorganisms at the interface between plant functioning and atmospheric trace gas dynamics. *Front. Microbiol.* 6. doi: 10.3389/fmicb.2015.00486

Cernava, T., Erlacher, A., Soh, J., Sensen, C. W., Grube, M., and Berg, G. (2019). Enterobacteriaceae dominate the core microbiome and contribute to the resistome of arugula (Eruca sativa mill.). *Microbiome* 7, 13. doi: 10.1186/s40168-019-0624-7

Chen, W., Ren, K., Isabwe, A., Chen, H., Liu, M., and Yang, J. (2019). Stochastic processes shape microeukaryotic community assembly in a subtropical river across wet and dry seasons. *Microbiome* 7, 138. doi: 10.1186/s40168-019-0749-8

Chin, C. H., Chen, S. H., Wu, H. H., Ho, C. W., Ko, M. T., and Lin, C. Y. (2014). CytoHubba: Identifying hub objects and sub-networks from complex interactome. *BMC Syst. Biol.* 8 Suppl 4, S11. doi: 10.1186/1752-0509-8-S4-S11

Copeland, J. K., Yuan, L., Layeghifard, M., Wang, P. W., and Guttman, D. S. (2015). Seasonal community succession of the phyllosphere microbiome. *Mol. Plant Microbe Interact.* 28, 274–285. doi: 10.1094/MPMI-10-14-0331-FI

Dai, Y. F., Wu, X. M., Wang, H. C., Li, W. H., Cai, L. T., Li, J. X., et al. (2022). Spatio-temporal variation in the phyllospheric microbial biodiversity of alternaria alternata-infected tobacco foliage. *Front. Microbiol.* 13. doi: 10.3389/fmicb.2022.920109

Douglas, G. M., Maffei, V. J., Zaneveld, J. R., Yurgel, S. N., Brown, J. R., Taylor, C. M., et al. (2020). PICRUSt2 for prediction of metagenome functions. *Nat. Biotechnol.* 38, 685–688. doi: 10.1038/s41587-020-0548-6

Edgar, R. C. (2013). UPARSE: Highly accurate OTU sequences from microbial amplicon reads. *Nat. Methods* 10, 996–998. doi: 10.1038/nmeth.2604

Enya, J., Shinohara, H., Yoshida, S., Tsukiboshi, T., Negishi, H., Suyama, K., et al. (2007). Culturable leaf-associated bacteria on tomato plants and their potential as biological control agents. *Microb. Ecol.* 53, 524–536. doi: 10.1007/s00248-006-9085-1

Erlacher, A., Cardinale, M., Grube, M., and Berg, G. (2015). Biotic stress shifted structure and abundance of enterobacteriaceae in the lettuce microbiome. *PloS One* 10, e118068. doi: 10.1371/journal.pone.0118068

Friedman, J., and Alm, E. J. (2012). Inferring correlation networks from genomic survey data. *PloS Comput. Biol.* 8, e1002687. doi: 10.1371/journal.pcbi.1002687

Fürnkranz, M., Wanek, W., Richter, A., Abell, G., Rasche, F., and Sessitsch, A. (2008). Nitrogen fixation by phyllosphere bacteria associated with higher plants and their colonizing epiphytes of a tropical lowland rainforest of Costa Rica. *ISME. J.* 2, 561–570. doi: 10.1038/ismej.2008.14

Gupta, A. K., Verma, J., Srivastava, A., Srivastava, S., and Prasad, V. (2021). A comparison of induced antiviral resistance by the phytoprotein CAP-34 and isolate P1f of the rhizobacterium pseudomonas putida. *3. Biotech.* 11, 509. doi: 10.1007/s13205-021-03057-3

Haefele, D. M., and Lindow, S. E. (1987). Flagellar motility confers epiphytic fitness advantages upon pseudomonas syringae. *Appl. Environ. Microbiol.* 53, 2528–2533. doi: 10.1128/aem.53.10.2528-2533.1987

Han, T., You, C., Zhang, L., Feng, C., Zhang, C., Wang, J., et al. (2016). Biocontrol potential of antagonist bacillus subtilis Tpb55 against tobacco black shank. *BioControl* 61, 195–205. doi: 10.1007/s10526-015-9705-0

Hsu, C. K., and Micallef, S. A. (2017). Plant-mediated restriction of salmonella enterica on tomato and spinach leaves colonized with pseudomonas plant growth-promoting rhizobacteria. *Int. J. Food Microbiol.* 259, 1–6. doi: 10.1016/j.ijfoodmicro.2017.07.012

Kõljalg, U., Larsson, K. H., Abarenkov, K., Nilsson, R. H., Alexander, I. J., Eberhardt, U., et al. (2005). UNITE: A database providing web-based methods for the molecular identification of ectomycorrhizal fungi. *New Phytol.* 166, 1063–1068. doi: 10.1111/j.1469-8137.2005.01376.x

Kong, Y. (2011). Btrim: A fast, lightweight adapter and quality trimming program for next-generation sequencing technologies. *Genomics* 98, 152–153. doi: 10.1016/j.ygeno.2011.05.009

Kumar, Y. V., Krishna, J. R., Kaushik, P., Altalayan, F. H., Al, B. T., and Alam, P. (2021). Traversing arbuscular mycorrhizal fungi and pseudomonas fluorescens for carrot production under salinity. *Saudi. J. Biol. Sci.* 28, 4217–4223. doi: 10.1016/j.sjbs.2021.06.025

Liu, T., Gu, Y., Zhou, Z., Liu, Z., Yin, H., Qin, C., et al. (2021). Ecological strategies of biological and chemical control agents on wildfire disease of tobacco (Nicotiana tabacum l.). *BMC Microbiol.* 21, 184. doi: 10.1186/s12866-021-02237-8

Liu, H., Jiang, J., An, M., Li, B., Xie, Y., Xu, C., et al. (2022). Bacillus velezensis SYL-3 suppresses alternaria alternata and tobacco mosaic virus infecting nicotiana tabacum by regulating the phyllosphere microbial community. *Front. Microbiol.* 13. doi: 10.3389/fmicb.2022.840318

Liu, L., Yang, J., Yu, X., Chen, G., and Yu, Z. (2013). Patterns in the composition of microbial communities from a subtropical river: Effects of environmental, spatial and temporal factors. *PloS One* 8, e81232. doi: 10.1371/journal.pone.0081232

Logares, R., Lindström, E. S., Langenheder, S., Logue, J. B., Paterson, H., Laybourn-Parry, J., et al. (2013). Biogeography of bacterial communities exposed to progressive long-term environmental change. *Isme. J.* 7, 937–948. doi: 10.1038/ismej.2012.168

Lucas, J. A., García-Villaraco, A., Ramos-Solano, B., Akdi, K., and Gutierrez-Mañero, F. J. (2022). Lipo-chitooligosaccharides (LCOs) as elicitors of the enzymatic activities related to ROS scavenging to alleviate oxidative stress generated in tomato plants under stress by UV-b radiation. *Plants (Basel).* 11. doi: 10.3390/plants11091246

Luo, L., Zhang, Z., Wang, P., Han, Y., Jin, D., Su, P., et al. (2019). Variations in phyllosphere microbial community along with the development of angular leaf-spot of cucumber. *AMB. Express.* 9, 76. doi: 10.1186/s13568-019-0800-y

McSpadden, G. B., Mavrodi, D. V., Thomashow, L. S., and Weller, D. M. (2001). A rapid polymerase chain reaction-based assay characterizing rhizosphere populations of 2,4-diacetylphloroglucinol-producing bacteria. *Phytopathology* 91, 44–54. doi: 10.1094/PHYTO.2001.91.1.44

Medina-Martínez, M. S., Allende, A., Barberá, G. G., and Gil, M. I. (2015). Climatic variations influence the dynamic of epiphyte bacteria of baby lettuce. *Food Res. Int.* 68, 54–61. doi: 10.1016/j.foodres.2014.06.009

Ottesen, A. R., González Peña, A., White, J. R., Pettengill, J. B., Li, C., Allard, S., et al. (2013). Baseline survey of the anatomical microbial ecology of an important food plant: Solanum lycopersicum (tomato). *BMC Microbiol.* 13, 114. doi: 10.1186/1471-2180-13-114

Pritchard, L., Liu, H., Booth, C., Douglas, E., François, P., Schrenzel, J., et al. (2009). Microarray comparative genomic hybridisation analysis incorporating genomic organisation, and application to enterobacterial plant pathogens. *PloS Comput. Biol.* 5, e1000473. doi: 10.1371/journal.pcbi.1000473

Priya, H., Prasanna, R., Ramakrishnan, B., Bidyarani, N., Babu, S., Thapa, S., et al. (2015). Influence of cyanobacterial inoculation on the culturable microbiome and growth of rice. *Microbiol. Res.* 171, 78–89. doi: 10.1016/j.micres.2014.12.011

Rastogi, G., Sbodio, A., Tech, J. J., Suslow, T. V., Coaker, G. L., and Leveau, J. H. (2012). Leaf microbiota in an agroecosystem: Spatiotemporal variation in bacterial community composition on field-grown lettuce. *Isme. J.* 6, 1812–1822. doi: 10.1038/ismej.2012.32

Redford, A. J., and Fierer, N. (2009). Bacterial succession on the leaf surface: A novel system for studying successional dynamics. *Microbial. Ecol.* 58, 189–198. doi: 10.1007/s00248-009-9495-y

Remus-Emsermann, M. N. P., and Schlechter, R. O. (2018). Phyllosphere microbiology: At the interface between microbial individuals and the plant host. *New Phytol.* 218, 1327–1333. doi: 10.1111/nph.15054

Roguet, A., Laigle, G. S., Therial, C., Bressy, A., Soulignac, F., Catherine, A., et al. (2015). Neutral community model explains the bacterial community assembly in freshwater lakes. *FEMS Microbiol. Ecol.* 91. doi: 10.1093/femsec/fiv125

Stoitsova, S. O., Braun, Y., Ullrich, M. S., and Weingart, H. (2008). Characterization of the RND-type multidrug efflux pump MexAB-OprM of the plant pathogen pseudomonas syringae. *Appl. Environ. Microbiol.* 74, 3387–3393. doi: 10.1128/AEM.02866-07

Tao, J., Yu, S., Jin, J., Lu, P., Yang, Z., Xu, Y., et al. (2022). The wilt pathogen induces different variations of root-associated microbiomes of plant. *Front. Plant Sci.* 13. doi: 10.3389/fpls.2022.1023837

Toju, H., Okayasu, K., and Notaguchi, M. (2019). Leaf-associated microbiomes of grafted tomato plants. *Sci. Rep.* 91787. doi: 10.1038/s41598-018-38344-2

Truchado, P., Gil, M. I., Reboleiro, P., Rodelas, B., and Allende, A. (2017). Impact of solar radiation exposure on phyllosphere bacterial community of red-pigmented baby leaf lettuce. *Food Microbiol.* 66, 77–85. doi: 10.1016/j.fm.2017.03.018

Vogel, C., Innerebner, G., Zingg, J., Guder, J., and Vorholt, J. A. (2012). Forward genetic in planta screen for identification of plant-protective traits of

sphingomonas sp. strain Fr1 against pseudomonas syringae DC3000. *Appl. Environ. Microbiol.* 78, 5529–5535. doi: 10.1128/AEM.00639-12

Vorholt, J. A. (2012). Microbial life in the phyllosphere. *Nat. Rev. Microbiol.* 10, 828–840. doi: 10.1038/nrmicro2910

Wang, Z., and Song, Y. (2022). Toward understanding the genetic bases underlying plant-mediated "cry for help" to the microbiota. *IMeta* 1, e8. doi: 10.1002/imt2.8

Whipps, J. M., Hand, P., Pink, D. A., and Bending, G. D. (2008). Human pathogens and the phyllosphere. *Adv. Appl. Microbiol.* 64, 183–221. doi: 10.1016/S0065-2164(08)00407-3

Xiang, L. G., Wang, H. C., Wang, F., Cai, L. T., Li, W. H., Hsiang, T., et al. (2022). Analysis of phyllosphere microorganisms and potential pathogens of tobacco leaves. *Front. Microbiol.* 13. doi: 10.3389/fmicb.2022.843389

Xing, L., Yang, J., Jia, Y., Hu, X., Liu, Y., Xu, H., et al. (2021). Effects of ecological environment and host genotype on the phyllosphere bacterial communities of cigar tobacco (Nicotiana tabacum l.). *Ecol. Evol.* 11, 10892–10903. doi: 10.1002/ece3.7861

Xing, L., Zhi, Q., Hu, X., Liu, L., Xu, H., Zhou, T., et al. (2022). Influence of association network properties and ecological assembly of the foliar fugal community on crop quality. *Front. Microbiol.* 13. doi: 10.3389/fmicb.2022.783923

Xu, N., Zhao, Q., Zhang, Z., Zhang, Q., Wang, Y., Qin, G., et al. (2022). Phyllosphere microorganisms: Sources, drivers, and their interactions with plant hosts. *J. Agric. Food Chem.* 70, 4860–4870. doi: 10.1021/acs.jafc.2c01113

Zhang, W., Pan, Y., Yang, J., Chen, H., Holohan, B., Vaudrey, J., et al. (2018). The diversity and biogeography of abundant and rare intertidal marine microeukaryotes explained by environment and dispersal limitation. *Environ. Microbiol.* 20, 462–476. doi: 10.1111/1462-2920.13916

Zheng, Y., Wang, J., Zhao, W., Cai, X., Xu, Y., Chen, X., et al. (2022). Effect of bacterial wilt on fungal community composition in rhizosphere soil of tobaccos in tropical yunnan. *Plant Pathol. J.* 38, 203–211. doi: 10.5423/PPJ.OA.03.2022.0035

frontiers | Frontiers in Plant Science

TYPE Original Research
PUBLISHED 17 February 2023
DOI 10.3389/fpls.2022.1106985

OPEN ACCESS

EDITED BY
Delong Meng,
Central South University, China

REVIEWED BY
Peng Zeng,
Central South University Forestry and Technology, China
Shulan Shi,
China University of Mining and, Technology, China

*CORRESPONDENCE
Jun Fang
fangjun1973@hunau.edu.cn
Shuming Liu
liushuming@stu.hunau.edu.cn

SPECIALTY SECTION
This article was submitted to Plant Symbiotic Interactions, a section of the journal Frontiers in Plant Science

RECEIVED 24 November 2022
ACCEPTED 28 December 2022
PUBLISHED 17 February 2023

CITATION
Xiao Y, Chen L, Li C, Ma J, Chen R, Yang B, Liu G, Liu S and Fang J (2023) Role of the rhizosphere bacterial community in assisting phytoremediation in a lead-zinc area. *Front. Plant Sci.* 13:1106985. doi: 10.3389/fpls.2022.1106985

Role of the rhizosphere bacterial community in assisting phytoremediation in a lead-zinc area

Yunhua Xiao[1], Liang Chen[1], Chunxiao Li[1], Jingjing Ma[1], Rui Chen[1], Bo Yang[1], Gang Liu[1], Shuming Liu[2*] and Jun Fang[1*]

[1]College of Bioscience and Biotechnology, Hunan Agricultural University, Changsha, China, [2]College of Chemical and Environmental Sciences, YiLi Normal University, YiLi, China

Heavy metals (HMs) contamination and vegetation destruction in the mining area caused by mining activities are severely increasing. It is urgent to restore vegetation and stabilize HMs. In this study, we compared the ability of HMs phytoextraction/phytostabilization of three dominant plants, including *Artemisia argyi* (LA), *Miscanthus floridulus* (LM), and *Boehmeria nivea* (LZ) in a lead-zinc mining area in Huayuan County (China). We also explored the role of the rhizosphere bacterial community in assisting phytoremediation using 16S rRNA sequencing technology. Bioconcentration factor (BCF) and translocation factor (TF) analysis showed that LA preferred accumulating Cd, LZ preferred accumulating Cr and Sb, and LM preferred accumulating Cr and Ni. Significant ($p < 0.05$) differences were found among the rhizosphere soil microbial communities of these three plants. The key genera of LA were *Truepera* and *Anderseniella*, that of LM were *Paracoccus* and *Erythrobacter*, and of LZ was *Novosphingobium*. Correlation analysis showed some rhizosphere bacterial taxa (e.g., *Actinomarinicola*, *Bacillariophyta* and *Oscillochloris*) affected some soil physicochemical parameters (e.g., organic matter and pH) of the rhizosphere soil and enhanced the TF of metals. Functional prediction analysis of soil bacterial community showed that the relative abundances of genes related to the synthesis of some proteins (e.g., manganese/zinc-transporting P-type ATPase C, nickel transport protein and 1-aminocyclopropane-1-carboxylate deaminase) was positively correlated with the phytoextraction/phytostabilization capacity of plants for heavy metals. This study provided theoretical guidance on selecting appropriate plants for different metal remediation applications. We also found some rhizosphere bacteria might enhance the phytoremediation of multi-metals, which could provide a reference for subsequent research.

KEYWORDS

Muti-metals contamination, Bioconcentration and translocation factors, Rhizosphere ecological characteristics, Phytoremediation, Bacterial community

1 Introduction

Due to the continuous mining activities, heavy metals (HMs) contamination and vegetation destruction are severely increasing. It is a severe threat to ecological biodiversity and human health. Therefore, soil restoration and governance need urgently be solved (Xiang et al., 2021; Zerizghi et al., 2022). The primary remediation methods for metal-contaminated soils include physical, chemical and biological strategies.

In general, physical and chemical remediation methods are costly, unfriendly to the environment, and can easily lead to secondary pollution, so that many researchers now focus on bioremediation strategies (González Henao and Ghneim-Herrera, 2021; Azhar et al., 2022). Phytoremediation has been widely used due to its advantages of being cost-effective, economical, eco-friendly, and sustainable (Ahemad, 2019; Shrivastava et al., 2019). Currently, As hyperaccumulators such as *Pteris vittata* and *Pteris cretica*, Zn hyperaccumulator *Sedum alfredii*, Cd hyperaccumulator *Viola baoshanensis*, and Mn hyperaccumulator *Phytolacca acinose* have been found in China for the phytoremediation of mine tailings (Niu et al., 2021). The effectiveness of phytoremediation depends on the chemical and physical properties of the plant, the bioavailability of metals in the soil, and the ability of rhizosphere soil microorganisms to absorb, transfer and detoxify metals (Subpiramaniyam, 2021). The removal of HMs by microorganisms has the advantages of easy use, low cost, large adsorption capacity, and high efficiency. Among these, bacteria, fungi and algae are widely used (Yin et al., 2019). In general, heavy metal ions can be adsorbed and combined by some functional groups of bacterial polysaccharide mucus layer, e.g., carboxyl, amino, phosphate, and sulfate (Yue et al., 2015). The adsorbed heavy metal ions can enter the microbial cells by metal-related enzymes or proteins, changing the redox state of heavy metal ions and thereby reducing their toxicity.

In practical applications, plants and microorganisms for bioremediation are more efficient (Vaid et al., 2022). Usually, microorganisms can improve plant extraction by increasing the availability of HMs in plants and increasing plant biomass (Wood et al., 2016; Mishra et al., 2017). Previous studies have shown that *Patescibacteria* increased the availability of HMs in the rhizosphere and promoted the remediation of heavy metal-contaminated soil by *Sedum alfredii* (Tian et al., 2022). Moreover, the plant preference for some HMs is influenced by the rhizosphere ecological characteristics, including the specific hormones, root exudates, soil nutrients, soil properties and rhizosphere soil microbes (Bais et al., 2006). The phytoremediation efficiency was regulated by soil enzyme activity and beneficial rhizosphere-associated microorganisms *Trifolium repens* L. (Lin et al., 2021). Therefore, the combined plant-microbes method can improve the heavy metal resistance of plants and achieve an ideal remediation effect. In recent years, it has also been found the limited efficiency of phytoremediation with a single plant (Buscaroli et al., 2017; Rizwan et al., 2019; Hosseinniaee et al., 2022) and the co-planting pattern of complementary plants for metals enrichment may be more efficient. The co-plantation of *Solanum nigrum* with *Quercus nuttallii* or *Quercus pagoda* effectively improved the enrichment of cadmium (>40%) and zinc (>30%) (Qu et al., 2021).

The environmental problem is severe in the lead-zinc mining area in Huayuan County, Hunan Province, China. This area is a super large ore deposit with many tailings ponds. Wastewater and ore sand was discharged through tunnels and village ditches, accumulating in the surrounding crops and villagers. Barbaric mining and poor management caused environmental pollution, damaged mine landforms, reduced vegetation coverage, soil erosion, and other problems. Therefore, we aim to explore the relationships among metals uptake of the dominant plants, rhizosphere bacterial community and the soil environment under the long-term HMs stress, analyze the ecological characteristics of the rhizosphere (physicochemical properties, soil enzyme activities and bacterial community structure), and the major microbial groups and metabolisms responsible for the oxidoreduction/detoxification/tolerance of HMs in the rhizosphere and absorption/translocation of HMs of plants.

2 Materials and methods

2.1 Sample collection and pretreatment

The Pb-Zn mining area was located in Huayuan County, Hunan Province (China), with a subtropical monsoon climate with an average temperature of 16.0°C and an average rainfall of 1363.8 mm. Environmental conditions and vegetation patterns were studied through field sampling. The vegetation pattern and distribution at different study sites were analyzed by quadratic analysis to identify dominant plant species, including *Artemisia argyi* (LA, 109°22′31.31″ E and 28°31′59.47″ N), *Boehmeria nivea* (LZ, 109°22′31.31″ E and 28°31′41.25″ N) and *Miscanthus floridulus* (LM, 109°21′41.12″ E and 28°30′46.47″ N) (Figure S1). There were eight replicates for each plant and the corresponding rhizospheric soil. Soil samples were collected from rhizosphere soil (5-20 cm). All soil and plant samples were sealed into clean polyethylene bags and transported to the laboratory at a low temperature (<5°C). Fresh plants were rinsed with tap water and deionized water. Then the plant samples were dried at a high temperature of 105°C for 30 minutes and then dried at 65°C to constant weight. The dried plant tissue was then separated into roots and shoots, ground to a fine powder, and placed in polyethylene bags for further analysis. Soil samples were air-dried, ground to a particle size of less than 0.147 mm (Xiao et al., 2018), and stored in polyethylene bags until analysis. The remained soil samples were stored at -80 °C for microbial analysis.

2.2 Measurements of HMs in plant tissues and soil properties

Plant samples (0.5 g) were digested with 10 mL mixed acid (HNO_3: $HClO_4$, vol/vol, 4:1). The contents of HMs were measured by inductively coupled plasma atomic emission spectrometry (ICAP 7200, Thermo Fisher Scientific, England) (Li G. et al., 2020).

Soil pH was measured by a pH meter (PHS-25, Shanghai Yidi Scientific Instrument Co., Ltd., China). 5.0 g soil was dried at 65°C to constant weight to measure the moisture content (MC). Soil-available phosphorus (AP), soil-available potassium (AK), soil acid phosphatase (S.ACP), soil catalase (S.CAT) and soil peroxidase (S.POD) were measured with the test kit (Shanghai zcibio technology co., Ltd. China). Analysis of soil organic matter (OM) was measured as described by Walz et al. (Walz et al., 2017). Total nitrogen was determined using the Kjeldahl method (Bremner, 2009). Soil HMs were determined regarding the method used by Sungur et al. (Sungur et al., 2020).

2.3 DNA extraction and Illumina MiSeq sequencing

DNA extraction and Illumina MiSeq sequencing of soil microorganisms were performed by Shenzhen E-Gene Technology Co., Ltd., using a 16S rRNA high throughput sequencing technique. Briefly, PCR was performed using primer pair 515 F (50- GTGCCAGCMGCCGCGGTAA-30) and 806 R (50-GGACTACHVGGGTWTCTAAT-30). PCR reaction conditions were as follows: 3 min of denaturation at 95 °C , 27 cycles of 30 s at 95 °C , 30 s for annealing at 55 °C , and 45 s for elongation at 72 °C , and a final extension at 72 °C for 10 min. The raw data were deposited in the Sequence Read Archive of the National Center for Biotechnology Information database (accession number: PRJNA904575).

2.4 Molecular ecological network

2.4.1 Network construction

In this study, the relative abundances of bacterial OTUs in the soil were used to construct phylogenetic molecular ecological networks (PMEN) using a network approach based on random matrix theory (RMT). This method can automatically identify keystone OTUs and determine the topological properties of the network. The detailed operation methods were referred to the previous study by Deng et al. (2012). In our study, the OTUs detected in equal or more than 3 of the 8 biological replicates were kept for network construction. The default similarity threshold is 0.98. Finally, the network interactions were visualized using Cytoscape 3.9.1 and Gephi 0.9.5.

2.4.2 Module detection and keystone microorganism identification

Molecular ecological networks consist of many OTUs/genes (nodes) and interactions (links) (Dunne et al., 2008). A module is a group of nodes that have similar functions and effects. Maximum modularity can separate the OTU into multiple dense subgraphs (Tao et al., 2018). Within a module, the role of a node is characterized by its intra-module connectivity (Zi) and inter-module connectivity (Pi). Based on Zi and Pi, nodes in the network could be classified into four different roles: peripheral nodes ($Zi \leq 2.5$ and $Pi \leq 0.62$, nodes have only a few links with other nodes within their modules); connectors ($Zi \leq 2.5$ and $Pi > 0.62$, nodes highly connected to several modules); module hubs ($Zi > 2.5$ and $Pi \leq 0.62$, nodes highly connected to many nodes within their own modules); and network hubs ($Zi > 2.5$ and $Pi > 0.62$, nodes act as both module hubs and connectors (Olesen et al., 2007). Nodes playing the roles of connectors, module hubs, and network hubs might act as keystone taxa to maintain the network structure and function (Faust and Raes, 2012).

2.5 Functional profiling

Before functional gene prediction using PICRUSt (phylogenetic investigation of communities by reconstruction of unobserved states) described by Langille et al. (2013), the detected OTUs were reclassified using the GREENGENES reference database. Subsequently, PICRUSt used 16S rRNA genes to infer metagenome gene functional content from phylogenetic information. The predictions were precalculated for genes in databases, including the Kyoto Encyclopaedia of Genes and Genomes (KEGG). The input data were first normalized by copy number by dividing each OTU by the known 16S copy number abundance before metagenome predictions and subsequent collapse into different functional pathways. The output of PICRUSt consisted of a table of functional gene counts as KEGG orthologs (KOs). The Nearest Sequenced Taxon Index (NSTI) value was used to validate the reliability of predicted metagenomes and functional pathways.

2.6 Statistical analysis

A completely randomized experimental design with eight replicates per treatment was used. Statistical analysis was conducted using analysis of variance (Markowitz et al., 2014). Multiple comparison analyses among treatments were performed using IBM SPSS Statistics 26 with Tukey's test. The translocation factors (TF) and bioconcentration factors (BCF) of three plants were calculated to evaluate the restoration potential of plants. TF evaluates the ability of plants to transport and enrich HMs from underground to aboveground. BCF reflects the ability of plants to absorb and transfer HMs into plant tissues.

BCF and TF were calculated as follows: BCF= C plant/C soil; TF= C shoot/C root.

The Shannon and Simpson diversity index analysis showed species abundance and evenness. The Chord diagram of the species relationship map was used to analyze the species composition of each sample in the microbial community. A Venn diagram was used to show the general relationship between the different treatments. It was commonly used to visualize common or unique information from multiple samples. Ternary phase diagrams showed the relative abundance of species in different groups. Principal Component Analysis (PCA) and Non-metric multidimensional scaling (NMDS) analysis were used to reflect the distances of the bacterial communities among samples. LEfse analysis (LDA Effect Size analysis) was conducted to find the species with significant differences in abundance between groups. Correlation analysis was conducted to show the Spearman correlation coefficient among environmental variables and the Mantel correlation coefficient among microbial species, predicting functional genes, environmental variables and BCF/TF. All the above mapping analysis was conducted using Origin 64 and Rstudio 4.2.0.

3 Results

3.1 The contents of HMs in the shoots and roots.

The contents of HMs in the shoots and roots of plants were shown in Table 1. For the shoot, the content of Pb in the LA group reached 144.43 mg/kg, significantly ($p < 0.05$) higher than that in the LZ and LM groups. The content of Zn (635.81 mg/kg), Cu (81.29 mg/kg), Fe (5529.07 mg/kg) and Mn (501.26 mg/kg) in the LZ group was significantly ($p < 0.05$) higher than that in the LA group. The content of Cr (654.82 mg/kg) and Ni (90.8676 mg/kg) in the LM group was significantly ($p < 0.05$) higher than that in the LA and LZ groups. Except for Mn, the contents of other HMs in the roots of LA were significantly ($p < 0.05$) higher than those of LZ and LM in the root. Among them,

TABLE 1 The contents of different heavy metals in three plants.

Parameter	HMs(mg/kg)	LA	LZ	LM
Shoot	As	3.28 ± 0.86 a	5.09 ± 2.64 a	5.12 ± 2.77 a
	Cd	5.3 ± 3.3 a	3.61 ± 2.75 ab	2.04 ± 0.72 b
	Cr	503.16 ± 11.33 b	549.47 ± 28.09 b	654.82 ± 82.22 a
	Cu	1063986 60.72 ± 2.59 b	81.29 ± 10.75 a	69.38 ± 25.26 ab
	Fe	2032.94 ± 864.74 b	5529.07 ± 2380.7 a	2698.95 ± 1317.88 b
	Mn	219.84 ± 77.14 b	501.26 ± 117.42 a	401.84 ± 63.64 a
	Ni	11.91 ± 3.69 b	32.98 ± 9.96 b	90.87 ± 37.45 a
	Pb	144.43 ± 56.53 a	37.06 ± 16.33 b	61.29 ± 26.96 b
	Sb	7.17 ± 1.84 a	8.46 ± 2.59 a	10.88 ± 4.57 a
	Zn	317.7 ± 43.28 b	635.81 ± 371.61 a	371.9 ± 68.1 ab
Root	As	9.86 ± 5.26 a	2.01 ± 1.37 b	2.01 ± 0.88 b
	Cd	4.56 ± 2.01 a	1.04 ± 0.88 b	1.74 ± 1.05 b
	Cr	598.18 ± 56.12 a	354.78 ± 29.29 b	355.63 ± 18.32 b
	Cu	85.04 ± 15.39 a	45.13 ± 6.81 b	40.82 ± 5.21 b
	Fe	15352.6 ± 8704.41 a	4166.79 ± 1767.31 b	3620.98 ± 1272.64 b
	Mn	12.66 ± 4.35 b	20.37 ± 5.87 b	51.11 ± 30.5 a
	Ni	58.09 ± 24.07 a	26.51 ± 18.31 b	27.41 ± 8.81 b
	Pb	1265.88 ± 410.09 a	32.67 ± 13.28 b	100.18 ± 51.92 b
	Sb	8.64 ± 3.94 a	3.41 ± 1.08 b	4.95 ± 0.95 b
	Zn	1053.39 ± 410.54 a	255.99 ± 96.69 b	360.55 ± 181.34 b

Values in the table represent mean ± standard deviation, and different lowercase letters in the table represent significant differences.

the contents of Zn and Pb reached 1053.40 mg/kg and 1265.88 mg/kg, respectively.

3.2 Soil physicochemical/biochemical properties

The physicochemical properties in the rhizosphere soil were shown in Table 2. The MC (2.75%-15.88%), pH (4.89-6.37), OM (3.47-21.55) and TN (0.36-2.29) were different in rhizosphere soils of different plants, and they were significantly ($p < 0.05$) higher in the LZ group than those of LM. The soil AK contents showed no significant ($p > 0.05$) difference among the three groups, but the soil AP content in the LZ and LM groups was significantly ($p < 0.05$) higher than that of LA by 18.77% and 22.53%, respectively. The activity of S-ACP in the LA and LZ groups were significantly ($p < 0.05$) higher than that in the LM group, but the activities of S-CAT and S-POD showed no significant ($p > 0.05$) differences.

In addition, the contents of As (11.17 mg/kg), Cd (2.53 mg/kg), Cr (3.83 mg/kg), Cu (29.32 mg/kg), Fe (14148.06 mg/kg), Mn (761.88 mg/kg), and Ni (21.69 mg/kg) in the LA group were significantly ($p < 0.05$) lower than those in the LZ or LM group. The Pb content in the LZ group was 392.18 mg/kg, which was significantly ($p < 0.05$) lower than that of LA and LM.

3.3 Translocation factor and Bioconcentration factor

The results of BCF and TF were shown in Table 3. The BCFs of Cd (2.31), Cr (105.40), Cu (2.93) and Ni (1.66) were greater than 1 in the LA group, while only the BCFs of Cr (11.04) and Sb (1.74) in the LZ group and the BCF of Cr (16.36) and Sb (3.08) in the LM group were greater than 1. In addition, LZ also has strong TF (TF > 1) for all other metals, LM has strong TF (TF > 1) for all metals except Mn and Sb, and LA has strong TF (TF > 1) for Cd and Zn. The TFs of Cr, Cu, and Ni in LA also reached 0.84, 0.71, and 0.83, which were relatively higher than the TFs of other HMs in the same plant species. It was found that the TF of LZ for Cd, Cu, Mn, Ni, Pb, Sb, and Zn were higher than those of LA and LM, while the TF of LM for As, and Cr, was the strongest.

TABLE 2 Physiological and biochemical indexes of soil.

Parameter	LA	LZ	LM
MC (%)	15.88 ± 1.44 a	15.35 ± 1.52 a	2.75 ± 1.12 b
pH	5.52 ± 0.85 ab	6.37 ± 0.6 a	4.89 ± 0.83 b
OM (g/kg)	6.42 ± 3.01 b	21.55 ± 2.22 a	3.47 ± 1.32 c
TN (g/kg)	0.63 ± 0.21 b	2.29 ± 0.91 a	0.36 ± 0.15 b
AP (μmol/g)	0.28 ± 0.02 b	0.33 ± 0.05 a	0.34 ± 0.03 a
AK (mg/kg)	10.85 ± 0.2 a	10.78 ± 0.13 a	10.8 ± 0.14 a
As (mg/kg)	11.17 ± 3.94 b	16.51 ± 2.42 b	34.41 ± 10.44 a
Cd (mg/kg)	2.53 ± 1.08 c	7.42 ± 0.52 a	4.03 ± 1.2 b
Cr (mg/kg)	3.83 ± 6.95 b	44.06 ± 12.25 a	40.77 ± 20.47 a
Cu (mg/kg)	29.32 ± 13.64 c	93.68 ± 11.55 a	71.18 ± 10.62 b
Fe (mg/kg)	14148.06 ± 4733.69 b	45100.6 ± 1821 a	40984.16 ± 10974.14 a
Mn (mg/kg)	761.88 ± 300.12 c	2321.23 ± 360.87 a	1368.95 ± 320.17 b
Ni (mg/kg)	21.69 ± 5.29 b	45.67 ± 1.15 a	49.54 ± 13.21 a
Pb (mg/kg)	1130.67 ± 492.75 a	392.18 ± 32.72 b	807.54 ± 250.25 a
Sb (mg/kg)	6.24 ± 2.04 a	3.6 ± 0.97 b	3.9 ± 1.69 b
Zn (mg/kg)	917.67 ± 303.19 b	1351.12 ± 53.11 a	796.31 ± 296.53 b
S-ACP (nmol/d·g)	6000.73 ± 345.23 a	6788.41 ± 512.17 a	4351.27 ± 954.43 b
S-CAT (U/g)	110.69 ± 0.68 a	109.74 ± 0.96 a	110.86 ± 1.15 a
S-POD (μmol/d/g)	401.24 ± 200.31 a	430.33 ± 174.42 a	350.84 ± 97.79 a

Values in the table represent mean ± standard deviation, and different lowercase letters in the table represent significant differences.

TABLE 3 Translocation factors and Bioconcentration factors.

	Treatment	As	Cd	Cr	Cu	Fe	Mn	Ni	Pb	Sb	Zn
TF	LA	0.33	**1.16**	0.84	0.71	0.21	0.11	0.83	0.3	0.13	**17.36**
	LZ	**2.53**	**3.47**	**1.55**	**1.8**	**1.24**	**1.13**	**2.48**	**2.48**	**1.33**	**24.61**
	LM	**2.54**	**1.17**	**1.84**	**1.7**	**3.31**	0.61	**2.2**	**1.03**	0.75	**7.86**
BCF	LA	0.64	**2.31**	**105.4**	**2.93**	0.72	0.19	**1.66**	0.9	**1.4**	0.76
	LZ	0.23	0.32	**11.04**	0.68	0.11	0.12	0.65	0.09	**1.74**	0.33
	LM	0.12	0.51	**16.36**	0.79	0.09	0.18	**1.35**	0.1	**3.08**	0.51

Bold font means that BCF is greater than 1 or TF is greater than 1.

3.4 Overview of bacterial community in the rhizosphere soil

Simpson Index showed no significant ($p > 0.05$) differences among the three groups, but the Simpson Index in the LM group reached 65.51, which was higher than the other two groups. The Shannon Index showed that the microbial diversity of LA, LM, and LZ were 4.11, 4.18, and 4.44, respectively. Among them, LM had the most abundant diversity and was significantly higher than LA (Figure 1A). According to the Venn diagram, there were 26 duplicated OTUs in 864 OTUs (Figure 1C). The abundance chord chart showed that soil bacterial communities mainly consisted of *Armatimonadetes_gp4*, *Gp3*, and *Thermanaerothrix*, and the dominant genera were different among three groups (Figure 1B): they were *Ornatilinea* (4.47%), *Gp16* (3.63%), and *Saccharibacteria_genera_incertae_sedis* (3.60%) in the LA group; they were *Armatimonadetes_gp4* (6.92%), *Gp3* (4.93%), and *Thermanaerothrix* (3.43%) in the LM group; They were *Gp3* (4.66%), *Bacillariophyta* (4.30%), and *Iphinoe* (3.50%) in the LZ group. A ternary plot analysis performed on the phylum level showed that Actinobacteria, Cyanobacteria/Chloroplast, Chloroflexi, Firmicutes, and Proteobacteria were the dominant phyla (Figure 1D). Armatimonadetes dominated LM, and Planctomycetes dominated LZ. Results of PCA showed that points of samples in the three groups separated from each other group (Figure 1E), and similar results were obtained by dissimilarity tests, suggesting that significant ($p < 0.05$) differences occurred in the rhizosphere bacterial community structure of different plant (Table S1).

Further LEfse analysis at the genus level was shown in Figure 2. The cladogram (Figure 2A) compares the differences of genera between three plants, and LDA analysis (Figure 2B)

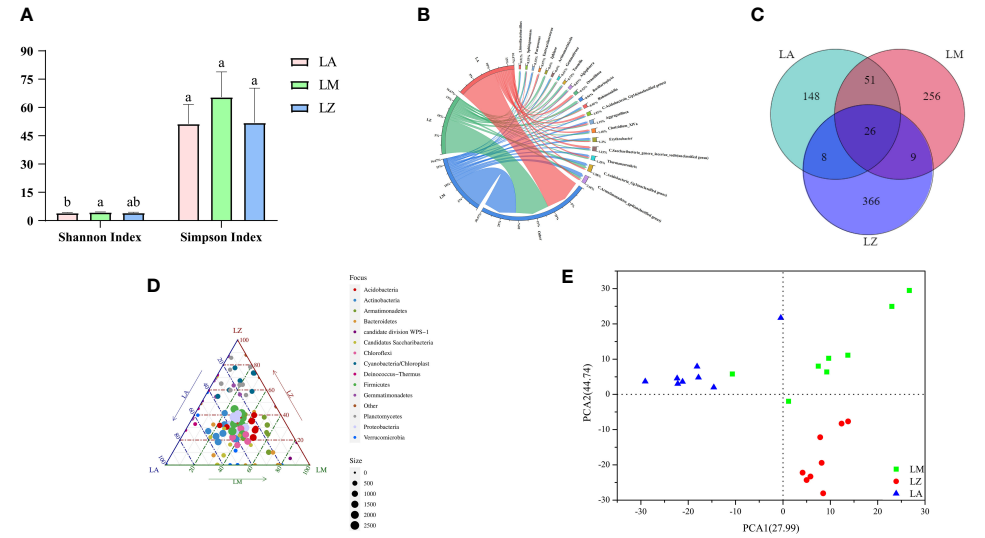

FIGURE 1
Structure, diversity and composition of rhizospheric soil bacterial communities in three dominant plants. **(A)** Shannon Index and Simpson Index; **(B)** The abundance of microorganisms at the genus level; **(C)** Venn diagram; **(D)** The ternary map of microorganisms at the phylum level; **(E)** Principal Component Analysis. In the ternary phase diagram, different points represent different species, the size of the points represents the average abundance of the species in different groups, the gray points represent the non-enrichment, and the points of each color respectively represent the enriched groups.

shows the main genera with significant ($p < 0.05$) differences. The relative abundances of genera (e.g., *Ornatilinea*, *Gp16*, *Enteractinococcus*) were highest in the LA group; The relative abundances of genera (e.g., *Armatimonadetes_gp4*, *Aggregatilinea*, *Paracoccus*) were highest in the LM group; The relative abundances of genera (e.g., *Bacillariophyta*, *Iphinoe*, *Gemmatirosa*) were highest in the LZ group.

3.5 Co-occurrence networks analysis

Microbial population data were analyzed using the RMT-based network approach to discern the ecological network. Three networks were constructed based on the 16S rRNA gene sequencing data of three plans, respectively (Figure 3A). Major topological properties of the empirical MENs of microbial communities in the eight groups are shown in Table S2. With the same threshold (0.980), their correlation values were more than 0.580, indicating that the degree of distributions in the constructed molecular ecological networks fits the power law model well. There were 134 links and 67 nodes in the LA group, of which the positive links accounted for 70.07%, and the negative links accounted for 29.93%. There were 137 links and 80 nodes in the LM group, of which the positive links accounted for 53.71%, and the negative links accounted for 46.29%. There were 175 links and 88 nodes in the LZ group, of which the positive links accounted for 63.52% and the negative links accounted for 36.48% (Figure 3A). The network indexes showed that the microbial network of LZ was the most complex, but the number of modules in the LM group was higher than that of LA and LZ (Table S2). Results of ZP analysis showed that there were 6, 7 and 27 key OTUs in the LA, LM and LZ groups (Figure 3B). Sub-network analysis of key OTUs revealed that OTU167 (*Geothermobacterium*, 4 connections, 4 positive correlations) and OTU89 (*Clostridium XlVa*, 5 connections, 4 positive correlations) were the core OTUs in the LA group. OTU77 (*Paracoccus*, 8 connections, 7 positive correlations) and OTU12 (*Algisphaera*, 4 connections, 4 positive correlations) were the core OTUs in the LM group. The core OTUs in the LZ group were OTU57 (*Iphinoe*, 19 connections, 16 positive correlations), OTU61 (*Paracoccus*, 18 connections, 14 positive correlations), OTU268 (*Pseudoscardovia*, 6 connections, 6 positive correlations), OTU111 (*Limosilactobacillus*, 7 connections, 6 positive correlations) (Figure 3C). Venn diagram analysis of essential microorganisms showed that 10 key OTUs were shared by LA, LM, and LZ (Figure 3D), which belonged to the genera, including *Armatimonadetes_gp4*, *Gp3*, *Algisphaera*, *Clostridium XlVa*, *Robinsoniella*, *Taonella*, *Verrucosispora*, *Erythrobacter*, and *Thermanaerothrix*.

3.6 Correlation analysis

According to the correlation analysis (Figure 4A), it was shown that the key microorganisms were mainly related to the BCF of Cu, Cr, Cd, Fe, Ni and Zn, and the TF of As, Cd, Cr, Cu, Mn, Ni, Pb and Zn. S.ACP, S.CAT, pH, MC, OM, AP and TN were also significantly ($p < 0.05$) correlated to the key microorganisms. The diversity of the bacterial community was mainly related to the TF of Ni and Sb, as well as MC and AP. Bacterial community structures were significantly ($p < 0.05$) correlated to the TF of Ni, the activity of S.ACP, soil pH, and the contents of MC. Most HMs were mainly related to the contents of AP and MC in soil (Figure 4A). TF_Cd was significantly ($p < 0.05$) positively correlated to the contents of OM/TN, soil pH, and the activity of S.ACP. TF_Fe was significantly ($p < 0.05$) positively correlated with TN, BCF_Mn, and BCF_Ni were significantly ($p < 0.05$) negatively correlated with the content of OM ($p < 0.05$). There was no significant ($p > 0.05$) correlation between BCF_Sb and soil physicochemical properties. Similarly, there was no significant ($p > 0.05$) difference between the TF and BCF of HMs and the soil contents of AK. Further correlation tests explored the relationships among microorganisms, HMs,

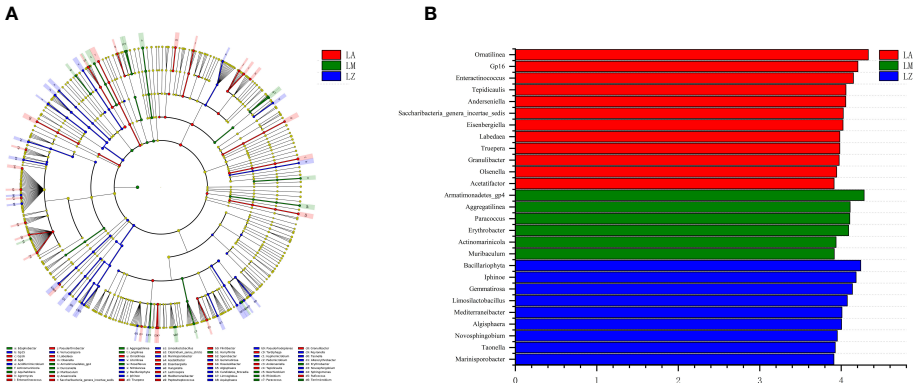

FIGURE 2
Linear discriminant analysis effect size (LEfSe). **(A)** The evolutionary branching diagram, and **(B)** the distribution histogram.

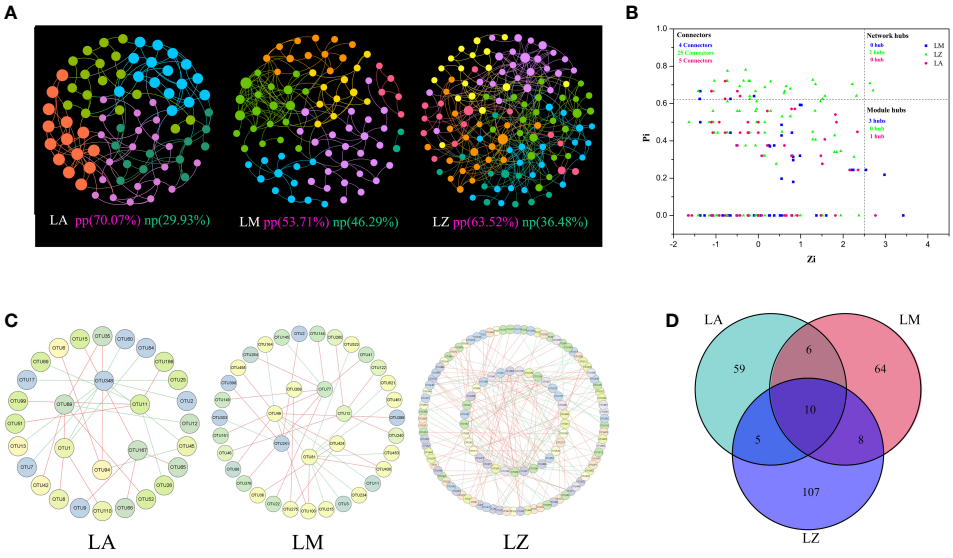

FIGURE 3
Co-occurrence Networks analysis. **(A)** Co-occurrence network; **(B)** ZP diagram; **(C)** Sub-network analysis diagram; **(D)** Venn diagram of key nodes. Different colors represent different modules, and the key nodes indicated Zi>2.5 or Pi>0.62.

and physiochemical properties in soil. It was found that the essential microorganisms were mainly negatively correlated with S.CAT, positively correlated with the TF of HMs, and had no significant ($p > 0.05$) correlation with S.POD. Interestingly, the Bacteroidetes was significantly ($p < 0.05$) negatively associated with soil nutrients. Furthermore, most microbiotas were negatively correlated with the BCF of HMs. The correlations between microorganisms and environmental factors/BCF/TF were shown in Figure 4B. Some microorganisms (e.g., *Actinomarinicola*, *Bacillariophyta* and *Oscillochloris*) were positively related to organic matter, pH and the TF of metals, while were negatively related to the BCF of metals.

3.7 Analysis of predictive functional genes

NMDS analysis showed significant inter-group differences in the predictive functional genes contained in soil microorganisms from different plant rhizosphere, while intra-group differences were slight (Figure 5A). There were significant ($p < 0.05$) differences in the relative abundances of some functional genes in different microbial communities (Table S3). The relative abundances of the genes about 1-aminocyclopropane-1-carboxylate deaminase (ACC deaminase), tryptophan synthase alpha/beta chain, nickel transport protein and manganese/Zinc-

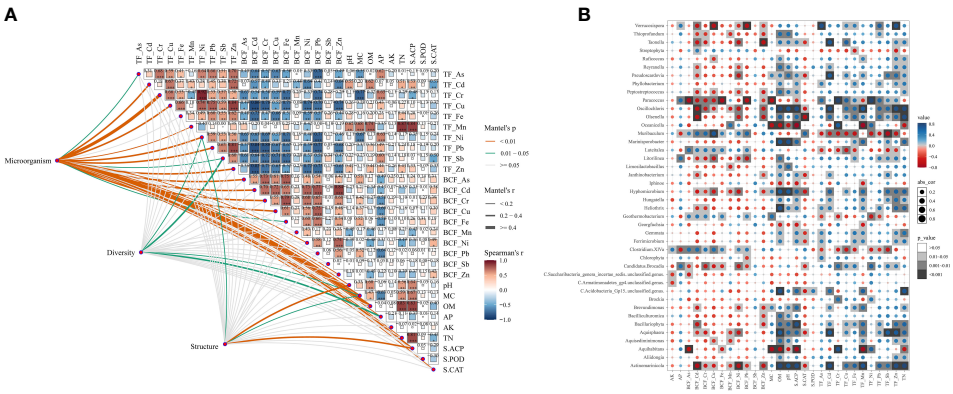

FIGURE 4
Correlation analysis among bacterial communities, TFs and BCFs of heavy metals, and soil physicochemical properties. **(A)** The relationships among the different parameters (microorganism, diversity, structure), HMs TFs, BCFs and soil environmental parameters by Mantel tests; **(B)** Spearman correlations of genus and soil environmental factors.

transporting P-type ATPase C were the most abundant in LA. The relative abundances of the genes about nonribosomal peptide synthetases were the highest in LZ (Table 4). Furthermore, some genes were further selected to make fitting curves with the contents of HMs in plant root tissues (Figure 5B). The relative abundance of the gene about manganese/zinc-transporting P-type ATPase C was significantly ($p < 0.01$) positively correlated with the contents of Cd, Zn, and Pb, and the relative abundance of the gene about nickel transport protein was significantly ($p < 0.01$) positively correlated with the contents of Ni.

4 Discussion

In recent decades, our demand for metal resources has been increasing, which accelerated the mining of metal mines. The continuous expansion of mining areas led to more and more arable land facing environmental pollution (Diaz-Morales et al., 2021; Li et al., 2022). The increase in HMs will stimulate the production of a large number of reactive oxygen species, which will seriously impact the quality of crops and vegetables (Clemens and Ma, 2016) and lead to human health risks (Xiang et al., 2021). Phytoremediation is a sustainable approach to remediating contaminated sites (Hasnaoui et al., 2020). Thus, the study of the interaction between the hyperaccumulators and microorganisms can help formulate effective remediation strategies for mining areas (Xuan et al., 2021). In this study, we investigated the rhizosphere ecological characteristics of the dominant plants around the mining area and further explored their potential for multi-metal(loid)s phytoremediation. It was found that As, Cd, Cu, Pb and Zn have reached potentially hazardous levels (Table 1). We found that *Artemisia argyi, Miscanthus floridulus*, *Boehmeria nivea* are the dominant enrichment plants in this area, and the application of dominant plants combined with microbial communities for the bioremediation of soil pollution was explored (Figure 6).

Microorganisms can directly or indirectly change the availability of metals and promote plant growth and absorption of HMs by regulating soil physicochemical properties or secretion of secondary metabolites. Our study found that Cyanobacteria/Chloroplast, Chloroflexi and Acidobacteria were key phyla for the plant to accumulate HMs. Different plants had different dominant rhizosphere flora, which affected the remediation of different HMs. The dominant phylum Cyanobacteria/Chloroplast in LZ was significantly ($p<0.05$) positively correlated with TF of Cd, Cu, Mn, Pb and Zn (Figure S2). However, few studies reported the responses of Cyanobacteria/Chloroplast and their roles in phytoremediation under HMs stress, and it might need further study to verify. Chloroflexi was the dominant phylum in the LA group (Figure 1B), significantly ($p < 0.05$) higher than in LM and LZ (Figure 2B). Studies have found that Chloroflexi had an obvious advantage in polluted soil (Hemmat-Jou et al., 2018; Koner et al., 2022), which could rapidly adapt to heavy metal stress and affect the content of organic matter to control the practical availability of Cr and Pb for plants (Tang et al., 2019). It is consistent with this study, where Chloroflexi was also significantly ($p < 0.05$) positively correlated with the organic matter (Figure S2). Acidobacteria was the dominant phylum in the LM group (Figure 1B) and was significantly ($p < 0.05$) positively correlated with BCF of Cr (Figure S2). Previous research found that the relative abundance of Acidobacteria was inversely related to pH (Debnath et al., 2016). Sun et al. (2022) found that the relative abundance of Acidobacteria was positively correlated to the contents of total Cr and available Cr, and Acidobacteria could cut down soil pH. The key genera of LA

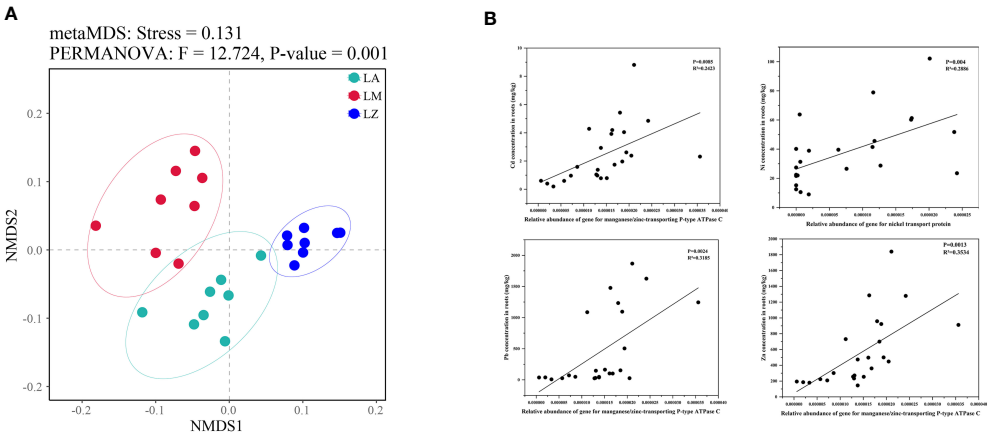

FIGURE 5
NMDS analysis of the structure in predicting genes **(A)** and the correlations between some genes and the contents of heavy metals in plant roots **(B)**.

TABLE 4 Relative abundance of key functional genes in different rhizosphere microbial communities.

Genes for proteins/enzymes	LA	LM	LZ
ACC deaminase	7.96E-05a	5.35E-05b	7.53E-05a
Tryptophan synthase alpha/beta chain	6.71E-04a	5.82E-04b	4.89E-04c
Nonribosomal peptide synthetases	8.82E-04b	7.33E-04b	1.21E-03a
Nickel transport protein	1.72E-05a	3.72E-06b	3.47E-07b
Manganese/Zinc-transporting P-type ATPase C	2.06E-05a	7.48E-06b	1.51E-05a

were *Truepera* and *Anderseniella*, that of LM were *Paracoccus* and *Erythrobacter*, and of LZ was *Novosphingobium*. The oxidation-reduction and nitrogen fixation activities of *Truepera* allow it to support plant growth (Zhou et al., 2022). *Anderseniella* can eliminate metabolic wastes, heavy metals, and aromatic chemicals (Karimi et al., 2019). *Paracoccus* can produce acid, alter the chemical and physical parameters in the soil and encourage plants to absorb heavy metals (Carvalho et al., 2018). *Erythrobacter* is an iron metabolism bacterium that can secrete iron carriers and promote plant growth (Li L. et al., 2020). *Novosphingobium* has strong antioxidant activity and can slow down the toxic effect of heavy metals on plants (Petruk et al., 2018).

Except for the dominant flora of different plants, the study found that they shared the same vital microorganisms (Figure 3D). These microorganisms (e.g., Proteobacteria, Acidobacteria and Firmicutes) could assist plants in accumulating HMs. Studies have found that in the harsh tailings environment, the colonies mentioned above belonged to the dominant flora and could benefit the expression of metal resistance genes (Guo et al., 2017; Jiang et al., 2021; Koner et al., 2022). HMs in the soil can affect the growth of microorganisms through protein denaturation, cell membrane damage and inhibition of RNA expression and metabolism (Wang et al., 2020; Duan et al., 2022). It has also been studied that HMs stress enhanced the functional fitness of endophytic bacterial communities (Yao et al., 2022). Most microorganisms were positively correlated to the contents of soil organic matter so that we might stabilize soil microbial communities and increase the abundance of beneficial bacteria by improving soil fertility. Notably, the research found that the abundance of Bacteroidetes increased in extremely harsh soils, and Bacteroidetes transferred and enriched a large amount of Ni (Figure S2), which is consistent with Jiao et al. (2022) findings. Besides, Tang et al. (2019) found that Bacteroidetes also affected the availability of Cu and Zn.

Okkeri and Haltia (1999; 2006) found that the zinc-transporting P-type ATPase C was not only related to the transport of Zn but also to Cd and Pb, which is consistent with our genetic prediction. Similarly, nickel transport protein is a novel metal regulatory protein associated with heavy metal Ni transport (Dosanjh and Michel, 2006; Wang et al., 2014). In addition, there are functional genes secreting siderophore (Carroll and Moore, 2018), indoleacetic acid (Estenson et al., 2018) and ACC deaminase (Glick, 2005) in rhizosphere soil microorganisms. It is indicated that many plant growth-

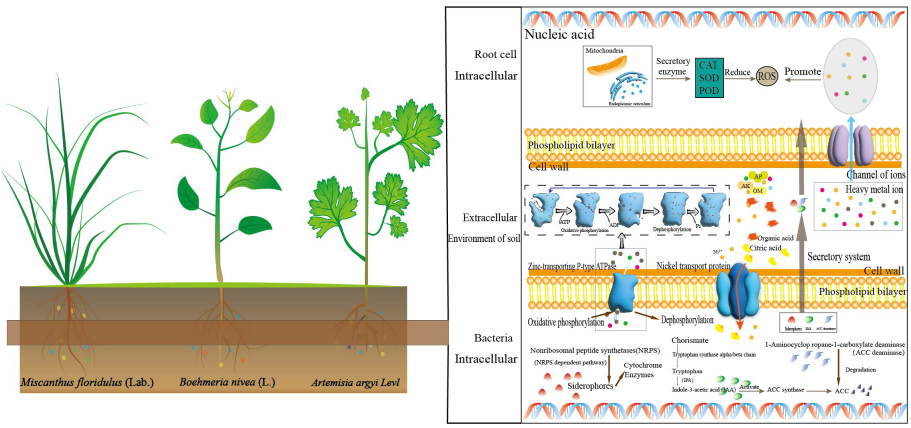

FIGURE 6
Schematic plot of the interaction between rhizosphere bacteria and plants in multi-HMs contaminated soil.

promoting bacteria (PGPB) resist HMs in rhizosphere soil. They significantly improved plant growth in heavy metal-contaminated soils and could enhance heavy metal phytoremediation by binding super-enriched plants (Ahemad, 2019). Xu et al. (2022) found that Actinobacteriota and Gemmatimonadota promoted plant growth and fixed Cd in rhizosphere soil. Li et al. (2022) found that *Sphingomonas* promoted plant growth and degraded organometallic compounds to remediate soil HMs contamination. Similarly, Ham et al. (2022) found that *Pseudopyroactor* promoted plant growth and improved antioxidant capacity. PGPB significantly improve plant growth in heavy metal-contaminated soils (Ahemad, 2019) and may represent potential bacterial strain resources in plant-PGPR combined remediation of HM-contaminated soils.

The presence of HMs significantly destabilizes network structure (Jiang et al., 2020; Caili et al., 2022). A more complex network represents that microbial activities and interactions are more active and intensive, which might have beneficial functions in the phytoremediation of HMs in soils (Hou et al., 2019). Plants consistently interact with a core set of microbes contributing to plant performance (Luo et al., 2022). We found that the network of LZ was the most complex (Figure 3C), and *Boehmeria nives* (L.) showed higher TFs of all ten metals. Thus, a good rhizosphere ecological network might be helpful for plants to absorb heavy metals.

5 Conclusion

According to our investigation of BCF and TF for metals, LA preferred accumulating Cd, LZ preferred accumulating Cr and Sb, and LM preferred accumulating Cr and Ni. The bioaccumulating capacity for multi-metals of *Artemisia argyi* Levl was more potent, while the translocating capacity was weaker than that of *Miscanthus floridulus* (Lab.) and *Boehmeria nives* (L.). The dominant bacterial groups, ecological networks and soil properties (e.g., available phosphorus and moisture content) were different in the rhizosphere soil of these three plants. A higher proportion of positive links in the ecological network might enhance the metal uptake of plants. PICRUSt analysis and correlation tests indicated that genes related to the synthesis of proteins (e.g., manganese/zinc-transporting P-type ATPase C, nickel transport protein and ACC deaminase) could also promote phytoremediation. The rhizosphere bacterial community contained genera, such as *Truepera*, *Anderseniella*, *Paracoccus*, *Erythrobacter* and *Novosphingobium*, which may represent potential bacterial strain resources for plant-microbes combined remediation of HM-contaminated soils.

Data availability statement

The datasets presented in this study can be found in online repositories. The names of the repository/repositories and accession number(s) can be found in the article/Supplementary Material.

Author contributions

YX, JF, and SL contributed to the study's conception and design. Research, material preparation, data collection, and analysis were performed by LC, CL, RC, JM and GL. The first draft of the manuscript was written by LC, YX, BY commented on previous versions of the manuscript. All aforementioned authors read and approved the final manuscript. All authors contributed to the article and approved the submitted version.

Funding

The study was supported by the National Natural Science Foundation of China (No. 41807135), the Scientific Research Fund of Hunan Provincial Education Department (No. 21A0142, 20A233, 18B107), the Natural Science Foundation of Hunan province, China (No. 2019JJ50220) and Science and Technology of Hunan Branch of China National Tobacco Corporation (XX2022-2024Aa01).

Conflict of interest

The authors declare that this study received funding from Science and Technology of Hunan Branch of China National Tobacco Corporation. The funder was not involved in the study design, collection, analysis, interpretation of data, the writing of this article, or the decision to submit it for publication.

Publisher's note

Supplementary material

The Supplementary Material for this article can be found online at: https://www.frontiersin.org/articles/10.3389/fpls.2022.1106985/full#supplementary-material

References

Ahemad, M. (2019). Remediation of metalliferous soils through the heavy metal resistant plant growth promoting bacteria: Paradigms and prospects. *ARAB J. Chem.* 12 (7), 1365–1377. doi: 10.1016/j.arabjc.2014.11.020

Azhar, U., Ahmad, H., Shafqat, H., Babar, M., Shahzad Munir, H. M., Sagir, M., et al. (2022). Remediation techniques for elimination of heavy metal pollutants from soil: A review. *Environ. Res.* 214 (Pt 4), 113918. doi: 10.1016/j.envres.2022.113918

Bais, H. P., Weir, T. L., Perry, L. G., Gilroy, S., and Vivanco, J. M. (2006). The role of root exudates in rhizosphere interactions with plants and other organisms. *Annu. Rev. Plant Biol.* 57, 233–266. doi: 10.1146/annurev.arplant.57.032905.105159

Bremner, J. M. (2009). Determination of nitrogen in soil by the kjeldahl method. *J. AGR SCI-CAMBRIDGE.* 55 (01), 11. doi: 10.1017/s0021859600021572

Buscaroli, A., Zannoni, D., Menichetti, M., and Dinelli, E. (2017). Assessment of metal accumulation capacity of *Dittrichia viscosa* (L.) greuter in two different Italian mine areas for contaminated soils remediation. *J. GEOCHEM. Explor.* 182, 123–131. doi: 10.1016/j.gexplo.2016.10.001

Caili, S., Pan, W., Guanghao, W., and Xingjie, K. (2022). Heavy metal pollution decreases the stability of microbial co-occurrence networks in the rhizosphere of native plants. *Front. Environ. Sci.* 1631. doi: 10.3389/fenvs.2022.979922

Carroll, C. S., and Moore, M. M. (2018). Ironing out siderophore biosynthesis: a review of non-ribosomal peptide synthetase (NRPS)-independent siderophore synthetases. *Crit. Rev. Biochem. Mol. Biol.* 53 (4), 356–381. doi: 10.1080/10409238.2018.1476449

Carvalho, G., Pedras, I., Karst, S. M., Oliveira, C. S. S., Duque, A. F., Nielsen, P. H., et al. (2018). Functional redundancy ensures performance robustness in 3-stage PHA-producing mixed cultures under variable feed operation. *New Biotechnol.* 40, 207–217. doi: 10.1016/j.nbt.2017.08.007

Clemens, S., and Ma, J. F. (2016). Toxic heavy metal and metalloid accumulation in crop plants and foods. *Annu. Rev. Plant Biol.* 67, 489–512. doi: 10.1146/annurev-arplant-043015-112301

Debnath, R., Yadav, A., Gupta, V. K., Singh, B. P., Handique, P. J., and Saikia, R. (2016). Rhizospheric bacterial community of endemic *Rhododendron arboreum* sm. ssp. delavayi along eastern himalayan slope in tawang. *Front. Environ. Sci.* 07. doi: 10.3389/fpls.2016.01345

Deng, Y., Jiang, Y.-H., Yang, Y., He, Z., Luo, F., and Zhou, J. (2012). Molecular ecological network analyses. *BMC Bioinf.* 13 (1), 113. doi: 10.1186/1471-2105-13-113

Diaz-Morales, D. M., Erasmus, J. H., Bosch, S., Nachev, M., Smit, N. J., Zimmermann, S., et al. (2021). Metal contamination and toxicity of soils and river sediments from the world's largest platinum mining area. *Environ. pollut.* 286, 117284. doi: 10.1016/j.envpol.2021.117284

Dosanjh, N. S., and Michel, S. L. (2006). Microbial nickel metalloregulation: NikRs for nickel ions. *Curr. Opin. Chem. Biol.* 10 (2), 123–130. doi: 10.1016/j.cbpa.2006.02.011

Duan, C., Wang, Y., Wang, Q., Ju, W., Zhang, Z., Cui, Y., et al. (2022). Microbial metabolic limitation of rhizosphere under heavy metal stress: Evidence from soil ecoenzymatic stoichiometry. *Environ. pollut.* 300, 118978. doi: 10.1016/j.envpol.2022.118978

Dunne, J. A., Williams, R. J., Martinez, N. D., Wood, R. A., and Erwin, D. H. (2008). Compilation and network analyses of cambrian food webs. *PloS Biol.* 6 (4), e102. doi: 10.1371/journal.pbio.0060102

Estenson, K., Hurst, G. B., Standaert, R. F., Bible, A. N., Garcia, D., Chourey, K., et al. (2018). Characterization of indole-3-acetic acid biosynthesis and the effects of this phytohormone on the proteome of the plant-a microbe pantoea sp. YR343. *J. Proteome Res.* 17 (4), 1361–1374. doi: 10.1021/acs.jproteome.7b00708

Faust, K., and Raes, J. (2012). Microbial interactions: from networks to models. *Nat. Rev. Microbiol.* 10 (8), 538–550. doi: 10.1038/nrmicro2832

Glick, B. R. (2005). Modulation of plant ethylene levels by the bacterial enzyme ACC deaminase. *FEMS Microbiol. Lett.* 251 (1), 1–7. doi: 10.1016/j.femsle.2005.07.030

González Henao, S., and Ghneim-Herrera, T. (2021). Heavy metals in soils and the remediation potential of bacteria associated with the plant microbiome. *Front. Environ. Sci.* 9. doi: 10.3389/fenvs.2021.604216

Guo, H., Nasir, M., Lv, J., Dai, Y., and Gao, J. (2017). Understanding the variation of microbial community in heavy metals contaminated soil using high throughput sequencing. *Ecotoxicol. Environ. Saf.* 144, 300–306. doi: 10.1016/j.ecoenv.2017.06.048

Ham, S. H., Yoon, A. R., Oh, H. E., and Park, Y. G. (2022). Plant growth-promoting microorganism *Pseudarthrobacter* sp. NIBRBAC000502770 enhances the growth and flavonoid content of *Geum aleppicum*. *Microorganisms* 10 (6), 1241. doi: 10.3390/microorganisms10061241

Hasnaoui, S. E., Fahr, M., Keller, C., Levard, C., Angeletti, B., Chaurand, P., et al. (2020). Screening of native plants growing on a Pb/Zn mining area in eastern Morocco: Perspectives for phytoremediation. *Plants (Basel)* 9 (11), 1458. doi: 10.3390/plants9111458

Hemmat-Jou, M. H., Safari-Sinegani, A. A., Mirzaie-Asl, A., and Tahmourespour, A. (2018). Analysis of microbial communities in heavy metals-contaminated soils using the metagenomic approach. *Ecotoxicology.* 27 (9), 1281–1291. doi: 10.1007/s10646-018-1981-x

Hosseinniaee, S., Jafari, M., Tavili, A., Zare, S., Cappai, G., and De Giudici, G. (2022). Perspectives for phytoremediation capability of native plants growing on angouran Pb-zn mining complex in northwest of Iran. *J. Environ. Manage* 315, 115184. doi: 10.1016/j.jenvman.2022.115184

Hou, J., Liu, W., Wu, L., Ge, Y., Hu, P., Li, Z., et al. (2019). Rhodococcus sp. NSX2 modulates the phytoremediation efficiency of a trace metal-contaminated soil by reshaping the rhizosphere microbiome. *Appl. Soil Ecol.* 133, 62–69. doi: 10.1016/j.apsoil.2018.09.009

Jiang, X., Liu, W., Xu, H., Cui, X., Li, J., Chen, J., et al. (2021). Characterizations of heavy metal contamination, microbial community, and resistance genes in a tailing of the largest copper mine in China. *Environ. pollut.* 280, 116947. doi: 10.1016/j.envpol.2021.116947

Jiang, R., Wang, M., Chen, W., Li, X., and Balseiro-Romero, M. (2020). Changes in the integrated functional stability of microbial community under chemical stresses and the impacting factors in field soils. *Ecol. Indic.* 110, 105919. doi: 10.1016/j.ecolind.2019.105919

Jiao, A., Gao, B., Gao, M., Liu, X., Zhang, X., Wang, C., et al. (2022). Effect of nitrilotriacetic acid and tea saponin on the phytoremediation of Ni by Sudan grass (*Sorghum sudanense* (Piper) stapf.) in Ni-pyrene contaminated soil. *Chemosphere* 294, 133654. doi: 10.1016/j.chemosphere.2022.133654

Karimi, E., Keller-Costa, T., Slaby, B. M., Cox, C. J., da Rocha, U. N., Hentschel, U., et al. (2019). Genomic blueprints of sponge-prokaryote symbiosis are shared by low abundant and cultivatable *Alphaproteobacteria*. *Sci. Rep.* 9 (1), 1999. doi: 10.1038/s41598-019-38737-x

Koner, S., Tsai, H.-C., Chen, J.-S., Hussain, B., Rajendran, S. K., and Hsu, B.-M. (2022). Exploration of pristine plate-tectonic plains and mining exposure areas for indigenous microbial communities and its impact on the mineral-microbial geochemical weathering process in ultramafic setting. *Environ. Res.* 214 (Pt 2), 113802. doi: 10.1016/j.envres.2022.113802

Langille, M. G., Zaneveld, J., Caporaso, J. G., McDonald, D., Knights, D., Reyes, J. A., et al. (2013). Predictive functional profiling of microbial communities using 16S rRNA marker gene sequences. *Nat. Biotechnol.* 31 (9), 814–821. doi: 10.1038/nbt.2676

Li, L., Bai, S., Li, J., Wang, S., Tang, L., Dasgupta, S., et al. (2020). Volcanic ash inputs enhance the deep-sea seabed metal-biogeochemical cycle: A case study in the yap trench, western pacific ocean. *Mar. Geol.*. 430, 106340. doi: 10.1016/j.margeo.2020.106340

Li, G., Dongping, Q., Xusong, Y., and Gang, Y. (2020). Determination of heavy metals in the plant sample pretreatment methods. *J. Phys.: Conf. Series.* 1549 (2), 022008. doi: 10.1088/1742-6596/1549/2/022008

Li, Q., Xiang, P., Zhang, T., Wu, Q., Bao, Z., Tu, W., et al. (2022). The effect of phosphate mining activities on rhizosphere bacterial communities of surrounding vegetables and crops. *Sci. Total Environ.* 821, 153479. doi: 10.1016/j.scitotenv.2022.153479

Lin, H., Liu, C., Li, B., and Dong, Y. (2021). *Trifolium repens l.* regulated phytoremediation of heavy metal contaminated soil by promoting soil enzyme activities and beneficial rhizosphere associated microorganisms. *J. Hazard Mater.* 402, 123829. doi: 10.1016/j.jhazmat.2020.123829

Luo, J., Gu, S., Guo, X., Liu, Y., Tao, Q., Zhao, H.-P., et al. (2022). Core microbiota in the rhizosphere of heavy metal accumulators and its contribution to plant performance. *Environ. Sci. Technol.* 56, 18, 12975–12987. doi: 10.1021/acs.est.1c08832

Markowitz, V. M., Chen, I. M., Chu, K., Szeto, E., Palaniappan, K., Pillay, M., et al. (2014). IMG/M 4 version of the integrated metagenome comparative analysis system. *Nucleic Acids Res.* 42 (Database issue), D568–D573. doi: 10.1093/nar/gkt919

Mishra, J., Singh, R., and Arora, N. K. (2017). Alleviation of heavy metal stress in plants and remediation of soil by rhizosphere microorganisms. *Front. Microbiol.* 8. doi: 10.3389/fmicb.2017.01706

Niu, H., Leng, Y., Li, X., Yu, Q., Wu, H., Gong, J., et al. (2021). Behaviors of cadmium in rhizosphere soils and its interaction with microbiome communities in

phytoremediation. *Chemosphere* 269, 128765. doi: 10.1016/j.chemosphere.2020.128765

Okkeri, J., and Haltia, T. (1999). Expression and mutagenesis of ZntA, a zinc-transporting p-type ATPase from *Escherichia coli*. *Biochemistry*. 38 (42), 14109–14116. doi: 10.1021/bi9913956

Okkeri, J., and Haltia, T. (2006). The metal-binding sites of the zinc-transporting p-type ATPase of *Escherichia coli*. Lys693 and Asp714 in the seventh and eighth transmembrane segments of ZntA contribute to the coupling of metal binding and ATPase activity. *Biochim. Biophys. Acta* 1757 (11), 1485–1495. doi: 10.1016/j.bbabio.2006.06.008

Olesen, J. M., Bascompte, J., Dupont, Y. L., and Jordano, P. (2007). The modularity of pollination networks. *PNAS*. 104 (50), 19891–19896. doi: 10.1073/pnas.0706375104

Petruk, G., Roxo, M., De Lise, F., Mensitieri, F., Notomista, E., Wink, M., et al. (2018). The marine gram-negative bacterium novosphingobium sp. PP1Y as a potential source of novel metabolites with antioxidant activity. *Biotechnol. Lett*. 41 (2), 273–281. doi: 10.1007/s10529-018-02636-4

Qu, H., Ma, C., Xiao, J., Li, X., Wang, S., and Chen, G. (2021). Co-Planting of *Quercus nuttallii*, *Quercus pagoda* with *Solanum nigrum* enhanced their phytoremediation potential to multi-metal contaminated soil. *Int. J. Phytoremed.* 23 (10), 1104–1112. doi: 10.1080/15226514.2021.1878105

Rizwan, M., ElShamy, M. M., and Abdel-Aziz, H. M. M. (2019). Assessment of trace element and macronutrient accumulation capacity of two native plant species in three different Egyptian mine areas for remediation of contaminated soils. *Ecol. Indic.* 106, 105463. doi: 10.1016/j.ecolind.2019.105463

Shrivastava, M., Khandelwal, A., and Srivastava, S. (2019). Heavy metal hyperaccumulator plants: the resource to understand the extreme adaptations of plants towards heavy metals. *Plant-Metal Interact.* 79–97. doi: 10.1007/978-3-030-20732-8_5

Subpiramaniyam, S. (2021). *Portulaca oleracea* l. for phytoremediation and biomonitoring in metal-contaminated environments. *Chemosphere* 280, 130784. doi: 10.1016/j.chemosphere.2021.130784

Sungur, A., Vural, A., Gundogdu, A., and Soylak, M. (2020). Effect of antimonite mineralization area on heavy metal contents and geochemical fractions of agricultural soils in gümüşhane province, Turkey. *Catena* 184, 104255. doi: 10.1016/j.catena.2019.104255

Sun, H., Shao, C., Jin, Q., Li, M., Zhang, Z., Liang, H., et al. (2022). Response of microbial community structure to chromium contamination in panax ginseng-growing soil. *Environ. Sci. pollut. Res.* 29, 61122–61134. doi: 10.1007/s11356-022-20187-0

Tang, Z., Xi, B., Huang, C., Tan, W., Xia, X., Yang, T., et al. (2019). Linking phytoavailability of heavy metals with microbial community dynamics during municipal sludge composting. *Process Saf. Environ. Prot*. 130, 288–296. doi: 10.1016/j.psep.2019.08.026

Tao, J., Meng, D., Qin, C., Liu, X., Liang, Y., Xiao, Y., et al. (2018). Integrated network analysis reveals the importance of microbial interactions for maize growth. *Appl. Microbiol. Biotechnol.* 102 (8), 3805–3818. doi: 10.1007/s00253-018-8837-4

Tian, Z., Li, G., Tang, W., Zhu, Q., Li, X., Du, C., et al. (2022). Role of *Sedum alfredii* and soil microbes in the remediation of ultra-high content heavy metals contaminated soil. *gric Ecosyst. Environ*. 339, 108090. doi: 10.1016/j.agee.2022.108090

Vaid, N., Sudan, J., Dave, S., Mangla, H., and Pathak, H. (2022). Insight into microbes and plants ability for bioremediation of heavy metals. *Curr. Microbiol.* 79 (5), 141. doi: 10.1007/s00284-022-02829-1

Walz, J., Knoblauch, C., Böhme, L., and Pfeiffer, E.-M. (2017). Regulation of soil organic matter decomposition in permafrost-affected Siberian tundra soils - impact of oxygen availability, freezing and thawing, temperature, and labile organic matter. *Soil Boil Biochem.* 110, 34–43. doi: 10.1016/j.soilbio.2017.03.001

Wang, X., Cui, Y., Zhang, X., Ju, W., Duan, C., Wang, Y., et al. (2020). A novel extracellular enzyme stoichiometry method to evaluate soil heavy metal contamination: Evidence derived from microbial metabolic limitation. *Sci. Total Environ.* 738, 139709. doi: 10.1016/j.scitotenv.2020.139709

Wang, K., Sitsel, O., Meloni, G., Autzen, H. E., Andersson, M., Klymchuk, T., et al. (2014). Structure and mechanism of Zn^{2+}-transporting p-type ATPases. *Nature* 514 (7523), 518–522. doi: 10.1038/nature13618

Wood, J. L., Tang, C., and Franks, A. E. (2016). Microbial associated plant growth and heavy metal accumulation to improve phytoextraction of contaminated soils. *Soil Boil Biochem.* 103, 131–137. doi: 10.1016/j.soilbio.2016.08.021

Xiang, M., Li, Y., Yang, J., Lei, K., Li, Y., Li, F., et al. (2021). Heavy metal contamination risk assessment and correlation analysis of heavy metal contents in soil and crops. *Environ. pollut.* 278, 116911. doi: 10.1016/j.envpol.2021.116911

Xiao, R., Shen, F., Du, J., Li, R., Lahori, A. H., and Zhang, Z. (2018). Screening of native plants from wasteland surrounding a zn smelter in feng county China, for phytoremediation. *Ecotoxicol. Environ. Saf.* 162, 178–183. doi: 10.1016/j.ecoenv.2018.06.095

Xuan, Z., Baiquan, Z., Hui, L., Jing, H., Lijuan, J., Xian, Z., et al. (2021). Soil heavy metals and phytoremediation by *Populus deltoides* alter the structure and function of bacterial community in mine ecosystems. *Appl. Soil Ecol. L.* 172, 104359. doi: 10.1016/j.apsoil.2021.104359

Xu, Z. M., Zhang, Y. X., Wang, L., Liu, C. G., Sun, W. M., Wang, Y. F., et al. (2022). Rhizobacteria communities reshaped by red mud based passivators is vital for reducing soil cd accumulation in edible amaranth. *Sci. Total Environ.* 826, 154002. doi: 10.1016/j.scitotenv.2022.154002

Yao, Y., Zhang, X., Huang, Z., Li, H., Huang, J., Corti, G., et al. (2022). A field study on the composition, structure, and function of endophytic bacterial community of *Robinia pseudoacacia* at a composite heavy metals tailing. *Sci. Total Environ.* 850, 157874. doi: 10.1016/j.scitotenv.2022.157874

Yin, K., Wang, Q., Lv, M., and Chen, L. (2019). Microorganism remediation strategies towards heavy metals. *Chem. Eng. J.* 360, 1553–1563. doi: 10.1016/j.cej.2018.10.226

Yue, Z. B., Li, Q., Li, C. C., Chen, T. H., and Wang, J. (2015). Component analysis and heavy metal adsorption ability of extracellular polymeric substances (EPS) from sulfate reducing bacteria. *Biores. Technol.* 194, 399–402. doi: 10.1016/j.biortech.2015.07.042

Zerizghi, T., Guo, Q., Tian, L., Wei, R., and Zhao, C. (2022). An integrated approach to quantify ecological and human health risks of soil heavy metal contamination around coal mining area. *Sci. Total Environ.* 814, 152653. doi: 10.1016/j.scitotenv.2021.152653

Zhou, S., Song, Z., Li, Z., Qiao, R., Li, M., Chen, Y., et al. (2022). Mechanisms of nitrogen transformation driven by functional microbes during thermophilic fermentation in an ex situ fermentation system. *Biores. Technol.* 350, 126917. doi: 10.1016/j.biortech.2022.126917

frontiers | Frontiers in Plant Science

TYPE Original Research
PUBLISHED 20 June 2023
DOI 10.3389/fpls.2023.1200136

OPEN ACCESS

EDITED BY
Delong Meng,
Central South University, China

REVIEWED BY
Anton Hartmann,
Ludwig Maximilian University of Munich, Germany
Jing Cong,
Qingdao University of Science and Technology, China

*CORRESPONDENCE
Yunhua Xiao
huazipiaoling.123@163.com
Wu Chen
chenwuwarrior@163.com

†These authors have contributed equally to this work

RECEIVED 04 April 2023
ACCEPTED 31 May 2023
PUBLISHED 20 June 2023

CITATION
Tang Q, Liu T, Teng K, Xiao Z, Cai H, Wang Y, Xiao Y and Chen W (2023) Microbial interactions and metabolisms in response to bacterial wilt and black shank pathogens in the tobacco rhizosphere. *Front. Plant Sci.* 14:1200136. doi: 10.3389/fpls.2023.1200136

Microbial interactions and metabolisms in response to bacterial wilt and black shank pathogens in the tobacco rhizosphere

Qianjun Tang[1†], Tianbo Liu[1,2†], Kai Teng[2], Zhipeng Xiao[2], Hailin Cai[2], Yunsheng Wang[1], Yunhua Xiao[3*] and Wu Chen[1*]

[1]College of Plant Protection, Hunan Agricultural University, Changsha, China, [2]Laboratory of Plant Protection, Hunan Tobacco Science Institute, Changsha, China, [3]College of Bioscience and Biotechnology, Hunan Agricultural University, Changsha, China

Background: Tobacco bacterial wilt (TBW) and black shank (TBS) are responsible for substantial economic losses worldwide; however, microbial interactions and metabolisms in response to TBW and TBS pathogens in the tobacco rhizosphere remain unclear.

Methods: We explored and compared the response of rhizosphere microbial communities to these two plant diseases with the incidences in moderate and heavy degrees by sequencing of 16S rRNA gene amplicons and bioinformatics analysis.

Results and discussions: We found that the structure of rhizosphere soil bacterial communities was significantly ($p < 0.05$) changed from the incidences of TBW and TBS, which also led to decreased Shannon diversity and Pielou evenness. Compared with the healthy group (CK), the OTUs with significantly ($p < 0.05$) decreased relative abundances were mostly affiliated with Actinobacteria (e.g., *Streptomyces* and *Arthrobacter*) in the diseased groups, and the OTUs with significantly ($p < 0.05$) increased relative abundances were mainly identified as Proteobacteria and Acidobacteria. Also, molecular ecological network analysis showed that the nodes (<467) and links (<641) were decreased in the diseased groups compared with the control group (572; 1056), suggesting that both TBW and TBS weakened bacterial interactions. In addition, the predictive functional analysis indicated that the relative abundance of genes related to the biosynthesis of antibiotics (e.g., ansamycins and streptomycin) was significantly ($p < 0.05$) decreased due to incidences of TBW and TBS, and antimicrobial tests showed that some Actinobacteria strains (e.g., *Streptomyces*) and their secreted antibiotics (e.g., streptomycin) could effectively inhibit the growth of these two pathogens.

KEYWORDS

bacterial wilt, black shank, actinobacteria, bacterial interaction, biosynthesis of antibiotics

Introduction

Soil-borne diseases caused by bacteria or fungi often occur in agriculture and bring huge economic losses, and plant resistance mechanisms to plant diseases are complex (Deverall, 1987). Many researchers showed that the incidence of plant soil-borne diseases was closely related to plant species and soil environments (Kyselková et al., 2009; Schreiter et al., 2018). For plant autoimmune mechanisms, plants can recognize pathogen-associated molecular patterns and pathogen-delivered effectors to stimulate corresponding responses. Plants can strengthen existing defenses, elicit other defense mechanisms (Gómez-Gómez and Boller, 2002) mediated by secondary signal molecules such as salicylic acid, ethylene, and jasmonic acid, and fine-tune their defense responses (Wang et al., 2002).

The soil environment, including biotic (e.g., populations of bacteria and fungi) and abiotic (e.g., soil type and nutrients) factors, is critical to impacting disease incidence (Choi et al., 2020; Gu et al., 2022; Kim et al., 2022; Ren et al., 2022; Zhang et al., 2022). Microbes in the rhizosphere soil are the first protective screen against plant soil-borne pathogens (Kwak et al., 2018), and they can hinder pathogen growth through competent (e.g., nutrient and space) and antagonistic (e.g., antimicrobial peptide and phenolic acid antibacterial agent) actions. Many microbial ecological agents have recently been isolated from rhizosphere soil samples to control plant diseases (Tan et al., 2021; Wang et al., 2021; Kim et al., 2022). For example, *Bacillus* spp., isolated from wheat soil samples, could effectively reduce the growth of *Fusarium graminearum* strains causing fusarium head blight (Stumbriene et al., 2018), and *Flavobacterium* sp. TRM1, isolated from rhizosphere soil, could suppress *Ralstonia solanacearum* disease development (Kwak et al., 2018). Therefore, it is necessary to understand rhizosphere soil microbial communities and their associations with plant disease incidence.

Some soil-borne diseases often co-occur, making disease management more difficult. Many methods, e.g., promoting plant immune reaction, optimizing agronomic management, and developing biocontrol agents, were studied to prevent disease incidence. The plant immune system is determined by plant genes (Deverall, 1987), which need direct and hard genetic manipulation. The disease inhibiting efficiency of optimizing agronomic management is limited. Therefore, more and more researchers have focused on the beneficial rhizosphere soil or endophytic microbes. The anti-pathogen mechanism of microbes is expected to be complex, especially for different pathogens (Bacon and White, 2016). For example, some antibiotics are broad-spectrum antimicrobials, and some are limited (Yao et al., 2016; Cao et al., 2022). Therefore, high abundances and diverse species of probiotics in the rhizosphere soil may effectively prevent and control multiple diseases. Besides, disease incidence or infection was largely related to indigenous ecological interactions and stability disrupted by pathogens, and in return, close interactions and strong stability of soil microbial communities may be necessary to suppress disease incidences or infections for plants (Miliute et al., 2015; Xiao et al., 2018).

Tobacco (*Nicotiana tobacum*) is an economically important crop worldwide. Tobacco bacterial wilt (TBW) and tobacco black shank (TBS), respectively caused by the bacterial pathogen *Ralstonia solanacearum* (Yin et al., 2022) and fungal pathogen *Phytophthora nicotianae* (Jin and Shew, 2021), are two accompanying of the most devastating soil-borne diseases resulting in severe losses in yield and quality of tobacco. Although many previous studies found a difference in rhizosphere microbial diversity after the infection of pathogenic bacteria and pathogenic fungi, few studies were conducted in the same field, crop, and period. In this study, we explored the composition and interactions of rhizosphere soil microbial communities in response to incidences of TBW and TBS in the same field, crop, and period by sequencing of 16S rRNA gene amplicons. Our results indicated that the diseased rhizosphere microbial communities decreased diversity and interactions as well as decreased functional species for the biosynthesis of antibiotics, leading to incidences of both bacterial and fungal diseases, and these plant pathogens could further weaken community functions. This study provides new insights into our understanding of broad-spectrum Actinobacteria and has important implications for controlling TBW and TBS with microbes.

Materials and methods

Rhizosphere soil sampling

Rhizosphere soil samples were collected from a long-term ecological research site for a tobacco (*N. tabacum* cultivar K326) consecutive monoculture experiment located in Xiangxi, Hunan, China. Soil type of this research site was clayey and climate is humid subtropical monsoon. Fertilizer consisted of 50 kg/mu special basal fertilizer, 20 kg/mu special top dressing, 15 kg/mu bioorganic fertilizer, and 5 kg/mu hole-applied fertilizer. Its N:P:K (N, P_2O_5, and K_2O) was 1:1.2:2.43. Transplanted tobacco was irrigated with 300 kg/mu water and 5 kg/mu hole-applied fertilizer. No pest or disease controls was applied during the whole experiment. *N. tabacum* cultivar K326 was introduced by Northup King Seed Company (America) to Yunnan province (China) in 1985. It was now preserved in the Tobacco Research Institute, Chinese Academy of Agricultural Sciences, where we obtained and used seeds with permission.

At the *N. tabacum* harvesting stage in July 2017, we investigated the disease index of each tobacco plant in an area planted with 100 tobacco plants. The bacterial wilt and black shank disease index of each plant were determined based on the Chinese national standard GB/T 23222-2008, as described by Gao et al. (2015), ranging from 0 (lowest) to 9 (highest). In this study, moderate infection with a disease index of 1, 3 and 5, and heavy infection with a disease index of 7 and 9.

We designed five groups: the group with no disease (CK), the group moderately infected by TBW (BWM), the group heavily infected by TBW (BWH), the group moderately infected by TBS (BSM), and the group of heavily infected by TBS (BSH). Eight

rhizosphere soil samples were collected using a clean spade for each group following Kwak et al. (2018). The whole roots of each tobacco plant were collected at a soil depth of 0–20 cm. The loose soil particles adhering to the roots were shaken off. Afterward, the roots were placed in a 200-mL tube containing 100 mL of phosphate buffered saline buffer, and washed 3 times with shaking at 180 r/min. Finally, the rhizosphere soils were obtained after centrifuged at 10 000 r/min for 10 min and removing the supernatant. The rhizosphere soil samples were stored at -80°C before DNA extraction.

DNA extraction, amplification, 16S rRNA gene sequencing and data processing

DNA extraction, amplification, 16S rRNA gene amplicon sequencing, and data processing followed by Xiao et al. (2018). The rhizosphere soil from each root collection was homogenized, and 1.0 g from each sample was used for DNA extraction using a PowerSoil DNA Isolation Kit (MO BIO, San Diego, USA). DNA extracts were purified by electrophoresis on a 0.7% agarose gel using a DNA gel extraction kit (OMEGA, USA). The 16S rRNA gene was amplified with primer pair 515F (5'-GTGCCAGCMGCCGCGGTAA-3') and 806R (5'-GGACTACHVGGGTWTCTAAT-3'), combined with Illumina adapter sequences, a pad and a linker of two bases, and barcodes on the reverse primer. PCR products were purified, and the concentration was quantified with a NanoDrop ND-1000 spectrophotometer (NanoDrop Technologies, Wilmington, USA). The products were sequenced on a MiSeq machine (Illumina, San Diego, CA) using a 500-cycle kit. All 16S rRNA gene sequences were submitted to the Sequence Read Archive (SRA) of NCBI, and the accession number is PRJNA899683.

Molecular ecological network construction and characterization

Random matrix theory (RMT)-based approaches were used for network construction (Yin et al., 2015), hub and connector OTU identification and the topological property were determined with a similar threshold (0.95). OTUs, presented in 8 out of 8 replicates, were used for network analysis to ensure data reliability. Various network properties were characterized, such as average degree, average path distance, average clustering coefficient, and modularity index. The network modules were generated using rapid greedy modularity optimization. The experimental data used for constructing phylogenetic molecular ecological networks (pMENs) were based on 16S rRNA gene sequences, and Gephi 0.9.2 software was used to visualize network graphs. The pMENs were constructed separately based on sequencing data of five treatments to reveal the effects of different disease incidences on the microbial network interactions.

Functional profiling

Prior to functional gene prediction using PICRUSt (phylogenetic investigation of communities by reconstruction of unobserved states) described by Langille et al. (2013), the detected OTUs were reclassified using the GREENGENES reference database. Subsequently, PICRUSt uses 16S rRNA genes to infer metagenome gene functional content from phylogenetic information. The predictions are precalculated for genes in databases, including the Kyoto Encyclopaedia of Genes and Genomes (KEGG). The input data were first normalized by copy number by dividing each OTU by the known 16S rRNA copy number abundance before metagenome predictions and subsequent collapse into functional pathways. The output of PICRUSt consists of a table of functional gene counts as KEGG orthologs (KOs). The Nearest Sequenced Taxon Index (NSTI) value was used to validate the reliability of predicted metagenomes and functional pathways.

Species isolation and identification

According to data analysis, Actinobacteria could play a key role in inhibiting *P. nicotianae* and *R. solanacearum* growth. We isolated some Actinobacteria strains from the rhizosphere soil of healthy tobacco plants in the above sampling site using GAUZE's Medium NO.1. *P. nicotianae* HD1 and *R. solanacearum* GMI1000 were obtained originally from diseased *N. tabacum* roots. The single-species antagonism experiments were conducted as the description in our previous study (Liu et al., 2020). And the antagonistic isolates were identified following Ghodhbane-Gtari et al. (2010) based on 16S rRNA gene sequences against the NCBI database. The 16S rDNA sequence was amplified by PCR using primers 27F (5-AGAGTTTGATCACTGGCTCAG-3) and 1492R (5-CGGCTTACCTTGTTACGACTT-3).

Antimicrobial tests of antibiotics

The antimicrobial effect of several antibiotics was tested by the filtering paper method. Antibiotics included streptomycin, tetracycline and novobiocin, which are biosynthesized by Actinobacteria. The pathogens were *P. nicotianae* (incubated in the PDA medium) and bacterial pathogen *R. solanacearum* (incubated in the LB Agar).

Pot experiments

The effect of antagonistic strain on TBW and TBS was investigated by a pot experiment in the greenhouse. The cultivated tobacco seedlings (5 to 6 true leaves) were transplanted into pots with sterilized soil. Fifteen days after transplantation, the root was rinsed with the bacterial solution of strain 4-9 (1×10^8 CFU/mL). The treatment with sterile distilled water replaced bacterial solution was a negative control (CK). Eighteen seedlings of each treatment were repeated 3 times, and 50 mL bacterial solution or sterile distilled water was applied to each plant. 24 h after root irrigation, zoospore/bacterial suspensions were inoculated with a concentration of 1×10^4/mL (20 mL per plant). The incidence of TBS was observed 30 days after inoculation with *P. nicotiana*, and the

incidence of TBW was observed 15 days after inoculation with *R. solanacearum*. Disease classification was according to the Chinese national standard GB/T 23222-2008, further calculating the incidence, disease index and prevention effect.

Statistical analysis

The community diversity was assessed using the Shannon diversity index (*H'*) and species diversity index. Differences in diversity and relative abundances of bacterial composition based on Tukey's test were conducted by a one-way analysis of variance (ANOVA) and response ratio analysis (Deng et al., 2012). Detrended correspondence analysis (DCA) and dissimilarity tests were conducted to analyze the bacterial community structure. Linear regression analysis was carried out to explore relationships between disease suppression and microbial diversity (Barberán et al., 2014; Wagg et al., 2014; Cui et al., 2016). All analyses were performed using R v.3.6.3 and STAMP v 2.1.3. The functional/key OTUs were identified following Sheng et al. (2008) by comparing their 16S rRNA gene sequences to the NCBI database, and the phylogenetic tree was constructed using MEGA 5.2 (Kumar et al., 2018).

Results

Overview of rhizosphere soil bacterial communities

After clustering at the 97% sequence identity, 4955 OTUs were identified to comprise the soil bacterial community. The α-diversity index, including Shannon diversity and Pielou evenness, were shown in Table 1. Compared with the CK group (*H'*: 6.387; *J'*: 0.824), the Shannon diversity index was significantly ($p < 0.05$) decreased in the BWH (5.830), BSM (6.054) and BSH (5.679) groups, and Pielou evenness index was significantly ($p < 0.05$) reduced in the BSH group (0.758). DCA showed that the CK samples were segregated from the BWM and BWH samples (Figure 1A), and the BWM and BWH samples were also segregated from each other. Similarly, the CK samples were separated from the BSM and BSH samples (Figure 1B). Further dissimilarity tests showed that although the structure of BWM or BSM microbial communities was not significantly ($p < 0.05$) different, the CK group was significantly ($p < 0.05$) different from the other four pathogenic groups, and the heavily infected groups (BWH and BSH) were significantly ($p < 0.05$) different (Additional file 1), indicating the structure of rhizosphere soil bacterial communities was influenced by plant diseases at different degrees.

TABLE 1 Shannon diversity and Pielou evenness of microbial communities in the five groups.

Sample	Shannon diversity (H')	Pielou evenness (J')
CK	6.387 ± 0.341a	0.824 ± 0.034a
BWM	5.867 ± 0.253ab	0.784 ± 0.031ab
BWH	5.83 ± 0.196b	0.776 ± 0.03ab
BSM	6.054 ± 0.501b	0.783 ± 0.05ab
BSH	5.679 ± 0.311b	0.758 ± 0.036b

"a" and "b" indicated the significant ($p < 0.05$) difference.

The Venn diagram showed that there were 936, 175 and 335 unique OTUs in the CK, BWM and BWH groups, respectively, and the number of core OTUs was 2165 (Figure 1C), occupying the relative abundance up to 99%. Similarly, there were 665, 456 and 201 unique OTUs in the CK, BSM and BSH groups, respectively (Figure 1D), and 2295 core OTUs, occupying up to 99% relative abundance.

The compositions of rhizosphere soil bacterial communities shifted under the incidence of TBW and TBS

At the phylum level, the bacterial composition of five groups consisted of 26 phyla, which were mostly dominated by Proteobacteria (26.0~53.8%), Actinobacteria (8.0~33.6%), Acidobacteria (5.1~19.8%), Chloroflexi (1.2~15.1%), Bacteroidetes (1.4~9.3%), Thaumarchaeota (0.1~18.6%), and Verrucomicrobia (0.7~7.5%) (Figure 2A). However, compared with the CK group, the relative abundances of some phyla were changed under the incidence of plant diseases. ANOVA results showed that the average relative abundances of four phyla (Verrucomicrobia, BRC1, Latescibacteria, and Armatimonadetes) were significantly ($p < 0.05$) lower, and two (Chloroflexi and WPS-2) were significantly ($p < 0.05$) higher in the BWM group (Figure 2D); the average relative abundances of five phyla (Actinobacteria, Verrucomicrobia, BRC1, Latescibacteria, and Armatimonadetes) were significantly ($p < 0.05$) lower, and six (Chloroflexi, Thaumarchaeota, Firmicutes, Euryarchaeota, Parcubacteria and WPS-2) were significantly ($p < 0.05$) higher (Figure 2E) in the BWH group; the average relative abundance of one phylum (BRC1) were significantly ($p < 0.05$) lower, and two (Chloroflexi and Chlamydiae) were significantly ($p < 0.05$) higher in the BSM group (Figure 2F); the average relative abundances of six phyla (Acidobacteria, Verrucomicrobia, BRC1, Latescibacteria, Armatimonadetes and WPS-1) were significantly ($p < 0.05$) lower, and three (Chloroflexi, Parcubacteria and WPS-2) were significantly ($p < 0.05$) higher in the BSH group (Figure 2G). Besides, only one phylum showed a significant ($p < 0.05$) difference between BWM and BSM groups and two phyla between BWH and BSH groups (Figures 2H, I).

At the genus level (Figure 2B), compared with the CK group, the relative abundances of some genera were also changed by plant diseases. ANOVA results showed that: the average relative abundances of 84 genera (e.g., *Gp6*, *Streptomyces* and *Gp4*) were significantly ($p < 0.05$) lower and 43 (e.g., *Rhodanobacter*, *Gp1*, and *Gp2*) were significantly ($p < 0.05$) higher in the BWM group (Additional file 2); the average relative abundances of 91 genera (e.g., *Streptomyces*, *Gp6*, and *Gp4*) were significantly ($p < 0.05$) lower and 26 (e.g., *Nitrososphaera*, *Gp1* and *Rhodanobacter*) were significantly ($p < 0.05$) higher in the BWH group (Additional file 3); the average relative abundance of 60 genera (e.g., Gp6, Gp4 and

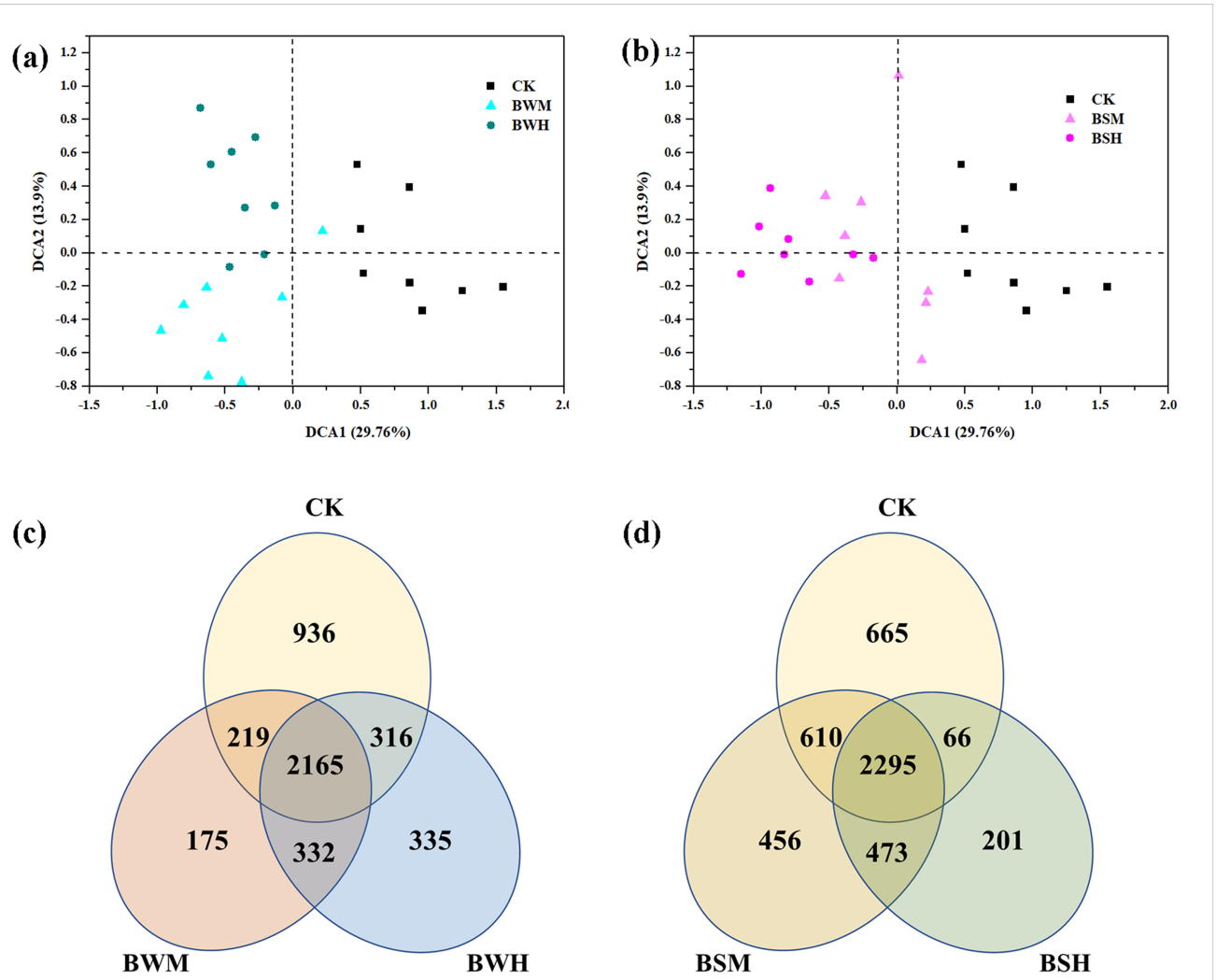

FIGURE 1
The ordination plots of all samples for the community structure analyzed by detrended correspondence analysis **(A, B)** and Venn diagram **(C, D)**. CK: control group; BWM: the group of moderately infected by TBW; BWH: the group of heavily infected by TBW; BSM: the group of moderately infected by TBS; BSH: the group of heavily infected by TBS.

Spartobacteria_genera_incertae_sedis) were significantly ($p < 0.05$) lower, and 27 (e.g., *Ktedonobacter*, *Geothrix* and *Terriglobus*) were significantly ($p < 0.05$) higher in the BSM group (Additional file 4); the average relative abundances of 113 genera (e.g., *Gp6*, *Streptomyces* and *Gp4*) were significantly ($p < 0.05$) lower, and 37 (e.g., *Rhodanobacter*, *Gp1* and *Ktedonobacter*) were significantly ($p < 0.05$) higher in the BSH group (Additional file 5).

At the OTU level (Figure 2C), compared with the CK group, the composition of the other four groups was significantly ($p < 0.05$) different. ANOVA results showed that: the average relative abundances of 691 OTUs were significantly lower, and 239 were significantly ($p < 0.05$) higher in the BWM group (Additional file 6); the average relative abundances of 654 OTUs were significantly ($p < 0.05$) lower, and 197 were significantly ($p < 0.05$) higher in the BWH group (Additional file 7); the average relative abundance of 456 OTUs were significantly ($p < 0.05$) lower, and 198 were significantly higher in the BSM group (Additional file 8); the average relative abundances of 821 OTUs were significantly ($p < 0.05$) lower, and 128 were significantly ($p < 0.05$) higher in the BSH group (Additional file 9).

We further aligned the 16S rRNA sequences of top 10 OTUs with the largest decrease (15 OTUs, Figure 3) or increase (19 OTUs, Figure 4) of relative abundances compared with the CK group to the NCBI database. The top 10 decreased OTUs were identical in the BWM, BWH, and BSH groups (Figures 3B, C, E), suggesting their importance in controlling the incidence of TBW and TBS. The phylogenetic tree (Figure 3A) indicated that six OTUs (OTU_8, OTU_16, OTU_17, OTU_34, OTU_42, and OTU_3189) were identified as Actinobacteria (*Amycolatopsis*, *Lentzea*, *Arthrobacter*, *Janibacter*, *Streptomyces*), two OTUs (OTU_74 and OTU_155) were identified as Acidobacteria (*Gp4* and *Gp6*), and one OTU (OTU_6) was identified as proteobacteria (*Sphingobium*). In the BSM group, five OTUs were the same as the other three groups, and five were different (Figure 3D). The top 10 increased OTUs (19 OTUs in total) were different in the different groups (Figures 4B–E), but most of them were identified as Proteobacteria (6 OTUs) and Acidobacteria (5 OTUs) (Figure 4A). The relative abundances of OTU_2 (Thaumarchaeota) and OTU_18 (Acidobacteria_*Geothrix*) were increased in the four diseased groups.

10.3389/fpls.2023.1200136

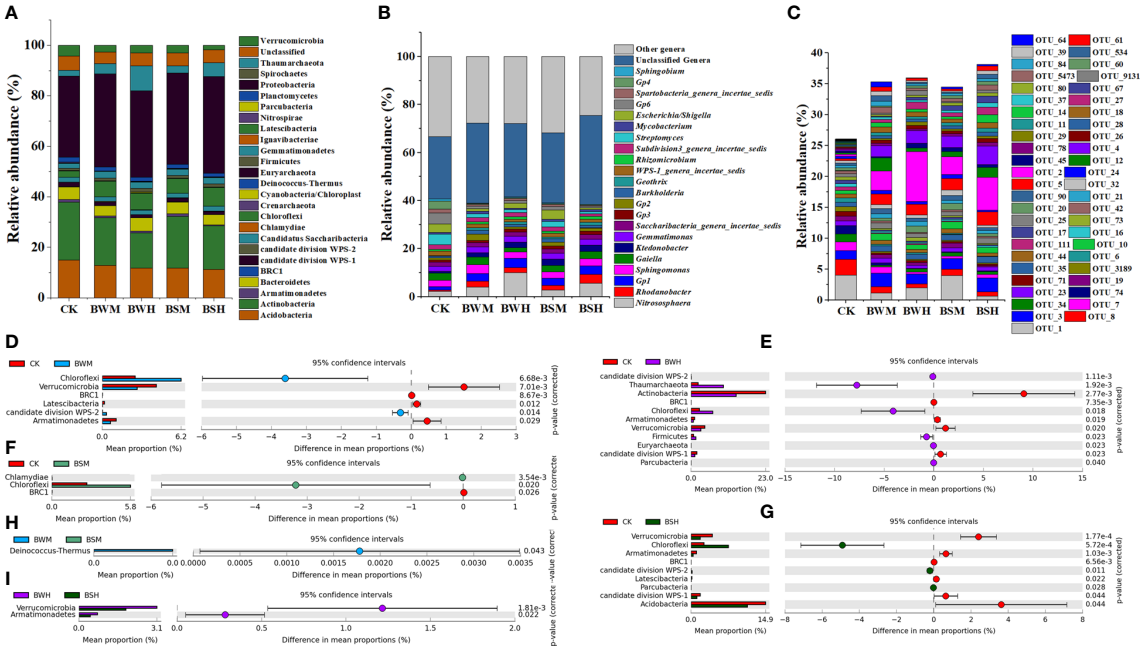

FIGURE 2
The compositions of microbial communities in phylum **(A)**, genus **(B)**, OTU **(C)** levels, and the significant phyla between each two groups **(D–I)**.

Network interactions of bacterial communities shifted under the incidence of TBW and TBS

To discern possible microbial interactions in response to TBW and TBS, molecular ecological networks (MENs) were constructed with 16S rRNA sequencing data using the RMT-based network approaches (Figures 5A–E). Major topological properties of empirical MENs of microbial communities in the nine groups were shown in Table 2. With the same threshold (0.900), their correlations were more than 0.750, indicating that the degree distributions in both constructed molecular ecological networks fitted the power-law model well. There were more nodes and links in the CK group (572 nodes and 1056 links) than those in the BWM

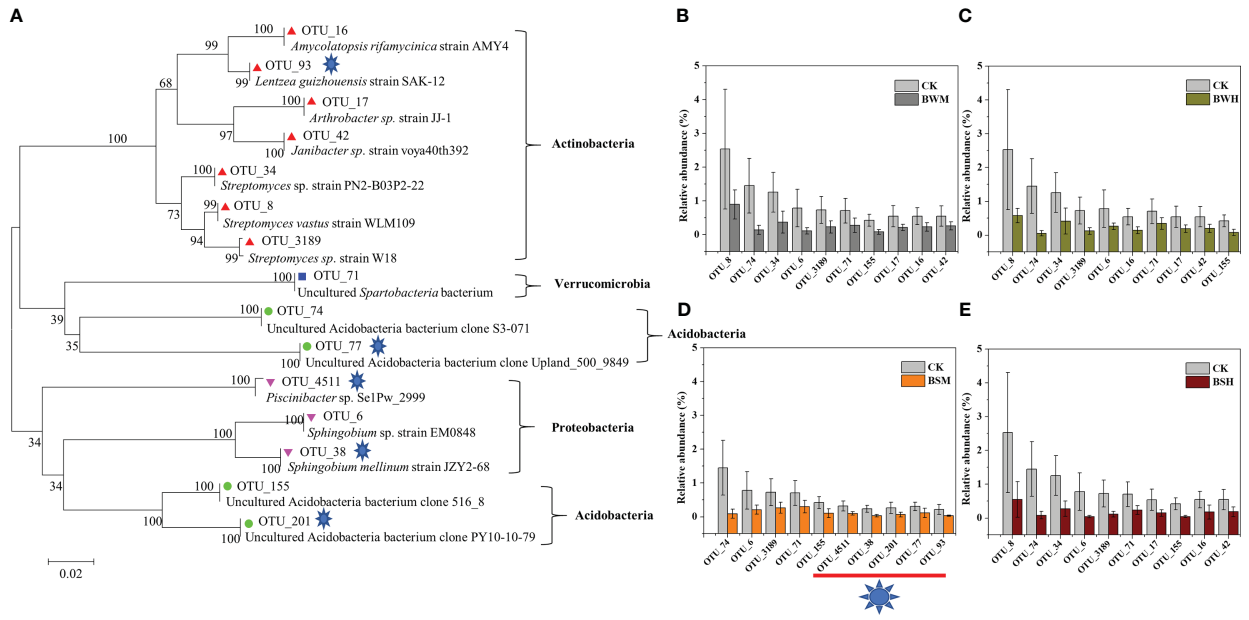

FIGURE 3
Phylogenetic tree **(A)** of the top 10 decreased OTUs in BWM **(B)**, BWH **(C)**, BSM **(D)**, and BSH **(E)** groups, compared with the CK group.

10.3389/fpls.2023.1200136

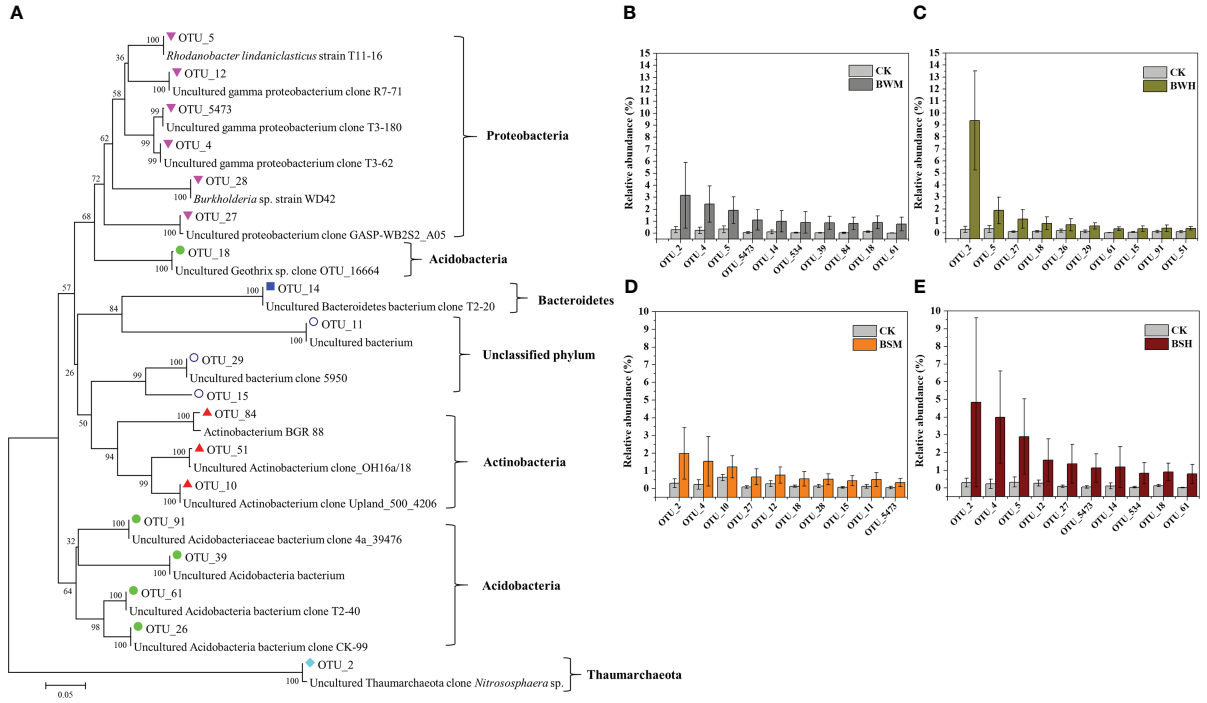

FIGURE 4
Phylogenetic tree **(A)** of the top 10 increased OTUs in BWM **(B)**, BWH **(C)**, BSM **(D)**, and BSH **(E)** groups, compared with the CK group.

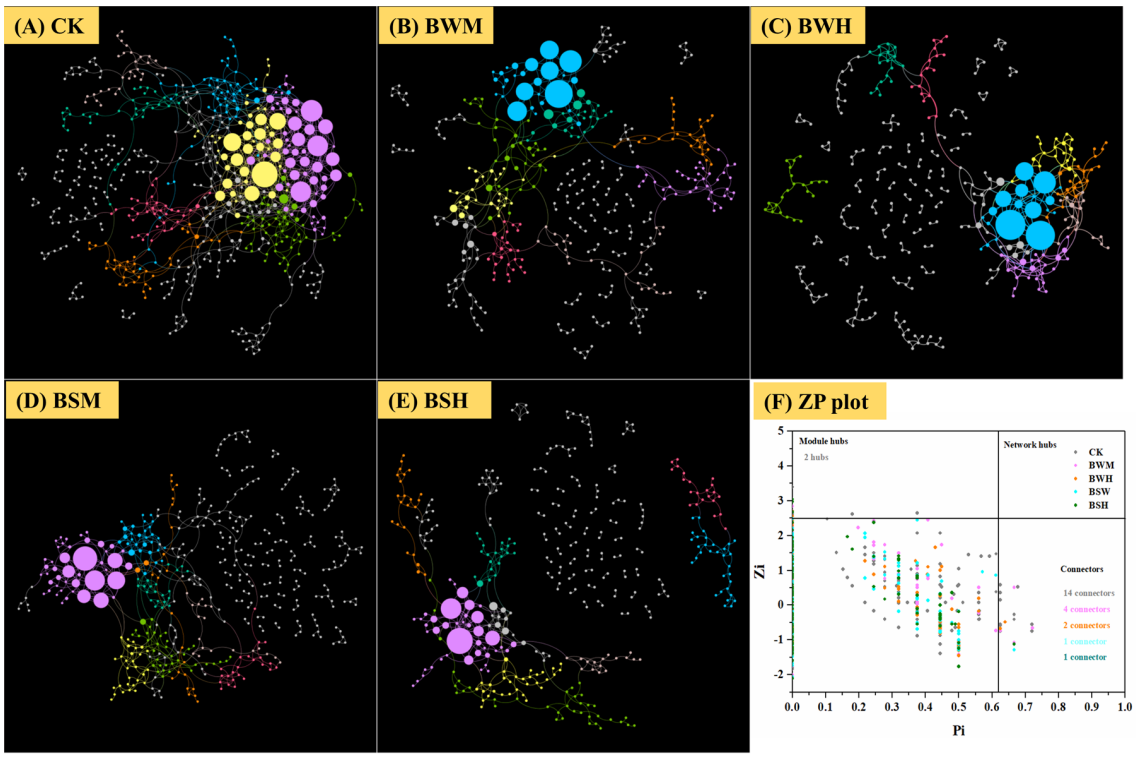

FIGURE 5
Molecular ecological networks in CK **(A)**, BWM **(B)**, BWH **(C)**, BSM **(D)**, and BSH **(E)** groups, and the *Z-P* plot showing the distribution of OTUs based on their topological roles **(F)**. The color of the circle represented the module in the network interaction. The topological role of each OTU was determined according to the scatter plot of within-module connectivity (Zi) and among-module connectivity (Pi).

TABLE 2 Topological properties of the empirical pMENs of soil bacterial communities in five groups.

Network Indexes	CK	BWM	BWH	BSM	BSH
Total nodes	572	396	346	466	392
Total links	1056	521	435	640	512
Threshold	0.900	0.900	0.900	0.900	0.900
R square of power-law	0.84	0.755	0.869	0.82	0.859
moduel	46	49	56	63	61
modurity	0.742	0.846	0.848	0.829	0.859
Average degree (avgK)	3.692	2.631	2.514	2.747	2.612
Average clustering coefficient (avgCC)	0.237	0.201	0.223	0.182	0.229
Average path distance (GD)	7.692	8.381	7.557	7.357	7.609
Connectedness (Con)	0.731	0.527	0.242	0.415	0.31
Efficiency	0.993	0.992	0.98	0.99	0.986

(396 and 521), BWH (346 and 435), BSM (466 and 640), and BSH (392 and 512) groups. It showed interactions of rhizosphere soil microbial communities could be disrupted by pathogens of plant diseases, and the higher degree of plant diseases could lead to more network destruction compared to the CK group.

There were also more module hubs (2 hubs) and connectors (14 connectors) in the CK group (Figure 5F). We further aligned the 16S rRNA sequences of all hubs and connectors (23 OTUs; 16 in CK; 4 in BWM; 2 in BWH; 1 in BSM; 1 in BSH) to the NCBI database (Additional file 10), and found that 11 OTUs were associated with Actinobacteria, and the other 12 OTUs with Proteobacteria (3 OTUs), Acidobacteria (3 OTUs), Verrucomicrobia (2 OTUs), Firmicutes (1 OTU), Gematimonadetes(1 OTU), Armatimonadetes(1 OTU), and unclassified phylum (1 OTU). OTU_48 (Proteobacteria_*Ramlibacter*) was a connector in both CK and BSM groups. Among the 23 OTUs, 14 OTUs (OTU_624, OTU_42, OTU_7584, OTU_2102, OTU_48, OTU_7351, OTU_9474, OTU_631, OTU_483, OTU_38, OTU_96, OTU_48, OTU_279, and OTU_671) were significantly ($p < 0.05$) different between the CK group and the diseased groups, and interestingly, the other 13 OTUs were higher in the CK group except OTU_671 (Additional file 10).

Metabolic diversity

Based on the 16S rRNA sequences, potential functions were predicted to explore changes of functional diversity and composition by plant pathogens. Although the functional diversity index showed no significant difference among these five groups (Additional file 11), DCA results showed that the CK samples were segregated from the diseased samples (Figures 6A, B), which was further verified using the dissimilarity tests (Additional file 12). There were about 6900 core genes in these groups, and more unique genes (121/126) were in the CK group compared with the other diseased groups (Figures 6C, D). Compared with the CK group, the relative abundance of genes related to metabolisms of carbohydrate, terpenoids and polyketides was significantly ($p < 0.05$) decreased in the diseased groups, especially in the BWH group. In contrast, the relative abundance of genes related to cell process (e.g., cell motility) was significantly ($p < 0.05$) increased (Additional file 13) in the diseased groups.

We further explored the change in gene abundances related to antibiotics biosynthesis pathways (metabolism of terpenoids and polyketides and biosynthesis of other secondary metabolites). ANOVA results showed that the relative abundances of 6 pathways, including biosynthesis of 12-, 14- and 16-membered macrolides, biosynthesis of ansamycins, polyketide sugar unit biosynthesis, biosynthesis of enediyne antibiotics, streptomycin biosynthesis, and penicillin and cephalosporin biosynthesis, were significantly decreased in all diseased groups (Table 3). Besides, 13 pathways (e.g., tetracycline biosynthesis and carbapenem biosynthesis) were also weakened, and three pathways (caffeine metabolism, tropane, piperidine and pyridine alkaloid biosynthesis, and isoflavonoid biosynthesis) were enhanced in individual diseased groups (Table 3).

Antagonistic effects of Actinobacteria and inhibition effects of antibiotics

Six strains were obtained after isolation on GAUZE's medium NO. 1 of the rhizosphere soils in healthy tobacco plants. Through antagonism experiments, four strains could inhibit the growth of *P. nicotianae* HD1 (Figure 7A). After identification, two strains (3-13 and 3-17) had the highest similarity to *Streptomyces sakaiensis* (99%), one (4-9) similarity to *Streptomyces acidiscabies* (99%), and one (4-2) similarity to *Stenotrophomonas maltophilia* (99%). A further experiment found that three strains could inhibit the growth of *R. solanacearum* GMI1000 (Figure 7B).

Filtering paper methods (Figures 7C, D) showed that streptomycin (100 μg/ml), tetracycline (100 μg/ml), novobiocin (300 μg/ml) and vancomycin (100 μg/ml) could inhibit the growth

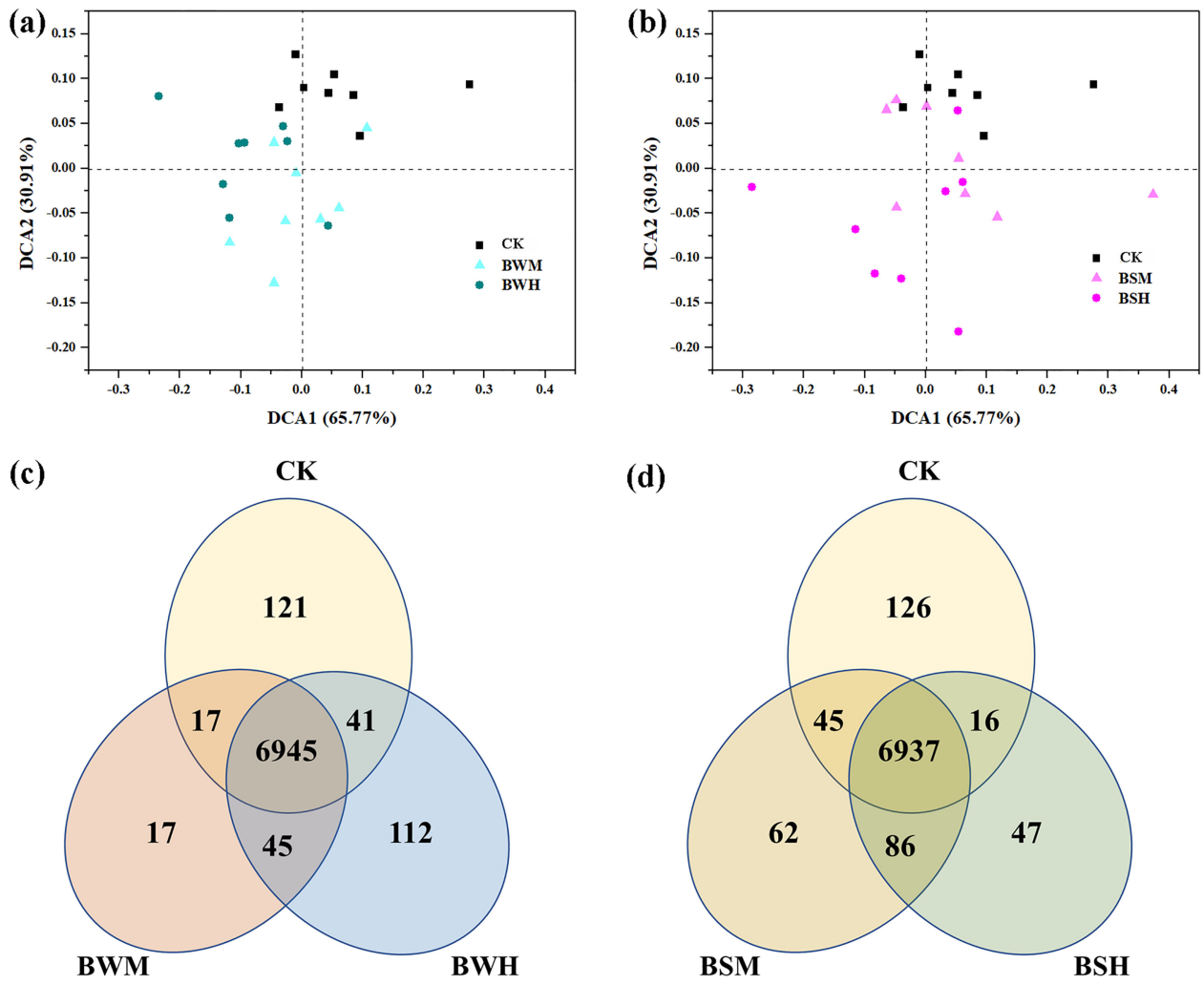

FIGURE 6
The ordination plots of all samples for the predicted genes analyzed by detrended correspondence analysis **(A, B)** and Venn diagram **(C, D)**.

of *R. solanacearum* GMI1000, and streptomycin (50 mg/ml) and novobiocin (100 mg/ml) could inhibit the growth of *P. nicotianae* HD1.

Results of the pot experiment indicated that compared with the CK group, the index and incidence of TBW (62.76%; 45.53%) and TBS (12.1%; 20.36%) in the group inoculated with strain 4-9 were significantly decreased (Figures 7E, F). The control efficiency of strain 4-9 was 60.40% on TBS and 30.67% on TBW.

Discussion

Previous studies focused on using microbial antagonists for controlling soil-borne diseases, and many biocontrol agents were found virtually for plant disease biocontrol against a single pathogen (Dunne et al., 1997; Liu et al., 2007; Shanks et al., 2012; Han et al., 2016). However, managing just one of the pathogens may not fully solve the problem since different pathogens often co-occur on the same plant, resulting in a disease complex causing synergistic yield losses (Shen et al., 2022). An environmentally friendly alternative could be using multiple strains with a broad spectrum of antagonism against multiple pathogens, which may provide excellent and new options for soil-borne disease control. TBW is a bacterial disease, and TBS is a fungal disease, which usually results in severe losses of yield and quality of tobacco, so that TBW and TBS can be excellent model for biocontrol research. The first task is to find effectively broad-spectrum microorganisms (Zheng et al., 2021; Shi et al., 2022). In this study, we studied the response of rhizosphere soil microbial communities to these two plant diseases.

The relationship between rhizosphere soil bacterial community composition/structure and crop disease incidence was well studied (Mengesha et al., 2017; Ma et al., 2018; Xiao et al., 2018). It is clear that rhizosphere soil microbial communities generally differ between healthy and diseased plants (Niu et al., 2017; Yang et al., 2017). After plants are infected, the soil microbial diversity and the abundance of probiotics decrease, and microbial interactions could be destroyed (Niu et al., 2017), which is also found in this study. It was also indicated that the change in rhizosphere soil microbial communities was more evident with the increased disease index. Although rhizosphere soil microbial communities showed some

TABLE 3 The key pathways with significant ($p < 0.05$) differences between the CK group and each diseased group.

Metabolism	Pathway	CK vs. BWM (%)	CK vs. BWH (%)	CK vs. BSM (%)	CK vs. BSH (%)
Metabolism of terpenoids and polyketides	Biosynthesis of 12-, 14- and 16-membered macrolides	9.07E-05	1.16E-04	7.45E-05	1.11E-04
	Biosynthesis of type II polyketide backbone	6.10E-03	7.15E-03	–	7.84E-03
	Biosynthesis of ansamycins	7.62E-04	1.35E-03	8.25E-04	1.24E-03
	Tetracycline biosynthesis	1.21E-04	–	–	9.48E-05
	Polyketide sugar unit biosynthesis	2.71E-02	3.09E-02	1.71E-02	3.19E-02
	Biosynthesis of vancomycin group antibiotics	3.00E-03	2.89E-03	–	3.26E-03
	Biosynthesis of enediyne antibiotics	8.15E-04	1.00E-03	7.15E-04	9.47E-04
	Type I polyketide structures	–	1.62E-03	–	1.76E-03
	Insect hormone biosynthesis	5.82E-06	–	5.82E-06	–
	Biosynthesis of type II polyketide products	–	3.00E-03	–	–
	Limonene and pinene degradation	–	1.31E-03	–	–
	Geraniol degradation	–	3.68E-03	–	–
Biosynthesis of other secondary metabolites	Carbapenem biosynthesis	1.07E-03	1.08E-03	–	1.22E-03
	Biosynthesis of secondary metabolites-other antibiotics	1.33E-03	1.57E-03	–	1.67E-03
	Caffeine metabolism	-9.96E-05	–	–	-1.61E-04
	Streptomycin biosynthesis	3.30E-04	3.91E-04	3.09E-04	3.61E-04
	Tropane, piperidine and pyridine alkaloid biosynthesis	-3.83E-03	–	–	-4.86E-03
	Penicillin and cephalosporin biosynthesis	5.90E-03	1.12E-02	7.00E-03	8.02E-03
	Novobiocin biosynthesis	–	5.91E-05	5.34E-05	6.16E-05
	Isoflavonoid biosynthesis	–	–	–	-4.06E-03
	Indole alkaloid biosynthesis	4.91E-06	–	–	5.88E-06
	Phenylpropanoid biosynthesis	1.33E-03	–	–	–
	Betalain biosynthesis	-2.69E-03	–	–	–

CK vs. BWM, BWH, BSM, or BSH indicated the relative abundance of genes in the CK group minus that in the BWM, BWH, BSM, or BSH group, respectively.

differences between different types (caused by fungi or bacteria) of plant diseases, they offered much more similarities. It is hypothesized that bacterial and fungal diseases would have different effects on rhizosphere soil microecology. Indeed, the composition and structure of rhizosphere soil microbial communities were different between the BWH and BSH groups, and three possible mechanisms are: the invasive ability of various pathogens is different; the plant immunocompetence to various pathogens are different; the effective probiotics are different (Horst and Kenneth, 1990; Keen et al., 1993; Ojiambo and Scherm, 2006). However, in our study, many results suggest that after different diseases are outbursts, the rhizosphere soil microbial community alters in a similar direction. The diversity index did not show differences between the TBS and TBW groups (Table 1); microbial interactions appeared to be simple; most of the varied populations (e.g., Actinobacteria) were found to be similar; most varied pathways (e.g., biosynthesis of secondary metabolites, biosynthesis of ansamycins) were almost the same among diseased groups.

The resistance mechanisms to plant diseases are complex, mainly depending on the plant-soil-microbe interaction in the soil system (Rasmussen et al., 2019). After the plants were transplanted in the same area, some were healthy, some were lightly diseased, and some were heavily diseased, which seems stochastic. Once pathogens occur in plant tissues, root exudates will be influenced (Gulati et al., 2020). Root exudates have specialized roles in nutrient cycling and signal transduction between a root and its surrounding soil (Jonasson et al., 1999), as well as in plant responses to environmental stresses (Liu et al., 2020). Root exudates play essential roles in the root-root, root-microbe, and microbe-microbe interactions (Bais et al., 2004). Some secretions, e.g., cutin, are screened against plant pathogens (Maurel et al., 1994). The diversity and stability of normal plant flora are

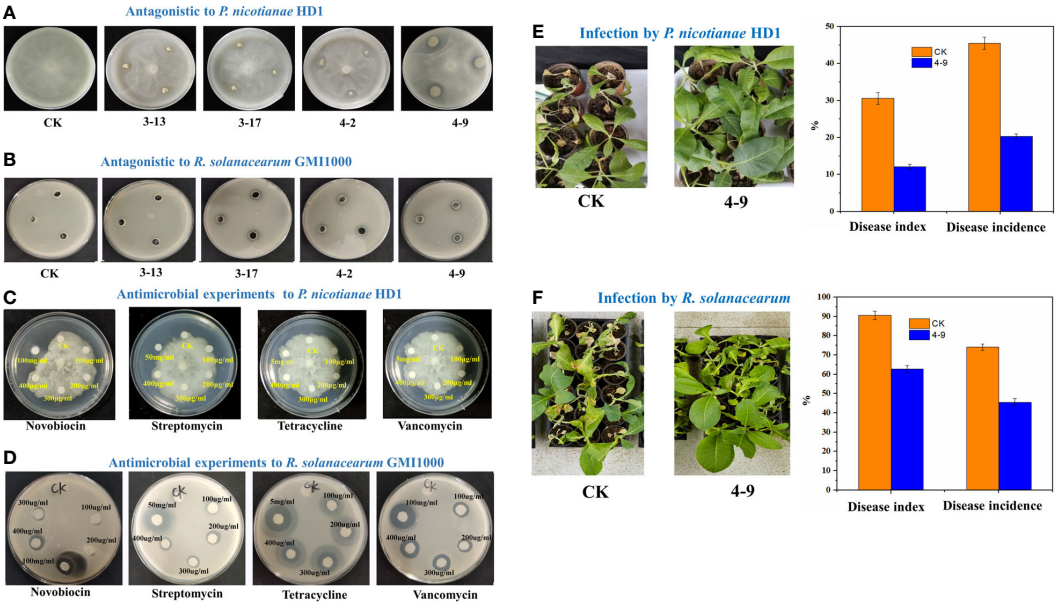

FIGURE 7
Antagonistic effects. The plate-antagonistic effects of isolated Actinobacteria strains on *P. nicotianae* HD1 **(A)** and *R. solanacearum* GMI1000 **(B)**; The plate-inhibition experiments of some antibiotics on *P. nicotianae* HD1 **(C)** and *R. solanacearum* GMI1000 **(D)**; The pot-antagonistic effects of strain 4-9 on *P. nicotianae* HD1 **(E)** and *R. solanacearum* GMI1000 **(F)**.

other factors to inhibit or kill pathogens (Tilman and Downing, 1994; Tilman et al., 1997; Fitter et al., 2005). Generally, the more closely and stable this system is, the stronger its protective ability is. Also, probiotics and their secondary metabolites play important roles in decreasing the infection of pathogens (Fravel, 1988; Howell, 2003). A well-conditioned cycle should be that normal root exudates improve soil nutrients and soil microecological environments and are beneficial for probiotics to grow, which protects the plant from pathogen infection and accelerates plant growth. Otherwise, a vicious cycle may be that the changed and bad root exudates, as toxic resources, decrease soil nutrients, promote pathogen growth, inhibit probiotics, destroy the stability of soil microecology, and further aggravate the plant disease. Therefore, although the appearance of pathogens or their types is random, the plant-soil-microbe interaction determines the colonization of pathogens and the occurrence of plant diseases.

Analyses of high-throughput sequencing data suggested that Actinobacteria (e.g., *Amycolatopsis*, *Lentzea*, *Arthrobacter Mycobacterium*, and *Streptomyces*) and their biosynthesis of antimicrobial peptides (e.g., ansamycins, novobiocin, streptomycin, tetracycline) played crucial roles in inhibiting both TBS and TBW. We further emphasized that some isolated Actinobacteria and some antimicrobial peptides (e.g., novobiocin, streptomycin) could inhibit both *P. nicotianae* HD1. and *R. solanacearum* GMI1000. The researches for Actinobacteria as biological control agents of plant disease are of interest, given their ability to colonize healthy plant tissues and produce antibiotics *in situ* (Trujillo et al., 2015; Jose et al., 2021; Yadav et al., 2021). For example, *Streptomyces* isolated from healthy banana plants could produce antifungal molecules that inhibited the growth of *Fusarium oxysporum* (Cao et al., 2005). Yacine et al. (2014) found that *Streptomyces* were isolated from tomatoes and native plants of the *Algerian Sahara* and screened for biocontrol activity against *Rhizotocnia solani*. Actinobacteria are the source of two-thirds of naturally derived antibiotics and a range of antihelminthic, antifungal, antibacterial, anticancer, and immunosuppressive drugs (Ventura et al., 2007). The impressive list of important anti-infective compounds synthesized by Actinobacteria includes streptomycin, tetracyclines, chloramphenicol, novobiocin, ansamycins, erythromycin, vancomycin, and kanamycin, and some of these (e.g., ansamycins) are broad-spectrum antibiotics (Mahajan and Balachandran, 2012). Our pot experiment also showed *Streptomyces acidiscabies* 4-9 could effectively control TBW and TBS. Therefore, some broad-spectrum Actinobacteria may be biocontrol agents for both tobacco bacterial and fungal diseases in the future. However, since in the final pot experiments sterilized soil was applied and heavy inoculation with selected Streptomyces strains was used, there is still a long way to a practical application of Streptomyces strains for biocontrol of wilt and black shark diseases of tobacco.

Conclusions

Compared with healthy plants, the composition and structure of rhizosphere soil microbial communities showed some differences in diseased plants infected with TBW or TBSwith decreased species diversity, destructive networks, and decreased functionality involved in the biosynthesis of antibiotics, which might be the characteristics of the diseased soils. Actinobacteria (e.g., *Amycolatopsis*, *Arthrobacter Mycobacterium, Streptomyces*) were

the effective probiotics, and their biosynthesis of antimicrobial peptides (e.g., novobiocin and streptomycin) played crucial roles in controlling the growth of bacterial and fungal pathogens.

Data availability statement

The data presented in the study are deposited in the Sequence Read Archive (SRA) of NCBI repository, accession number PRJNA899683.

Author contributions

WC and QT contributed to the study's conception and design. Research, material preparation, data collection and analysis were performed by TL, KT, ZX, and HC. The first draft of the manuscript was written by YX. TL, QT, YW and WC commented on previous versions of the manuscript. All authors contributed to the article and approved the submitted version.

Funding

This study was supported by the key Research project of Hunan Province (2021NK1040), the key project of Science and Technology Project of China National Tobacco Corporation [110202101050 (LS-10) and 110202201019 (LS-03)], the key project of Science and Technology of Hunan Branch of China National Tobacco Corporation (CS2022KJ02 and XX2022-2024Aa01), Scientific Research Project of Education Department of Hunan Province (21A0142).

Acknowledgments

Hunan Engineering & Technology Research Center for Agricultural Big Data Analysis & Decision-making, and Tobacco Technology Center of Xiangxi provided field space.

Conflict of interest

The authors declare that the research was conducted in the absence of any commercial or financial relationships that could be construed as a potential conflict of interest.

Publisher's note

Supplementary material

The Supplementary Material for this article can be found online at: https://www.frontiersin.org/articles/10.3389/fpls.2023.1200136/full#supplementary-material

References

Bacon, C. W., and White, J. F. (2016). Functions, mechanisms and regulation of endophytic and epiphytic microbial communities of plants. *Symbiosis* 68, 87–98. doi: 10.1007/s13199-015-0350-2

Bais, H. P., Park, S., Weir, T. L., Callaway, R. M., and Vivanco, J. M. (2004). How plants communicate using the underground information superhighway. *Trends Plant Sci.* 9, 26–32. doi: 10.1016/j.tplants.2003.11.008

Barberán, A., Ramirez, K. S., Leff, J. W., Bradford, M. A., Wall, D. H., and Fierer, N. (2014). Why are some microbes more ubiquitous than others? predicting the habitat breadth of soil bacteria. *Ecol. Lett.* 17, 794–802. doi: 10.1111/ele.12282

Cao, X., Landick, R., and Campbell, E. A. (2022). A roadmap for designing narrow-spectrum antibiotics targeting bacterial pathogens. *Microbial Cell* 9, 136–138. doi: 10.15698/mic2022.07.780

Cao, L., Qiu, Z., You, J., Tan, H., and Zhou, S. (2005). Isolation and characterization of endophytic streptomycete antagonists of fusarium wilt pathogen from surface-sterilized banana roots. *FEMS Microbiol. Lett.* 247, 147. doi: 10.1016/j.femsle.2005.05.006

Choi, K., Choi, J., Lee, P. A., Roy, N., Khan, R., Lee, H. J., et al. (2020). Alteration of bacterial wilt resistance in tomato plant by microbiota transplant. *Front. Plant Sci.* 11. doi: 10.3389/fpls.2020.01186

Cui, P., Fan, F., Yin, C., Song, A., Huang, P., Tang, Y. J., et al. (2016). Long-term organic and inorganic fertilization alters temperature sensitivity of potential N_2O emissions and associated microbes. *Soil Biol. Biochem.* 93, 131–141. doi: 10.1016/j.soilbio.2015.11.005

Deng, Y., He, Z., Xu, M., Qin, Y., Van Nostrand, J. D., Wu, L. Y., et al. (2012). Elevated carbon dioxide alters the structure of soil microbial communities. *Appl. Environ. Microbiol.* 78, 2991–2995. doi: 10.1128/AEM.06924-11

Deverall, B. J. (1987). Book review - mechanisms of resistance to plant diseases. *Australas. Plant Pathol.* 16, 68. doi: 10.1071/APP9870068

Dunne, C., Crowley, J. J., Moenne-Loccoz, Y., Dowling, D. N., Bruijn, S., and Fergal, O. (1997). Biological control of *Pythium ultimum* by *Stenotrophomonas maltophilia* W81 is mediated by an extracellular proteolytic activity. *Microbiology* 143, 3921–3931. doi: 10.1099/00221287-143-12-3921

Fitter, A. H., Gilligan, C. A., Hollingworth, K., Kleczkowski, A., Twyman, R. M., and Pitchford, J. W. (2005). Biodiversity and ecosystem function in soil. *Funct. Ecol.* 19, 369–377. doi: 10.1111/j.0269-8463.2005.00969.x

Fravel, D. R. (1988). Role of antibiosis in the biocontrol of plant diseases. *Annu. Rev. Phytopathol.* 26, 75–91. doi: 10.1146/annurev.py.26.090188.000451

Gao, Y., Wang, B., Xu, Z., Li, M., Song, Z., Li, W. Z., et al. (2015). Tobacco serine/threonine protein kinase gene NrSTK enhances black shank resistance. *Genet. Mol. Res.* 14, 16415. doi: 10.4238/2015.December.9.11

Ghodhbane-Gtari, F., Essoussi, I., Chattaoui, M., Chouaia, B., Jaouani, A., Daffonchio, D., et al. (2010). Isolation and characterization of non-frankia actinobacteria from root nodules of *Alnus glutinosa*, *Casuarina glauca* and *Elaeagnus angustifolia*. *Symbiosis* 50, 51–57. doi: 10.1007/s13199-009-0029-7

Gómez-Gómez, L., and Boller, T. (2002). Flagellin perception: a paradigm for innate immunity. *Trends Plant Sci.* 7, 251–256. doi: 10.1016/S1360-1385(02)02261-6

Gu, Y., Liu, Y., Li, J., Cao, M., Wang, Z., Li, J., et al. (2022). Mechanism of intermittent deep tillage and different depths improving crop growth from the perspective of rhizosphere soil nutrients, root system architectures, bacterial communities, and functional profiles. *Front. Microbiol.* 12. doi: 10.3389/fmicb.2021.759374

Gulati, S., Ballhausen, M., Kulkarni, P., Grosch, R., and Garbeva, P. (2020). A non-invasive soil-based setup to study tomato root volatiles released by healthy and infected roots. *Sci. Rep.* 10, 12704. doi: 10.1038/s41598-020-69468-z

Han, T., You, C., Zhang, L., Feng, C., Zhang, C., Wang, J., et al. (2016). Biocontrol potential of antagonist bacillus subtilis Tpb55 against tobacco black shank. *BioControl* 61, 195–205. doi: 10.1007/s10526-015-9705-0

Horst, R. K. (1990). Plant diseases and their pathogens. In: *Westcott's Plant Disease Handbook*. (Boston, MA: Springer). doi: 10.1007/978-1-4615-8143-7_4

Howell, C. R. (2003). Mechanisms employed by *Trichoderma* species in the biological control of plant diseases: the history and evolution of current concepts. *Plant Dis.* 87, 4–10. doi: 10.1094/PDIS.2003.87.1.4

Jin, J., and Shew, H. D. (2021). Components of aggressiveness in *Phytophthora nicotianae* during adaptation to multiple sources of partial resistance in tobacco. *Plant Dis.* 105, 1960–1966. doi: 10.1094/PDIS-09-20-1929-RE

Jonasson, S., Michelsen, A., Schmidt, I. K., and Nielsen, E. V. (1999). Responses in microbes and plants to changed temperature, nutrient, and light regimes in the arctic. *Ecology* 80, 1828. doi: 10.2307/176661

Jose, P. A., Maharshi, A., and Jha, B. (2021). Actinobacteria in natural products research: progress and prospects. *Microbiological Res.* 246, 126708. doi: 10.1016/j.micres.2021.126708

Keen, N. T., Bent, A., and Staskawicz, B. (1993). Plant disease resistance genes: interactions with pathogens and their improved utilization to control plant diseases. *Discrete Appl. Mathematics* 157, 341–352. doi: 10.1007/978-3-540-77120-3_31

Kim, B., Park, A. R., Song, C. W., Song, H., and Kim, J. (2022). Biological control efficacy and action mechanism of *Klebsiella pneumoniae* JCK-2201 producing meso-2,3-Butanediol against tomato bacterial wilt. *Front. Microbiol.* 13. doi: 10.3389/fmicb.2022.914589

Kumar, S., Stecher, G., Li, M., Knyaz, C., and Tamura, K. (2018). MEGA X: molecular evolutionary genetics analysis across computing platforms. *Mol. Biol. Evol.* 35, 1547–1549. doi: 10.1093/molbev/msy096

Kwak, M., Kong, H. G., Choi, K., Kwon, S., Song, J. Y., Lee, J., et al. (2018). Rhizosphere microbiome structure alters to enable wilt resistance in tomato. *Nat. Biotechnol.* 36, 1100–1109. doi: 10.1038/nbt.4232

Kyselková, M., Kopecký, J., Frapolli, M., Défago, G., Ságovámarecková, M., Grundmann, G. L., et al. (2009). Comparison of rhizobacterial community composition in soil suppressive or conducive to tobacco black root rot disease. *Isme J.* 3, 1127–1138. doi: 10.1038/ismej.2009.61

Langille, M. G. I., Zaneveld, J., Caporaso, J. G., Mcdonald, D., Knights, D., Joshua, R., et al. (2013). Predictive functional profiling of microbial communities using 16S rRNA marker gene sequences. *Nat. Biotechnol.* 31, 814–821. doi: 10.1038/nbt.2676

Liu, C. H., Chen, X., Liu, T. T., Lian, B., Gu, Y., Caer, V., et al. (2007). Study of the antifungal activity of *Acinetobacter baumannii* LCH001 *in vitro* and identification of its antifungal components. *Appl. Microbiol. Biotechnol.* 76, 459–466. doi: 10.1007/s00253-007-1010-0

Liu, T., Xiao, Y., Yin, J., Yi, T., Zhou, Z., Hsiang, T., et al. (2020). Effects of cultured root and soil microbial communities on the disease of nicotiana tabacum caused by *Phytophthora nicotianae*. *Front. Microbiol.* 11. doi: 10.3389/fmicb.2020.00929

Liu, W., Zhao, Q., Zhang, Z., Li, Y., Xu, N., Qu, Q., et al. (2020). Enantioselective effects of imazethapyr on arabidopsis thaliana root exudates and rhizosphere microbes. *Sci. Total Environ.* 716, 137121. doi: 10.1016/j.scitotenv.2020.137121

Ma, L., Zhang, H., Zhou, X., Yang, C., Zheng, S., Duo, J. L., et al. (2018). Biological control tobacco bacterial wilt and black shank and root colonization by bio-organic fertilizer containing bacterium *Pseudomonas aeruginosa* NXHG29. *Appl. Soil Ecol.* 129, 136–144. doi: 10.1016/j.apsoil.2018.05.011

Mahajan, G. B., and Balachandran, L. (2012). Antibacterial agents from actinomycetes - a review. *Front. Bioscience* 4 (1), 240–53. doi: 10.2741/373

Maurel, C., Leblanc, N., Barbier-Brygoo, H., Perrot-Rechenmann, C., Bouvier-Durand, M., and Guern, J. (1994). Alterations of auxin perception in rolB-transformed tobacco protoplasts (Time course of rolB mRNA expression and increase in auxin sensitivity reveal multiple control by auxin). *Plant Physiol.* 105, 1209–1215. doi: 10.1104/pp.105.4.1209

Mengesha, W. K., Powell, S. M., Evans, K. J., and Barry, K. M. (2017). Diverse microbial communities in non-aerated compost teas suppress bacterial wilt. *World J. Microbiol. Biotechnol.* 33 (3), 49. doi: 10.1007/s11274-017-2212-y

Miliute, I., Buzaite, O., Baniulis, D., and Stanys, V. (2015). Bacterial endophytes in agricultural crops and their role in stress tolerance: a review. *Zemdirbyste-Agriculture* 102, 465–478. doi: 10.13080/z-a.2015.102.060

Niu, J., Chao, J., Xiao, Y., Chen, W., Zhang, C., Liu, X., et al. (2017). Insight into the effects of different cropping systems on soil bacterial community and tobacco bacterial wilt rate. *J. Basic Microbiol.* 57, 3–11. doi: 10.1002/jobm.201600222

Ojiambo, P. S., and Scherm, (2006). Biological and application-oriented factors influencing plant disease suppression by biological control: a meta-analytical review. *Phytopathology*. 96 (11), 1168–1174. doi: 10.1094/PHYTO-96-1168

Rasmussen, P. U., Bennett, A. E., and Tack, A. J. M. (2019). The impact of elevated temperature and drought on the ecology and evolution of plant–soil microbe interactions. *J. Ecol.* 108, 337–352. doi: 10.1111/1365-2745.13292

Ren, X., Wang, J., Zhu, F., Wang, Z., Mei, J., Xie, Y., et al. (2022). β-aminobutyric acid (BABA)-induced resistance to tobacco black shank in tobacco (*Nicotiana tabacum* l.). *PloS One* 17, e267960. doi: 10.1371/journal.pone.0267960

Schreiter, S., Babin, D., Smalla, K., and Grosch, R. (2018). Rhizosphere competence and biocontrol effect of *Pseudomonas* sp. RU47 independent from plant species and soil type at the field scale. *Front. Microbiol.* 9. doi: 10.3389/fmicb.2018.00097

Shanks, R. M. Q., Dashiff, A., Alster, J. S., and Kadouri, D. E. (2012). Isolation and identification of a bacteriocin with antibacterial and antibiofilm activity from *Citrobacter freundii*. *Arch. Microbiol.* 194, 575–587. doi: 10.1007/s00203-012-0793-2

Shen, M., Shi, Y., Bo, G., and Liu, X. (2022). Fungal inhibition of agricultural soil pathogen stimulated by nitrogen-reducing fertilization. *Front. Bioengineering Biotechnol.* 10. doi: 10.3389/fbioe.2022.866419

Sheng, X. F., Jiang, C. Y., and He, L. Y. (2008). Characterization of plant growth-promoting *Bacillus edaphicus* NBT and its effect on lead uptake by Indian mustard in a lead-amended soil. *Can. J. Microbiol.* 54, 417–422. doi: 10.1139/W08-020

Shi, H., Xu, P., Wu, S., Yu, W., Cheng, Y., Chen, Z., et al. (2022). Analysis of rhizosphere bacterial communities of tobacco resistant and non-resistant to bacterial wilt in different regions. *Sci. Rep.* 12, 18309. doi: 10.1038/s41598-022-20293-6

Stumbriene, K., Gudiukaite, R., Semaskiene, R., Svegzda, P., Jonaviciene, A., and Suproniene, S. (2018). Screening of new bacterial isolates with antifungal activity and application of selected bacillus sp. cultures for biocontrol of *Fusarium graminearum* under field conditions. *Crop Prot.* 113, 22–28. doi: 10.1016/j.cropro.2018.07.006

Tan, L., Zeng, W., Xiao, Y., Li, P., Gu, S., Wu, S., et al. (2021). Fungi-bacteria associations in wilt diseased rhizosphere and endosphere by interdomain ecological network analysis. *Front. Microbiol.* 12. doi: 10.3389/fmicb.2021.722626

Tilman, D., and Downing, J. A. (1994). Biodiversity and stability in grasslands. *Nature* 367, 363–365. doi: 10.1038/367363a0

Tilman, D., Knops, J., Wedin, D., Reich, P., Ritchie, M., and Siemann, E. (1997). The influence of functional diversity and composition on ecosystem processes. *Sci. (American Assoc. Advancement Science)* 277, 1300–1302. doi: 10.1126/science.277.5330.1300

Trujillo, M. E., Riesco, R., Benito, P., and Carro, L. (2015). Endophytic actinobacteria and the interaction of micromonospora and nitrogen fixing plants. *Front. Microbiol.* 6. doi: 10.3389/fmicb.2015.01341

Ventura, M., Canchaya, C., Tauch, A., Chandra, G., Fitzgerald, G. F., Chater, K. F., et al. (2007). Genomics of actinobacteria: tracing the evolutionary history of an ancient phylum. *Microbiol. Mol. Biol. Rev.* 71, 495–548. doi: 10.1128/MMBR.00005-07

Wagg, C., Bender, S. F., Widmer, F., and van der Heijden, M. G. A. (2014). Soil biodiversity and soil community composition determine ecosystem multifunctionality. *Proc. Natl. Acad. Sci.* 111, 5266–5270. doi: 10.1073/pnas.1320054111

Wang, K. L. C., Li, H., and Ecker, J. R. (2002). Ethylene biosynthesis and signaling networks. *Plant Cell* 14, S131–S151. doi: 10.1105/tpc.001768

Wang, Y., Zhao, A., Morcillo, R. J. L., Yu, G., Xue, H., Rufian, J. S., et al. (2021). A bacterial effector protein uncovers a plant metabolic pathway involved in tolerance to bacterial wilt disease. *Mol. Plant* 14, 1281–1296. doi: 10.1016/j.molp.2021.04.014

Xiao, Y., Liu, X., Meng, D., Tao, J., Gu, Y., Yin, H., et al. (2018). The role of soil bacterial community during winter fallow period in the incidence of tobacco bacterial wilt disease. *Appl. Microbiol. Biotechnol.* 102, 2399–2412. doi: 10.1007/s00253-018-8757-3

Yacine, G., Omrane, T., Amine, Y., Nasserdine, S., Florence, M., and Abdelghani, Z. (2014). Biocontrol of *Rhizoctonia solani* damping-off and promotion of tomato plant growth by endophytic actinomycetes isolated from native plants of Algerian Sahara. *Microbiological Res.* 169 (1), 59–65. doi: 0.1016/j.micres.2013.06.014

Yadav, K. K. (2021). Actinobacteria interventions in plant and environment fitness. Microbiomes and plant health. In: M. K. Solanki, P. L. Kashyap and B. Kumari (Eds.), *Panoply and their Applications*. Academic Press, pp. 397–427. doi: 10.1016/B978-0-12-819715-8.00014-8

Yang, H., Li, J., Xiao, Y., Gu, Y., Liu, H., Liang, Y., et al. (2017). An integrated insight into the relationship between soil microbial community and tobacco bacterial wilt disease. *Front. Microbiol.* 8. doi: 10.3389/fmicb.2017.02179

Yao, J., Carter, R. A., Vuagniaux, G., Barbier, M., Rosch, J. W., Rock, C. O., et al. (2016). A pathogen-selective antibiotic minimizes disturbance to the microbiome. *Antimicrob. Agents Chemother.* 60, 4264–4273. doi: 10.1128/AAC.00535-16

Yin, H., Niu, J., Ren, Y., Cong, J., Zhang, X., Fan, F., et al. (2015). An integrated insight into the response of sedimentary microbial communities to heavy metal contamination. *Sci. Rep.* 5, 93–102. doi: 10.1038/srep14266

Yin, J., Zhang, Z., Guo, Y., Chen, Y., Xu, Y., Chen, W., et al. (2022). Precision probiotics in agroecosystems: multiple strategies of native soil microbiotas for conquering the competitor *Ralstonia solanacearum*. *MSystems* 7 (3), e01159–21. doi: 10.1128/msystems.01159-21

Zhang, S., Liu, X., Zhou, L., Deng, L., Zhao, W., Liu, Y., et al. (2022). Alleviating soil acidification could increase disease suppression of bacterial wilt by recruiting potentially beneficial rhizobacteria. *Microbiol. Spectr.* 10 (2), e02333-21. doi: 10.1128/spectrum.02333-21

Zheng, Y., Han, X., Zhao, D., Wei, K., Yuan, Y., Li, Y., et al. (2021). Exploring biocontrol agents from microbial keystone taxa associated to suppressive soil: a new attempt for a biocontrol strategy. *Front. Plant Sci.* 12. doi: 10.3389/fpls.2021.655673

frontiers | Frontiers in Plant Science

TYPE Original Research
PUBLISHED 21 June 2023
DOI 10.3389/fpls.2023.1109467

OPEN ACCESS

EDITED BY
Mengting Maggie Yuan,
University of California, Berkeley,
United States

REVIEWED BY
Jianjun Yang,
Chinese Academy of Agricultural Sciences (CAAS), China
Anne Kakouridis,
Sound Agriculture, Emeryville, CA,
United State

*CORRESPONDENCE
Klaudia Debiec-Andrzejewska
klaudia.debiec@uw.edu.pl

RECEIVED 27 November 2022
ACCEPTED 26 May 2023
PUBLISHED 21 June 2023

CITATION
Zakrzewska M, Rzepa G, Musialowski M, Goszcz A, Stasiuk R and Debiec-Andrzejewska K (2023) Reduction of bioavailability and phytotoxicity effect of cadmium in soil by microbial-induced carbonate precipitation using metabolites of ureolytic bacterium *Ochrobactrum* sp. POC9. *Front. Plant Sci.* 14:1109467. doi: 10.3389/fpls.2023.1109467

Reduction of bioavailability and phytotoxicity effect of cadmium in soil by microbial-induced carbonate precipitation using metabolites of ureolytic bacterium *Ochrobactrum* sp. POC9

Marta Zakrzewska[1], Grzegorz Rzepa[2], Marcin Musialowski[3], Aleksandra Goszcz[3,4], Robert Stasiuk[3] and Klaudia Debiec-Andrzejewska[3]*

[1]Department of Environmental Microbiology and Biotechnology, Institute of Microbiology, Faculty of Biology, University of Warsaw, Warsaw, Poland, [2]Department of Mineralogy, Petrography and Geochemistry, Faculty of Geology, Geophysics and Environmental Protection, AGH University of Science and Technology, Krakow, Poland, [3]Department of Geomicrobiology, Institute of Microbiology, Faculty of Biology, University of Warsaw, Warsaw, Poland, [4]Department of Ecotoxicology, Institute of Environmental Biology, Faculty of Biology, University of Warsaw, Warsaw, Poland

The application of ureolytic bacteria for bioremediation of soil contaminated with heavy metals, including cadmium (Cd), allows for the efficient immobilization of heavy metals by precipitation or coprecipitation with carbonates. Microbially-induced carbonate precipitation process may be useful also in the case of the cultivation of crop plants in various agricultural soils with trace but legally permissible Cd concentrations, which may be still uptaken by plants. This study aimed to investigate the influence of soil supplementation with metabolites containing carbonates (MCC) produced by the ureolytic bacterium *Ochrobactrum* sp. POC9 on the Cd mobility in the soil as well as on the Cd uptake efficiency and general condition of crop plants (*Petroselinum crispum)*. In the frame of the conducted studies (i) carbonate productivity of the POC9 strain, (ii) the efficiency of Cd immobilization in soil supplemented with MCC, (iii) crystallization of cadmium carbonate in the soil enriched with MCC, (iv) the effect of MCC on the physico-chemical and microbiological properties of soil, and (v) the effect of changes in soil properties on the morphology, growth rate, and Cd-uptake efficiency of crop plants were investigated. The experiments were conducted in soil contaminated with a low concentration of Cd to simulate the natural environmental conditions. Soil supplementation with MCC significantly reduced the bioavailability of Cd in soil with regard to control variants by about 27-65% (depending on the volume of MCC) and reduced the Cd uptake by plants by about 86% and 74% in shoots and roots, respectively. Furthermore, due to the decrease in soil toxicity and improvement of soil nutrition with other metabolites produced during the urea degradation (MCC), some microbiological properties of soil (quantity and activity of soil

microorganisms), as well as the general condition of plants, were also significantly improved. Soil supplementation with MCC enabled efficient Cd stabilization and significantly reduced its toxicity for soil microbiota and plants. Thus, MCC produced by POC9 strain may be used not only as an effective Cd immobilizer in soil but also as a microbe and plant stimulators.

KEYWORDS

heavy metals immobilization, ureolytic bacteria, crop plants protection, plants growth promoting bacteria, agricultural soil treatment, remediation in situ

1 Introduction

Cadmium (Cd) is considered a highly toxic and hazardous element due to its damaging properties on proteins' and nucleic acids' structure (Lee et al., 2012; Balali-Mood et al., 2021), high bioavailability (Godt et al., 2006; Tran and Popova, 2013) and cancerogenic properties (Lunn et al., 2022). The main routes of human exposure to Cd are smoking and consuming certain crop plants grown in Cd-contaminated soil (Satarug and Moore, 2004; Chaney, 2012; European Food Safety Authority, 2012). The elevated concentration of Cd is more and more frequently observed in agricultural soil (Tran and Popova, 2013) as a result of anthropological activities, e.g. using of sludge and phosphate fertilizers (e.g. superphosphates), which may contain up to 10 mg/kg Cd (Satarug et al., 2003).

According to the current guidelines of the United Nations Economic Commission for Europe, the total concentration of Cd in agricultural soil should not exceed 0.9 mg/kg (de Vries et al., 2003) but the maximum permissible concentration (MPC) for Cd in soil, crop plants and other food types should be set at the lowest possible level (Satarug et al., 2017). Even at trace concentrations, plants can successfully uptake Cd from the soil, often without any visible phytotoxic effects (Benavides et al., 2005). Cadmium phytoextraction rate may be increased by certain environmental conditions, e.g. long periods of drought (Tudoreanu and Phillips, 2004; Henry et al., 2007; Bashir et al., 2019). Drought stress triggers plant roots' exudation of compounds that not only secure the soil against further water loss (Williams and de Vries, 2020), but also enhance nutrition (Kohli et al., 2012). Secretion of organic acids (e.g. citric, malic, tartaric, oxalic, phenolic) causes local soil acidification, increasing mobility not only of nutrients but also hazardous elements, e.g. Cd, which are more effectively absorbed by plants (Fageria et al., 2002; Tudoreanu and Phillips, 2004; Bashir et al., 2019).

The commonly known remediation methods dedicated to soils contaminated with Cd are often unsuitable for agricultural soils for many reasons (Megharaj and Naidu, 2017) since they significantly change soil physical, chemical, and (micro)biological quality (Dhaliwal et al., 2020). While in the case of post-industrial soils, it is not of great importance, in the case of agricultural soils, changing even one of the above-mentioned parameters may exclude the soil from agricultural use for many years (Dhaliwal et al., 2020). Thus, the treatment of Cd-contaminated agricultural soil should be provided with the use of an effective, highly selective, and environmentally friendly remediation method that does not change the natural soil properties (Hou et al., 2020). An additional benefit of the method could be the improvement of plant nutrition and microbiological fitness of the soil.

Soil bioconsolidation based on microbial-induced carbonate precipitation (MICP) leads to the immobilization of heavy metals, including Cd, in the form of carbonate salts (Liu et al., 2021). MICP is based on the microbiological urea hydrolysis reaction (through the urea decomposition produces ammonia and carbonate ions) and may contribute to the reduction of bioavailable forms of heavy metals in soil (Wang et al., 2019a). MICP is generally regarded as an efficient, environmentally safe, and highly selective method (Rajasekar et al., 2021) and thus it seems to be very promising in the remediation of agricultural soil. Furthermore, in contrast to other remediation methods e.g. surface capping (Li et al., 2019), encapsulation (Khan et al., 2004), or soil-washing (Hashim et al., 2011), MICP may be used for soil treatment even in trace concentrations of contaminants. The high effectiveness of the MICP process has been already verified in the efficient immobilization of copper, arsenic, cadmium, lead and zinc from contaminated soils (Achal et al., 2011; Achal et al., 2012a; Achal et al., 2012b; Kumari et al., 2014; Liu et al., 2021).

The MICP process may contribute not only to the immobilization of Cd and other heavy metals in soil (Kang et al., 2014b) but also, by the use of an appropriate bacterial strain and a proper methodology of soil supplementation, may potentially also stimulate soil microbiota and improve the nutrition of crop plants. Among the metabolites co-produced during the urea decomposition (and simultaneous carbonates production) is not only ammonia (Liu et al., 2021), which is the most easily digestible source of nitrogen for soil microorganisms and plants (Robertson and Groffman, 2015), but also various types of secondary metabolites, such as organic acids, ligands, alcohols, short-chain peptides, and unsaturated fatty acids (Yang et al., 2021) that may enrich the agricultural soil with additional nutrients. Thus, the MICP method with the use of MCC may have a potentially triple beneficial effect on plants growth and development, not only by reducing Cd toxicity and additional nutrition but also by the improvement of the general condition of soil microbiota, eg. quantity and activity. Due to the controlled production of MCC

and its reproducibility, the use of metabolites could be superior to inoculation with urea-degrading microorganisms for bioremediation purposes. Since microbial ureolytic activity in soil is influenced by various factors, the outcome of microorganisms' introduction is difficult to predict (Zhao et al., 2022).

The main aim of the study was to verify the hypothesis about soil microbiota stimulation and crop plants (root parsley) growth promotion by the utilization of the MICP method based on soil supplementation with MCC. The experiments were performed with the use of model crop plants cultivated in agricultural soil contaminated with low concentrations of Cd, which was supplemented with MCC produced by the ureolytic and metabolically versatile bacterium *Ochrobactrum* sp. POC9, isolated from sewage sludge. The ability of the POC9 strain to the production of various potentially beneficial secondary metabolites has been already described in our previous study (Yang et al., 2021). In this study, detailed research aimed at (i) the optimization of carbonate production by *Ochrobactrum* POC9, (ii) the selection of the method for supplementation of Cd-contaminated soil with POC9 metabolites to obtain effective Cd immobilization, (iii) the confirmation of the presence of cadmium carbonate in soil, and (iv) verification of the impact of soil enrichment with POC9 metabolites on the Cd bioavailability, quantity and activity of soil microbes, general condition of plants and the efficiency of Cd uptake by plants were performed. The presented study was realized in the context of the development of an effective method of remediation and nutrition of soils, contaminated with trace concentration of Cd, useful for agricultural purposes.

2 Materials and methods

2.1 Characteristics of the *Ochrobactrum* sp. POC9 and optimization of its carbonate productivity

As an efficient carbonate producer, the ureolytic bacterium *Ochrobactrum* sp. POC9 was applied. POC9 strain was isolated from raw sewage sludge samples collected from the wastewater treatment plant "Czajka" (Warsaw, Poland). Genomic and physiological characteristics of the *Ochrobactrum* sp. POC9 in the context of sewage sludge utilization (Poszytek et al., 2018) and enhancing biogas production (Poszytek et al., 2019) were previously described. Furthermore, the possibility of utilizing the ureolytic activity of POC9 for the treatment of acidic leachates (Yang et al., 2020) and stimulating the activity of sulfates-reducing bacteria (Yang et al., 2021) was also verified. In our previous paper, the composition of MCC produced on a medium containing urea was also analyzed. Among identified metabolites (alcohols, organic acids, unsaturated hydrocarbons as well as nitrogen and sulfur-containing organic compounds), no organic compounds with Cd immobilizing properties were found (Yang et al., 2020).

The inoculum of the POC9 strain was used for various experiments described in this paper. It was prepared by routine overnight cultivation of the strain in lysogeny broth (LB) medium at room temperature, to reach the appropriate initial optical density (OD) measured spectrophotometrically at wavelength 600 nm (OD_{600nm} >1). Then, the inoculum was used for inoculation of various microbial media containing urea. Bacterial cultures in media with urea were carried out for 72 hours, with shaking 150 rpm, in 100 ml final volume of the medium. Urea-containing media was enriched with sodium chloride (5 g/l), phosphate salt (KH_2PO_4 2 g/l) and peptone (1 g/l) (Christensen, 1946; Yang et al., 2020).

The effect of various physical, chemical and microbiological factors on the carbonate productivity of *Ochrobactrum* sp. POC9 in batch cultures was investigated. The carbonate production efficiency depending on the (i) urea concentration (0.5, 1, 2 and 5%), (ii) pH of the medium (5, 5.5, 6, 6.8 and 7.5), (iii) temperature of the culture (22, 30 and 37 °C) and (iv) initial quantity of microorganisms (optical density - OD_{600nm}: 0.01; 0.03; 0.06; 0.08; 0.1) was determined. The pH of the media was adjusted as needed with 0.1M HCl or NaOH. Uninoculated media were used as chemical controls. All batch cultures were performed in triplicates. During the batch culture cultivation, the concentration of carbonate was monitored at the end of the experiments (after 72 hours) using Nanocolor® kits (Macherey-Nagel, Germany) according to the instructions given by the manufacturer. As a result of these experiments various compositions of metabolites containing carbonates (MCC) were obtained.

2.2 Physico-chemical and microbiological characteristics of Cd-contaminated soil

Commercially available, potted garden soil (fractions< 2 mm) was used in the experiments. The soil was artificially contaminated with Cd in concentration reflecting the natural, environmental conditions in agricultural soil. An aqueous cadmium chloride solution ($CdCl_2$*$2H_2O$) was added to the air-dry soil to achieve a final Cd concentration of 2 mg/kg of dry-weight soil. Then, the soil was thoroughly mixed to homogenize its entire volume. The soil was incubated at room temperature under a cover and systematically watered with distilled water to maintain a constant humidity of about 50%. Additionally, to further soil homogenization and maintain humidity, the soil was thoroughly mixed every 3 days. Soil conditioning with Cd was carried out for 30 days.

Basic physico-chemical and microbiological parameters of Cd-contaminated soil were determined. The elemental contents of carbon, nitrogen, and sulfur, the total solids, volatile solids, pH, bulk density and porosity of the soil as well as microbiological parameters in the form of heterotrophic bacteria and fungi quantity and dehydrogenase activity of soil microbes were presented in Table 1.

Elementary CHNS analysis was performed by Elemental Analyzer EA1112 (Thermo Finnigan). Total solids were determined by drying the soil sample at 50°C until constant weight. Volatile solids were determined by the thermal treatment of the dried soil sample at 550°C for 6 hours. pH was measured in water by pH-meter (Mettler Toledo F-20, Switzerland) with a compatible pH electrode (LE438). Bulk density was calculated on the basis of the ratio of solid soil weight to total soil volume. Soil

TABLE 1 Physico-chemical and microbiological characterization of soil contaminated with Cd, including percentage concentration of carbon, nitrogen, and sulfur, total solids [TS], volatile solids [VS], pH, bulk density, soil porosity, the quantity of heterotrophic microorganisms and activity of dehydrogenase in soil.

Parameters	Units	Values
C	% [v/w]	55.03
N	% [v/w]	13.00
S	% [v/w]	0.66
TS	% fresh mass	52.60
VS	% total solids	13.91
pH	–	5.30
Bulk density	g/cm^3	0.48
Soil porosity	%	34.29
Quantity of heterotrophic microorganisms	CFU/ml	$1.32*10^8$
Dehydrogenase activity	INTF $h^{-1}g^{-1}$	11.581

porosity was determined based on the specific density and bulk density of the soil.

The quantity of heterotrophic (facultatively or obligatorily) aerobic and cultivable microorganisms (bacteria and fungi) in the soil was determined using the method of plating soil extracts on plates with unselective LB Agar medium. To prepare soil extracts, 5 g of fresh soil was placed in sterile flasks, and then 45 ml of 0.85% NaCl solution was added. The samples were shaken (150 rpm) overnight at room temperature. Then, serial dilutions from the obtained inoculum were prepared and plated per 100 µl on plates. The dishes were incubated at room temperature for 96 hours and then grown colonies were counted. The results were averaged and presented as values in CFU/ml (as colony-forming units per 1 milliliter). The dehydrogenase activity of soil microbes (bacteria, fungi and others) was determined according to the method described by von Mersi and Schinner (1991). All analyses were performed in triplicates.

2.3 Optimization of the soil supplementation with MCC

In the frame of the preliminary studies, before soil supplementation with MCC, the process of cadmium precipitation in solution enriched with MCC was investigated. Detailed experimental methodology and results of obtained precipitates analysis were presented in Supplementary Materials.

Optimization of soil supplementation was performed with the use of MCC obtained in conditions selected in the frame of the experiment described in section 2.1. They were as follows: 2% urea, OD_{600nm} 0.06, pH 6.8, temperature 23°C. The obtained mixture of MCC was characterized by pH 9.1, Ec 47.6 mS, and carbonate concentration 12 770 mg/l. 200 g of Cd-contaminated soil was supplemented with MCC in the following volume ratios: 0:1 (soil without MCC supplementation), 1:1, 2:1, 3:1, 7:1, 8:1 and 10:1 w/v. The soils enriched with MCC were incubated under constant humidity (50%) and temperature conditions (22°C). The experiment was conducted for 14 days. Soil samples for physico-chemical and microbiological analysis were collected. In the frame of physico-chemical analysis, pH of the soil and the bioavailability of Cd were determined. pH and microbiological analysis of soil were determined according to the methods described in section 2.2.

2.4 Investigation of the presence of cadmium carbonate in soil

Due to the low expected concentration of Cd in the studied soil, it was impossible to apply standard analyzes of the phase composition like X-ray diffractometry. Therefore, in order to establish the forms (speciations) of Cd in the soil, Fourier-transform infrared spectroscopy (FTIR) and scanning electron microscopy (SEM) were chosen instead.

Infrared spectra were collected using Thermo Scientific Nicolet 7600 spectrometer in the range of 400–4000 cm^{-1}. The spectra reported are the resultant of 64 scans at the resolution of 1 cm^{-1}. Prior to analysis, KBr discs were obtained by homogenizing 200 mg of ground potassium bromide with 2 mg of the sample. Scanning electron microscope (SEM) analyses of powder samples were carried out in low vacuum mode, using a FEI 200 Quanta FEG microscope equipped with an EDS/EDAX spectrometer. The acceleration voltage was 15-20 kV, and the pressure 60 Pa. The samples were not coated with any conductive layer SEM and FTIR analysis were performed for Cd-contaminated soil supplemented with MCC in three selected soil:MCC ratios, 1:1, 3:1 and 7:1. Since low concentrations of Cd are undetectable by neither of these methods, soils with much higher final Cd concentrations of 50, 500, 5000 and 10000 mg/kg were used in these experiments.

2.5 Plants cultivation experimental setup

As a model of crop plants that could be potentially exposed to Cd phytotoxicity effect, root parsley (*Petroselinum crispum*) was

used. The species is representative of plants with edible hypocotyl parts which are particularly exposed to contaminants (Dghaim et al., 2015; Lizarazo et al., 2020). Furthermore, due to the direct surrounding of potential contaminants in soil, nutrients uptake by roots and relatively low translocation factor, the concentration of contaminants in underground parts of plants is usually higher than in their aboveground parts (Zare et al., 2018; Parihar et al., 2021).

Plants were cultivated in Cd-contaminated soil (2 mg kg^{-1}) enriched with MCC in a ratio 7:1 (soil:MCC). The ratio was selected based on the results of the experiment described in Section 2.3. As control variants, the soils uncontaminated and/or unsupplemented with MCC were used. Plant cultivations were performed in small pots containing 200 g of soil each. All 4 variants of the experiment (1- soil with plants, 2 - soil with MCC and plants, 3 – Cd-contaminated soil with plants, 4 - Cd-contaminated soil with MCC and plants) were carried out in 5 replicates. In every pot, five plants were grown (25 plants per experimental variant). The experiment was carried out for 14 weeks. Plant cultivation was deliberately prolonged in order to investigate the chemical stability of cadmium carbonate and observe the eventual secondary mobilization of Cd as a result of root secretion and/or soil microbiota activity. The soil and plant samples were collected at the beginning of the experiment, after 7 and/or 14 weeks.

During the plants' cultivation experiment (i) dry mass of roots and aboveground parts of plants, (ii) water content on both parts of plants, (iii) total chlorophyll concentration as well as (iv) the total Cd concentration in plants and soil were measured. Furthermore, the analysis of soil including the pH, Cd bioavailability, quantity and activity of microorganisms was performed. Total chlorophyll concentration in plant leaves was determined *in vivo* using CI-710s SpectraVue Leaf Spectrometer (CID Bio-Science, USA) with compatible software. Spectrophotometric measurements were performed after 7 and 14 weeks of the experiment on all living leaves, with 5 single measurements per leaf.

To estimate the efficiency of cadmium uptake by plants from the soil, the bioconcentration factor (BCF) was determined. These values were calculated based on the values of total Cd concentration in soil and plant according to the equation (1):

$$BCF = \frac{total\ Cd\ concentration\ in\ roots\ and\ green\ parts\ of\ plants}{total\ Cd\ concentration\ in\ soil} \quad (1)$$

2.6 Cadmium bioavailability in soil and total cadmium concentration analysis

The bioavailability of Cd in soil was determined by extraction using 100 mM $CaCl_2$ solution (Chen et al., 2018). To 1 g of the soil 5 ml of calcium chloride was added and then, samples were vigorously mixed and incubated for 4 hours. Then, soil samples were centrifuged (8000 rpm, 5 minutes) and the supernatant was filtered through laboratory paper filters (Whatman 41 Grade, 150 mm diameter). The filtered samples of the soil extracts were stabilized by the addition of 69% nitric acid in a volume ratio of 4:1 and stored at a 4°C prior to the analysis.

The total Cd concentration in soil extracts, soils and plants (roots and green parts) samples was determined with the use of Atomic Absorption Spectrometry with Graphite Furnace (GF-AAS) method applying Thermo Fisher ICE 3300 spectrometer. The digestion of soil and plant samples (about 0.3 g of soil and 0.1 g of plants) was carried out with 5 ml of a mixture of 69% HNO_3 and 30% H_2O_2 (4.5:0.5 v/w ratio) at 180°C for 30 min in a closed microwave system (Milestone Ethos Plus). Digested samples were transferred to plastic tubes and stored below 4°C prior to measurements. Cadmium standard solutions (Merck, Darmstadt, Germany) were prepared in 3% HNO_3.

2.7 Statistical analysis

Statistical analysis of the results was performed using RStudio 2022.02.2 software. The significance of the differences between experimental groups was statistically evaluated by one-way analysis of variance (ANOVA) at $p \leq 0.05$ and was represented by an asterisk under the respective group (*** - $p < 0.001$, ** - $p \leq 0.01$, * - $p \leq 0.05$, no asterisk - $p > 0.05$). The pairwise significance of the differences between experimental variants was assessed by Tukey's Honestly Significant Difference (HSD) test at $p \leq 0.05$ and indicated by letters above the bars. The results were presented on graphs obtained with ggplot2 v3.3.5 (Wickham, 2016).

3 Results

3.1 Carbonate productivity of *Ochrobactrum* sp. POC9

At first, the productivity of carbonate ions depending on the initial amount of urea was evaluated (Figure 1A). It has been noticed that the urea concentration in the medium increased the amount of CO_3^{2-} in practically direct proportion. The highest amount of carbonates was produced with the addition of 5% urea (av.16168,33 mg/l), followed by the variant with 2% urea (av. 12371 mg/l). Next in order were variants with 1% urea (av. 9641 mg/l), and the least with 0,5% urea (av. 5458 mg/l). The most divergent (between replicates) results occurred in the version with 1% urea.

The effect of initial pH on carbonate production was also investigated (Figure 1B). It has been noted that out of the 5 investigated variants, three in the middle showed the highest carbonate concentrations. The highest concentration of carbonate occurred at pH 5.5 (av. 12638 mg/l) and 6 (av. 11827 mg/l). However, these results were less reproducible in comparison to the variants with an initial pH of 6.8 (av. 11135 mg/l). The result of the variant with the most alkaline pH was almost two times lower (av. 6645 mg/l) than the previous one.

No significant differences in carbonate productivity were observed among the variants at various temperatures (Figure 1C). The lowest concentration of carbonates occurred in cultures incubated at 30°C (av. 8010 mg/l). In the variant with incubation at room temperature slightly higher productivity (av. 8959 mg/l) than the previous one was found. Although the highest carbonate productivity was detected in microbial

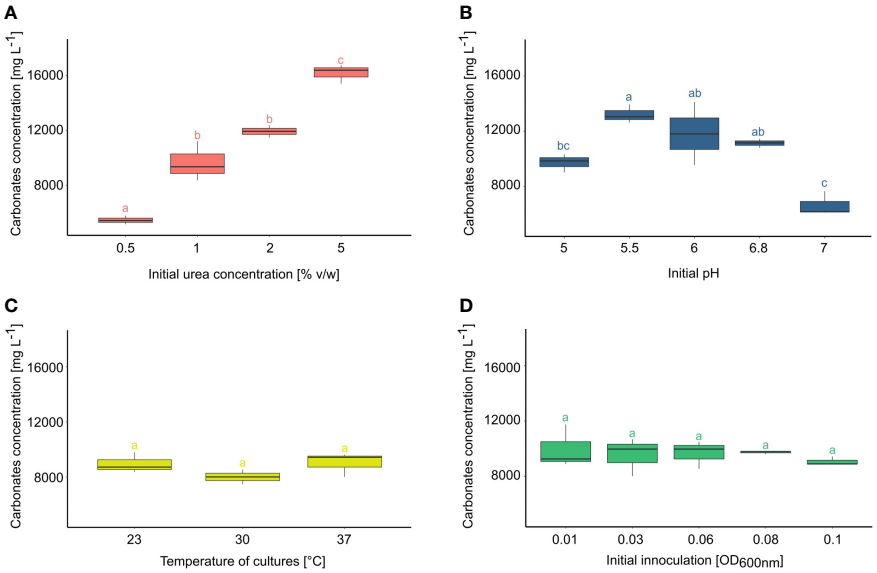

FIGURE 1
Carbonate productivity of *Ochrobactrum* sp. POC9 under the influence of various initial urea concentrations **(A)**, pH **(B)**, temperature **(C)**, and initial quantity of microorganisms **(D)**. Statistical analysis: Tukey HSD test (letters above the bars, $p \leq 0.05$).

cultures incubated at 37 °C (av. 9018 mg/l), the observed differences were statistically insignificant.

The effect of the initial inoculation ratio on carbonate production efficiency was also evaluated (Figure 1D). Changes in initial optical density, related to the quantity of microorganisms, did not show notable differences in carbonate contents in microbial cultures. A variant with an initial OD_{600nm} 0.01 occurred as the one with the most uneven results. The repeatability improved with higher initial OD values. From initial OD_{600nm} 0.08, carbonate productivity seemed to be lower.

3.2 FTIR and SEM-EDS analysis of Cd compounds in the soil

FTIR spectra of contaminated soil at Cd concentrations of 50 and 500 mg/kg did not virtually differ from the spectrum of non-contaminated soil. Therefore, additional analyzes of Cd-contaminated soils with cadmium at concentrations of 10,000 mg/kg were performed. Even at these high cadmium levels all the spectra were very similar (Figure 2). However, the spectra of Cd-contaminated soil revealed an additional weak band at ca. 875 cm^{-1} which was not observed in uncontaminated soil spectrum. The feature could be attributed to out of plane bending vibrations ν_2 of carbonate (CO_3^{2-}) group, proving the presence of (secondary) carbonate in the soil.

As with FTIR analysis, the SEM observations did not reveal the presence of any separate cadmium compounds in the soils contaminated with Cd at concentrations of 50 and 500 mg/kg. Again, additional observations and analyzes were then carried out on highly contaminated soils (5000 and 10,000 mg/kg). It has been found that cadmium was apparently dispersed within organic matter, but was also incorporated, in significantly variable amounts, in inorganic compounds. Among the latter, calcium carbonate seemed to be the most common. At lower cadmium loads and/or at lower MCC/soil ratios small (up to a few micrometers in size) crystals of almost pure calcium carbonate have been encountered (Figures 3A, B). They showed only traces of Cd since the Cd/Ca molar ratios calculated on the basis of semi-quantitative EDS analyses are usually below 0.02–0.03. In the soil contaminated with Cd at the highest level (i.e. 10,000 mg/kg), especially at higher MCC/soil ratios, another type of carbonate accumulation has been found as well (Figures 3C–E). These consisted of very small, often elongated crystallites forming isometric, quasispherical or fan-like aggregates with a diameter not exceeding approximately 5–6 micrometers. Much higher concentrations of cadmium have been found in their chemical

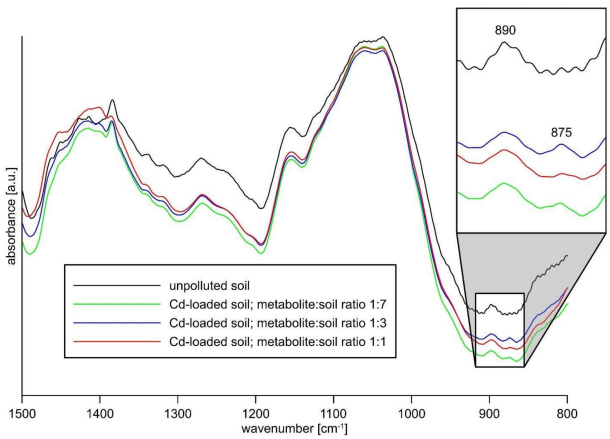

FIGURE 2
FTIR spectra of uncontaminated and Cd-contaminated (10,000 mg/kg) soil.

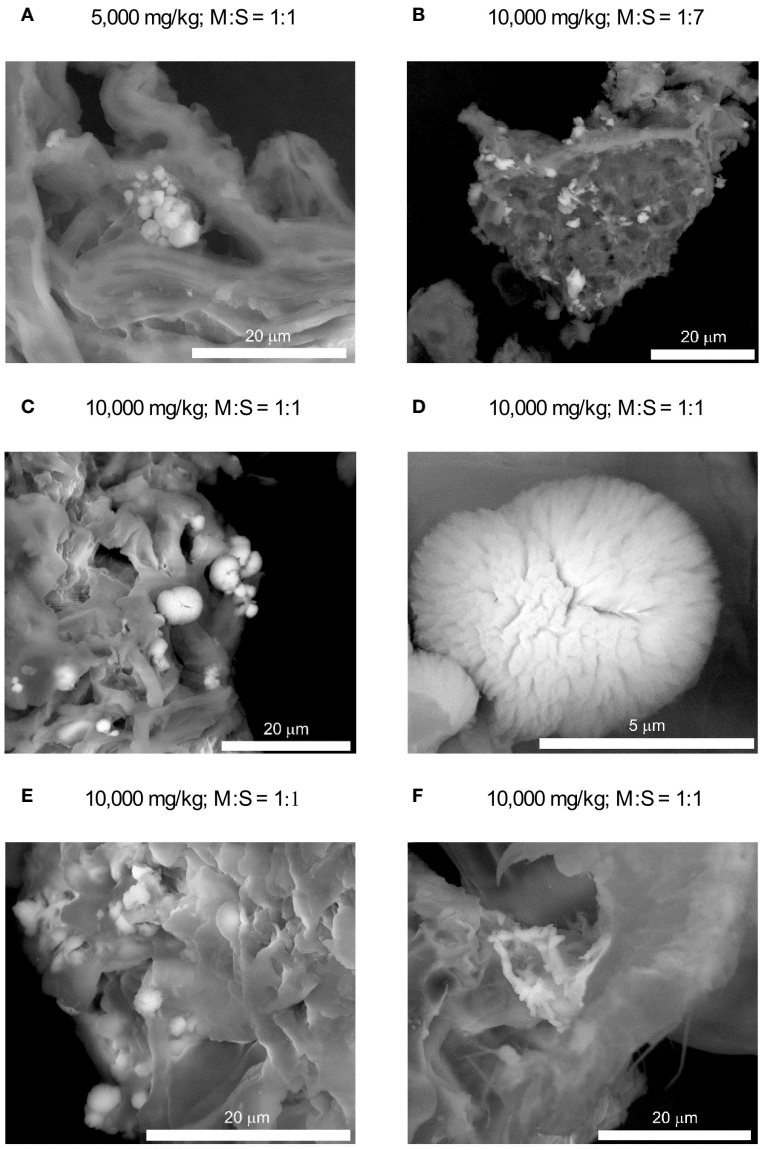

FIGURE 3
SEM images of inorganic Cd carriers in the soil (brighter crystallites). **(A, B)** – low-Cd carbonates; **(C–E)** – high-Cd carbonates, **(F)** – phosphates. M:S denotes metabolite–soil ratio.

composition, as the Cd/Ca molar ratios range between 0.2 and 0.8. They usually also contain phosphate admixtures. Another inorganic cadmium carriers were apparently apatite-type calcium phosphates (Figure 3F). Cadmium concentrations in the phosphates are, however, rather low – Cd/Ca molar ratios did not usually exceed 0.05.

3.3 The effect of MCC on the pH and Cd mobility in soil

The soil supplementation with MCC contributed to the significant reduction of the Cd mobility (Figure 4A). The higher volume of MCC supplemented to the soil, the higher degree of Cd immobilization was observed. The most effective Cd immobilization was shown for the highest soil supplementation with MCC, in a ratio of 1:1. The level of Cd mobility in this experimental variant decreased by about 65% with regard to the control variant (0:1). A similar degree of Cd immobilization in soil was observed in the cases of ratios 2:1 and 3:1. For the 7:1 and 10:1 ratios, Cd mobility was reduced by about 51% and 29%, respectively compared to the control variant. Cadmium mobility reduction was also observed in variants with soil supplementation with urea medium used for bacteria cultivation. Furthermore, in these experimental variants, a similar correlation was found as in soil supplemented with MCC- the higher volume of medium the higher degree of Cd immobilization. In the soil supplemented with bacterial medium, the efficiency of Cd immobilization was significantly lower compared with soil enriched with MCC, regardless the soil:medium/MCC ratio. The highest Cd mobility

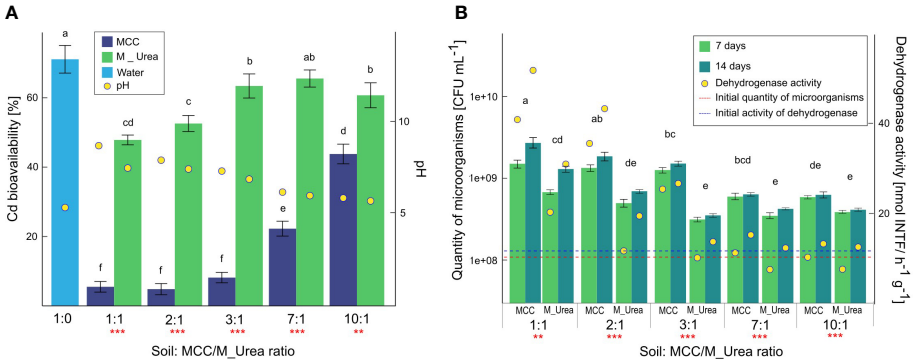

FIGURE 4
Cadmium bioavailability in soil correlated with the pH **(A)** and microbiological quantity and activity in soil **(B)** and under the influence of Cd-contaminated soil supplementation with various volumes of MCC or M_UREA after 7 and 14 days of soil incubation. Statistical analysis: ANOVA (*** - $p < 0.001$, ** - $p \leq 0.01$) and Tukey HSD test (letters above the bars, $p \leq 0.05$).

reduction in soil supplemented with the microbial medium was found in ratios 1:1 and 2:1 (ca. 22% and 19%, respectively, compared to the control variant). For ratios 3:1, 7:1 and 10:1 the level of Cd mobility was similar and decreased by about 6-10% compared to the control variant.

The degree of Cd immobilization was strongly correlated with the pH of the soil solution resulting from its supplementation with MCC or microbial medium. It was shown that the higher the volume of MCC or medium in soil, the higher pH of the soil solution. In the case of the highest soil supplementation with MCC, the pH value increased from 5.30 to 8.54. For ratios 2:1, 3:1, and 7:1 pH values increased up to 7.76, 7.18, and 6.05, respectively. In the case of a ratio 10:1, the change in the pH value was insignificant and was 5.73. A stronger soil alkalization was observed in the soil enriched with MCC than in soil supplemented with the microbial medium. In soils supplemented with bacterial medium, the highest pH values were found in the case of a ratio 1:1, which was 7.34. The amplitudes of pH values in other soil:medium ratios were significantly lower with regard to soil supplementation with MCC and the pH in the ratio 10:1 was only slightly higher than in control soil.

3.4 Changes in quantity and activity of microbes in Cd-contaminated soil under the influence of MCC

The soil supplementation with MCC strongly affected the quantity and activity of soil microbiota (Figure 4B). Soil supplementation with MCC or bacterial medium (control variant) in various proportions contributed to the increase of the quantity of microorganisms. Furthermore, the increase in the quantity of microorganisms in the soil was directly proportional to the volumes of supplemented liquids (MCC or microbial medium). In the case of soil supplementation with MCC in the highest volume (1:1) the quantity of microorganisms increased by about an order of magnitude after 7 days of the experiment with regard to the beginning quantity (marked as a red line in Figure 4B). After 14 days the value increased almost twice with regard to the result obtained after 7 days, that the final quantity of microbes was $2.77*10^9$ CFU/ml. Similar correlations in the cases of 2:1 and 3:1 were observed. A lower volume of MCC also stimulated the quantity of microorganisms in the soil but the increase was lower and after 14 days of the experiment the quantities of microbes were $6.51*10^8$ CFU/ml and $3.43*10^8$ CFU/ml for 7:1 and 10:1 ratios, respectively. Thus, it was shown that even the lowest soil supplementation with MCC increased the quantity of microorganisms almost three times with regard to unsupplemented soil. The stimulation of the microbes quantity was also observed in the case of soil enrichment with bacterial medium with various volumes corresponding with MCC supplementation. Although the increase of the soil microorganisms quantity was noticeable in cases of both types of soil supplementation, the degree of biostimulation in soil enriched with the microbial medium was lower than in the case of soil supplemented with MCC by about 23-53%, depending on the soil: medium ratio.

The quantity of microorganisms directly reflected the level of the activity of microbes in the soil. This correlation was confirmed by the analysis of dehydrogenase activity in soil (Figure 4B). The highest activity of dehydrogenase was shown in soil supplemented with MCC in the highest volume (1:1). After 7 days of the experiment, this value was quadrupled and after 14 days increased fivefold with regard to the initial activity of dehydrogenase in unsupplemented soil. In cases of lower soil: MCC ratios, the increase of dehydrogenase activity was also significant but this decreased with the lower volumes of MCC supplemented to the soil. It was also shown that the longer soil incubation with MCC the more intensive stimulation of the activity of microorganisms. On the other hand, the soil enrichment with microbial medium with urea also contributed to the increase in dehydrogenase activity. The degree of the biostimulation of microbial activity also depended on the volume of microbial medium supplemented to the soil, but the efficiency was significantly lower compared to soil supplementation with MCC, regardless of the ratio. In cases 7:1 and 10:1, values of

dehydrogenase activity in soil enriched with microbial medium after 7 days of the experiment were even below the initial value of dehydrogenase in unsupplemented soil.

3.5 Plants reaction to the soil supplementation with MCC

Soil supplementation with MCC strongly promoted plant growth and increased the biomass of both shoots and roots (Figures 5A, B), regardless of the Cd presence in soil. Furthermore, plant growth stimulation by the soil supplementation with MCC increased with time so the highest effect of MCC was noted after 14 weeks of the experiment. Uncontaminated soil enrichment with MCC increased the shoots biomass more than eight times with regard to shoots of plants cultivated in unsupplemented soil (Figure 5A). This effect was noticed after 14 weeks of the experiment – after 7 weeks of the experiment differences in shoots biomass were not observed. A similar effect of MCC was found in the case of shoots of plants grown in Cd-contaminated soil. Despite the pronounced phytotoxic effect of cadmium on plant biomass, the soil supplementation with MCC contributed to increasing shoots biomass and their dry weight was almost 15 times higher than in contaminated but unsupplemented soil. The soil enrichment in MCC also caused root growth stimulation (Figure 5B). The biomass of roots of plants cultivated in uncontaminated soil after 14 weeks of the experiment increased triple under the influence of MCC soil supplementation. In the case of the roots of plants grown in soil contaminated with Cd, their dry weight increased fourfold. Similarly, as in the case of shoots biomass, these differences were not observed before the end of the experiment.

Morphological changes of plants were confirmed by their physiological reaction in the form of a reduction of the water content in tissues (Figure 5C) and chlorophyll concentration in shoots (Figure 5D). Analysis of water content in plant tissues confirmed the phytotoxic effect of cadmium (Figure 5C). Although the turgor of shoots of plants cultivated in Cd surrounding was not changed before the end of the experiment, the strong reduction of water content in roots after just 7 weeks was observed. The soil supplementation with MCC strongly affected the general condition of plants which was confirmed by the significantly higher water content in roots already after 7 weeks of cultivation and shoots after 14 weeks of the experiment. After 14 weeks of plant cultivation, the effect of MCC enrichment was more visible since the positive influence of bacterial metabolites on the water content was observed both in the case of shoots and roots of plants grown both in pure and Cd-contaminated soil. In the case of plants cultivated in Cd-contaminated soil, the MCC contributed to the increase of turgor shoots and roots by about 12% and 48%, respectively. Furthermore, the turgor of plant roots grown in contaminated and supplemented soil was higher even than plants cultivated in pure soil. Thus, the high improvement of the general condition of plants under the influence of soil supplementation with MCC was shown.

Regarding the effect of soil supplementation with MCC on the chlorophyll concentration in plants, the positive influence was found only in the case of plants cultivated in Cd-contaminated soil (Figure 5D). The presence of MCC in soil contributed to an increase in chlorophyll concentration both after 7 and 14 weeks of the experiment. In the middle of the experiment, the difference in the value was twice but at the end of the experiment, there was

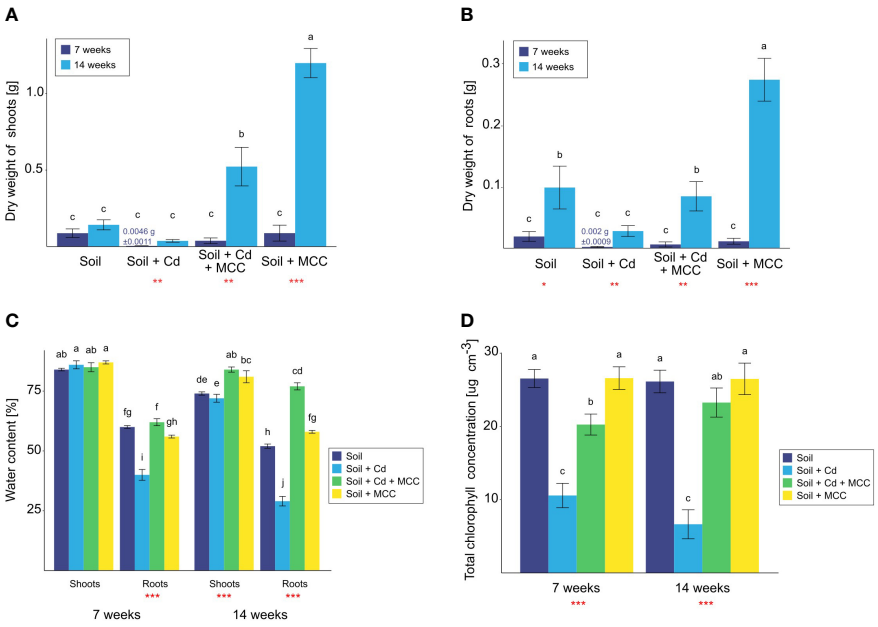

FIGURE 5
Biomass of shoots **(A)** and roots **(B)**, water content **(C)** and chlorophyll concentration **(D)** of plants cultivated in soil (un)contaminated with Cd and/or (un)supplemented with MCC after 7 and 14 days of the experiment. Statistical analysis: ANOVA (***p< 0.001, **p ≤ 0.01, *p ≤ 0.05, no asterisk - p>0.05) and Tukey HSD test (letters above the bars, p ≤ 0.05).

already a fourfold difference. The effect of MCC enrichment on plants grown in uncontaminated soil was not confirmed.

3.6 The effect of the MCC on the Cd uptake by plants, Cd bioavailability in the soil as well as quantity and activity of soil microbes

The soil enrichment with MCC strongly inhibited Cd uptake by plants (Figure 6A). Significantly lower concentrations of Cd were detected both in the roots and shoots of plants cultivated in Cd-contaminated soil, both after 7 and 14 weeks of the experiment. After 7 weeks of plant cultivation, soil supplementation with MCC contributed to the decrease of Cd concentration in shoots more than threefold while in roots the difference was twice. At the end of the experiment, the effect of soil enrichment with MCC was stronger and the differences between shoots and roots were more than sevenfold and almost fourfold, respectively, in favor of plants grown in MCC-enriched soil.

Based on the total Cd concentration in soil and plants the values of the bioconcentration factor (BCF) were calculated. BCF for plants cultivated for 7 weeks in MCC-enriched soil and in soil without MCC supplementation were 15.54 and 32.96, respectively. After 14 weeks of cultivation, BF for plants cultivated in both types of soil were lower with regard to values obtained in the middle of the experiment and were 4.74 and 21.14, respectively.

The lower Cd uptake by plants cultivated in MCC-supplemented soil was strongly correlated with the bioavailability of Cd in soil (Figure 6B). It has been shown that the soil enrichment with MCC significantly decreased Cd mobility both in soil without plants and in the presence of plants. These differences were visible from the beginning of the experiment, but they became more significant after 7 and 14 weeks of plant cultivation. After 7 weeks of the experiment, the difference in Cd bioavailability in soil without plants was more than twice but after 14 weeks was already almost threefold in favor of the MCC-supplemented soil. In the case of soil with plants a similar correlation was observed but differences between MCC-enriched and unenriched soil were even more significant. They were fourfold and almost fivefold, respectively. On the other hand, it was also noticed, that after 14 weeks of the experiment, the presence of plants contributed to the increase of the Cd bioavailability in the soil. In this case, the appropriate soil supplementation with MCC also reduced the cadmium bioavailability.

MCC supplementation of soil significantly affected the quantity and activity of microbes inhabiting both Cd-contaminated (Figure 6C) and uncontaminated soil (Figure 6D) regardless of the presence of plants. Furthermore, the effect of MCC on Cd-contaminated soil seemed to be stronger with regard to pure soil. In uncontaminated soil after 7 weeks of the experiment, the MCC supplementation increased the quantity of microorganisms only in soil with plants, but after 14 weeks, the effect of MCC was noticeable both in soil with and without plants (Figure 6C). At the end of the experiment, MCC supplementation contributed to the increase of microorganisms quantity in both types of soil by about one order of magnitude. In the case of Cd-contaminated soil, the significant effect of MCC was observed already after 7 weeks of the experiment, both in soil with and without plants (Figure 6D). Soil

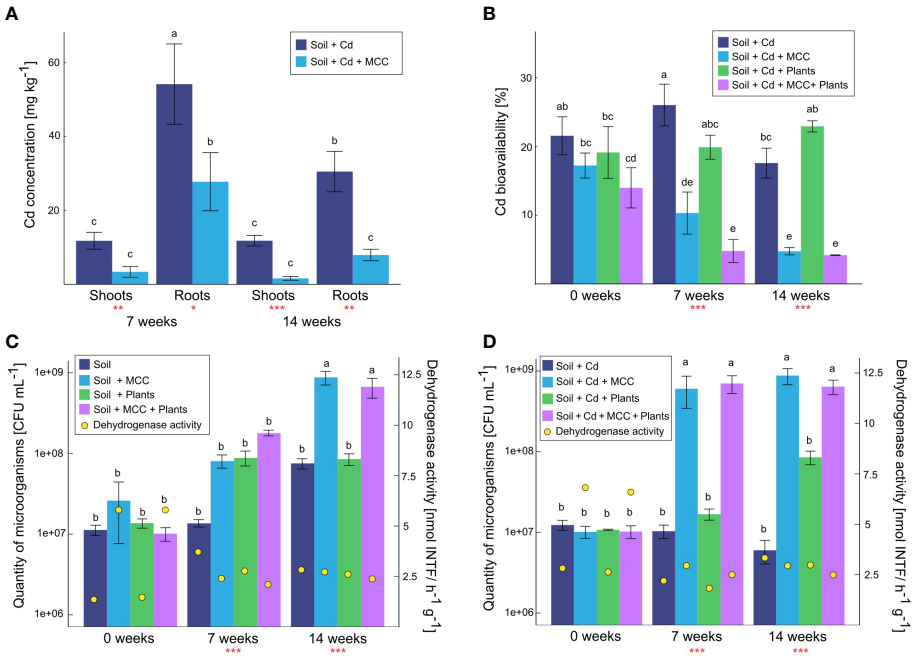

FIGURE 6
Total Cd concentration in plants cultivated in soil (un)supplemented with MCC **(A)**, cadmium bioavailability in soil **(B)**, microbiological quantity and activity in uncontaminated **(C)** and Cd-contaminated soil **(D)** after 7 and 14 weeks of plants cultivation. Statistical analysis: ANOVA (**p< 0.001, **p ≤ 0.01, *p ≤ 0.05, no asterisk - p>0.05) and Tukey HSD test (letters above the bars, p ≤ 0.05).

supplementation with MCC contributed in both cases to an increase in the quantity of microorganisms by almost two orders of magnitudes. After 14 weeks of the experiment, similar correlations were observed, however in this case the impact of the plants themselves on the microorganisms' quantity was also significantly noticeable. It has been shown that the presence of plants in soil unsupplemented with MCC increased the quantity of microbes in the soil by about one order of magnitude, however, the soil enrichment with MCC increased the value by an additional one order of magnitude.

Regarding the activity of dehydrogenases, a similar effect of MCC was found both in Cd-contaminated and uncontaminated soil only at the beginning of the experiment. The activity of dehydrogenases was then higher in both types of soil under the supplementation of MCC. After 7 weeks of the experiment, significant differences in contaminated and uncontaminated soil were found. Higher activity of dehydrogenases in soil uncontaminated and unsupplemented with MCC was found, but in the case of contaminated soil, the opposite tendency was observed. Thus, in this sampling point, the positive effect of MCC supplementation was confirmed only for Cd-contaminated soil. After 14 weeks of the experiment, the positive effect of MCC supplementation in contaminated soil had been nullified, thus no effect of soil supplementation with MCC on the dehydrogenase activity in soil was found.

4 Discussion

4.1 Carbonate productivity by *Ochrobactrum* sp. POC9

As a result of urea hydrolysis in presence of urease, ammonium and carbonate ions are created (Zambelli et al., 2011) that directly affect cadmium mobility in soil. Ammonium ions increase the pH of soil, contributing to the reduction of cadmium mobility whereas carbonate enables the precipitation of insoluble cadmium carbonate (Li et al., 2013). Changing conditions of the urea hydrolysis reaction affect the activity of urease, which corresponds directly to the content of both types of products in the solution (Krajewska, 2009). In our study, a positive correlation between the amount of urea and the concentration of carbonate in the medium was observed. This phenomenon is an effect of the Michaelis–Menten equation, which indicates that at a constant enzyme content, the efficiency of the reaction depends, within certain limits, on the substrate concentration (Krajewska, 2016). A similar correlation was found in other ureolytic bacteria strains NB33, LPB21, NB28, NB30 belonging to *Sporosarcina pasteurii* and *Bacillus lentus*. In these cases, the lowest urease activity at 2% of urea concentration, and highest at 6 or 8% initial urea concentrations was detected (Omoregie et al., 2017). With 10% of the initial urea concentration, the amount of hydrolyzed urea decreased, probably by the inhibition of the ureolysis reaction by the products (Krajewska, 2016). The carbonate production efficiency of the *Ochrobactrum* POC9 strain was maximally 16168.33 mg/l when the medium contained 5% of urea. The carbonate efficiency was a bit higher than in other previously described strains, e.g., *Bacillus pasteuri* (Yi et al., 2021).

For the MICP process, the change in the initial pH of the microbial medium can affect the activity of urease, and through it the amount of carbonate ions (Barazorda-Ccahuana et al., 2020). We showed that pH range 5.5- 6.8 is optimal for *Ochrobactrum* sp. POC9 growth. Previous studies of urease enzyme kinetics confirmed that ureolysis is a pH dependent process (Fidaleo et al., 2003; Lauchnor et al., 2015). Furthermore, the optimum pH for cell-free extract was narrower than this in the presence of bacteria and was more vulnerable to changes in pH to acidic values (van Paassen, 2009). This was one of the reasons why cell-free supernatant was used in our study. The activity of urease may vary in various bacteria species depending on the pH (Sachs et al., 2001). For *Pararhodobacter* sp. maximum urease activity was found at pH 8 (Fujita et al., 2017). For *Bacillus pasteurii* ATCC11859 optimum pH range was 7.0-9.0 (Yi et al., 2021) and for *Sporosarcina pasteurii* optimal is pH 9.25, and when pH raised to 10, the growth of bacteria was stopped (Wiley and Stokes, 1962). *Micrococcus yunnanensis* showed the highest urease activity on pH 7 (Imran et al., 2019). It is regarded that urease activity is significantly lower in acidic conditions (lower than 5) and alkaline (over 8), which was also confirmed in our study.

No significant differences in carbonate production efficiency were observed between various temperature variants. A few other experimental results showed that the temperature was positively correlated with the ureolysis rate (van Paassen, 2009; Krajewska, 2016) and microbial cultures incubated at the higher temperature (e.g., 37 °C) gave the best results. Differences in response to this factor can be seen between *Sporosarcina pasteurii* and *Bacillus megaterium* (Sun et al., 2019). The urease activity of *B. megaterium* was lower in temperatures between 25 and 30 °C but in the case of *S. pasteurii*, the activity of the enzyme increased with the temperature. For *Bacillus pasteurii* optimal temperature was 30 °C (Yi et al., 2021). Furthermore, in this temperature, the highest urease activity has been noticed.

Changes in initial optical density, related to the quantity of microorganisms, did not show notable differences in carbonate contents in POC9 cultures. The most probable explanation is the difference in bacterial growth rate and the relative abundance of nutrients available for the bacterial population. In variants with a higher quantity of bacteria, nutrient availability was lower than in variants with a less initial quantity of microbes (Allen and Waclaw, 2019). In other studies, an initial optical density of cultures strongly affected the urease activity, eg. in *Pararhodobacter* sp. culture (Fujita et al., 2017). Urease activity increased almost in directly proportional to the increase of bacterial optical density variants. For *Sporosarcina pasteurii* (DSM 33) the effect of three initial optical densities (OD_{600nm} 0.2, 1.0, 3.0) on the growth and urease activity was tested (Wang et al., 2021). It has been shown that in the variant with the lowest initial OD_{600nm} bacteria growth was the most intensive. The highest examined variant had the lowest bacterial growth rate and the fastest entered the lethal phase. This result was explained again by shortages in nutrients.

4.2 Cadmium carbonate detection in the soil by SEM and FTIR analysis

The presence of a carbonate mineral in the Cd-contaminated soil is evidenced by the emergence of an additional feature at ca. 875 cm^{-1} in the FTIR spectra (Russell, 1977; Bucca et al., 2009; Liu et al., 2017; Pérez-Villarejo et al., 2018). Due to a very low intensity and significant blurring of this band, it is not possible to precisely determine its position and consequently to determine which carbonate is present. The approximate position at ca. 875 cm^{-1} is, however, close to those reported for both calcium (calcite 876–878 cm^{-1}, vaterite 877 cm^{-1}) and cadmium (otavite 860–863 cm^{-1}) carbonates (Jones and Jackson, 1993; Russell and Fraser, 1994; Moreno et al., 2018; Liu and Lian, 2019). Although this value is closer to calcium carbonates, the clear asymmetry of the band (Figure 2) might suggest the crystallization of a $CaCO_3$-$CdCO_3$ solid solution as well. Such a possibility is favored by the close similarity of calcium and cadmium divalent cations, especially by small difference between Cd^{2+} and Ca^{2+} ionic radii which are 0.95 Å and 0.99 Å, respectively (Shannon, 1976; Tesoriero and Pankow, 1996). Therefore complete miscibility of $(Ca,Cd)CO_3$ has been evidenced experimentally (Sackey et al., 2019; Mergelsberg et al., 2021). Since the soil contains much more calcium than cadmium, the supply of carbonate to the system results in the crystallization of larger amounts of calcium carbonate. However, due to the clear difference in the solubility products (K_{SP}) of both compounds ($10^{-8.48}$ for $CaCO_3$ vs $10^{-12.24}$ for $CdCO_3$), it can be assumed that cadmium will be preferentially incorporated into precipitating calcium carbonate. The formation of $(Ca,Cd)CO_3$ solid solution at the surface of calcium carbonate crystals is also possible via Ostwald ripening during recrystallization processes (Kang et al., 2014a).

Scanning electron microscopic observations confirmed crystallization of carbonate minerals on the surface of Cd-contaminated soil (Figure 3). Lower Cd concentrations in the soil and/or at lower soil:MCC ratios resulted in the formation of small blocky or platy crystals with recognizable rhombohedral habits and a low Cd admixture (Figures 3A, B). Such a morphology, combined with the FTIR feature at ca. 875 cm^{-1} (Figure 2), suggests that the carbonate is calcite. This is consistent with previous studies since calcite is apparently the most common product of MICP (Kumari et al., 2014; Krajewska, 2018). Higher Cd levels and higher soil:MCC ratios favored crystallization of $(Ca,Cd)CO_3$ that revealed other habits - acicular or columnar crystals that form isometric or fan-like aggregates (Figures 3C–E). The morphology combined with EDS chemical analyses suggest calcite-otavite solid solution. A distinct change in morphology of Cd-substituted Ca carbonates was observed previously (e.g. Kim et al., 2021; Natsi and Koutsoukos, 2022) and resulted probably from a change in crystallization kinetics. Both Ca and Ca-Cd carbonates are apparently more common in samples of higher soil:MCC ratios. This is more likely due to the alkalizing effect of metabolites on the soil solution (Figure 4A), which in turn favors the precipitation of carbonates.

4.3 The efficiency of Cd immobilization in soil with the use of MICP

The reduction of Cd mobility in soil with the use of MICP method is caused by the increase of pH in soil and the precipitation of cadmium carbonate (Lyu et al., 2022). Due to the high-efficiency Cd immobilization even in low concentration in soil, recently MICP is more and more frequently used for the treatment of soil dedicated to agricultural purposes (Liao et al., 2023). In our study, the MICP was used for Cd immobilization in agricultural soil, and furthermore, the soil bioconsolidation method based on MICP was optimized not only in the context of the carbonate production maximization but also regarding the soil supplementation manner.

The results of Cd bioavailability in soil reflected an increased degree of immobilization of this element under the influence of soil supplementation with MCC produced by the POC9 strain. Application of MCC to Cd-contaminated soil contributed to the significant reduction of the Cd bioavailability; however, the efficiency of the process strongly depended on the soil:MCC volume ratio. Reduction of the Cd bioavailability ranged from 28 to 65% depending on the volume of MCC supplemented to the soil. The positive effect of MICP in regard to Cd immobilization was confirmed also for many other bacterial strains belonged i.e. to *Bacillus* (Zhao et al., 2017; Wang et al., 2019b), *Lysinibacillus* (Kang et al., 2014b), *Pseudomonas* (Bravo et al., 2018), *Serratia* (Bhattacharya et al., 2018), and *Sporosarcina* (Kang et al., 2014a) genus, but those studies concerned the Cd precipitation in various solutions/media, not in soil. In solutions, the possibility of Cd precipitation with carbonates is usually easier and more effective than in soil since the higher mobility of both types of molecules in a liquid matrix (Yang et al., 2016; Ghorbanzadeh et al., 2020). Regarding the soil experiments, the obtained Cd precipitation with the use of MCC produced by the POC9 strain was comparable with other previously described bacteria as eg. *Enterobacter* spp. (56.10%) (Peng et al., 2020), *Sporosarcina pasteurii* (61.1-89.3% (Ghorbanzadeh et al., 2020) or 13.6%-29.9% (Liu et al., 2021), and soil autochthonous microbiota (59.8%) (Lyu et al., 2022).

The positive effect of Cd-contaminated soil supplementation with medium containing urea without MCC was also found. In these experimental variants, the effect of biostimulation of autochthonous microbiota by the additional nutrition was observed. It has been shown that soil enrichment with 2% of urea stimulated the ureolytic activity of autochthonous soil microorganisms, which contributed to increased Cd immobilization. In our study, the efficiency of this process was significantly lower with regard to soil supplementation with MCC but still noticeable. Immobilization of Cd and other heavy metals by MICP based on the activity on the autochthonous soil microbiota was previously described (Kim and Lee, 2019; Lyu et al., 2022) and the efficiency of the process were comparable with data obtained in this study.

Most of the so far described MICP applications for heavy metal immobilization in soil utilized culture breeding (bacterial cells suspended in metabolites solution) directly to contaminated soil (Kumari et al., 2014; Liu et al., 2021; Qiao et al., 2021). In some cases, soil enrichment with the exogenous pool of microbes may have a negative effect on the soil's autochthonous microbiome condition, by disturbing its natural community structure (Lourenço et al., 2018; Seitz et al., 2022). The appropriate microbiome composition is particularly important in the context of the treatment of agricultural soil since microbes directly interact with crop plants and affect their productivity (Trivedi et al., 2020; Glick and Gamalero, 2021). Furthermore, the unfavorable effect may be enhanced by autochthonous and exogenous microbes competition about space and/or nutrients (Mawarda et al., 2022; Nunes et al., 2022), which may also affect the MICP efficiency (Liu et al., 2019). In our study, a filtered MCC solution was applied to Cd-contaminated soil, thus minimization of the interference of allochthonous microorganisms in the soil ecosystem was ensured.

4.4 Biostimulation of soil microbiota by MCC

The addition of external carbon sources is essential for the proper growth and activity of soil microbes (Bandara et al., 2021). Application of various organic amendments to soil results in the improvement of bacterial community structure, diversity and quantity (Omori et al., 2016; Macias-Benitez et al., 2020; Tao et al., 2020; Readyhough et al., 2021). The addition of MCC to soil was correlated with a significant increase in microorganism quantity, observed in soil contaminated with Cd and uncontaminated. Soil supplementation with MCC provided an additional nutrient pool, which could stimulate bacterial growth. As was shown in our previous studies, various secondary metabolites were produced during the decomposition of urea by *Ochrobactrum* sp. POC9 (Yang et al., 2021). Among them, unsaturated hydrocarbons were one of the major groups. These compounds could be used by various ecological groups of bacteria as energy sources (Widdel and Musat, 2016). Secondary metabolites of *Ochrobactrum* sp. POC9 also contained a high amount of organic acids, which could be an easily-accessible carbon and energy source for microorganisms (Macias-Benitez et al., 2020). It was also shown that organic acids play a crucial role in the stimulation and recruitment of plant-growth-promoting rhizobacteria, being one of the major components of plant roots exudates (Macias-Benitez et al., 2020; Sharma et al., 2020). Alcohols were another major group of organic compounds found in secondary metabolites of *Ochrobactrum* sp. POC9. Bacteria with various lifestyles are able to degrade alcohols (Fisk et al., 2009; Yakushi and Matsushita, 2010) and use them as an energy source (Yakushi and Matsushita, 2010; Schuchmann and Müller, 2016).

The increase in the quantity of microorganisms was also observed in soil contaminated with Cd due to decreased bioavailability of this heavy metal. High concentrations of Cd have toxic effects on bacterial cells, possibly causing DNA damage, disturbed cell division, inhibition of respiration and enzymatic activity, mainly through binding to sulfhydryl groups in proteins (Trevors et al., 1986; Fazeli et al., 2011). The presence of extensive Cd in soil has also impacted entire microbial communities, reshaping their structure and activity resulting in decreased bacterial biomass and diversity (Pal et al., 2005; Yu et al., 2021). The addition of MCC to soil was correlated with a decrease in Cd bioavailability, which is a crucial factor for its toxicity (Bandara et al., 2021). This created more optimal conditions for microbial communities to grow and resulted

in greater microbial quantities. In other papers, it has been shown that the reduction of Cd bioavailability improved soil microbiome in terms of quality and quantity (Bandara et al., 2021; Sun et al., 2021). An increase in microbial basal respiration and biomass was observed in soils, as an effect of the addition of biochar, which decreased Cd bioavailability (Bandara et al., 2021). Stabilization of Cd could also have an indirect positive impact on soil microbiota in the plant rhizosphere. Reduced toxicity of Cd for plants results in their stimulated growth. This elevates the level of soil plants residues and root exudates, providing nutrients for various soil microbes (Sun et al., 2021).

In contrast to the observed stimulation of the number of microorganisms in the presence of plants, a decrease was observed in dehydrogenase activity (DHA). DHA play a key role in the oxidation of organic matter mediating the transfer of hydrogen from the substrates to acceptors. DHA is involved in the transfer of hydrogen atoms to coenzymes such as NAD^+, $NADP^+$ or FAD^+, which are the first acceptors of the electrons in cellular respiration (Furtak and Gajda, 2017). Therefore, it is considered that the activity of dehydrogenase is indirectly connected with soil microorganisms quantity (Skujins and McLaren, 1967). The activity of DHA in soil depends on many factors, including pH, soil hydration level, redox potential, oxygen diffusion rate, organic matter content, or temperature. In this work, it was shown that despite the increase in the quantity of microorganisms in the soil, the activity of the DHA decreased during the experiment. In several studies, the optimal soil pH for DHA activity was neutral or slightly alkaline and was in a range of 7-8.5 (Włodarczyk et al., 2002; Ros et al., 2003). Moreover, low activity of DHA has been observed below pH 6.6 and above pH 9.5 (Trevors, 1984). These correlations may explain the decrease in DHA activity during experiments, despite the increase in the quantity of microorganisms. After the initial addition of MCC to the soil, its pH increased providing optimal conditions for the activity of DHA. In the course of the experiment, a decrease in the soil pH was observed, resulting in suboptimal conditions and lowering the DHA activity.

4.5 Effect of MCC on the general plants' conditions and Cd uptake efficiency

Cadmium contamination of soil negatively affects seed germination and the synthesis of photosynthetic pigments, reduces crop plant growth and number of leaves as well as inhibits root elongation (Mani et al., 2012; He et al., 2017; el Rasafi et al., 2020). Cadmium is regarded as highly toxic and its accumulation in plant tissues results in disturbance of various intracellular processes.

Cadmium stress induces the overproduction of reactive oxygen species (ROS), which eventually leads to damage and destruction of cell membranes, organelles and biomolecules (Abbas et al., 2018). In this study, Cd presence in the soil also caused a significant inhibition of crop plants development, observed already after 7 weeks of cultivation, compared to plants grown in soil supplemented with MCC. The presence of MCC had a highly positive effect on the overall condition of plants. The biomass of plants grown in soil without MCC was significantly lower and leaves discoloration was observed, in contrast to the plants grown in soil with MCC, which remained in good condition throughout the experiment. A similar correlation was observed for the plants grown in unpolluted soils with and without the supplementation, but this effect was found after 14 weeks of cultivation. The deterioration of the condition of plants at the end of the experiment could have been the result of a shortage of micro- and macroelements in the soil (Kumar et al., 2021). Due to the addition of MCC, the plants were supplied with the necessary building components until the end of the cultivation, so their development was not inhibited (Styczynski et al., 2022).

Supplementation of MCC to soil provided also an additional source of nitrogen, which is a crucial element for plant growth and development (Xu et al., 2012; Kiba and Krapp, 2016; Feng et al., 2020). Ammonium ions are directly introduced with MCC to soil, where they are present as a product of urea hydrolysis (Zambelli et al., 2011). Ammonium is considered as a preferred nitrogen source for plants, because it does not have to undergo further transformation after uptake inside of the plant cells (Xu et al., 2012; Kiba and Krapp, 2016). This direct utilization of ammonium by plant limits energy expenditure on nitrogen assimilation (Hachiya and Sakakibara, 2017). However, in several studies it was shown that uptake of nitrate is also important for plant growth, despite the necessity of its reduction to ammonium either in roots or leaves (Hachiya and Sakakibara, 2017; Feng et al., 2020). MCC could also indirectly contribute to the supply of nitrate in soil available for plant uptake. Soil is inhabited by nitrifying bacteria, which are able to oxidize ammonium delivered with MCC to nitrite and nitrate (Beeckman et al., 2018; Wendeborn, 2020). MCC also creates preferential conditions for oxidation, by alkalization of soil. Neutral to slightly alkaline soil pH is correlated with highest efficiency of soil nitrification (Norton and Stark, 2011).

The results regarding water and chlorophyll content indicated a positive effect of MCC supplementation. The presence of MCC allowed for maintaining constant hydration of the plants and photosynthetic activity throughout the cultivation period. This could be connected with mitigation of Cd toxicity in plants. It has been shown that exposure to Cd in soil could lead to osmotic stress and lowering of water content in shoots (Rizwan et al., 2016; Haider et al., 2021). Cadmium also affects chlorophyll content, mainly by hindering the uptake and metabolism of sulfur and iron, which are crucial for chlorophyll biosynthesis (Gallego et al., 2012; Haider et al., 2021). The beneficial effect of a representative of the genus *Ochrobactrum* on plant growth was also described in cucumber culture supplementation with *Ochrobactrum* sp. NW-3. Furthermore, NW-3 has been classified as plant growth-promoting bacteria (PGPB) (Xu et al., 2015). Other examples of PGPB strains may be *Bacillus* sp. UR21, which contributed to the increase in the biomass and chlorophyll content in pakchoi plants cultivated in Cd-contaminated soil (Wei et al., 2022) or *Pseudomonas grimontii* Bc09, *Pantoea vagans* So23, *Pseudomonas veronii* E02, and *Pseudomonas fluorescens* Oj24 that had a positive effect on acetic acid production, 1-aminocyclopropane-1-carboxylic acid deaminase (ACCD) activity and phosphate solubilization by *Panicum virgatum L.* cultivated in Cd-contaminated soil (Begum et al., 2018).

In this study, we showed that most of the Cd ions absorbed by plants were retained in the root system. The reason for this is structural elements of the cell wall, including pectin compounds and proteins, protect plants against contaminant translocation (el Rasafi et al., 2020). MCC soil supplementation resulted in a strong inhibition of Cd uptake by plants and significantly lowered accumulation of Cd in the tissues, both in the root and shoot parts. Literature data also indicate a positive effect of the use of ureolytic bacteria *Bacillus* sp. UR21 and eggshell waste on the reduction of Cd uptake by pakchoi plants (*Brassica chinensis* L.) (Wei et al., 2022). A similar correlation was also confirmed in the case of *Bacillus* sp. TZ5, which effectively increased the biomass of ryegrass and decreased Cd accumulation in those plants (Ma et al., 2020) or in the case of *Pantoea agglomerans*, which promoted rice growth and reduced Cd concentration in rice grain (Tian et al., 2022).

5 Conclusions

The soil supplementation with MCC produced by *Ochrobactrum* sp. POC9 as a result of the hydrolysis reaction contributed to the significant reduction of Cd bioavailability in soil and improved its microbiological properties by the increase in the quantity of soil microorganisms. Both cadmium immobilization in the form of carbonates, as well as additional nutrition of soil by its enrichment with MCC, resulted in the better growth of plants and a significant reduction in Cd uptake. It has been shown that appropriate soil supplementation with MCC produced by the POC9 strain may bring a quadruple beneficial effect in the form of Cd toxicity reduction, stimulation of the soil microbes growth, reduction in the Cd uptake by plants, and promotion of plants' growth. Furthermore, the soil supplementation with MCC did not negatively affect the properties of the soil and thus this method may be successfully applied in soil dedicated to agricultural purposes.

Data availability statement

The raw data supporting the conclusions of this article will be made available by the authors, without undue reservation.

Author contributions

Conceptualization: KD-A. Data curation: MZ, GR, MM, AG, RS. Formal analysis: KD-A. Funding acquisition: KD-A, GR. Investigation: MZ, GR, MM, AG, RS. Methodology: MZ, GR, KD-A. Project administration, resources and supervision: KD-A.

Validation: MZ, GR, MM, AG, RS, KD-A. Visualization: GR, MM, KD-A. Writing—original draft: MZ, GR, MM, AG, KD-A. Writing—review & editing: MZ, GR, MM, RS, KD-A. All authors contributed to the article and approved the submitted version.

Funding

This work was supported by (i) the National Centre for Research and Development (Poland) in the frame of the LIDER program, grant no. LIDER/13/0051/L-11/NCBR/2020 and (ii) the University of Warsaw, Excellence Initiative – Research University (Poland), grant no. BOB-IDUB-622-199/2022. SEM and FTIR analyses were supported by AGH-UST grant no. 16.16.140.315. Funding for open access charge: University of Warsaw.

Conflict of interest

MZ and KD-A are holders of a patent application related to this work P.442546.

The remaining authors declare that the research was conducted in the absence of any commercial or financial relationships that could be construed as a potential conflict of interest.

Publisher's note

Supplementary material

The Supplementary Material for this article can be found online at: https://www.frontiersin.org/articles/10.3389/fpls.2023.1109467/full#supplementary-material

References

Abbas, T., Rizwan, M., Ali, S., Adrees, M., Zia-ur-Rehman, M., Qayyum, M. F., et al. (2018). Effect of biochar on alleviation of cadmium toxicity in wheat (*Triticum aestivum* l.) grown on cd-contaminated saline soil. *Environ. Sci. Pollut. Res.* 25 (26), 25668–25680. doi: 10.1007/S11356-017-8987-4/TABLES/3

Achal, V., Pan, X., Fu, Q., and Zhang, D. (2012a). Biomineralization based remediation of As(III) contaminated soil by *Sporosarcina ginsengisoli*. *J. Hazardous Materials* 201-202, 178–184. doi: 10.1016/J.JHAZMAT.2011.11.067

Achal, V., Pan, X., and Zhang, D. (2011). Remediation of copper-contaminated soil by *Kocuria flava* CR1, based on microbially induced calcite precipitation. *Ecol. Eng.* 37 (10), 1601–1605. doi: 10.1016/J.ECOLENG.2011.06.008

Achal, V., Pan, X., Zhang, D., and Fu, Q. (2012b). Bioremediation of Pb-contaminated soil based on microbially induced calcite precipitation. *J. Microbiol. Biotechnol.* 22 (2), 244–247. doi: 10.4014/JMB.1108.08033

Allen, R. J., and Waclaw, B. (2019). Bacterial growth: a statistical physicist's guide. *Reports on progress in physics. Phys. Soc. (Great Britain)* 82 (1). doi: 10.1088/1361-6633/AAE546

Balali-Mood, M., Naseri, K., Tahergorabi, Z., Khazdair, M. R., and Sadeghi, M. (2021). Toxic mechanisms of five heavy metals: mercury, lead, chromium, cadmium, and arsenic. *Front. Pharmacol.* 12. doi: 10.3389/FPHAR.2021.643972/BIBTEX

Bandara, T., Franks, A., Xu, J., Chathurika, J. B. A. J., and Tang, C. (2021). Biochar aging alters the bioavailability of cadmium and microbial activity in acid contaminated soils. *J. Hazardous Materials* 420, 126666. doi: 10.1016/J.JHAZMAT.2021.126666

Barazorda-Ccahuana, H. L., Gómez, B., Mas, F., and Madurga, S. (2020). Effect of pH on the supramolecular structure of *Helicobacter pylori* urease by molecular dynamics simulations. *Polymers* 12 (11), 1–13. doi: 10.3390/POLYM12112713

Bashir, S., Adeel, M., Gulshan, A. B., Iqbal, J., Khan, S., Rehman, M., et al. (2019). Effects of organic and inorganic passivators on the immobilization of cadmium in contaminated soils: a review. *Environ. Eng. Sci.* 36 (9), 986–998. doi: 10.1089/EES.2018.0483

Beeckman, F., Motte, H., and Beeckman, T. (2018). Nitrification in agricultural soils: impact, actors and mitigation. *Curr. Opin. Biotechnol.* 50, 166–173. doi: 10.1016/J.COPBIO.2018.01.014

Begum, N., Afzal, S., Zhao, H., Lou, L., and Cai, Q. (2018). Shoot endophytic plant growth-promoting bacteria reduce cadmium toxicity and enhance switchgrass (*Panicum virgatum* l.) biomass. *Acta Physiologiae Plantarum* 40 (9), 1–16. doi: 10.1007/S11738-018-2737-1/FIGURES/5

Benavides, M. P., Gallego, S. M., and Tomaro, M. L. (2005). Cadmium toxicity in plants. *Braz. J. Plant Physiol.* 17 (1), 21–34. doi: 10.1590/S1677-04202005000100003

Bhattacharya, A., Naik, S. N., and Khare, S. K. (2018). Harnessing the bio-mineralization ability of urease producing *Serratia marcescens* and *Enterobacter cloacae* EMB19 for remediation of heavy metal cadmium (II). *J. Environ. Manage.* 215, 143–152. doi: 10.1016/J.JENVMAN.2018.03.055

Bravo, D., Pardo-Díaz, S., Benavides-Erazo, J., Rengifo-Estrada, G., Braissant, O., and Leon-Moreno, C. (2018). Cadmium and cadmium-tolerant soil bacteria in cacao crops from northeastern Colombia. *J. Appl. Microbiol.* 124 (5), 1175–1194. doi: 10.1111/JAM.13698

Bucca, M., Dietzel, M., Tang, J., Leis, A., and Köhler, S. J. (2009). Nucleation and crystallization of otavite, witherite, calcite, strontianite, hydrozincite, and hydrocerussite by CO_2 membrane diffusion technique. *Chem. Geology* 266, 143–156. doi: 10.1016/j.chemgeo.2009.06.002

Chaney, R. L. (2012). Food safety issues for mineral and organic fertilizers. *Adv. Agron.* 117, 51–116. doi: 10.1016/B978-0-12-394278-4.00002-7

Chen, H., Yang, X., Wang, P., Wang, Z., Li, M., and Zhao, F. J. (2018). Dietary cadmium intake from rice and vegetables and potential health risk: a case study in xiangtan, southern China. *Sci. Total Environ.* 639, 271–277. doi: 10.1016/J.SCITOTENV.2018.05.050

Christensen, W. B. (1946). Urea decomposition as a means of differentiating Proteus and paracolon cultures from each other and from salmonella and shigella types 1. *J. Bacteriology* 52, 461–466. doi: 10.1128/jb.52.4.461-466.1946

de Vries, W., Schütze, G., Lots, S., Meili, M., Römkens, P., Farret, R., et al. (2003). Critical limits for cadmium, lead and mercury related to ecotoxicological effects on soil organisms, aquatic organisms, plants, animals and humans. *Agris*, 29–78. Availbale at: https://edepot.wur.nl/52354.

Dghaim, R., Rasool, H., and Khan, M. A. (2015). Determination of heavy metals concentration in traditional herbs commonly consumed in the united Arab Emirates. *J. Environ. Public Health* 2015. doi: 10.1155/2015/973878

Dhaliwal, S. S., Singh, J., Taneja, P. K., and Mandal, A. (2020). Remediation techniques for removal of heavy metals from the soil contaminated through different sources: a review. *Environ. Sci. Pollut. Res. Int.* 27 (2), 1319–1333. doi: 10.1007/S11356-019-06967-1

el Rasafi, T., Oukarroum, A., Haddioui, A., Song, H., Kwon, E. E., Bolan, N., et al. (2020). Cadmium stress in plants: a critical review of the effects, mechanisms, and tolerance strategies. *Crit. Rev. Environ. Sci. Technol.* 52 (5), 675–726. doi: 10.1080/10643389.2020.1835435

European Food Safety Authority (2012). Cadmium dietary exposure in the European population. *EFSA J.* 10 (1), 2551. doi: 10.2903/j.efsa.2012.2551

Fageria, N. K., Baligar, C., and Clark, R. B. (2002). Micronutrients in crop production. *Adv. Agron.* 77, 185–268. doi: 10.1016/S0065-2113(02)77015-6

Fazeli, M., Hassanzadeh, P., and Alaei, S. (2011). Cadmium chloride exhibits a profound toxic effect on bacterial microflora of the mice gastrointestinal tract. *Hum. Exp. Toxicol.* 30 (2), 152–159. doi: 10.1177/0960327110369821

Feng, H., Fan, X., Miller, A. J., and Xu, G. (2020). Plant nitrogen uptake and assimilation: regulation of cellular pH homeostasis. *J. Exp. Bot.* 71 (15), 4380. doi: 10.1093/JXB/ERAA150

Fidaleo, M., Lavecchia, R., and Lellis, S. C. (2003). Kinetic study of enzymatic urea hydrolysis in the pH range 4-9. *Chem. Biochem. Eng. Q.* 17, 311–318. doi: 10.15255/CABEQ.2014.599

Fisk, P. R., Wildey, R. J., Girling, A. E., Sanderson, H., Belanger, S. E., Veenstra, G., et al. (2009). Environmental properties of long chain alcohols. part 1: physicochemical, environmental fate and acute aquatic toxicity properties. *Ecotoxicology Environ. Saf.* 72 (4), 980–995. doi: 10.1016/J.ECOENV.2008.09.025

Fujita, M., Nakashima, K., Achal, V., and Kawasaki, S. (2017). Whole-cell evaluation of urease activity of pararhodobacter sp. isolated from peripheral beachrock. *Biochem. Eng. J.* 124, 1–5. doi: 10.1016/J.BEJ.2017.04.004

Furtak, K., and Gajda, A. M. (2017). Activity of dehydrogenases as an indicator of soil environment quality. *Polish J. Soil Sci.* 50 (1), 33. doi: 10.17951/PJSS.2017.50.1.33

Gallego, S. M., Pena, L. B., Barcia, R. A., Azpilicueta, C. E., Iannone, M. F., Rosales, E. P., et al. (2012). Unravelling cadmium toxicity and tolerance in plants: insight into regulatory mechanisms. *Environ. Exp. Bot.* 83, 33–46. doi: 10.1016/J.ENVEXPBOT.2012.04.006

Ghorbanzadeh, N., Abduolrahimi, S., Forghani, A., and Farhangi, M. B. (2020). Bioremediation of cadmium in a sandy and a clay soil by microbially induced calcium carbonate precipitation after one week incubation. *Arid Land Res. Manage.* 34 (3), 309–335. doi: 10.1080/15324982.2020.1720866

Glick, B. R., and Gamalero, E. (2021). Recent developments in the study of plant microbiomes. *Microorganisms* 9, 533. doi: 10.3390/MICROORGANISMS9071533

Godt, J., Scheidig, F., Grosse-Siestrup, C., Esche, V., Brandenburg, P., Reich, A., et al. (2006). The toxicity of cadmium and resulting hazards for human health. *J. Occup. Med. Toxicol.* 1 (1). doi: 10.1186/1745-6673-1-22

Hachiya, T., and Sakakibara, H. (2017). Interactions between nitrate and ammonium in their uptake, allocation, assimilation, and signaling in plants. *J. Exp. Bot.* 68 (10), 2501–2512. doi: 10.1093/JXB/ERW449

Haider, F. U., Liqun, C., Coulter, J. A., Cheema, S. A., Wu, J., Zhang, R., et al. (2021). Cadmium toxicity in plants: impacts and remediation strategies. *Ecotoxicology Environ. Saf.* 211, 111887. doi: 10.1016/J.ECOENV.2020.111887

Hashim, M. A., Mukhopadhyay, S., Sahu, J. N., and Sengupta, B. (2011). Remediation technologies for heavy metal contaminated groundwater. *J. Environ. Manage.* 92 (10), 2355–2388. doi: 10.1016/J.JENVMAN.2011.06.009

He, S., Yang, X., He, Z., and Baligar, V. C. (2017). Morphological and physiological responses of plants to cadmium toxicity: a review. *Pedosphere* 27 (3), 421–438. doi: 10.1016/S1002-0160(17)60339-4

Henry, A., Doucette, W., Norton, J., and Bugbee, B. (2007). Changes in crested wheatgrass root exudation caused by flood, drought, and nutrient stress. *J. Environ. Qual.* 36 (3), 904–912. doi: 10.2134/JEQ2006.0425SC

Hou, D., O'Connor, D., Igalavithana, A. D., Alessi, D. S., Luo, J., Tsang, D. C. W., et al. (2020). Metal contamination and bioremediation of agricultural soils for food safety and sustainability. *Nat. Rev. Earth Environ.* 1 (7), 366–381. doi: 10.1038/s43017-020-0061-y

Imran, M., Nakashima, K., Evelpidou, N., and Kawasaki, S. (2019). Factors affecting the urease activity of native ureolytic bacteria isolated from coastal areas. *Geomechanics Eng.* 17 (5), 421–427. doi: 10.12989/GAE.2019.17.5.421

Jones, G. C., and Jackson, B. (1993). *Infrared transmission spectra of carbonate minerals* (London: Chapman & Hall).

Kang, C. H., Choi, J. H., Noh, J. G., Kwak, D. Y., Han, S. H., and So, J. S. (2014a). Microbially induced calcite precipitation-based sequestration of strontium by *Sporosarcina pasteurii* WJ-2. *Appl. Biochem. Biotechnol.* 174 (7), 2482–2491. doi: 10.1007/S12010-014-1196-4

Kang, C. H., Han, S. H., Shin, Y., Oh, S. J., and So, J. S. (2014b). Bioremediation of cd by microbially induced calcite precipitation. *Appl. Biochem. Biotechnol.* 172 (4), 1929–1937. doi: 10.1007/S12010-013-0626-Z

Khan, F. I., Husain, T., and Hejazi, R. (2004). An overview and analysis of site remediation technologies. *J. Environ. Manage.* 71 (2), 95–122. doi: 10.1016/J.JENVMAN.2004.02.003

Kiba, T., and Krapp, A. (2016). Plant nitrogen acquisition under low availability: regulation of uptake and root architecture. *Plant Cell Physiol.* 57 (4), 707. doi: 10.1093/PCP/PCW052

Kim, Y., Kwon, S., and Roh, Y. (2021). Effect of divalent cations (Cu, zn, Pb, cd, and Sr) on microbially induced calcium carbonate precipitation and mineralogical properties. *Front. Microbiol.* 12. doi: 10.3389/fmicb.2021.646748

Kim, J. H., and Lee, J. Y. (2019). An optimum condition of MICP indigenous bacteria with contaminated wastes of heavy metal. *J. Material Cycles Waste Manage.* 21 (2), 239–247. doi: 10.1007/S10163-018-0779-5/FIGURES/9

Kohli, A., Narciso, J. O., Miro, B., and Raorane, M. (2012). Root proteases: reinforced links between nitrogen uptake and mobilization and drought tolerance. *Physiologia Plantarum* 145 (1), 165–179. doi: 10.1111/J.1399-3054.2012.01573.X

Krajewska, B. (2009). Ureases i. functional, catalytic and kinetic properties: a review. *J. Mol. Catalysis B: Enzymatic* 59 (1–3), 9–21. doi: 10.1016/J.MOLCATB.2009.01.003

Krajewska, B. (2016). A combined temperature-pH study of urease kinetics. assigning pKa values to ionizable groups of the active site involved in the catalytic reaction. *J. Mol. Catalysis B: Enzymatic* 124, 70–76. doi: 10.1016/J.MOLCATB.2015.11.021

Krajewska, B. (2018). Urea-aided calcium carbonate mineralization for engineering applications: a review. *J. Advanced Research* 13, 59–67. doi: 10.1016/j.jare.2017.10.009

Kumar, S., Kumar, S., and Mohapatra, T. (2021). Interaction between macro- and micro-nutrients in plants. *Front. Plant Sci.* 12. doi: 10.3389/FPLS.2021.665583

Kumari, D., Pan, X., Lee, D. J., and Achal, V. (2014). Immobilization of cadmium in soil by microbially induced carbonate precipitation with *Exiguobacterium undae* at low temperature. *Int. Biodeterioration Biodegradation* 94, 98–102. doi: 10.1016/J.IBIOD.2014.07.007

Landrigan, P. J. (1982). Occupational and community exposures to toxic metals: lead, cadmium, mercury and arsenic. *Western J. Med.* 137 (6), 531.

Lauchnor, E. G., Topp, D. M., Parker, A. E., and Gerlach, R. (2015). Whole cell kinetics of ureolysis by *Sporosarcina pasteurii*. *J. Appl. Microbiol.* 118 (6), 1321–1332. doi: 10.1111/JAM.12804

Lee, J. C., Son, Y. O., Pratheeshkumar, P., and Shi, X. (2012). Oxidative stress and metal carcinogenesis. *Free Radical Biol. Med.* 53 (4), 742–757. doi: 10.1016/J.FREERADBIOMED.2012.06.002

Li, M., Cheng, X., and Guo, H. (2013). Heavy metal removal by biomineralization of urease producing bacteria isolated from soil. *Int. Biodeterioration Biodegradation* 76, 81–85. doi: 10.1016/J.IBIOD.2012.06.016

Li, C., Zhou, K., Qin, W., Tian, C., Qi, M., Yan, X., et al. (2019). A review on heavy metals contamination in soil: effects, sources, and remediation techniques. *Soil Sediment Contamination: Int. J.* 28 (4), 380–394. doi: 10.1080/15320383.2019.1592108

Liao, Z., Wu, S., Xie, H., Chen, F., Yang, Y., and Zhu, R. (2023). Effect of phosphate on cadmium immobilized by microbial-induced carbonate precipitation: mobilization or immobilization? *J. Hazardous Materials* 443, 130242. doi: 10.1016/J.JHAZMAT.2022.130242

Liu, Y., Chen, Y., Huang, X., and Wu, G. (2017). Biomimetic synthesis of calcium carbonate with different morphologies and polymorphs in the presence of bovine serum albumin and soluble starch. *Materials Sci. Eng. C* 79, 457–464. doi: 10.1016/j.msec.2017.05.085

Liu, R., and Lian, B. (2019). Immobilization of Cd(II) on biogenic and abiotic calcium carbonate. *J. Hazardous Materials* 378, 120707. doi: 10.1016/j.jhazmat.2019.05.100

Liu, P., Shao, G. h., and Huang, R. p (2019). Study of the interactions between *S. pasteurii* and indigenous bacteria and the effect of these interactions on the MICP. *Arabian J. Geosciences* 12 (23), 1–10. doi: 10.1007/S12517-019-4840-Z/FIGURES/9

Liu, P., Zhang, Y., Tang, Q., and Shi, S. (2021). Bioremediation of metal-contaminated soils by microbially-induced carbonate precipitation and its effects on ecotoxicity and long-term stability. *Biochem. Eng. J.* 166, 107856. doi: 10.1016/J.BEJ.2020.107856

Lizarazo, M. F., Herrera, C. D., Celis, C. A., Pombo, L. M., Teherán, A. A., Piñeros, L. G., et al. (2020). Contamination of staple crops by heavy metals in sibaté, Colombia. *Heliyon* 6 (7). doi: 10.1016/J.HELIYON.2020.E04212

Lourenço, K. S., Suleiman, A. K. A., Pijl, A., van Veen, J. A., Cantarella, H., and Kuramae, E. E. (2018). Resilience of the resident soil microbiome to organic and inorganic amendment disturbances and to temporary bacterial invasion. *Microbiome* 6 (1). doi: 10.1186/S40168-018-0525-1

Lunn, R. M., Mehta, S. S., Jahnke, G. D., Wang, A., Wolfe, M. S., and Berridge, B. R. (2022). Cancer hazard evaluations for contemporary needs: highlights from new national toxicology program evaluations and methodological advancements. *J. Natl. Cancer Institute* 114 (11), 1441–1448. doi: 10.1093/JNCI/DJAC164

Lyu, C., Qin, Y., Chen, T., Zhao, Z., and Liu, X. (2022). Microbial induced carbonate precipitation contributes to the fates of cd and Se in cd-contaminated seleniferous soils. *J. Hazardous Materials* 423 (Pt A). doi: 10.1016/J.JHAZMAT.2021.126977

Ma, H., Wei, M., Wang, Z., Hou, S., Li, X., and Xu, H. (2020). Bioremediation of cadmium polluted soil using a novel cadmium immobilizing plant growth promotion strain bacillus sp. TZ5 loaded on biochar. *J. Hazardous Materials* 388, 122065. doi: 10.1016/j.jhazmat.2020.122065

Macias-Benitez, S., Garcia-Martinez, A. M., Caballero Jimenez, P., Gonzalez, J. M., Tejada Moral, M., and Parrado Rubio, J. (2020). Rhizospheric organic acids as biostimulants: monitoring feedbacks on soil microorganisms and biochemical properties. *Front. Plant Sci.* 11. doi: 10.3389/FPLS.2020.00633/BIBTEX

Mani, D., Sharma, B., Kumar, C., and Balak, S. (2012). Cadmium and lead bioaccumulation during growth stages alters sugar and vitamin c content in dietary vegetables. *Proc. Natl. Acad. Sci. India Section B - Biol. Sci.* 82 (4), 477–488. doi: 10.1007/S40011-012-0057-6/TABLES/4

Mawarda, P. C., Mallon, C. A., Le Roux, X., van Elsas, J. D., and Salles, J. F. (2022). Interactions between bacterial inoculants and native soil bacterial community: the case of spore-forming bacillus spp. *FEMS Microbiol. Ecol.* 98 (12), 1–11. doi: 10.1093/FEMSEC/FIAC127

Megharaj, M., and Naidu, R. (2017). Soil and brownfield bioremediation. *Microbial Biotechnol.* 10 (5), 1244. doi: 10.1111/1751-7915.12840

Mergelsberg, S. T., Riechers, S. L., Graham, T. R., Prange, M. P., and Kerisit, S. N. (2021). Effect of cd on the nucleation and transformation of amorphous calcium carbonate. *Crystal Growth Design* 21, 3384–3393. doi: 10.1021/acs.cgd.1c00169

Moreno, O. P., Pérez, R. G., Portillo, M. C., García, M. E. A., Moreno, G. E., Cruz, S. C., et al. (2018). Morphological, optical and structural analysis in CdS, CdS-$CdCO_3$ and

$CdCO_3$ thin solid films grown by chemical bath. *Optik* 157, 388–399. doi: 10.1016/j.ijleo.2017.11.036

Natsi, P. D., and Koutsoukos, P. G. (2022). Calcium carbonate crystallization on a microalgal matrix: the effects of heavy metal presence. *Crystals* 12, 1424. doi: 10.3390/cryst12101424

Norton, J. M., and Stark, J. M. (2011). Regulation and measurement of nitrification in terrestrial systems. *Meth. Enzymol.* 486, 343–362.

Nunes, I., Hansen, V., Bak, F., Bonnichsen, L., Su, J., Hao, X., et al. (2022). Succession of the wheat seed-associated microbiome as affected by soil fertility level and introduction of *Penicillium* and *Bacillus* inoculants in the field. *FEMS Microbiol. Ecol.* 98 (3), 1–14. doi: 10.1093/FEMSEC/FIAC028

Omoregie, A. I., Khoshdelnezamiha, G., Senian, N., Ong, D. E. L., and Nissom, P. M. (2017). Experimental optimization of various cultural conditions on urease activity for isolated *Sporosarcina pasteurii* strains and evaluation of their biocement potentials. *Ecol. Eng.* 109, 65–75. doi: 10.1016/J.ECOLENG.2017.09.012

Omori, W. P., Camargo, A. F., Goulart, K. C. S., Lemos, E. G. D. M., and Souza, J. A. M. (2016). Influence of vinasse application in the structure and composition of the bacterial community of the soil under sugarcane cultivation. *Int. J. Microbiol.*, 2349514. doi: 10.1155/2016/2349514

Pal, A., Dutta, S., Mukherjee, P. K., and Paul, A. K. (2005). Occurrence of heavy metal-resistance in microflora from serpentine soil of Andaman. *J. Basic Microbiol.* 45 (3), 207–218. doi: 10.1002/JOBM.200410499

Parihar, J. K., Parihar, P. K., Pakade, Y. B., and Katnoria, J. K. (2021). Bioaccumulation potential of indigenous plants for heavy metal phytoremediation in rural areas of shaheed bhagat singh nagar, punjab (India). *Environ. Sci. Pollut. Res.* 28 (2), 2426–2442. doi: 10.1007/S11356-020-10454-3/FIGURES/5

Peng, D., Qiao, S., Luo, Y., Ma, H., Zhang, L., Hou, S., et al. (2020). Performance of microbial induced carbonate precipitation for immobilizing cd in water and soil. *J. Hazardous Materials* 400, 123116. doi: 10.1016/J.JHAZMAT.2020.123116

Pérez-Villarejo, L., Takabait, F., Mahtout, L., Carrasco-Hurtado, B., Eliche-Quesada, D., and Sánchez-Soto, P. J. (2018). Synthesis of vaterite $CaCO_3$ as submicron and nanosized particles using inorganic precursors and sucrose in aqueous medium. *Ceramic Int.* 44, 5291–5296. doi: 10.1016/j.ceramint.2017.12.142

Poszytek, K., Karczewska-Golec, J., Ciok, A., Decewicz, P., Dziurzynski, M., Gorecki, A., et al. (2018). Genome-guided characterization of ochrobactrum sp. POC9 enhancing sewage sludge utilization–biotechnological potential and biosafety considerations. *Int. J. Environ. Res. Public Health* 15 (7). doi: 10.3390/ijerph15071501

Poszytek, K., Karczewska-Golec, J., Dziurzynski, M., Stepkowska-Kowalska, O., Gorecki, A., Decewicz, P., et al. (2019). Genome-wide and functional view of proteolytic and lipolytic bacteria for efficient biogas production through enhanced sewage sludge hydrolysis. *Molecules* 24 (14). doi: 10.3390/MOLECULES24142624

Qiao, S., Zeng, G., Wang, X., Dai, C., Sheng, M., Chen, Q., et al. (2021). Multiple heavy metals immobilization based on microbially induced carbonate precipitation by ureolytic bacteria and the precipitation patterns exploration. *Chemosphere* 274. doi: 10.1016/J.CHEMOSPHERE.2021.129661

Rajasekar, A., Wilkinson, S., and Moy, C. K. S. (2021). MICP as a potential sustainable technique to treat or entrap contaminants in the natural environment: a review. *Environ. Sci. Ecotechnology* 6, 100096. doi: 10.1016/J.ESE.2021.100096

Readyhough, T., Neher, D. A., and Andrews, T. (2021). Organic amendments alter soil hydrology and belowground microbiome of tomato (*Solanum lycopersicum*). *Microorganisms* 9 (8). doi: 10.3390/MICROORGANISMS9081561

Rizwan, M., Ali, S., Abbas, T., Zia-ur-Rehman, M., Hannan, F., Keller, C., et al. (2016). Cadmium minimization in wheat: a critical review. *Ecotoxicology Environ. Saf.* 130, 43–53. doi: 10.1016/J.ECOENV.2016.04.001

Robertson, G. P., and Groffman, P. M. (2015). Nitrogen transformations chapter contents. *Soil Microbiol. Ecol. Biochem.* 421–446. doi: 10.1016/B978-0-12-415955-6.00014-1

Ros, M., Hernandez, M. T., and García, C. (2003). Soil microbial activity after restoration of a semiarid soil by organic amendments. *Soil Biol. Biochem.* 35 (3), 463–469. doi: 10.1016/S0038-0717(02)00298-5

Russell, J. (1977). H.W. van der marel and h. beutelspache (1976). atlas of infrared spectroscopy of clay minerals and their admixtures. elsevier, Amsterdam 1976. *Clay Minerals* 12 (3), 279–280. doi: 10.1180/claymin.1977.012.3.11

Russell, J. D., and Fraser, A. R. (1994). "Infrared methods," in *Clay mineralogy: spectroscopic and chemical determinative methods*. Ed. M. J. Wilson (London: Chapman & Hall), 11–67.

Sachs, G., Scott, D. R., Weeks, D. L., Rektorscheck, M., and Melchers, K. (2001). Regulation of urease for acid habitation. *Helicobacter Pylori*, 277–283. doi: 10.1128/9781555818005.ch25

Sackey, J., Maaza, M., Ngillirabanga, J., and Gibaud, A. (2019). Analysis of the miscibility of Cd^{2+} ions in $CaCO_3$. *Surfaces Interfaces* 17, 100356. doi: 10.1016/j.surfin.2019.100356

Satarug, S., Baker, J. R., Urbenjapol, S., Haswell-Elkins, M., Reilly, P. E. B., Williams, D. J., et al. (2003). A global perspective on cadmium pollution and toxicity in non-occupationally exposed population. *Toxicol. Lett.* 137 (1–2), 65–83. doi: 10.1016/S0378-4274(02)00381-8

Satarug, S., and Moore, M. R. (2004). Adverse health effects of chronic exposure to low-level cadmium in foodstuffs and cigarette smoke. *Environ. Health Perspect.* 112 (10), 1099. doi: 10.1289/EHP.6751

Satarug, S., Vesey, D. A., and Gobe, G. C. (2017). Health risk assessment of dietary cadmium intake: do current guidelines indicate how much is safe? *Environ. Health Perspect.* 125 (3), 284–288. doi: 10.1289/EHP108

Schuchmann, K., and Müller, V. (2016). Energetics and application of heterotrophy in acetogenic bacteria. *Appl. Environ. Microbiol.* 82 (14), 4056–4069. doi: 10.1128/AEM.00882-16/ASSET/10323180-8FC3-4FA6-B9FC-7E62C3979554/ASSETS/GRAPHIC/ZAM9991172840006.JPEG

Seitz, T. J., Schütte, U. M. E., and Drown, D. M. (2022). Unearthing shifts in microbial communities across a soil disturbance gradient. *Front. Microbiol.. 13* 781051. doi: 10.3389/FMICB.2022.781051/FULL

Shannon, R. D. (1976). Revised effective ionic radii and systematic studies of interatomic distances in halides and chalcogenides. *Acta Crystallographica A32*, 751–767. doi: 10.1107/S0567739476001551

Sharma, M., Saleh, D., Charron, J. B., and Jabaji, S. (2020). A crosstalk between *Brachypodium* root exudates, organic acids, and *Bacillus velezensis* B26, a growth promoting bacterium. *Front. Microbiol.* 11. doi: 10.3389/FMICB.2020.575578/BIBTEX

Skujins, J. J., and McLaren, A. D. (1967). Enzyme reaction rates at limited water activities. *Science* 158 (3808), 1569–1570. doi: 10.1126/SCIENCE.158.3808.1569

Styczynski, M., Biegniewski, G., Decewicz, P., Rewerski, B., Debiec-Andrzejewska, K., and Dziewit, L. (2022). Application of psychrotolerant Antarctic bacteria and their metabolites as efficient plant growth promoting agents. *Front. Bioengineering Biotechnol.* 10. doi: 10.3389/FBIOE.2022.772891

Sun, X., Miao, L., Tong, T., and Wang, C. (2019). Study of the effect of temperature on microbially induced carbonate precipitation. *Acta Geotechnica* 14 (3), 627–638. doi: 10.1007/S11440-018-0758-Y/FIGURES/9

Sun, L., Song, K., Shi, L., Duan, D., Zhang, H., Sun, Y., et al. (2021). Influence of elemental sulfur on cadmium bioavailability, microbial community in paddy soil and cd accumulation in rice plants. *Sci. Rep.* 11 (1), 1–9. doi: 10.1038/s41598-021-91003-x

Tao, C., Li, R., Xiong, W., Shen, Z., Liu, S., Wang, B., et al. (2020). Bio-organic fertilizers stimulate indigenous soil *Pseudomonas* populations to enhance plant disease suppression. *Microbiome* 8 (1), 1–14. doi: 10.1186/S40168-020-00892-Z/FIGURES/6

Tesoriero, A. T., and Pankow, J. F. (1996). Solid solution partitioning of Sr^{2+}, Ba^{2+}, and Cd^{2+} in calcite. *Geochimica Cosmochimica Acta* 60 (6), 1053–1063. doi: 10.1016/0016-7037(95)00449-1

Tian, W., Li, L., Xiao, X., Wu, H., Wang, Y., Hu, Z., et al. (2022). Identification of a plant endophytic growth-promoting bacteria capable of inhibiting cadmium uptake in rice. *J. Appl. Microbiol.* 132 (1), 520–531. doi: 10.1111/JAM.15201

Tran, T. A., and Popova, L. P. (2013). Functions and toxicity of cadmium in plants: recent advances and future prospects. *Turkish J. Bot.* 37 (1), 1–13. doi: 10.3906/BOT-1112-16

Trevors, J. T. (1984). Effect of substrate concentration, inorganic nitrogen, O_2 concentration, temperature and pH on dehydrogenase activity in soil. *Plant Soil* 77 (2), 285–293. doi: 10.1007/BF02182931

Trevors, J. T., Stratton, G. W., and Gadd, G. M. (1986). Cadmium transport, resistance, and toxicity in bacteria, algae, and fungi. *Can. J. Microbiol.* 32 (6), 447–464. doi: 10.1139/M86-085

Trivedi, P., Leach, J. E., Tringe, S. G., Sa, T., and Singh, B. K. (2020). Plant–microbiome interactions: from community assembly to plant health. *Nat. Rev. Microbiol.* 18 (11), 607–621. doi: 10.1038/s41579-020-0412-1

Tudoreanu, L., and Phillips, C. J. C. (2004). Modeling cadmium uptake and accumulation in plants. *Adv. Agron.* 84, 121–157. doi: 10.1016/S0065-2113(04)84003-3

van Paassen, L. A. (2009) *Biogrout, ground improvement by microbial induced carbonate precipitation*. Available at: https://repository.tudelft.nl/islandora/object/uuid%3A5f3384c4-33bd-4f2a-8641-7c665433b57b.

von Mersi, W., and Schinner, F. (1991). An improved and accurate method for determining the dehydrogenase activity of soils with iodonitrotetrazolium chloride. *Biol. Fertility Soils* 11 (3), 216–220. doi: 10.1007/BF00335770

Wang, Y., Soga, K., DeJong, J. T., and Kabla, A. J. (2021). Effects of bacterial density on growth rate and characteristics of microbial-induced $CaCO_3$ precipitates: particle-scale experimental study. *J. Geotechnical Geoenvironmental Eng.* 147 (6), 04021036. doi: 10.1061/(ASCE)GT.1943-5606.0002509

Wang, M., Wu, S., Guo, J., Zhang, X., Yang, Y., Chen, F., et al. (2019a). Immobilization of cadmium by hydroxyapatite converted from microbial precipitated calcite. *J. Hazardous Materials* 366, 684–693. doi: 10.1016/J.JHAZMAT.2018.12.049

Wang, M., Wu, S., Guo, J., Zhang, X., Yang, Y., Chen, F., et al. (2019b). Immobilization of cadmium by hydroxyapatite converted from microbial precipitated calcite. *J. Hazardous Materials* 366, 684–693. doi: 10.1016/J.JHAZMAT.2018.12.049

Wei, T., Li, H., Yashir, N., Li, X., Jia, H., Ren, X., et al. (2022). Effects of urease-producing bacteria and eggshell on physiological characteristics and cd accumulation of pakchoi (*Brassica chinensis* l.) plants. *Environ. Sci. pollut. Res.* 29 (42), 63886–63897. doi: 10.1007/S11356-022-20344-5/FIGURES/5

Wendeborn, S. (2020). The chemistry, biology, and modulation of ammonium nitrification in soil. *Angewandte Chemie Int. Edition* 59 (6), 2182–2202. doi: 10.1002/ANIE.201903014

Wickham, H. (2016). "ggplot2: elegant graphics for data analysis," in *Use r! series* (Springer-Verlag New York). Available at: http://had.co.nz/ggplot2/book.

Widdel, F., and Musat, F. (2016). Diversity and common principles in enzymatic activation of hydrocarbons: an introduction. *Aerobic Utilization Hydrocarbons Oils Lipids*, 1–30. doi: 10.1007/978-3-540-77587-4_70

Wiley, W. R., and Stokes, J. L. (1962). Requirement of an alkaline pH and ammonia for substrate oxidation by *Bacillus pasteurii*. *J. Bacteriology* 84 (4), 730–734. doi: 10.1128/JB.84.4.730-734.1962

Williams, A., and de Vries, F. T. (2020). Plant root exudation under drought: implications for ecosystem functioning. *New Phytol.* 225 (5), 1899–1905. doi: 10.1111/NPH.16223

Włodarczyk, T., Stłpniewski, W., and Brzezińska, M. (2002). Dehydrogenase activity, redox potential, and emissions of carbon dioxide and nitrous oxide from *Cambisols* under flooding conditions. *Biol. Fertility Soils* 36 (3), 200–206. doi: 10.1007/S00374-002-0513-1

Xu, G., Fan, X., and Miller, A. J. (2012). Plant nitrogen assimilation and use efficiency. *Annu. Rev. Plant Biol.* 63, 153–182. doi: 10.1146/ANNUREV-ARPLANT-042811-105532

Xu, S., Liu, Y., Wang, J., Yin, T., Han, Y., Wang, X., et al. (2015). Isolation and potential of ochrobactrum sp. NW-3 to increase the growth of cucumber. *Int. J. Agric. Policy Res.* 3 (9), 341–350. doi: 10.15739/IJAPR.059

Yakushi, T., and Matsushita, K. (2010). Alcohol dehydrogenase of acetic acid bacteria: structure, mode of action, and applications in biotechnology. *Appl. Microbiol. Biotechnol.* 86 (5), 1257–1265. doi: 10.1007/S00253-010-2529-Z

Yang, Z., Liu, Z., Dabrowska, M., Debiec-Andrzejewska, K., Stasiuk, R., Yin, H., et al. (2021). Biostimulation of sulfate-reducing bacteria used for treatment of hydrometallurgical waste by secondary metabolites of urea decomposition by ochrobactrum sp. POC9: from genome to microbiome analysis. *Chemosphere* 282, 131064. doi: 10.1016/J.CHEMOSPHERE.2021.131064

Yang, J., Pan, X., Zhao, C., Mou, S., Achal, V., Al-Misned, F. A., et al. (2016). Bioimmobilization of heavy metals in acidic copper mine tailings soil. *Geomicrobiology J.* 33 (3–4), 261–266. doi: 10.1080/01490451.2015.1068889

Yang, Z., Uhrynowski, W., Jakusz, G., Retka, J., Karczewska-Golec, J., Debiec-Andrzejewska, K., et al. (2020). Biochemical treatment of leachates from hydrometallurgical recycling of spent alkaline batteries. *Hydrometallurgy* 191. doi: 10.1016/J.HYDROMET.2019.105223

Yi, H., Zheng, T., Jia, Z., Su, T., and Wang, C. (2021). Study on the influencing factors and mechanism of calcium carbonate precipitation induced by urease bacteria. *J. Crystal Growth* 564, 126113. doi: 10.1016/J.JCRYSGRO.2021.126113

Yu, X., Zhao, J. T., Liu, X., Sun, L. X., Tian, J., and Wu, N. (2021). Cadmium pollution impact on the bacterial community structure of arable soil and the isolation of the cadmium resistant bacteria. *Front. Microbiol.* 12. doi: 10.3389/FMICB.2021.698834

Zambelli, B., Musiani, F., Benini, S., and Ciurli, S. (2011). Chemistry of Ni2+ in urease: sensing, trafficking, and catalysis. *Accounts Chem. Res.* 44 (7), 520–530. doi: 10.1021/AR200041K/SUPPL_FILE/AR200041K_SI_001.PDF

Zare, A. A., Khoshgoftarmanesh, A. H., Malakouti, M. J., Bahrami, H. A., and Chaney, R. L. (2018). Root uptake and shoot accumulation of cadmium by lettuce at various Cd:Zn ratios in nutrient solution. *Ecotoxicology Environ. Saf.* 148, 441–446. doi: 10.1016/J.ECOENV.2017.10.045

Zhao, R., Liu, J., Xu, N., He, T., Meng, J., and Liu, Z. (2022). Urea hydrolysis in different farmland soils as affected by long-term biochar application. *Front. Environ. Sci.* 10. doi: 10.3389/fenvs.2022.950482

Zhao, Y., Yao, J., Yuan, Z., Wang, T., Zhang, Y., and Wang, F. (2017). Bioremediation of cd by strain GZ-22 isolated from mine soil based on biosorption and microbially induced carbonate precipitation. *Environ. Sci. Pollut. Res. Int.* 24 (1), 372–380. doi: 10.1007/S11356-016-7810-Y

frontiers | Frontiers in Plant Science

TYPE Original Research
PUBLISHED 11 August 2023
DOI 10.3389/fpls.2023.1196130

OPEN ACCESS

EDITED BY
Patrizia Cesaro,
University of Eastern Piedmont, Italy

REVIEWED BY
Flavio Anastasia,
Università del Piemonte Orientale, Italy
Huanyun Yu,
Chinese Academy of Sciences (CAS), China

*CORRESPONDENCE
Juan Li
adalee619@163.com

RECEIVED 29 March 2023
ACCEPTED 25 July 2023
PUBLISHED 11 August 2023

CITATION
Li P, Xiong Z, Tian Y, Zheng Z, Liu Z, Hu R, Wang Q, Ao H, Yi Z and Li J (2023) Community-based mechanisms underlying the root cadmium uptake regulated by Cd-tolerant strains in rice (*Oryza sativa*. L). *Front. Plant Sci.* 14:1196130. doi: 10.3389/fpls.2023.1196130

Community-based mechanisms underlying the root cadmium uptake regulated by Cd-tolerant strains in rice (*Oryza sativa*. L)

Peng Li[1], Ziqin Xiong[1], Yunhe Tian[1], Zhongyi Zheng[1], Zhixuan Liu[2], Ruiwen Hu[1], Qiming Wang[1], Hejun Ao[1], Zhenxie Yi[1] and Juan Li[1]*

[1]College of Agronomy, Hunan Agricultural University, Changsha, China, [2]Hunan Rice Research Institute, Hunan Academy of Agricultural Sciences, Changsha, China

In recent years, the problem of Cd pollution in paddy fields has become more and more serious, which seriously threatens the safe production of food crops and human health. Using microorganisms to reduce cadmium pollution in rice fields is a green, safe and efficient method, the complicated interactions between the microbes in rice roots throughout the process of cadmium absorption by rice roots are poorly understood. In this investigation, a hydroponic pot experiment was used to examine the effects of bacteria R3 (*Herbaspirillum* sp) and T4 (*Bacillus cereus*) on cadmium uptake and the endophytic bacterial community in rice roots. The results showed that compared with CK (Uninoculated bacterial liquid), the two strains had significant inhibitory or promotive effects on cadmium uptake in rice plant, respectively. Among them, the decrease of cadmium content in rice plants by R3 strain reached 78.57-79.39%, and the increase of cadmium content in rice plants by T4 strain reached 140.49-158.19%. Further investigation showed that the cadmium content and root cadmium enrichment coefficient of rice plants were significantly negatively correlated with the relative abundances of *Burkholderia* and *Acidovorax*, and significantly positively correlated with the relative abundances of *Achromobacter*, *Agromyces* and *Acidocella*. Moreover, a more complex network of microbes in rice roots inhibited rice plants from absorbing cadmium. These results suggest that cadmium uptake by rice plants is closely related to the endophytic bacterial community of roots. This study provides a reference scheme for the safe production of crops in cadmium contaminated paddies and lays a solid theoretical foundation for subsequent field applications.

KEYWORDS

rice, cadmium pollution, microbiological control, endophytic bacterial community, interaction

1 Introduction

Cadmium (Cd) is not essential to plant growth, but is toxic to plants (Huang et al., 2020). When a specific concentration is reached, it hurts plant cell structure and disrupts normal cell physiological processes, and lead to abnormal growth and development of plants or death (Wan and Zhang, 2012). Further entry into people and animals via the food chain will seriously threaten their life and health (Kukusamude et al., 2021). As a significant food crop, rice (*Oryza sativa* L.) is one of the main sources of Cd buildup in the human body (Li et al., 2017). A better understanding of the mechanism of Cd uptake and accumulation in rice is essential for developing strategies to prevent excessive Cd from entering the food chain. Plant roots are the most critical site for Cd absorption and accumulation (Song et al., 2016). Therefore, it is crucial to comprehend the process by which Cd is absorbed by rice roots. The employment of microorganisms to control Cd absorption by crops has sparked a lot of attention due to its low cost, significant effect, and ecological environmental protection (Cheng et al., 2021b; Wang et al., 2022). At present, numerous research has revealed that adding strains to rice's rhizosphere not only helps the plant grow and develop (Kuang et al., 2016), but also increases the plant's ability to withstand Cd while lowering its Cd content (Ma et al., 2016; El-Esawi et al., 2020; Cheng et al., 2021a).

Microbial control of Cd pollution in rice is mainly achieved through two aspects. First, microorganisms can interact with Cd in the environment to passivate or chelate Cd ions, as a result, the bioavailability of Cd in the environment is reduced, increasing rice tolerance to Cd and reducing Cd absorption by roots to meet the goal of maintaining normal rice development and expansion and lowering the Cd content of rice grains (Xu et al., 2018; Zhang et al., 2018; Cui et al., 2020; Li et al., 2021). Meanwhile, microorganisms can also secrete organic acids that release Cd into ionic form, increasing its bioavailability and promote its absorption by plants (Chen et al., 2014; He et al., 2020), thereby reducing the Cd content in paddy fields. Microorganisms with this latter function are often used in conjunction with other crops before rice production to reduce Cd content in the paddy field, to achieve the goal of lowering the Cd content of rice when replanting rice. Second, microorganisms can directly interact with plants to influence the expression of key channel proteins involved in Cd uptake and transport, hence influencing Cd uptake and transport in plants (Chatterjee et al., 2020; Zhou et al., 2020). Furthermore, the structure and function of the plant endophytic bacterial community are linked to Cd uptake and transport (Teixeira et al., 2014). The structure and function of this community will change according to the interaction between exogenous endophytic bacteria and their own endophytic bacteria, thus either limiting or boosting Cd absorption and transport by plants (He et al., 2022).

In this study, we used Cd-tolerant endophytic bacteria previously isolated from rice seeds in the laboratory and selected two strains with strong comprehensive physiological functions for rice hydroponic pot experiments, to investigate the impact of inoculation on Cd absorption in rice and analyze the microbial community of rice roots after inoculation. Overall, the goal of this research is to: (1) Analyze the growth and Cd accumulation of rice plants at the highest tillering stage after inoculation with abovementioned strains; (2) Explore the effect of endophytic bacterial inoculation on the endophytic bacterial community in the roots of rice plants; (3) Elucidate the possible mechanism(s) by which inoculation of endophytic bacteria affect Cd uptake in rice plants. This work offers a new method for controlling Cd pollution in rice fields, reducing Cd buildup in rice grains, and a new practical value for the utilization of moderately and mildly Cd-contaminated farmland. It is of great significance for mitigating environment problems and ensuring food security.

2 Materials and methods

2.1 Experiment material

The tested rice (*Oryza sativa*. L Huanghuazhan), a thermosensitive conventional rice variety that readily accumulates Cd, was provided by the Hunan Rice Research Institute. The water sorting method was used to screen out the full-grained rice seeds, after that, the seeds were disinfected by soaking them in a 5% solution of sodium hypochlorite for 15 minutes and then rinsing them 8-10 times with purified water to make sure that no sodium hypochlorite solution remained. After soaking the sterilized seeds for 2-3 days in clean water, they were laid flat in a germination box and incubated in a constant temperature incubator (30°C) until they reached the three-leaf stage. Rice seedlings with identical development and size were chosen for pot experiments.

Cd-resistant endophytic bacterial strains R3 (*Herbaspirillum* sp) and T4 (*Bacillus cereus*) were screened from Huanghuazhan rice seeds in a previous study. All organisms stocks were stored at -80°C. The two strains were seeded into 500 mL of LB liquid solution at 5% before the test and shaken for 36 hours at 30°C and 180 rpm. Low-temperature high-speed centrifugation was used to remove the fermentation broth. The bacteria were resuspended in 0.85% KCl solution, the cell counting plate was used to determine the concentration under the optical microscope, and 1×10^8 cfu·mL^{-1} bacterial solution was prepared for use. The nutrient solution tested was Kimura B (Yue et al., 2015), and exogenous Cd was added as $CdCl_2$ to provide a nutritional solution with a Cd content of 0.3 mg·L^{-1} (Simulate farmland with moderate cadmium pollution in China).

2.2 Pot experiment design

Rice hydroponic pot trials were conducted in a greenhouse at Hunan Agricultural University in April 2017, with daytime temperatures of 29-40°C and nighttime temperatures of 24-29°C, and a relative humidity of 65-85%. The pot was a polyethylene (PE) cuboid basin with an inner length of 65 cm, a width of 40 cm, and a height of 16 cm. Each basin was divided into 20 L Kimura B nutrient solution (Cd concentration 0.3 mg·L^{-1}, pH 7.0). The rice seedlings were transplanted into hydroponic pots and fixed with foam plates

and planting baskets, after one week of culture, the strains were inoculated on the roots of the rice seedlings (100 mL 1×10^8 cfu·mL^{-1} bacterial suspension). Three treatment groups were established: (1) R3: Inoculate R3 strain; (2) T4: Inoculate T4 strain; (3) CK: The blank control group was not inoculated with strain, and the same amount of distilled water was added. For each treatment, eight replicate pots were put up. During the rice growing time, the rice was cultured to the highest tillering stage by regularly adding the same amount of nutrient solution. Random sampling was used to measure the dry matter weight of rice plants and the Cd content of various plant components, and further analysis was done on changes in the endophytic microbial community of rice roots.

2.3 Sampling

For each treatment, random sampling was done when the rice was at its highest tillering stage, 8 plants was used to detect dry matter weight and cadmium content, and 4 plants was used to detect microbial community. The entire rice plant was split into roots and aboveground components, then thoroughly cleaned using distilled water, packed into a clean envelope bag, respectively, placed in an oven at 105°C for 30 minutes, dried to a constant weight at 80°C, and then the dry weight of each portion was measured. Each sample was then pulverized into a powder, and after further processing, the Cd content of each part of the plant was detected.

For surface sterilization and disinfection, the rice roots of each treatment were first washing for three minutes in 5% NaClO after being rinsed with pure water, followed by 5 minutes in 75% ethanol. Finally, the roots were repeatedly rinsed with pure water to remove any remaining chemicals from the root surface. The roots were pounded into a powder in a sterile mortar using liquid nitrogen for subsequent DNA extraction.

2.4 Detection of biomass and Cd content

Rice roots and aboveground sections were weighed using an electronic balance to assess their dry matter content. 0.5 g samples of various sections of the rice plant were weighed into polytetrafluoroethylene jars, to which 5 mL of premium pure nitric acid (GR, 99.7%) were added, after which the jars were sealed and left overnight. Next morning 1 mL of H_2O_2 was added and the samples then placed in a microwave digestion apparatus (Changzhou, DTD-50). After the digestion was complete, it was allowed to cool, before slowly opening the tank cover to exhaust. The digestion tank was placed on a temperature-controlled electric hot plate at 150 °C to reduce the acid concentration in the solution. After cooling again, after being transferred to a 10.0 mL volumetric flask, the digestion solution, and the digestion tank was washed 3 times with a small amount of distilled water, combine the washings in the volumetric flask (50 mL) and diluted to the mark, and mixed well. By using inductively coupled plasma mass spectrometry (ICP-MS, EXPEC 7200, China), the Cd concentration was measured (Peng et al., 2014).

2.5 Detection of endogenous microbial communities

The Plant Genome DNA Extraction Kit (TransGen Biotech) was used to extract DNA from various parts of the rice plant, and the extracted genomic DNA was used as a template for PCR amplification. The V5-V7 region was selected for amplification of 16S rRNA gene using specific primers 799 F (5 '-AACmGG attagataccCGG-3') and 1115 R (5 '-AGGGTTGCGCTCGTTG-3') (Kembel et al., 2014). The length and concentration of PCR amplification products were detected by 1% agarose-gel electrophoresis. After qualified detection, a library was constructed. Finally, PE250 sequencing was performed on the constructed amplified library using Illumina Nova 6000 platform.

2.6 Data processing and statistical analysis

The data were processed under the guidance of Zheng (Zheng et al., 2022), as detailed in the Supplementary Material.

3 Results

3.1 Effects of endophytic bacteria on dry matter weight and Cd uptake and transport in rice plants

The strains were inoculated after transplanting of the three-leaf period of rice seedlings, and they were cultured until the plants reached their highest tillering stage. The action time of the strains was 24 days. According to Table 1, compared to CK, the inoculation of strains R3 and T4 had no significant effect on the dry matter weight of the roots and aboveground portions of rice plants ($P < 0.05$).

Table 1 shows that for each treatment, the roots of the rice plants had a higher Cd content than the aboveground sections. However, the Cd uptake of rice plants showed two divergent trends, promotion and inhibition, with the inoculation of the different strains. Inoculation with strain R3 may dramatically lower the Cd content of rice roots and aboveground portions when compared to CK ($P < 0.05$), with reduction rates reaching 78.29% and 79.36%, respectively, while the Cd content of rice roots and aboveground sections may be greatly increased by inoculation with strain T4 ($P < 0.05$), at rates of 158.19% and 140.79%, respectively. When rice is in its highest tillering stage, compared with CK, Cd accumulation in roots and aboveground parts of rice plants treated with both strains changed significantly ($P < 0.05$), and Cd was mainly enriched in the roots of rice plants (Table S1). Among them, the inoculation of R3 strain significantly reduced the cadmium accumulation in the roots and aboveground parts of rice plants, and the inoculation of T4 strain significantly increased the cadmium accumulation in the roots and aboveground parts of rice plants ($P < 0.05$). In comparison to CK, inoculation with strain R3 considerably reduced and inoculation with strain T4 dramatically raised the Cd enrichment coefficient of rice roots,

respectively (Table 1) ($P < 0.05$). There was no significant change in the Cd transfer coefficient from roots to shoots of rice plants treated with either strain compared with CK (Table 1) ($P < 0.05$). These findings demonstrate that strain R3 inoculation mainly reduces the absorption of Cd by rice roots, while strain T4 inoculation mostly boosts rice roots' ability to absorb Cd. Therefore, the root system is the key compartment influencing Cd absorption in rice plants.

3.2 Overall changes in the microbial community of rice roots under the action of endophytic bacteria

To further analyze the underlying mechanism of the effects of inoculated strains on Cd uptake in rice roots, we analyzed the overall changes in the endophytic microbial community in rice roots of inoculated and uninoculated treatments. We obtained an average of 22,372 raw sequences per sample, the resampling depth of each sample was 10203 sequences, and the cluster was 587 OTUs.

The rarefaction curves in Figure S1 demonstrated that the sequencing depth was enough for the future analysis. Alpha-diversity analysis of the endophytic bacterial community in rice roots showed that the Shannon index, Richness index, Pielou evenness and Simpson index of the rice root microbial community after inoculation with strains R3 and T4 did not change significantly compared with the control (Figures 1A, B, Figure S2) ($P < 0.05$). PCoA (Figure 1C) analysis showed that the samples between the three treatments were intermixed. There was no significant change in bacterial community structure between the CK, R3, and T4 treatments were shown to be inconsequential by the different tests of MRPP, ANOSIM, and ADONIS (three nonparametric multivariate statistical tests) based on the Bray-Curtis matrix (Table S2). At the genus level, the most abundant genera in rice roots were *Escherichia/Shigella*, *Acinetobacter*, *Rhodanobacter*, *Achromobacter*, *Pseudomonas*, *Burkholderia*, *Alicyclobacillus*, *Agromyces* and *Curtobacterium*, which together accounted for more than 77% of the total abundance (Figure 1D). Compared with CK, the abundance of *Escherichia/Shigella* and *Acinetobacter* were increased in R3 treatment, while the numbers of *Rhodanobacter*, *Achromobacter* and *Pseudomonas* were decreased. The abundances of *Escherichia/Shigella*, *Acinetobacter* and *Achromobacter* were increased in the T4 treatment, while the abundance of *Rhodanobacter*, *Pseudomonas* and *Burkholderia* were decreased (Table S3) ($P < 0.05$). The results showed that inoculating R3 and T4 had no significant influence on microbial community diversity in rice plant roots, but did modify the relative abundances of their endophytic bacterial populations.

3.3 Correlation between rice plant-related indicators and root bacterial taxa

The relative abundance of bacterial taxa in rice roots was substantially linked with some rice plant characteristics, according to Pearson's correlation analysis (Figure 2). The results revealed that among the three sample groups, the bacterial groups connected with rice plant dry matter weight and Cd-related variables differed at the genus level. Rice plant dry matter weight was strongly negatively connected with *Escherichia/Shigella* and *Acinetobacter*, and considerably favorably correlated with *Rhodanobacter*, *Pseudomonas*, *Alicyclobacillus*, and *Massilia*. The Cd content and root Cd enrichment coefficient of rice plants were strongly favorably correlated with *Achromobacter*, *Agromyces* and *Acidocella*, and considerably negatively correlated with *Burkholderia* and *Acidovorax*. The Cd accumulation in rice plants was strongly favorably correlated with *Achromobacter* and *Acidocella*, and significantly negatively correlated with *Acidovorax*, and the Cd accumulation in rice roots was also negatively correlated with *Burkholderia*. The Cd transport coefficient from roots to aboveground parts of rice plants was negatively correlated with *Agromyces* and *Buttiauxella*. These results showed that rice plant Cd absorption is influenced by the structure and changes of the endophytic bacterial community in the roots, among them, more microorganism species and quantity (Figure 2, Table S3) exhibited a strong link with Cd absorption in rice roots, fewer microorganism kinds and numbers (Figure 2, Table S3) exhibited a significant link with the cadmium transfer coefficient from the root to the aboveground parts of rice. among them, the types and quantities of more flora (Figure 2, Table S3) were significantly correlated with Cd uptake by rice roots. The types and quantities of less flora (Figure 2, Table S3) were significantly correlated with the Cd transport coefficient from roots to aboveground parts in rice.

3.4 Topological characteristics of the microbial networks in rice roots under different strain treatments

To investigate whether the topological structure of interactions between endophytic bacteria in the roots of uninoculated and treated

TABLE 1 Effects of endophytic bacteria on dry matter weight and Cd uptake in rice plants.

Treatment	Dry matter weight/g·plant^{-1}		Cd concentration/mg·kg^{-1}		BCF	TF
	Root	Aboveground part	Root	Aboveground part		
CK	0.66 ± 0.05a	2.59 ± 0.16a	28.01 ± 1.31b	2.28 ± 0.27b	93.36 ± 4.36b	0.082 ± 0.012a
R3	0.64 ± 0.04a	2.44 ± 0.17a	6.08 ± 0.81c	0.47 ± 0.09c	20.25 ± 2.72c	0.079 ± 0.022a
T4	0.63 ± 0.02a	2.52 ± 0.21a	72.32 ± 7.21a	5.49 ± 0.74a	241.01 ± 24.04a	0.076 ± 0.008a

According to the Duncan test, mean values (± S.D., n = 8) with distinct letters differ substantially between CK, R3 and T4 treatments (P < 0.05). BCF of rice root to Cd in Nutrient solution, TF of Cd from rice roots to aboveground parts.

10.3389/fpls.2023.1196130

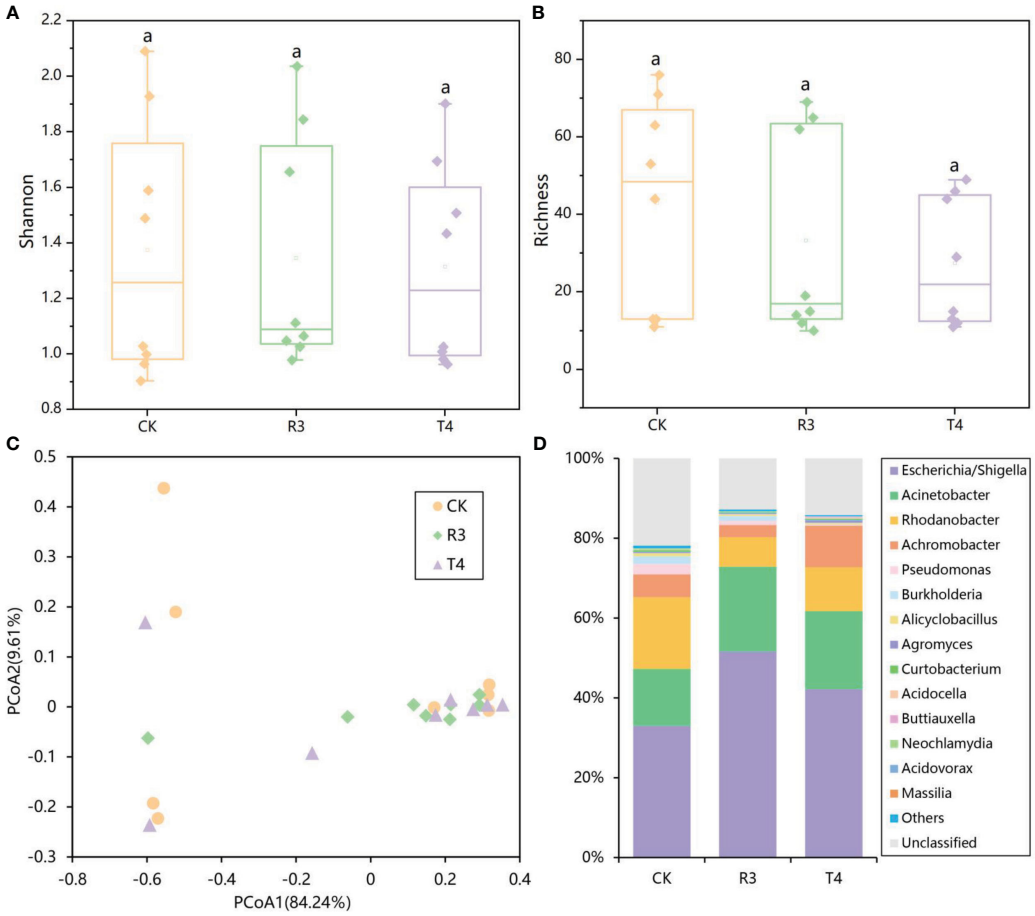

FIGURE 1
(A) Shannon-Wiener index, **(B)** Richness index, **(C)** 16S rRNA Gene Sequence Data using Principal Coordinates Analysis (PCoA) and **(D)** a detailed analysis of the relative abundance of endophytic populations at the genus level showing differences in the endophytic microbial community among rice roots with or without inoculation of test strains.

rice plants were different, we constructed endophytic bacterial community-related networks (Figure 3), which showed that endophytic bacterial interactions were different in response to the inoculated strains. The network inoculated with strain R3 had more links than CK, while the harmonic geodesic distance and average path distance were lower than CK. Compared with CK, the network inoculated with the T4 strain had fewer links and increased harmonic geodesic distance and average path distance (Table S4). Potential interactions within both the R3 and T4 treated endophytic bacterial communities had higher positive correlations compared with CK (Figure 3). Interestingly, only 5-8 phyla per treatment participated in the network, which may have been due to the dominance of these phyla in the respective endophytic bacterial communities, and further implied their critical roles in root function and ecological processes for rice. Compared with the CK interaction network, in the R3 treatment network, the frequency of *Acidobacteria* and *Deinococcus-Thermus* decreased, *Firmicutes* increased, and *Bacteroidetes* were absent, while *Nitrospirae* appeared. Compared with CK, in the T4 treatment network, the frequency of *Proteobacteria* and *Firmicutes* increased, while *Actinobacteria* decreased, and *Acidobacteria* and *Deinococcus-Thermus* were absent (Figure 3). Furthermore, we determined the topological role of each OTU in the endophytic bacterial network for each of the three treatment groups by RMT-based network analysis (Figure 4) and found that only one key taxon, OUT_471 (*Proteobacteria*), was detected in CK.

3.5 Association between network structure and Cd content in rice roots

The network's complexity may be represented by links, nodes, average path distance, and so on. A larger number of links and nodes, as well as a shorter average path distance, imply that a network is more sophisticated (Ye et al., 2012). According to Pearson correlation analysis, the number of links in the network was significantly inversely associated with Cd content in rice roots (P=0.009) (Figure 5), implying that lower Cd content in rice plants was correlated with more intricate networks in rice roots.

4 Discussion

This research evaluated the impact of two distinct bacterial strains on Cd buildup in rice plants and discovered that they had

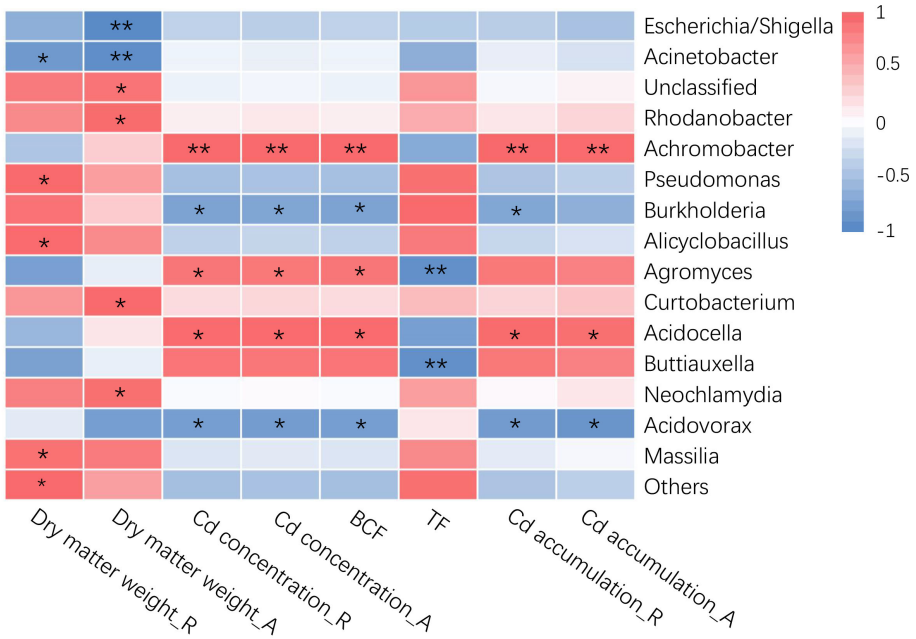

FIGURE 2
Correlations between root-specific enriched taxa (genus level) and plant variables of rice. "R" represents the root of rice, "A" represents the aboveground part of rice. The color represents the Pearson correlation coefficients (r). The asterisks in the grids show Pearson's correlations that are significant: *, $P<0.05$; **, $P<0.01$.

opposite effects. The inoculation of strain R3 exhibited a strong inhibitory impact on rice plant Cd absorption, and it could potentially be used as an exogenous additive to directly reduce the Cd content in rice plants. The rice plants' ability to absorb Cd was greatly enhanced by strain T4 inoculation, and this strain was able to interact with heavy metal hyperaccumulators, allowing plants to efficiently enrich Cd in paddy soil. The Cd content of rice plants may be indirectly reduced by lowering the Cd content of the paddy soil by harvesting and disposing the Cd-enriched plants. Therefore, both strains have potential value in controlling Cd pollution in rice.

4.1 The overall impact of inoculated strains on rice growth and Cd uptake

As a heavy metal, Cd places stress on plant growth and development, and can also lead to plant death at high concentrations (Andresen and Küpper, 2013). Some microorganisms can mitigate the toxicity of Cd through biosorption, precipitation, complexation and chelation (Siripornadulsil and Siripornadulsil, 2013), meanwhile, there are also microorganisms that can promote plant growth through symbiotic interactions, auxin synthesis, and improved disease and stress resistance (Shan et al., 2020). In this study, the tested strains, R3 and T4, were endophytic bacteria screened from seeds of the rice variety Huanghuazhan, with functions such as tolerance to high Cd concentration, siderophore production, phosphorus dissolution and nitrogen fixation (Table S5). In the hydroponic pot experiment, after the rice roots were inoculated with the respective strains, it was discovered that there was no significant influence on rice growth and development. This may be because the nutrients in the growth solution were all in the form of ions, which could have been easily absorbed by the rice plants, and, as such, the phosphorus-solubilization, nitrogen fixation and other functions of the strains were not fully exerted, so no obvious growth-promoting effects were shown (Table 1).

Recent studies have found that microorganisms have a significant effect on Cd uptake by plants. For example, exogenous application of Bacillus *thuringiensis* X30 and Serratia *liquefaciens* CL-1 could significantly reduce soil available Cd content and rape Cd accumulation (Han et al., 2018). Similarly, *Bacillus strain* XT4 inoculation reduced soil available Cd content and Cd content in *Brassica rapa* (Zhang et al., 2021). However, it was discovered in another study that inoculating various strains of arbuscular mycorrhizal (AM) fungus considerably enhanced the absorption efficiency of Cd by *Sedum alfredii* Hance (Hu et al., 2013). The promotion or inhibition of Cd absorption from the environment by plants is mainly achieved by the adsorption, fixation or dissolution of Cd by various microorganisms, some of which modify the form of Cd, reducing its bioavailability, or fixing it with their own cells through adsorption, lowering the Cd content in the environment, as a result, lowering plant absorption of Cd (Li et al., 2018; Yuan et al., 2018; Wang et al., 2021), while other microorganisms can dissolve $CdCO_3$ and solid Cd in the environment, increasing Cd's environmental bioavailability (Yang et al., 2018), promoting the absorption of Cd by plants. Meanwhile, by fostering the growth of plant roots, some Plant Growth-Promoting Bacteria (PGPB) can enhance plants' resistance to Cd stress and Cd buildup (Prapagdee et al., 2013). In order to verify whether the strains tested in the current

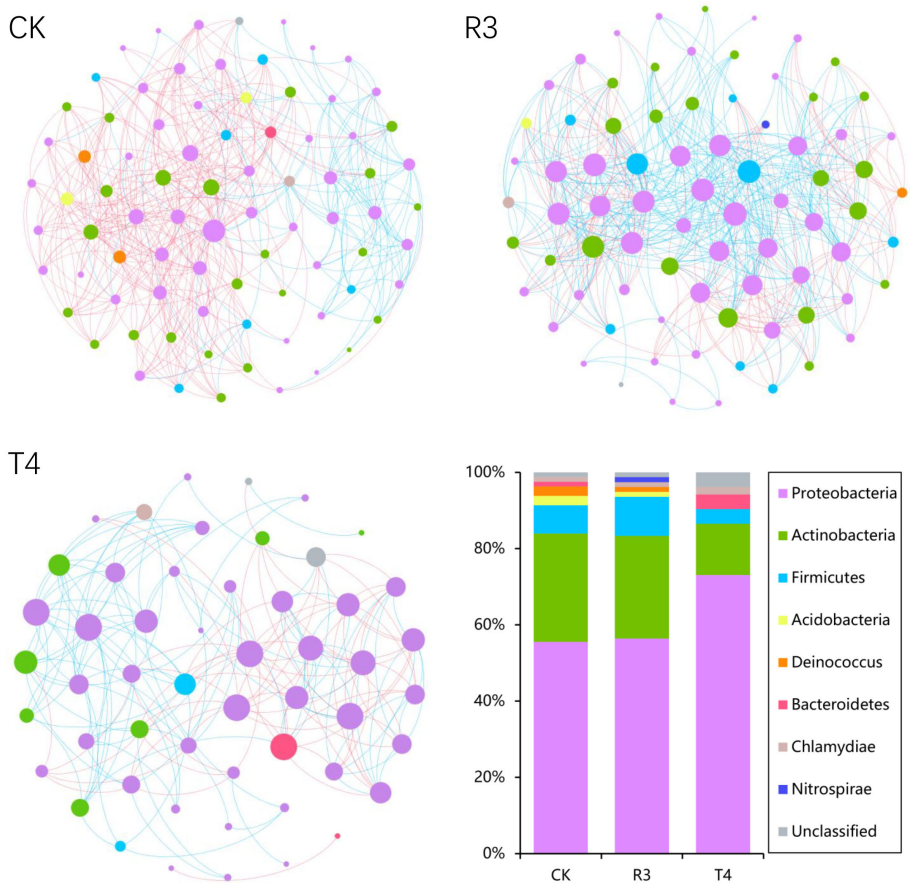

FIGURE 3
The co-occurrence networks for CK, R3 and T4, colored by phylum. A connection indicates a strong (Spearman's |r|>0.8) and significant (P <0.01) correlation. Positive correlations are represented by blue lines, while negative correlations are represented by red lines. The node size represents the degree of OTUs.

study had an effect on the morphological transformation of Cd, we used *E. coli* as a positive control for a Cd^{2+} adsorption experiment. The findings demonstrated that strains R3 and T4 inoculation did not change the content of available Cd in the nutrient solution (Figure S3), therefore, it is first rejected that these two strains may have an impact on the Cd bioavailable in the environment. In our study, it was found that compared with CK, inoculation of the R3 strain could significantly lower the Cd concentration in each rice plant part that was examined for this study, while not significantly affecting the Cd transfer coefficient from the roots to the aboveground part, but significantly decreasing the Cd enrichment coefficient of roots to the environment (Table 1). It showed that strain R3 could reduce the Cd level of every region of the rice plant, mostly through diminishing rice roots' ability to absorption of Cd from the environment. Compared with CK, the inoculation with the T4 strain significantly increased Cd content in all parts of the rice plant. While the transport coefficient of Cd from the root to the aboveground part did not change significantly, the Cd enrichment ability of the root to the environment was greatly increased (Table 1), indicating that strain T4 increased Cd content in all parts of rice plants mainly by enhancing the Cd uptake ability of rice roots. Therefore, one of the major affecting the Cd content of rice plants is the capacity of rice roots to accumulate Cd from the environment.

4.2 Effects of bacterial community structure and interaction in rice roots on Cd accumulation

The accumulation of Cd in rice plants mainly depends on the availability ofCd in the environment (Zhu et al., 2016; Wang et al., 2019), rice variety (Chen et al., 2019), rice planting management systems (Honma et al., 2016; Spanu et al., 2018; Wang et al., 2020b), physiological and ecological conditions of the rice plants (He et al., 2008; Uraguchi et al., 2009; Bari et al., 2020), and the endophytic microbial community (Zhou et al., 2020; Su et al., 2021). The effective Cd content in the environment did not significantly change in this study, and the rice varieties and planting management conditions were all the same. Therefore, variations in the endophytic bacterial community of the rice roots across the various treatments may be the reason for differences in Cd accumulation in rice plants. Studies have shown that plants rely on useful interactions between roots and microbes to acquire nutrients, stimulate growth and development, and withstand abiotic and biotic stresses (Edwards et al., 2015), therefore, the root microbial community is important in Cd accumulation in rice. However, little is known about how to root microorganisms influence Cd buildup in rice plants.

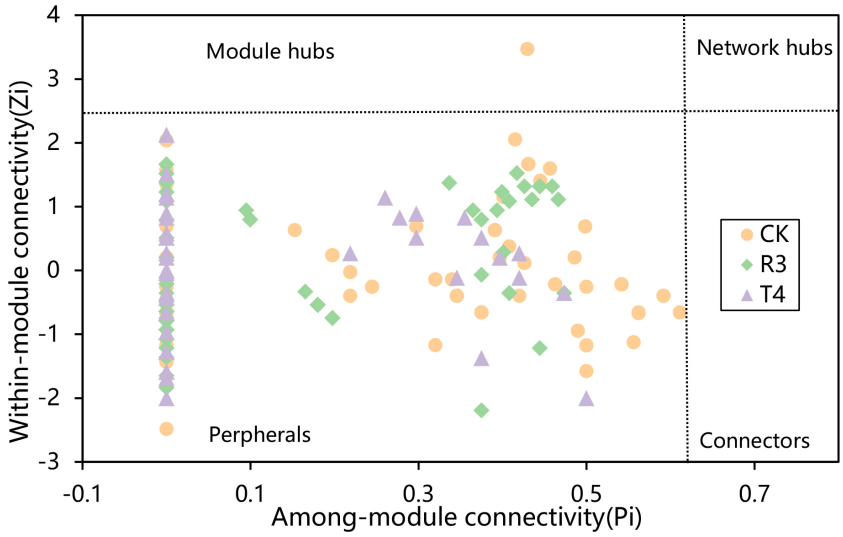

FIGURE 4
The distribution of OTUs in the three groups of samples was displayed using Zi-Pi plots based on their topological network roles. The Zi and Pi threshold values for classifying OTUs were 2.5 and 0.62, respectively.

In this research, when compared with CK, neither of the rice root endophytic bacterial communities treated with strains R3 or T4 showed significantly altered diversity (Figures 1A–C, Table S2), indicating that the diversity of endophytic bacterial communities in rice roots was not a key factor affecting Cd uptake by rice. This was consistent with a study where it was shown *Sedum plumbizincicola*'s accumulation of Cd and Zn to be unrelated to the diversity of the endophytic bacterial community (Hou et al., 2017). However, the relative abundance of different endophytic bacteria in the roots of rice inoculated with strains R3 and T4 changed significantly (Figure 1D). This may be due to the fact that exogenous strains enter the tissues of rice through the lenticels or wounds (Compant et al., 2005), disrupting the makeup of the original microbial community, and forming a new stable community structure after a certain period of interaction. Studies have shown that inoculation with specific bacteria can alter the microbial community of plant roots, thereby altering symbiotic relationships involved in the turnover of soil organic matter (Ibekwe et al., 2013). Thus, we speculate that the different relative abundances of specific bacterial taxa were one of the explanations for the discrepancies in Cd accumulation in the rice plants.

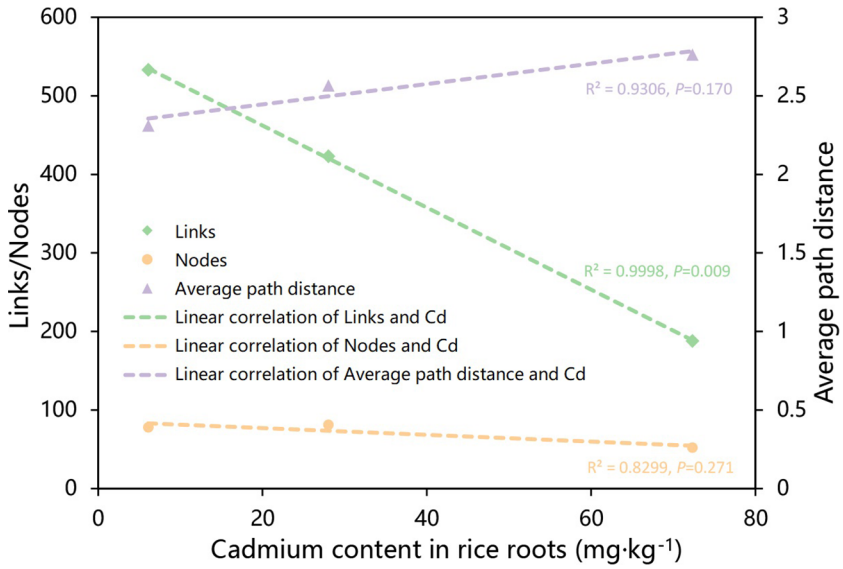

FIGURE 5
Plots of linear regression analysis illustrating the correlations between the nodes, links, and average path distance of the molecular ecological network and the Cd content of the rice. Linear regressions were detected for parameters that linked with rice Cd concentration considerably (*P* value < 0.05).

Previous research has revealed a significant link between the Cd level of rice roots and the endophytic bacterial taxa (Chu et al., 2021). We discovered that there was a strong link between the bacterial taxa in rice roots and the Cd concentration in rice plants using Pearson correlation analysis (Figure 2). The results revealed that the Cd concentration and root Cd enrichment coefficient of rice plants were strongly favorably connected with *Achromobacter*, *Agromyces*, and *Acidocella*, and considerably negatively linked with *Burkholderia* and *Acidovorax*. At present, other studies have found that these bacterial groups interact with Cd. For example, *Achromobacter* has a strong Cd adsorption action (Abyar et al., 2012); *Agromyces* has a dissolving action on Cd and can improve plant Cd absorption (Kuffner et al., 2008; De Maria et al., 2011); *Burkholderia* Y4 can limit Cd accumulation in rice by boosting nutrient absorption, resulting in a competitive impact (Wang et al., 2020a). The variations in the physiological functions and relative abundances of various bacterial groups may be one of the key explanations for the discrepancies in Cd accumulation in rice, and the interaction of specific bacterial groups with crops and Cd requires further study.

Interactions between microorganisms have important roles in plant health (Durán et al., 2018), including plant growth synergistic effects (Van der Heijden et al., 2015) and microbiological pathogen antagonistism (Santhanam et al., 2015), and the mutual competition and cooperation between microorganisms contributes greatly to the entire microbial community (Hassani et al., 2018). In our study, we found that, while the number of nodes in the microbial network of rice roots treated with strain R3 did not change much in comparison with CK, the number of links increased significantly, and the average path distance decreased. In comparison, the rice treated with strain T4 has considerably fewer nodes and links in its root microbial network, and the average path distance increased (Figure 3). This indicated that after inoculation with strain R3, endophytic bacteria in rice roots interacted more complexly and closely, however, the interaction between endophytic bacteria in rice roots became simpler following inoculation with strain T4. According to relevant research, complex networks can better adapt to environmental changes (Berry and Widder, 2014; Zheng et al., 2022) or can better resist the damage of soil diseases to plants (Yang et al., 2017). The average path distance and the number of links between network nodes were both connected with the amount of Cd present in rice plants, as can be shown in Figure 5, whereas the network's size was not the main factor impacting Cd absorption in rice. Therefore, there was a significant link between the network's intricacy and the Cd content in rice plants.

It's interesting to note that either strain inoculation significantly increased the positive (positively correlated) interactions in the rice root network (Figure 1). Positive interactions tend to indicate complementation or cooperation between nodes, while negative (negatively correlated) interactions imply predation or competition. Compared with CK, the root endophytes of both treatments had more harmonious symbiotic patterns (Ye et al., 2012). We speculate that the two strains' inoculation initially altered the relative abundance of some endophytic bacteria that interact with Cd in rice roots, and that these changes may cause rice Cd uptake to exhibit the two different effects, either inhibiting or promoting uptake, and that the greater number of positive interactions may lead to more synergy between endophytic bacteria to jointly inhibit or promote Cd absorption and transport, thus causing the significant differences in Cd content of rice plants treated with the inoculated strains. These results suggest that inoculation of R3 and T4 strains not only had a significant impact on the functional structure of rice plant root microbial endophytic communities, but also on their microbial network interactions, with changes in these functional structures and interactions being significantly related to Cd concentration in rice plants. Further research on the physiological and biochemical properties of rice roots and the expression of genes associated to Cd absorption and transport will help to reveal the respective molecular mechanisms in rice of Cd uptake inhibition or promotion by the R3 and T4 strains.

5 Conclusion

Our research analyzed the influence of endophytic bacteria inoculation on Cd content in rice plants, and explored the effect of endophytic microbial communities in rice roots on rice plant Cd accumulation. The results indicated that the two strains, R3 and T4, respectively, exhibited significant inhibitory and promotion effects on Cd uptake in rice, and that this significant difference was mainly due to the altered relative abundance of endophytic bacterial taxa and their interactions in the rice roots. The higher the relative abundance of *Agromyces*, *Achromobacter* and *Acidocella* in the roots of rice plants and the simpler the network structure, the higher the Cd content of rice plants, but the higher the relative abundance of *Burkholderia* and *Acidovorax* in the root endophytic communities, and the more complex the network structure, the lower the Cd content of rice plants. Our findings imply that modulating the composition and interaction of root endophytic bacteria can efficiently minimize Cd buildup in rice plants without adverse effects. This study offers a different strategy to guarantee the cultivation of crops safely in paddy fields polluted by Cd, and a new microecological criterion for evaluating the role of exogenously added strains in Cd-contaminated remediation.

Data availability statement

The datasets presented in this study can be found in online repositories. The names of the repository/repositories and accession number(s) can be found in the article/Supplementary Material.

Author contributions

PL: Data curation, writing-original draft preparation. JL: Writing-reviewing and editing, validation. ZX, YT, ZZ, ZL and RH: Data collation and verification. QW, HA and ZY: Writing guidance. All authors contributed to the article and approved the submitted version.

Funding

This research was supported by the Hunan Province Innovation Platform and Talent Plan—Hunan Young Talents (2020RC3073), the General project of Natural Science Foundation of Hunan Province (2020JJ4038), and the National Natural Science Foundation of China (32172107).

Conflict of interest

The authors declare that the research was conducted in the absence of any commercial or financial relationships that could be construed as a potential conflict of interest.

Publisher's note

Supplementary material

The Supplementary Material for this article can be found online at: https://www.frontiersin.org/articles/10.3389/fpls.2023.1196130/full#supplementary-material

References

Abyar, H., Safahieh, A., Zolgharnein, H., and Zamani, I. (2012). Isolation and Identification of Achromobacter denitrificans and Evaluation of its Capacity in Cadmium Removal. *Polish J. Environ. Stud.* 21, 1523–1527.

Andresen, E., and Küpper, H. (2013). "Cadmium Toxicity in Plants," in *Cadmium: From Toxicity to Essentiality* (Germany: Springer Netherlands), 395–413.

Bari, M. A., Prity, S. A., Das, U., Akther, M. S., Sajib, S. A., Reza, M. A., et al. (2020). Silicon induces phytochelatin and ROS scavengers facilitating cadmium detoxification in rice. *Plant Biol.* 22, 472–479. doi: 10.1111/plb.13090

Berry, D., and Widder, S. (2014). Deciphering microbial interactions and detecting keystone species with co-occurrence networks. *Front. Microbiol.* 5, 219. doi: 10.3389/fmicb.2014.00219

Chatterjee, S., Kumari, S., Rath, S., Priyadarshanee, M., and Das, S. (2020). Diversity, structure and regulation of microbial metallothionein: metal resistance and possible applications in sequestration of toxic metals. *Metallomics* 12, 1637–1655. doi: 10.1039/d0mt00140f

Chen, L., Wu, W., Han, F., Li, J., Ye, W., Fu, H., et al. (2019). Agronomic management and rice varieties controlling cd bioaccumulation in rice. *Int. J. Environ. Res. Public Health* 16, 2376. doi: 10.3390/ijerph16132376

Chen, B., Zhang, Y., Rafiq, M. T., Khan, K. Y., Pan, F., Yang, X., et al. (2014). Improvement of cadmium uptake and accumulation in Sedum alfredii by endophytic bacteria Sphingomonas SaMR12 : Effects on plant growth and root exudates. *Chemosphere* 117, 367–373. doi: 10.1016/j.chemosphere.2014.07.078

Cheng, C., Wang, R., Sun, L., He, L., and Sheng, X. (2021b). Cadmium-resistant and arginine decarboxylase-producing endophytic Sphingomonas sp. C40 decreases cadmium accumulation in host rice (Oryza sativa Cliangyou 513). *Chemosphere* 275, 130109. doi: 10.1016/j.chemosphere.2021.130109

Cheng, C., Wang, Q., Wang, Q. X., He, L. Y., and Sheng, X. F. (2021a). Wheat-associated Pseudomonas Taiwanensis WRS8 reduces cadmium uptake by increasing root surface cadmium adsorption and decreasing cadmium uptake and transport related gene expression in wheat. *Environ. pollut.* 268, 115850. doi: 10.1016/j.envpol.2020.115850

Chu, C., Fan, M., Song, C., Li, N., Zhang, C., Fu, S., et al. (2021). Unveiling endophytic bacterial community structures of different rice cultivars grown in a cadmium-contaminated paddy field. *Front. Microbiol.* 12. doi: 10.3389/fmicb.2021.756327

Compant, S. P., Reiter, B., Sessitsch, A., Nowak, J., Cleíment, C., and Ait Barka, E. d. (2005). Endophytic Colonization of Vitis vinifera L. by Plant Growth-Promoting Bacterium Burkholderia sp. Strain PsJN. *Appl. Environ. Microbiol.* 71, 1685–1693. doi: 10.1128/AEM.71.4.1685-1693.2005

Cui, H., Ou, Y., Wang, L., Yan, B., Li, Y., and Ding, D. (2020). The passivation effect of heavy metals during biochar-amended composting: Emphasize on bacterial communities. *Waste Manage.* 118, 360–368. doi: 10.1016/j.wasman.2020.08.043

De Maria, S., Rivelli, A. R., Kuffner, M., Sessitsch, A., Wenzel, W. W., Gorfer, M., et al. (2011). Interactions between accumulation of trace elements and macronutrients in Salix caprea after inoculation with rhizosphere microorganisms. *Chemosphere* 84, 1256–1261. doi: 10.1016/j.chemosphere.2011.05.002

Durán, P., Thiergart, T., Garrido Oter, R., Agler, M., Kemen, E., Schulze Lefert, P., et al. (2018). Microbial interkingdom interactions in roots promote arabidopsis survival. *Cell* 175, 973–983.e14. doi: 10.1016/j.cell.2018.10.020

Edwards, J., Johnson, C., Santos Medellín, C., Lurie, E., Podishetty, N. K., Bhatnagar, S., et al. (2015). Structure, variation, and assembly of the root-associated microbiomes of rice. *Proc. Natl. Acad. Sci.* 112, E911–E920. doi: 10.1073/pnas.1414592112

El-Esawi, M. A., Elkelish, A., Soliman, M., Elansary, H. O., Zaid, A., and Wani, S. H. (2020). Serratia marcescens BM1 enhances cadmium stress tolerance and phytoremediation potential of soybean through modulation of osmolytes, leaf gas exchange, antioxidant machinery, and stress-responsive genes expression. *Antioxidants* 9, 43. doi: 10.3390/antiox9010043

Han, H., Wang, Q., He, L., and Sheng, X. (2018). Increased biomass and reduced rapeseed Cd accumulation of oilseed rape in the presence of Cd-immobilizing and polyamine-producing bacteria. *J. Hazardous Materials* 353, 280–289. doi: 10.1016/j.jhazmat.2018.04.024

Hassani, M. A., Durán, P., and Hacquard, S. (2018). Microbial interactions within the plant holobiont. *Microbiome* 6, 58. doi: 10.1186/s40168-018-0445-0

He, J. Y., Ren, Y. F., Wang, F. J., Pan, X. B., Zhu, C., and Jiang, D. A. (2008). Characterization of Cadmium Uptake and Translocation in a Cadmium-Sensitive Mutant of Rice (Oryza sativa L. ssp. japonica). *Arch. Environ. Contamination Toxicol.* 57, 299–306. doi: 10.1007/s00244-008-9273-8

He, T., Xu, Z. J., Wang, J. F., Wang, F. P., Zhou, X. F., Wang, L. L., et al. (2022). Improving cadmium accumulation by Solanum nigrum L. via regulating rhizobacterial community and metabolic function with phosphate-solubilizing bacteria colonization. *Chemosphere* 287, 132209. doi: 10.1016/j.chemosphere.2021.132209

He, X., Xu, M., Wei, Q., Tang, M., Guan, L., Lou, L., et al. (2020). Promotion of growth and phytoextraction of cadmium and lead in Solanum nigrum L. mediated by plant-growth-promoting rhizobacteria. *Ecotoxicology Environ. Saf.* 205, 111333. doi: 10.1016/j.ecoenv.2020.111333

Honma, T., Ohba, H., Kaneko Kadokura, A., Makino, T., Nakamura, K., and Katou, H. (2016). Optimal soil eh, pH, and water management for simultaneously minimizing arsenic and cadmium concentrations in rice grains. *Environ. Sci. Technol.* 50, 4178–4185. doi: 10.1021/acs.est.5b05424

Hou, J., Liu, W., Wu, L., Hu, P., Ma, T., Luo, Y., et al. (2017). Modulation of the efficiency of trace metal phytoremediation by Sedum plumbizincicola by microbial community structure and function. *Plant Soil* 421, 285–299. doi: 10.1007/s11104-017-3466-8

Hu, J., Wu, S., Wu, F., Leung, H. M., Lin, X., and Wong, M. H. (2013). Arbuscular mycorrhizal fungi enhance both absorption and stabilization of Cd by Alfred stonecrop (Sedum alfredii Hance) and perennial ryegrass (Lolium perenne L.) in a Cd-contaminated acidic soil. *Chemosphere* 93, 1359–1365. doi: 10.1016/j.chemosphere.2013.07.089

Huang, S., Wang, P., Yamaji, N., and Ma, J. F. (2020). Plant nutrition for human nutrition: Hints from rice research and future perspectives. *Mol. Plant* 13, 825–835. doi: 10.1016/j.molp.2020.05.007

Ibekwe, A. M., Bodenhausen, N., Horton, M. W., and Bergelson, J. (2013). Bacterial communities associated with the leaves and the roots of arabidopsis thaliana. *PLoS One* 8, 2. doi: 10.1371/journal.pone.0056329

Kembel, S. W., O'Connor, T. K., Arnold, H. K., Hubbell, S. P., Wright, S. J., and Green, J. L. (2014). Relationships between phyllosphere bacterial communities and plant functional traits in a neotropical forest. *Proc. Natl. Acad. Sci.* 111, 13715–13720. doi: 10.1073/pnas.1216057111

Kuang, X. L., Gu, J. D., Tie, B. Q., Yao, B. S., and Shao, J. H. (2016). Interactive effects of cadmium and Microcystis aeruginosa (cyanobacterium) on the growth, antioxidative responses and accumulation of cadmium and microcystins in rice seedlings. *Ecotoxicology* 25, 1588–1599. doi: 10.1007/s10646-016-1714-y

Kuffner, M., Puschenreiter, M., Wieshammer, G., Gorfer, M., and Sessitsch, A. (2008). Rhizosphere bacteria affect growth and metal uptake of heavy metal accumulating willows. *Plant Soil* 304, 35–44. doi: 10.1007/s11104-007-9517-9

Kukusamude, C., Sricharoen, P., Limchoowong, N., and Kongsri, S. (2021). Heavy metals and probabilistic risk assessment via rice consumption in Thailand. *Food Chem.* 334, 127402. doi: 10.1016/j.foodchem.2020.127402

Li, T., Chang, Q., Yuan, X., Li, J., Ayoko, G. A., Frost, R. L., et al. (2017). Cadmium transfer from contaminated soils to the human body through rice consumption in southern Jiangsu Province, China. *Environ. Science: Processes Impacts* 19, 843–850. doi: 10.1039/C6EM00631K

Li, X., Lan, X., Feng, X., Luan, X., Cao, X., and Cui, Z. (2021). Biosorption capacity of Mucor circinelloides bioaugmented with Solanum nigrum L. for the cleanup of lead, cadmium and arsenic. *Ecotoxicology Environ. Saf.* 212, 112014. doi: 10.1016/j.ecoenv.2021.112014

Li, L., Wang, S., Li, X., Li, T., and Yong, T. (2018). Effects of Pseudomonas chenduensis and biochar on cadmium availability and microbial community in the paddy soil. *Sci. Total Environ.* 640, 1034–1043. doi: 10.1016/j.scitotenv.2018.05.287

Ma, Y., Rajkumar, M., Zhang, C., and Freitas, H. (2016). Beneficial role of bacterial endophytes in heavy metal phytoremediation. *J. Environ. Manage.* 174, 14–25. doi: 10.1016/j.jenvman.2016.02.047

Peng, X. L., Cheng, P., Pharmacy, D. O., and Vocationalamp, Z. R. (2014). Icp-aes and icp-ms analysis of mineral elements in rice. *J. henan Univ. technology (natural Sci. edition)* 34, 4. doi: 10.16433/j.cnki.issn1673-2383.2013.04.024

Prapagdee, B., Chanprasert, M., and Mongkolsuk, S. (2013). Bioaugmentation with cadmium-resistant plant growth-promoting rhizobacteria to assist cadmium phytoextraction by Helianthus annuus. *Chemosphere* 92, 659–666. doi: 10.1016/j.chemosphere.2013.01.082

Santhanam, R., Luu, V. T., Weinhold, A., Goldberg, J., Oh, Y., and Baldwin, I. T. (2015). Native root-associated bacteria rescue a plant from a sudden-wilt disease that emerged during continuous cropping. *Proc. Natl. Acad. Sci.* 112, E5013–E5020. doi: 10.1073/pnas.1505765112

Shan, S., Guo, Z., Lei, P., Li, Y., Wang, Y., Zhang, M., et al. (2020). Increased biomass and reduced tissue cadmium accumulation in rice via indigenous Citrobacter sp. XT1-2-2 and its mechanisms. *Sci. Total Environ.* 708, 135224. doi: 10.1016/j.scitotenv.2019.135224

Siripornadulsil, S., and Siripornadulsil, W. (2013). Cadmium-tolerant bacteria reduce the uptake of cadmium in rice: Potential for microbial bioremediation. *Ecotoxicology Environ. Saf.* 94, 94–103. doi: 10.1016/j.ecoenv.2013.05.002

Song, Y., Jin, L., and Wang, X. (2016). Cadmium absorption and transportation pathways in plants. *Int. J. Phytoremediation* 19, 133–141. doi: 10.1080/15226514.2016.1207598

Spanu, A., Valente, M., Langasco, I., Barracu, F., Orlandoni, A. M., and Sanna, G. (2018). Sprinkler irrigation is effective in reducing cadmium concentration in rice (Oryza sativa L.) grain: A new twist on an old tale? *Sci. Total Environ.* 628-629, 1567–1581. doi: 10.1016/j.scitotenv.2018.02.157

Su, Z. Z., Dai, M., Zhu, J. N., Liu, X. H., and Lin, F. C. (2021). Dark septate endophyte Falciphora oryzae-assisted alleviation of cadmium in rice. *J. Hazardous Materials* 419, 126435. doi: 10.1016/j.jhazmat.2021.126435

Teixeira, C., Almeida, C. M. R., Nunes da Silva, M., Bordalo, A. A., and Mucha, A. P. (2014). Development of autochthonous microbial consortia for enhanced phytoremediation of salt-marsh sediments contaminated with cadmium. *Sci. Total Environ.* 493, 757–765. doi: 10.1016/j.scitotenv.2014.06.040

Uraguchi, S., Mori, S., Kuramata, M., Kawasaki, A., Arao, T., and Ishikawa, S. (2009). Root-to-shoot Cd translocation via the xylem is the major process determining shoot and grain cadmium accumulation in rice. *J. Exp. Bot.* 60, 2677–2688. doi: 10.1093/jxb/erp119

Van der Heijden, M. G. A., Bruin, S. d., Luckerhoff, L., van Logtestijn, R. S. P., and Schlaeppi, K. (2015). A widespread plant-fungal-bacterial symbiosis promotes plant biodiversity, plant nutrition and seedling recruitment. *ISME J.* 10, 389–399. doi: 10.1038/ismej.2015.120

Wan, L., and Zhang, H. (2012). Cadmium toxicity: effects on cytoskeleton, vesicular trafficking and cell wall construction. *Plant Signaling Behav.* 7, 345–348. doi: 10.4161/psb.18992

Wang, S., Dai, H., Wei, S., Skuza, L., and Chen, Y. (2022). Effects of Cd-resistant fungi on uptake and translocation of Cd by soybean seedlings. *Chemosphere* 291, 132908. doi: 10.1016/j.chemosphere.2021.132908

Wang, X., Deng, S., Zhou, Y., Long, J., Ding, D., Du, H., et al. (2020b). Application of different foliar iron fertilizers for enhancing the growth and antioxidant capacity of rice and minimizing cadmium accumulation. *Environ. Sci. pollut. Res.* 28, 7828–7839. doi: 10.1007/s11356-020-11056-9

Wang, C., Huang, Y., Yang, X., Xue, W., Zhang, X., Zhang, Y., et al. (2020a). Burkholderia sp. Y4 inhibits cadmium accumulation in rice by increasing essential nutrient uptake and preferentially absorbing cadmium. *Chemosphere* 252, 126603. doi: 10.1016/j.chemosphere.2020.126603

Wang, J., Wang, P. M., Gu, Y., Kopittke, P. M., Zhao, F. J., and Wang, P. (2019). Iron–Manganese (Oxyhydro)oxides, Rather than Oxidation of Sulfides, Determine Mobilization of Cd during Soil Drainage in Paddy Soil Systems. *Environ. Sci. Technol.* 53, 2500–2508. doi: 10.1021/acs.est.8b06863

Wang, Y., Zheng, X., He, X., Lü, Q., Qian, X., Xiao, Q., et al. (2021). Effects of Pseudomonas TCd-1 on rice (Oryza sativa) cadmium uptake, rhizosphere soils enzyme activities and cadmium bioavailability under cadmium contamination. *Ecotoxicol Environ. Saf.* 218, 112249. doi: 10.1016/j.ecoenv.2021.112249

Xu, P., Lai, C., Zeng, G., Huang, D., Chen, M., Song, B., et al. (2018). Enhanced bioremediation of 4-nonylphenol and cadmium co-contaminated sediment by composting with Phanerochaete chrysosporium inocula. *Bioresource Technol.* 250, 625–634. doi: 10.1016/j.biortech.2017.11.069

Yang, H., Li, J., Xiao, Y., Gu, Y., Liu, H., Liang, Y., et al. (2017). An Integrated Insight into the Relationship between Soil Microbial Community and Tobacco Bacterial Wilt Disease. *Front. Microbiol.* 8. doi: 10.3389/fmicb.2017.02179

Yang, P., Zhou, X. F., Wang, L. L., Li, Q. S., Zhou, T., Chen, Y. K., et al. (2018). Effect of phosphate-solubilizing bacteria on the mobility of insoluble cadmium and metabolic analysis. *Int. J. Environ. Res. Public Health* 15, 1330. doi: 10.3390/ijerph15071330

Ye, D., Jiang, Y. H., Yang, Y., He, Z., Luo, F., and Zhou, J. (2012). Molecular ecological network analyses. *BMC Bioinf.* 13, 113. doi: 10.1186/1471-2105-13-113

Yuan, C., Liu, T., Li, F., Liu, C., Yu, H., Sun, W., et al. (2018). Microbial iron reduction as a method for immobilization of a low concentration of dissolved cadmium. *J. Environ. Manage* 217, 747–753. doi: 10.1016/j.jenvman.2018.04.023

Yue, G., Zhu, C., Gan, L., Ng, D., and Xia, K. (2015). Effects of exogenous gibberellic acid3 on iron and manganese plaque amounts and iron and manganese uptake in rice. *PLoS One* 10, e0118177. doi: 10.1371/journal.pone.011817

Zhang, X., Li, X., Yang, H., and Cui, Z. (2018). Biochemical mechanism of phytoremediation process of lead and cadmium pollution with Mucor circinelloides and Trichoderma asperellum. *Ecotoxicology Environ. Saf.* 157, 21–28. doi: 10.1016/j.ecoenv.2018.03.047

Zhang, J., Wang, X., Zhang, L. X., and Zhao, F. J. (2021). Reducing cadmium bioavailability and accumulation in vegetable by an alkalizing bacterial strain. *Sci. Total Environ.* 758, 143596. doi: 10.1016/j.scitotenv.2020.143596

Zheng, Z., Li, P., Xiong, Z., Ma, T., Mathivanan, K., Praburaman, L., et al. (2022). Integrated network analysis reveals that exogenous cadmium-tolerant endophytic bacteria inhibit cadmium uptake in rice. *Chemosphere* 301, 134655. doi: 10.1016/j.chemosphere.2022.134655

Zhou, J., Li, P., Meng, D., Gu, Y., Zheng, Z., Yin, H., et al. (2020). Isolation, characterization and inoculation of Cd tolerant rice endophytes and their impacts on rice under Cd contaminated environment. *Environ. pollut.* 260, 113990. doi: 10.1016/j.envpol.2020.113990

Zhu, H., Chen, C., Xu, C., Zhu, Q., and Huang, D. (2016). Effects of soil acidification and liming on the phytoavailability of cadmium in paddy soils of central subtropical China. *Environ. pollut.* 219, 99–106. doi: 10.1016/j.envpol.2016.10.043

Frontiers in Plant Science

Cultivates the science of plant biology and its applications

The most cited plant science journal, which advances our understanding of plant biology for sustainable food security, functional ecosystems and human health.

Discover the latest Research Topics

See more →

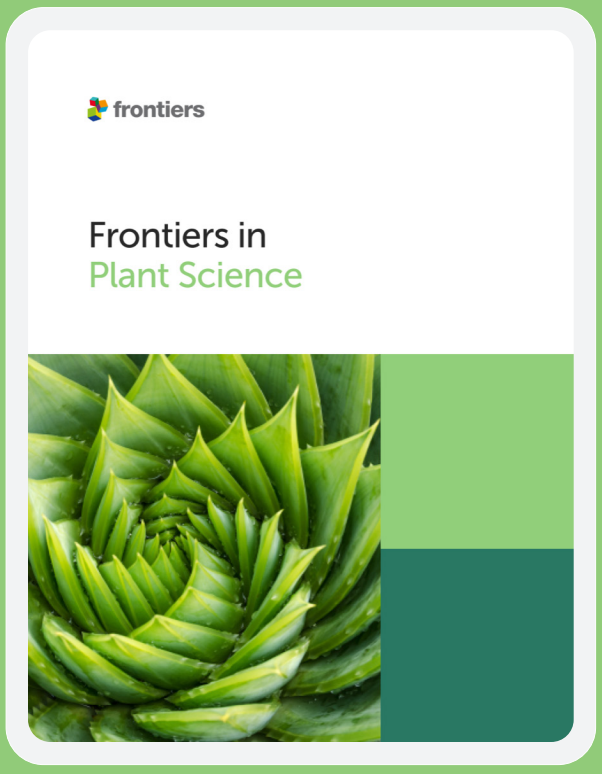

Frontiers

Avenue du Tribunal-Fédéral 34
1005 Lausanne, Switzerland
frontiersin.org

Contact us

+41 (0)21 510 17 00
frontiersin.org/about/contact